HiTASC

High Temperature Advanced Structural Composites

Rensselaer Polytechnic Institute
Troy, N. Y. 12180-3590

Final Report

Book 3 of 3: *Mechanics*

University Research Initiative

Contract No.: N00014-86-K-0770
October, 1986 - June, 1992

Sponsored by: The Defense Advanced Research Projects Agency

Monitored by: Office of Naval Research

FINAL REPORT

University Research Initiative
Contract No. N00014—86—K—0770
October 1, 1986 — June 13, 1992

High Temperature Advanced Structural Composites

vol. 3 of 3

sponsored by
Office of Naval Research and
Defense Advanced Research Projects Agency

SECURITY CLASSIFICATION OF THIS PAGE

REPORT DOCUMENTATION PAGE

Form Approved OMB No. 0704-0188

1a. REPORT SECURITY CLASSIFICATION Unclassified	1b. RESTRICTIVE MARKINGS
2a. SECURITY CLASSIFICATION AUTHORITY	3. DISTRIBUTION / AVAILABILITY OF REPORT Unrestricted
2b. DECLASSIFICATION / DOWNGRADING SCHEDULE	
4. PERFORMING ORGANIZATION REPORT NUMBER(S)	5. MONITORING ORGANIZATION REPORT NUMBER(S)
6a. NAME OF PERFORMING ORGANIZATION Center for Composite Materials and Structures Rensselaer Polytechnic Institute 6b. OFFICE SYMBOL (If applicable)	7a. NAME OF MONITORING ORGANIZATION Office of Naval Research
6c. ADDRESS (City, State, and ZIP Code) Rensselaer Polytechnic Institute Troy, NY 12180-3590	7b. ADDRESS (City, State, and ZIP Code) 800 North Quincy Street Arlington, VA 22217-5000
8a. NAME OF FUNDING / SPONSORING ORGANIZATION Advanced Research Projects Agency 8b. OFFICE SYMBOL (If applicable)	9. PROCUREMENT INSTRUMENT IDENTIFICATION NUMBER #N00014-86-K-0770
8c. ADDRESS (City, State, and ZIP Code) 1400 Wilson Blvd. Arlington, Virginia 22209	10. SOURCE OF FUNDING NUMBERS PROGRAM ELEMENT NO. / PROJECT NO. / TASK NO. / WORK UNIT ACCESSION NO.

11. TITLE (Include Security Classification)
High Temperature Advanced Structural Composites

12. PERSONAL AUTHOR(S)
George J. Dvorak and R. Judd Diefendorf

13a. TYPE OF REPORT	13b. TIME COVERED	14. DATE OF REPORT (Year, Month, Day)	15. PAGE COUNT
Final	FROM 861001 TO 920613	930402	748

16. SUPPLEMENTARY NOTATION

17. COSATI CODES			18. SUBJECT TERMS (Continue on reverse if necessary and identify by block number)
FIELD	GROUP	SUB-GROUP	High temperature composites, Fibers, Matrices, Interfaces, Processing, Thermomechanical and Environmental behavior

19. ABSTRACT (Continue on reverse if necessary and identify by block number)

Final results obtained on the High Temperature Advanced Structural Composites Program at Rensselaer Polytechnic Institute are described in three volumes. Volume one contains the Executive Summary and reprints of papers on Intermetallic Compounds. Volume two contains reprints of papers on Ceramic Matrix Composites, Fiber Processing and Properties and on Interfaces. The third volume contains reprints of papers on Mechanics.

20. DISTRIBUTION / AVAILABILITY OF ABSTRACT ☒ UNCLASSIFIED/UNLIMITED ☐ SAME AS RPT. ☐ DTIC USERS	21. ABSTRACT SECURITY CLASSIFICATION Unclassified
22a. NAME OF RESPONSIBLE INDIVIDUAL	22b. TELEPHONE (Include Area Code) / 22c. OFFICE SYMBOL

DD Form 1473, JUN 86 Previous editions are obsolete. SECURITY CLASSIFICATION OF THIS PAGE

HiTASC

HIGH TEMPERATURE ADVANCED STRUCTURAL COMPOSITES

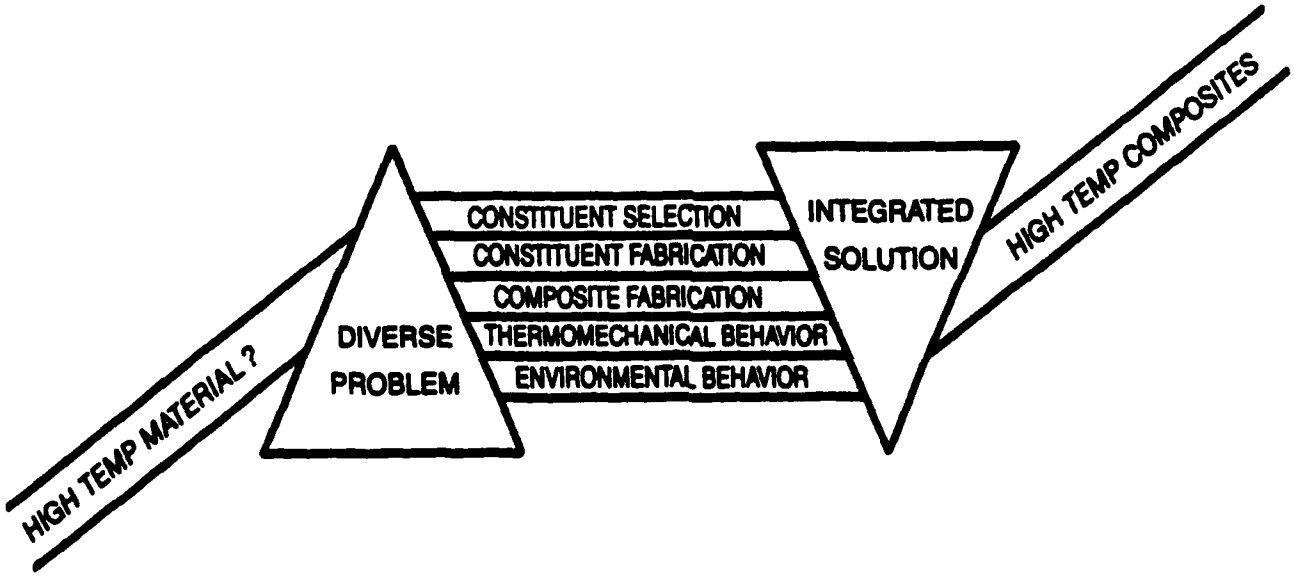

RENSSELAER POLYTECHNIC INSTITUTE
TROY, N.Y. 12180-3590

Sponsored by
ONR/DARPA

FINAL REPORT

University Research Initiative
CONTRACT NO. N00014-86-K-0770
OCTOBER 1, 1986 – JUNE 13, 1992

Volume 3 of 3

HiTASC

HIGH TEMPERATURE ADVANCED STRUCTURAL COMPOSITES

Professor George J. Dvorak
Program Director

Professor R. J. Diefendorf
Program Director (1986–1989)

Program Monitors

Dr. William Coblenz, Defense Advanced Research Projects Agency

and

Dr. Steven Fishman, Office of Naval Research

RENSSELAER POLYTECHNIC INSTITUTE

Troy, N.Y. 12180

SUMMARY

OF

TABLE OF CONTENTS

BOOK 3

TABLE OF CONTENTS

MECHANICS

MODELLING

Benveniste, Y. and Dvorak, G.J., "Some Remarks on a Class of Uniform Fields in Fibrous Composites," Journal of Applied Mechanics, 59, 1030–1032 (1992).

Bahei–El–Din, Y.A., Dvorak, G.J., "Local Fields in Uncoated and Coated High Temperature Fibrous Composite Systems," AD–Vol. 25–2, Damage and Oxidation Protection in High Temperature Composites – Vol. 2, ASME, 21–34 (1991).

Bahei–El–Din, Y.A., "Uniform Fields, Yielding, and Thermal Hardening in Fibrous Composite Laminates," International Journal of Plasticity, 8, 867–892 (1992).

Benveniste, Y. and Dvorak, G.J., "On a Correspondence Between Mechanical and Thermal Fields in Composites with Slipping Interfaces," Inelastic Deformation of Composite Materials, G.J. Dvorak, ed., IUTAM Symposium, Troy, New York, May 29–June 1, 1990, Springer–Verlag, New York, NY, 1991, pp. 77–98.

Dvorak, G.J. and Benveniste, Y., "On the Thermomechanics of Composites with Imperfectly Bonded Interfaces and Damage," International Journal of Solids and Structures, 29, 2907–2919 (1992).

Pijaudier–Cabot, G. and Dvorak, G.J., "A Variational Approximation of Stress Intensity Factors in Cracked Laminates," European Journal of Mechanics, A/Solids, 9 517–535 (1990).

THERMOVISCOPLASTICITY OF METAL METRIX LAMINATES

Krempl, E. and Lee, K.D., "Thermal, Viscoplastic Analysis of Composite Laminates," Materials Research Society Symposium Proceedings, Vol. 120, Materials Research Society, Pittsburgh, PA, 1988, pp. 129–136.

Krempl, E. and Yeh, N.–M., "Residual Stresses in Fibrous Metal Matrix Composites: A Thermoviscoplastic Analysis," Inelastic Deformation of Composite Materials, G.J. Dvorak, ed., IUTAM Symposium, Troy, New York, May 29–June 1, 1990, Springer–Verlag, New York, NY, 1991, pp. 411–443.

Lee, K.–D. and Krempl, E., "Thermomechanical, Time–Dependent Analysis of Layered Metal Matrix Composites," Thermal and Mechanical Behavior of Metal Matrix and Ceramic Matrix Composites, American Society for Testing and Materials, Philadelphia, 1990, pp. 40–55.

Lee, K.–D. and Krempl, E., "Uniaxial Thermomechanical Loading. Numerical Experiments Using the Thermal Viscoplasticity Theory Based on Overstress," European Journal of Mechanics, A/Solids, Vol. 10, 1991, pp. 173–192.

Yeh, N.–M. and Krempl, E., "A Numerical Simulation of the Effects of Volume Fraction, Creep and Thermal Cycling on the Behavior of Fibrous Metal–Matrix Composites," Journal of Composite Materials, Vol. 26, 1992, pp. 900–915.

Yeh, N.–M. and Krempl, E., "Thermoviscoplasticity Based on Overstress Applied to the Analysis of Fibrous Metal–Matrix Composites," Journal of Composite Materials, Vol. 26, 1992, pp. 969–990.

Yeh, N.–M. and Krempl, E., "The Influence of Cool–Down Temperature Histories on the Residual Stresses in Fibrous Metal Matrix Composites," Journal of Composite Materials, (to appear) (32 pp.).

Yeh, N.–M. and Krempl, E., "An Incremental Life Prediction Law for Multiaxial Creep–Fatigue Interaction and Thermomechanical Loading," Proceedings for the Symposium on Multiaxial Fatigue, ASTM, San Diego, CA 1991,(in press) (25 pp.).

Krempl, E. and Yeh, N.–M., "Residual Stresses Effects on Thermal Cycling Behavior of Laminated Metal Matrix Composites. A Thermoviscoplastic Analysis.," Residual Stresses – III, ICRS 3, Vol. 1, Ed. H. Fujiwara, T. Abe and K. Tanaka, Elsevier Science Publishers, Ltd., London, England, pp. 64–69 (1992).

Yeh, N.–M. and Krempl, E., "A Thermomechanical Analysis of Laminated Metal Matrix Composites Using the Viscoplasticity Theory Based on Overstress," Mechanics of Composites at Elevated and Cryogenic Temperatures, AMD–Vol. 118, ASME 1991, pp. 9–22.

Yeh, N.M. and Krempl, E., "A Thermoviscoplastic Analysis of Uniaxial Ratchetting Behavior of SiC/Ti Fibrous Metal Matrix Composites," Proceedings, American Society for Composites 6th Technical Conference on Composite Materials, Albany, New York, October 6–9, 1991, pp. 329–337.

MECHANICS

MODELLING

Reprinted from June 1989, Vol. 111, Journal of Applied Mechanics

Thermal Expansion of Three-Phase Composite Materials

George J. Dvorak
Fellow, ASME

Tungyang Chen
Graduate Research Assistant

Department of Civil Engineering,
Rensselaer Polytechnic Institute,
Troy, N.Y. 12180

Exact expressions are found for overall thermal expansion coefficients of a composite medium consisting of three perfectly-bonded transversely isotropic phases of cylindrical shape and arbitrary transverse geometry. The results show that macroscopic thermal expansion coefficients depend only on the thermoelastic constants and volume fractions of the phases, and on the overall compliance. The derivation is based on a decomposition procedure which indicates that spatially uniform elastic strain fields can be created in certain heterogeneous media by superposition of uniform phase thermal strains with local strains caused by piecewise uniform stress fields, which are in equilibrium with prescribed surface tractions. The procedure also allows evaluation of thermal stress fields in the aggregate in terms of known local fields caused by axisymmetric overall stresses. Finally, averages of local fields are found with the help of known mechanical stress and strain concentration factors.

1 Introduction

In his 1967 paper, Levin found that macroscopic thermal expansion coefficients of an elastic heterogeneous composite medium, consisting of two distinct, perfectly-bonded isotropic phases of arbitrary shape, depend in a unique way on the overall elastic moduli of the aggregate and on the thermoelastic constants of the phases. Such coefficients are the average overall strains caused by a uniform thermal change of unit magnitude in a traction-free composite. Levin's results, and their extension to binary systems with anisotropic constituents (Rosen and Hashin 1970), permit a direct evaluation of these coefficients in terms of the known overall elastic moduli and local thermoelastic constants. However, the approach cannot be applied to composites of three or more constituents without additional information about local stress concentration factors. Thermoelastic constants of such multiphase media can be bounded with the help of thermoelastic extremum principles (Schapery 1968, Rosen and Hashin 1970), or evaluated in terms of estimated values of phase stress concentration factors which are indicated by certain averaging techniques (Christensen, 1979), but their direct evaluation appears possible only in a few special cases. For example, Hashin (1984) recently found an exact relation between the thermal expansion coefficients and the bulk moduli of certain statistically isotropic polycrystalline aggregates.

This work is concerned with the macroscopic response of three-phase fibrous composite materials which are subjected to simultaneous increments of uniform thermal change and uniform overall stress or strain. In particular, we derive relationships between overall thermal expansion coefficients and the overall elastic moduli of a composite medium which consists of three perfectly-bonded cylindrical phases of arbitrary cross-section. Similar connections are found between mechanical and thermal microstress fields. Each of the phases can be transversely isotropic or isotropic; phase properties are assumed to be temperature independent within the applied increment. Unidirectional hybrid fiber composites, or binary systems reinforced by coated aligned fibers, can be regarded as particular examples of such three-phase media.

2 Governing Equations

The composite material under consideration consists of three perfectly-bonded homogeneous phases. Each of the phases is of cylindrical shape and is, at most, transversely isotropic about the "fiber" direction x_3 of a Cartesian coordinate system. In the transverse x_1x_2-plane, the cross-sections and the distributions of the phases can be arbitrary, providing that all such transverse sections are identical and the composite can be regarded as statistically homogeneous and free of voids. Overall isotropy in the transverse plane is permissible but not required; thus, the composite medium may have only one plane of elastic symmetry. The thermoelastic constants of the phases are known. Also, the overall elastic stiffness tensor $\mathbf{L}$ and the compliance tensor $\mathbf{M}$ of the aggregate are assumed to be known; they can be determined experimentally or estimated by various averaging methods. For example, the self-consistent method (Hershey, 1954; Budiansky, 1965; Hill, 1965), the Mori-Tanaka (1973) procedure, and the differential scheme (McLaughlin, 1977; Norris, 1985) lead to such

Contributed by the Applied Mechanics Division of THE AMERICAN SOCIETY OF MECHANICAL ENGINEERS for presentation at the Joint ASCE/ASME Applied Mechanics, Biomechanics, and Fluids Engineering Conference, San Diego, CA, July 9 to 12, 1989.

Discussion of this paper should be addressed to the Editorial Department, ASME, United Engineering Center, 345 East 47th Street, New York, N.Y. 10017, and will be accepted until two months after final publication of the paper itself in the JOURNAL OF APPLIED MECHANICS. Manuscript received by ASME Applied Mechanics Division, April 28, 1988; final revision, September 14, 1988.
Paper No. 89-APM-30.

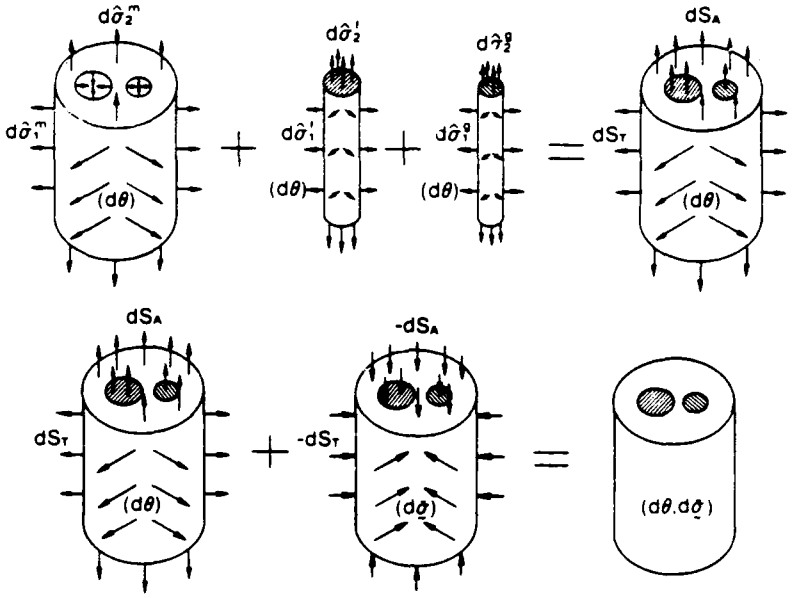

Fig. 1 Scheme of decomposition procedure

estimates. Also, Walpole (1984) gives bounds on overall mechanical properties of some of the multiphase materials considered herein.

A representative volume element V of the composite is selected and subjected to certain uniform overall stress $\bar{\sigma}_o$ or strains $\bar{\epsilon}_o$ which are imposed by prescribed surface tractions or displacements applied at the surface S of volume V. Also, a certain uniform thermal change has been applied such that θ_o is the current uniform temperature in V. Suppose that at this particular point of the loading sequence, the aggregate is subjected to simultaneous, uniform, infinitesimal increments of $d\theta$ and $d\bar{\sigma}$, or of $d\theta$ and $d\bar{\epsilon}$. The response of the aggregate to these load increments is described by the constitutive equations

$$d\bar{\epsilon} = \mathbf{M}d\bar{\sigma} + \mathbf{m}d\theta, \quad d\bar{\sigma} = \mathbf{L}d\bar{\epsilon} - \mathbf{l}d\theta, \tag{1}$$

where $\mathbf{L}$, $\mathbf{M}$ are the known (6×6) overall stiffness and compliance matrices, and $\mathbf{l}$, $\mathbf{m}$ are (6×1) overall thermal stress and strain vectors which are to be found in terms of $\mathbf{L}$ or $\mathbf{M}$, and the thermoelastic constants and volume fractions of the phases.

The thermoelastic properties and response of the transversely isotropic phases can be described by phase variants of equation (1). A particular form, which will be useful in the sequel, relates the axisymmetric stress and strain invariants of the transversely isotropic medium (Dvorak, 1986):

$$\begin{Bmatrix} d\epsilon_1 \\ d\epsilon_2 \end{Bmatrix} = \frac{1}{kE} \begin{bmatrix} n & -l \\ -l & k \end{bmatrix} \begin{Bmatrix} d\sigma_1 \\ d\sigma_2 \end{Bmatrix} + \begin{Bmatrix} \alpha \\ \beta \end{Bmatrix} d\theta \tag{2}$$

$$\begin{Bmatrix} d\sigma_1 \\ d\sigma_2 \end{Bmatrix} = \begin{bmatrix} k & l \\ l & n \end{bmatrix} \begin{Bmatrix} d\epsilon_1 \\ d\epsilon_2 \end{Bmatrix} - \begin{bmatrix} k\alpha + l\beta \\ l\alpha + n\beta \end{bmatrix} d\theta \tag{3}$$

where k, l, n are Hill's (1964) elastic moduli, $E = n - l^2/k$, $\alpha = 2\alpha_T$, $\beta = \alpha_L$, and α_T, α_L are the linear coefficients of thermal expansion in the transverse plane and in the longitudinal direction, respectively. For an isotropic phase with the usual elastic constants K, G, and ν, one finds that $k = G/(1-2\nu)$, $l = K - 2G/3$, and $n = K + 4G/3$. The strain and stress invariants are defined as:

$$d\epsilon_1 = d\epsilon_{11} + d\epsilon_{22}, \quad d\epsilon_2 = d\epsilon_{33},$$
$$d\sigma_1 = \tfrac{1}{2}(d\sigma_{11} + d\sigma_{22}), \; d\sigma_2 = d\sigma_{33}. \tag{4}$$

In the sequel, the three phases will be denoted by letters f, g, and m, or by a single letter $r = f, g, m$. For example, the phase volume fractions $c_f + c_g + c_m = 1$. Equations (2), (3), with appropriate values of thermoelastic constants, will describe the response of each phase to the respective axisymmetric invariants (4).

3 Decomposition Procedure

The unknown thermal stress and strain vectors $\mathbf{l}$, $\mathbf{m}$ of the three-phase composite medium will be found with a special form of the decomposition procedure of Dvorak (1983, 1986, 1987). In the first step of the procedure which is illustrated in Fig. 1, the three phases are separated and surface tractions or displacements which preserve the current local stresses σ_o^r and strains ϵ_o^r are applied to each phase $r = f, g, m$. Then, a uniform thermal change $d\theta$ is applied to each phase. This causes uniform, but dissimilar thermal strains or stresses (2), (3), in the phases, so that the phases are no longer compatible and cannot be reassembled. To make the phases compatible, auxiliary uniform stress increments of as yet unknown magnitude are applied to each phase simultaneously with $d\theta$. These stress increments are limited to the components which appear in (4), and are axisymmetric, i.e., $d\sigma_{11} = d\sigma_{22}$. Therefore, the corresponding strains are also limited to those in (4), with $d\epsilon_{11} = d\epsilon_{22}$, and follow from (2). The auxiliary uniform fields in the separated phases, which are denoted in the sequel by top hats, are thus given by:

$$d\hat{\epsilon}_1^f = (n_f d\hat{\sigma}_1^f - l_f d\hat{\sigma}_2^f)/k_f E_f + \alpha_f d\theta, \tag{5}$$
$$d\hat{\epsilon}_1^g = (n_g d\hat{\sigma}_1^g - l_g d\hat{\sigma}_2^g)/k_g E_g + \alpha_g d\theta, \tag{6}$$
$$d\hat{\epsilon}_1^m = (n_m d\hat{\sigma}_1^m - l_m d\hat{\sigma}_2^m)/k_m E_m + \alpha_m d\theta, \tag{7}$$
$$d\hat{\epsilon}_2^f = (-l_f d\hat{\sigma}_1^f + k_f d\hat{\sigma}_2^f)/k_f E_f + \beta_f d\theta \tag{8}$$
$$d\hat{\epsilon}_2^g = (-l_g d\hat{\sigma}_1^g + k_g d\hat{\sigma}_2^g)/k_g E_g + \beta_g d\theta \tag{9}$$
$$d\hat{\epsilon}_2^m = (-l_m d\hat{\sigma}_1^m + k_m d\hat{\sigma}_2^m)/k_m E_m + \beta_m d\theta. \tag{10}$$

We recall that each of the contributing fields in (5) to (10) is axisymmetric and spatially uniform. Therefore, internal

equilibrium and compatibility of the phases can be assured by the following conditions which relate the total uniform fields:

$$d\hat{\varepsilon}_1^f = d\hat{\varepsilon}_1^g = d\hat{\varepsilon}_1^m \tag{11}$$

$$d\hat{\sigma}_1^f = d\hat{\sigma}_1^g = d\hat{\sigma}_1^m = dQ_T \tag{12}$$

$$d\hat{\varepsilon}_2^f = d\hat{\varepsilon}_2^g = d\hat{\varepsilon}_2^m \tag{13}$$

$$c_f d\hat{\sigma}_2^f + c_g d\hat{\sigma}_2^g + c_m d\hat{\sigma}_2^m = dQ_A. \tag{14}$$

Here, dQ_A, dQ_T are the overall stress components which must be applied to the surface S of V while $d\hat{\sigma}_1^r$ and $d\hat{\sigma}_2^r$ are applied to the phases. They are defined by the overall forms of $(4_3, 4_4)$, but unless the composite medium has an axis of rotational symmetry x_3 they are not necessarily invariant in the overall stress space.

The fourteen equations (5) to (14) can be solved for the twelve stresses and strains $d\hat{\sigma}_1^r$, $d\hat{\sigma}_2^r$, $d\hat{\varepsilon}_1^r$, $d\hat{\varepsilon}_2^r$, and for dQ_A, dQ_T. The solution gives the magnitudes of the overall stress components dQ_A, and dQ_T, which, if applied together with the uniform thermal change $d\theta$, would create a spatially uniform incremental strain field in the heterogeneous medium. In reality, such overall stresses are not prescribed. Therefore, they must be eventually removed by application of $-dQ_A$, and $-dQ_T$ to the surface S of V.

The existence of the solution of the system of equations should be verified in each case, but if there are no special relationships between phase properties, the solution exists and can be found as follows: Equations (5) to (7) are substituted into (11), and (8) to (10) into (12). These, together with (13) and (14) are then solved in terms of $d\theta$. The result is:

$$dQ_A = s_A d\theta \tag{15}$$

$$dQ_T = s_T d\theta \tag{16}$$

where,

$$s_A = [(a_2 b_1 - a_1 b_2)s_T + a_3 b_1 - a_1 b_3]/(b_1 - a_1) \tag{17}$$

$$s_T = (B_{fm}C_{gf} - B_{fg}C_{mf})/(A_{gf}B_{fm} - B_{fg}A_{mf}) \tag{18}$$

with scalar quantities

$$A_{pq} = \left[\left(\frac{n_p}{k_p E_p} - \frac{n_q}{k_q E_q}\right) - \frac{l_p}{k_p}\left(\frac{l_p}{k_p E_p} - \frac{l_q}{k_q E_q}\right)\right] \tag{19}$$

$$B_{pq} = (l_p/k_p - l_q/k_q)/E_p \tag{20}$$

$$C_{pq} = l_p(\beta_q - \beta_p)/k_p + (\alpha_q - \alpha_p) \tag{21}$$

where the subscripts p, q, assume the phase designations f, g, m for the phase moduli k_r, l_r, n_r, and E_r; $p \neq q$.

The remaining terms in (17) are:

$$a_1 = c_f + c_g \frac{l_f}{k_f E_f}\cdot\frac{k_g E_g}{l_g} + c_m \frac{l_f}{k_f E_f}\cdot\frac{k_m E_m}{l_m} \tag{22}$$

$$a_2 = c_g \frac{k_g E_g}{l_g}\left(\frac{n_g}{k_g E_g} - \frac{n_f}{k_f E_f}\right) + c_m \frac{k_m E_m}{l_m}\left(\frac{n_m}{k_m E_m} - \frac{n_f}{k_f E_f}\right) \tag{23}$$

$$a_3 = c_g k_g E_g(\alpha_g - \alpha_f)/l_g + c_m k_m E_m (\alpha_m - \alpha_f)/l_m \tag{24}$$

$$b_1 = c_f + c_g E_g/E_f + c_m E_m/E_f \tag{25}$$

$$b_2 = c_g E_g \left(\frac{l_g}{k_g E_g} - \frac{l_f}{k_f E_f}\right) + c_m E_m \left(\frac{l_m}{k_m E_m} - \frac{l_f}{k_f E_f}\right) \tag{26}$$

$$b_3 = c_g E_g(\beta_f - \beta_g) + c_m E_m (\beta_f - \beta_m). \tag{27}$$

The solution of the system (5) to (14) can be written in the following form which reflects a change from the invariants (4) to the (6×1) vectors. The local auxiliary strain fields are:

$$\begin{aligned}
d\hat{\varepsilon}_{11}^f &= d\hat{\varepsilon}_{22}^f = \frac{1}{2}\, d\hat{\varepsilon}_1^f = h_1 d\theta \\
d\hat{\varepsilon}_{33}^f &= d\hat{\varepsilon}_2^f = h_2 d\theta \\
d\hat{\varepsilon}_{11}^g &= d\hat{\varepsilon}_{22}^g = \frac{1}{2}\, d\hat{\varepsilon}_1^g = h_1 d\theta \\
d\hat{\varepsilon}_{33}^g &= d\hat{\varepsilon}_2^g = h_2 d\theta \\
d\hat{\varepsilon}_{11}^m &= d\hat{\varepsilon}_{22}^m = \frac{1}{2}\, d\hat{\varepsilon}_1^m = h_1 d\theta \\
d\hat{\varepsilon}_{33}^m &= d\hat{\varepsilon}_2^m = h_2 d\theta
\end{aligned} \tag{28}$$

where

$$h_1 = \frac{1}{2}\left(n_f s_T - l_f \frac{A_{gf}C_{mf} - A_{mf}C_{gf}}{A_{gf}B_{fm} - A_{mf}B_{fg}}\right)/(k_f E_f) + \frac{1}{2}\alpha_f \tag{29}$$

$$h_2 = \left(k_f \frac{A_{gf}C_{mf} - A_{mf}C_{gf}}{A_{gf}B_{fm} - A_{mf}B_{fg}} - l_f s_T\right)/(k_f E_f) + \beta_f. \tag{30}$$

The local auxiliary stress fields are:

$$\begin{aligned}
d\hat{\sigma}_{11}^f &= d\hat{\sigma}_{22}^f = d\hat{\sigma}_1^f = s_T d\theta \\
d\hat{\sigma}_{33}^f &= d\hat{\sigma}_2^f = \gamma s_T d\theta \\
d\hat{\sigma}_{11}^g &= d\hat{\sigma}_{22}^g = d\hat{\sigma}_1^g = s_T d\theta \\
d\hat{\sigma}_{33}^g &= d\hat{\sigma}_2^g = \rho s_T d\theta \\
d\hat{\sigma}_{11}^m &= d\hat{\sigma}_{22}^m = d\hat{\sigma}_1^m = s_T d\theta \\
d\hat{\sigma}_{33}^m &= d\hat{\sigma}_2^m = \psi s_T d\theta
\end{aligned} \tag{31}$$

where

$$\gamma = (A_{gf}C_{mf} - A_{mf}C_{gf})/(B_{fm}C_{gf} - B_{fg}C_{mf}) \tag{32}$$

$$\rho = D_{gf}/B_{gf} + C_{fg}/(s_T B_{gf}) \tag{33}$$

$$\psi = D_{mf}/B_{mf} + C_{fm}/(s_T B_{mf}) \tag{34}$$

and, with reference to the notation used in (19) to (21):

$$D_{pg} = \left[\left(\frac{n_p}{k_p E_p} - \frac{n_g}{k_g E_g}\right) - \frac{l_g}{k_g}\left(\frac{l_p}{k_p E_p} - \frac{l_g}{k_g E_g}\right)\right]. \tag{35}$$

The final results that appear in the sequel assume a more concise form with the definitions:

$$\begin{aligned}
\mathbf{h} &= [h_1, h_1, h_2, 0, 0, 0]^T \\
\mathbf{s} &= [s_T, s_T, s_A, 0, 0, 0]^T \\
\boldsymbol{\gamma} &= [1, 1, \gamma, 0, 0, 0]^T \\
\boldsymbol{\rho} &= [1, 1, \rho, 0, 0, 0]^T \\
\boldsymbol{\psi} &= [1, 1, \psi, 0, 0, 0]^T
\end{aligned} \tag{36}$$

where $[\,]^T$ denotes a transpose and the coefficients appear in (17), (18), and (32) to (34).

In the final step of the decomposition procedure, the phases are reassembled and the auxiliary surface tractions are removed by application of overall stresses $-dQ_A$, $-dQ_T$. This leads to the results described in the next section.

4 Overall Properties and Local Fields

The aforementioned results make it possible to write directly the expression for the overall strain increment caused in the composite by superposition of simultaneous increments of $d\theta$ and $d\boldsymbol{\vartheta}$, and also the expression for the overall stress increment in a composite subjected to simultaneous changes $d\theta$ and $d\boldsymbol{\varepsilon}$:

$$d\boldsymbol{\varepsilon} = \mathbf{h}\, d\theta + \mathbf{M}(d\boldsymbol{\vartheta} - \mathbf{s}\, d\theta) \tag{37}$$

$$d\boldsymbol{\vartheta} = \mathbf{s}\, d\theta + \mathbf{L}(d\boldsymbol{\varepsilon} - \mathbf{h}\, d\theta). \tag{38}$$

A comparison with (1) yields the unknown overall thermal strain and stress vectors, which contain the desired overall thermal expansion coefficients:

$$\mathbf{m} = \mathbf{h} - \mathbf{M}\,\mathbf{s} \tag{39}$$

$$\mathbf{l} = -\mathbf{s} + \mathbf{L}\,\mathbf{h}. \tag{40}$$

To facilitate applications we note that the overall thermal strain vector

$$\mathbf{m} = [\alpha_1, \alpha_2, \alpha_3, \alpha_4, \alpha_5, \alpha_6]^T \tag{41}$$

and

$$\mathbf{l} = \mathbf{L}\,\mathbf{m}. \tag{42}$$

If the medium has only one plane of elastic symmetry perpendicular to x_3, then the overall compliance $\mathbf{M}$ in (39) depends on 13 independent elastic coefficients. Examples in Section 5 show that, in this case, $\alpha_4 = \alpha_5 = 0$. On the other hand, if the medium is transversely isotropic, then $\mathbf{m}$ can be written in the form

$$\mathbf{m} = [\alpha_T, \alpha_T, \alpha_A, 0, 0, 0]^T \tag{43}$$

where α_T, α_A are the overall linear coefficients of thermal expansion in the transverse plane and in the longitudinal directions, respectively. Then, using (39), one can find these coefficients in the explicit form:

$$\alpha_T = h_1 - \frac{1}{2(nk - l^2)}\,(ns_T - ls_A) \tag{44}$$

$$\alpha_A = h_2 - \frac{1}{nk - l^2}\,(ks_A - ls_T). \tag{45}$$

If the volume fraction of one of the phases is reduced to zero, then one recovers from these formulae the results for binary composites given by Dvorak (1986).

Note also that the decomposition procedure suggests the following connection between thermal microstress fields in the composite and mechanical microstress fields under axisymmetric uniform overall stresses. In particular, suppose that latter are written in the form

$$d\boldsymbol{\sigma}(x_i) = \mathbf{B}(x_i)\,d\bar{\boldsymbol{\sigma}} \tag{46}$$

where $\mathbf{B}(x_i)$ describes the spatial distribution of the local stresses under any overall stress $d\bar{\boldsymbol{\sigma}}$. As a minimum, $\mathbf{B}(x_i)$ must describe the response to axisymmetric uniform stresses $d\bar{\sigma}_{11} = d\bar{\sigma}_{22} = d\bar{\sigma}_1$, and $d\bar{\sigma}_{33} = d\bar{\sigma}_2$. According to the decomposition sequence, the local thermal stresses after the reassembly of the aggregate are given by (31). In the final step, one must remove the axisymmetric surface stresses dQ_A, dQ_T, represented by $\mathbf{s}$ in (36). Of course, that can be done using (46) to yield:

$$\begin{aligned}
&\text{In phase } f\text{: } d\boldsymbol{\sigma}(x_i) = s_T\,\boldsymbol{\gamma} + \mathbf{B}(x_i)(d\bar{\boldsymbol{\sigma}} - \mathbf{s}\,d\theta)\\
&\text{In phase } g\text{: } d\boldsymbol{\sigma}(x_i) = s_T\,\boldsymbol{\rho} + \mathbf{B}(x_i)(d\bar{\boldsymbol{\sigma}} - \mathbf{s}\,d\theta)\\
&\text{In phase } m\text{: } d\boldsymbol{\sigma}(x_i) = s_T\,\boldsymbol{\psi} + \mathbf{B}(x_i)(d\bar{\boldsymbol{\sigma}} - \mathbf{s}\,d\theta)
\end{aligned} \tag{47}$$

where $d\theta$ and $d\bar{\boldsymbol{\sigma}}$ are the prescribed uniform thermal change and overall stress vector, respectively.

Similarly, if instead of (46), there is a known connection between local and overall strains in the form:

$$d\boldsymbol{\epsilon}(x_i) = \mathbf{A}(x_i)\,d\bar{\boldsymbol{\epsilon}} \tag{48}$$

then one finds from (28) and (36) the local strain field in the aggregate loaded by a uniform thermal change $d\theta$ and an arbitrary overall strain $d\bar{\boldsymbol{\epsilon}}$:

$$d\boldsymbol{\epsilon}(x_i) = \mathbf{h}\,d\theta + \mathbf{A}(x_i)(d\bar{\boldsymbol{\epsilon}} - \mathbf{h}\,d\theta). \tag{49}$$

These results can be readily reduced to those for average stresses and strains in the phases. If the mechanical stress and strain concentration factors $\mathbf{B}_r$ and $\mathbf{A}_r$ of the phases are known, then the local averages can be written in the form

$$\begin{aligned}
d\boldsymbol{\sigma}_r &= \mathbf{B}_r\,d\bar{\boldsymbol{\sigma}} + \mathbf{b}_r\,d\theta\\
d\boldsymbol{\epsilon}_r &= \mathbf{A}_r\,d\bar{\boldsymbol{\epsilon}} - \mathbf{a}_r\,d\theta \qquad (r = f,g,m)
\end{aligned} \tag{50}$$

where the phase thermal stress concentration factors are:

$$\begin{aligned}
\mathbf{b}_f &= s_T\boldsymbol{\gamma} - \mathbf{B}_f\mathbf{s}\\
\mathbf{b}_g &= s_T\boldsymbol{\rho} - \mathbf{B}_g\mathbf{s}\\
\mathbf{b}_m &= s_T\boldsymbol{\psi} - \mathbf{B}_m\mathbf{s}\\
\mathbf{a}_r &= (\mathbf{A}_r - \mathbf{I})\mathbf{h}, \qquad r = (f,g,m).
\end{aligned} \tag{51}$$

5 Examples

To illustrate the results (39) to (42) we consider first a three-phase composite with transversely isotropic phases. Overall material symmetry elements are limited to a single plane of elastic symmetry with the normal x_3. The overall compliance matrix $\mathbf{M}$ has the following form:

$$\mathbf{M} = \begin{bmatrix}
M_{11} & M_{12} & M_{13} & 0 & 0 & M_{16}\\
M_{12} & M_{22} & M_{23} & 0 & 0 & M_{26}\\
M_{13} & M_{23} & M_{33} & 0 & 0 & M_{36}\\
0 & 0 & 0 & M_{44} & M_{45} & 0\\
0 & 0 & 0 & M_{45} & M_{55} & 0\\
M_{16} & M_{26} & M_{36} & 0 & 0 & M_{66}
\end{bmatrix}. \tag{52}$$

The stiffness matrix $\mathbf{L}$ is formally similar to $\mathbf{M}$. Now, $\mathbf{h}$ is taken from (36) and substituted, together with $\mathbf{M}$, into (39). That leads to an explicit form of (41):

$$\mathbf{m} = \begin{bmatrix}
h_1 - M_{11}s_T - M_{12}s_T - M_{13}s_A\\
h_1 - M_{12}s_T - M_{22}s_T - M_{23}s_A\\
h_2 - M_{13}s_T - M_{23}s_T - M_{33}s_A\\
0\\
0\\
-M_{16}s_T - M_{26}s_T - M_{36}s_A
\end{bmatrix}. \tag{53}$$

One also finds from (40) that

$$\mathbf{l} = \begin{bmatrix}
-s_T + L_{11}h_1 + L_{12}h_1 + L_{13}h_2\\
-s_T + L_{12}h_1 + L_{22}h_1 + L_{23}h_2\\
-s_A + L_{13}h_1 + L_{23}h_1 + L_{33}h_2\\
0\\
0\\
L_{16}h_1 + L_{26}h_1 + L_{36}h_2
\end{bmatrix}. \tag{54}$$

If the arrangement of the three transversely isotropic phases is such that the composite medium is transversely isotropic, then the coefficients $M_{16} = M_{26} = M_{36} = M_{45} = 0$ in (50) and also, $L_{16} = L_{26} = L_{36} = L_{45} = 0$. The specific forms of (41) and (42) then follow in an obvious manner from (53) and (54).

6 Conclusion

The results represent exact connections between overall elastic thermal stress and strain vectors, overall stiffness $\mathbf{L}$ or compliance $\mathbf{M}$, and phase thermoelastic properties of a three-phase composite medium consisting of perfectly-bonded cylindrical phases of arbitrary transverse geometry. They remain formally unchanged, except for $\mathbf{L}$ and $\mathbf{M}$, if the overall elastic symmetry properties of the composite are modified within the indicated constraints. Application of the decomposition procedure is limited to such combinations of phase properties for which the governing equations can be solved. The exceptional cases can be established by examination of (17) and (18). For example, one such exception would arise if all three phases were isotropic and if any two of them had the same Poisson's ratio. Another such exception occurs when the three phases have identical mechanical properties but different thermal expansion coefficients. Furthermore, in an n-phase fibrous medium the decomposition leads to $5n - 1$ equations for $4n + 2$ unknowns. Hence, the system can be solved for $n = 3$, and it

allows a choice of an additional constraint if $n = 2$. This last property was utilized by Dvorak (1986) in an application of this procedure to binary fibrous systems with an elastic-plastic matrix.

A particularly useful result is given by (47) and (49) which show that not only the overall response (37) and (38), but also the local thermal fields can be evaluated from known mechanical fields by a modification of the overall stress or strain increment, and by an addition of a piecewise uniform stress field or a uniform strain field.

Acknowledgments

The authors wish to acknowledge useful discussions with Prof. Yakov Benveniste. Funding for this work was provided in part, by the DARPA-HiTASC program at RPI, and by the Mechanics Division of the Office of Naval Research.

References

Budiansky, B., 1965, "On the Elastic Moduli of Some Heterogeneous Materials," *Journal of the Mechanics and Physics of Solids*, Vol. 13, p. 223.

Christensen, R. M., 1979, *Mechanics of Composite Materials*, John Wiley and Sons, New York.

Dvorak, G. J., 1983, "Metal Matrix Composites: Plasticity and Fatigue," *Mechanics of Composite Materials: Recent Advances*, Z. Hashin and C. T. Herakovich, eds., Pergamon Press, pp. 73-91.

Dvorak, G. J., 1986, "Thermal Expansion of Elastic-Plastic Composite Materials," ASME JOURNAL OF APPLIED MECHANICS, Vol. 53, pp. 737-743.

Dvorak, G. J., 1987, "Thermomechanical Deformation and Coupling in Elastic-Plastic Composite Materials," *Thermomechanical Couplings in Solids*, H. D. Bin, and Q. S. Nguyen, eds., North-Holland, pp. 43-54

Hashin, Z., 1984, "Thermal Expansion of Polycrystalling Aggregates. I. Exact Analysis," *Journal of the Mechanics and Physics of Solids*, Vol. 32, pp. 149-158.

Hershey, A. V., 1954, "The Elasticity of an Isotropic Aggregate of Anisotropic Cubic Crystals," ASME JOURNAL OF APPLIED MECHANICS, Vol. 21, pp. 236-240.

Hill, R., 1964, "Theory of Mechanical Properties of Fiber-Strengthened Materials: I. Elastic Behaviour," *Journal of the Mechanics and Physics of Solids*, Vol. 12, pp. 199-212.

Hill, R., 1965, "A Self-Consistent Mechanics of Composite Materials," *Journal of the Mechanics and Physics of Solids*, Vol. 13, pp. 213-222.

Levin, V. M., 1967, "Thermal Expansion Coefficients of Heterogeneous Materials," *Mekhanika Tverdogo Tela*, Vol. 2, pp. 88-94.

McLaughlin, R., 1977, "A Study of the Differential Scheme for Composite Materials," *International Journal of Engineering Science*, Vol. 15, pp. 237-244.

Mori, T., and Tanaka, K., 1973, "Average Stress in Matrix and Average Elastic Energy of Materials with Misfitting Inclusions," *Acta Metal*, Vol. 21, p. 571.

Norris, A. N., 1985, "A Differential Scheme for the Effective Moduli of Composites," *Mechanics of Materials*, Vol. 4, pp. 1-16.

Rosen, B. W., and Hashin, Z., 1970, "Effective Thermal Expansion Coefficients and Specific Heats of Composite Materials," *International Journal of Engineering Science*, Vol. 8, pp. 157-173.

Schapery, R. A., 1968, "Thermal Expansion Coefficients of Composite Materials Based on Energy Principles," *Journal of Composite Materials*, Vol. 2, pp. 380-404.

Walpole, L. J., 1984, "The Analysis of the Overall Elastic Properties of Composite Materials," *Fundamentals of Deformation and Fracture*, B. A. Bilby, K. J. Miller, J. R. Willis, eds., pp. 91-107.

PROCEEDINGS

of the

I PAN AMERICAN CONGRESS OF APPLIED MECHANICS

(PACAM)

Sponsored by

American Academy of Mechanics

Associação Brasileira de Ciências Mecânicas

Hosted by

Departamento de Engenharia Civil

Pontifícia Universidade Católica do Rio de Janeiro

PUC-Rio

Rio de Janeiro, Brazil

January 3-6, 1989

Conference Chairman A.W. Leissa

Conference Vice-Chairman M.R.M. Crespo da Silva

Chairman of the Local Arragements Committee M.A. Souza

Editorial Committee Co-Chairmen

C.R. Steele

L. Bevilacqua

COEFFICIENTS OF THERMAL EXPANSION OF THREE-PHASE COMPOSITE MATERIALS

George J. Dvorak and Tungyang Chen
Professor and Graduate Research Assistant
Department of Civil Engineering
Rensselaer Polytechnic Institute
Troy, NY 12180, U.S.A.

ABSTRACT

Exact expressions are found for overall thermal expansion coefficients of a composite medium consisting of three perfectly bonded, transversely isotropic phases of cylindrical shape and arbitrary transverse geometry.

INTRODUCTION

In his 1967 paper, Levin [1] found that macroscopic thermal expansion coefficients of an elastic heterogeneous composite medium, consisting of two distinct perfectly bonded isotropic phases of arbitrary shape, depend in a unique way on the overall elastic moduli of the aggregate and on thermoelastic constants of the phases. Such coefficients are the average overall strains caused by a uniform thermal change of unit magnitude in a traction free composite. Levin's results, and their extension to binary systems with anisotropic constituents [2], permit a direct evaluation of these coefficients in terms of the known overall elastic moduli and local thermoelastic constants. However, the approach cannot be applied to composites of three or more constituents. Thermoelastic constants of such multiphase media can be bounded with the help of thermoelastic extremum principles [2,3], or estimated with certain averaging techniques [4], but their direct evaluation appears possible only in few special cases. For example, Kushin [5] had recently found an exact relation between the thermal expansion coefficient and the bulk modulus of certain statistically isotropic polycrystalline aggregates.

The present work develops an exact relationship between overall thermal expansion coefficients and the overall elastic moduli of a composite medium which consists of three perfectly bonded cylindrical phases of arbitrary cross section. Unidirectional hybrid fiber composites, or binary systems reinforced by aligned coated fibers can be regarded as particular examples of such three-phase media.

The unknown thermal stress and strain vectors $\underline{l}$, $\underline{m}$ of the three-phase composite medium will be found with a special form of the decomposition procedure of Dvorak [7]. In the first step of the procedure, the three phases are separated and surface tractions or displacements which preserve the current local stresses $\underline{\sigma}^0$ and strains $\underline{\varepsilon}^0$ are applied to each phase $r = f,g,m$. Also, a uniform thermal change $d\theta$ is applied to each phase. This causes uniform but dissimilar thermal strains or stresses (2) in the phases, so that the phases are no longer compatible and cannot be reassembled. To make the phases compatible, auxiliary uniform stress increments of as yet unknown magnitude are applied to each phase simultaneously with $d\theta$. (The auxiliary uniform fields are denoted by top hats.) This causes the following strain increments in the separated phases:

$$d\hat{\varepsilon}_1^f = (n_f d\hat{\sigma}_1^f - l_f d\hat{\sigma}_2^f)/k_f E_f + \alpha_f d\theta, \quad d\hat{\varepsilon}_2^f = (-l_f d\hat{\sigma}_1^f + k_f d\hat{\sigma}_2^f)/k_f E_f + \beta_f d\theta$$

$$d\hat{\varepsilon}_1^g = (n_g d\hat{\sigma}_1^g - l_g d\hat{\sigma}_2^g)/k_g E_g + \alpha_g d\theta, \quad d\hat{\varepsilon}_2^g = (-l_g d\hat{\sigma}_1^g + k_g d\hat{\sigma}_2^g)/k_g E_g + \beta_g d\theta \qquad (4)$$

$$d\hat{\varepsilon}_1^m = (n_m d\hat{\sigma}_1^m - l_m d\hat{\sigma}_2^m)/k_m E_m + \alpha_m d\theta, \quad d\hat{\varepsilon}_2^m = (-l_m d\hat{\sigma}_1^m + k_m d\hat{\sigma}_2^m)/k_m E_m + \beta_m d\theta$$

Each of the contributing fields in (4) is spatially uniform. Therefore, internal equilibrium and compatibility of the phases can be assured by the following conditions:

$$d\hat{\varepsilon}_1^f = d\hat{\varepsilon}_1^g = d\hat{\varepsilon}_1^m \quad , \quad d\hat{\varepsilon}_2^f = d\hat{\varepsilon}_2^g = d\hat{\varepsilon}_2^m$$

$$d\hat{\sigma}_1^f = d\hat{\sigma}_1^g = d\hat{\sigma}_1^m = dQ_T \quad , \quad c_f d\hat{\sigma}_2^f + c_g d\hat{\sigma}_2^g + c_m d\hat{\sigma}_2^m = dQ_A \qquad (5)$$

Here, dQ_T, dQ_A are the overall stress components which must be applied to the surface S of V while $d\hat{\rho}_1^r$ and $d\hat{\sigma}_2^r$ are applied to the phases. They are defined by the overall forms of (3), but unless the composite medium has an axis of rotational symmetry x_3, they are not necessarily invariant in the overall stress space. The fourteen equations (4) and (5) can be solved for the twelve stresses and strains $d\hat{\sigma}_1^r$, $d\hat{\sigma}_2^r$, $d\hat{\varepsilon}_1^r$, $d\hat{\varepsilon}_2^r$, and for dQ_T, dQ_A. The solution gives the magnitudes of the overall stress components dQ_T, and dQ_A which, if applied together with the uniform thermal change $d\theta$, would create spatially uniform incremental stress and strains fields in the heterogeneous medium. In reality, such overall stresses are not prescribed. Therefore, they must be removed by application of $-dQ_T$, and $-dQ_A$ to the surface S of V. After some algebra one finds:

$$dQ_T = s_T d\theta, \qquad d\hat{\sigma}_1^r = g_1 d\theta, \qquad d\hat{\varepsilon}_1^r = h_1 d\theta$$

$$dQ_A = s_A d\theta, \qquad d\hat{\sigma}_2^r = g_2 d\theta, \qquad d\hat{\varepsilon}_2^r = h_2 d\theta \qquad (6)$$

where $r = f,g,m$, and the constants s_T, s_A, h_1, h_2, g_1, g_2 depend only on the thermoelastic constants and volume fractions of the phases. Space limitation prevents complete listing of the constants.

GOVERNING EQUATIONS

The composite material under consideration consists of three perfectly bonded homogeneous phases. Each of the phases is of cylindrical shape and is at most transversely isotropic about the "fiber" direction x_3 of a Cartesian coordinate system. In the transverse x_1x_2-plane, the cross section and the distributions of the phases can be arbitrary, providing that all such transverse sections are identical and the composite can be regarded as statistically homogeneous and free of voids. Overall isotropy in the transverse plane is permissible but not required; thus the composite medium may have only one plane of elastic symmetry. The thermoelastic constants of the phases are known. Also, the overall elastic stiffness tensor $\underset{\sim}{L}$ and the compliance tensor $\underset{\sim}{M}$ of the aggregate are assumed to be known; they can be found by several available averaging methods [6].

A representative volume element V of the composite is selected and subjected to certain uniform overall stresses $\underset{\sim}{\sigma}^o$ or strains $\underset{\sim}{\varepsilon}^o$ which are imposed by prescribed surface tractions or displacements applied at the surface S of volume V. Also, a certain uniform thermal change has been applied such that θ_o is the current uniform temperature in V. Suppose that at this particular point of the loading sequence, the aggregate is subjected to simultaneous, uniform, infinitesimal increments of $d\theta$ and $d\overline{\underset{\sim}{\sigma}}$, or of $d\theta$ and $d\overline{\underset{\sim}{\varepsilon}}$. The response of the aggregate to these load increments is described by the constitutive equations

$$d\overline{\underset{\sim}{\varepsilon}} = \underset{\sim}{M}\, d\overline{\underset{\sim}{\sigma}} + \underset{\sim}{m}\, d\theta\,, \qquad d\overline{\underset{\sim}{\sigma}} = \underset{\sim}{L}\, d\overline{\underset{\sim}{\varepsilon}} - \underset{\sim}{l}\, d\theta\,, \tag{1}$$

where $\underset{\sim}{L}$, $\underset{\sim}{M}$ are the known (6x6) overall stiffness and compliance matrices, and $\underset{\sim}{l}$, $\underset{\sim}{m}$ are (6x1) overall thermal stress and strain vectors which are to be found in terms of $\underset{\sim}{L}$ or $\underset{\sim}{M}$, and the thermoelastic constants and volume fractions of the phases.

The thermoelastic properties and response of the transversely isotropic phases can be described by phase variants of (1). A particular form, which will be useful in the sequel, relates the axisymmetric stress and strain invariants of the transversely isotropic medium [7]:

$$\begin{Bmatrix} d\varepsilon_1 \\ d\varepsilon_2 \end{Bmatrix} = \frac{1}{kE} \begin{bmatrix} n & -l \\ -l & k \end{bmatrix} \begin{Bmatrix} d\sigma_1 \\ d\sigma_2 \end{Bmatrix} + \begin{Bmatrix} \alpha \\ \beta \end{Bmatrix} d\theta \tag{2}$$

where k, l, n are Hill's elastic moduli, $E = n - l^2/k$, $\alpha = 2\alpha_T$, $\beta = \alpha_L$, and α_T, α_L are the linear coefficients of thermal expansion in the transverse plane and in the longitudinal direction, respectively. The strain and stress invariants are defined as:

$$d\varepsilon_1 = d\varepsilon_{11} + d\varepsilon_{22}, \quad d\varepsilon_2 = d\varepsilon_{33}, \quad d\sigma_1 = \frac{1}{2}(d\sigma_{11} + d\sigma_{22}), \quad d\sigma_2 = d\sigma_{33} \tag{3}$$

In the sequel, the three phases will be denoted by letters f, g, and m, or by a single letter r = f,g,m. For example, the phase volume fractions $c_f + c_g + c_m = 1$. Equations (2), with appropriate values of thermoelastic constants, will describe the response of each phase to the respective axisymmetric invariants (3).

OVERALL PROPERTIES AND LOCAL FIELDS

The above results make it possible to write the expression for the overall strain increment $d\bar{\underline{\varepsilon}}$ caused in the composite by superposition of simultaneous increments of $d\theta$ and $d\bar{\underline{\sigma}}$, and also the expression for the overall stress increment $d\bar{\underline{\sigma}}$ in a composite subjected to simultaneous changes $d\theta$ and $d\bar{\underline{\varepsilon}}$:

$$d\bar{\underline{\varepsilon}} = \underline{h}\, d\theta + \underline{M}(d\bar{\underline{\sigma}} - \underline{s}_a d\theta) \quad ; \quad d\bar{\underline{\sigma}} = \underline{s}_a d\theta + \underline{L}(d\bar{\underline{\varepsilon}} - \underline{h}\, d\theta) \tag{7}$$

where

$$\underline{h} = [h_1, h_1, h_2, 0, 0, 0]^T \quad , \quad \underline{s}_a = [s_T, s_T, s_A, 0, 0, 0]^T$$

A comparison with (1) yields the unknown overall thermal strain and stress vectors, which contain the desired overall thermal expansion coefficients. One can also easily recover expressions for averages of local fields in the phases caused by the above changes in $d\theta$ and $d\bar{\underline{\sigma}}$, or in $d\theta$ and $d\bar{\underline{\varepsilon}}$.

CONCLUSION

The results represent exact connections between overall elastic thermal stress and strain vectors, overall stiffness $\underline{L}$ or compliance $\underline{M}$, and phase thermoelastic properties of a three-phase composite medium consisting of perfectly bonded cylindrical phases of arbitrary transverse geometry. They remain unchanged, except for $\underline{L}$ and $\underline{M}$, if the composite becomes transversely isotropic, as in the case of hybrid unidirectional plies or of unidirectional binary systems with coated fibers.

Acknowledgements: Funding for this work was provided by the Mechanics division of the Office of Naval Research. Dr. Yapa Rajapakse was program monitor.

REFERENCES

1. Levin, V.M., Thermal expansion coefficients of heterogeneous materials, Mekhanika Tverdogo Tela, Vol. 2, pp. 88-94 (1967).
2. Rosen, B.W., and Hashin, Z., Effective thermal expansion coefficients and specific heats of composite materials, Intl. Jnl. Engng. Sci., Vol. 8, pp. 157-173 (1970).
3. Schapery, R.A., Thermal expansion coefficients of composite materials based on energy principles, Jnl. Composite Mater., Vol. 2, pp. 380-404 (1968).
4. Budiansky, B., Thermal and thermoelastic properties of isotropic composites, Jnl. Composite Mater., Vol. 4, pp. 286-295 (1970).
5. Hashin, Z., Thermal expansion of polycrystalling aggregates. I. Exact analysis, Jnl. Mech. Phys. Solids, Vol. 32, pp. 149-158 (1984).
6. Christensen, R.M., Mechanics of Composite Materials, John Wiley & Sons, 348 pp. (1979).
7. Dvorak, G.J., Thermal expansion of elastic-plastic composite materials, Jnl. Appl. Mech., Vol. 53 (1986).

Mechanics of Materials 7 (1989) 305–317
North-Holland

STRESS FIELDS IN COMPOSITES WITH COATED INCLUSIONS

Y. BENVENISTE *, G.J. DVORAK and T. CHEN

Department of Civil Engineering, Rensselaer Polytechnic Institute Troy, NY 12180-3590, U.S.A.

Received 30 August 1988

A micromechanics model is presented for the prediction of stress fields in coated fiber composites. The method is based on the "average stress in the matrix" concept of Mori and Tanaka and is formulated for the case of thermoelastic loading. A general description of the model is first given for three-phase materials and then specialized to the case of coated fiber composites. Results are presented for typical coated fiber composite systems under a variety of mechanical loading situations and uniform temperature change.

1. Introduction

Micromechanics analysis of composite materials often relies on Eshelby's (1957) finding that the strain field in an ellipsoidal inclusion bonded to a uniformly strained infinite medium is also uniform. This result is commonly used to evaluate overall properties and average local fields in composite aggregates in terms of the phase strain and stress concentration factor tensors, which have been determined for many practically useful inclusion shapes. Unfortunately, the above result no longer holds when the inclusion is surrounded by a layer of coating which is then bonded to the surrounding medium. Local fields in coated inclusions are generally not uniform, hence the phase concentration factors cannot be easily evaluated. Therefore, analysis of composites reinforced by coated fibers or particles is one of the more difficult problems in micromechanics.

Available solutions of problems of this kind can be found in the papers by Walpole (1978) and Hatta and Taya (1986). Walpole considers a composite with dilute reinforcement under mechanical loading. He develops his solution from the assumption that a very thin coating has no effect on strain distribution in the particles. The analysis thus becomes similar to that of an uncoated particle, and the fields in the coating are found using Hill's (1972) interface conditions. As Walpole remarks, the procedure does not give reliable results even for thin coatings when the coating is either extremely weak or extremely strong. Hatta and Taya consider the heat conduction problem in composites reinforced by short coated fibers, in the context of the original Mori–Tanaka method.

The present paper is concerned with evaluation of local fields and overall thermomechanical properties of composites reinforced by coated fibers or particles. The results are derived from a variant of Benveniste's (1987) reexamination of Mori–Tanaka's method. In particular, the local fields in a coated inclusion are approximated by those found when the coated inclusion is embedded in an unbounded matrix medium subjected to the average matrix stresses (or strains) at infinity. The advantage of this approach is that the local fields in the coating and inclusion, and in the adjacent matrix can be evaluated by using the solution of a single coated particle in an infinite matrix and particle interaction is taken into account through the yet unknown average matrix stresses. The first two sections describe, respectively, the procedure for evaluation of local fields, and overall or effective thermomechanical properties, of matrix-based composites consisting of three anisotropic phases of arbitrary geometry. We show that the results are consistent in that the overall

* On sabbatical leave from Tel-Aviv University.

compliance tensor is the inverse of the stiffness tensor, and that the required connections between the predicted overall thermal strain tensors and stiffness tensors are satisfied. Then, specific results are found for systems reinforced by aligned coated fibers, where the phases are isotropic. The case of coated anisotropic fibers will be considered elsewhere.

2. Stress and strain fields in three-phase composites

Consider a three-phase composite material consisting of a continuous matrix phase m, in which there are embedded inhomogeneities of a particle or fiber phase f, and a third phase g which, in Section 4, will represent a layer of coating that encapsulates each particle or fiber of the f phase. However, the results of this and the next section are valid for any microstructural geometry of a matrix-based three-phase medium, so the phases f and g can be thought of as two different reinforcement materials. The thermoelastic constitutive equations of the phases are given in the form

$$\boldsymbol{\sigma}_r = \boldsymbol{L}_r\boldsymbol{\epsilon}_r + \boldsymbol{l}_r\theta \tag{1}$$

$$\boldsymbol{\epsilon}_r = \boldsymbol{M}_r\boldsymbol{\sigma}_r + \boldsymbol{m}_r\theta \tag{2}$$

where $r = \mathrm{f}, \mathrm{g}, \mathrm{m}$; $\boldsymbol{L}_r$, and $\boldsymbol{M}_r = (\boldsymbol{L}_r)^{-1}$ are the stiffness and compliance tensors; $\boldsymbol{l}_r$ is the thermal stress tensor and $\boldsymbol{m}_r$ is the thermal strain tensor of the expansion coefficients, such that

$$\boldsymbol{l}_r = -\boldsymbol{L}_r\boldsymbol{m}_r. \tag{3}$$

Define the following thermomechanical loading problems:

$$\boldsymbol{u}(S) = \boldsymbol{\epsilon}_0\boldsymbol{x}, \qquad \theta(S) = \theta_0 \tag{4}$$

$$\boldsymbol{\sigma}_n(S) = \boldsymbol{\sigma}_0\boldsymbol{n}, \qquad \theta(S) = \theta_0, \tag{5}$$

where $\boldsymbol{\sigma}_n(S)$ and $\boldsymbol{u}(S)$ are the traction and displacement vectors at the external boundary S of a representative volume V of the composite under consideration, $\boldsymbol{n}$ is the outer normal unit vector to S; $\boldsymbol{\sigma}_0$ and $\boldsymbol{\epsilon}_0$ are the applied constant stress and strain fields; $\boldsymbol{x}$ denotes the coordinate system; $\theta(S)$ is the temperature rise at S, and θ_0 is a constant quantity.

The composite medium is statistically homogeneous, with arbitrary phase geometry. The inclusion phases can in principle have a certain distribution in the orientation of the symmetry axis but are chosen herein, for simplicity, to possess a fixed orientation.

Our first objective is to find certain general relations between the local and overall stress and strain fields in the aggregate. These relations will be established using the concepts which were introduced by Mori and Tanaka (1973), and reexamined by Benveniste (1987).

Consider the composite subjected to boundary conditions (4) and denote the solution for the strain field in the phases symbolically as

$$\boldsymbol{\epsilon}_r(\boldsymbol{x}) = \boldsymbol{A}_r(\boldsymbol{x})\boldsymbol{\epsilon}_0 + \boldsymbol{a}_r(\boldsymbol{x})\theta_0, \quad r = \mathrm{f}, \mathrm{g}, \mathrm{m}, \tag{6}$$

where $\boldsymbol{A}_r(\boldsymbol{x})$ and $\boldsymbol{a}_r(\boldsymbol{x})$ are fourth and second order tensors, respectively, whose volume averages $\boldsymbol{A}_r$ and $\boldsymbol{a}_r$ (no argument $\boldsymbol{x}$) are usually referred to as mechanical and thermal strain concentration factors. Determination of the tensors $\boldsymbol{A}_r(\boldsymbol{x})$ and $\boldsymbol{a}_r(\boldsymbol{x})$ is achieved in this paper in an approximate way by using the ideas in the original work of Mori and Tanaka (1973). Specifically, the strain field in each part of the reinforcement phases f or g, i.e., in each particle or fiber, are assumed to be equal to the fields in a single inclusion of phase f or g which is embedded in an unbounded matrix medium m and subjected to remotely applied strains $\boldsymbol{\epsilon}_m$ which are equal to the yet unknown average strain in the matrix, and also to a uniform temperature change θ_0.

Suppose therefore that the single inclusion is surrounded by a large matrix volume V' with surface S', Fig. 1a. The boundary conditions are

$$\boldsymbol{u}(S') = \boldsymbol{\epsilon}_m\boldsymbol{x}, \qquad \theta(S') = \theta_0, \tag{7}$$

where $\boldsymbol{\epsilon}_m$ is the unknown average matrix strain. In analogy with (6) we write the solution in the symbolic form

$$\boldsymbol{\epsilon}_r(\boldsymbol{x}) = \boldsymbol{T}_r(\boldsymbol{x})\boldsymbol{\epsilon}_m + \boldsymbol{t}_r(\boldsymbol{x})\theta_0, \quad r = \mathrm{f}, \mathrm{g}. \tag{8}$$

where $\mathrm{T}_r(\boldsymbol{x})$ and $\boldsymbol{t}_r(\boldsymbol{x})$ relate to single particles in an infinite matrix and have phase volume averages $\boldsymbol{T}_r$, $\boldsymbol{t}_r$ which are the strain concentration factors.

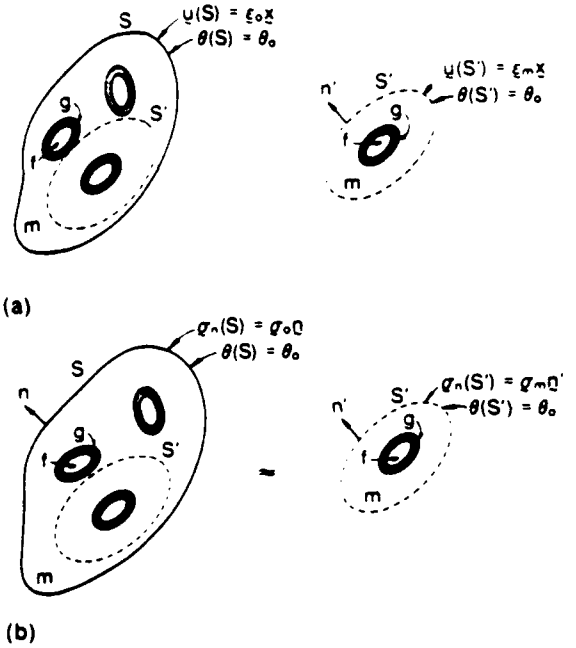

Fig. 1. A schematic representation of Mori–Tanaka's method for thermoelastic problems.

To determine ϵ_m, we recall that the overall uniform strain ϵ and the local average strains ϵ_r, which were found in the solution of the original problem (4) are connected by the relations

$$\epsilon = \sum_r c_r \epsilon_r = \epsilon_0, \quad r = \text{f, g, m,} \tag{9}$$

where c_r denote the phase volume fractions, $c_f + c_g + c_m = 1$. When (6) is averaged over the volume of each phase, and the result introduced into (7), one finds the unknown average matrix strain as

$$\epsilon_m = \left[\sum_r c_r T_r\right]^{-1}\left[\epsilon_0 - \theta_0 \sum_r c_r t_r\right], \quad r = \text{f, g m.} \tag{10}$$

Since the T_r and t_r tensors refer to a single inclusion in volume V' of the matrix, the state of strain in the matrix is affected only in a small volume adjacent to the inclusion, hence it follows that in this special case

$$T_m \doteq I, \qquad t_m \doteq 0, \tag{11}$$

where I is the fourth-order unit tensor defined by

$$I_{ijkl} = \tfrac{1}{2}(\delta_{ik}\delta_{jl} + \delta_{il}\delta_{jk}) \tag{12}$$

and δ_{ij} is the Kronecker symbol. Finally, substitution of (10) in (8) yields the desired approximation for $\epsilon_r(x)$.

An entirely similar procedure can be applied under stress boundary conditions (5). For the composite aggregate we write in place of (6)

$$\sigma_r(x) = B_r(x)\sigma_0 + b_r(x)\theta_0, \quad r = \text{f, g, m,} \tag{13}$$

where $B_r(x)$ and $b_r(x)$ have volume phase averages B_r and b_r which are referred to as the mechanical and thermal stress concentration factors. In the limiting case of a single inclusion in volume V' surrounded by S', Fig. 1b, the solution assumes the form

$$\sigma_r(x) = W_r(x)\sigma_m + w_r(x)\theta_0, \quad r = \text{f, g,} \tag{14}$$

The tensors $W_r(x)$ and $w_r(x)$ are related to their counterparts in (8) by (Benveniste, 1987)

$$W_r(x) = L_r T_r(x) M_m, \quad r = \text{f, g, m,} \tag{15}$$

$$w_r(x) = L_r T_r(x) m_m + L_r t_r(x) + l_r. \tag{16}$$

Of course, according to the arguments leading to (11) there is

$$W_m \doteq I, \qquad w_m \doteq 0. \tag{17}$$

Next, write (9) in terms of stresses for the problem (5):

$$\sigma = \sum_r c_r \sigma_r = \sigma_0, \quad r = \text{f, g, m,} \tag{18}$$

and use (14) to find the unknown average matrix stress in the aggregate. The result is:

$$\sigma_m = \left[\sum_r c_r W_r\right]^{-1}\left[\sigma_0 - \theta_0 \sum_r c_r w_r\right], \tag{19}$$

which, when substituted into (14) gives the desired approximation of $\sigma_r(x)$.

3. Effective thermomechanical properties

In analogy with (1) and (2), define the thermoelastic constitutive relations of the composite medium as

$$\sigma = L\epsilon + l\theta \tag{20}$$

$$\epsilon = M\sigma + m\theta, \tag{21}$$

where σ, ϵ and θ denote representative volume averages, and L, M, and l, m have the same interpretation in the overall sense as their counterparts in (1) and (2) had locally.

To find L and l, note that under boundary conditions (4), the uniform field $\theta(x) = \theta_0$ is a solution of the problem in the representative volume. Also, from (1), (9), and (20):

$$\sum_r c_r(L_r\epsilon_r + l_r\theta_0) = L\epsilon_0 + l\theta_0, \quad r = \text{f, g, m.} \tag{22}$$

The volume average of (8), together with (10), can be substituted into (22) to give

$$L = \left[\sum_r c_r L_r T_r\right]\left[\sum_r c_r T_r\right]^{-1}, \tag{23}$$

$$l = \left[\sum_r c_r L_r T_r\right]\left[\sum_r c_r T_r\right]^{-1}\left[-\sum_r c_r t_r\right] + \sum_r c_r(L_r t_r + l_r). \tag{24}$$

Similarly, under boundary conditions (5), one can use (2), (18) and (21) to find that

$$\sum_r c_r(M_r\sigma_r + m_r\theta_0) = M\sigma_0 + m\theta_0, \tag{25}$$

which, through (14) and (19) furnishes

$$M = \left[\sum_r c_r M_r W_r\right]\left[\sum_r c_r W_r\right]^{-1}, \tag{26}$$

$$m = \left[\sum_r c_r M_r W_r\right]\left[\sum_r c_r W_r\right]^{-1}\left[-\sum_r c_r w_r\right] + \sum_r c_r(M_r w_r + m_r). \tag{27}$$

We now prove the consistency of the method which requires that the relations

$$M = L^{-1}, \tag{28a}$$

$$l = -Lm \tag{28b}$$

be satisfied by the effective properties L, M, and l, m.

Rearrange (26) to get

$$M\left[\sum_r c_r W_r\right] = \left[\sum_r c_r M_r W_r\right]. \tag{29}$$

Similarly, (15) and (29) lead to

$$M\left[\sum_r c_r L_r T_r\right] = \left[\sum_r c_r T_r\right], \tag{30}$$

which allows one to write (23) in the form

$$L\left[\sum_r c_r T_r\right] = \left[\sum_r c_r L_r T_r\right], \tag{31}$$

and thus show that (28a) is indeed satisfied.

To prove that (28b) is fulfilled by the l and m found in (24) and (27), substitute (26) and (16) into (27) and write

$$m = -M\left[\sum_r c_r(L_r T_r m_r + L_r t_r + l_r) + \sum_r c_r(T_r m_r + t_r)\right]. \tag{32}$$

Multiply both sides of (32) by $L = M^{-1}$, and recall (23) to get

$$-Lm = \sum_r c_r(L_r t_r + l_r) - L\sum_r c_r t_r, \tag{33}$$

which is equal to the right hand side of (24).

We now examine certain limitations of the results found with the Mori–Tanaka method. First, when the matrix volume fractions $c_m \to 0$, and $c_f + c_g = 1$, one would expect to recover the properties of a binary composite consisting of the latter phases in which the matrix properties would play no role. However, according to their definitions, the tensors T_f, T_g, and t_f, t_g, depend on matrix properties, but not on c_m. Therefore, composite properties would contain elements of matrix properties even in the limit $c_m \to 0$. Of course, the method does not admit the phases on equal footing, it reserves a distinct role for the matrix and is not applicable to aggregates without a continuous matrix phase. Therefore, the above limit can be taken only with the understanding that one of the remaining phases assumes the role of the matrix. However, it is interesting to note that in the limit $c_m = c_g \to 0$, one recovers $L = L_f$, $m = m_f$, etc. Also, it can be proven that the matrix properties happen to cancel out when the limit $c_m \to 0$ is taken in Mori–Tanaka estimates of the properties of a composite reinforced by coated spherical particles.

We mention here that Benveniste (1987) has proved that the Mori–Tanaka predictions of effective stiffnesses and compliances of two-phase composites with randomly orientated inclusions are bracketed by the Hashin–Shtrikman bounds (Hashin and Shtrikman, 1963). For a discussion of Mori–Tanaka's method in multiphase composites, see also a recent work by Norris (1989). Effective moduli estimates by this method in the case of uncoated composites have been shown to exhibit satisfactory agreement with experimental results (Weng, 1984); Tandon and Weng, 1986). Finally, in connection to thermomechanical problems in coated-fiber composites it should be mentioned that recent results by Dvorak and Chen (1988) show that in three-phase fibrous composites made of cylindrical phases, the overall l and m, can be derived in a unique way from local thermomechanical moduli, volume fractions, and the overall L and M without the knowledge of the respective mechanical concentration factors A_r, B_r. Furthermore, the tensors $a(x)$, $b(x)$, $t(x)$, $\omega(x)$, and their phase volume averages can be derived in a similar unique way in terms of the corresponding mechanical concentration factors.

4. Application to coated fiber composites

4.1. Solution procedure

We now turn our attention to a specific three-phase composite and consider a system reinforced by coated cylindrical fibers of circular cross-section. The fibers are aligned and distributed in the matrix in a statistically homogeneous manner. We assume that each of the three distinct phases is isotropic.

The composite is subjected to traction boundary conditions and to a uniform change in temperature. We wish to find the stress distribution in the fiber (f), coating (g) and in the matrix (m) which surrounds the periphery of the coated fiber. Also, we find the overall effective properties of the system. The problem is linear and therefore solved as a superposition of the following loading cases:

Case 1 - Transverse hydrostatic stress, Fig. 2a.
Case 2 - Transverse shear stress, Fig. 2b.
Case 3 - Transverse normal stress, Fig. 2c.

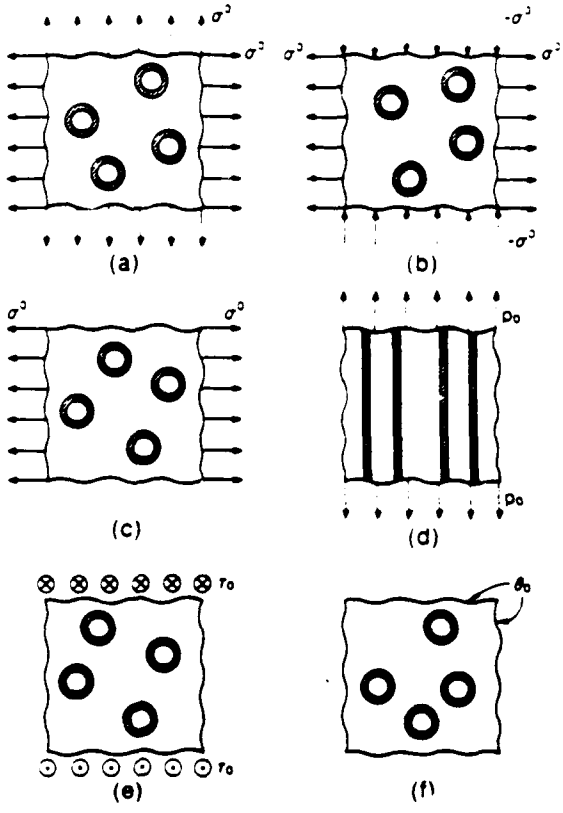

Fig. 2. Mechanical and thermal loading configurations.

Case 4 - Axial normal stress, Fig. 2d.
Case 5 - Longitudinal shear stress, Fig. 2e.
Case 6 - Uniform change in temperature, Fig. 2f.

The solution of Case 3 can be obtained as a superposition of Cases 1 and 2. The implementation of the Mori–Tanaka theory calls for the solution of auxiliary problems in which a single coated fiber is bonded as an inclusion to an infinite medium which is subjected, in turn, to the six loading cases listed above. The information needed in Cases 1, 4, and 6 can be obtained by solving the auxiliary problem shown in Fig. 3. Cases 2 and 5 call for solution of two additional auxiliary problems described in Fig. 4.

4.2. Auxiliary problems

(i) *Cases 1, 4, and 6*

Let a denote the outer radius of the fiber, and b the outer radius of the coating. In what follows,

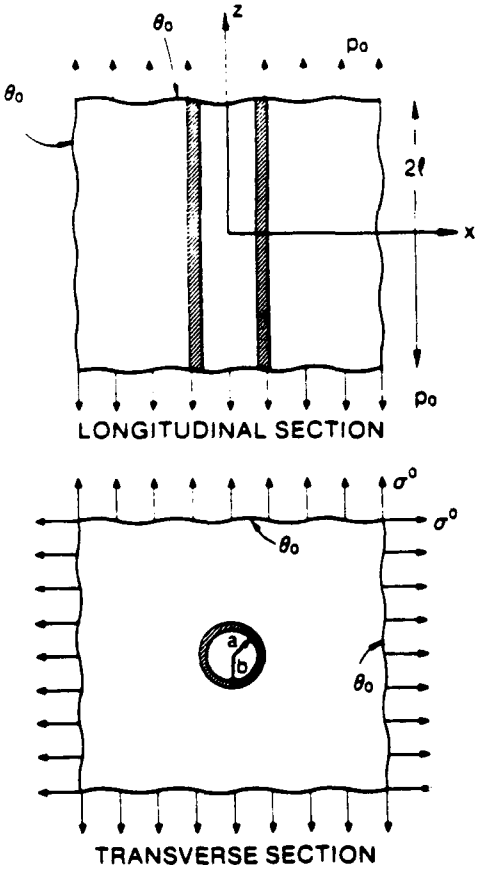

Fig. 3. Auxiliary problem for Cases 1, 4, and 6.

the cylindrical coordinate directions are r, θ, and z; when they appear with the respective stress or strain components they are always written as subscripts, whereas the phase designation symbol r is always written as a superscript. The boundary conditions on the surface S' which surrounds the matrix with the single coated fiber are, Fig. 3:

$$\begin{aligned} &\sigma_{xx}|_{r\to\infty} = \sigma_0 \qquad \sigma_{zz}|_{z=\pm l} = p_0 \\ &\sigma_{yy}|_{r\to\infty} = \sigma_0 \qquad \theta(S') = \theta_0. \end{aligned} \tag{34}$$

A simple solution of the above boundary value problem, valid away from the boundaries $z = \pm l$, can be derived from the following axisymmetric displacement field:

$$\begin{aligned} &u_r^f = A_f r \qquad && u_r^m = A_m r + B_m/r \\ &u_r^g = A_g r + B_g/r \qquad && u_z^r = \epsilon_{zz}^0 z, \end{aligned} \tag{35}$$

where $r = 0$ is the fiber axis, and u_r^r, with the superscript $r = f, g, m$, are the radial displacements in the respective phases; u_z^r denotes the axial displacements in the z direction, ϵ_{zz}^0 is a uniform strain field to be determined together with the constants A_r, B_r. The third boundary condition in (34) cannot be satisfied pointwise by the present solution. Instead, we demand that the average stress $\sigma_{zz}(\pm l)$ be equal to p_0. This is a generalized plane strain problem in which the stresses do not depend on the z coordinate, hence

$$\sigma_{zz}^m = p_0. \tag{36}$$

In addition, the solution must satisfy the following five equations: four equations of continuity of radial stresses and displacements at the two interfaces, and the condition that $\sigma_{rr}^m = \sigma^0$ at $r \to \infty$. It can be readily verified that the displacement field (35) causes uniform σ_{zz} stresses in each phase, so (36) is readily implemented.

Define now the stress invariant σ_T^r

$$\sigma_T^r = \sigma_{xx}^r + \sigma_{yy}^r = \sigma_{rr}^r + \sigma_{\theta\theta}^r, \tag{37}$$

where all stresses denote phase averages and let σ_L^r stand for the average longitudinal stress σ_{zz}^r. The solution of the auxiliary problem can now be written in the form

$$\begin{aligned} \sigma_T^r &= W_{TL}^r p_0 + W_{TT}^r \sigma_T^0 + w_T^r \theta_0 \\ \sigma_L^r &= W_{LL}^r p_0 + W_{LT}^r \sigma_T^0 + w_L^r \theta_0, \end{aligned} \tag{38}$$

where, for example, W_{TL}^r denotes the average stress σ_T^r due to a unit longitudinal stress p_0 and σ_T^0 is given by $\sigma_T^0 = 2\sigma^0$; w_T and w_L define, respectively, the average stresses σ_T and σ_L due to a unit temperature change.

We note that equation (38) is a special case of the general equation (14) where the coefficients must be found from the solution of the auxiliary problem. These components of the tensors W_r and w_r will be used in the implementation of the Mori–Tanaka method in the sequel.

(ii) *Loading Case 2*

The solution of this problem depends on the coordinate θ, but it can be obtained from an existing solution to a similar problem found by

Christensen and Lo (1979). The corresponding displacement field is

$$u_r^f = (b\sigma^0/4\mu_f)\left[a_1(\eta_f - 3)\left(\frac{r}{b}\right)^3 + d_1\left(\frac{r}{b}\right)\right] \times \cos 2\theta, \quad 0 \leqslant r \leqslant a \tag{39}$$

$$u_\theta^f = (b\sigma^0/4\mu_f)\left[a_1(\eta_f + 3)\left(\frac{r}{b}\right)^3 - d_1\left(\frac{r}{b}\right)\right] \sin 2\theta \tag{40}$$

$$u_r^g = (b\sigma^0/4\mu_g)\left[a_2(\eta_g - 3)\left(\frac{r}{b}\right)^3 + d_2\left(\frac{r}{b}\right) + c_2(\eta_g + 1)\left(\frac{b}{r}\right) + b_2\left(\frac{b}{r}\right)^3\right] \times \cos 2\theta, \quad a \leqslant r \leqslant b \tag{41}$$

$$u_\theta^g = (b\sigma^0/4\mu_g)\left[a_2(\eta_g + 3)\left(\frac{r}{b}\right)^3 - d_2\left(\frac{r}{b}\right) - c_2(\eta_g - 1)\left(\frac{b}{r}\right) + b_2\left(\frac{b}{r}\right)^3\right] \times \sin 2\theta \tag{42}$$

$$u_r^m = (b\sigma^0/4\mu_m) \times \left[2\left(\frac{r}{b}\right) + (\eta_m + 1)a_3\left(\frac{b}{r}\right) + c_3\left(\frac{b}{r}\right)^3\right] \times \cos 2\theta, \quad b \leqslant r \leqslant \infty \tag{43}$$

$$u_\theta^m = (b\sigma^0/4\mu_m)\left[-2\left(\frac{r}{b}\right) - (\eta_m - 1)a_3\left(\frac{b}{r}\right) + c_3\left(\frac{b}{r}\right)^3\right] \sin 2\theta \tag{44}$$

$$u_z^{(1)} = 0, \tag{45}$$

where a and b denote the inner and outer radii of the coating, a_i, b_i, c_i, d_i are unknown constants, μ_r are phase shear moduli, and

$$\eta_r = 3 - 4\nu_r \tag{46}$$

where ν_r denote Poisson's ratio.

The interface conditions to be satisfied are the continuity requirements for the stresses σ_{rr}, $\sigma_{r\theta}$ and displacements u_r, u_θ at interfaces $r = a$ and $r = b$. These yield eight equations for the constants. It can be readily verified that the displacement field (40) to (46) results in vanishing overall σ_{zz} stress

$$\sigma_{zz} = 0 \tag{47}$$

and fulfills

$$\sigma_{xx}|_{r\to\infty} = \sigma_0, \qquad \sigma_{yy}|_{r\to\infty} = -\sigma_0. \tag{48}$$

We now write the solution as

$$\sigma_{xx}^r = W_{TS}^r\sigma_0, \qquad \sigma_{yy}^r = -W_{TS}^r\sigma_0, \quad r = \text{f, g,} \tag{49}$$

where now the subscript TS simply refers to transverse shear, and in the last equation σ_{xx}^r, σ_{yy}^r denote phase averages.

(iii) *Loading Case 5*

It can be verified that the displacement field

$$\begin{aligned} u_z^f &= A_f r \sin\theta \\ u_z^g &= \left(A_g r + \frac{B_g}{r}\right)\sin\theta \\ u_z^m &= \left(A_m r + \frac{B_m}{r}\right)\sin\theta \\ u_x^r &= u_y^r = 0 \qquad\qquad r = \text{f, g, m,} \end{aligned} \tag{50}$$

satisfies the Navier equations for displacements, which in the present case turns out to be a Laplace equation. The five constants, A_f, A_g, A_m, B_g, B_m, are again obtained from continuity of the u_z displacement and the σ_{rz} stresses at interfaces $r = a$, and $r = b$, as well as from the boundary condition $\sigma_{yz} = \sigma_0$ at $r \to \infty$. The σ_{zz} stresses are identically equal to zero in this case.

The solution is

$$\sigma_{yz}^r = W_{LS}^r\tau_0, \quad r = \text{f, g,} \tag{51}$$

where the subscript LS denotes the longitudinal shear loading case and σ_{yz}^r is again the stress average in phase r.

4.3. Stress fields and effective properties

(i) *Loading Cases 1, 4 and 6*

For each of the loading cases listed in Section 4.1, we now find the stress fields in the phases and also the overall moduli of the composite which

can be detected under the particular loading conditions. As in 4.2 (i), Cases 1, 4, and 6 can be treated in a unified manner using the boundary conditions (34). Specific values are obtained by setting, in turn, two of the three loading parameters σ_0, p_0, θ_0 equal to zero. With the coefficients defined in (38), the average of equation (14) can be written in the form

$$\sigma_T^r = W_{TL}^r \sigma_L^m + W_{TT}^r \sigma_T^m + w_T^r \theta_0 \tag{52}$$

$$\sigma_L^r = W_{LL}^r \sigma_L^m + W_{LT}^r \sigma_T^m + w_L^r \theta_0, \tag{53}$$

where σ_T^r is given by (37) and σ_L^r stands again for σ_{zz}^r.

We now use the relations

$$\sigma_{zz} = p_0, \qquad \sigma_T = \sigma_T^0 = 2\sigma_0 \tag{54}$$

to find a special form of (19):

$$\left(c_g W_{TL}^g + c_f W_{TL}^f\right)\sigma_L^m + \left(c_m + c_g W_{TT}^g + c_f W_{TT}^f\right)\sigma_T^m = \sigma_T^0 - \left(c_f w_T^f + c_g w_T^g\right)\theta_0, \tag{55}$$

$$\left(c_m + c_g W_{LL}^g + c_f W_{LL}^f\right)\sigma_L^m + \left(c_g W_{LT}^g + c_f W_{LT}^f\right)\sigma_T^m = p_0 - \left(c_f w_L^f + c_g w_L^g\right)\theta_0, \tag{56}$$

which can be solved for σ_L^m and σ_T^m.

The method presented in 4.2(i) is now implemented with the help of another solution of the problem of single coated fiber in an infinite matrix, this time under boundary conditions

$$\begin{aligned} &\sigma_{xx}|_{r\to\infty} = \sigma_T^m/2 \qquad \sigma_{zz}|_{z=\pm l} = \sigma_L^m \\ &\sigma_{yy}|_{r\to\infty} = \sigma_T^m/2 \qquad \theta(S') = \theta_0, \end{aligned} \tag{57}$$

where σ_T^m and σ_L^m are solutions of (55) and (56). The results represent the actual stresses in the fiber, coating, and in the surrounding matrix, under external loads applied in Cases 1, 4, and 6.

One can also find estimates of the effective properties. The axial Young's modulus E follows from the relation

$$\epsilon_{zz} = \sigma_{zz}/E = c_f \epsilon_{zz}^f + c_g \epsilon_{zz}^g + c_m \epsilon_{zz}^m. \tag{58}$$

Since $\bar{\sigma}_{zz} = p_0$, this can be written as

$$p_0/E = \sum_r c_r\left[(\sigma_L^r/E_r) - (\sigma_T^r \nu_r/E_r)\right], \qquad r = \text{f, g, m}. \tag{59}$$

The stresses σ_T^m, σ_L^m found by solving (55) and (56) for $\sigma_T^0 = 0$, $\theta_0 = 0$ depend only on the external load p_0. The stresses σ_T^r, σ_L^r, r = f, g, in the other two phases are given by (52) and (53). When these expressions are substituted into (59), p_0 cancels out and there remains one equation for the modulus E.

A similar procedure yields the effective plane stress bulk modulus k

$$\frac{\sigma_T^0}{2\bar{k}} \sum_r c_r\left[(1-\nu_r)\sigma_T^r/E_r - (\nu_r \sigma_L^r/E_r)\right], \tag{60}$$

where, in this case, σ_T^m, σ_L^m are solutions of (55) and (56) for $p_0 = 0$, $\theta_0 = 0$, and σ_T^r, σ_L^r are again given by (52).

The effective transverse and longitudinal coefficients of thermal expansion α_T, α_L are obtained from

$$2\alpha_T \theta_0 = \sum_r c_r(\epsilon_{rr}^r + \epsilon_{\theta\theta}^r) \qquad r = \text{f, g, m} \tag{61}$$

$$\alpha_L \theta_0 = \sum_r c_r \epsilon_{zz}^r. \tag{62}$$

Consequently,

$$2\alpha_T \theta_0 = \sum_r c_r\left\{\left[(1-\nu_r)\sigma_T^r/E_r\right] - (2\nu_r/E_r)\sigma_L^r + 2\alpha_r\theta_0\right\} \tag{63}$$

$$\alpha_L \theta_0 = \sum_r c_r\left[(\sigma_L^r/E_r) - (\sigma_T^r \nu_r/E_r) + \alpha_r \theta_0\right], \tag{64}$$

where again σ_L^m, σ_T^m are solutions of (55) and (56), but for $p_0 = \sigma_T^0 = 0$. The stresses σ_T^r, σ_L^r follow from (52) and (53), where α_r are the linear expansion coefficients of the isotropic phases.

(ii) *Loading Case 2*

We now use the definitions (49) to implement the average of (14) in the form

$$\sigma_{xx}^r = W_{TS}^r \sigma_{xx}^m \quad r = \text{f, g}, \tag{65}$$

where again the stresses denote average quantities. Note that

$$\sigma_{xx} = \sigma_0 \tag{66}$$

to obtain

$$\sigma_{xx}^m = \left(c_m + c_f W_{TS}^f + c_g W_{TS}^g\right)^{-1} \sigma_0. \tag{67}$$

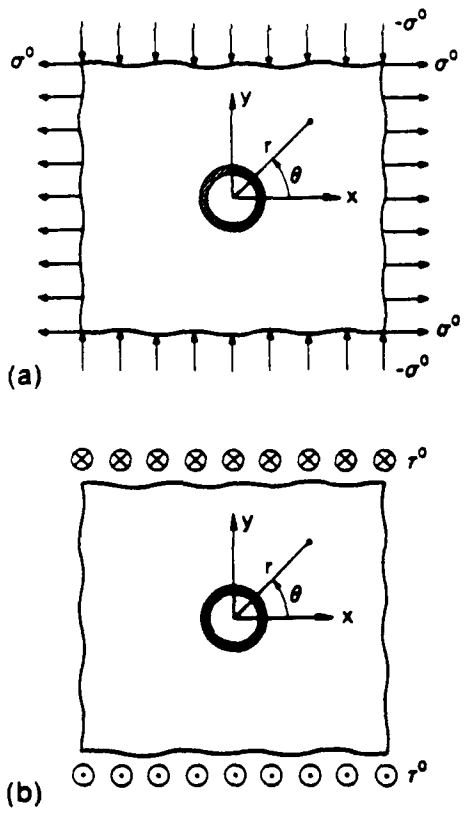

Fig. 4. Auxiliary problems for Case 2(a); and Case 5(b).

The stress field in the coated fiber now follows if the load in Fig. 4a is redefined as

$$\pm\sigma_0 = \pm\sigma_{xx}^{m}, \tag{68}$$

and if the previous solution of (39)–(45) is now used with (68).

The effective transverse shear modulus μ_T then follows from

$$\frac{1}{2\mu_T} = \left(c_m\frac{1}{2\mu_m} + c_f\frac{1}{2\mu_f}W_{TS}^{f} + c_g\frac{1}{2\mu_g}W_{TS}^{g}\right) \cdot\left(c_m + c_fW_{TS}^{f} + c_gW_{TS}^{g}\right)^{-1}, \tag{69}$$

where μ_r are the phase shear moduli. This equation takes advantage of the fact that in the auxiliary problem of Fig. 4a, the shear stress $\sigma_{x'y'}^{r}$, in a coordinate system rotated by 45° about z is equal to σ_{xx}^{r}.

(iii) *Loading Case 6*

Here we use definitions (51) and write the average of (14) in the form

$$\sigma_{yz}^{r} = W_{LS}^{r}\sigma_{yz}^{m}, \quad r = f, g. \tag{70}$$

Note now that

$$\sigma_{yz} = \tau_0 \tag{71}$$

and find

$$\sigma_{yz}^{m} = \left(c_m + c_fW_{LS}^{f} + c_gW_{LS}^{g}\right)^{-1}\tau_0. \tag{72}$$

The stress field in the coated fiber is obtained by redefining τ_0 in Fig. 4b as $\tau_0 = \sigma_{yz}^{m}$ and by using the solution of (50) with this value.

The effective longitudinal shear modulus turns out to be

$$\frac{1}{2\mu_L} = \left(c_m\frac{1}{2\mu_m} + c_f\frac{1}{2\mu_f}W_{LS}^{f} + c_g\frac{1}{2\mu_g}W_{LS}^{g}\right) \cdot\left(c_m + c_fW_{LS}^{f} + c_gW_{LS}^{g}\right)^{-1}. \tag{73}$$

4.4. Numerical results

Stress distributions and effective moduli of coated-fiber composites are illustrated for several systems whose properties are given in Table 1. It is noted that all of the constituents are isotropic except for the transversely isotropic fiber in system 2. The fiber volume fraction is 0.4 throughout.

Numerical results are presented only for transverse shear loading (Case 2), transverse normal loading (Case 3), longitudinal shear loading (Case 5) and a uniform change in temperature of 1°C (Case 6).

Figures 5–7 illustrate the average stresses in the coating as a function of the angle θ, for the case of system 4 (Table 1).

Figure 8 illustrates the stresses in the coating and in the immediate surrounding fiber and matrix for the case of uniform temperature change of 1°C, in system 4 (Table 1). The average stresses in the fiber, coating and matrix for thermal loading in all of the four composite systems have been summarized in Table 2. It should be noted here that system 2 has a transversely isotropic fiber and

Table 1
Stress distributions and effective moduli of coated-fiber composites

System		E_A (Gpa)	E_T (Gpa)	G_A (Gpa)	G_T (Gpa)	α_T (10^{-6} 1/°C)	α_A (10^{-6} 1/°C)	c (Volume fraction)
1	Nicalon fiber	172.38	172.38	71.78	71.78	3.8	3.8	0.4
	Carbon coating	34.48	34.48	14.34	14.34	3.3	3.3	0.01616
	LAS matrix	103.43	103.43	43.09	43.09	2.8	2.8	0.583384
2	Carbon fiber	689.5	7.58	15.17	3.99	11.0	−1.32	0.4
	Ytria coating	172.38	172.38	71.83	71.83	6.0	6.0	0.084
	SiC matrix	482.65	482.65	201.10	201.10	4.8	4.8	0.516
3	Tungsten fiber	345.0	345.0	135.0	135.0	5.0	5.0	0.4
	Carbon coating	34.48	34.48	14.34	14.34	3.3	3.3	0.0107
	Nickel matrix	214.0	214.0	81.6	81.6	13.3	13.3	0.5893
4	SiC fiber	431.0	431.0	172.0	172.0	4.86	4.86	0.4
	Carbon coating	34.48	34.48	14.34	14.34	3.3	3.3	0.0107
	Titanium aluminate matrix	96.5	96.5	37.1	37.1	9.25	9.25	0.5893

Table 2
Uniform thermal change +1°C

Material	MPa						
	$\bar{\sigma}^{f}_{zz}$ [a]	$\bar{\sigma}^{s}_{zz}$	$\bar{\sigma}^{m}_{zz}$	$\bar{\sigma}^{s}_{rr}$	$\bar{\sigma}^{s}_{\theta\theta}$	$\sigma^{f}_{\theta\theta}$ (interface)	$\sigma^{m}_{\theta\theta}$ (interface)
1	−0.0968	−0.00603	0.0665	−0.0405	0.00458	−0.0410	0.0968
2	2.064	−0.791	−1.471	−0.0394	−0.225	−0.0302	0.137
3	1.826	0.412	−1.247	0.774	0.304	0.777	−1.845
4	0.583	0.157	−0.399	0.200	0.126	0.201	−0.479

[a] Top bars indicate phase stress averages

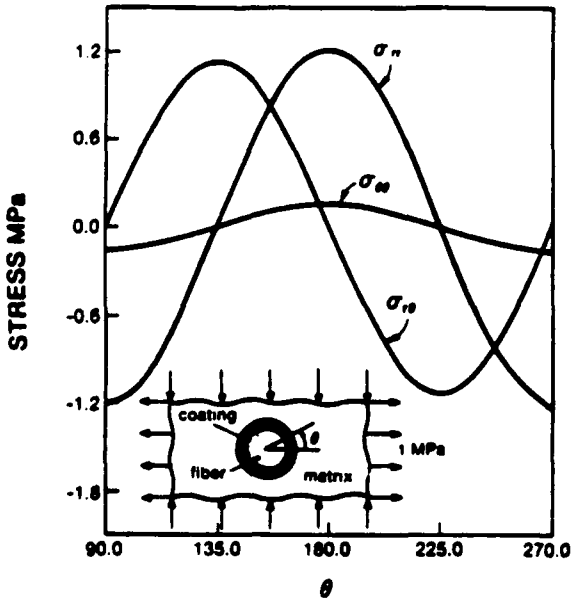

Fig. 5. Average stress distributions in the coating for transverse shear loading (1 MPa) versus the angle θ in the case of composite system 4 (Table 1).

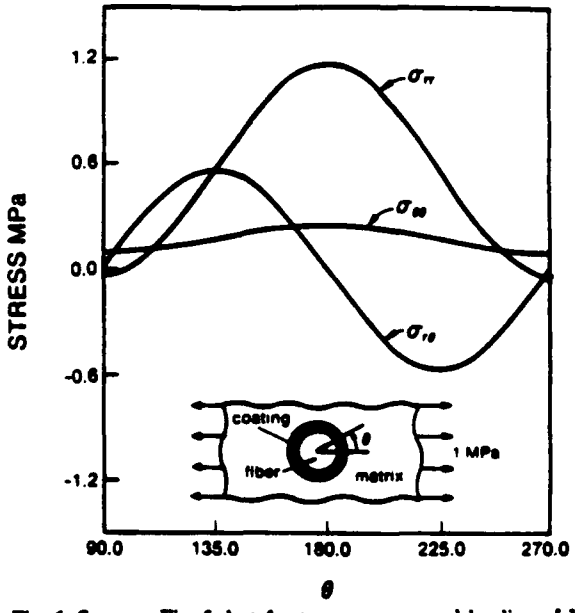

Fig. 6. Same as Fig. 5, but for transverse normal loading of 1 MPa.

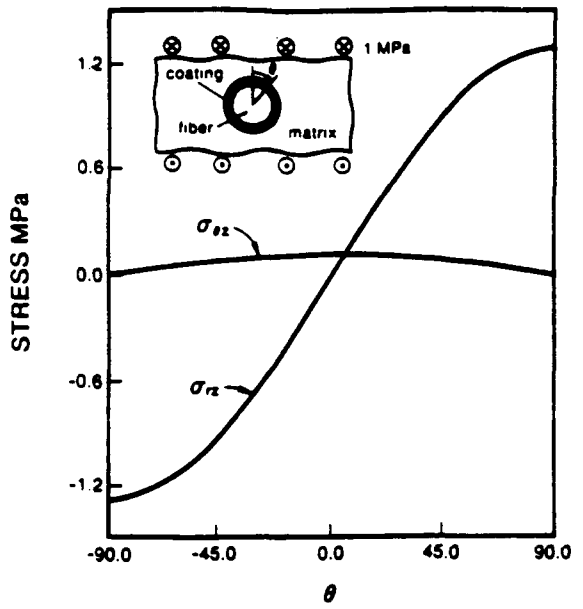

Fig. 7. Same as Fig. 5, but for longitudinal shear loading of 1 MPa.

Table 3
Comparison of Effective Properties Predications by Mori-Tanaka Method and Composite Cylinder Assemblage (C.C.A.) Model

	Material	Mori-Tanaka	C.C.A.
E_A/E_m	1	1.255	1.249
	3	1.236	1.234
	4	2.379	2.376
$\tilde{k}/\mu_m$	1	1.766	1.739
	3	2.158	1.996
	4	3.073	2.979
μ_L/μ_m	1	1.188	1.188
	3	1.171	1.171
	4	1.655	1.655
$\alpha_T[°C^{-1}]$	1	0.3224×10^{-5}	0.3222×10^{-5}
	3	0.1009×10^{-4}	0.1008×10^{-4}
	4	0.7638×10^{-5}	0.7637×10^{-5}
$\alpha_L[°C^{-1}]$	1	0.3332×10^{-5}	0.3327×10^{-5}
	3	0.9071×10^{-6}	0.9074×10^{-5}
	4	0.5998×10^{-5}	0.5999×10^{-5}

Key: E_A longitudinal Young's modulus, $\tilde{k}$ plane stress bulk modulus, μ_L longitudinal shear modulus, α_T transverse linear thermal expansion coefficient, and α_L longitudinal linear thermal expansion coefficient.

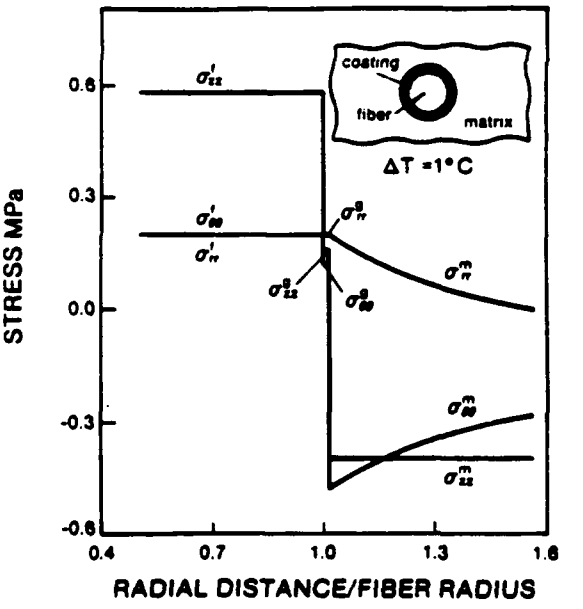

Fig. 8. Stress distributions in system 4 (Table 1) for the case of uniform temperature change of 1°C.

the analysis given in 4.2(i) can be applied with the same displacement field (35) with the proper constitutive equation for the fiber.

The effective moduli and thermal expansion coefficients of the coated fiber composites have also been calculated using the method presented in the paper. Due to the very small thickness of the coating in the considered systems the effective properties are almost equal to their counterparts in the uncoated fiber case. Results for the composite systems 1, 3, 4, without the coating are exhibited in Table 3 and compared to the corresponding composite cylinder assemblage results (Hashin and Rosen, 1964) in loading situations for which they exist.

Acknowledgements

The first author is indebted to Professor G.J. Dvorak for the visiting appointment at the Civil Engineering Department at RPI during 1987/1988. Support from the DARPA-HiTASC program is gratefully acknowledged.

References

Benveniste, Y. (1987), A new approach to the application of Mori–Tanaka's theory in composite materials, *Mech. Mater.* 6, 147.

Christensen, R.M. and K.H. Lo (1979), Solutions for the effective shear properties of three-phase sphere and cylinder models, *J. Mech. Phys. Solids 27*, 315.

Dvorak, G.J. and T. Chen (1988), Thermal expansion of three-phase composite materials, *J. Appl. Mech.*, to appear.

Eshelby, J.D. (1957), The determination of the elastic field of an ellipsoidal inclusion and related problems, *Proc. R. Soc. London A241*, 376.

Hashin, Z. and B.W. Rosen (1964), The elastic moduli of fiber-reinforced materials, *J. Appl. Mech. 31*, 223.

Hashin, Z. and S. Shtrikman (1963), A variational approach to the theory of elastic behavior of multiphase materials, *J. Mech. Phys. Solids 11*, 127.

Hatta, H. and M. Taya (1986), Thermal conductivity of coated filler composites, *J. Appl. Phys. 59*, 1851–1860.

Hill, R. (1972), An invariant treatment of interfacial discontinuities in elastic composites, in: L.I. Sedov, ed., *Continuum Mechanics and Related Problems of Analysis*, Academy of Sciences SSSR, Moscow, 597.

Mori, T. and K. Tanaka (1973), Average stress in matrix and average elastic energy of materials with misfitting inclusions, *Acta Metall. 21*, 571.

Norris, A.N. (1989), An examination of the Mori–Tanaka effective medium approximation for multiphase composites, *J. Appl. Mech.*, to appear.

Tandon, G.P. and G.J. Weng (1986), Average stress in the matrix and effective moduli of randomly oriented composites, *Compos. Sci. Tecnol. 27*, 111–132.

Walpole, L.J. (1978), A coated inclusion in an elastic medium, *Math. Proc. Comb. Phil. Soc. 83*, 495–506.

Weng, G.J. (1984), Some elastic properties of reinforced solids, with special reference to isotropic ones containing spherical inclusions, *Int. J. Eng. Sci. 22*, 845.

Addendum

We address here the question of symmetry of the L and l tensors in equations (23) and (24). In particular, we prove that the diagonal symmetry of the L tensor ($L_{ijkl} = L_{klij}$) exists in the following cases:

a. Multiphase composites reinforced by anisotropic ellipsoidal inclusions of identical shape and orientation.

b. Two-phase composites reinforced by anisotropic ellipsoidal inclusions with aligned axis of anisotropy, but several different shapes which may be non-aligned.

The remaining symmetries of L ($L_{ijkl} = L_{jikl} = L_{ijlk}$) can be shown to follow from the corresponding symmetries of the L_r and T_r tensors, and are always satisfied. Similarly, the symmetry of the second order tensor l depends on the relations $L^{(r)}_{ijkl} = L^{(r)}_{jikl}$ and $l^{(r)}_{ij} = l^{(r)}_{ji}$, and is again automatically satisfied.

So far, we are not in the position to make a conclusive statement about the diagonal symmetry of the L tensor of coated fiber composites, predicted by the Mori–Tanaka theory. The outcome depends on the structure of the T_r tensors which are generally not available in explicit form. We should point out, however, that recent numerical results for the case of coated cylindrical fibers with a circular cross-section confirm the symmetry of the L tensor in this situation.

It is clear that similar comments can be made about the M and m tensors given by eqns. (26) and (27). The proofs of symmetry of L in the two systems can be obtained as follows.

Case a.

Let (23) represents a multiphase medium with $r = 0, 1, \ldots, N$, where $r = 0$ denotes the matrix phase. Recall that the tensor T_r for inclusions of ellipsoidal shape is given by

$$T_r = \left[I + SL_0^{-1}(L_r - L_0) \right]^{-1}, \tag{A.1}$$

where S is the Eshelby tensor. Note that S depends only on the elastic moduli of the matrix, and on the aspect ratios of the ellipsoid. Therefore, it is identical for all inclusions. Define the tensor L_0^0 as

$$L_0^0 = L_0 S^{-1} - L_0. \tag{A.2}$$

Since $L_0 S^{-1}$ is diagonally symmetric (see, for example, Walpole, 1981), it follows that L_0^0 is also diagonally symmetric. T_r can be also written as

$$T_r = \left[L_0^0 + L_r \right]^{-1} \left[L_0^0 + L_0 \right]. \tag{A.3}$$

Substitution of this equation into (23), and some algebra eventually yield the following expression for L:

$$L = \left[\sum_r c_r \left(L_r + L_0^0 \right)^{-1} \right]^{-1} - L_0^0. \tag{A.4}$$

which proves the diagonal symmetry of $\boldsymbol{L}$. This form of the Mori–Tanaka model for multiphase composites was noted by Norris (1989).

Case b.

Write (23) in the form

$$\boldsymbol{L} = \boldsymbol{L}_0 + \sum_{r=1}^{M} c_r(\boldsymbol{L}_r - \boldsymbol{L}_0)\boldsymbol{T}_r\left[c_0\boldsymbol{I} + \sum_{s=1}^{M} c_s\boldsymbol{T}_s\right]^{-1} \tag{A.5}$$

which for a two-phase system, with anisotropic inclusions having aligned axis of symmetry, can be reduced to

$$\boldsymbol{L} = \boldsymbol{L}_0 + (\boldsymbol{L}_p - \boldsymbol{L}_0)\sum_{r=1}^{M} c_r\boldsymbol{T}_r\left[c_0\boldsymbol{I} + \sum_{s=1}^{M} c_s\boldsymbol{T}_s\right]^{-1} \tag{A.6}$$

where $\boldsymbol{L}_p$ and $\boldsymbol{L}_0$ denote the stiffness tensors of the particulate and matrix phase, respectively. Recall that the inclusions may have different shape, and let c_r, $r = 1, 2, \ldots, M$, denote the volume fraction of the set particles of the same shape. $\boldsymbol{T}_r$ is the partial concentration factor for that set. After some algebra, eqn. (6) assumes the form

$$\boldsymbol{L} = \boldsymbol{L}_0 + \left[c_0\left[(\boldsymbol{L}_p - \boldsymbol{L}_0)\sum_{r=1}^{N} c_r\boldsymbol{T}_r\right]^{-1} + (\boldsymbol{L}_p - \boldsymbol{L}_0)^{-1}\right]^{-1}. \tag{A.7}$$

We further recall that the tensor $\boldsymbol{T}_r$ can be written as

$$\boldsymbol{T}_r = \left[\boldsymbol{I} + \boldsymbol{P}_r(\boldsymbol{L}_0 - \boldsymbol{L}_p)\right], \tag{A.8}$$

such that $\boldsymbol{P}_r$ is a diagonally symmetric tensor related to the $\boldsymbol{P} = \boldsymbol{S}\boldsymbol{L}_0^{-1}$ tensor by (Walpole, 1981):

$$\boldsymbol{P}(\boldsymbol{L}_p - \boldsymbol{L}_0)\boldsymbol{P}_r = \boldsymbol{P} - \boldsymbol{P}_r \tag{A.9}$$

Substitution of (A.8) into (A.7) gives

$$\boldsymbol{L} = \boldsymbol{L}_0 + \left[c_0\left[\sum_{r=1}^{M} c_r(\boldsymbol{L}_p - \boldsymbol{L}_0) - c_r(\boldsymbol{L}_p - \boldsymbol{L}_0)\boldsymbol{P}_r(\boldsymbol{L}_p - \boldsymbol{L}_0)\right]^{-1} + (\boldsymbol{L}_0 - \boldsymbol{L}_p)^{-1}\right]^{-1} \tag{A.10}$$

which shows that $\boldsymbol{L}$ is diagonally symmetric.

Additional Reference

L.J. Walpole (1981), Elastic behavior of composite materials: Theoretical foundations, in: C.S. Yih, ed., *Advances in Applied Mechanics*, Academic Press Inc., New York, Vol. *21*, 169–243.

Proceedings of American Society for Composites, Technomic Pub. Co., 1989, pp. 139-147

Thermal Stresses in Coated Fiber Composites

Tungyang Chen[1], George J. Dvorak[2] and Yakov Benveniste[3]

Institute Center for Composite Materials and Structures
Rensselaer Polytechnic Institute
Troy, N.Y. 12180

March 1989

1 Graduate Research Assistant
2 Professor and Head, Dept. of Civil Eng., R.P.I.
3 Professor, Dept. of Solid Mechanics, Materials and Structures
Tel-Aviv University, ISRAEL

ABSTRACT

This paper presents a micromechanical analysis of stress fields in coated and uncoated fiber composites subjected to both mechanical and thermal load fluctuations. The analysis of unidirectional materials is based on the 'average stress in the matrix' concept of Mori and Tanaka (1973) [6]. In the present work, the concept is extended to coated fibers. The advantage of this approach is that it permits one to introduce exact elasticity solutions of the coated fiber problem into the analysis. Such relations were derived for the case of distinct transversely isotropic phases. All possible mechnaical loadings, and a uniform temperature change were considered. Results are given for several specific systems.

INTRODUCTION

Micromechanics analyses of composite materials are often related to Eshelby's (1957) [4] result that the strain field in an ellipsoidal inclusion bonded to a uniformly strained infinite medium is also uniform. This result is commonly used to evaluate overall properties and average local fields in composite aggregates in terms of the phase stress and strain concentration tensors. Unfortunately, local fields in coated inclusions are generally not uniform, hence the phase concentration tensors cannot be easily evaluated. Therefore, the analysis of composite reinforced by coated fibers or particles is one of the more difficult problems in micromechanics.

Walpole (1978) [8] was among the first to consider problems of this kind. He assumed that a very thin coating has no effect on strain distribution in the inclusion. Hatta and Taya (1986) [5] considered the heat conduction problem in composites reinforced by short coated fibers in the context of the original Mori-Tanaka method. Recently, Pagano and Tandon (1988) [7] analyzed a multidirectional coated fiber composite by means of a three-phase concentric cylinder model.

The present paper is concerned with evaluation of local fields and overall properties of composites reinforced by coated fibers . The results are derived from a variant of Benveniste's (1987) [1] reexamination of the Mori-Tanaka's method. In particular, the local fields in a coated inclusions are approximated by those found when the coated inclusion is embedded in an unbounded matrix medium subjected to the average matrix stresses at infinity. The advantage of this approach is that the local fields in the coating and inclusion,

[1] Graduate Research Assistant
[2] Professor, Dept. of Civil Eng., R.P.I.,Troy, N. Y.
[3] Professor, Tel-Aviv University, ISRAEL

and in the matrix can be evaluated by using the solution for a single coated fiber in an infinite matrix. Specific results are found for systems reinforced by aligned coated fibers, where the phases are isotropic or transversely isotropic elastic solids. We also consider the possibility of plastic yielding in the unidirectional composites.

STRESS AND STRAIN FIELDS IN THREE-PHASE COMPOSITES

Consider a three-phase composite material consisting of a continuous matrix phase m, in which there are embedded a fiber phase f, and a third phase g which represents a layer of coating that encapsulates each fiber of the f phase. The fibers have a circular crosssection. The phases are assumed elastic and perfectly bonded during deformation. The composite medium is statistically homogeneous. The thermoelastic constitutive equations of the phases are given in the form

$$\sigma_r = L_r \varepsilon_r + l_r \theta \tag{1}$$

$$\varepsilon_r = M_r \sigma_r + m_r \theta \tag{2}$$

where r=f, g, m; L_r and $M_r=(L_r)^{-1}$ are the stiffness and compliance tensors; l_r is the thermal stress vector and m_r is the thermal strain vector of the expansion coefficients, such that

$$l_r = -L_r m_r \tag{3}$$

Define the following thermomechanical loading problems

$$\sigma_n(S) = \sigma_o n \qquad \theta(S) = \theta_o \tag{4}$$

where $\sigma_n(S)$ is the traction at the external boundary S of a representative volume V of the composite under consideration, n denotes the exterior normal to the surface S; σ_o is the applied uniform stress field; $\theta(S)$ is the temperature rise at S, and θ_o is a constant quantity.

The composite is subjected to boundary conditions (4). The solution for the stress field in the phases can be expressed in the form:

$$\sigma_r(x) = B_r(x)\, \sigma_o + b_r(x)\, \theta_o \qquad r = f, g, m \tag{5}$$

where $B_r(x)$ and $b_r(x)$ are fourth and second order tensors, respectively. Their volume averages B_r and b_r are usually referred to as mechanical and thermal stress concentration factors.

In the Mori-Tanaka method,, the stress fields in phases f and g are assumed to be equal to the fields in a single coated fiber which is embedded in an unbounded matrix medium and subjected to remotely applied stresses which are equal to the yet unknown average stress in the matrix. Also a uniform temperature change is applied.

Suppose that the single inclusion is surrounded by a large matrix volume V' with surface S', Fig 1. The solutions of this dilute problem assumes the form

$$\sigma_r(x) = W_r(x)\,\sigma_m + w_r(x)\,\theta_o \qquad r = f, g \tag{6}$$

we will solve this auxiliary problem in the next section. To determine σ_m, we recall that the overall uniform stress and the local average stress are connected by the relations

$$\sum_r c_r \sigma_r = \sigma_o \qquad r = f, g, m \tag{7}$$

where c_r denote the phase volume fractions, $c_f+c_g+c_m=1$. From equations (6) into (7), one finds that the unknown matrix stress is equal to

$$\sigma_m = \left[\sum_r c_r W_r\right]^{-1} \left[\sigma_o - \theta_o \sum_r c_r w_r\right] \tag{8}$$

This opens the way for evaluation of the partial stress concentration factors in (6) and of the average matrix stress (8). One can then obtain the solution (5). An entirely similar procedure can be applied under strain boundary conditions.

The effective thermoelastic constitutive relations of the composite medium are defined as:

$$\sigma = L\varepsilon + l\theta \tag{9}$$

$$\varepsilon = M\sigma + m\theta \tag{10}$$

where σ, ε and θ denote representative volume averages and L, M, l, m are overall stiffness, compliance, thermal stress and thermal strain tensors, respectively. Using equations (6), (7), and (8), one can derive :

$$M = \left[\sum_r c_r M_r W_r\right]\left[\sum_r c_r W_r\right]^{-1} \tag{11}$$

$$m = \left[\sum_r c_r M_r W_r\right]\left[\sum_r c_r W_r\right]^{-1}\left[-\sum_r c_r w_r\right] + \sum_r c_r (M_r w_r + m_r) \tag{12}$$

We note here that Benveniste et al (1989) [2] has proved that the results are consistent in that the overall compliance tensor is the inverse of stiffness tensor. Also, we have numerically verified that the effective stiffness L and compliance M are symmetric.

AUXILIARY PROBLEMS

In the evaluation of W_T and w_T, the composite is subjected to several traction boundary conditions and to a uniform temperature change. We wish to find the stress distribution in the fiber, coating and matrix which surrounds the periphery of the coated fiber. The loading cases are shown in Fig. 2 :

Case 1 - Transverse hydrostatic stress
Case 2 - Transverse shear stress
Case 3 - Transverse normal stress
Case 4 - Axial normal stress
Case 5 - Longitudinal shear stress
Case 6 - Uniform change in temperature

Case 3 can be obtained as a superposition of cases 1 and 2. In what follows, the cylindrical coordinates r, θ, z are used; the respective stress or strain components are always written as subscripts, while the phase designation is always written as a supercript.

(i) Cases 1,4,6

The solution of the above boundary value problems can be derived from the following admissible displacement field:

$$u_r^f = A_f r \qquad u_r^m = A_m r + B_m/r$$
$$u_r^g = A_g r + B_g/r \qquad u_z^r = \varepsilon_z^o \tag{13}$$

where $u_r^{(i)}$, with the superscript (i)=f,g,m, are the radial displacements in the phases; $u_z^{(i)}$ denotes the axial displacement in the z direction . The constants A_f, A_g, A_m, B_g, B_m and ε_z^o are to be determined from the conditions of continuity of displacements and tractions at the two interfaces, and from the traction boundary conditions at infinity.

(ii) Case 2

The admissible displacement field of this problem has the form given by Christensen and Lo (1979) [3] :

$$u_r^f = (b\sigma^o/4\mu_T)\left[a_1(\eta_f - 3)\left[\frac{r}{b}\right]^3 + d_1\left[\frac{r}{b}\right]\right]\cos 2\theta \quad , \quad 0 \le r \le a \tag{14}$$

$$u_\theta^f = (b\sigma^o/4\mu_T)\left[a_1(\eta_f + 3)\left[\frac{r}{b}\right]^3 - d_1\left[\frac{r}{b}\right]\right]\sin 2\theta \quad , \quad 0 \le r \le a \tag{15}$$

$$u_r^g = (b\sigma^o/4\mu_g)\left[a_2(\eta_g - 3)\left[\frac{r}{b}\right]^3 + d_2\left[\frac{r}{b}\right] + c_2(\eta_g + 1)\left[\frac{b}{r}\right] + b_2\left[\frac{b}{r}\right]^3\right]\cos 2\theta \tag{16}$$

$$u_\theta^g = (b\sigma^\circ/4\mu_g)\left[a_2(\eta_g+3)\left[\frac{r}{b}\right]^3 - d_2\left[\frac{r}{b}\right] - c_2(\eta_g-1)\left[\frac{b}{r}\right] + b_2\left[\frac{b}{r}\right]^3\right]\sin 2\theta \qquad (17)$$

$$u_r^m = (b\sigma^\circ/4\mu_m)\left[2\left[\frac{r}{b}\right] + (\eta_m+1)a_3\left[\frac{b}{r}\right] + c_3\left[\frac{b}{r}\right]^3\right]\cos 2\theta \qquad (18)$$

$$u_\theta^m = -(b\sigma^\circ/4\mu_m)\left[2\left[\frac{r}{b}\right] + (\eta_m-1)a_3\left[\frac{b}{r}\right] - c_3\left[\frac{b}{r}\right]^3\right]\sin 2\theta \qquad (1.$$

$$u_z^{(i)} = 0 \qquad (20)$$

where a and b denote the inner and outer radii of the coating, μ_r are phase shear moduli, and $\eta_r = 3 - 4\nu_r$; ν_r denotes the Poisson's ratio; a_i, b_i, c_i, and d_i are unknown constants to be determined from the interface conditions.

(iii) Case 5

The general displacement field of anti-plane shear is

$$u_z^f = A_f r \sin\theta \qquad u_z^g = \left(A_g r + \frac{B_g}{r}\right)\sin\theta$$
$$u_z^m = \left(A_m r + \frac{B_m}{r}\right)\sin\theta \qquad u_x^r = u_y^r = 0 \qquad (21)$$

The five constants A_f, A_g, A_m, B_g, B_m are obtained from continuity of the u_z displacement and the σ_{rz} stress at the interfaces, as well as from the boundary condition $\sigma_{yz} = \sigma^\circ$ at $r = \infty$.

NUMERICAL RESULTS

The stress distributions in coated and uncoated composites are illustrated for several systems. The fiber volume fraction is assumed to be 0.4 .

Table 1 shows the thermal stresses in the fiber, coating and matrix under uniform temperature change of 1°C. Since the volume fraction of the coating is very small (less than 1%), the results for coated fiber composites are not much different from those for the uncoated fiber composites. However, very different stress magnitudes are found in different systems.

Figure 3 illustrates the thermal stress distribution in the radial direction for the system consisting of SiC fiber, carbon coating and Ti_3Al matrix. The coating thickness is 1 μm; fiber radius is 75 μm. The fiber stresses are uniform in this case. Table 2 presents the average thermal stress caused by cooling from the processing temperature to the room temperature, for 4 different uncoated systems. Figures 4 and 5 show yield stress and the

effective stress vs temperature during cooling in a system consisting of an Al_2O_3 fiber, in a Ti_3Al or Ni_3Al matrix. These results indicate that yielding may take place during cooling.

ACKNOWLEDGEMENTS

Support for this work was provided by the DARPA - HiTASC program at R.P.I. .

REFERENCES

1.Benveniste, Y.,1987, "A New Approach to The Application of Mori-Tanaka's Theory in Composite Materias, " Mechanics of Materials, Vol. 6, pp. 147-157.

2.Benveniste, Y., Dvorak, G. J. and Chen, T., 1989, "Stress fields in Composites with coated Inclusions, " Mechanics of Materials, in press.

3.Christensen, R. M. and Lo , K. H.,1979, " Solutions for the Effective Shear Properties of Three-Phase Sphere and Cylinder Models, " Journal of Mechanics and Physics of Solids, Vol. 27, pp. 315.

4.Eshelby, J. D.,1957, " The Determination of the Elastic Field of an Ellipsoidal Inclusion and Related Problems, " Proceedings of the Royal Society, London, series A, Vol. 241, pp. 376-396.

5.Hatta, H and Taya, M.,1986, "Thermal Conductivity of Coated Filler Composites, "Journal of Applied Physics, Vol. 59, pp. 1851-1860.

6.Mori, T. and Tanaka K.,1973, " Average Stress in Matrix and Average Elastic Energy of Materials With Misfitting Inclusions, " Acta Metallurgica, Vol. 21, pp. 571-574.

7.Pagano, N. J. and Tandon, G. P.,1988,"Elastic Response of Multi-directional Coated-fiber Composites," Composite Science and Technology, Vol.31, pp.273-293.

8.Walpole, L. J., 1978, "A Coated Inclusion in an Elastic Medium," Mathematical Proceeding Camb. Phil. Society, Vol. 83, pp. 495-506.

MPa/°C	$\bar{\sigma}_{rr}^{c}$	$\bar{\sigma}_{\theta\theta}^{c}$	$\sigma_{\theta\theta}^{f}$	$\sigma_{\theta\theta}^{m}$
Nicalon f. Carbon c. LAS matrix	-0.0405 (-0.03)	-0.2205	0.0218 (0.0246)	-0.043 (-0.058)
Graphite f. Yttria c. SiC matrix	2.673 (3.069)	2.577	2.923 (3.074)	-6.855 (-7.079)
Tungsten f. Carbon c. Nickel matrix	0.789 (0.7961)	0.288	0.771 (0.797)	-1.814 (1.848)
SiC f. Carbon c. Ti_3Al m.	0.1936 (0.1960)	0.1064	0.1942 (0.1980)	-0.4516 (-0.4523)

() — without coating

Table 1 Average Thermal Stresses in the fiber and coating and matrix stresses at interfaces after a temperature change of $+1^0$ C

MPa	PT(°C) YT(°C) ΔT_a(°C)	STRESS EVALUATION ΔT(°C)	σ_{rr}^{f}	σ_{rr}^{m}	$\sigma_{\theta\theta}^{f}$ interface	$\sigma_{\theta\theta}^{m}$ interface	$\sigma_{\theta\theta}^{f}$	$\sigma_{\theta\theta}^{m}$
Al_2O_3 Ti_3Al	900 X -600	-100	-12.91	-6.01	-12.91	26.82	-40.07	21.58
SCS-6 Ti_3Al	900 722.4 -216.6	-100	-43.19	-20.09	-43.19	89.72	-139.43	75.08
SCS-6 Ni_3Al	1200 1000 -102	-100	-73.85	-34.35	-73.85	153.39	-207.19	111.55
Al_2O_3 Ni_3Al	1200 977.7 -222.3	-100	-46.75	-21.75	-46.75	97.11	-129.61	67.79

Table 2 Thermal stresses after cooling 100^0 C

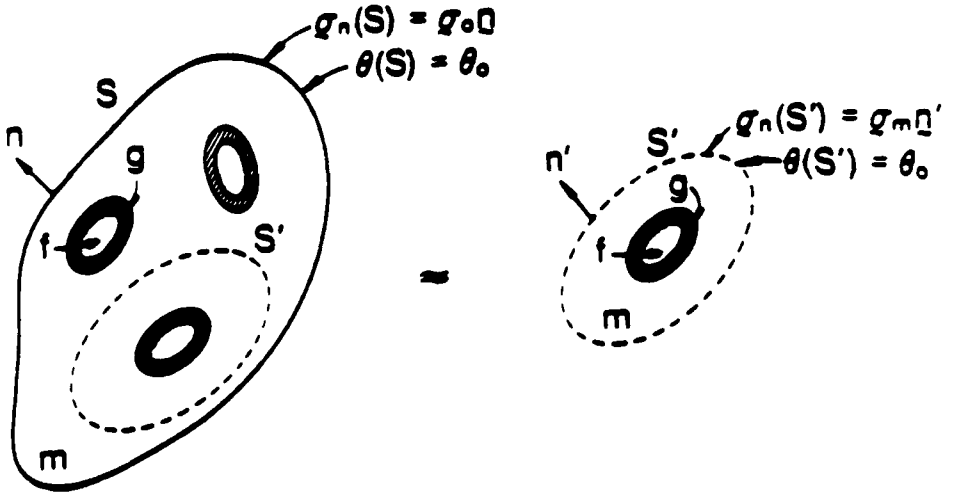

Fig. 1 A schematic representation of Mori–Tanaka's method for thermoelastic problems

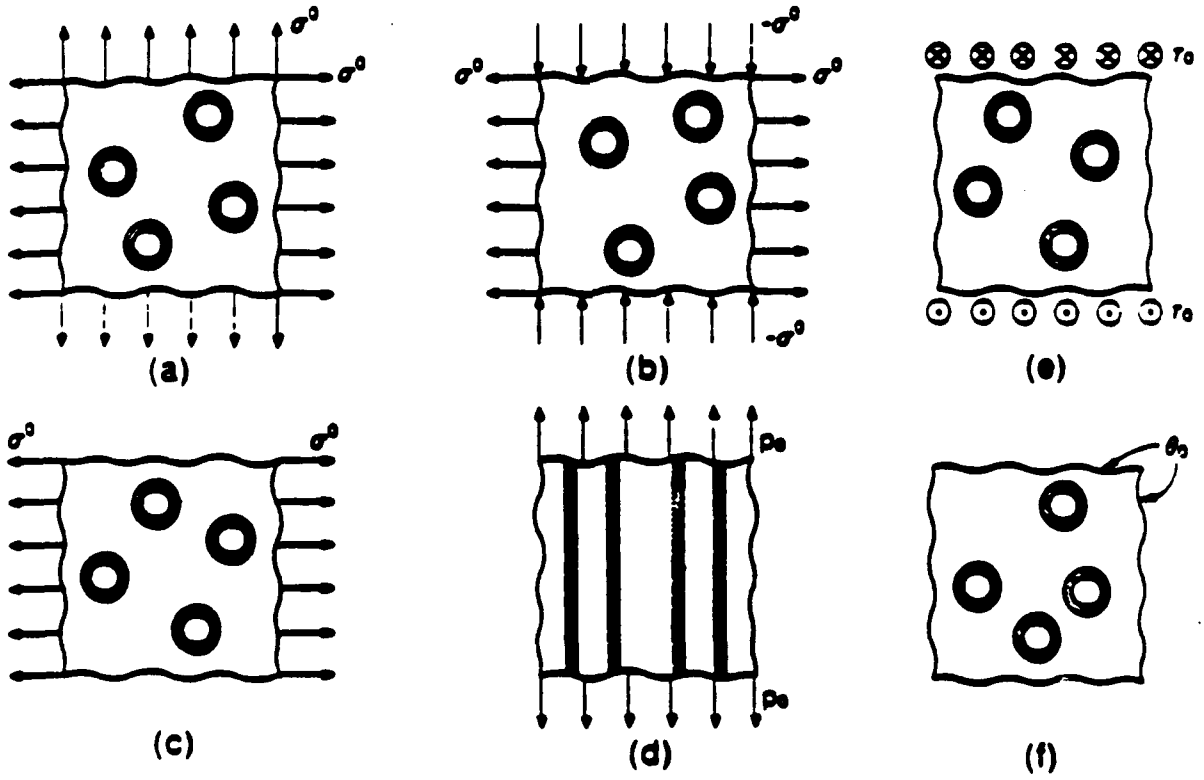

Fig. 2 Mechanical and thermal loading configurations

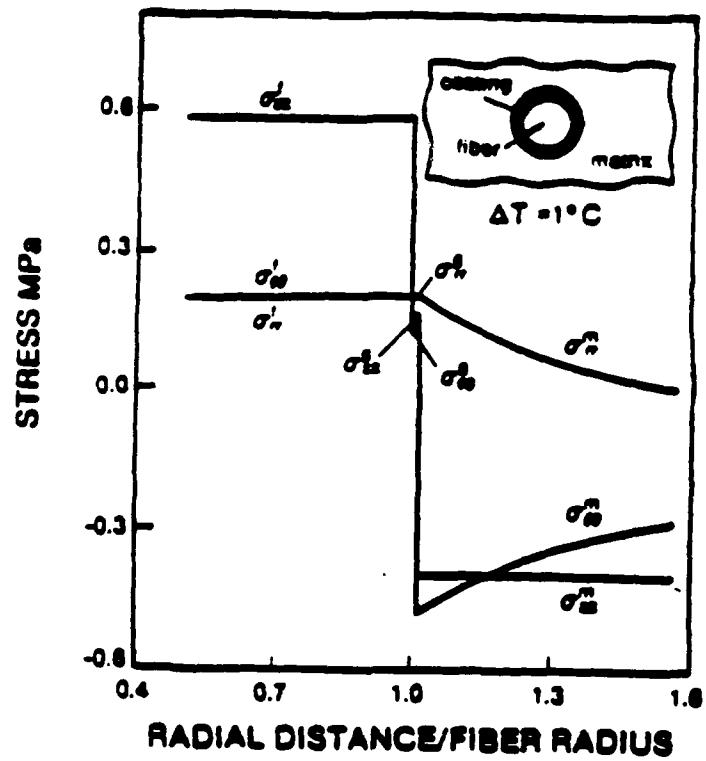

Fig. 3 Stress distribution for uniform temperature change of +1° C in the SiC fiber, carbon coating and Ti_3Al matrix system

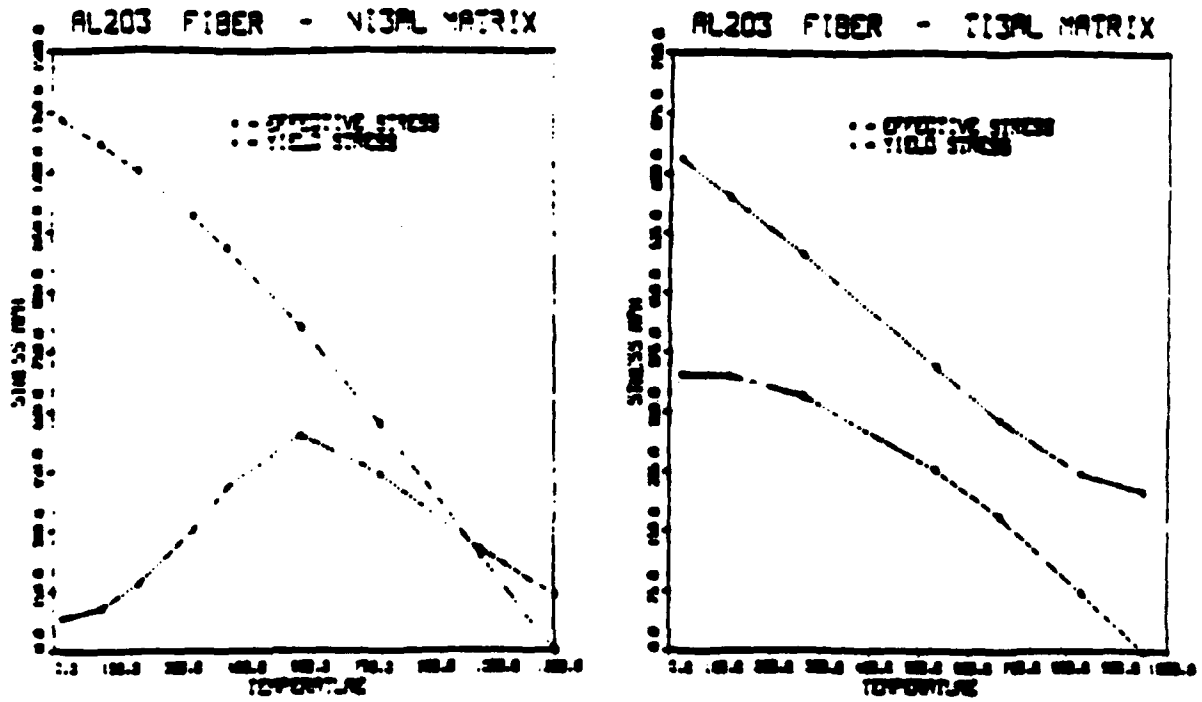

Fig. 4 . 5 Effective stress at the matrix-coating interface during cooling

The effective thermal conductivity of composites reinforced by coated cylindrically orthotropic fibers

Y. Benveniste, T. Chen, and G. J. Dvorak
Department of Solid Mechanics, Material and Structures, Faculty of Engineering, Tel-Aviv University, Ramat Aviv, 69978, Israel, and Department of Civil Engineering, Rensselaer Polytechnic Institute, Troy, New York 12180-3590

(Received 24 August 1989; accepted for publication 17 November 1989)

The present paper is concerned with coated-fiber composites in which the fibers possess cylindrical orthotropy and may have an arbitrary orientation distribution. A micromechanics model is developed which predicts the effective thermal conductivity and estimates the local fields of such composites which may be subjected to uniform heat fluxes on its boundary. The micromechanics model is based on the Mori–Tanaka mean-field concept [T. Mori and K. Tanaka, Acta Metall. **21**, 571 (1973)] and provides explicit expressions for the effective conductivity of the considered composite aggregate which is highly complicated. The analysis shows that special care is needed in formulating an effective theory of composites with constituents possessing curvilinear anisotropy.

I. INTRODUCTION

The subject of the effective thermal conductivity of composites is one of the classical problems in heterogeneous media which has recently drawn renewed interest due to the increasing importance of high-temperature systems. For an extensive list of references in the subject, the reader is referred to the works of Hatta and Taya,[1,2] Miloh and Benveniste,[3] and Benveniste and Miloh.[4]

Highly complicated systems of coated-fiber composites in which the fiber may have cylindrical orthotropy are now in use, and there is a need for rational micromechanics models which predict the effective thermal conductivity and also provide information on the local fields. Systems of such coated fibers which are aligned have recently been analyzed by the authors in the context of the mechanical properties.[5]

The fiber arrangement in a composite aggregate can, however, have a certain orientation distribution which may be due to processing. The present paper presents a micromechanics model of a composite containing coated fibers which are nonaligned and possess cylindrical orthotropy. The first section of the paper presents a general framework for the determination of the effective thermal conductivity of such composites. It is specially seen that particular care is needed in dealing with constituents which possess curvilinear anisotropy and also have an orientation distribution. The second section formulates the employed micromechanics model which is based on the mean-field concept of Mori and Tanaka.[6] The analysis given here is in the spirit of the application of this theory to heat-conduction problems by Benveniste.[7] The treatment in both sections is general and applicable, in principle, to short-fiber composites. The last section illustrates the method for the case of cylindrical coated fibers with a circular cross section. The effective thermal conductivity is given for some chosen examples of fiber distribution, and an example for the local fields is also presented.

II. GENERAL THEORY

A. Curvilinearly anisotropic constituents

Consider a composite reinforced with coated carbon fibers which are transversely isotropic or cylindrically orthotropic and which may be aligned or have a certain orientation distribution. In order to evaluate the effective thermal conductivity and temperature fields in various systems of this kind which may be subjected to certain heat fluxes on their boundaries, we develop in this paper a micromechanical analysis of coated-fiber composites in which the fiber may be at most cylindrically orthotropic and the coating and/or matrix transversely isotropic.

The phase constitutive relations for a cylindrically orthotropic fiber is given by

$$\begin{Bmatrix} q_r \\ q_\phi \\ q_z \end{Bmatrix} = \begin{bmatrix} k_r & 0 & 0 \\ 0 & k_\phi & 0 \\ 0 & 0 & k_z \end{bmatrix} \begin{Bmatrix} H_r \\ H_\phi \\ H_z \end{Bmatrix}, \tag{1}$$

where the vector $\mathbf{q}$ is the heat-flux vector expressed in a cylindrical coordinate system (r,ϕ,z) (see Fig. 1). $\mathbf{H}$ is the intensity, defined as

$$\mathbf{H} = -\nabla\theta = -\begin{Bmatrix} \dfrac{\partial\theta}{\partial r} \\ \dfrac{1}{r}\dfrac{\partial\theta}{\partial\phi} \\ \dfrac{\partial\theta}{\partial z} \end{Bmatrix}, \tag{2}$$

where θ is the temperature, and k_r, k_ϕ, and k_z, are the conductivities in the r, ϕ, and z directions, respectively. It is seen that three constants of conductivity describe this kind of cylindrical orthotropy which is characterized by the fact that properties in tangential, radial, and axial directions are different from each other; in other words, the material is

 0021-8979/90/062878-07$03.00

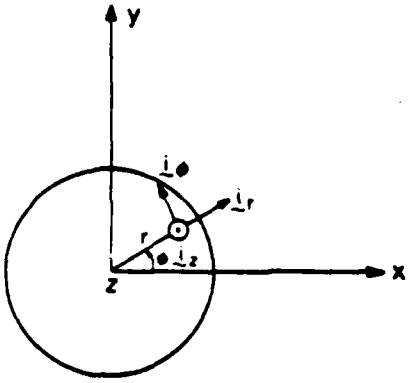

FIG. 1. A cylindrically orthotropic fiber.

orthotropic in a Cartesian axis located at a generic point within the fiber with the three axes pointing in the axial, tangential, and radial directions, respectively. If $k_r > k_\phi$, the material is radially orthotropic, and if $k_r < k_\phi$, it is called circumferentially orthotropic. In the special case of transverse isotropy, we have $k_r = k_\phi$, and for isotropic solids, of course $k_r = k_\phi = k_z$ prevails.

In general, the determination of the effective conductivity of a system containing phases with curvilinear anisotropy requires special attention since from a fixed Cartesian system point of view such a phase is like an inhomogeneous medium. We now proceed to establish a framework of the determination of the effective conductivity of such systems.

Let the composite be subjected on its outside boundary S to homogeneous temperature or flux boundary conditions, defined as

$$\theta(S) = -\mathbf{H}_0\mathbf{x}, \quad q_n = \mathbf{q}_0\mathbf{n}, \tag{3}$$

where x denotes the components of a fixed Cartesian system in the composite, n is the outside normal to S, and $\mathbf{H}_0$ and $\mathbf{q}_0$ are constant intensity and heat flux vectors. In this paper when two quantities A and B are vectors, AB will denote the dot product A_iB_i; when A is a second-order tensor and B is a vector, then AB will mean $A_{ij}B_j$. As it is known, the boundary conditions (3) are useful in the determination of the effective behavior of the composite. We will now show that under such boundary conditions, and as far as the computation of the effective properties are concerned, it is useful to represent a phase with curvilinear anisotropy by an effective rectilinearly anisotropic phase. To this end, suppose that the heat flux and intensity fields in the composite under $(3)_1$ and $(3)_2$ are known in a current curvilinear system ξ [Fig. 2(a)] and are denoted by primed quantities $\mathbf{q}'(\xi)$ and $\mathbf{H}'(\xi)$.

Similarly, let the conductivity tensor $\mathbb{K}'$ and resistivity tensor $\mathbb{R}' = (\mathbb{K}')^{-1}$ in such a system be defined by

$$\mathbf{q}'_s(\xi) = \mathbb{K}'_s\mathbf{H}'_s(\xi), \quad \mathbf{H}'_s(\xi) = \mathbb{R}'_s\mathbf{q}'_s(\xi), \tag{4}$$

where the subscript s denotes a certain phase.

Since in this paper we will be eventually concerned with cylindrically orthotropic fibers with a certain orientation distribution, it is useful to introduce an additional auxiliary Cartesian coordinate system (η) whose η_3 axis coincides

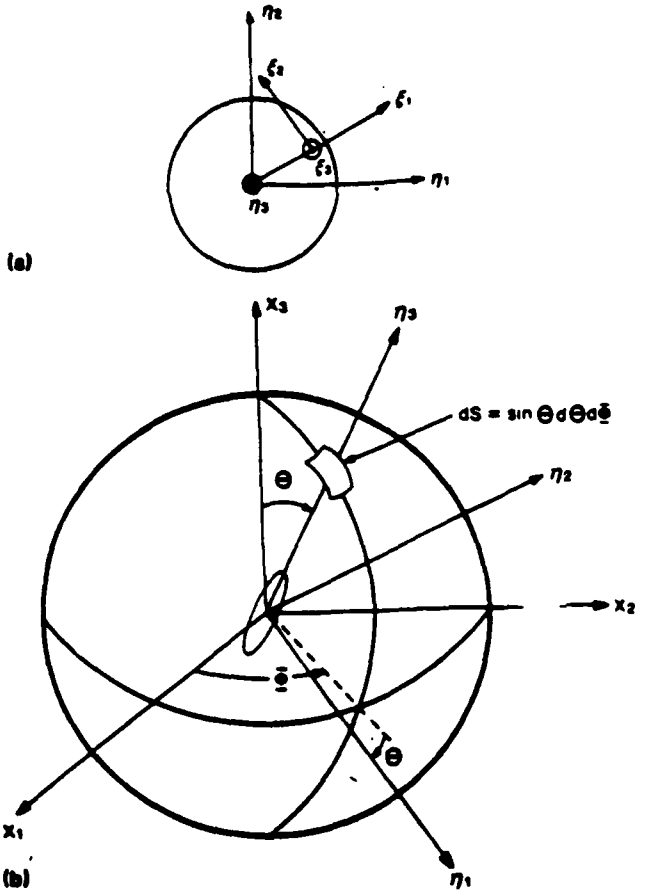

FIG. 2. (a) Local coordinates in a curvilinearly anisotropic system (ξ) and a Cartesian system (η) fixed in a phase. (b) The orientation of a fiber in a fixed Cartesian system (x).

with the axis of symmetry of the fiber (Fig. 2). More generally, this system can be thought of as a local Cartesian system which is fixed in a certain phase. Field quantities in this Cartesian system will be denoted by a tilde and the transformation between the current curvilinear and Cartesian components of the fields denoted by a prime and a tilde, respectively, and are described by

$$\tilde{\mathbf{q}}_s(\xi) = \mathbf{Q}\mathbf{q}'_s(\xi), \quad \tilde{\mathbf{H}}_s(\eta) = \mathbf{Q}\mathbf{H}'_s(\xi), \tag{5}$$

where Q is the orthogonal transformation matrix between the η and ξ systems and defined as

$$\eta = \mathbf{Q}\xi. \tag{6}$$

Note that Q is usually a function of ξ; for example, if the transformation is between the cylindrical and Cartesian system, Q is a function of the angle ϕ.

The constitutive laws in the ξ system can be now described by

$$\mathbf{q}'_s = \mathbb{K}'_s\mathbf{H}'_s, \quad \text{or} \quad \mathbf{H}'_s = \mathbb{R}'_s\mathbf{q}'_s, \tag{7}$$

with $\mathbb{R}'_s = (\mathbb{K}'_s)^{-1}$. Equations (5) and (7) yield

$$\tilde{\mathbf{q}}_s = \mathbf{Q}\mathbb{K}'_s\mathbf{Q}^{-1}\tilde{\mathbf{H}}_s, \quad \tilde{\mathbf{H}}_s = \mathbf{Q}\mathbb{R}'\mathbf{Q}^{-1}\tilde{\mathbf{q}}_s, \tag{8}$$

at any point η in phase s. As mentioned above Q is usually a function of ξ (or η). For the sake of simplicity in notation, however, these quantities will be denoted without the argu-

ment η in the sequel.

Averaging (8) over the volume of the phases yields

$$\tilde{\mathbf{q}}_r = \frac{1}{V_r}\int_{V_r} \mathbf{Q}\mathbf{K}_r'\mathbf{Q}^{-1}\tilde{\mathbf{H}}_r(\eta)dV_r,$$
$$\tilde{\mathbf{H}}_r = \frac{1}{V_r}\int_{V_r} \mathbf{Q}\mathbf{R}_r'\mathbf{Q}^{-1}\tilde{\mathbf{q}}_r(\eta)dV_r. \tag{9}$$

Let now the local flux and intensity fields in the composite aggregate be related to the applied uniform fields through certain influence functions $\tilde{\mathbf{A}}_r(\eta)$, $\tilde{\mathbf{B}}_r(\eta)$, given by

$$\tilde{\mathbf{H}}_r(\eta) = \tilde{\mathbf{A}}_r(\eta)\tilde{\mathbf{H}}_0, \quad \tilde{\mathbf{q}}_r(\eta) = \tilde{\mathbf{B}}_r(\eta)\tilde{\mathbf{q}}_0, \tag{10}$$

under $(3)_1$ and $(3)_2$, respectively, where the overall intensity and flux vectors have also been referred to the η frame relative to phase r. Similar relations can be written for average quantities

$$\tilde{\mathbf{H}}_r = \tilde{\mathbf{A}}_r\tilde{\mathbf{H}}_0, \quad \tilde{\mathbf{q}}_r = \tilde{\mathbf{B}}_r\tilde{\mathbf{q}}_0. \tag{11}$$

In this paper we will denote local fields with an argument and quantities without an argument will refer to averages. The tensors $\tilde{\mathbf{A}}_r$ and $\tilde{\mathbf{B}}_r$ in (11) are called concentration factors.

Next let us write the average flux and intensity under $(3)_1$ and $(3)_2$, respectively:

$$\tilde{\mathbf{q}}_r = \left(\frac{1}{V_r}\int_{V_r} \mathbf{Q}\mathbf{K}_r'\mathbf{Q}^{-1}\tilde{\mathbf{A}}_r(\eta)dV_r\right)\tilde{\mathbf{H}}_0, \tag{12}$$

$$\tilde{\mathbf{H}}_r = \left(\frac{1}{V_r}\int_{V_r} \mathbf{Q}\mathbf{R}_r'\mathbf{Q}^{-1}\tilde{\mathbf{B}}_r(\eta)dV_r\right)\tilde{\mathbf{q}}_0. \tag{13}$$

Solving for $\tilde{\mathbf{H}}_0$ and $\tilde{\mathbf{q}}_0$ in (11), and substituting in (12) and (13), respectively, yields

$$\tilde{\mathbf{q}}_r = \tilde{\mathbf{K}}_r\tilde{\mathbf{H}}_r, \quad \tilde{\mathbf{H}}_r = \tilde{\mathbf{R}}_r\tilde{\mathbf{q}}_r, \tag{14}$$

where the effective properties $\tilde{\mathbf{K}}_r$ and $\tilde{\mathbf{R}}_r$ have been defined as

$$\tilde{\mathbf{K}}_r = \left(\frac{1}{V_r}\int_{V_r} \mathbf{Q}\mathbf{K}_r'\mathbf{Q}^{-1}\tilde{\mathbf{A}}_r(\eta)dV_r\right)\tilde{\mathbf{A}}_r^{-1}, \tag{15}$$

$$\tilde{\mathbf{R}}_r = \left(\frac{1}{V_r}\int_{V_r} \mathbf{Q}\mathbf{R}_r'\mathbf{Q}^{-1}\tilde{\mathbf{B}}_r(\eta)dV_r\right)\tilde{\mathbf{B}}_r^{-1}. \tag{16}$$

Note that in view of their definition in (15) and (16), $\tilde{\mathbf{K}}_r$ and $\tilde{\mathbf{R}}_r$ are second-order tensors. Very much like the overall effective behavior of the composite aggregate, those effective tensors depend on the nature of the influence functions $\tilde{\mathbf{A}}_r(\eta)$ and $\tilde{\mathbf{B}}_r(\eta)$. Since these functions are approximated differently in different micromechanics models, $\tilde{\mathbf{K}}_r$ and $\tilde{\mathbf{R}}_r$ may vary from model to model. Furthermore, to qualify as effective properties, the reciprocity relation $\tilde{\mathbf{K}}_r = \tilde{\mathbf{R}}_r^{-1}$ needs to be proved in the context of the used theory. Such a reciprocity relation is also usually necessary to prove that the overall conductivity tensor and resistivity tensor as predicted by the model are the inverse of each other.

With the quantities $\tilde{\mathbf{K}}_r$ and $\tilde{\mathbf{R}}_r$ defined in (15) and (16), a proper framework can be now formulated for the computation of the effective conductivity and resistivity tensors.

B. Coated fibers with curvilinearly anisotropic fiber and given orientation and distribution

Let us first start with a proper definition of average quantities in a composite in which the fibers may assume some given orientation distribution. Recall that a Cartesian frame $\mathbf{x}$ and an auxiliary one η, whose η_3 axis coincides with the fiber axis, have already previously been defined. The transformation between the $\mathbf{x}$ and η systems is described as

$$\mathbf{x} = \mathbf{D}\eta, \tag{17}$$

with $\mathbf{D}$ being given by [see Fig. 2(b)]:

$$\mathbf{D} = \begin{pmatrix} \cos\Theta\cos\Phi & -\sin\Phi & \sin\Theta\cos\Phi \\ \cos\Theta\sin\Phi & \cos\Phi & \sin\Theta\sin\Phi \\ -\sin\Theta & 0 & \cos\Theta \end{pmatrix}. \tag{18}$$

The framework presented in this section is valid for short spheroidal coated fibers with an axis of symmetry. Implementation of the method in the last section will be given for the case of long cylindrical fibers with circular cross sections.

Consider now a quantity $\psi_r(\Theta, \Phi)$, be it scalar, vector, or tensor, which has already been averaged over the fiber core or coating of a single fiber, and which depends on the specific orientation (Θ, Φ) of that fiber. The average of this quantity over all possible fiber orientations will be now sought. To this end, define an orientation distribution by the function of $\rho(\Theta, \Phi)$ which represents the number of fibers intersecting a unit area of the unit sphere in Fig. 2(b). The average of the quantity $\psi_r(\Theta, \Phi)$ over all possible fiber orientations is therefore given by

$$\langle\psi_r(\Theta,\Phi)\rangle = \frac{\int_0^{\pi/2}\int_0^{2\pi}\psi_r(\Theta,\Phi)\rho(\Theta,\Phi)\sin\Theta\, d\Theta\, d\Phi}{\int_0^{\pi/2}\int_0^{2\pi}\rho(\Theta,\Phi)\sin\Theta\, d\Theta\, d\Phi}. \tag{19}$$

Consider next the boundary condition $(3)_1$, under which the average intensity $\mathbf{H}$ is given by

$$\mathbf{H} = \mathbf{H}_0, \tag{20}$$

with

$$\mathbf{H} = c_m\mathbf{H}_m + \sum_{r=f,g} c_r\langle\mathbf{H}_r(\Theta,\Phi)\rangle, \tag{21}$$

where all the intensity fields are referred now to the fixed coordinate system. In (21), $\mathbf{H}$ denotes the overall intensity, $\mathbf{H}_m$ is the average intensity in the matrix, and $\mathbf{H}_r(\Theta,\Phi)$ are the average intensities in the fiber and coating of a coated fiber which has an orientation (Θ,Φ). Using the proper transformation between the $\mathbf{H}_r$ and $\tilde{\mathbf{H}}$ vectors, and invoking $(11)_1$ and (20) in (21) provides

$$c_m\mathbf{H}_m = \left(\mathbf{I} - \sum_{r=f,g} c_r\langle\mathbf{D}\tilde{\mathbf{A}}_r\mathbf{D}^{-1}\rangle\right)\mathbf{H}_0. \tag{22}$$

Next define an overall conductivity tensor $\mathbf{K}$ referred to the fixed coordinate system $\mathbf{x}$:

$$\mathbf{q} = \mathbf{K}\mathbf{H} = \mathbf{K}\mathbf{H}_0. \tag{23}$$

Writing (23) in the form

$$\mathbf{K}\mathbf{H}_0 = c_m\mathbf{K}_m\mathbf{H}_m + \sum_{r=f,g} c_r\langle\mathbf{q}_r\rangle, \tag{24}$$

and using proper transformation between coordinate systems together with $(14)_1$ and (22) provides, after some manipulations,

$$\mathbf{K} = \mathbf{K}_m + \sum_{s=f,g} c_s \langle (\mathbf{D}\tilde{\mathbf{K}}_s \mathbf{D}^{-1})(\mathbf{D}\tilde{\mathbf{A}}_s \mathbf{D}^{-1}) \rangle - \mathbf{K}_m \sum_{s=f,g} c_s \langle \mathbf{D}\tilde{\mathbf{A}}_s \mathbf{D}^{-1} \rangle, \tag{25}$$

where in the above development the matrix is assumed to be homogeneous and rectilinearly anisotropic.

Under boundary conditions $(3)_2$, using

$$\mathbf{q} = c_m \mathbf{q}_m + \sum_{s=f,g} c_s \langle \mathbf{q}_s(\Theta,\Phi) \rangle = \mathbf{q}_0, \tag{26}$$

and $(11)_2$ and $(14)_2$, yields the following equation for the effective resistivity tensor $\mathbf{R}$:

$$\mathbf{R} = \mathbf{R}_m + \sum_{s=f,g} c_s \langle (\mathbf{D}\tilde{\mathbf{R}}_s \mathbf{D}^{-1})(\mathbf{D}\tilde{\mathbf{B}}_s \mathbf{D}^{-1}) \rangle - \mathbf{R}_m \sum_{s=f,g} c_s \langle \mathbf{D}\tilde{\mathbf{B}}_s \mathbf{D}^{-1} \rangle, \tag{27}$$

which is counterpart to (25).

III. THE MICROMECHANICS MODEL

We employ here the Mori–Tanaka mean-field theory to determine the effective thermal conductivity of the above-described composite systems. The essential assumption of this theory consists in estimating the concentration factors in (11) by those obtained in an auxiliary configuration of one fiber in an infinite matrix subjected at infinity to

$$\theta(S) = \mathbf{H}_m \mathbf{x}, \quad \text{or} \quad q_n(S) = \mathbf{q}_m \mathbf{n}, \tag{28}$$

where $\mathbf{H}_m$ and $\mathbf{q}_m$ are the average intensity and the flux vectors in the matrix to be determined.

Consider first the boundary conditions $(3)_1$ and let the intensity in the fiber core and surrounding coating of a single coated fiber embedded in an infinite matrix subjected to $(28)_1$ be given by

$$\tilde{\mathbf{H}}_s(\eta) = \tilde{\mathbf{T}}_s(\eta)\tilde{\mathbf{H}}_m = \tilde{\mathbf{T}}_s(\eta)\mathbf{D}^{-1}\mathbf{H}_m. \tag{29}$$

Use of (29) and (21) provides

$$\mathbf{H}_m = \left(c_m \mathbf{I} + \sum_{s=f,g} c_s \langle \mathbf{D}\tilde{\mathbf{T}}_s \mathbf{D}^{-1} \rangle \right)^{-1} \mathbf{H}_0. \tag{30}$$

Substitution of (30) back in (29) and recalling the definition of $\tilde{\mathbf{A}}_s$ in (11) gives

$$\tilde{\mathbf{A}}_s(\eta) = \tilde{\mathbf{T}}_s(\eta)\mathbf{D}^{-1}\left(c_m \mathbf{I} + \sum_{s=f,g} \langle \mathbf{D}\tilde{\mathbf{T}}_s \mathbf{D}^{-1} \rangle \right)^{-1} \mathbf{D}. \tag{31}$$

Finally, employing (31) in (25) provides the following expression for $\mathbf{K}$:

$$\mathbf{K} = \mathbf{K}_m + \left(\sum_{s=f,g} c_s \langle (\mathbf{D}\tilde{\mathbf{K}}_s \mathbf{D}^{-1})(\mathbf{D}\tilde{\mathbf{T}}_s \mathbf{D}^{-1}) \rangle - \mathbf{K}_m \sum_{s=f,g} c_s \langle \mathbf{D}\tilde{\mathbf{T}}_s \mathbf{D}^{-1} \rangle \right) \times \left(c_m \mathbf{I} + \sum_{s=f,g} c_s \langle \mathbf{D}\tilde{\mathbf{T}}_s \mathbf{D}^{-1} \rangle \right)^{-1}. \tag{32}$$

Similarly, under boundary conditions $(3)_2$, defining the $\tilde{\mathbf{W}}_s$ tensor, counterpart to $\tilde{\mathbf{T}}_s$ in (29), as

$$\tilde{\mathbf{q}}_s(\eta) = \tilde{\mathbf{W}}_s(\eta)\tilde{\mathbf{q}}_m, \tag{33}$$

yields equations for $\tilde{\mathbf{q}}_m$ and $\tilde{\mathbf{B}}_m$ and the resistivity tensor $\mathbf{R}$ counterpart to (30), (31), and (32):

$$\mathbf{q}_m = {}_m\mathbf{I} + \sum_{s=f,g} c_s \langle \mathbf{D}\tilde{\mathbf{W}}_s \mathbf{D}^{-1} \rangle \Big)^{-1} \mathbf{q}_0, \tag{34}$$

$$\tilde{\mathbf{B}}_s(\eta) = \tilde{\mathbf{W}}_s(\eta)\mathbf{D}^{-1}\left(c_m \mathbf{I} + \sum_{s=f,g} \langle \mathbf{D}\tilde{\mathbf{W}}_s \mathbf{D}^{-1} \rangle \right)^{-1} \mathbf{D}^{-1}, \tag{35}$$

$$\mathbf{R} = \mathbf{R}_m + \left(\sum_{s=f,g} c_s \langle (\mathbf{D}\tilde{\mathbf{R}}_s \mathbf{D}^{-1})(\mathbf{D}\tilde{\mathbf{W}}_s \mathbf{D}^{-1}) \rangle - \mathbf{R}_m \sum_{s=f,g} c_s \langle \mathbf{D}\tilde{\mathbf{W}}_s \mathbf{D}^{-1} \rangle \right) \times \left(c_m \mathbf{I} + \sum_{s=f,g} c_s \langle \mathbf{D}\tilde{\mathbf{W}}_s \mathbf{D}^{-1} \rangle \right)^{-1}. \tag{36}$$

Two consistency properties need now to be proved: first, that the effective phase properties as predicted by the model in conjunction with (15), (16), (31), and (35) satisfy

$$\tilde{\mathbf{K}}_s = \tilde{\mathbf{R}}_s^{-1}, \tag{37}$$

and second, that the predicted effective properties (32) and (36) satisfy a similar relation:

$$\mathbf{K} = \mathbf{R}^{-1}. \tag{38}$$

Let us first prove (37). Substitution of (31) into (15) and (35) into (16) yields

$$\tilde{\mathbf{K}}_s = \left(\frac{1}{V_s} \int_{V_s} \mathbf{Q}\mathbf{K}_s' \mathbf{Q}^{-1} \tilde{\mathbf{T}}_s(\eta) dV_s \right) \tilde{\mathbf{T}}_s^{-1}, \tag{39}$$

$$\tilde{\mathbf{R}}_s = \left(\frac{1}{V_s} \int_{V_s} \mathbf{Q}\mathbf{R}_s' \mathbf{Q}^{-1} \tilde{\mathbf{W}}_s(\eta) dV_s \right) \tilde{\mathbf{W}}_s^{-1}, \tag{40}$$

Consider now (29) and transform it consecutively to the following equivalent forms:

$$\tilde{\mathbf{H}}_s(\eta) = \tilde{\mathbf{T}}_s(\eta)\tilde{\mathbf{H}}_m, \quad \mathbf{Q}\mathbf{H}_s' = \tilde{\mathbf{T}}_s(\eta)\tilde{\mathbf{R}}_m \tilde{\mathbf{q}}_m,$$
$$\mathbf{Q}\mathbf{R}_s'\mathbf{q}_s' = \tilde{\mathbf{T}}_s(\eta)\tilde{\mathbf{R}}_m \tilde{\mathbf{q}}_m, \quad \mathbf{Q}\mathbf{R}_s'\mathbf{Q}^{-1}\tilde{\mathbf{q}}_s = \tilde{\mathbf{T}}_s(\eta)\tilde{\mathbf{R}}_m \tilde{\mathbf{q}}_m,$$
$$\tilde{\mathbf{q}}_s = \mathbf{Q}\mathbf{K}_s'\mathbf{Q}^{-1}\tilde{\mathbf{T}}_s(\eta)\tilde{\mathbf{R}}_m \tilde{\mathbf{q}}_m, \tag{41}$$

which, when compared with (33), implies that

$$\tilde{\mathbf{W}}_s(\eta) = \mathbf{Q}\mathbf{K}_s'\mathbf{Q}^{-1}\tilde{\mathbf{T}}_s(\eta)\tilde{\mathbf{R}}_m. \tag{42}$$

Substitution of (42) into (40) provides, after some manipulation,

$$\tilde{\mathbf{R}}_s = \tilde{\mathbf{T}}_s \left(\frac{1}{V_s} \int_{V_s} \mathbf{Q}\mathbf{K}_s' \mathbf{Q}^{-1} \tilde{\mathbf{T}}_s(\eta) dV_s \right)^{-1}, \tag{43}$$

whose comparison with (39) shows that (37) is fulfilled.

Let us now prove that $\mathbf{K}$ and $\mathbf{R}$ as given by (32) and (36) fulfill (38). To this end, write first (36) as

$$\mathbf{R}\left(c_m \mathbf{I} + \sum_{s=f,g} c_s \langle \mathbf{D}\tilde{\mathbf{W}}_s \mathbf{D}^{-1} \rangle \right) = \left(\mathbf{R}_m c_m + \sum_{s=f,g} \mathbf{R}_m c_s \langle \mathbf{D}\tilde{\mathbf{W}}_s \mathbf{D}^{-1} \rangle \right) + \left(\sum_{s=f,g} c_s \langle (\mathbf{D}\tilde{\mathbf{R}}_s \mathbf{D}^{-1})(\mathbf{D}\tilde{\mathbf{W}}_s \mathbf{D}^{-1}) \rangle - \mathbf{R}_m \sum_{s=f,g} c_s \langle \mathbf{D}\tilde{\mathbf{W}}_s \mathbf{D}^{-1} \rangle \right), \tag{44}$$

Next note that integrating (42) over V_s and comparing with (39) provides

$$\tilde{\mathbf{W}}_s = \tilde{\mathbf{K}}_s \tilde{\mathbf{T}}_s \tilde{\mathbf{R}}_m. \tag{45}$$

Substitute now (45) in (44), and obtain, after some manipulations,

$$\mathbf{R}\left(c_m \mathbf{K}_m + \sum_{s=f,g} c_s \langle (\mathbf{D}\tilde{\mathbf{K}}_s \mathbf{D}^{-1})(\mathbf{D}\tilde{\mathbf{T}}_s \mathbf{D}^{-1}) \rangle\right) = \left(c_m \mathbf{I} + \sum_{s=f,g} c_s \langle \mathbf{D}\tilde{\mathbf{T}}_s \mathbf{D}^{-1} \rangle\right), \tag{46}$$

where we have used the fact that $\langle \mathbf{D}\tilde{\mathbf{K}}_s \tilde{\mathbf{T}}_s \mathbf{D}^{-1} \tilde{\mathbf{R}}_m \mathbf{D}^{-1} \rangle = \langle \mathbf{D}\tilde{\mathbf{K}}_s \tilde{\mathbf{T}}_s \mathbf{D}^{-1} \rangle \mathbf{R}_m$. Noting finally that (32) can be written as

$$\mathbf{K}\left(c_m \mathbf{I} + \sum_{s=f,g} c_s \langle \mathbf{D}\tilde{\mathbf{T}}_s \mathbf{D}^{-1} \rangle\right) = \left(c_m \mathbf{K}_m + \sum_{s=f,g} c_s \langle (\mathbf{D}\tilde{\mathbf{K}}_s \mathbf{D}^{-1})(\mathbf{D}\tilde{\mathbf{T}}_s \mathbf{D}^{-1}) \rangle\right), \tag{47}$$

and comparing (46) and (47) shows that (38) is fulfilled.

The local fields in a coated fiber and the immediate surrounding matrix can be obtained in the framework of the present model, by solving the auxiliary problem of a single coated fiber taken at an orientation (Θ,Φ) and embedded in an infinite matrix, and subjecting it at infinity to boundary conditions $(28)_1$. The implementation of the theory presented herein for the case of cylindrical coated fibers with circular cross section will be presented in the next section.

IV. APPLICATION: COMPOSITES WITH COATED FIBERS OF CYLINDRICAL SHAPE WITH A CIRCULAR CROSS SECTION

Let us now consider long coated fibers in which the fiber core is cylindrically orthotropic, the coating is transversely isotropic, and the matrix is isotropic. The conductivities of the phases are, respectively, denoted by $k_r^{(f)}$, $k_\phi^{(f)}$, $k_z^{(f)}$; $k^{(g)}$; $(k_z)^g$; $k^{(m)}$. We will be concerned in this section with boundary conditions of type $(3)_1$ only and chose to implement Eq. (32). The temperature field θ in the coated fiber and surrounding matrix can be obtained by solving the problem of a single coated fiber in an infinite matrix and subjecting it to $(28)_1$, with $\mathbf{H}_m$ given in (30).

The solution of the auxiliary problem leading to the tensor $\tilde{\mathbf{T}}_s$ is given in the Appendix. It turns out that

$$\tilde{\mathbf{T}}_f = \begin{pmatrix} d^{(f)}a^{\lambda-1} & 0 & 0 \\ 0 & d^{(f)}a^{\lambda-1} & 0 \\ 0 & 0 & 1 \end{pmatrix}, \qquad \tilde{\mathbf{T}}_g = \begin{pmatrix} d^{(g)} & 0 & 0 \\ 0 & d^{(g)} & 0 \\ 0 & 0 & 1 \end{pmatrix}, \tag{48}$$

where λ is given by $\lambda = (k_\phi^{(f)}/k_r^{(f)})^{1/2}$, and $d^{(f)}$ with $d^{(g)}$ are constants defined as

$$d^{(f)} = \frac{4k^{(m)}k^{(g)}a^{1-\lambda}}{(k^{(m)}+k^{(g)})(\lambda k_r^{(f)}+k^{(g)}) - (a^2/b^2)(k^{(m)}-k^{(g)})(\lambda k_r^{(f)}-k^{(g)})}, \tag{49}$$

$$d^{(g)} = \frac{2k^{(m)}(\lambda k_r^{(f)}+k^{(g)})}{(k^{(m)}+k^{(g)})(\lambda k_r^{(f)}+k^{(g)}) - (a^2/b^2)(k^{(m)}-k^{(g)})(\lambda k_r^{(f)}-k^{(g)})}, \tag{50}$$

and a and b denote the inner and outer radii of the coating.

The effective conductivity $\tilde{\mathbf{K}}_s$ of the cylindrically orthotropic fiber is obtained from (15) with $\tilde{\mathbf{A}}_f$ being defined in (31), resulting in

$$\tilde{\mathbf{K}}_f = \left(\frac{1}{V_s}\int_{V_s} \mathbf{Q}\mathbf{K}_s'\mathbf{Q}^{-1}\tilde{\mathbf{T}}_f(\eta)dV_s\right)\tilde{\mathbf{T}}_f^{-1}, \tag{51}$$

where an expression for the $\tilde{\mathbf{T}}(\eta)$ tensor depending on the position within the fiber is again to be found in the Appendix. After performing the integration in (51), $\tilde{\mathbf{K}}_f$ results as a diagonal matrix with

$$(\tilde{\mathbf{K}}_f)_{11} = (\tilde{\mathbf{K}}_f)_{22} = \frac{k_r^{(f)}\lambda + k_\phi^{(f)}}{1+\lambda}, \quad (\tilde{\mathbf{K}}_f)_{33} = k_z, \tag{52}$$

so that Eq. (32) can readily be implemented.

In the case of completely random distribution, the explicit form of (32) is given as

$$K_{11} = K_{22} = K_{33} = k^{(m)} + c_f\left[\tfrac{1}{3}(k^{(f)}-k^{(m)})d^{(f)}a^{\lambda-1} + \tfrac{1}{3}(k_z^{(f)}-k^{(m)})\right]A + c_g\left[\tfrac{1}{3}(k^{(g)}-k^{(m)})d^{(g)} + \tfrac{1}{3}(k_z^{(g)}-k^{(m)})\right]A, \tag{53}$$

where

$$A = \left[c_m + c_f(\tfrac{1}{3}d^{(f)}a^{\lambda-1}+\tfrac{1}{3}) + c_g(\tfrac{1}{3}d^{(g)}+\tfrac{1}{3})\right]^{-1}, \tag{54}$$

$$k^{(f)} = \frac{k_r^{(f)}\lambda + k_\phi^{(f)}}{1+\lambda}. \tag{55}$$

For cosine-type distribution, $\rho = \rho_0 \cos\Theta$, the effective conductivities in transverse and axial direction have the form

$$K_{11} = K_{22} = k^{(m)} + c_f\left[\tfrac{1}{2}(k^{(f)}-k^{m})d^{(f)}a^{\lambda-1} + \tfrac{1}{4}(k_z^{(f)}-k^{(m)})\right]B + c_g\left[\tfrac{1}{2}(k^{(g)}-k^{(m)})d^{(g)} + \tfrac{1}{4}(k_z^{(g)}-k^{(m)})\right]B, \tag{56}$$

$$K_{33} = k^{(m)} + c_f\left[\tfrac{1}{2}(k^{(f)}-k^{(m)})d^{(f)}a^{\lambda-1} + \tfrac{1}{2}(k_z^{(f)}-k^{(m)})\right]C + c_g\left[\tfrac{1}{2}(k^{(g)}-k^{(m)})d^{(g)} + \tfrac{1}{2}(k_z^{(g)}-k^{(m)})\right]C, \tag{57}$$

where

$$B = \left[c_m + c_f(\tfrac{1}{2}d^{(f)}a^{\lambda-1}+\tfrac{1}{2}) + c_g(\tfrac{1}{2}d^{(g)}+\tfrac{1}{2})\right]^{-1}, \tag{58}$$

$$C = \left[c_m + c_f\left(\tfrac{1}{2}d^{(f)}a^{\lambda-1} + \tfrac{1}{2}\right) + c_g\left(\tfrac{1}{2}d^{(g)} + \tfrac{1}{2}\right)\right]^{-1}. \quad (59)$$

For binary systems with uncoated cylindrical fibers with circular cross section and isotropic constituents, Eqs. (53), (56), and (57) reduce to Eqs. (25), (30), (31), (35), and (36) of Hatta and Taya.[1]

Just as an illustration, numerical results are given for the following chosen parameters: $k_r^{(f)}/k^{(m)} = 10$, $k_\phi^{(f)}/k^{(m)} = 20$, $k_z^{(f)}/k^{(m)} = 20$, $k_r^{(g)}/k^{(m)} = k_\phi^{(g)}/k^{(m)} = 10$, $k_z^{(g)}/k^{(m)} = 15$, and $b/a = 1.1$. Figure 3 illustrates the effective thermal conductivities of completely random and cosine-type distribution of fibers in which $\rho(\Theta,\Psi) = \rho_0 \cos\Theta$ in Eq. (19). In Fig. 4 we consider the case of unidirectionally reinforced composite with an applied intensity transverse to the fiber; the figure illustrates the thermal intensity distribution in the fiber, coating, and matrix along the angles $\phi = 0°$ and 90°.

ACKNOWLEDGMENT

Support from the DARPA-HiTASC program at Rensselaer is gratefully acknowledged.

APPENDIX

We derive in this Appendix the temperature flux and intensity fields in a coated cylindrical fiber with a circular cross section which is embedded in an infinite matrix and subjected at infinity to a constant intensity [see Fig. A1(a)]. The core of the fiber is cylindrically orthotropic and described by Eq. (1), the coating is transversely isotropic, and the matrix is isotropic.

In accordance to the notation used in the paper, a Cartesian system η is centered at the fiber with the η_3 axis coinciding with its axis of symmetry, and the intensity field at infin-

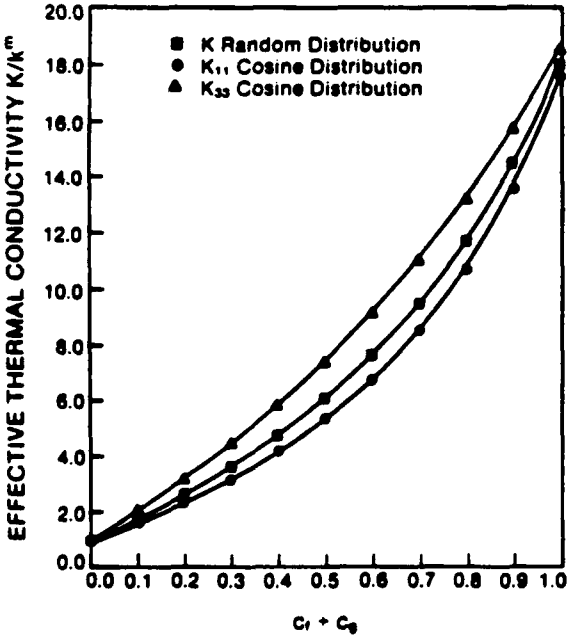

FIG. 3. A composite with fibers which are randomly oriented. The nondimensionalized effective thermal conductivity K/k_m vs the volume fraction of the coated fiber $c_f + c_g$.

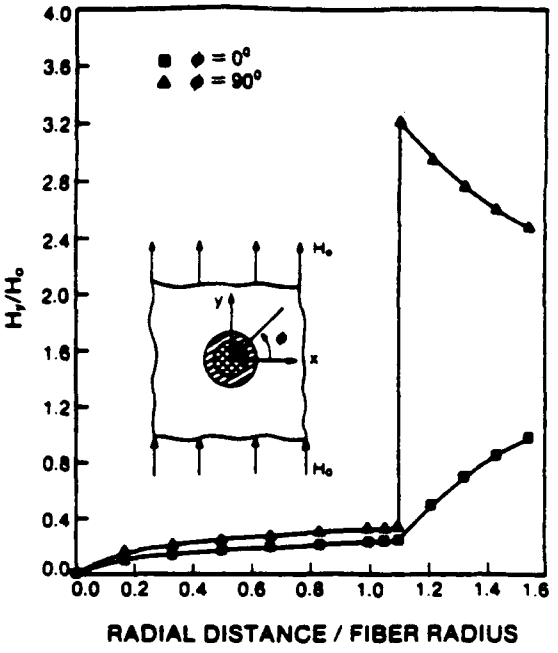

FIG. 4. Uniaxially reinforced composite. The nondimensionalized thermal intensity field H_r/H_0 vs the ratio of the radial distance to the fiber radius, given at locations $\phi = 0°$ and 90°.

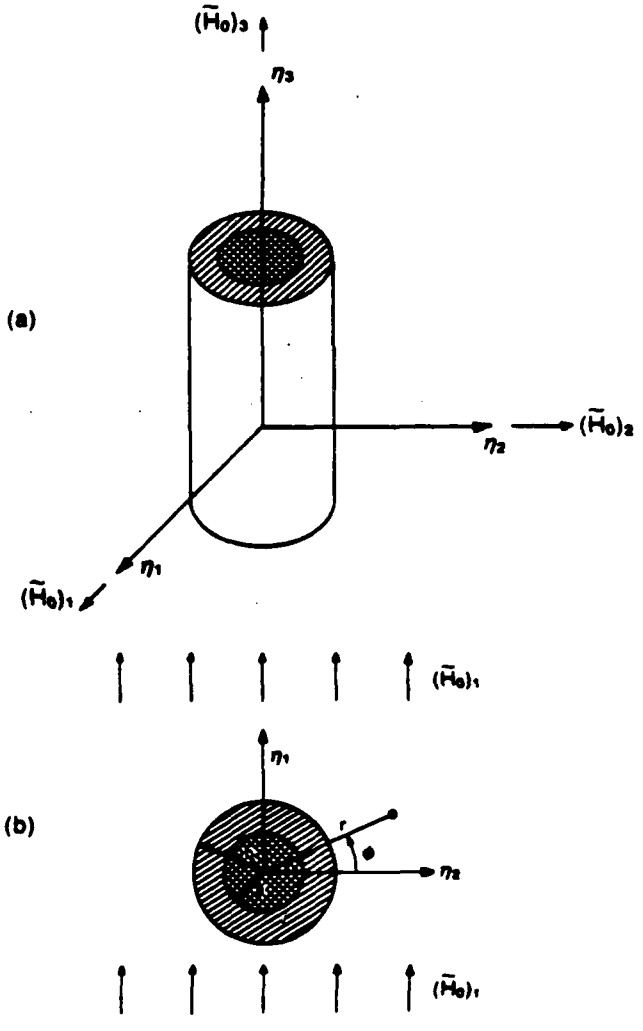

FIG. A1. The auxiliary problem of a single coated fiber in infinite matrix.

ity is described by $(\mathbf{H}_0)$. Due to the axisymmetric nature of the described boundary-value problem, it is sufficient to consider only an external intensity in the form $[(\tilde{H}_0)_1, 0, (\tilde{H}_0)_3]$. The solution due to $(\tilde{H}_0)_3$ is trivial and consists in

$$\mathbf{H}^{(s)} = [0,0,(\tilde{H}_0)_3], \quad \mathbf{q}^{(s)} = [0,0,k_z^{(s)}(\tilde{H}_0)_3], \quad \text{(A1)}$$

so that we will solve here the problem due to a transverse intensity $(\tilde{H}_0)_1$ [see Fig. A1(b)].

The described problem is therefore two dimensional with the heat flux in each phase being given by

$$\begin{Bmatrix} \tilde{q}_r \\ \tilde{q}_\phi \end{Bmatrix}^{(s)} = \begin{bmatrix} k_r^{(s)} & 0 \\ 0 & k_\phi^{(s)} \end{bmatrix} \begin{Bmatrix} \tilde{H}_r \\ \tilde{H}_\phi \end{Bmatrix}^{(s)}, \quad \text{(A2)}$$

where $k_r^{(f)} \neq k_\phi^{(f)}$ in this case, $k_r^{(g)} = k_\phi^{(g)} \neq k_z^{(g)}$ in the coating, and $k_r^{(m)} = k_\phi^{(m)} = k_z^{(m)}$ in the matrix. Under steady-state conditions,

$$\nabla \cdot \mathbf{q} = 0 \quad \text{(A3)}$$

prevails. Using the expressions given for $\mathbf{H}$ in (2) and writing (A2) in a cylindrical coordinate system provides

$$k_r^{(s)} \frac{\partial^2 \theta^{(s)}}{\partial r^2} + k_r^{(s)} \left(\frac{1}{r}\right) \frac{\partial \theta^{(s)}}{\partial r} + k_\phi^{(s)} \left(\frac{1}{r^2}\right) \frac{\partial^2 \theta^{(s)}}{\partial \phi^2} = 0. \quad \text{(A4)}$$

Using separation of variables,

$$\theta^{(s)} = F^{(s)}(r) G^{(s)}(\phi), \quad \text{(A5)}$$

yields the following solutions for the temperature field in each phase:

$$\begin{aligned} \theta^{(f)} &= d^{(f)} r^\lambda \sin \phi, \\ \theta^{(g)} &= \left[d^{(g)} r + \frac{e^{(g)}}{r} \right] \sin \phi, \\ \theta^{(m)} &= \left[d^{(m)} r + \frac{e^{(m)}}{r} \right] \sin \phi, \end{aligned} \quad \text{(A6)}$$

where $d^{(s)}$ and $e^{(s)}$ are five constants to be determined from the interface conditions and boundary conditions at infinity. Continuity of the temperature field and radial heat flux at material interfaces demand

$$\begin{aligned} &\theta^{(f)} = \theta^{(g)}, \quad \text{at } r = a, \\ &\theta^{(g)} = \theta^{(m)}, \quad \text{at } r = b, \\ &k_r^{(f)} \frac{\partial \theta^{(f)}}{\partial r} = k^{(g)} \frac{\partial \theta^{(g)}}{\partial r}, \quad \text{at } r = a, \\ &k^{(g)} \frac{\partial \theta^{(g)}}{\partial r} = k^{(m)} \frac{\partial \theta^{(m)}}{\partial r}, \quad \text{at } r = b, \end{aligned} \quad \text{(A7)}$$

where a and b denote the radius of the fiber core and radius of the coating-matrix interface, respectively. The condition at infinity, on the other hand, requires

$$d^{(m)} = -\tilde{H}_0^{(1)}. \quad \text{(A8)}$$

Solution of (A7) and (A8) provides the constants of interest, and the expression for the $\tilde{\mathbf{T}}^{(s)}$ tensor therefore results as given in (48).

[1] H. Hatta and M. Taya, J. Appl. Phys. 58, 2478 (1985).
[2] H. Hatta and M. Taya, J. Appl. Phys. 59, 1851 (1986).
[3] T. Miloh and Y. Benveniste, J. Appl. Phys. 63, 789 (1988).
[4] Y. Benveniste and T. Miloh, J. Appl. Phys. 66, 176 (1989).
[5] T. Chen, G. J. Dvorak, and Y. Benveniste, Mech. Mater. (to be published).
[6] T. Mori and K. Tanaka, Acta Metall. 21, 571 (1973).
[7] Y. Benveniste, J. Appl. Phys. 61, 2840 (1987).

Mechanics of Materials 9 (1990) 17–32
Elsevier

STRESS FIELDS IN COMPOSITES REINFORCED BY COATED CYLINDRICALLY ORTHOTROPIC FIBERS

T. CHEN, G.J. DVORAK and Y. BENVENISTE *

Department of Civil Engineering, Rensselaer Polytechnic Institute, Troy, NY 12180, U.S.A.

Received 25 August 1989; revised version received 15 November 1989

Local fields and effective thermoelastic properties are derived for coated fiber composites with cylindrically orthotropic fibers and transversely isotropic coating and matrix phases. Thermomechanical loading situations are considered in which a uniform stress and a uniform temperature change are applied to the boundary of the composite aggregate. A micromechanical model, based on the Mori and Tanaka's concept of average stress in the matrix, is used to account for phase interaction. It is found that a special treatment is needed in formulation of effective properties of composites reinforced by constituents which are curvilinearly anisotropic. Results are presented for a pitch precursor carbon fiber, carbon coating and titanium aluminate matrix system.

1. Introduction

The present paper is a continuation of our earlier study of stress fields in composites reinforced by coated inclusions (Benveniste et al., 1989), which will be referred to as (I) in the sequel. In that work we evaluated the overall properties of such composites, and examined in detail the local fields in fibrous composites with isotropic phases. A general overall uniform stress state and a uniform temperature change represented the external loads. The results are useful in applications to many actual systems, but not in situations where the phases are anisotropic. A particular example is a composite reinforced by carbon fibers which are transversely isotropic or cylindrically orthotropic, and also a system which contains carbon-coated fibers. To evaluate the local fields and overall properties in various systems of this kind, we develop herein a micromechanical analysis of coated fiber composites in which the fiber may be at most cylindrically orthotropic, and the coating and/or matrix transversely isotropic.

* Permanent address: Department of Solid Mechanics, Materials and Structures, Faculty of Engineering, Tel-Aviv University, Ramat-Aviv 69978, Israel.

0167-6636/90/$3.50

In addition to the earlier studies of coated fiber composites described in (I), we mention here the work of Avery and Herakovich (1986) who considered a single composite cylinder, with a cylindrically orthotropic fiber, under uniform thermal change. Pagano and Tandon (1988) treat a thermomechanically loaded system reinforced by randomly oriented short coated fibers in which the constituents may be transversely isotropic. Mikata and Taya (1985a, 1986) used the Boussinesq–Sadowsky stress functions to find stress fields in coated ellipsoidal inclusion in an infinite matrix under transverse dilatational, axial and thermal loadings. In another paper (Mikata and Taya, 1985b), they considered the problem of four concentric cylinders with transversely isotropic phases as a model of a composite reinforced by aligned coated fibers; overall stresses were limited to uniform temperature change and to axisymmetric mechanical loading.

In contrast, the present results are not limited to special loading conditions. The applied load may consist of any uniform overall state of stress, and a uniform change in temperature. As in (I), the micromechanical model employed here is based on the Mori–Tanaka approximation. The stresses in the fiber and coating are derived from the

solution of an auxiliary dilute problem in which the coated fiber is embedded in a large volume of matrix. The interaction between fibers is accounted for in an approximate way: The actual stress in the matrix is replaced by its average value σ_m, which is applied together with the prescribed uniform thermal change at the remote boundaries of the matrix. The magnitude of σ_m is obtained from the Mori–Tanaka model described in the sequel. The advantage of this approach is that the approximation affects only the boundary conditions of the modified dilute problem, but the problem itself can be solved exactly for the stress field in the fiber and coating, in the adjacent volume of the matrix, and at the respective interfaces.

The paper starts with the solution of several auxiliary dilute problems which focus on a single coated fiber while certain uniform overall stress states, and a uniform temperature change are applied to the matrix at infinity. These solutions show that even under uniform overall states, the local fields in the phases are not uniform. The results are found in cylindrical coordinates associated with the fiber axis, whereas the evaluation of overall properties must be based on phase stress averages in Cartesian coordinates. In the cylindrically orthotropic fiber, the phase properties are not uniform in the Cartesian system, and the transformation of the stress fields and phase properties requires special attention. This opens the way for implementation of the Mori–Tanaka scheme, and for a proof of its consistency. Finally, examples of computed overall properties and local stress fields are presented for a pitch precursor carbon fiber, carbon coating and titanium aluminide matrix system which is of interest in applications.

2. Auxiliary dilute problems

2.1. Phase properties

We now proceed to find solutions to the dilute problems in which the coated fiber is embedded in a large volume of matrix subjected to certain remotely applied tractions derived from uniform stress states. Invariably, the analysis will be performed in cylindrical coordinates, r, ϕ, z, where the z direction coincides with the fiber axis.

The phase constitutive equations employed in the analysis can be summarized as follows. The cylindrically orthotropic fiber is a particular example of a cylindrically anisotropic solid with the constitutive equation written as:

$$\begin{Bmatrix} \sigma_r \\ \sigma_\phi \\ \sigma_z \\ \sigma_{r\phi} \\ \sigma_{z\phi} \\ \sigma_{rz} \end{Bmatrix} = \begin{bmatrix} C_{rr} & C_{r\phi} & C_{rz} & 0 & 0 & 0 \\ C_{\phi r} & C_{\phi\phi} & C_{\phi z} & 0 & 0 & 0 \\ C_{zr} & C_{z\phi} & C_{zz} & 0 & 0 & 0 \\ 0 & 0 & 0 & G_{r\phi} & 0 & 0 \\ 0 & 0 & 0 & 0 & G_{z\phi} & 0 \\ 0 & 0 & 0 & 0 & 0 & G_{rz} \end{bmatrix} \times \begin{Bmatrix} \epsilon_r - \alpha_r\theta_0 \\ \epsilon_\phi - \alpha_\phi\theta_0 \\ \epsilon_z - \alpha_z\theta_0 \\ 2\epsilon_{r\phi} \\ 2\epsilon_{z\phi} \\ 2\epsilon_{rz} \end{Bmatrix} \tag{1}$$

where C_{ij}, $G_{r\phi}$, and G_{rz} are the stiffness coefficients, α_i are linear coefficients of thermal expansion, and θ_0 is the prescribed change in temperature. Nine stiffness coefficients and three thermal expansion coefficients describe this kind of anisotropy. Cylindrical orthotropy is characterized by the fact that the properties in the tangential, radial and axial directions are distinct; in other words, the material is orthotropic in a Cartesian system which is located at any point within the fiber, with the three axes pointing in the axial, tangential and radial direction respectively. If $C_{rr} > C_{\phi\phi}$, then the material is called radially orthotropic, and if $C_{rr} < C_{\phi\phi}$ it is called circumferentially orthotropic.

In the special case of transversely isotropic solids, which may represent the coating and the matrix, as well as some fibers, the nine independent constants in (1) are related by the connections

$$\begin{aligned} &C_{rr} = C_{\phi\phi}, \qquad C_{rz} = C_{\phi z}, \\ &G_{z\phi} = G_{rz}, \qquad C_{rr} - C_{r\phi} = 2G_{r\phi}. \end{aligned} \tag{2}$$

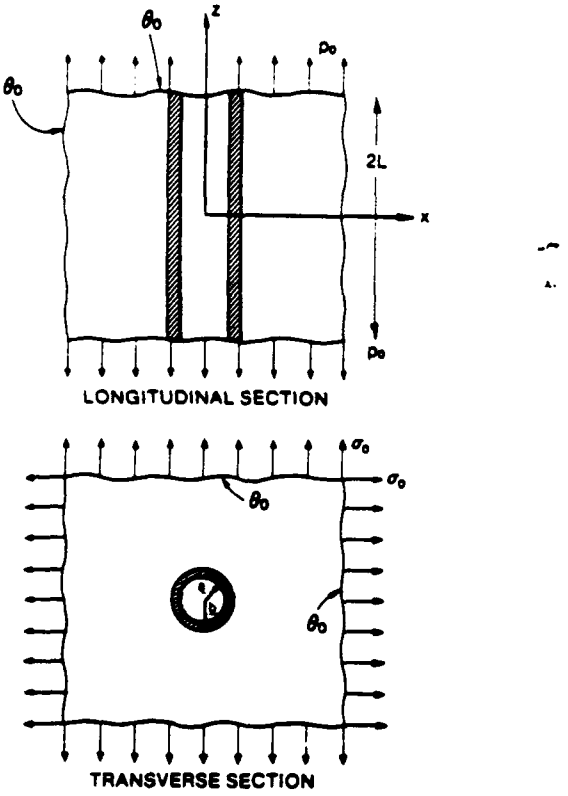

Fig. 1. The auxiliary problem for axisymmetric loading.

This reduces the number of independent constants to five. It is often convenient to represent the stiffness coefficients of a transversely isotropic solid by Hill's (1964) moduli k, l, m, n, and p, as:

$$C_{rr} = k + m, \quad C_{r\phi} = k - m, \quad C_{rz} = l$$
$$C_{zz} = n, \quad G_{rz} = p, \quad G_{r\phi} = m. \tag{3}$$

2.2. Axisymmetric deformation

We refer to Fig. 1 for definition of the geometry of the coated fiber assemblage, and of the applied loads. The cylindrical coordinates are denoted by the symbols r, ϕ, z; they appear as subscripts when used with the respective stress or strain components. The phase designation symbol $s = f, g, m$ for fiber, coating and matrix, is always written as a superscript. The boundary conditions on the surface which surrounds the large matrix volume are:

$$\sigma_r = \sigma_0 \quad \text{at } r \to \infty$$
$$\sigma_z = p_0 \quad \text{at } z \to \pm L, \quad \theta(S') = \theta_0. \tag{4}$$

It should be emphasized here that in this auxiliary problem and in those which will follow the stresses at infinity are denoted by σ_0. The stress fields in the composite will be derived from the solution of the same auxiliary problems but this time, according to the main assumption of Mori–Tanaka's method, the average stress in the matrix σ_m will replace σ_0.

A general solution to the above boundary value problem, valid away from the fiber ends $z = \pm L$, can be derived by substituting (1) into the equations of equilibrium with the boundary condition that the hoop displacement u_ϕ is zero. Also, the stresses and strains must be independent of ϕ. Cohen and Hyer (1934) found such a general form of the axisymmetric displacement field, for a cross-ply composite tube. This field can be utilized in the present situation:

$$u_r^f = A^f r^\eta + H_1 \epsilon_z^0 r + H_2 r\theta_0$$
$$u_r^g = A^g r + B^g/r \tag{5}$$
$$u_r^m = A^m r + B^m/r$$
$$u_z^s = \epsilon_z^0 r \quad s = f, g, m.$$

where $r = 0$ is the fiber axis z, and $u_r^{(s)}$, $u_z^{(s)}$ denote the radial and axial displacements in the phases s. A^s, B^s, and the uniform strain ϵ_z^0 are unknown constants which follow from the boundary conditions (4) and from the usual displacement and traction continuity conditions at the interfaces $r = a$, and $r = b$. If the fiber is transversely isotropic, then H_1 and H_2 in (5) are reduced to zero, and $\eta = 1$. As in (I) the second boundary condition in (4) cannot be satisfied pointwise by the present solution. Instead, we demand that the average stress $\sigma_z(\pm L)$ be equal to p_0. Since an infinite matrix surrounds a single coated fibers, this latter condition is implemented by simply demanding that the σ_z stress in the matrix (which turns out to be constant in the

present case) be equal to p_0. The additional constants in (5) are defined as:

$$\eta = \sqrt{C_{\phi\phi}/C_{rr}}$$

$$H_1 = \frac{C_{\phi z} - C_{rz}}{C_{rr} - C_{\phi\phi}}$$

$$H_2 = \{(C_{rr} - C_{\phi r})\alpha_r + (C_{r\phi} - C_{\phi\phi})\alpha_\phi + (C_{rz} - C_{\phi z})\alpha_z\} \times (C_{rr} - C_{\phi\phi})^{-1}. \quad (6)$$

The stress fields in the three phases are now obtained from the above displacement fields as:

$$\sigma_r^f = (C_{rr}\eta r^{\eta-1} + C_{r\phi} r^{\eta-1}) A^f + (C_{rr}H_1 + C_{r\phi}H_1 + C_{rz})\epsilon_z^0 + [C_{rr}(H_2 - \alpha_r) + C_{r\phi}(H_2 - \alpha_\phi) - C_{rz}\alpha_z]\theta_0$$

$$\sigma_\phi^f = (C_{r\phi}\eta r^{\eta-1} + C_{\phi\phi} r^{\eta-1}) A^f + (C_{r\phi}H_1 + C_{\phi\phi}H_1 + C_{\phi z})\epsilon_z^0 + [C_{r\phi}(H_2 - \alpha_r) + C_{\phi\phi}(H_2 - \alpha_\phi) - C_{\phi z}\alpha_z]\theta_0 \quad (7)$$

$$\sigma_z^f = (C_{rz}\eta r^{\eta-1} + C_{\phi z} r^{\eta-1}) A^f + (C_{rz}H_1 + C_{\phi z}H_1 + C_{zz})\epsilon_z^0 + [C_{rz}(H_2 - \alpha_r) + C_{\phi z}(H_2 - \alpha_\phi) - C_{zz}\alpha_z]\theta_0$$

$$\sigma_r^s = 2k^s A^s - 2m^s \frac{B^s}{r^2} + l^s\epsilon_z^0 - (2k^s\alpha_T^s + l^s\alpha_L^s)\theta_0$$

$$\sigma_\phi^s = 2k^s A^s + 2m^s \frac{B^s}{r^2} + l^s\epsilon_z^0 - (2k^s\alpha_T^s + l^s\alpha_L^s)\theta_0 \quad (8)$$

$$\sigma_z^s = 2l^s A^s + n^s\epsilon_z^0 - (2l^s\alpha_T^s + n^s\alpha_L^s)\theta_0$$

$$\sigma_r^m = 2k^m A^m - 2m^m \frac{B^m}{r^2} + l^m\epsilon_z^0 - (2k^m\alpha_T^m + l^m\alpha_L^m)\theta_0$$

$$\sigma_\phi^m = 2k^m A^m + 2m^m \frac{B^m}{r^2} + l^m\epsilon_z^0 - (2k^m\alpha_T^m + l^m\alpha_L^m)\theta_0 \quad (9)$$

$$\sigma_z^m = 2l^m A^m + n^m\epsilon_z^0 - (2l^m\alpha_T^m + n^m\alpha_L^m)\theta_0.$$

There are several axisymmetric solutions in micromechanics of fibrous media which have been found for transversely isotropic fibers. To provide contact between those ar the present results, we evaluate in the Appendix the effective thermomechanical properties of a substitute transversely isotropic fiber which, if used in the present axisymmetric loading case, would preserve the stress fields (8) and (9) in the coating and matrix. Under axisymmetric loading, the substitute fiber has the same overall response as the cylindrically orthotropic fiber, and the uniform stress and strain found in the substitute fiber is equal to the fiber volume average of the field (7).

Chen and Diefendorf (1985) pointed out that a nonuniform thermal stress field, similar but not identical to (7), may develop in a cylindrically orthotropic fiber which is not bonded to a matrix. The existence of such fields in embedded fibers is accounted for by the present solution.

2.3. Transverse shear loading

The statically admissible displacement field in the cylindrically orthotropic fiber, and in the transversely isotropic coating and matrix, for the loading described in Fig. 2, can be found as follows. For a homogeneous elastic medium subjected to a uniform field of simple shear deformation, the displacement components are defined by:

$$u_x = cx \quad u_y = -cy \quad u_z = 0, \quad (10)$$

where c is a constant. In cylindrical coordinates this becomes:

$$u_r = cr\cos 2\phi \quad u_\phi = -cr\sin 2\phi \quad u_z = 0. \quad (11)$$

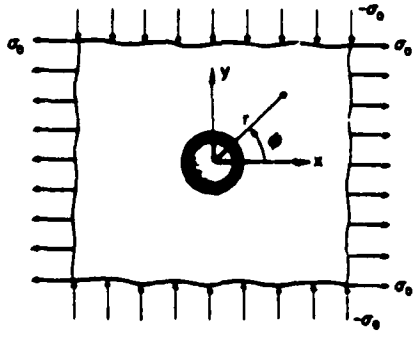

Fig. 2. The auxiliary problem for transverse shear loading.

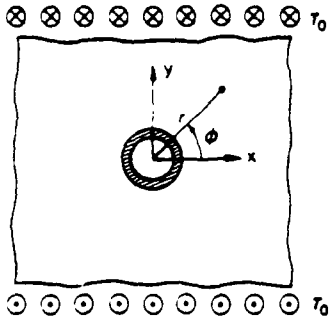

Fig. 3. The auxiliary problem for longitudinal shear loading.

In the semi-inverse solution of the present problem, Fig. 3, we therefore assume that the displacement field in the anisotropic phases will have the form

$$u_r^{(s)} = U_r^{(s)}(r)\cos 2\phi$$
$$u_\phi^{(s)} = U_\phi^{(s)}(r)\sin 2\phi \qquad (12)$$
$$u_z^{(s)} = 0,$$

where $U_r^{(s)}(r)$, $U_\phi^{(s)}(r)$ are unknown functions of r which need to be determined from the equations of equilibrium. In particular, the substitution of (12) in the stress–strain relations of the fiber (1) gives stresses which, when substituted into the equations of equilibrium in cylindrical coordinates, provide the following equations for evaluation of $U_r^{(s)}(r)$, $U_\phi^{(s)}(r)$:

$$C_{rr}\frac{d^2U_r^{(s)}}{dr^2} + \frac{C_{rr}}{r}\frac{dU_r^{(s)}}{dr} - \left(\frac{4}{r^2}G_{r\phi} + \frac{1}{r^2}C_{\phi\phi}\right)U_r^{(s)} + \frac{2(C_{r\phi}+G_{r\phi})}{r}\frac{dU_\phi^{(s)}}{dr} - \frac{2}{r^2}(G_{r\phi}+C_{\phi\phi})U_\phi^{(s)} = 0 \qquad (13)$$

$$-\frac{2(G_{r\phi}+C_{r\phi})}{r}\frac{dU_r^{(s)}}{dr} - \frac{2(G_{r\phi}+C_{\phi\phi})}{r^2}U_r^{(s)} + G_{r\phi}^{(s)}\frac{d^2U_\phi^{(s)}}{dr^2} + \frac{G_{r\phi}}{r}\frac{dU_\phi^{(s)}}{dr} - \frac{G_{r\phi}+4C_{\phi\phi}}{r^2}U_\phi^{(s)} = 0. \qquad (14)$$

Note that a change in temperature does not contribute to the present loading case. Moreover, according to our original intent, we admit cylindrical orthotropy only in the fiber domain and use a reduced form of the general solution to recover the fields in the transversely isotropic coating and matrix.

The above equations can be solved using the substitution $r = e^t$; this yields two coupled ordinary differential equations with constant coefficients for the unknown functions. The result is:

$$U_r(r) = 2\left[(G_{r\phi}+C_{\phi\phi}) - \eta_1(C_{r\phi}+G_{r\phi})\right]Ar^{\eta_1} + 2\left[(G_{r\phi}+C_{\phi\phi}) + \eta_1(C_{r\phi}+G_{r\phi})\right]Br^{-\eta_1} + 2\left[(G_{r\phi}+C_{\phi\phi}) - \eta_2(C_{r\phi}+G_{r\phi})\right]Cr^{\eta_2} + 2\left[(G_{r\phi}+C_{\phi\phi}) + \eta_2(C_{r\phi}+G_{r\phi})\right]Dr^{-\eta_2} \qquad (15)$$

$$U_\phi(r) = \left[C_{rr}\eta_1^2 - (4G_{r\phi}+C_{\phi\phi})\right]Ar^{\eta_1} + \left[C_{rr}\eta_1^2 - (4G_{r\phi}+C_{\phi\phi})\right]Br^{-\eta_1} + \left[C_{rr}\eta_2^2 - (4G_{r\phi}+C_{\phi\phi})\right]Cr^{\eta_2} + \left[C_{rr}\eta_2^2 - (4G_{r\phi}+C_{\phi\phi})\right]Dr^{-\eta_2} \qquad (16)$$

where η_1^2 and η_2^2 are the roots of

$$C_{rr}G_{r\phi}\eta^4 + \left[4C_{r\phi}^2 + 8C_{r\phi}G_{r\phi} - 4C_{rr}C_{\phi\phi} - G_{r\phi}(C_{rr}+C_{\phi\phi})\right]\eta^2 + 9G_{r\phi}C_{\phi\phi} = 0,$$

and A, B, C and D are certain constants.

As already noted, (15) and (16) are admitted only in the fiber domain. However, to assure boundedness of the displacements at the origin, the terms which contain the negative powers of η_1 and η_2 must be excluded. The displacements in the coating and matrix domains are special forms of (15) and (16). The resulting admissible displacement fields in the phases can be eventually summarized as:

$$u_r^I = \frac{b\sigma_0}{4G_{r\phi}}\left\{2\left[(G_{r\phi}+C_{\phi\phi}) - \eta_1(C_{r\phi}+G_{r\phi})\right] \times a_1\left(\frac{r}{b}\right)^{\eta_1} + 2\left[(G_{r\phi}+C_{\phi\phi}) - \eta_2(C_{r\phi}+G_{r\phi})\right]c_1\left(\frac{r}{b}\right)^{\eta_2}\right\}\cos 2\phi \qquad (17)$$

$$u_\phi^f = \frac{b\sigma_0}{4G_{r\phi}}\left\{\left[C_{rr}\eta_1^2 - (4G_{r\phi} + C_{\phi\phi})\right]a_1\left(\frac{r}{b}\right)^{\eta_1} + \left[C_{rr}\eta_2^2 - (4G_{r\phi} + C_{\phi\phi})\right]c_1\left(\frac{r}{b}\right)^{\eta_2}\right\}\sin 2\phi$$

$$u_z^f = 0$$

$$u_r^g = \frac{b\sigma_0}{4m^g}\left[(\xi_g - 3)\left(\frac{r}{b}\right)^3 a_2 + \left(\frac{r}{b}\right)d_2 + (\xi_g + 1)\left(\frac{b}{r}\right)c_2 + \left(\frac{b}{r}\right)^3 b_2\right]\cos 2\phi$$

$$u_\phi^g = \frac{b\sigma_0}{4m^g}\left[(\xi_g + 3)\left(\frac{r}{b}\right)^3 a_2 - \left(\frac{r}{b}\right)d_2 - (\xi_g - 1)\left(\frac{b}{r}\right)c_2 + \left(\frac{b}{r}\right)^3 b_2\right]\sin 2\phi \tag{18}$$

$$u_z^g = 0$$

$$u_r^m = \frac{b\sigma_0}{4m^m}\left[\frac{2}{b}r + (\xi_m + 1)\frac{b}{r}a_3 + \left(\frac{b}{r}\right)^3 c_3\right]\cos 2\phi$$

$$u_\phi^m = \frac{b\sigma_0}{4m^m}\left[-\frac{2}{b}r - (\xi_m - 1)\frac{b}{r}a_3 + \left(\frac{b}{r}\right)^3 c_3\right]\sin 2\phi \tag{19}$$

$$u_z^m = 0$$

where

$$\xi_g = (2m^g + k^g)/k^g, \quad \xi_m = (2m^m + k^m)/k^m$$

and σ_0 is normal transverse stress applied at infinity, Fig. 2.

Observe also that the equations have been written in terms of a nondimensional radial coordinate (r/b), and that as yet unknown constants a_1, a_2, a_3, b_2, c_1, c_2, c_3, and d_2 have been introduced to replace the A, B, C, D constants in (15) and (16).

Since both the coating and the matrix are regarded as transversely isotropic, we have used the connections (2) between elastic constants to introduce the Hill's moduli k^g, k^m, and m^g, m^m. We finally mention that when applied to isotropic phases, eqns. (17) to (19) become identical with (39) to (45) in (I), and are also in agreement with the results obtained by Christensen and Lo (1979, 1986). The latter were obtained for an isotropic fiber and coating in a transversely isotropic matrix.

The stress fields for overall transverse shear loading can be derived from the displacement fields (17) to (19), using the appropriate constitutive relations (1) or (3). Since these fields are of interest in applications, and their derivation is cumbersome, we reproduce them here:

$$\sigma_r^f = \left\{\left[C_{rr}f_1\eta_1 + C_{r\phi}(2g_1 + f_1)\right]a_1\frac{r^{\eta_1 - 1}}{b^{\eta_1}} + \left[C_{rr}f_2\eta_2 + C_{r\phi}(2g_2 + f_2)\right]c_1\frac{r^{\eta_2 - 1}}{b^{\eta_2}}\right\} \times \sigma_0\cos 2\phi$$

$$\sigma_\phi^f = \left\{\left[C_{\phi r}f_1\eta_1 + C_{\phi\phi}(2g_1 + f_1)\right]a_1\frac{r^{\eta_1 - 1}}{b^{\eta_1}} + \left[C_{\phi r}f_2\eta_2 + C_{\phi\phi}(2g_2 + f_2)\right]c_1\frac{r^{\eta_2 - 1}}{b^{\eta_2}}\right\} \times \sigma_0\cos 2\phi$$

$$\sigma_z^f = \left\{\left[C_{zr}f_1\eta_1 + C_{z\phi}(2g_1 + f_1)\right]a_1\frac{r^{\eta_1 - 1}}{b^{\eta_1}} + \left[C_{zr}f_2\eta_2 + C_{z\phi}(2g_2 + f_2)\right]c_1\frac{r^{\eta_2 - 1}}{b^{\eta_2}}\right\} \times \sigma_0\cos 2\phi$$

$$\sigma_{r\phi}^f = G_{r\phi}\left[(-2f_1 + g_1\eta_1 - g_1)a_1\frac{r^{\eta_1 - 1}}{b^{\eta_1}} + (-2f_2 + g_2\eta_2 - g_2)c_1\frac{r^{\eta_2 - 1}}{b^{\eta_2}}\right]\sigma_0\sin 2\phi \tag{20}$$

$$\sigma_r^g = \left\{\left[3k^g(\xi_g - 1) - 6m^g\right]\frac{r^2}{b^3}a_2 + m^g\frac{d_2}{b} - \left[k^g(\xi_g - 1) + 2m^g\right]\frac{b}{r^2}c_2 - 3m^g\frac{b^3}{r^4}b_2\right\} \times \frac{b\sigma_0}{2m^g}\cos 2\phi$$

$$\sigma_\phi^g = \left\{\left[3k^g(\xi_g - 1) + 6m^g\right]\frac{r^2}{b^3}a_2 - m^g\frac{d_2}{b} - \left[k^g(\xi_g - 1) - 2m^g\right]\frac{b}{r^2}c_2 + 3m^g\frac{b^3}{r^4}b_2\right\} \times \frac{b\sigma_0}{2m^g}\cos 2\phi$$

$$\sigma_r^s = \left[3(\xi_s - 1)\frac{r^2}{b^3}a_2 - (\xi_s - 1)\frac{b}{r^2}c_2\right] \times \frac{bl^s}{2m^s}\sigma_0 \cos 2\phi$$

$$\sigma_{r\phi}^s = \left[6\frac{r^2}{b^3}a_2 - \frac{d_2}{b} - 2\frac{b}{r^2}c_2 - 3\frac{b^3}{r^4}b_2\right] \times \frac{b}{2}\sigma_0 \sin 2\phi \tag{21}$$

$$\sigma_r^m = \left\{\frac{2m^m}{b} - \left[k^m(\xi_m - 1) + 2m^m\right]\frac{b}{r^2}a_3 - 3m^m\frac{b^3}{r^4}c_3\right\}\frac{b\sigma_0}{2m^m}\cos 2\phi$$

$$\sigma_\phi^m = \left\{-\frac{2m^m}{b} - \left[k^m(\xi_m - 1) - 2m^m\right]\frac{b}{r^2}a_3 + 3m^m\frac{b^3}{r^4}c_3\right\}\frac{b\sigma_0}{2m^m}\cos 2\phi$$

$$\sigma_z^m = \left[(1 - \xi_m)\frac{b^2}{r^2}a_3\right]\frac{l^m\sigma_0}{2m^m}\cos 2\phi$$

$$\sigma_{r\phi}^m = -\left[\left(1 + \left(\frac{b}{r}\right)^2 a_3\right) + \frac{3}{2}\left(\frac{b}{r}\right)^4 c_3\right]\sigma_0 \sin 2\phi \tag{22}$$

where

$$f_1 = \frac{b}{2G_{r\phi}}\left[(G_{r\phi} + C_{\phi\phi}) - \eta_1(C_{r\phi} + G_{r\phi})\right]$$

$$f_2 = \frac{b}{2G_{r\phi}}\left[(G_{r\phi} + C_{\phi\phi}) - \eta_2(C_{r\phi} + G_{r\phi})\right]$$

$$g_1 = \frac{b}{4G_{r\phi}}\left[C_{rr}\eta_1^2 - (4G_{r\phi} + C_{\phi\phi})\right] \tag{23}$$

$$g_2 = \frac{b}{4G_{r\phi}}\left[C_{rr}\eta_2^2 - (4G_{r\phi} + C_{\phi\phi})\right].$$

The interface conditions to be satisfied are the continuity requirements for the stresses σ_{rr}, $\sigma_{r\phi}$ and the displacements u_r, u_ϕ at interfaces $r = a$ and $r = b$. These conditions provide the equations for evaluation of the eight unknown constants, but the solution is best obtained numerically. It can be verified that the displacements (17) to (19) guarantee that the average of the stress σ_{zz} in the solution domain does vanish, and that at infinity there is:

$$\sigma_{xx}|_{r\to\infty} = \sigma_0, \quad \sigma_{yy}|_{r\to\infty} = -\sigma_0. \tag{24}$$

2.4. Longitudinal shear loading

For this loading case, which is described in Fig. 3, we retrace the steps outlined in the previous sections. The displacement field has only one nonvanishing component, which must have the form:

$$u_r = 0, \quad u_\phi = 0, \quad u_z = u_z(r, \phi). \tag{25}$$

The corresponding nonvanishing strain components are:

$$\epsilon_{rz} = \frac{1}{2}\frac{\partial u_z}{\partial r}, \quad \epsilon_{\phi z} = \frac{1}{2r}\frac{\partial u_z}{\partial \phi} \tag{26}$$

and the stresses are:

$$\sigma_{rz} = G_{rz}\frac{\partial u_z}{\partial r}, \quad \sigma_{\phi z} = \frac{G_{\phi z}}{r}\frac{\partial u_z}{\partial \phi}. \tag{27}$$

Note that these stresses automatically satisfy the first two equilibrium equations in cylindrical coordinates, while the third equation

$$\frac{\partial \sigma_{rz}}{\partial r} + \frac{1}{r}\frac{\partial \sigma_{\phi z}}{\partial \phi} + \frac{\partial \sigma_{zz}}{\partial \phi} + \frac{\sigma_{rz}}{r} = 0 \tag{28}$$

yields the relation

$$r^2\frac{\partial^2 u_z}{\partial r^2} + r\frac{\partial u_z}{\partial r} + q^2\frac{\partial^2 u_z}{\partial \phi^2} = 0 \tag{29}$$

for the unknown displacement u_z, where $q = \sqrt{G_{\phi z}/G_{rz}}$.

Letting

$$u_z = R(r)\Phi(\phi) \tag{30}$$

leads readily to the solution

$$u_z^l = A^l r^q \sin \phi$$

$$u_z^s = \left(A^s r + \frac{B^s}{r}\right)\sin \phi \tag{31}$$

$$u_z^m = \left(A^m r + \frac{B^m}{r}\right)\sin \phi.$$

The stresses are then obtained as

$$\sigma_{rz}^l = G_{rz}A^l q r^{q-1} \sin \phi$$

$$\sigma_{\phi z}^l = G_{\phi z}A^l r^{q-1} \cos \phi$$

$$\sigma_{rz}^s = p^s\left(A^s - \frac{B^s}{r^2}\right)\sin \phi$$

$$\sigma^{s}_{\phi z} = p^{s}\left(A^{s} + \frac{B^{s}}{r^2}\right)\cos\phi$$

$$\sigma^{m}_{rz} = p^{m}\left(A^{m} - \frac{B^{m}}{r^2}\right)\sin\phi$$

$$\sigma^{m}_{\phi z} = p^{m}\left(A^{m} + \frac{B^{m}}{r^2}\right)\cos\phi \qquad (32)$$

where, we recall, p^{s}, p^{m} are the longitudinal shear moduli of the phases.

This completes the solution of the auxiliary problems. The solutions will be implemented in the micromechanic model described in Section 4, in order to obtain the effective properties and stress fields in the composite.

3. Phase stress and strain averages

The stress fields obtained in Section 2, and the phase properties employed in finding the fields, were both written in the cylindrical coordinates associated with the fiber axis. However, utilization of such fields in evaluation of overall properties, e.g., by the Mori–Tanaka method, requires that they be written in the Cartesian system. Furthermore, since the composites contain a curvilinearly anisotropic phase, special care is needed in the determination of effective properties. This section presents the framework for dealing with such systems.

A representative volume of the composite is subjected to homogeneous displacement or traction boundary conditions and to a uniform temperature change defined as

$$\begin{aligned} u(S) &= \epsilon_0 x \qquad \theta(S) = \theta_0 \\ \sigma_n(S) &= \sigma_0 n \qquad \theta(S) = \theta_0, \end{aligned} \qquad (33)$$

where u and σ_n denote the displacement and traction vectors respectively, ϵ_0, σ_0 and θ_0 are uniform strain, stress and temperature fields and n denotes the outside normal of S. Suppose that the actual stress and strain fields in the phases are known in the current coordinate system and are denoted by primed letters $\sigma'(\xi)$ and $\epsilon'(\xi)$. The phase properties in the ξ system are denoted by L', M', m' and l'. For example, if the system is identified with the cylindrical coordinates of Section 2, then (1) and the phase stress fields obtained in the solution of the auxiliary problems represent such primed fields. The corresponding quantities in the Cartesian coordinates are denoted by similar but unprimed letters.

Let the transformation between the current and the Cartesian components of the fields at any point in a given phase s be described by as:

$$\sigma_s(x) = R\sigma'_s(\xi), \quad \epsilon_s(x) = Q\epsilon'_s(\xi), \qquad (34)$$

where, according to the conventional use in the literature, with the factor 2 in the shear terms of the 6×1 strain vector, the transformation matrices R and Q are related by $R^{T} = Q^{-1}$. In a transformation between the cylindrical and Cartesian systems, R and Q are functions of the angle ϕ.

Next, write the phase constitutive relations, such as (1), in the symbolic form:

$$\begin{aligned} \sigma'_s(\xi) &= L'_s(\xi)\epsilon'_s(\xi) + l'_s(\xi)\theta_0, \\ \epsilon'_s(\xi) &= M'_s(\xi)\sigma'_s(\xi) + m'_s(\xi)\theta_0 \end{aligned} \qquad (35)$$

where

$$M'_s = L'^{-1}_s \text{ and } l'_s = -L'_s m'_s$$

Equations (34) and (35) provide the relations

$$\begin{aligned} \sigma_s(x) &= RL'_sQ^{-1}\epsilon_s(x) + Rl'_s\theta_0, \\ \epsilon_s(x) &= QM'_sR^{-1}\sigma_s(x) + Qm'_s\theta_0 \end{aligned} \qquad (36)$$

at each point x. Note that Q, R, L'_s, l'_s and m'_s may now be functions of x, but for brevity in notation the argument will be omitted in the sequel. Averages over the volume of the phases are given by the expressions:

$$\begin{aligned} \sigma_s &= \frac{1}{V_s}\int_{V_s}\sigma_s(x)\,dV_s = \frac{1}{V_s}\int_{V_s} RL'_sQ^{-1}\epsilon_s(x)\,dV_s \\ &\quad + \frac{1}{V_s}\int_{V_s} Rl'_s\theta_0\,dV_s \\ \epsilon_s &= \frac{1}{V_s}\int_{V_s}\epsilon_s(x)\,dV_s = \frac{1}{V_s}\int_{V_s} QM'_sR^{-1}\sigma_s(x)\,dV_s \\ &\quad + \frac{1}{V_s}\int_{V_s} Qm'_s\theta_0\,dV_s. \end{aligned} \qquad (37)$$

The local fields (36) in the composite aggregate are related to the uniform fields through certain influence functions $A_s(x)$, $a_s(x)$, $B_s(x)$, $b_s(x)$ given by

$$\epsilon_s(x) = A_s(x)\epsilon_0 + a_s(x)\theta_0$$
$$\sigma_s(x) = B_s(x)\sigma_0 + b_s(x)\theta_0. \tag{38}$$

In this paper strain and stress symbols followed by the argument (x) will denote local fields and those without an argument will refer to averages. Similar relations can also be written for the phase volume averages

$$\epsilon_s = A_s\epsilon_0 + a_s\theta_0$$
$$\sigma_s = B_s\sigma_0 + b_s\theta_0 \tag{39}$$

where the constant tensors A_s, a_s, B_s, b_s are the concentration factors. The average stress in the phases under boundary condition (33_1), is given in accordance to (37_1) and (38_1) by

$$\sigma_s = \frac{1}{V_s}\int_{V_s} RL_s'Q^{-1}\left[A_s(x)\epsilon_0 + a_s(x)\theta_0\right] dV_s + \frac{1}{V_s}\int_{V_s} Rl_s'\theta_0\, dV_s, \tag{40}$$

where we have used the fact that a uniform temperature field $\theta = \theta_0$ prevails in the composite. Similarly, the average strain ϵ_s under (37_2) is:

$$\epsilon_s = \frac{1}{V_s}\int_{V_s} QM_s'R^{-1}\left[B_s(x)\sigma_0 + b_s(x)\theta_0\right] dV_s + \frac{1}{V_s}\int_{V_s} Qm_s'\theta_0\, dV_s. \tag{41}$$

Solve for ϵ_0 and σ_0 in (39) and substitute in (40) and (41):

$$\sigma_s = L_s\epsilon_s + l_s\theta_0$$
$$\epsilon_s = M_s\sigma_s + m_s\theta_0, \tag{42}$$

where

$$L_s = \left[\frac{1}{V_s}\int_{V_s} RL_s'Q^{-1}A_s(x)\, dV_s\right]A_s^{-1}$$
$$l_s = \left\{\left[-\frac{1}{V_s}\int_{V_s} RL_s'Q^{-1}A_s(x)\, dV_s\right]A_s^{-1}a_s + \frac{1}{V_s}\int_{V_s} RL_s'Q^{-1}a_s(x)\, dV_s + \frac{1}{V_s}\int_{V_s} Rl_s'\, dV_s\right\} \tag{43}$$

$$M_s = \left[\frac{1}{V_s}\int_{V_s} QM_s'R^{-1}B_s(x)\, dV_s\right]B_s^{-1}$$
$$m_s = \left\{\left[-\frac{1}{V_s}\int_{V_s} QM_s'R^{-1}B_s(x)\, dV_s\right]B_s^{-1}b_s + \frac{1}{V_s}\int_{V_s} QM_s'R^{-1}b_s(x)\, dV_s + \frac{1}{V_s}\int_{V_s} Qm_s'\, dV_s\right\}. \tag{44}$$

Note that in view of their definitions in (43) and (44), the quantities L_s and M_s are fourth order tensors and l_s and m_s are second order tensors. Like the overall effective behavior of the composite aggregate, these effective tensors depend on the nature of the influence functions $A_s(x)$, $B_s(x)$, $a_s(x)$, and $b_s(x)$. Since the latter are approximated differently in different micromechanical models, L_s, M_s, l_s, and m_s may vary from model to model. Furthermore for these tensors to qualify as effective properties, they must obey the relation

$$L_s = M_s^{-1}, \quad l_s = -L_s m_s^{-1} \tag{45}$$

in the context of the used theory. Proofs of similar relations between the overall effective properties tensors may also be needed.

4. The micromechanical model

The effective properties and stress fields will be calculated using the Mori–Tanaka model. This method of evaluation of the influence functions in (38) and of the effective properties of the composite aggregate has been described in (I). Here we summarize only those expressions which will be needed in the sequel. The first step is the evaluation of local fields in the dilute problem, where a single coated fiber is embedded in a large volume of matrix, Fig. 4. A uniform stress σ_m or strain ϵ_m and temperature change θ_0 are applied to the matrix at infinity, such that σ_m and ϵ_m are the as yet unknown averages stress and strain in the matrix, while the composite is subjected to the boundary condition (33_1) and (33_2), respectively. The solution of this dilute problem can be ex-

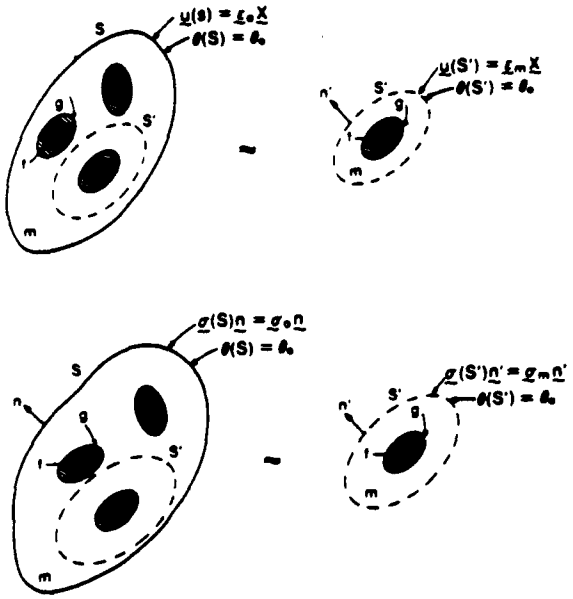

Fig. 4. A schematic representation of the Mori–Tanaka's method for thermoelastic problems.

pressed in terms of the influence functions $T_s(x)$, $t_s(x)$, $W_s(x)$, $w_s(x)$ as follows:

$$\epsilon_s(x) = T_s(x)\epsilon_m + t_s(x)\theta_0$$
$$\sigma_s(x) = W_s(x)\sigma_m + w_s(x)\theta_0. \tag{46}$$

The magnitudes of ϵ_m and σ_m are derived from the requirement that

$$\epsilon = \sum_s c_s\epsilon_s = \epsilon_0$$
$$\sigma = \sum_s c_s\sigma_s = \sigma_0, \quad s = \mathrm{f, g, m}, \tag{47}$$

where c_s are the phase volume fractions such that $\Sigma c_s = 1$, and ϵ_s and σ_s are the phase volume averages of the local strains and stresses. The final result is

$$\epsilon_m = \left[\sum_s c_s T_s\right]^{-1}\left[\epsilon_0 - \theta_0\sum_s c_s t_s\right]$$
$$\sigma_m = \left[\sum_s c_s W_s\right]^{-1}\left[\sigma_0 - \theta_0\sum_s c_s w_s\right], \quad s = \mathrm{f, g, m}. \tag{48}$$

Note that in the dilute configuration there is

$$T_m \doteq I, \; t_m = 0$$
$$W_m \doteq I, \; w_m = 0 \tag{49}$$

where I is the identity tensor.

In this way, the evaluation of the quantities of interest in (38) is reduced to finding of the concentration factors T_s, t_s, W_s and w_s, which are defined as the phase volume averages of the influence functions $T_s(x)$, $t_s(x)$, $W_s(x)$ and $w_s(x)$ in (46).

Substitution of (48) into (46) provides the influence functions indicated by the Mori–Tanaka model. These are:

$$A_s = T_s(x)\left[\sum_s c_s T_s\right]^{-1}$$
$$a_s = -T_s(x)\left[\sum_s c_s T_s\right]^{-1}\left[\sum_s c_s t_s\right] + t_s(x) \tag{50}$$
$$B_s = W_s(x)\left[\sum_s c_s W_s\right]^{-1}$$
$$b_s = -W_s(x)\left[\sum_s c_s W_s\right]^{-1}\left[\sum_s c_s w_s\right] + w_s(x). \tag{51}$$

Use of (50) and (51) and (43) and (44) gives

$$L_s = \left[\frac{1}{V_s}\int_{V_s} RL_s'Q^{-1}T_s(x)\,\mathrm{d}V_s\right]T_s^{-1}$$
$$l_s = -L_s t_s + \frac{1}{V_s}\int_{V_s} RL_s'Q^{-1}t_s(x)\,\mathrm{d}V_s + \frac{1}{V_s}\int_{V_s} Rl_s'\,\mathrm{d}V_s \tag{52}$$

$$M_s = \left[\frac{1}{V_s}\int_{V_s} QM_s'R^{-1}W_s(x)\,\mathrm{d}V_s\right]W_s^{-1}$$
$$m_s = -M_s w_s + \frac{1}{V_s}\int_{V_s} QM_s'R^{-1}w_s(x)\,\mathrm{d}V_s + \frac{1}{V_s}\int_{V_s} Qm_s'\,\mathrm{d}V_s. \tag{53}$$

On the other hand, knowledge of the local fields (46) results in the prediction of the effective

stiffness and compliance tensors L, M, and effective thermal tensors l and m. These are

$$L = \left[\sum_s c_s L_s T_s\right]\left[\sum_s c_s T_s\right]^{-1}$$
$$l = \left[\sum_s c_s L_s T_s\right]\left[\sum_s c_s T_s\right]^{-1}\left[-\sum_s c_s l_s\right] + \left[\sum_s c_s (L_s l_s + l_s)\right] \tag{54}$$
$$M = \left[\sum_s c_s M_s W_s\right]\left[\sum_s c_s W_s\right]^{-1}$$
$$m = \left[\sum_s c_s M_s W_s\right]\left[\sum_s c_s W_s\right]^{-1}\left[-\sum_s c_s w_s\right] + \left[\sum_s c_s (M_s w_s + m_s)\right]. \tag{55}$$

We now prove that L_s, l_s, M_s and m_s, as predicted by the micromechanical model in (52) and (53), satisfy:

$$L_s = M_s^{-1}, \quad l_s = -L_s m_s. \tag{56}$$

Consider (46_1), with $\theta_0 = 0$, and write this equation in an equivalent form:

$$\epsilon_s(x) = T_s(x)\epsilon_m$$
$$\sigma_s(x) = RL_s' Q^{-1} T_s(x) M_m \epsilon_m, \tag{57}$$

Table 1
Thermoelastic constants

	Fiber	Coating	Matrix
E_R (GPa)	13.8	34.4	96.5
E_ϕ (GPa)	772.2	34.4	96.5
E_z (GPa)	772.2	34.4	96.5
$G_{r\phi}$ (GPa)	20.7	14.3	37.1
$G_{\phi z}$ (GPa)	68.9	14.3	37.1
G_{rz} (GPa)	20.7	14.3	37.1
$\nu_{r\phi}$	0.25	0.2	0.3
$\nu_{\phi z}$	0	0.2	0.3
ν_{rz}	0.25	0.2	0.3
α_r (10^{-6}/°C)	28.0	3.3	9.3
α_ϕ (10^{-6}/°C)	−1.8	3.3	9.3
α_z (10^{-6}/°C)	−1.8	3.3	9.3

Pitch precursor carbon fiber $c_f = 0.4$
Carbon coating $c_s = 0.0107$
Titanium aluminide matrix $c_m = 0.5893$

which, when compared with (46_2) under $\theta_0 = 0$, implies that

$$W_s(x) = RL_s' Q^{-1} T_s(x) M_m. \tag{58}$$

Substitution of this last equation into (53_1) yields

$$M_s = T_s\left[\frac{1}{V_s}\int_{V_s} RL_s' Q^{-1} T_s(x)\, dV_s\right]^{-1}. \tag{59}$$

Finally, compare (59) with (52_1), to show that (56_1), is in fact satisfied.

Let us now proceed to prove the second relation in (56). Start with (46_1), let $\epsilon_m = 0$, and write it in the following equivalent forms:

$$\epsilon_s(x) = t_s(x)\theta_0$$
$$\sigma_s(x) = RL_s' Q^{-1} t_s(x)\theta_0 - RL_s' m_s'\theta_0 \tag{60}$$

or

$$\sigma_s(x) = RL_s' Q^{-1} t_s(x)\theta_0 - RL_s' m_s'\theta_0 + W_s(x) l_m \theta_0 - W_s(x) l_m \theta_0, \tag{61}$$

where it should be noted that $l_m\theta_0$ is the stress induced on the outside boundary of the matrix by a temperature change under zero overall strain. Compare (61) with the last of (46):

$$w_s(x) = RL_s' Q^{-1} t_s(x) - RL_s' m_s' - W_s(x) l_m. \tag{62}$$

Integrate now (62) over V_s to get w_s and substitute both w_s and $w_s(x)$ into (53_2):

$$m_s = -M_s\left[\frac{1}{V_s}\int_{V_s} RL_s' Q^{-1} t_s(x)\, dV_s\right] + M_s \frac{1}{V_s}\int_{V_s} RL_s' m_s'\, dV_s + M_s \frac{1}{V_s}\int_{V_s} W_s(x)\, dV_s l_m + \frac{1}{V_s}\int_{V_s} t_s(x)\, dV_s - \frac{1}{V_s}\int_{V_s} RM_s' R^{-1} W_s(x)\, dV_s l_m. \tag{63}$$

Finally, multiply (63) from the left by $-L_s$, recall the definition of M_s in (53_1), and compare with (52_2), to show that (56_2) is in fact fulfilled. Since (56) are satisfied by the model, the proof of con-

sistency relations $L = M^{-1}$, $l = -Lm$, between the effective properties follows along the lines shown in (I).

It should finally be noted that the thermal stress influence functions $a_s(x)$, $b_s(x)$ and effective thermal stress tensors could also be found from a correspondence between mechanical and thermal fields in heterogeneous aggregates. We follow here the direct approach; the latter route, outlined by Dvorak and Chen (1989), gives entirely equivalent results, but the quantities of interest are obtained from exact connections between $b_s(x)$ and $B_s(x)$, and also between m and M. The results in that work have been derived only for systems with transversely isotropic phases, but they can be extended to composites with cylindrically orthotropic fibers if the actual fiber properties are expressed by effective ones, as outlined in the Appendix. The resulting forms are very simple, this may be preferable in some applications.

It is now necessary to assemble the W_s and w_s tensors from the solutions of the auxiliary problems, and also to construct the M_s and m_s tensors in accordance with (44). To this end, suppose that we have already obtained from (33_2) the Cartesian components of the local stresses in the auxiliary problems. Let the external boundary stresses p_0 in Fig. 1 with $\theta_0 = 0$ be denoted by $\sigma_0(1)$, and the Cartesian components of the local stresses, under a unit load $\sigma_0(1) = 1$, be given by $\sigma_s(1)$. Similarly, $\sigma_0(2)$ denotes stress σ_0 in Fig. 1 with $\theta_0 = 0$, and $\sigma_s(2)$ the corresponding local Cartesian stress field under $\sigma_0(2) = 1$. The external stresses in Figs. 2 and 3 are respectively denoted by $\sigma_0(3)$ and $\sigma_0(4)$, and the corresponding local Cartesian stresses under external loads by $\sigma_s(3)$, $\sigma_s(4)$.

The external stress vector in the Cartesian system can be therefore written as

$$\begin{Bmatrix} \sigma_x^0 \\ \sigma_y^0 \\ \sigma_z^0 \\ \sigma_{xz}^0 \\ \sigma_{yz}^0 \\ \sigma_{xy}^0 \end{Bmatrix} = \begin{Bmatrix} [\sigma_0(2) + \sigma_0(3)]/2 \\ [\sigma_0(2) - \sigma_0(3)]/2 \\ \sigma_0(1) \\ \sigma_0(4) \\ \sigma_0(4) \\ \sigma_0(3)' \end{Bmatrix} \tag{64}$$

where $\sigma_0(3)'$ denotes the external loading configuration in Fig. 2 rotated by 45°. Denote the average of these stresses over the fiber and matrix by $\bar{\sigma}_s$ (s = f, g). By definition, the W_s tensor represents the resulting average Cartesian stresses in the constituents due to a unit Cartesian stress tensor at infinity. Therefore the columns of the (6×6) W_s matrix can be written as:

$$\begin{aligned} &W_s^{(1)} = [\bar{\sigma}_s(2) + \bar{\sigma}_s(3)]/2 \quad s = \text{f, g} \\ &W_s^{(2)} = [\bar{\sigma}_s(2) - \bar{\sigma}_s(3)]/2 \\ &W_s^{(3)} = \bar{\sigma}_s(1),\ W_s^{(4)} = \bar{\sigma}_s(4),\ W_s^{(5)} = \bar{\sigma}_s(4), \\ &W_s^{(6)} = \bar{\sigma}_s(3)', \end{aligned} \tag{65}$$

with the last column $W_s^{(6)}$ being equal to the average stress tensor $\bar{\sigma}_s(3)$ rotated by 45° about the fiber axis. Finally the vector w_s (s = f, g) is equal to the average Cartesian stress components in the fiber and coating due to a unit temperature $\theta_0 = 1$ at infinity.

This completes the derivation of the concentration tensors W_s and w_s. The stress fields can now be obtained from (46), where the average matrix stress σ_m is determined from (48). Numerical results for these fields under different loading con-

Table 2
Effective compliance matrix

$$\begin{bmatrix} 0.01139 & -0.004253 & -0.0005519 & 0 & 0 & 0 \\ -0.004253 & 0.01139 & -0.0005519 & 0 & 0 & 0 \\ -0.0005519 & -0.0005519 & 0.002717 & 0 & 0 & 0 \\ 0 & 0 & 0 & 0.02450 & 0 & 0 \\ 0 & 0 & 0 & 0 & 0.02450 & 0 \\ 0 & 0 & 0 & 0 & 0 & 0.03130 \end{bmatrix} \text{MPa}^{-1}$$

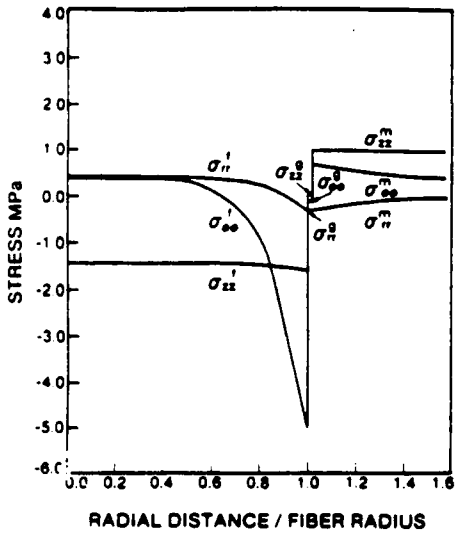

Fig. 5. Stress distributions for the case of uniform temperature change $-1°C$.

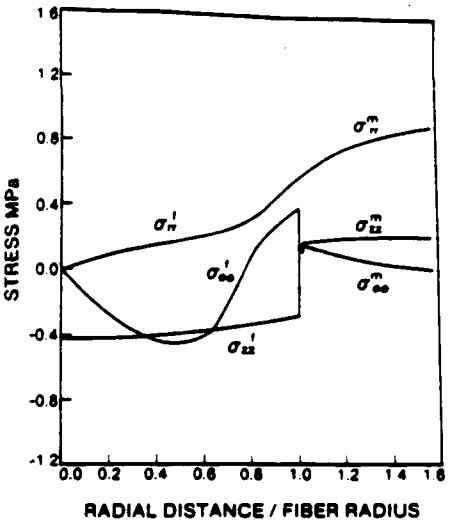

Fig. 7. Stress distribution for transverse normal loading 1 MPa along $\phi = 0°$.

figurations will be given in the last section of the paper, together with the effective compliance tensor M for the system considered.

Finally, we mention here that numerical calculations show that the resulting M matrix as predicted by the Mori–Tanaka model is symmetric. Such behavior was also observed in (I), in the simpler system made of isotropic constituents. Unfortunately, due to the complicated nature of the concentration factors, an analytical proof of this property cannot be given for the present systems.

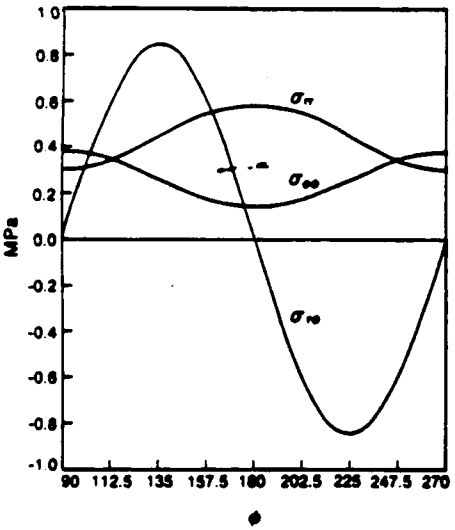

Fig. 6. Average stress in the coating for transverse normal loading 1 MPa versus the angle ϕ.

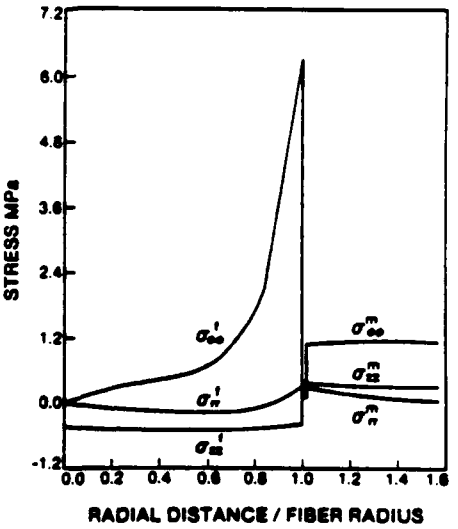

Fig. 8. Stress distribution for transverse normal loading 1 MPa along $\phi = 90°$.

5. Numerical results

We consider a fibrous system made of pitch precursor carbon fiber, carbon coating and titanium aluminide matrix. Stress fields are evaluated both for thermal changes and for typical mechanical loading situations. Of particular interest are the thermal stresses caused in these systems by a uniform temperature change.

Table 1 shows the thermomechanical properties and phase volume fractions of the constituents of this system; the fibers are cylindrically orthotropic, the coating and the matrix are isotropic. Material constants do not vary with temperature. The values of material constants were taken from work in progress by Diefendorf (1989). When material properties are functions of temperature, the results developed here can be readily implemented in an incremental form, using the procedure described in Dvorak et al. (1989).

The effective compliance matrix predicted by the model is given in Table 2. For axisymmetric loading, however, the replacement scheme described in the Appendix can also be used to obtain certain effective properties. For the system considered, the properties of the equivalent transversely isotropic fiber, as furnished by eqns. (A.9) and (A.10) are:

$$k = 53.4\ \text{GPa},\ l = 26.7\ \text{GPa},\ n = 786.2\ \text{GPa},$$
$$\alpha_A = -1.69 \times 10^{-6}/^\circ\text{C}\ \ \alpha_T = 2.086 \times 10^{-6}/^\circ\text{C}. \tag{66}$$

With these values, eqns. (7–10) can be readily evaluated, in the form applicable to systems with transversely isotropic properties.

Local field are illustrated in Figs. 5–8. Figure 5 shows the thermal stress distribution as a function of a normalized radial distance for the case of a uniform temperature change of -1°C. It is seen that the hoop stress attains a maximum at the fiber–coating interface and that the stress field is not uniform within the fiber. We note here that for radially orthotropic fibers ($C_{rr} > C_{\phi\phi}$), the stress field becomes infinite at the center of the fiber, as already pointed out by Avery and Herakovich (1986), for the case of a single fiber. This may require a reexamination of the present solution.

Figures 6–8 show the average stress in the coating for the case of pure mechanical loading in simple tension. Figure 6 shows the stresses in the coating as a function of ϕ, and Figs. 7 and 8 give the stresses in the fiber, coating and matrix under simple tension at $\phi = 0^\circ$, and $\phi = 90^\circ$, respectively. Since, both η_1 and η_2 are greater than 1 in the present system (see eqn. 16), it is interesting to observe that the radial and hoop stress become zero at the center of the fiber. We note, however, that $\eta_1 = 1$, $\eta_2 = 3$, in an isotropic fiber, and the stresses at the center of the fiber have a finite value. If for certain material properties η_1 and η_2 are less than 1, the stresses at the center of the fiber become singular.

Acknowledgement

Support from the DARPA-HiTASC program at Rensselaer is gratefully acknowledged.

References

Avery, W.B. and C.T. Herakovich (1986), Effect of fiber anisotropy on thermal stresses in fibrous composites, *J. Appl. Mech. 53*, 751.

Benveniste, Y., G.J. Dvorak and T. Chen (1989), Stress field in composites with coated inclusions, *Mech. Mater. 7*, 305.

Chen, K.J. and R.J. Diefendorf (1985), A theoretical calculation of residual stresses in carbon fibers, in: Proc. 17th Biennial Conference on Carbon, American Carbon Society, p. 387.

Christensen, R.M. and K.H. Lo (1979), Solutions for effective shear properties in three phase sphere and cylinder models, *J. Mech. Phys. Solids 27*, 315.

Christensen, R.M. and K.H. Lo (1986), Erratum to Christensen and Lo (1979), *J. Mech. Phys. Solids 34*, 639.

Cohen, D. and M.W. Hyer (1984), Residual stresses in cross-ply composite tubes, Report CCMS-84-04, Virginia Polytechnic Institute and State University, Blacksburg, VA.

Diefendorf, R.J. (1989), Private communication.

Dvorak, G.J. and T. Chen (1989), Thermal expansion of three-phase composite materials, *J. Appl. Mech. 56*, 418.

Dvorak, G.J., T. Chen and J. Teply (1989), Thermomechanical stress fields in high temperature fibrous composites: I. Unidirectional laminates, to be published.

Hill, R. (1964), Theory of mechanical properties of fiber strengthened materials: I. Elastic behavior, *J. Mech. Phys. Solids 13*, 189.

Norris, A.N. (1989), An examination of the Mori–Tanaka effective medium approximation for multiphase composites, *J. Appl. Mech. 56*, 83.

Mikata, Y. and M. Taya (1985a), Stress field in a coated continuous fiber composite subjected to thermo-mechanical loadings, *J. Compos. Mater. 19*, 554.

Mikata, Y. and M. Taya (1985b), Stress field in and around a coated short fiber in an infinite matrix subjected to uniaxial and biaxial loadings, *J. Appl. Mech. 52*, 19.

Mikata, Y. and M. Taya (1986), Thermal stresses in a coated short fiber composite, *J. Appl. Mech. 53*, 681.

Pagano, N.J. and G.P. Tandon (1988), Elastic response of multi-directional coated-fiber composites, *Compos. Sci. Technol. 31*, 273.

Appendix

In this Appendix we prove a result which is of interest when the fibers are cylindrically orthotropic.

Consider a composite specimen containing aligned fibers of circular cylindrical shape and let the specimen be subjected to an axisymmetric loading together with a uniform temperature change (see Fig. A.1). The loading conditions on the specimen are

$$\sigma_{rr}(C) = \sigma_r^0, \quad \sigma_{zz}(\pm H) = 0 \tag{A.1}$$

where C denotes the cross-section of the specimen perpendicular to the fibers and $2H$ is the height of the specimen. For sufficiently long fibers the loading condition $(A.1_2)$ can be replaced by $\bar{\sigma}_z = 0$, so that it is satisfied in the St. Venant's sense. We will now show that it is possible to replace the cylindrically orthotropic fiber by an equivalent transversely isotropic fiber, without changing the stress field in the surrounding matrix. To achieve this, proceed in the following manner. Take out a single orthotropic fiber, load it by certain radial tractions σ^0, and uniform temperature change θ_0 and also allow a linear displacement in the z-direction given by

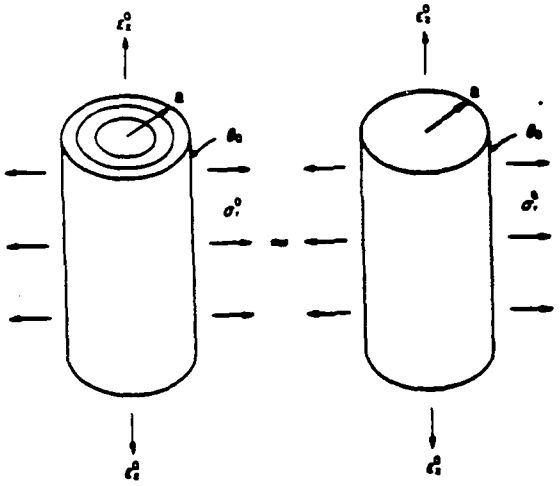

Fig. A.1. A schematic representation of equivalent fiber.

$$u_z = \epsilon_z^0 z. \tag{A.2}$$

Then, obtain the solution for the radial displacement $u_r|_{r=a}$ and $\bar{\sigma}_z^f$ where the latter denotes the average longitudinal stress in the fiber. Next, consider a transversely isotropic fiber with as yet unknown properties, load it again with σ_r^0, θ_0 and ϵ_z^0, and compute the radial displacement and average axial stress, now denoted by $u_r'|_{r=a}$ and $\bar{\sigma}_z^{f'}$.

Demand the equality

$$u_r|_{r=a} = u_r'|_{r=a}, \quad \bar{\sigma}_z^f = \bar{\sigma}_z^{f'} \tag{A.3}$$

as a basis for obtaining the properties of the transversely isotropic fiber. The following derivation shows that if the overall load remains axisymmetric it is indeed possible to replace the cylindrically orthotropic fiber with one which is transversely isotropic.

The results developed in the paper provide, after considerable manipulation:

$$\begin{aligned} u_r|_{r=a} = {} & \frac{a}{C_{rr}\eta + C_{r\phi}}\sigma_r^0 \\ & + \left[H_1 - \frac{C_{rr}H_1 + C_{r\phi}H_1 + C_{rz}}{C_{rr}\eta + C_{r\phi}}\right] a\epsilon_z^0 \\ & + \Big[H_2 + \big[(C_{rr}\alpha_r + C_{r\phi}\alpha_\phi + C_{rz}\alpha_z) \\ & \qquad - (C_{rr} + C_{r\phi})H_2\big] \\ & \times \{C_{rr}\eta + C_{r\phi}\}^{-1}\Big] a\theta_0 \end{aligned} \tag{A.4}$$

$$\bar{\sigma}_z^f = \frac{C_{rz}\eta + C_{\phi z}}{C_{rr}\eta + C_{r\phi}} \frac{2}{1+\eta}\sigma_r^0 + \left[(C_{rz}H_1 + C_{\phi z}H_1 + C_{zz}) - \frac{2}{1+\eta}\frac{C_{rz}\eta + C_{\phi z}}{C_{rr}\eta - C_{r\phi}} \times (C_{rr}H_1 + C_{r\phi}H_1 + C_{rz}) \right] \epsilon_z^0 + \theta_0 \Big\{ (C_{rz} + C_{\phi z})H_2 - (C_{rz}\alpha_r + C_{\phi z}\alpha_\phi + C_{zz}\alpha_z) + \frac{2}{1+\eta}\frac{C_{rz}\eta + C_{\phi z}}{C_{rr}\eta + C_{r\phi}} \times \left[(C_{rr}\alpha_r + C_{r\phi}\alpha_\phi + C_{rz}\alpha_z) - (C_{rr} + C_{r\phi})H_2 \right] \Big\} \tag{A.5}$$

$$u_r'|_a = \frac{a}{2k}\sigma_r^0 - \frac{a}{2}\frac{l}{k}\epsilon_z^0 + a\left(\alpha_T + \frac{l}{2k}\alpha_A\right)\theta_0 \tag{A.6}$$

$$\bar{\sigma}_z^{f\prime} = \frac{l}{k}\sigma_r^0 + \left(n - \frac{l^2}{k}\right)\epsilon_z^0 - \left(n - \frac{l^2}{k}\right)\alpha_A\theta_0 \tag{A.7}$$

where

$$\eta = \sqrt{\frac{C_{\phi\phi}}{C_{rr}}}, \quad H_1 = \frac{C_{\phi z} - C_{rz}}{C_{rr} - C_{\phi\phi}}$$

$$H_2 = \{(C_{rz} - C_{\phi z})\alpha_z + (C_{r\phi} - C_{\phi\phi})\alpha_\phi + (C_{rr} - C_{r\phi})\alpha_r\} \times \{C_{rr} - C_{\phi\phi}\}^{-1}. \tag{A.8}$$

Five constants k, l, n, α_T and α_A need to be determined, yet if one demands that the coefficients of σ_r^0, ϵ_z^0 and θ_0 be equal to each other in the respective expressions, then (A.4, A.5) and (A.6, A.7) give six equalities. Interestingly enough, it turns out that the second term in equation (A.4) is related to the first term in (A.5), which in turn is identical to the relation between the second term in (A.6) and the first term in (A.7). This fact, which can be proved after certain manipulations, reduces the number of equations to five, and provides a unique way for obtaining the effective properties of the cylindrically orthotropic fiber.

The resulting properties are:

$$k = (C_{rr}\eta + C_{r\phi})/2, \quad l = \frac{C_{rz}\eta + C_{\phi z}}{C_{rr}\eta + C_{r\phi}}\frac{2}{1+\eta}k$$

$$n = \frac{l^2}{k} + \left[(C_{rz}H_1 + C_{\phi z}H_1 + C_{zz}) - \frac{2}{1+\eta}\frac{C_{rz}\eta + C_{\phi z}}{C_{rr}\eta + C_{r\phi}} \times (C_{rr}H_1 + C_{r\phi}H_1 + C_{rz}) \right] \tag{A.9}$$

$$\alpha_A = -\left(n - \frac{l^2}{k}\right)^{-1} \times \Big\{ (C_{rz} + C_{\phi z})H_2 - (C_{rz}\alpha_r + C_{\phi z}\alpha_\phi + C_{zz}\alpha_z) + \frac{2}{1+\eta}\frac{(C_{rz}\eta + C_{\phi z})}{(C_{rr}\eta + C_{r\phi})} \times \left[(C_{rr}\alpha_r + C_{r\phi}\alpha_\phi + C_{rz}\alpha_z) - (C_{rr} + C_{r\phi})H_2 \right] \Big\} \tag{A.10}$$

$$\alpha_T = \left\{ H_2 + \left[(C_{rr}\alpha_r + C_{r\phi}\alpha_\phi + C_{rz}\alpha_z) - (C_{rr} + C_{r\phi})H_2 \right] \{C_{rr}\eta + C_{r\phi}\}^{-1} \right\} - \frac{l}{2k}\alpha_A.$$

Mechanics of Materials 12 (1991) 289–297
Elsevier

On effective properties of composites with coated cylindrically orthotropic fibers

Y. Benveniste [1], G.J. Dvorak and T. Chen

Department of Civil Engineering, Rensselaer Polytechnic Institute, Troy, NY 12180-3590, USA

Received 18 October 1990; revised version received 10 July 1991

Composite systems consisting of a matrix phase and coated inclusions with curvilinear anisotropy are considered, and a concise framework is established for analysis of their effective thermomechanical behavior. An exact relation between the effective thermal stress tensor and the purely mechanical influence functions of such media is derived. The presented analysis includes as a special case some previous work by the authors on composites with coated and cylindrically orthotropic fibers, e.g., carbon fibers. Furthermore, it allows to prove analytically certain symmetry and consistency properties of the effective thermomechanical tensors of such systems as approximated by the Mori–Tanaka micromechanical model.

1. Introduction

The present paper is the conclusion of two previous studies by the authors, Benveniste et al. (1989), and Chen et al. (1990) (denoted (I) and (II), respectively, in the following), on micromechanical modeling of composite systems reinforced with coated fibers which may be curvilinearly anisotropic. Interest in problems of this kind is motivated by the use of coated carbon fibers which may possess circumferential or radial orthotropy; see for example, Avery and Herakovich (1986), Hashin (1990), and other references cited in (I) and (II).

In the previous studies, we evaluated both the effective moduli and the local stresses in the phases in terms of the Mori–Tanaka (1973) estimates, within the framework developed by Benveniste (1987) and Benveniste and Dvorak (1990). However, the diagonal symmetry of the effective stiffness tensor $\boldsymbol{L}$ was verified only by numerical examples. Furthermore, the effective thermal stress tensor $\boldsymbol{l}$ was evaluated by a direct application of the Mori–Tanaka method, but consistency of the obtained results with the alternative provided by a Levin-type procedure was not established (Levin, 1967).

The paper has three major objectives: (a) to establish a transparent and concise framework for computation of the effective thermomechanical moduli of composite systems reinforced by curvilinearly anisotropic, coated inclusions; (b) to extend the validity of the Levin-type relationship to composites of this kind; and (c) for the fibrous systems considered in (I) and (II), and for the micromechanics model used therein, to establish analytically the diagonal symmetry of the predicted $\boldsymbol{L}$ tensor, and consistency between the "direct" and Levin's derivations of the effective thermal stress tensor $\boldsymbol{l}$.

2. Effective thermomechanical behavior of composite media with curvilinear anisotropy

Let us consider a composite medium consisting of a rectilinear matrix phase and inhomogeneous inclusions. The term "inhomogeneous inclusion" is used here to describe a reinforcing particle or fiber which has variable thermomechanical moduli

[1] Visiting from Department of Solid Mechanics, Materials and Structures, Faculty of Engineering, Tel-Aviv University, Tel-Aviv, Israel.

in a fixed Cartesian coordinate system, or which consists of several homogeneous phases.

In general, the local thermoelastic constitutive equations in such systems can be described as:

$$\begin{aligned} \sigma_m(x) &= L_m \epsilon_m(x) + l_m \theta, \\ \sigma_f(x) &= L_f(x)\, \epsilon_f(x) + l_f(x)\theta, \end{aligned} \tag{1}$$

where σ_s, ϵ_s, θ, L_s, l_s, with $s = f, m$, denote respectively the stresses, strains, temperature, and the stiffness and thermal stress tensors in the inhomogeneous inclusion (f) and matrix (m), respectively, all written with respect to a fixed Cartesian system. Note that the L_m and l_m tensors, being rectilinearly anisotropic, are independent of x.

Examples of such systems are composites consisting of a rectilinearly anisotropic matrix reinforced by non-coated or coated cylindrically orthotropic carbon fibers, or simply reinforced by coated fibers with an isotropic core and coating. In a cylindrically orthotropic carbon fiber, the stiffness and thermal stress tensors are constant when written in terms of a coordinate system located at the center of the fiber with the three axis pointing in the axial, tangential and radial directions respectively. There are nine stiffness and three thermal expansion coefficients, (see (II), for example). Obviously, the space dependent Cartesian $L_f(x)$, $l_f(x)$ tensors are related to these constants through the usual transformation law which depends on the polar coordinate ϕ, itself a function of the generic point x. A coated fiber on the other hand, even if it consists of an isotropic and homogeneous core and coating, may also be considered as an "inhomogeneous inclusion." In this case the tensors $L_f(x)$ and $l_f(x)$ are equal to the constant tensors of the core (L_c, l_c) or the coating (L_g, l_g), depending on the position of the generic point x within the fiber. Such a coated fiber is therefore an "inhomogeneous inclusion" possessing piecewise constant materials properties.

In this section we provide a framework for the computation of the effective properties of the type of composite systems described above. The inhomogeneous inclusions will be formally denoted by the tensors $L_f(x)$ and $l_f(x)$, irrespective of their internal structure. These inclusions may be uncoated or coated inclusions with curvilinearly anisotropic constituents.

The effective behavior of the composite is given as

$$\bar{\sigma} = L\bar{\epsilon} + l\theta, \tag{2}$$

where L and l are overall stiffness and thermal strain tensors, and $\bar{\sigma}$, $\bar{\epsilon}$ denote volume averages of the local stresses and strains, over a representative volume element. These averages are given by:

$$\bar{\sigma} = c_f\bar{\sigma}_f + c_m\bar{\sigma}_m, \quad \bar{\epsilon} = c_f\bar{\epsilon}_f + c_m\bar{\epsilon}_m, \tag{3}$$

where $\bar{\sigma}_s$, $\bar{\epsilon}_s$, denote averages over the phases, and c_f, c_m denote the volume fractions of the inhomogeneous inclusions and matrix respectively.

Equations for the determination of L and l can be derived by considering homogeneous boundary conditions on a representative volume element of the composite as follows:

$$u(S) = \epsilon_0 x, \quad \theta(S) = \theta_0, \tag{4}$$

which results in

$$\bar{\epsilon} = \epsilon_0, \quad \theta(x) = \theta_0. \tag{5}$$

Define now the influence functions

$$\begin{aligned} \epsilon_f(x) &= A_f(x)\, \epsilon_0 + a_f(x)\, \theta_0, \\ \sigma_f(x) &= \tilde{A}_f(x)\, \epsilon_0 + \tilde{a}_f(x)\, \theta_0, \end{aligned} \tag{6}$$

so that, from $(1)_1$, it follows:

$$\begin{aligned} \tilde{A}_f(x) &= L_f(x)\, A_f(x), \\ \tilde{a}_f(x) &= L_f(x)\, a_f(x) + l_f(x). \end{aligned} \tag{7}$$

Equations (1)–(3) and (5) can be shown to provide

$$\begin{aligned} L &= L_m + c_f(\tilde{A}_f - L_m A_f), \\ l &= c_m l_m + c_f(\tilde{a}_f - L_m a_f), \end{aligned} \tag{8}$$

where the "concentration factors" $\tilde{A}_f$, A_f, $\tilde{a}_f$, a_f, without the argument (x), are the volume averages of the respective influence functions in the fiber:

$$\bar{\sigma}_f = \tilde{A}_f\epsilon_0 + \tilde{a}_f\theta_0, \quad \bar{\epsilon}_f = A_f\epsilon_0 + a_f\theta_0. \tag{9}$$

Equation (8) is the main result of this section. Together with Eq. (9), it allows us to treat the coated-fiber systems described above as two-phase

systems consisting of a rectilinearly anisotropic matrix reinforced by "inhomogeneous inclusions" characterized by $\boldsymbol{L}_f(\boldsymbol{x})$ and $\boldsymbol{l}_f(\boldsymbol{x})$.

In order to make more transparent the implementation of Eq. (8), consider, for example, a composite system consisting of a rectilinearly anisotropic matrix and aligned coated fibers with a cylindrically orthotropic core and coating. Suppose that we are interested in obtaining the dilute approximation $\boldsymbol{L}_{\text{dil}}$ for the effective stiffness tensor. To this end, we embed a coated fiber in the infinite matrix and subject it at infinity to (4) with $\theta_0 = 0$. Choosing, for convenience, a cylindrical coordinate system, this auxiliary problem is solved and the solution for strain and stress fields in the coated inclusion is obtained in terms of their cylindrical components. Next, using the usual transformation law, the Cartesian components $\boldsymbol{\epsilon}_f(\boldsymbol{x})$ and $\boldsymbol{\sigma}_f(\boldsymbol{x})$ of the strain and stress tensors and their average $\bar{\boldsymbol{\epsilon}}_f$ and $\bar{\boldsymbol{\sigma}}_f$ are recovered. Use of these values in (9) yields the desired tensors $\boldsymbol{A}_f$ and $\tilde{\boldsymbol{A}}_f$, and their substitution into $(8)_1$, provides the dilute approximation $\boldsymbol{L}_{\text{dil}}$. A detailed description of this procedure which is in fact valid for any micromechanics model is given in the Appendix.

Clearly, if the inclusion is homogeneous with its properties described by a pair of constant rectilinearly anisotropic Cartesian tensor $\boldsymbol{L}_f$ and $\boldsymbol{l}_f$, it follows from (7) that

$$\tilde{\boldsymbol{A}}_f = \boldsymbol{L}_f \boldsymbol{A}_f, \quad \tilde{\boldsymbol{a}}_f = \boldsymbol{L}_f \boldsymbol{a}_f + \boldsymbol{l}_f \tag{10}$$

so that the expressions in (8) reduce to their familiar forms:

$$\begin{aligned} \boldsymbol{L} &= \boldsymbol{L}_m + c_f(\boldsymbol{L}_f - \boldsymbol{L}_m)\, \boldsymbol{A}_f, \\ \boldsymbol{l} &= c_f \boldsymbol{l}_f + c_m \boldsymbol{l}_m + c_f(\boldsymbol{L}_f - \boldsymbol{L}_m)\, \boldsymbol{a}_f. \end{aligned} \tag{11}$$

A similar dual framework can be formulated for the compliance and thermal strain tensor $\boldsymbol{M}_s$ and $\boldsymbol{m}_s$ and their effective counterparts $\boldsymbol{M}$ and $\boldsymbol{m}$, but will be omitted here for brevity.

Finally, we should mention here that in dealing with coated fibrous composites, the analysis in (I) and (II) made in fact *implicit* use of (8). This could be best understood by recalling that the employed micromechanics model in these papers was Mori–Tanaka's theory which utilized the auxiliary configuration of a coated particle (as an entity) in an infinite matrix. The equations in (I) and (II) were however set up for the more general case of hybrid composites consisting of more than one type of reinforcement. We now believe that when dealing with coated inclusions the present framework gives a more concise method of dealing with such systems. It also allows us to discuss properties of general nature in Sections 3, 5 and 6 below. The present section, together with Sections 3, 5 and 6 achieve in fact the major objectives of this paper. For a detailed implementation of the Mori–Tanaka method to systems with coated and curvilinearly anisotropic inclusions the reader is referred to (I) and (II).

3. Exact relations between effective thermal and mechanical properties

It can now be shown that the effective thermal tensor $\boldsymbol{l}$ follows solely from the knowledge of the influence function $\boldsymbol{A}_f(\boldsymbol{x})$. This provides an alternative to Eq. $(8)_2$ and leads to an exact relation between certain averages of the mechanical and thermal influence functions.

These results can be found from the virtual work theorem, as done by Levin (1967) in composite media with isotropic consituents. The procedure is exactly the same, but the inhomogeneous inclusion is treated with regard to its space dependent moduli. To this end, two alternative boundary conditions are considered on the external surface S of the composite:

$$\boldsymbol{u}'(S) = \boldsymbol{\epsilon}' \boldsymbol{x}, \quad \theta'(S) = 0, \tag{12}$$

$$\boldsymbol{u}(S) = 0, \qquad \theta(S) = \theta_0. \tag{13}$$

According to the theorem of virtual work, we write

$$\int_V \sigma'_{ij}(\boldsymbol{x})\, \epsilon_{ij}(\boldsymbol{x})\, \mathrm{d}V = \int_S t'_i(\boldsymbol{x})\, u_i(\boldsymbol{x})\, \mathrm{d}S, \tag{14}$$

as well as

$$\int_V \sigma_{ij}(\boldsymbol{x})\, \epsilon'_{ij}(\boldsymbol{x})\, \mathrm{d}V = \int_S t_i(\boldsymbol{x})\, u'_i(\boldsymbol{x})\, \mathrm{d}S, \tag{15}$$

where t_i denotes the traction vector on S. The procedure described by Levin (1967), and (14) and (15) eventually provide

$$\boldsymbol{l} = c_m \boldsymbol{A}_m^T \boldsymbol{l}_m + c_f \frac{1}{V_f} \int_{V_f} \boldsymbol{A}_f^T(\boldsymbol{x})\, \boldsymbol{l}_f(\boldsymbol{x})\, dV, \tag{16}$$

where $\boldsymbol{A}_m^T$ is the transpose of the averaged influence function $\boldsymbol{A}_m$ defined under the boundary conditions (4), at $\theta_0 = 0$. Then,

$$\bar{\boldsymbol{\epsilon}}_m = \boldsymbol{A}_m \boldsymbol{\epsilon}_0, \tag{17}$$

that satisfies

$$c_m \boldsymbol{A}_m + c_f \boldsymbol{A}_f = \boldsymbol{I}, \tag{18}$$

where $\boldsymbol{I}$ is the fourth-order unit tensor.

Thus Eq. (16) can also be written as

$$\boldsymbol{l} = (\boldsymbol{I} - c_f \boldsymbol{A}_f^T)\boldsymbol{l}_m + c_f \frac{1}{V_f} \int_{V_f} \boldsymbol{A}_f^T(\boldsymbol{x})\, \boldsymbol{l}_f(\boldsymbol{x})\, dV. \tag{19}$$

This last expression provides an alternative to Eq. $(8)_2$ for evaluation of $\boldsymbol{l}$, and leads after some manipulation to the following exact relation between the mechanical and thermal influence functions and their averages:

$$(\boldsymbol{I} - \boldsymbol{A}_f^T)\boldsymbol{l}_m + \frac{1}{V_f} \int_{V_f} \boldsymbol{A}_f^T(\boldsymbol{x})\, \boldsymbol{l}_f(\boldsymbol{x})\, dV = \bar{\boldsymbol{a}}_f - \boldsymbol{L}_m \boldsymbol{a}_f. \tag{20}$$

It can be readily verified that for an inclusion which is described by a single pair of constant $\boldsymbol{L}_f$ and $\boldsymbol{l}_f$ tensors, Eq. (19) in conjunction with $(11)_1$ provides

$$\boldsymbol{l} = \boldsymbol{l}_m + (\boldsymbol{L}_m - \boldsymbol{L})(\boldsymbol{L}_f - \boldsymbol{L}_m)^{-1}(\boldsymbol{l}_m - \boldsymbol{l}_f), \tag{21}$$

while (20) gives another familiar form:

$$\boldsymbol{a}_f = (\boldsymbol{I} - \boldsymbol{A}_f)(\boldsymbol{L}_m - \boldsymbol{L}_f)^{-1}(\boldsymbol{l}_f - \boldsymbol{l}_m). \tag{22}$$

4. The Mori–Tanaka (MT) model

In the two recent papers (I) and (II), we have been concerned with modeling of coated carbon fiber composites, in which the fiber core was cylindrically orthotropic. Both the effective moduli and the local stresses were of interest, and were estimated by the Mori–Tanaka (1973) approximation, in the form developed by Benveniste (1987), and Benveniste and Dvorak (1990).

As mentioned in Section 2, the description of the Mori–Tanaka theory in (I) and (II) was given for general three-phase composite systems which may consist, for example, either of coated inclusions, or two kinds of fibers in a matrix. As explained in that work, this micromechanics model makes use of an "auxiliary configuration" in which a typical inclusion is embedded in an infinite matrix which is subjected at infinity to the average matrix strain. In the application of the model to the coated-fiber composites, the typical embedded inclusion *is* a coasted particle, and thus the implementation can be carried out in the framework of two-phase composites in which a matrix is reinforced by "inhomogeneous inclusions". The inhomogeneous inclusion is now the coated particle.

Specifically, the basic assumption of the micromechanics model amounts to expressing the average strains $\bar{\boldsymbol{\epsilon}}_f$ and stresses $\bar{\boldsymbol{\sigma}}_f$ in the coated inclusion in the form of:

$$\bar{\boldsymbol{\epsilon}}_f = \boldsymbol{T}\bar{\boldsymbol{\epsilon}}_m + \boldsymbol{t}\theta_0, \quad \bar{\boldsymbol{\sigma}}_f = \tilde{\boldsymbol{T}}\bar{\boldsymbol{\epsilon}}_m + \tilde{\boldsymbol{t}}\theta_0, \tag{23}$$

where the fourth- and second-order tensors $\boldsymbol{T}$, $\tilde{\boldsymbol{T}}$, $\boldsymbol{t}$ and $\tilde{\boldsymbol{t}}$ give the average strains and stresses in a single coated inclusion within an infinite matrix subjected to the conditions (4) at infinity. Specifically,

$$\bar{\boldsymbol{\epsilon}}_s = \boldsymbol{T}\boldsymbol{\epsilon}_0 + \boldsymbol{t}\theta_0, \quad \bar{\boldsymbol{\sigma}}_s = \tilde{\boldsymbol{T}}\boldsymbol{\epsilon}_0 + \tilde{\boldsymbol{t}}\theta_0, \tag{24}$$

where the subscript s indicates a solitary coated inclusion in an infinite matrix. It can be shown that Eq. (23), in conjunction with $(3)_2$, (5) and (8) provides after some manipulation the MT estimates

$$\boldsymbol{L} = \boldsymbol{L}_m + c_f \left\{ \left[(\tilde{\boldsymbol{L}} - \boldsymbol{L}_m)\boldsymbol{T} \right]^{-1} c_m + c_f (\tilde{\boldsymbol{L}} - \boldsymbol{L}_m)^{-1} \right\}^{-1}, \tag{25}$$

$$\boldsymbol{l} = c_f (\tilde{\boldsymbol{L}} - \boldsymbol{L})\boldsymbol{t} + c_m \boldsymbol{l}_m + c_f \tilde{\boldsymbol{l}}, \tag{26}$$

where the fourth- and second-order tensors $\tilde{\boldsymbol{L}}$ and $\tilde{\boldsymbol{l}}$ are defined as

$$\tilde{\boldsymbol{T}} = \tilde{\boldsymbol{L}}\boldsymbol{T}, \quad \tilde{\boldsymbol{l}} = \tilde{\boldsymbol{t}} - \tilde{\boldsymbol{L}}\boldsymbol{t}. \tag{27}$$

The tensors $\tilde{\boldsymbol{L}}$ and $\tilde{\boldsymbol{l}}$ interrelate the average stress, strain and temperature of a single inhomogeneous inclusion (or coated inclusion in the present case), when it is embedded in an infinite matrix which is subjected at infinity to boundary conditions, i.e.

$$\bar{\boldsymbol{\sigma}} = \tilde{\boldsymbol{L}}\bar{\boldsymbol{\epsilon}} + \tilde{\boldsymbol{l}}\theta_0. \tag{28}$$

Since $\tilde{\boldsymbol{L}}$ and $\tilde{\boldsymbol{l}}$ have been defined in this manner, they cannot be considered in general to represent the effective moduli of the inhomogeneous inclusion.

It should be noted that a somewhat different formalism, which is actually equivalent to that introduced in the present Eqs. (23), (25) and (26), was adopted in (II). The present treatment is more transparent and convenient to use in the subsequent proofs of diagonal symmetry of the predicted effective tensors.

From their definition in (23), it is clear that the $\boldsymbol{T}$, $\tilde{\boldsymbol{T}}$, $\boldsymbol{t}$ and $\tilde{\boldsymbol{t}}$ tensors possess the following symmetry properties:

$$T_{ijkl} = T_{jikl} = T_{jilk}, \quad t_{ij} = t_{ji}, \tag{29}$$

$$\tilde{T}_{ijkl} = \tilde{T}_{jikl} = \tilde{T}_{jilk}, \quad \tilde{t}_{ij} = \tilde{t}_{ji},$$

so that from (27)

$$\tilde{L}_{ijkl} = \tilde{L}_{jikl} = \tilde{L}_{jilk}, \quad \tilde{l}_{ij} = \tilde{l}_{ji}. \tag{30}$$

Thus, Eqs. (25) and (26) imply that the approximate $\boldsymbol{L}$ and $\boldsymbol{l}$ tensors satisfy

$$L_{ijkl} = L_{jikl} = L_{jilk}, \quad l_{ij} = l_{ji}. \tag{31}$$

However, it is not obvious that the MT estimate of the $\boldsymbol{L}$ tensor is diagonally symmetric ($L_{ijkl} = L_{klij}$), this property needs to be investigated.

5. Diagonal symmetry of the $\boldsymbol{L}$ tensor

Suppose that the inhomogeneous inclusions are described by a space dependent tensor $\boldsymbol{L}_f(\boldsymbol{x})$ which is diagonally symmetric, and that the same property holds for the $\boldsymbol{L}_m$ tensor. An examination of (25) shows that the term $(\tilde{\boldsymbol{L}} - \boldsymbol{L}_m)\boldsymbol{T}$ on the right hand side is exactly identical to that which would appear in the dilute approximation formula:

$$\boldsymbol{L}_{dil} = \boldsymbol{L}_m + c_f(\tilde{\boldsymbol{L}} - \boldsymbol{L}_m)\boldsymbol{T}. \tag{32}$$

Since the diagonal symmetry of $\boldsymbol{L}_{dil}$ can be established from the reciprocal theorem of elasticity (Benveniste, Dvorak and Chen, 1991), it turns out that $(\tilde{\boldsymbol{L}} - \boldsymbol{L}_m)\,\boldsymbol{T}$ is diagonally symmetric. Therefore, the diagonal symmetry of the $\boldsymbol{L}$ tensor in (25) depends on the symmetry of the $\tilde{\boldsymbol{L}}$ tensor.

Unfortunately no general statement seems possible concerning the diagonal symmetry of $\tilde{\boldsymbol{L}}$. However, in the auxiliary problem of a solitary inclusion in an infinite matrix, one may consider specific circumstances under which the displacement field induced at the interface S_s of the inclusion and matrix is of the type

$$\boldsymbol{u}(S_s) = \boldsymbol{\epsilon}^* \boldsymbol{x}, \tag{33}$$

where $\boldsymbol{\epsilon}^*$ is a constant strain tensor. Then, Hill's (1963) formula suggests that

$$\frac{1}{V_s}\int_{V_s} \boldsymbol{\epsilon}_s \boldsymbol{\sigma}_s \, dV = \bar{\boldsymbol{\epsilon}}_s \bar{\boldsymbol{\sigma}}_s = \bar{\boldsymbol{\epsilon}}_s \tilde{\boldsymbol{L}} \bar{\boldsymbol{\epsilon}}_s, \tag{34}$$

which establishes the diagonal symmetry of the $\tilde{\boldsymbol{L}}$ tensor under the said conditions. This result will be useful in the sequel in proving the diagonal symmetry of the $\boldsymbol{L}$ tensor in (25) for the composite media analyzed in (I) and (II). We recall that the systems considered there consist of a matrix and aligned cylindrical fibers with a circular cross-section. The matrix and coating are at most transversely isotropic, while the fibers may be circumferentially or radially orthotropic.

Define now a Cartesian coordinate system (x_1, x_2, x_3) with the x_1-axis aligned along the direction of the fibers. Also, x_1 is the axis of overall rotational symmetry, and the effective composite medium is transversely isotropic. The overall properties are described by Hill's five elastic moduli k, l, n, G_L, and G_T, where n is the uniaxial modulus, l is the corresponding cross-modulus, and k, G_L, and G_T are respectively the plane strain bulk modulus, and longitudinal and transverse shear moduli.

The evaluation of n and l requires application of the following boundary conditions to the representative volume element of the composite:

$$u_1(S) = \epsilon_0 x_1, \quad u_2(S) = u_3(S) = 0, \tag{35}$$

whereas the determination of k, G_L and G_T calls, respectively, for the following boundary conditions on S:

$$u_1(S) = 0, \quad u_2(S) = \epsilon_0 x_2, \quad u_3(S) = \epsilon_0 x_3, \tag{36}$$

$$u_1(S) = \epsilon_0 x_3, \quad u_2(S) = 0, \quad u_3(S) = \epsilon_0 x_1, \tag{37}$$

$$u_1(S) = 0, \quad u_2(S) = \epsilon_0 x_2, \quad u_3(S) = -\epsilon_0 x_3. \tag{38}$$

For the auxiliary problem of a single cylindrical fiber in an infinite matrix with which we were concerned in (I) and (II), the boundary conditions (35) and (36) induce an axisymmetric displacement field, whereas (37) result in an anti-plane field. Both of these solutions produce at the interface S_s of the solitary fiber a displacement field of the type (33). Specific form of the solution appears in (II). Thus the $\tilde{L}$ tensor pertaining to these loading conditions is diagonally symmetric. Unfortunately, the last boundary condition (38) does not induce at the interface S_s a displacement field of the type (33). Therefore, a different way needs to be found to prove the symmetry of $\tilde{L}$ in this case. The argument which will be given here uses the rotational symmetry of the system, in conjunction with the loading configuration described by (38), to show that the average strain and stress tensors in the inhomogeneous fiber with rotational symmetry can be described by

$$\bar{\epsilon}_s = \begin{bmatrix} 0 & 0 & 0 \\ 0 & \alpha & 0 \\ 0 & 0 & -\alpha \end{bmatrix}, \quad \bar{\sigma}_s = \begin{bmatrix} \gamma & 0 & 0 \\ 0 & \beta & 0 \\ 0 & 0 & -\beta \end{bmatrix}. \tag{39}$$

With this result, the transformation between $\bar{\sigma}_s$ and $\bar{\epsilon}_s$ in (28), at $\theta_0 = 0$, can be explicitly written as

$$\begin{aligned} \gamma &= \tilde{L}_{1122}\alpha + \tilde{L}_{1133}(-\alpha), \\ \beta &= \tilde{L}_{2222}\alpha + \tilde{L}_{2233}(-\alpha), \\ -\beta &= \tilde{L}_{3322}\alpha + \tilde{L}_{3333}(-\alpha). \end{aligned} \tag{40}$$

However, rotational symmetry requires

$$\tilde{L}_{1122} = \tilde{L}_{1133}, \quad \tilde{L}_{2222} = \tilde{L}_{3333}. \tag{41}$$

This implies that $\gamma = 0$, together with

$$\beta = \tilde{L}_{2222}\alpha - \tilde{L}_{2233}\alpha, \quad -\beta = \tilde{L}_{3322}\alpha - \tilde{L}_{2222}\alpha. \tag{42}$$

Adding the last two equations yields

$$\tilde{L}_{3322} = \tilde{L}_{2233}. \tag{43}$$

We have therefore shown that under (38), the transformation (28), with $\theta_0 = 0$, reduces to

$$(\bar{\sigma}_{22})_s = \tilde{L}_{2222}(\bar{\epsilon}_{22})_s + \tilde{L}_{2233}(\bar{\epsilon}_{33})_s, \tag{44}$$

$$(\bar{\sigma}_{33})_s = \tilde{L}_{3322}(\bar{\epsilon}_{22})_s + \tilde{L}_{3333}(\bar{\epsilon}_{33})_s, \tag{45}$$

which, together with (43), establishes the diagonal symmetry of $\tilde{L}$ in this case.

This concludes the proof of the diagonal symmetry of $\tilde{L}$, and thus also of the MT estimate of L, for the systems considered in (I) and (II).

6. Consistency of the effective thermal strain tensor

We have shown in Section 3 that all derivations of the effective thermal stress tensor l must satisfy (20). Alternatively, it can be said that any model should predict the same effective thermal tensor either from (19), or by a direct application of the model to Eq. $(8)_2$. A general proof of such consistency property of the Mori–Tanaka method for arbitrarily shaped coated inclusions seems to be beyond reach. However, for the fibrous system with cylindrical fibers considered in (I) and (II), a consistency proof is given in the sequel.

First, note that Eq. (20) must hold for the dilute approximation, i.e.

$$(I - T^T)l_m + \frac{1}{V_f}\int_{V_f} T^T(x)\, l_f(x)\, dV = \tilde{l} - L_m t. \tag{46}$$

Since the dilute approximation makes recourse to an exact solution of the auxiliary problem, the boundary conditions (12) and (13), together with

(14) and (15), can be used (as in the derivation of (20)) to show that (46) is in fact valid.

Next, we recall that the concentration factors and influence function appearing in (20) are predicted in the framework of the Mori–Tanaka method as follows:

$$\boldsymbol{A}_f(x) = \boldsymbol{T}(x)(c_m\boldsymbol{I} + c_f\boldsymbol{T})^{-1},$$
$$\tilde{\boldsymbol{a}}_f - \boldsymbol{L}_m\boldsymbol{a}_f = \tilde{\boldsymbol{t}} - \boldsymbol{L}\boldsymbol{t}; \tag{47}$$

this may be found in (II). Therefore, the requirement that Eq. (20) be satisfied by the MT model reduces to

$$\left[\boldsymbol{I} - (c_m\boldsymbol{I} + c_f\boldsymbol{T}^T)^{-1}\boldsymbol{T}^T\right]^{-1}\boldsymbol{l}_m + \frac{1}{V_f}(c_m\boldsymbol{I} + c_f\boldsymbol{T}^T)^{-1}\int_{V_f}\boldsymbol{T}^T(x)\,\boldsymbol{l}_f(x)\,dV = \tilde{\boldsymbol{t}} - \boldsymbol{L}\boldsymbol{t}. \tag{48}$$

Unfortunately, it does not seem possible to prove that (46), by itself, implies validity of (48) for general systems with curvilinear anisotropy.

Therefore, we focus on the fibrous systems considered in (I) and (II) and prove the validity of (48) by exploiting the idea of the "replacement fiber," established in (II) and also independently by Hashin (1990). Under an axisymmetric stress state, a circular cylindrical fiber possessing radial or circumferential orthotropy can be replaced by an equivalent transversely isotropic fiber. This has no effect on either the average stress in the fiber, or on the local displacement and traction fields at its lateral surface. Therefore, the introduction of the replacement fiber does not affect the average strains and stresses in a fibrous system under a uniform thermal change.

The $\boldsymbol{T}$, $\boldsymbol{t}$ and $\tilde{\boldsymbol{t}}$ tensors in (46) and (48) relate to a single fiber in an infinite matrix under axisymmetric loading. Since they describe the average strain and stress within the fiber, they are not affected by introduction of the replacement fiber. Therefore,

$$\boldsymbol{T} = \boldsymbol{T}_R, \quad \tilde{\boldsymbol{t}} = \tilde{\boldsymbol{t}}_R, \quad \boldsymbol{t} = \boldsymbol{t}_R, \tag{49}$$

where the subscript R refers to the replacement fiber.

Note also that Eq. (46) is valid in the present circumstances, and write it first for the actual fiber with curvilinear anisotropy and then for the replacement fiber. From (49) it follows that

$$\int_{V_f}\boldsymbol{T}^T(x)\,\boldsymbol{l}_f(x)\,dV = \boldsymbol{T}_R^T(\boldsymbol{l}_f)_R V_f. \tag{50}$$

where $(\boldsymbol{l}_f)_R$ is the thermal stress tensor of the replacement fiber.

Coming back to Eq. (48), we recall that its validity for the case of transversely isotropic fibers has already been established in a recent paper by Benveniste et al. (1991), and that under axisymmetric loading the last term in (48) satisfies

$$\boldsymbol{L}_R\boldsymbol{t}_R = \boldsymbol{L}\boldsymbol{t} \tag{51}$$

where $\boldsymbol{L}_R$ is the effective modulus given by (25) for a system with the "replacement fibers". Rewriting of (48) for the replacement fiber gives:

$$\left[\boldsymbol{I} - (c_m\boldsymbol{I} + c_f\boldsymbol{T}_R^T)^{-1}\boldsymbol{T}_R^T\right]^{-1}\boldsymbol{l}_m + (c_m\boldsymbol{I} + c_f\boldsymbol{T}_R^T)^{-1}\left[\boldsymbol{T}_R^T(\boldsymbol{l}_f)_R V_f\right] = \tilde{\boldsymbol{t}}_R - \boldsymbol{L}_R\boldsymbol{t}_R. \tag{52}$$

Finally, compare (52) and (48) to show that the validity of (48) follows from (50); Q.E.D.

Acknowledgement

This work was supported by the ONR/DARPA-HiTASC program at Rensselaer.

References

Avery, N.B. and C.T. Herakovich (1986), Effect of fiber anisotropy on thermal stresses in fibrous composites, *J. Appl. Mech. 53*, 751.

Benveniste, Y. (1987), A new approach to the application of Mori–Tanaka's theory in composite materials, *Mech. Mater. 6*, 147.

Benveniste, Y., G.J. Dvorak and T. Chen (1989), Stress fields in composites with coated inclusions, *Mech. Mater. 7*, 305.

Benveniste, Y. and G.J. Dvorak (1990), On a correspondence between mechanical and thermal effects in two-phase composites, in: *Toshio Mura Anniversary Volume: Micromechanics and Inhomogeneity*, Eds. G.J. Weng, M. Taya and H. Abé, Springer, Berlin, pp. 65–81.

Benveniste, Y., G.J. Dvorak and T. Chen (1991), On diagonal and elastic symmetry of the approximate effective stiffness

tensor of heterogeneous media, *J. Mech. Phys. Solids*, in press.

Chen, T., G.J. Dvorak and Y. Benveniste (1990), Stress fields in composites reinforced by coated cylindrically orthotropic fibers, *Mech. Mater. 9*, 17.

Hashin, Z. (1990), Thermoelastic properties and conductivity of carbon/carbon fiber composites, *Mech. Materials 8*, 293.

Hill, R. (1963), Elastic properties of reinforced solids: some theoretical principles, *J. Mech. Phys. Solids 11*, 357.

Levin, V.M. (1967), Thermal expansion coefficients of heterogeneous materials, *Mekh. Tverd. Tela 2*, 88.

Mori, T. and K. Tanaka (1973), Average stress in matrix and average elastic energy of materials with misfitting inclusions, *Acta Metall. 21*, 571.

Appendix

Consider a coated cylindrical fiber with a core and coating which are cylindrically orthotropic. Let the fiber cross section be circular, with the core and outside radius being given by a and b. In this Appendix we will illustrate the tensors $\boldsymbol{L}_f(x)$ and $\boldsymbol{l}_f(x)$ for this system, also also explain in detail the procedure which leads to the representation of the $\boldsymbol{A}_f(x)$, $\boldsymbol{a}_f(x)$ and $\tilde{\boldsymbol{A}}_f(x)$, $\tilde{\boldsymbol{a}}_f(x)$ tensors.

Since both the core and the coating are cylindrically orthotropic, the constitutive equations are conveniently represented in terms of a cylindrical coordinate system located at the center of the fiber.

$$\begin{Bmatrix} \sigma_r \\ \sigma_\phi \\ \sigma_z \\ \sigma_{r\phi} \\ \sigma_{z\phi} \\ \sigma_{rz} \end{Bmatrix}^{(s)} = \begin{bmatrix} c_{rr} & c_{r\phi} & c_{rz} & 0 & 0 & 0 \\ c_{\phi r} & c_{\phi\phi} & c_{\phi z} & 0 & 0 & 0 \\ c_{zr} & c_{z\phi} & c_{zz} & 0 & 0 & 0 \\ 0 & 0 & 0 & G_{r\phi} & 0 & 0 \\ 0 & 0 & 0 & 0 & G_{z\phi} & 0 \\ 0 & 0 & 0 & 0 & 0 & G_{rz} \end{bmatrix}^{(s)} \times \begin{Bmatrix} \epsilon_r - \alpha_r\theta_0 \\ \epsilon_\phi - \alpha_\phi\theta_0 \\ \epsilon_z - \alpha_z\theta_0 \\ 2\epsilon_{r\phi} \\ 2\epsilon_{z\phi} \\ 2\epsilon_{rz} \end{Bmatrix}^{(s)}, \quad s = \mathrm{c}, \mathrm{g}, \tag{A.1}$$

where c_{ij}, $G_{r\phi}$, $G_{z\phi}$ and G_{rz} are the stiffness coefficients, α_i are the linear coefficients of thermal expansion, and c denotes the core whereas g denotes the coating (see (II)). This constitutive equation will be formally represented as

$$\boldsymbol{\sigma}_s'(\xi) = \boldsymbol{L}_s'(\xi)\,\boldsymbol{\epsilon}_s'(\xi) + \boldsymbol{l}_s'(\xi)\,\theta_0, \quad s = \mathrm{c}, \mathrm{g}, \tag{A.2}$$

where the primes indicate that all the quantities are referred to the cylindrical coordinate system which is now denoted by ξ.

Let the transformation between the current and the Cartesian components of the fields at any point within the fiber be described by

$$\boldsymbol{\sigma}_s(x) = \boldsymbol{R}\boldsymbol{\sigma}_s'(\xi), \quad \boldsymbol{\epsilon}_s(x) = \boldsymbol{Q}\boldsymbol{\epsilon}_s'(\xi) \tag{A.3}$$

Note that $\boldsymbol{R} \neq \boldsymbol{Q}$ since according to the conventional use in the literature there is a 2-term in the shear terms of the strain vector. In a transformation between the cylindrical and Cartesian systems, $\boldsymbol{R}$ and $\boldsymbol{Q}$ are functions of the angle ϕ and therefore of the x_1, x_2 Cartesian coordinates of the generic point. For this specific transformation it turns out that $\boldsymbol{R}^{\mathrm{T}} = \boldsymbol{Q}^{-1}$. Equations (A.2) and $(A.3)_1$ provide

$$\boldsymbol{\sigma}_s(x) = \boldsymbol{R}(x)\,\boldsymbol{L}_s'\boldsymbol{Q}^{-1}(x)\,\boldsymbol{\epsilon}_s(x) + \boldsymbol{R}(x)\,\boldsymbol{l}_s'\theta_0 \tag{A.4}$$

so that we can write $\boldsymbol{L}_f(x)$ and $\boldsymbol{l}_f(x)$ for the coated fiber as follows:

$$\begin{aligned} \boldsymbol{L}_f(x) &= \boldsymbol{R}(x)\,\boldsymbol{L}_c'\boldsymbol{Q}^{-1}(x)\,f_s(x) \\ &\quad + \boldsymbol{R}(x)\,\boldsymbol{L}_g'\boldsymbol{Q}^{-1}(x)\big[1 - f_s(x)\big], \\ \boldsymbol{l}_f(x) &= \boldsymbol{R}(x)\,\boldsymbol{l}_c' f_s(x) + \boldsymbol{R}(x)\boldsymbol{l}_g'\big[1 - f_s(x)\big], \end{aligned} \tag{A.5}$$

with $f_s(x)$ being defined as

$$f_x(x) = \begin{cases} 1, & \text{if } x \text{ is in the core,} \\ 0, & \text{if } x \text{ is in the coating.} \end{cases} \tag{A.6}$$

Suppose now that the composite is subjected to the boundary conditions (4), and the strain field in a representative fiber is described in a polar coordinate system located at the center of the fiber through the influence functions $\boldsymbol{A}_s'(\xi)$, $\boldsymbol{a}_s'(\xi)$

$$\boldsymbol{\epsilon}_s'(\xi) = \boldsymbol{A}_s'(\xi)\boldsymbol{\epsilon}_0 + \boldsymbol{a}_s'(\xi)\theta_0, \quad s = \mathrm{c}, \mathrm{g}. \tag{A.7}$$

Using $(A.3)_2$ and (A.7), we obtain the Cartesian components of the strain:

$$\epsilon_s(x) = \boldsymbol{Q}(x)\ \boldsymbol{A}'_s(x)\ \epsilon_0 + \boldsymbol{Q}(x)\ \boldsymbol{a}'_s(x)\ \theta_0, \quad s = c, g, \tag{A.8}$$

where it is assumed that the components of the polar coordinates ξ have been expressed in terms of the Cartesian one x. Recalling the definition of $\boldsymbol{A}_f$ and $\boldsymbol{a}_f$ in $(9)_2$, and taking an average of (A.8) over the fiber (core and coating) provides

$$\boldsymbol{A}_f = \sum_{s=c,g} \nu_s \left(\frac{1}{S_s} \int_{S_s} \boldsymbol{Q}(x)\ \boldsymbol{A}'_s(x)\ \mathrm{d}S_s \right),$$
$$\boldsymbol{a}_f = \sum_{s=c,g} \nu_s \left(\frac{1}{S_s} \int_{S_s} \boldsymbol{Q}(x)\ \boldsymbol{a}'_s(x)\ \mathrm{d}S_s \right), \tag{A.9}$$

where ν_s is given by

$$\nu_c = a^2/b^2, \quad \nu_g = (b^2 - a^2)/b^2 \tag{A.10}$$

and S_s denotes the cross sectional area of the core and coating.

Turning to the $\tilde{\boldsymbol{A}}_f$ and $\boldsymbol{Q}_f$ tensors, we write first the Cartesian stress either from (A.2), (A.7) and $(A.3)_1$, or directly from (A.4) and (A.8) as

$$\sigma_s(x) = \boldsymbol{R}(x)\ \boldsymbol{L}'_s \boldsymbol{A}'_s(x)\ \epsilon_0 + \left[\boldsymbol{R}(x)\ \boldsymbol{L}'_s \boldsymbol{a}'_s(x) + \boldsymbol{R}(x)\ \boldsymbol{l}'_s \right] \theta_0, \tag{A.11}$$

where we have expressed again the the components of ξ in terms of x.

Finally taking an average of (A.11) over the coated fiber and using the definition of $\tilde{\boldsymbol{A}}_f$ and $\tilde{\boldsymbol{a}}_f$ in $(9)_1$ provides

$$\tilde{\boldsymbol{A}}_f = \sum_{s=c,g} \nu_s \left(\frac{1}{S_s} \int_{S_s} \boldsymbol{R}(x)\ \boldsymbol{L}'_s \boldsymbol{A}'_s(x)\ \mathrm{d}S_s \right),$$
$$\tilde{\boldsymbol{a}}_f = \sum_{s=c,g} \nu_s \left(\frac{1}{S_s} \int_{S_s} \left[\boldsymbol{R}(x)\ \boldsymbol{L}'_s \boldsymbol{a}'_s(x) + \boldsymbol{R}(x)\ \boldsymbol{l}'_s \right] \mathrm{d}S_s \right) \tag{A.12}$$

Therefore once the influence functions $\boldsymbol{A}'_s(\xi)$, $\boldsymbol{a}'_s(\xi)$ of (A.7) are known through the use of some micromechanics model, substitution of (A.9) and (A.12) in (8) provides the desired effective tensors $\boldsymbol{L}$ and $\boldsymbol{l}$.

J. Mech. Phys. Solids Vol. 39, No. 7, pp. 927–946, 1991.
Printed in Great Britain.

0022-5096/91 $3.00 + 0.00

ON DIAGONAL AND ELASTIC SYMMETRY OF THE APPROXIMATE EFFECTIVE STIFFNESS TENSOR OF HETEROGENEOUS MEDIA

Y. BENVENISTE,† G. J. DVORAK and T. CHEN

Department of Civil Engineering, Rensselaer Polytechnic Institute, Troy, NY 12180-3590, U.S.A.

(*Received* 30 *January* 1990; *in revised form* 26 *July* 1990)

ABSTRACT

THE EXISTENCE of diagonal symmetry in estimates of overall stiffness tensors of heterogeneous media is examined for several micromechanical models. The dilute approximation gives symmetric estimates for all matrix-based multiphase media. The Mori–Tanaka and the self-consistent methods do so for all two-phase systems, but only for those multiphase systems where the dispersed inclusions have a similar shape and alignment. However, the differential schemes associated with the self-consistent method can predict diagonally symmetric overall stiffness and compliance for multiphase systems of arbitrary phase geometry. A related question is raised about the equivalence of two possible approaches to evaluation of the overall thermal stress and strain tensors. A direct estimate follows from each of the above models, whereas LEVIN's results [*Mechanics of Solids* **2**, 58 (1967)] permit an indirect evaluation in terms of the estimated overall mechanical properties or concentration factors and phase thermoelastic moduli. These two results are shown to coincide for those systems and models which return diagonally symmetric estimates of the overall stiffness. Finally, model predictions of the overall elastic symmetry of composite media are discussed with regard to the spatial distribution of the phases.

1. INTRODUCTION

IT IS well known that under uniform thermomechanical static loads, statistically homogeneous elastic composites can be regarded as macroscopically homogeneous media characterized by an effective stiffness or compliance tensor, and by an effective thermal stress or strain tensor. The reciprocal theorem of elasticity can be employed to show that the exact effective stiffness and compliance tensors of an actual composite must be diagonally symmetric if this property obtains in all constituent phases. However, the complex microstructural geometry of actual systems precludes an exact evaluation of these tensors. Instead, various approximate procedures, such as the dilute approximation, the self-consistent and Mori–Tanaka methods, and various differential schemes are often used to estimate the overall stiffness or compliance in terms of given phase moduli, volume fractions, and shapes. As they stand, these procedures do not guarantee diagonal symmetry of the estimated stiffness tensors.

† Visiting from Department of Solid Mechanics, Materials and Structures, Faculty of Engineering, Tel-Aviv University, Israel.

Trial calculations show that diagonal symmetry obtains in some systems and not in others, and the micromechanics literature does not seem to offer any general guidelines for an *a priori* identification of systems which admit a legitimate application of a particular approximate procedure.

A related problem arises in evaluation of the effective thermal tensors. These can be found in two distinct ways. A direct approach would employ one of the approximate methods to estimate these tensors. Alternatively, LEVIN's (1967) results can be used to relate these tensors in an exact manner to the actual or estimated overall elastic properties or mechanical concentration factors and to the known thermoelastic constants of the phases. These two predictions should always coincide, but again, no general proof of such coincidence appears to be available in the literature.

Although a given set of inclusions can be dispersed in a matrix to form aggregates with many different spatial arrangements and corresponding overall elastic symmetries, some of the approximate methods predict the moduli and thermal expansion coefficients of only one such aggregate. Again, it is not clear what might be the underlying internal structure of this particular system, and how the shapes and elastic properties of the phases influence its overall elastic symmetry.

The purpose of the present work is to offer some answers to these open questions. We show that the dilute model gives diagonally symmetric estimates of overall mechanical moduli tensors in all matrix-based heterogeneous systems. In contrast, the Mori–Tanaka and the self-consistent models return such diagonally symmetric results only for two-phase systems, and for those multiphase systems in which the dispersed phases are aligned and of similar shape. However, the differential schemes which employ successive dilute approximations, do always return a diagonally symmetric estimate of the overall stiffness. The coincidence of the two approaches to evaluation of the overall thermal stress and strain tensors is found to exist under similar circumstances. Finally, the overall elastic symmetry of the Mori–Tanaka model is shown to be determined by the lowest material and shape symmetry present among the phases.

It is important to mention that approximate methods based on variational principles should always yield a diagonally symmetric tensor; see for example, the self-consistent schemes based on the Hashin–Shtrikman principle and the closely related self-consistent quasicrystalline approximation (WILLIS, 1977, 1981, 1983, 1984). However, a specific implementation of such an approach to multiphase composites with inclusions of different shapes does not seem to exist at present.

2. SOME AVAILABLE RESULTS

We are concerned with the overall thermomechanical response of a representative volume of a perfectly bonded multiphase composite aggregate which is subjected to a uniform overall stress $\boldsymbol{\sigma}$ or strain $\boldsymbol{\varepsilon}$, and a uniform change in temperature θ. This is defined by

$$\boldsymbol{\sigma} = \mathbf{L}\boldsymbol{\varepsilon} + \mathbf{l}\theta, \quad \boldsymbol{\varepsilon} = \mathbf{M}\boldsymbol{\sigma} + \mathbf{m}\theta, \tag{1}$$

where $\mathbf{L}$ and $\mathbf{M}$, and $\mathbf{l}$, $\mathbf{m}$, are the effective overall stiffness and compliance, and the thermal stress and strain tensors. For consistency of (1), these must satisfy the relation

$\mathbf{L} = \mathbf{M}^{-1}$, and $\mathbf{l} = -\mathbf{L}\mathbf{m}$. Following HILL (1963) and LAWS (1973) one can show that the overall properties are related to the local moduli and volume fractions by

$$\mathbf{L} = \mathbf{L}_1 + \sum_{r=2}^{N} c_r(\mathbf{L}_r - \mathbf{L}_1)\mathbf{A}_r, \quad \mathbf{M} = \mathbf{M}_1 + \sum_{r=2}^{N} c_r(\mathbf{M}_r - \mathbf{M}_1)\mathbf{B}_r. \tag{2}$$

$$\mathbf{l} = \mathbf{l}_1 + \sum_{r=2}^{N} c_r(\mathbf{l}_r - \mathbf{l}_1) + \sum_{r=2}^{N} c_r(\mathbf{L}_r - \mathbf{L}_1)\mathbf{a}_r,$$

$$\mathbf{m} = \mathbf{m}_1 + \sum_{r=2}^{N} c_r(\mathbf{m}_r - \mathbf{m}_1) + \sum_{r=2}^{N} c_r(\mathbf{M}_r - \mathbf{M}_1)\mathbf{b}_r, \tag{3}$$

where $\mathbf{A}_r$, $\mathbf{B}_r$, $\mathbf{a}_r$, $\mathbf{b}_r$ represent the concentration factors which are the averages of certain influence functions to be defined below, and $\mathbf{L}_r$, $\mathbf{M}_r$, and $\mathbf{l}_r$, and $\mathbf{m}_r$ denote the properties of phase $s = 1, 2, \ldots, N$; in matrix-based composites, $s = 1$ denotes the matrix phase. These properties enter the phase constitutive relations as

$$\boldsymbol{\sigma}_r(\mathbf{x}) = \mathbf{L}_r\boldsymbol{\varepsilon}_r(\mathbf{x}) + \mathbf{l}_r\theta_r(\mathbf{x}), \quad \boldsymbol{\varepsilon}_r(\mathbf{x}) = \mathbf{M}_r\boldsymbol{\sigma}_r(\mathbf{x}) + \mathbf{m}_r\theta_r(\mathbf{x}). \tag{4}$$

Those are similar to (1), but relates the local fields rather than their overall averages. The local fields are connected to the overall average by certain mechanical and thermal influence functions

$$\boldsymbol{\varepsilon}_r(\mathbf{x}) = \mathbf{A}_r(\mathbf{x})\boldsymbol{\varepsilon} + \mathbf{a}_r(\mathbf{x})\theta, \quad \boldsymbol{\sigma}_r(\mathbf{x}) = \mathbf{B}_r(\mathbf{x})\boldsymbol{\sigma} + \mathbf{b}_r(\mathbf{x})\theta. \tag{5}$$

The phase averages $\boldsymbol{\sigma}_r$ and $\boldsymbol{\varepsilon}_r$ of the local fields satisfy analogous connections written in terms of the mechanical and thermal concentration factors $\mathbf{A}_r$, $\mathbf{B}_r$, $\mathbf{a}_r$, and $\mathbf{b}_r$, which appear in (2) and (3) above. In this paper, local fields will be denoted by an argument $(\mathbf{x})$, and quantities without an argument will refer to averages.

The phase properties are assumed to satisfy the symmetry relations

$$L^{(s)}_{ijkl} = L^{(s)}_{jikl} = L^{(s)}_{ijlk} = L^{(s)}_{klij}, \qquad l^{(s)}_{ij} = l^{(s)}_{ji},$$
$$M^{(s)}_{ijkl} = M^{(s)}_{jikl} = M^{(s)}_{ijlk} = M^{(s)}_{klij}, \quad m^{(s)}_{ij} = m^{(s)}_{ji}. \tag{6}$$

Also, both the influence functions in (5) and the concentration factors which are their phase volume averages, must satisfy the symmetry conditions

$$A^{(s)}_{ijkl} = A^{(s)}_{jikl} = A^{(s)}_{ijlk}, \quad a^{(s)}_{ij} = a^{(s)}_{ji},$$
$$B^{(s)}_{ijkl} = B^{(s)}_{jikl} = B^{(s)}_{ijlk}, \quad b^{(s)}_{ij} = b^{(s)}_{ji}, \tag{7}$$

but the diagonal symmetry relations are not necessarily satisfied: $A_{ijkl} \neq A_{klij}$, $B_{ijkl} \neq B_{klij}$.

To lead into the main topic of the paper, we recall the reciprocal theorem of elasticity. Suppose that a representative volume V of a heterogeneous medium is subjected to two different states of uniform overall stress σ_{ij} and σ'_{ij}, or conjugate overall uniform strain ε_{kl} and ε'_{kl}, at $\theta = 0$. The actual local fields are denoted as $\sigma_{ij}(\mathbf{x})$, $\varepsilon_{kl}(\mathbf{x})$, and $\sigma'_{ij}(\mathbf{x}), \varepsilon'_{kl}(\mathbf{x})$; they satisfy the connections

$$\sigma_{ij} = \frac{1}{V}\int_V L_{ijkl}(\mathbf{x})\varepsilon_{kl}(\mathbf{x})\,dV = L_{ijkl}\varepsilon_{kl}, \quad \sigma'_{ij} = \frac{1}{V}\int_V L_{ijkl}(\mathbf{x})\varepsilon'_{kl}(\mathbf{x})\,dV = L_{ijkl}\varepsilon'_{kl}. \tag{8}$$

The theorem states that the two sets of local elastic fields satisfy the relation

$$\int_V \sigma_{ij}(\mathbf{x})\varepsilon'_{ij}(\mathbf{x})\,dV = \int_V \sigma'_{ij}(\mathbf{x})\varepsilon_{ij}(\mathbf{x})\,dV,$$

or, since the boundary conditions are homogeneous

$$\sigma_{ij}\varepsilon'_{ij}V = \sigma'_{ij}\varepsilon_{ij}V. \tag{9}$$

This shows that $\mathbf{L}$ and $\mathbf{M}$ must also possess the symmetries indicated in (6), i.e.

$$\begin{aligned} L_{ijkl} &= L_{jikl} = L_{ijlk} = L_{klij}, \qquad l_{ij} = l_{ji}, \\ M_{ijkl} &= M_{jikl} = M_{ijlk} = M_{klij}, \quad m_{ij} = m_{ji}. \end{aligned} \tag{10}$$

Moreover, LEVIN (1967) and ROSEN and HASHIN (1970) found that the tensors $\mathbf{m}$ and $\mathbf{l}$ can be expressed as

$$\mathbf{l} = \sum_{s=1}^{N} c_s \mathbf{A}_s^T \mathbf{l}_s, \quad \mathbf{m} = \sum_{s=1}^{N} c_s \mathbf{B}_s^T \mathbf{m}_s \tag{11}$$

or, since

$$\sum_{s=1}^{N} c_s \mathbf{A}_s^T = \mathbf{I}, \quad \sum_{s=1}^{N} c_s \mathbf{B}_s^T = \mathbf{I},$$

$$\mathbf{l} = \mathbf{l}_1 + \sum_{s=2}^{N} c_s \mathbf{A}_s^T(\mathbf{l}_s - \mathbf{l}_1), \quad \mathbf{m} = \mathbf{m}_1 + \sum_{s=2}^{N} c_s \mathbf{B}_s^T(\mathbf{m}_s - \mathbf{m}_1). \tag{12}$$

In two-phase systems, (2) indicates that the concentration factors $\mathbf{A}_s$ and $\mathbf{B}_s$ can be replaced by overall $\mathbf{L}$ and $\mathbf{M}$ to yield

$$\begin{aligned} \mathbf{l} &= \mathbf{l}_1 + (\mathbf{L} - \mathbf{L}_1)(\mathbf{L}_2 - \mathbf{L}_1)^{-1}(\mathbf{l}_2 - \mathbf{l}_1), \\ \mathbf{m} &= \mathbf{m}_1 + (\mathbf{M} - \mathbf{M}_1)(\mathbf{M}_2 - \mathbf{M}_1)^{-1}(\mathbf{m}_2 - \mathbf{m}_1). \end{aligned} \tag{13}$$

BENVENISTE and DVORAK (1990) have recently established an exact relationship between the thermal and mechanical influence functions in two-phase systems:

$$\begin{aligned} \mathbf{a}_s(\mathbf{x}) &= [\mathbf{I} - \mathbf{A}_s(\mathbf{x})](\mathbf{L}_1 - \mathbf{L}_2)^{-1}(\mathbf{l}_2 - \mathbf{l}_1), \\ \mathbf{b}_s(\mathbf{x}) &= [\mathbf{I} - \mathbf{B}_s(\mathbf{x})](\mathbf{M}_1 - \mathbf{M}_2)^{-1}(\mathbf{m}_2 - \mathbf{m}_1), \end{aligned} \tag{14}$$

which can be readily extended to concentration factors.

In any actual system, the influence functions in (5), or the phase concentration factors are not known exactly. Instead, they are estimated by certain approximate procedures. The dilute approximation, together with the Mori–Tanaka and the self-consistent methods are often employed for this purpose. As they currently stand, neither guarantees that the estimates of overall $\mathbf{L}$ and $\mathbf{M}$ will satisfy the symmetry requirements (10).

The overall thermal tensors can be evaluated in two different ways. One approach would employ the above estimates of $\mathbf{A}_s$ and $\mathbf{B}_s$ in (11) and (12). Alternatively, $\mathbf{a}_s$ and $\mathbf{b}_s$ can be found directly from one of the above approximate procedures, and then utilized in a direct evaluation of $\mathbf{l}$ and $\mathbf{m}$ in (3). Again, it is not clear that these two approaches do always lead to the same result.

Therefore, one of the objectives of our inquiry is to find in which composite systems do the approximate procedures for evaluation of $\mathbf{A}_s$ and $\mathbf{B}_s$ produce symmetric estimates of $\mathbf{L}$ and $\mathbf{M}$ that satisfy (10). Also, we wish to establish when the direct estimates of $\mathbf{a}_s$, $\mathbf{b}_s$, $\mathbf{A}_s$ and $\mathbf{B}_s$ lead to identical values of $\mathbf{l}$ and $\mathbf{m}$ in (3) and (11) or (12), respectively.

3. The Dilute Approximation

A matrix-based multiphase medium is regarded here as a collection of non-interacting inhomogeneities. Each inclusion of phase $s = 2, 3, \ldots, N$ is considered in turn, embedded in a large volume of matrix ($s = 1$) which is subjected to a uniform overall strain $\boldsymbol{\varepsilon}$. The average strain in each such phase is defined in analogy to (5) as

$$\boldsymbol{\varepsilon}_s = \mathbf{T}_s\boldsymbol{\varepsilon} + \mathbf{t}_s\theta. \tag{15}$$

Since only two phases ($s = 1$ and $s \neq 1$) are involved in each application of (15), one can use (14_1) to write

$$\mathbf{t}_s = (\mathbf{I} - \mathbf{T}_s)(\mathbf{L}_1 - \mathbf{L}_s)^{-1}(\mathbf{l}_s - \mathbf{l}_1). \tag{16}$$

An estimate of the $\mathbf{L}$ tensor follows from (2) as

$$\mathbf{L} = \mathbf{L}_1 + \sum_{s=2}^{N} c_s(\mathbf{L}_s - \mathbf{L}_1)\mathbf{T}_s \tag{17}$$

while the $\mathbf{l}$ tensor can be estimated either from (12_1) as

$$\mathbf{l} = \mathbf{l}_1 + \sum_{s=2}^{N} c_s\mathbf{T}_s^T(\mathbf{l}_s - \mathbf{l}_1), \tag{18}$$

or from (16) and (3_1) as

$$\mathbf{l} = \mathbf{l}_1 + \sum_{s=2}^{N} c_s(\mathbf{l}_s - \mathbf{l}_1) + \sum_{s=2}^{N} c_s(\mathbf{L}_s - \mathbf{L}_1)(\mathbf{I} - \mathbf{T}_s)(\mathbf{L}_1 - \mathbf{L}_s)^{-1}(\mathbf{l}_s - \mathbf{l}_1). \tag{19}$$

We will now show that $\mathbf{L}$ in (17) satisfies the diagonal symmetry requirement in (10) and that (18) and (19) give identical estimates of $\mathbf{l}$. Consider first the symmetry properties of the product $(\mathbf{L}_s - \mathbf{L}_1)\mathbf{T}_s$. Recall that a single phase $s \neq 1$ is embedded in a large volume D_1 of the matrix phase $s = 1$ which is subjected to a uniform overall strain $\boldsymbol{\varepsilon}$, and $\theta = 0$. Suppose that two different overall strain states, ε_{ij} and ε'_{ij}, are applied. The reciprocal theorem (9) then shows that

$$[d_1\sigma_{ij}^{(1)} + d_s\sigma_{ij}^{(s)}]\varepsilon'_{ij} = [d_1(\sigma_{ij}^{(1)})' + d_s(\sigma_{ij}^{(s)})']\varepsilon_{ij}, \tag{20}$$

where $d_1 = D_1/D$ and $d_s = D_s/D$ denote the matrix ($s = 1$) and inclusion volume

fractions in the dilute configuration, $D = D_1 + D_r$; the $\sigma_{ij}^{(1)}$ and $\sigma_{ij}^{(r)}$ are the average phase stresses. From (4) and the relation $d_1\varepsilon_{ij}^{(1)} + d_r\varepsilon_{ij}^{(r)} = \varepsilon_{ij}$ for the auxiliary dilute configuration it follows that

$$L_{ijkl}^{(1)}\varepsilon_{kl}^{(1)} + d_r[L_{ijkl}^{(r)} - L_{ijkl}^{(1)}]T_{klmn}^{(r)}\varepsilon_{mn}^{(r)} = L_{ijkl}^{(1)}\varepsilon_{kl}^{(1)} + d_r[L_{ijkl}^{(r)} - L_{ijkl}^{(1)}]T_{klmn}^{(r)}\varepsilon_{mn}^{(1)}. \quad (21)$$

This shows that the product $(\mathbf{L}_r - \mathbf{L}_1)\mathbf{T}_r$, and therefore also the dilute approximation of $\mathbf{L}$ in (17), are indeed diagonally symmetric.

It is now easy to prove that the estimates (18) and (19) of $\mathbf{I}$ are equivalent. Rewrite (19) in the form

$$\mathbf{I} = \mathbf{I}_1 + \sum_{r=2}^{N} c_r(\mathbf{L}_r - \mathbf{L}_1)\mathbf{T}_r(\mathbf{L}_r - \mathbf{L}_1)^{-1}(\mathbf{I}_r - \mathbf{I}_1) \quad (22)$$

and recall that $(\mathbf{L}_r - \mathbf{L}_1)\mathbf{T}_r$ is symmetric; this provides the desired proof.

4. THE MORI-TANAKA METHOD

4.1. *Summary of the method*

MORI and TANAKA (1973) proposed the method in an attempt to find an estimate of matrix stress in a material containing precipitates with transformation strains. BENVENISTE (1987) reformulated the original approach, and more recently (BENVENISTE, 1990) he established certain unifying connections with the model proposed by LEVIN (1976) and the so-called closure approximation of lowest order of WILLIS (1981). The method enjoys widespread use. For example, BENVENISTE and DVORAK (1990), and BENVENISTE *et al.* (1989) applied it to thermal stress problems in two-phase and coated fiber systems. A comprehensive list of previous work on the Mori-Tanaka method in composites can be found in these papers.

As in the dilute approximation, an inclusion of each phase $s \neq 1$ is regarded as a solitary inhomogeneity in a large volume of matrix $s = 1$. However, the overall strain applied to the matrix is no longer the actual overall strain $\boldsymbol{\varepsilon}$ in the aggregate; instead, it is equal to the as yet unknown average matrix strain $\boldsymbol{\varepsilon}_1$. Therefore, in place of (15), the average phase strain is now equal to

$$\boldsymbol{\varepsilon}_r = \mathbf{T}_r\boldsymbol{\varepsilon}_1 + \mathbf{t}_r\theta. \quad (23)$$

Inasmuch as $\boldsymbol{\varepsilon} = \Sigma_r c_r\boldsymbol{\varepsilon}_r$, one can establish that

$$\boldsymbol{\varepsilon}_1 = \left[c_1\mathbf{I} + \sum_{r=2}^{N} c_r\mathbf{T}_r\right]^{-1}\left[\boldsymbol{\varepsilon} - \theta\sum_{r=2}^{N} c_r\mathbf{t}_r\right],$$

$$\mathbf{A}_r = \mathbf{T}_r\left[c_1\mathbf{I} + \sum_{r=2}^{N} c_r\mathbf{T}_r\right]^{-1},$$

$$\mathbf{a}_r = -\mathbf{T}_r\left[c_1\mathbf{I} + \sum_{r=2}^{N} c_r\mathbf{T}_r\right]^{-1}\left[\sum_{r=2}^{N} c_r\mathbf{t}_r\right] + \mathbf{t}_r. \quad (24)$$

A substitution of the above $\mathbf{A}_r$ into (2_1) then gives the Mori–Tanaka estimate of the overall stiffness $\mathbf{L}$ as

$$\mathbf{L} = \mathbf{L}_1 + \left[\sum_{r=2}^{N} c_r(\mathbf{L}_r - \mathbf{L}_1)\mathbf{T}_r\right]\left[c_1\mathbf{I} + \sum_{r=2}^{N} c_r\mathbf{T}_r\right]^{-1}. \tag{25}$$

or as

$$\mathbf{L} = \left[\sum_{r=1}^{N} c_r\mathbf{L}_r\mathbf{T}_r\right]\left[\sum_{r=1}^{N} c_r\mathbf{T}_r\right]^{-1}, \tag{26}$$

where we used the identities

$$\mathbf{T}_1 = \mathbf{I}, \quad \mathbf{t}_1 = \mathbf{0}. \tag{27}$$

Consider next the estimates of $\mathbf{I}$. The first option is to use $\mathbf{A}_r$ in (11_1) and after some algebra find

$$\mathbf{I} = \left[\sum_{r=1}^{N} c_r\mathbf{T}_r^T\right]^{-1}\left[\sum_{r=1}^{N} c_r\mathbf{T}_r^T\mathbf{I}_r\right]. \tag{28}$$

The second option is to substitute the direct estimate (24_1) of $\mathbf{a}_r$ into (3_1)

$$\mathbf{I} = \mathbf{L}\left[-\sum_{r=1}^{N} c_r\mathbf{t}_r\right] + \sum_{r=1}^{N} c_r(\mathbf{L}_r\mathbf{t}_r + \mathbf{I}_r) \tag{29}$$

with $\mathbf{L}$ taken from (26).

In the following paragraphs we show that the Mori–Tanaka estimates of $\mathbf{L}$ are symmetric only for those multiphase composites where all phases $s \neq 1$ are of similar shape. Also, we show that this property obtains in all two-phase systems, regardless of phase geometry.

4.2. *Aligned inclusions of similar shape*

Write the concentration factor $\mathbf{T}_r$ in the form

$$\mathbf{T}_r = [\mathbf{I} + \mathbf{P}(\mathbf{L}_r - \mathbf{L}_1)]^{-1}, \tag{30}$$

where $\mathbf{P} = \mathbf{P}^T$ is related to the constraint tensor $\mathbf{L}^*$ of a transformed homogeneous inclusion by

$$\mathbf{L}^* = \mathbf{P}^{-1} - \mathbf{L}_1 \tag{31}$$

and hence there is also $\mathbf{L}^* = (\mathbf{L}^*)^T$. The background related to the definition of the $\mathbf{P}$ tensor and associated concepts may be found in the comprehensive reviews by WALPOLE (1981) and WILLIS (1981). Of course, if the inclusion is of ellipsoidal shape, then $\mathbf{P} = \mathbf{S}\mathbf{L}_1^{-1}$, in terms of the Eshelby tensor $\mathbf{S}$, and the strain field inside such a solitary inclusion is uniform. However, this restriction is not required in the analysis which follows. What is required is that the tensor $\mathbf{P}$ be identical for all inclusions.

Thus the inclusions may have any similar shape, but each must have the same orientation in a fixed reference frame.

In any event, since $\mathbf{P}$ is identical for all $s \neq 1$, (30) and (31) provides

$$\mathbf{T}_s = (\mathbf{L}^* + \mathbf{L}_s)^{-1}(\mathbf{L}^* + \mathbf{L}_1). \tag{32}$$

Substitute this into (26) and after some algebra find the following diagonally symmetric form of the Mori–Tanaka estimate of $\mathbf{L}$ (NORRIS, 1989)

$$\mathbf{L} = \left[\sum_{s=1}^{N} c_s(\mathbf{L}^* + \mathbf{L}_s)^{-1}\right]^{-1} - \mathbf{L}^*. \tag{33}$$

Next, we proceed to show that the estimates (28) and (29) of $\mathbf{l}$ are equivalent. Take $\mathbf{T}_s$ from (32), recall that $\mathbf{L}_s$ and $\mathbf{L}^*$ are both diagonally symmetric, and write (28) as

$$\mathbf{l} = \left[\sum_{s=1}^{N} c_s(\mathbf{L}^* + \mathbf{L}_s)^{-1}\right]^{-1}\left[\sum_{s=1}^{N} c_s(\mathbf{L}^* + \mathbf{L}_s)^{-1}\mathbf{l}_s\right]. \tag{34}$$

Modify now (29) by noting that $\mathbf{t}_s$ in (16) can be rewritten with the help of (32) as

$$\mathbf{t}_s = -(\mathbf{L}^* + \mathbf{L}_s)^{-1}(\mathbf{l}_s - \mathbf{l}_1) \tag{35}$$

and substitute this together with $\mathbf{L}$ from (33) into (29). The result is

$$\mathbf{l} = \mathbf{l}_1 + \left[\sum_{s=1}^{N} c_s(\mathbf{L}^* + \mathbf{L}_s)^{-1}\right]^{-1}\left[\sum_{s=1}^{N} c_s(\mathbf{L}^* + \mathbf{L}_s)^{-1}(\mathbf{l}_s - \mathbf{l}_1)\right] \tag{36}$$

and, after expansion of the second bracket, it reduces to the form (34) which was derived from (28).

4.3. *Two-phase materials with inclusions of different shape*

The two phases are denoted by the subscript $r = \alpha, \beta$, where $r = \alpha$ denotes the matrix, and $r = \beta$ the dispersed phase which must have the same stiffness $\mathbf{L}_\beta$ in a fixed coordinate system. In an actual composite system, this last requirement is unlikely to be satisfied unless the phase $r = \beta$ is isotropic. The matrix phase resides in the region $s = 1$, while the second phase occupies various regions $s = 2, 3, \ldots, N$ of different shape. For each such region there exists a certain tensor $\mathbf{P}^s$.

It is convenient to introduce the tensor $\mathbf{P}_\alpha^s$ defined as

$$\mathbf{P}^s(\mathbf{L}_\alpha - \mathbf{L}_\beta)\mathbf{P}_\alpha^s = \mathbf{P}_\alpha^s - \mathbf{P}^s. \tag{37}$$

Since $\mathbf{P}^s = (\mathbf{P}^s)^T$, the definition shows that $\mathbf{P}_\alpha^s = (\mathbf{P}_\alpha^s)^T$. After some algebra, the tensor T_s in (30) assumes the form

$$\mathbf{T}_s = \mathbf{I} + \mathbf{P}_\alpha^s(\mathbf{L}_\alpha - \mathbf{L}_\beta). \tag{38}$$

First, we ask if the overall stiffness $\mathbf{L}$ defined by (25) is diagonally symmetric in the present system. Note that (25) can be rewritten as

$$\mathbf{L} = \mathbf{L}_\alpha + (\mathbf{L}_\alpha - \mathbf{L}_\beta)\left(c_\alpha \mathbf{I} - \sum_{s=1}^{N} c_s \mathbf{T}_s\right)\left(\sum_{s=1}^{N} c_s \mathbf{T}_s\right)^{-1}, \tag{39}$$

then transformed into

$$\mathbf{L} = \mathbf{L}_\beta + c_\alpha (\mathbf{L}_\alpha - \mathbf{L}_\beta)\left(\sum_{s=1}^{N} c_s \mathbf{T}_s\right)^{-1} \tag{40}$$

and with reference to (38) cast into the final form

$$\mathbf{L} = \mathbf{L}_\beta + c_\alpha \left[\sum_{s=1}^{N} c_s (\mathbf{L}_\alpha - \mathbf{L}_\beta)^{-1} + \mathbf{P}_\alpha^s\right]^{-1}, \tag{41}$$

which shows that indeed $\mathbf{L} = \mathbf{L}^T$.

Next, let us examine for the present system the two forms of $\mathbf{l}$ given by (28) and (29). If (38) is used in (28) together with $\mathbf{l}_s = \mathbf{l}_\beta$ for $s \neq 1$, then after much manipulation $\mathbf{l}$ becomes

$$\mathbf{l} = \mathbf{l}_\beta + c_\alpha \left[\sum_{s=1}^{N} c_s [(\mathbf{L}_\alpha - \mathbf{L}_\beta)^{-1} + \mathbf{P}_\alpha^s]\right]^{-1} (\mathbf{L}_\alpha - \mathbf{L}_\beta)^{-1} (\mathbf{l}_\alpha - \mathbf{l}_\beta). \tag{42}$$

On the other hand, if the identity $\mathbf{t}_\alpha = \mathbf{0}$ is used in (29), it follows that

$$\mathbf{l} = \mathbf{L}\left[-\sum_{s=1}^{N} c_s \mathbf{t}_s\right] + c_\alpha (\mathbf{l}_\alpha - \mathbf{l}_\beta) + \sum_{s=1}^{N} c_s (\mathbf{L}_\beta \mathbf{t}_s + \mathbf{l}_\beta), \tag{43}$$

where $\mathbf{t}_s$ can be evaluated from (16) with $\mathbf{T}_s$ taken from (38)

$$\mathbf{t}_s = \mathbf{P}_\alpha^s (\mathbf{l}_\alpha - \mathbf{l}_\beta). \tag{44}$$

Then, with $\mathbf{L}$ from (41), $\mathbf{l}$ becomes

$$\mathbf{l} = \mathbf{l}_\beta - c_\alpha \left\{\left[\sum_{s=1}^{N} c_s [(\mathbf{L}_\alpha - \mathbf{L}_\beta)^{-1} + \mathbf{P}_\alpha^s]\right]^{-1} \left[\sum_{s=1}^{N} c_s \mathbf{P}_\alpha^s\right] - \mathbf{I}\right\} (\mathbf{l}_\alpha - \mathbf{l}_\beta). \tag{45}$$

This can be cast into a form which is identical with (42); in the derivation it is helpful to write the identity tensor in (45) as

$$\mathbf{I} = \left[\sum_{s=1}^{N} c_s [(\mathbf{L}_\alpha - \mathbf{L}_\beta)^{-1} + \mathbf{P}_\alpha^s]\right]^{-1} \left[\sum_{s=1}^{N} c_s [(\mathbf{L}_\alpha - \mathbf{L}_\beta)^{-1} + \mathbf{P}_\alpha^s]\right]. \tag{46}$$

4.4. *Multiphase systems with inclusions of different shape*

In composites of this kind, where in each phase both the phase stiffness $\mathbf{L}_s$ and the tensor $\mathbf{P}^s$ vary with s, one can show that the overall $\mathbf{L}$ in (26) is generally not symmetric, and that (28) and (29) lead to different results. An analytic proof appears to be cumbersome, but the said properties can be conclusively demonstrated by a numerical example. To this end we consider a specific three-phase material consisting of a Ti_3Al matrix (phase 1), carbon circular disc (phase 2), with the normal of the

plane face of the disc in the direction x_3 of a Cartesian coordinate system, and continuous SiC fibers of circular cross-section (phase 3), aligned with x_3. Each phase is assumed to be isotropic. The phase moduli and volume fractions were selected as

$$E_1 = 96.5\,\text{GPa}, \quad G_1 = 37.1\,\text{GPa}, \quad \alpha_1 = 9.25 \times 10^{-6}\ \text{C}, \quad c_1 = 0.55,$$
$$E_2 = 34.4\,\text{GPa}, \quad G_2 = 14.3\,\text{GPa}, \quad \alpha_2 = 3.33 \times 10^{-6}\ \text{C}, \quad c_2 = 0.25,$$
$$E_3 = 431.0\,\text{GPa}, \quad G_3 = 172.0\,\text{GPa}, \quad \alpha_3 = 4.86 \times 10^{-6}\ \text{C}, \quad c_3 = 0.2. \tag{47}$$

The above constants give the following values of the coefficients of the (6×6) and (6×1) matrices defined by (26), and (28), (29), respectively

$$\mathbf{L} = \begin{bmatrix} 123.62 & 43.84 & 35.89 & 0 & 0 & 0 \\ 43.84 & 123.62 & 35.89 & 0 & 0 & 0 \\ 21.89 & 21.89 & 124.05 & 0 & 0 & 0 \\ 0 & 0 & 0 & 33.04 & 0 & 0 \\ 0 & 0 & 0 & 0 & 33.04 & 0 \\ 0 & 0 & 0 & 0 & 0 & 39.89 \end{bmatrix} \text{GPa}, \tag{48}$$

$$\mathbf{l} = (-0.14185, -0.14185, -0.12880, 0, 0, 0)^T \times 10^{-2}\,\text{GPa C} \quad \text{[from Eq. (28)]},$$

$$\mathbf{l} = (-0.14970, -0.14970, -0.08167, 0, 0, 0)^T \times 10^{-2}\,\text{GPa C} \quad \text{[from Eq. (29)]}.$$

The example shows that $\mathbf{L}$ is not symmetric, and that the $\mathbf{l}$ in (28) is different from $\mathbf{l}$ in (29).

We note that the only exception to this conclusion has been observed so far in systems where the phases 2 and 3 are combined in a coated fiber which is embedded in a continuous matrix (BENVENISTE *et al.*, 1989). In such systems, the tensors $\mathbf{T}_s$ and $\mathbf{t}_s$ of phases $s = 2, 3$ are obtained from an exact solution of an elasticity problem in which the coated fiber resides in a large volume of matrix which is loaded by an overall stress $\boldsymbol{\sigma}_1$ or strain $\boldsymbol{\varepsilon}_1$, and by a uniform temperature change θ. Clearly, this exact solution guarantees that the overall stiffness predicted by the dilute approximation of Section 3 is symmetric. A similar proof has not yet been established for the Mori–Tanaka method, but several numerical realizations of this method have consistently returned diagonally symmetric Mori–Tanaka estimates of $\mathbf{L}$, as well as agreements between (28) and (29). CHEN *et al.* (1990) obtained such results even for systems reinforced with cylindrically orthotropic fibers and transversely isotropic coatings in a transversely isotropic matrix.

5. THE SELF-CONSISTENT APPROXIMATION

5.1. *Review of the method*

This well known procedure has its origins in the work of BRUGGEMAN (1935) who used it to study conductivity of composites, HERSHEY (1954) and KRÖNER (1958) who applied it to polycrystals, and BUDIANSKY (1965) and HILL (1965) who formulated

the method for composite aggregates: see also the reviews of WALPOLE (1981), and WILLIS (1981) for further insights on the method.

In the theory, particle interaction is taken into account by assuming that an inclusion of each phase is embedded in an effective medium of initially unknown properties. As in the Mori–Tanaka method, mechanical and thermal concentration factors are derived from the solution of a dilute problem, but the solitary inclusion is now assumed to be bonded to a large volume of the effective medium of as yet unknown effective $\mathbf{L}$ and $\mathbf{l}$, which is loaded by the actual overall stress $\boldsymbol{\sigma}$ or strain $\boldsymbol{\varepsilon}$, and the temperature change θ.

The effective stiffness is again given by (2)

$$\mathbf{L} = \mathbf{L}_1 + \sum_{r=2}^{N} c_r(\mathbf{L}_r - \mathbf{L}_1)\mathbf{A}_r,$$

where the tensor $\mathbf{A}_r$ is now the actual concentration factor

$$\mathbf{A}_r = [\mathbf{I} + \mathbf{P}^r(\mathbf{L}_r - \mathbf{L})]^{-1} \tag{49}$$

and

$$\mathbf{P}^r = (\mathbf{L}_r^* + \mathbf{L})^{-1} \tag{50}$$

is a function of the overall moduli, but its form depends on the shape of the inclusions r. When used in (49) and then substituted into (2_1), this gives a system of nonlinear algebraic equations for the coefficients of $\mathbf{L}$. Explicit solutions have been obtained only for some common two-phase systems (HILL, 1965; WALPOLE, 1969), but a numerical procedure must be employed for more complex material combinations.

Once $\mathbf{L}$ is known, the effective thermal stress tensor $\mathbf{l}$ follows either from (12_1), or from (3_1) with $\mathbf{a}_r$ given by the expression

$$\mathbf{a}_r = (\mathbf{I} - \mathbf{A}_r)(\mathbf{L} - \mathbf{L}_r)^{-1}(\mathbf{l}_r - \mathbf{l}). \tag{51}$$

It is interesting to observe that if $\mathbf{L}$ is known, the first alternative [(12_1) and (49)] provides an explicit expression for $\mathbf{l}$, whereas the second one [(3_1), (49) and (51)] gives a linear algebraic equation for $\mathbf{l}$.

Again, two questions need to be answered. One pertains to the diagonal symmetry of the predicted $\mathbf{L}$, the other to the equivalence of the two alternative evaluations of $\mathbf{l}$. The first question can not be answered analytically for all systems, and numerical examples must be used instead. In any event, we show that the self-consistent prediction of $\mathbf{L}$ is symmetric in the same circumstances as the Mori–Tanaka prediction. The second question can be answered analytically. As in the Mori–Tanaka method, one obtains an affirmative answer for systems in Sections 4.2 and 4.3 when $\mathbf{L} = \mathbf{L}^T$. However, in multiphase materials with different $\mathbf{P}^r$ and $\mathbf{L}$, the two predictions of $\mathbf{l}$ would be different even if the overall $\mathbf{L}$ were symmetric.

For convenience, we first consider the multiphase systems of Section 4.4, and then the case of aligned inclusions and the two-phase systems.

5.2. *Multiphase systems of any phase geometry*

A numerical example will show that the method does not predict a symmetric overall stiffness tensor for this system. The numerical evaluation of $\mathbf{L}$ employs the following iterative procedure. In the first step, $\mathbf{P}^{s}$ is found in terms of the matrix moduli $\mathbf{L}_1$, i.e., as in the dilute approximation, and denoted by $(\mathbf{P}^{s})_1$; the subscript (1) refers to the first step. This is used in (49) and (2_1) to evaluate the first approximation of $\mathbf{L}$, denoted by $(\mathbf{L})_1$. In the second step, $\mathbf{P}^{s}$ is evaluated as a function of the new $(\mathbf{L})_1$, and used again in (49) and (2_1) to find the next approximation $(\mathbf{L})_2$ of $\mathbf{L}$. This is continued until a selected convergence criterion is satisfied.

Phase properties are selected as in Eq. (47). Again, phase 1 is the matrix, phase 2 has the shape of circular disc, and phase 3 forms aligned cylindrical fibers. The described iterative procedure gave the following results in steps 1, 2, and 23 when convergence was reached

$$(\mathbf{L})_1 = \begin{bmatrix} 118.46 & 39.47 & 24.59 & 0 & 0 & 0 \\ 39.47 & 118.46 & 24.59 & 0 & 0 & 0 \\ 24.59 & 24.59 & 122.60 & 0 & 0 & 0 \\ 0 & 0 & 0 & 31.96 & 0 & 0 \\ 0 & 0 & 0 & 0 & 31.96 & 0 \\ 0 & 0 & 0 & 0 & 0 & 39.50 \end{bmatrix} \text{GPa},$$

$$(\mathbf{L})_2 = \begin{bmatrix} 126.47 & 46.98 & 22.80 & 0 & 0 & 0 \\ 46.98 & 126.45 & 22.80 & 0 & 0 & 0 \\ 42.45 & 42.45 & 125.13 & 0 & 0 & 0 \\ 0 & 0 & 0 & 32.88 & 0 & 0 \\ 0 & 0 & 0 & 0 & 32.88 & 0 \\ 0 & 0 & 0 & 0 & 0 & 39.75 \end{bmatrix} \text{GPa},$$

$$(\mathbf{L})_{23} = \begin{bmatrix} 123.85 & 44.12 & 22.04 & 0 & 0 & 0 \\ 44.12 & 123.92 & 22.04 & 0 & 0 & 0 \\ 35.97 & 35.97 & 124.09 & 0 & 0 & 0 \\ 0 & 0 & 0 & 32.74 & 0 & 0 \\ 0 & 0 & 0 & 0 & 32.74 & 0 \\ 0 & 0 & 0 & 0 & 0 & 39.87 \end{bmatrix} \text{GPa}, \qquad (52)$$

which clearly shows lack of symmetry of the predicted $\mathbf{L}$. Note that even the second iteration gives a nonsymmetric $(\mathbf{L})_2$. However, this does not interfere with evaluation of $(\mathbf{P}^{s})_3$, because the coefficients L_{13}, L_{23}, L_{31}, and L_{32} are not involved.

We emphasize that the performance of the method must be evaluated for each particular application. For example, the above conclusion may not be reached in coated fiber composites, or in other three-phase systems where the interaction of two of the phases is evaluated from the solution of an exact elasticity problem.

Consider next the two alternatives in evaluation of the overall thermal stress tensor $\mathbf{l}$. The result (52) notwithstanding, we *assume* that the self-consistent estimate of the overall stiffness $\mathbf{L}$ is diagonally symmetric. The first alternative is suggested by (12_1), with $\mathbf{A}_r$ given by (49). If (50) is substituted into (49), then

$$\mathbf{A}_r = (\mathbf{L}_r^* + \mathbf{L}_r)^{-1}(\mathbf{L}_r^* + \mathbf{L}) \tag{53}$$

and (12_1) then becomes

$$\mathbf{l} = \mathbf{l}_1 + \sum_{r=2}^{N} c_r(\mathbf{L}_r^* + \mathbf{L})(\mathbf{L}_r^* + \mathbf{L}_r)^{-1}(\mathbf{l}_r - \mathbf{l}_1). \tag{54}$$

In the second alternative, $\mathbf{l}$ is found from (3_1), (51) and (53) as

$$\mathbf{l} = \mathbf{l}_1 + \sum_{r=2}^{N} c_r(\mathbf{l}_r - \mathbf{l}_1) + \sum_{r=2}^{N} c_r(\mathbf{L}_r - \mathbf{L}_1)(\mathbf{L}_r^* + \mathbf{L}_r)^{-1}(\mathbf{l} - \mathbf{l}_r). \tag{55}$$

To compare the last two forms, we recall the identity $\Sigma_{r=1}^{N} c_r \mathbf{A}_r = \mathbf{I}$ and use (53) to define the tensor $\mathbf{L}_1^*$ by

$$\sum_{r=1}^{N} c_r \mathbf{A}_r = \sum_{r=1}^{N} c_r(\mathbf{L}_r^* + \mathbf{L}_r)^{-1}(\mathbf{L}_r^* + \mathbf{L}) = \mathbf{I}. \tag{56}$$

This helps to reduce (54) to the form

$$\mathbf{l} = \sum_{r=1}^{N} c_r(\mathbf{L}_r^* + \mathbf{L})(\mathbf{L}_r^* + \mathbf{L}_r)^{-1}\mathbf{l}_r \tag{57}$$

and then to

$$\mathbf{l} = \left[\sum_{r=1}^{N} c_r(\mathbf{L}_r^* + \mathbf{L})(\mathbf{L}_r^* + \mathbf{L}_r)^{-1}\right]^{-1}\left[\sum_{r=1}^{N} c_r(\mathbf{L}_r^* + \mathbf{L})(\mathbf{L}_r^* + \mathbf{L}_r)^{-1}\mathbf{l}_r\right]. \tag{58}$$

In contrast, (56) and some algebra eventually convert (55) to the form

$$\mathbf{l} = \left[\sum_{r=1}^{N} c_r(\mathbf{L}_r^* + \mathbf{L}_1)(\mathbf{L}_r^* + \mathbf{L}_r)^{-1}\right]^{-1}\left[\sum_{r=1}^{N} c_r(\mathbf{L}_r^* + \mathbf{L}_1)(\mathbf{L}_r^* + \mathbf{L}_r)^{-1}\mathbf{l}_r\right], \tag{59}$$

which is different from (58). Thus we conclude that even if $\mathbf{L}$ were diagonally symmetric, the self-consistent method would still provide two conflicting estimates of $\mathbf{l}$ for general multiphase aggregates.

It should be noted here that in three-phase fibrous systems with arbitrary transverse phase geometry, the effective thermal tensor $\mathbf{l}$ can be found exactly in terms of the overall and local stiffnesses and volume fractions (DVORAK and CHEN, 1989). It remains to be verified, however, whether the use of the self-consistent method in conjunction with this result would coincide with its direct application to such systems.

5.3. *Aligned inclusions of similar shape*

In systems of this kind, all inclusions have the same constraint tensor $\mathbf{L}_r^* = \mathbf{L}^*$. For example, each grain in a polycrystalline aggregate may be regarded as a spherical

inclusion in an effective medium. However, in matrix-based composites reinforced by inclusions of the same shape and alignment, there is $\mathbf{L}_s^* = \mathbf{L}^*$ for the inclusions $s = 2, \ldots, N$, while $\mathbf{L}_1^*$ of the matrix ($s = 1$) needs to be determined. Following HILL (1965), we write

$$\boldsymbol{\sigma}_1 - \boldsymbol{\sigma} = \mathbf{L}_1^*(\boldsymbol{\varepsilon} - \boldsymbol{\varepsilon}_1), \quad \text{for } s = 1,$$
$$\boldsymbol{\sigma}_s - \boldsymbol{\sigma} = \mathbf{L}^*(\boldsymbol{\varepsilon} - \boldsymbol{\varepsilon}_s), \quad \text{for } s = 2, \ldots, N \tag{60}$$

and

$$\sum_{s=1}^{N} c_s(\boldsymbol{\sigma}_s - \boldsymbol{\sigma}) = 0, \quad \sum_{s=1}^{N} c_s(\boldsymbol{\varepsilon}_s - \boldsymbol{\varepsilon}) = 0. \tag{61}$$

Substitute from (60) into (61_1) and use (61_2) to find

$$c_1(\mathbf{L}_1^* - \mathbf{L}^*)(\boldsymbol{\varepsilon} - \boldsymbol{\varepsilon}_1) = \mathbf{0}$$

and

$$\mathbf{L}_1^* = \mathbf{L}^*. \tag{62}$$

Therefore, in composites of this kind the self-consistent method makes no distinction between the constraint tensors of the matrix and other inclusions. In this sense, all phases are admitted on the same footing.

It now follows that for the present system, the strain concentration factor (49) is

$$\mathbf{A}_s = [\mathbf{I} + \mathbf{P}(\mathbf{L}_s - \mathbf{L})]^{-1}, \quad \text{for } s = 1, \ldots, N, \tag{63}$$

where $\mathbf{P} = (\mathbf{L}^* + \mathbf{L})^{-1}$. This can be used to write

$$\mathbf{A}_s = (\mathbf{L}^* + \mathbf{L}_s)^{-1}(\mathbf{L}^* + \mathbf{L}) \quad \text{or} \quad \mathbf{A}_s = \mathbf{I} + \mathbf{P}_s(\mathbf{L} - \mathbf{L}_s), \tag{64}$$

where, as in (37)

$$\mathbf{P}_s - \mathbf{P} = \mathbf{P}(\mathbf{L} - \mathbf{L}_s)\mathbf{P}_s.$$

Now that all strain concentration factors are known, we invoke the identity (56) and establish that

$$\sum_{s=1}^{N} c_s(\mathbf{L}^* + \mathbf{L}_s)^{-1}(\mathbf{L}^* + \mathbf{L}) = \mathbf{I} \tag{65}$$

and

$$\sum_{s=1}^{N} c_s[\mathbf{I} + \mathbf{P}_s(\mathbf{L} - \mathbf{L}_s)] = \mathbf{I}. \tag{66}$$

Equation (65) can be recast as

$$\mathbf{L} = \left[\sum_{s=1}^{N} c_s(\mathbf{L}^* + \mathbf{L}_s)^{-1}\right]^{-1} - \mathbf{L}^*. \tag{67}$$

which provides an implicit form of $\mathbf{L}$. According to the definition, $\mathbf{L}^* = (\mathbf{L}^*)^T$, hence it follows that $\mathbf{L} = \mathbf{L}^T$.

An alternative form of $\mathbf{L}$ may be found when (2) is converted into the form $\sum_{r=1}^{N} c_r \mathbf{L}_r \mathbf{A}_r = \mathbf{L}$, and together with (64$_2$) it is utilized in finding

$$\mathbf{L} = \sum_{r=1}^{N} c_r \mathbf{L}_r + \sum_{r=1}^{N} c_r \mathbf{L}_r \mathbf{P}_r (\mathbf{L} - \mathbf{L}_r). \tag{68}$$

Now, multiply the left-hand side of (66) by $-\mathbf{L}$, add the result to (68), and recover

$$\mathbf{L} = \sum_{r=1}^{N} c_r \mathbf{L}_r - \sum_{r=1}^{N} c_r (\mathbf{L} - \mathbf{L}_r) \mathbf{P}_r (\mathbf{L} - \mathbf{L}_r). \tag{69}$$

According to the definition (37), $\mathbf{P}_r = \mathbf{P}_r^T$, hence it follows that $\mathbf{L} = \mathbf{L}^T$. This agrees with WALPOLE's (1981) self-consistent result for polycrystals, but in the present context the validity of the formula has been expanded to matrix-based systems reinforced by inclusions of the same shape and alignment. Equation (69) coincides with the several variants of the self-consistent approximation pointed out by WILLIS (1981), when all the particles are of the same shape and alignment, and the matrix itself is also embedded under the same shape as the particles.

The overall thermal stress tensor $\mathbf{I}$ is evaluated in the two ways indicated by say, (57) and (59). However, the existence of a single $\mathbf{L}^*$ for all phases guarantees that (57) can be written as

$$\mathbf{I} = (\mathbf{L}^* + \mathbf{L}) \sum_{r=1}^{N} c_r (\mathbf{L}^* + \mathbf{L}_r)^{-1} \mathbf{I} \tag{70}$$

and the same form is recovered from (59) with the help of (56).

The prediction of $\mathbf{I}$ are therefore consistent; this was also observed by LAWS (1973). Of course, in both cases the consistency holds if the predicted $\mathbf{L}$ is diagonally symmetric.

5.4. *Two-phase materials with inclusions of different shape*

Recall that systems of this type may have an arbitrary phase geometry, but that the material axes in each phase must be fixed. As in (37), (38), and (44), there is

$$\begin{aligned} \mathbf{a}_r &= \mathbf{P}_s^r (\mathbf{I} - \mathbf{I}_\beta) \\ \mathbf{P}^r (\mathbf{L} - \mathbf{L}_\beta) \mathbf{P}_s^r &= \mathbf{P}_s^r - \mathbf{P}^r, \quad s = 2, 3, \ldots, N, \\ \mathbf{A}_r &= \mathbf{I} + \mathbf{P}_s^r (\mathbf{L} - \mathbf{L}_\beta). \end{aligned} \tag{71}$$

Only a numerical evaluation of $\mathbf{L}$ will be presented with the phase properties in (47). Phase 1 is used as matrix, and phase 3 is present as fibers and circular discs. The first, second and the final, ninth iteration give the following estimates of $\mathbf{L}$:

$$(\mathbf{L})_1 = \begin{bmatrix} 245.70 & 87.88 & 71.07 & 0 & 0 & 0 \\ 87.88 & 245.70 & 71.07 & 0 & 0 & 0 \\ 71.07 & 71.07 & 224.60 & 0 & 0 & 0 \\ 0 & 0 & 0 & 53.95 & 0 & 0 \\ 0 & 0 & 0 & 0 & 53.95 & 0 \\ 0 & 0 & 0 & 0 & 0 & 78.91 \end{bmatrix} \text{GPa},$$

$$(\mathbf{L})_2 = \begin{bmatrix} 265.75 & 93.77 & 79.79 & 0 & 0 & 0 \\ 93.77 & 265.95 & 79.79 & 0 & 0 & 0 \\ 79.55 & 79.55 & 243.88 & 0 & 0 & 0 \\ 0 & 0 & 0 & 60.56 & 0 & 0 \\ 0 & 0 & 0 & 0 & 60.56 & 0 \\ 0 & 0 & 0 & 0 & 0 & 85.99 \end{bmatrix} \text{GPa},$$

$$(\mathbf{L})_9 = \begin{bmatrix} 269.95 & 95.45 & 82.80 & 0 & 0 & 0 \\ 95.45 & 269.95 & 82.80 & 0 & 0 & 0 \\ 82.80 & 82.80 & 249.24 & 0 & 0 & 0 \\ 0 & 0 & 0 & 64.44 & 0 & 0 \\ 0 & 0 & 0 & 0 & 64.44 & 0 \\ 0 & 0 & 0 & 0 & 0 & 87.25 \end{bmatrix} \text{GPa}. \tag{72}$$

which converges to a symmetric $\mathbf{L}$.

The first alternative evaluation of $\mathbf{l}$ follows from (3_1), where we take $\mathbf{a}$, from (71_1). This yields

$$\mathbf{l} = \left[\mathbf{I} - (\mathbf{L}_\beta - \mathbf{L}_2)\left(\sum_{s=2}^{N} c_s \mathbf{P}_2^s\right)\right]^{-1}\left[c_2\mathbf{l}_2 + (1-c_2)\mathbf{l}_\beta - (\mathbf{L}_\beta - \mathbf{L}_2)\left(\sum_{s=2}^{N} c_s \mathbf{P}_2^s\right)\mathbf{l}_\beta\right]. \tag{73}$$

The second alternative follows from (12_1) with $\mathbf{A}_s$ from (71_3). This eventually becomes

$$\mathbf{l} = c_2\mathbf{l}_2 + (1-c_2)\mathbf{l}_\beta + (\mathbf{L} - \mathbf{L}_\beta)\left[\sum_{s=2}^{N} c_s \mathbf{P}_2^s\right](\mathbf{l}_\beta - \mathbf{l}_2), \tag{74}$$

where $\mathbf{L}$ was assumed to be diagonally symmetric.

To show that (73) and (74) are equivalent, write $\mathbf{L}$ in the following form

$$\mathbf{L} = c_2\mathbf{L}_2 + c_\beta\mathbf{L}_\beta + (\mathbf{L}_\beta - \mathbf{L}_2)\left[\sum_{s=2}^{N} c_s \mathbf{P}_2^s\right](\mathbf{L} - \mathbf{L}_\beta), \tag{75}$$

which follows from (2_1) with $\mathbf{A}_s$ from (71_3). Solve this for $(\mathbf{L} - \mathbf{L}_\beta)$, and substitute into (74) to convert this equation into a form which coincides with (73). This proves the required consistency.

6. The Differential Scheme

An alternative to the direct evaluation of overall properties by the self-consistent or Mori–Tanaka methods is offered by various differential schemes (Roscoe, 1952; Boucher, 1974; McLaughlin, 1977; Cleary *et al.*, 1980; Norris, 1985). In principle, such schemes evaluate the final overall properties in many steps which involve removal of a small part of the current material volume, and its replacement by one or more of the inclusion phases. For example, an unreinforced matrix may serve as a starting point. A small volume is removed and replaced by one or more solitary inclusions of the other phases. The replacement starts with initial inclusions in the matrix, and is then incrementally repeated in the instantaneous effective medium. The process is repeated until the final volume fractions of all phases are reached.

Many specific procedures have been proposed, and the final outcome tends to depend on the path or removal/replacement sequence leading to the final material configuration. However, as long as the dilute approximation is employed at each step of the process, the predicted intermediate and final effective stiffness must be diagonally symmetric. In contrast to the Mori–Tanaka and self-consistent methods, the differential schemes may predict symmetric overall stiffness even for multiphase systems with inclusions of different shape.

As an illustration, we choose the procedure suggested by McLaughlin (1977), and extend it to a matrix-based ($s = 1$), three-phase composite. The overall stiffness is given by the following set of coupled nonlinear ordinary differential equations

$$\frac{\mathrm{d}\mathbf{L}}{\mathrm{d}c} = \frac{\mathrm{d}c_2}{(1-c)\,\mathrm{d}c}(\mathbf{L}_2-\mathbf{L})\mathbf{E}_2 + \frac{\mathrm{d}c_3}{(1-c)\,\mathrm{d}c}(\mathbf{L}_3-\mathbf{L})\mathbf{E}_3, \tag{76}$$

$$\mathbf{E}_r = [\mathbf{I}+\mathbf{P}_r(\mathbf{L}_r-\mathbf{L})]^{-1} = \mathbf{I}+\mathbf{P}_r(\mathbf{L}-\mathbf{L}_r), \quad \text{for } r = 2, 3, \tag{77}$$

with the initial condition $\mathbf{L} = \mathbf{L}_1$ at $c = 0$.

Here, $\mathbf{L}$ is the unknown overall stiffness, $\mathbf{L}_r$ are known phase properties, $c = \Sigma_2^3 c_r$ is the volume fraction of the inclusion phase, and the $\mathbf{E}_r$ define the intermediate strain concentration factors of the inclusion phases 2 and 3. Both inclusion phases may have different moduli and shape, but $\mathbf{P}_2$ and $\mathbf{P}_3$ are diagonally symmetric, as in (64). After substitution from (77) into (76) and rearrangement one finds

$$\frac{\mathrm{d}\mathbf{L}}{\mathrm{d}c} = \frac{1}{(1-c)}\sum_{r=2}^{3}\left(\frac{\mathrm{d}c_r}{\mathrm{d}c}(\mathbf{L}_r-\mathbf{L}) + (\mathbf{L}_r-\mathbf{L})\mathbf{P}_r(\mathbf{L}-\mathbf{L}_r)\right), \tag{78}$$

which suggests that each successive $\mathbf{L}$ will be diagonally symmetric, as long as the initial $\mathbf{L} = \mathbf{L}_1$ is diagonally symmetric. It can be proved that the formulation proposed by Norris (1985), will also lead to the same conclusion (Chen, 1990).

7. Overall Material Symmetry

Now that we have established some of the conditions which guarantee the diagonal symmetry of the various estimates of the overall stiffness, we proceed to examine the

elastic symmetry implied by these estimates. The motive is probably obvious. In any actual system, a given set of phases can be arranged in many different spatial configurations which may determine the overall material symmetry of the system. However, the dilute approximation and the Mori–Tanaka method are not explicitly concerned with the actual distribution of the phases. Indeed, through the dilute configuration which they typically employ, they focus on a single phase in a matrix. Therefore, it is of interest to find the overall material symmetries which are, or can be actually represented by the estimates.

To make progress, we first summarize the expressions which give an explicit estimate of $\mathbf{L}$. In the dilute approximation, $\mathbf{L}$ follows from (17), with

$$\mathbf{T}_r = [\mathbf{I} + \mathbf{P}^r(\mathbf{L}_r - \mathbf{L}_1)]^{-1}, \tag{79}$$

where $\mathbf{P}^r = \mathbf{S}\mathbf{L}_1^{-1}$, so that

$$\mathbf{L}_{\mathrm{DIL}} = \mathbf{L}_1 + \sum_{r=2}^{N} c_r[(\mathbf{L}_r - \mathbf{L}_1)^{-1} + \mathbf{P}^r]^{-1}. \tag{80}$$

In the Mori–Tanaka (MT) method, for systems with aligned inclusions of similar shape ($\mathbf{P}^r = \mathbf{P}$) in Section 4.2, Eq. (33) gives the result

$$\mathbf{L}_{\mathrm{MT}} = \left[\sum_{r=1}^{N} c_r(\mathbf{L}^* + \mathbf{L}_r)^{-1}\right]^{-1} - \mathbf{L}^*, \tag{81}$$

where [Eq. (31)]

$$\mathbf{L}^* = \mathbf{P}^{-1} - \mathbf{L}_1.$$

For two-phase systems of any geometry, Section 4.3, there is [Eq. (41)]

$$\mathbf{L}_{\mathrm{MT}} = \mathbf{L}_\beta + c_\gamma\left[\sum_{r=1}^{N} c_r(\mathbf{L}_\gamma - \mathbf{L}_\beta)^{-1} + \mathbf{P}_\gamma^\beta\right]^{-1},$$

where $\mathbf{P}_\gamma^\beta$ follows from (37) in the form

$$\mathbf{P}_\gamma^\beta = [(\mathbf{P}^\gamma)^{-1} - (\mathbf{L}_\gamma - \mathbf{L}_\beta)]^{-1}. \tag{82}$$

These explicit estimates indicate that, in the two cases, the material symmetry of $\mathbf{L}$ will coincide with the lowest symmetry or with the "highest anisotropy" found in any phase stiffness $\mathbf{L}_r$ and in the tensor $\mathbf{P}^r$, when all are written in a fixed overall coordinate system. For example, if $\mathbf{L}_r$ is at most transversely isotropic, and the structure of $\mathbf{P}^r$ resembles an orthotropic symmetry, then $\mathbf{L}$ is orthotropic. Similar conclusions can be verified for the tensor $\mathbf{I}$. However, there is no assurance that the estimates will reflect the effect that some special arrangement of the phases, e.g., in a cubic array, may have on the relative magnitude of some coefficients of $\mathbf{L}$; all such magnitudes follow directly from the respective expressions. In other words, each estimate provides information on the stiffness of only one of the many different systems which could be actually constructed from the same collection of phases and shapes. The outcome follows directly from the above expressions, it depends only on the prescribed magnitudes of c_r, $\mathbf{L}_r$, and $\mathbf{P}^r$, and it does not reveal the internal structure of this particular

system. Since no relevant information can be introduced, one may speculate that this system will have the most random arrangement of the phases permitted by the constraints that may be imposed by $\mathbf{L}_0$ and $\mathbf{P}'$.

As far as the self-consistent model is concerned, a variant of this method in which a certain periodic spatial distribution of inclusions is incorporated has recently been formulated by FASSI-FEHRI *et al.* (1989). In principle, the spatial distribution of particles can be incorporated into a micromechanics model through some statistical information: see the review papers by WILLIS (1981, 1983). However an implementation of such an approach to a specific system remains to be accomplished.

ACKNOWLEDGEMENTS

Funding for this work was provided, in part, by the ONR DARPA-HiTASC composites program at Rensselaer, and by the Air Force Office of Scientific Research.

REFERENCES

BENVENISTE, Y.	1987	*Mechanics of Materials* **6**, 147.
BENVENISTE, Y.	1990	*J. Appl. Mech.* **57**, 474.
BENVENISTE, Y. and DVORAK, G. J.	1990	In Toshio Mura Anniversary Volume: *Micromechanics and Inhomogenity* (edited by WENG, G. J., TAYA, M. and ABE, H.), pp. 65–81. Springer.
BENVENISTE, Y., DVORAK, G. J. and CHEN, T.	1989	*Mechanics of Materials* **7**, 305.
BOUCHER, S.	1974	*J. Comp. Mat.* **8**, 82.
BRUGGEMAN, D. A. G.	1935	*Annalen der Physik* **24**, 636.
BUDIANSKY, B.	1965	*J. Mech. Phys. Solids* **13**, 223.
CHEN, T.	1990	Ph.D. dissertation, Rensselaer Polytechnic Institute.
CHEN, T., DVORAK, G. J. and BENVENISTE, Y.	1990	*Mechanics of Materials* **9**, 17.
CLEARY, M. P., CHEN, I. W. and LEE, S. M.	1980	*J. Engng Mech.* **106**, 861.
DVORAK, G. J. and CHEN, T.	1989	*J. Appl. Mech.* **56**, 418.
FASSI-FEHRI, O., HIHI, A. and BERVEILLER, M.	1989	*Int. J. Engng Sci.* **27**, 495.
HERSHEY, A. V.	1954	*J. Appl. Mech.* **21**, 236.
HILL, R.	1963	*J. Mech. Phys. Solids* **11**, 357.
HILL, R.	1965	*J. Mech. Phys. Solids* **13**, 213.
KRÖNER, E.	1958	*Z. Phys.* **151**, 504.
LAWS, N.	1973	*J. Mech. Phys. Solids* **21**, 9.
LEVIN, V. M.	1967	*Mekhanika Tverdogo Tela* **2**, 88 (English translation: *Mechanics of Solids* **2**, 58).
LEVIN, V. M.	1976	*Mekhanika Tverdogo Tela*, **11**, 137 (English translation: *Mechanics of Solids* **11**, 119).
MCLAUGHLIN, R.	1977	*Int. J. Engng Sci.* **15**, 237.
MORI, T. and TANAKA, K.	1973	*Acta Metall.* **21**, 571.
NORRIS, A. N.	1985	*Mech. Mat.* **4**, 1.
NORRIS, A. N.	1989	*J. Appl. Mech.* **56**, 83.

ROSCOE, R. 1952 *Br. J. Appl. Phys.* **3**, 267.
ROSEN, B. W. and HASHIN, Z. 1970 *Int. J. Engng Sci.* **8**, 157.
WALPOLE, L. J. 1969 *J. Mech. Phys. Solids* **17**, 235.
WALPOLE, L. J. 1981 In *Advances in Applied Mechanics*, Vol. 21, p. 170 (edited by C. S. YIH). Academic Press, New York.
WILLIS, J. R. 1977 *J. Mech. Phys. Solids* **25**, 185.
WILLIS, J. R. 1981 In *Advances in Applied Mechanics*, Vol. 21, p. 1 (edited by C. S. YIH). Academic Press, New York.
WILLIS, J. R. 1983 *J. Appl. Mech.* **50**, 1202.
WILLIS, J. R. 1984 *J. Math. Phys.* **25**, 2116.

Reprinted from

G.J. Weng M. Taya H. Abé
Editors

Micromechanics and Inhomogeneity

The Toshio Mura 65th Anniversary Volume

Springer-Verlag
New York Berlin Heidelberg
London Paris Tokyo Hong Kong

On a Correspondence Between Mechanical and Thermal Effects in Two-Phase Composites

Y. BENVENISTE* and G. J. DVORAK
Department of Civil Engineering, Rensselaer Polytechnic Institute,
Troy, NY 12180-3590, U.S.A.

Abstract

This paper considers the thermomechanical loading problem of binary composites with any anisotropic elastic constituents and arbitrary phase geometry, subjected to homogeneous traction or displacement boundary conditions and uniform temperature change. It is shown that the solution of the thermomechanical problem is uniquely determined by the solution of the purely mechanical problem corresponding to zero temperature change. This result is used to obtain explicit relations between the effective thermal strain (or stress) coefficient tensor and the effective mechanical properties. The correspondence between thermomechanical and purely mechanical loads is also used to establish an important consistency property of the Mori–Tanaka model in the context of thermomechanical problems. Extensions of the results to composite systems with temperature-dependent properties is discussed.

1. Introduction

In recent papers, Dvorak (1983, 1986) has shown that for certain binary composites subjected to combined thermomechanical loading, the local thermal strain and stress concentration factors can be related in an exact way to the corresponding mechanical concentration factors. The considered systems were effectively isotropic binary composites with elastically isotropic phase but arbitrary phase geometry, and fibrous composites with elastically isotropic or transversely isotropic constituents of any cross section but of cylindrical geometry. The correspondence established in that paper between the concentration factors allows us to write expressions for the effective thermal expansion coefficients once the effective mechanical properties are known. Moreover, the derivation is made in a manner which makes the results applicable to inelastic systems.

The present paper generalizes the results obtained by Dvorak (1986) to

* On sabbatical leave from Tel-Aviv University.

binary composites with general anisotropic constituents and arbitrary phase geometry. The established results are then used to prove an important consistency property of the Mori–Tanaka micromechanics model in the context of thermomechanical problems.

In the second section of the paper the correspondence relations between thermomechanical problems and pure mechanical problems are obtained in a closed and simple form. Two types of loadings are considered:

(a) A combined thermomechanical loading with homogeneous traction boundary conditions and uniform temperature change (Equation (2.4)).
(b) A combined thermomechanical loading with homogeneous displacement boundary conditions and uniform temperature change (Equation (2.5)).

The purely mechanical problems are those corresponding to a zero temperature change.

The third section of the paper is concerned with evaluation of the tensor of effective thermal strain coefficients (thermal expansion) and the tensor of effective thermal stress coefficients, a subject which has drawn considerable interest in the literature in the last two decades. In a well-known paper, Levin (1967) has shown that in two-phase materials with arbitrary phase geometry the effective thermal expansion coefficients can be related to the effective elastic properties. This line of inquiry was extended by Schapery (1968), who derived bounds on thermal expansion coefficients of multiphase composites with isotropic phases, while Rosen and Hashin (1970) reviewed and extended Levin's result to general anisotropic phases. Laws (1973), on the other hand, has given a different treatment of the subject based on thermostatic considerations. We finally mention Craft and Christensen (1981) who considered the thermal expansion of composites with randomly oriented fibers. We show in the third section of the paper that the principle established in the second section allows a straightforward and elegant derivation of the results of Rosen and Hashin (1970) and Laws (1973). A dual formulation corresponding to zero traction or zero displacement boundary conditions is presented, resulting in expressions for the effective thermal strain and stress coefficient tensors.

The fourth section of the paper is concerned with the Mori–Tanaka (1973) model of composites in the context of thermomechanical problems. There exist several papers in the literature which predict the effective thermal coefficients of particulate composites by using the average matrix stress (or strain) concept of Mori and Tanaka (1973) (see Wakashima *et al.*, 1974; Takahashi *et al.*, 1985; Takao, 1985; Takao and Taya, 1985). These works base their derivation directly on eigenstrain concepts and the equivalent inclusion idea of Eshelby (1957), and do not make use of the results of Levin (1967) and Rosen and Hashin (1970). This section of the paper gives a concise derivation of the Mori–Tanaka micromechanics problem in the context of the thermomechanical properties, in the spirit of the exposition of this theory by Benveniste (1987) which dealt with the purely mechanical case. The correspondence relations established in the previous sections are then used to prove an

important consistency property of this micromechanical mode. Specifically, we show that the direct application of the model to the prediction of the effective thermal coefficients produces results which are in agreement with those that would have been obtained if the relations of Levin (1967) and Rosen and Hashin (1970) were used.

The paper concludes with some comments on applications of the results to composite systems with temperature-dependent properties.

2. Correspondence of Overall Mechanical and Thermomechanical Loading

Consider a two-phase composite consisting of perfectly bonded anisotropic constituents of arbitrary phase geometry such that the orientation of the respective material axes in each of the phases is fixed throughout the aggregate. Let the thermoelastic constitutive relations of the homogeneous phases, $r = 1, 2$, be given by

$$\boldsymbol{\sigma}_r = \mathbf{L}_r\boldsymbol{\varepsilon}_r + \mathbf{l}_r\theta, \tag{2.1}$$

$$\boldsymbol{\varepsilon}_r = \mathbf{M}_r\boldsymbol{\sigma}_r + \mathbf{m}_r\theta, \tag{2.2}$$

where $\mathbf{L}_r$ and $\mathbf{M}_r = (\mathbf{L}_r)^{-1}$ are the phase stiffness and compliance tensors, $\mathbf{m}_r$ is the thermal strain vector (of expansion coefficients), and $\mathbf{l}_r$ the thermal stress vector, such that

$$\mathbf{l}_r = -\mathbf{L}_r\mathbf{m}_r. \tag{2.3}$$

Define the following thermomechanical loading problems for a representative volume V of the composite aggregate:

Problem I

$$\boldsymbol{\sigma}_n(S) = \boldsymbol{\sigma}_0\mathbf{n}, \qquad \theta(S) = \theta_0. \tag{2.4}$$

Problem II

$$\mathbf{u}(S) = \boldsymbol{\varepsilon}_0\mathbf{x}, \qquad \theta(S) = \theta_0, \tag{2.5}$$

where $\boldsymbol{\sigma}_n(S)$ and $\mathbf{u}(S)$ are the traction and displacement vectors at the external boundary S of V, with an outer unit normal $\mathbf{n}$, $\boldsymbol{\sigma}_0$ and $\boldsymbol{\varepsilon}_0$ are constant uniform overall stress and strain fields, and $\mathbf{x}$ denotes a Cartesian coordinate; $\theta(S)$ is the thermal change at S, and θ_0 is a constant quantity.

Note first that the uniform field $\theta(\mathbf{x}) = \theta_0$ in the volume V is the stationary temperature distribution that satisfies the boundary conditions ((2.4_2), (2.5_2)). The local stresses and strains in the phase, which are caused, respectively, by the prescribed boundary conditions (2.4) and (2.5), can be written in the form

$$\boldsymbol{\sigma}_r(\mathbf{x}) = \mathbf{B}_r(\mathbf{x})\boldsymbol{\sigma}_0 + \mathbf{b}_r(\mathbf{x})\theta_0, \tag{2.6}$$

and

$$\boldsymbol{\varepsilon}_r(\mathbf{x}) = \mathbf{A}_r(\mathbf{x})\boldsymbol{\varepsilon}_0 + \mathbf{a}_r(\mathbf{x})\theta_0. \tag{2.7}$$

In the above equations, $\mathbf{A}_r(\mathbf{x})$ and $\mathbf{B}_r(\mathbf{x})$ are fourth-order tensors; their phase volume averages in a representative volume, $\mathbf{A}_r$ and $\mathbf{B}_r$ are usually called the mechanical strain and stress concentration factor tensors. The second-order

tensors $\mathbf{a}_r(\mathbf{x})$ and $\mathbf{b}_r(\mathbf{x})$, have representative phase volume averages $\mathbf{a}_r$ and $\mathbf{b}_r$ which are called the thermal strain and stress concentration factors. These tensors without the argument x will denote average quantities in the sequel of the paper.

We will now show that for statistically homogeneous two-phase composites with distinct anisotropic constituents and completely arbitrary phase geometry, the tensor $\mathbf{b}_r(\mathbf{x})$ can be uniquely determined in terms of $\mathbf{B}_r(\mathbf{x})$, $\mathbf{M}_r$, and $\mathbf{m}_r$. A similar relation will be derived between $\mathbf{a}_r(\mathbf{x})$ and the tensors $\mathbf{A}_r(\mathbf{x})$, $\mathbf{L}_r$, and $\mathbf{l}_r$. These results will be obtained from the decomposition procedure proposed by Dvorak (1986, Sect. 3), which is extended here to systems with arbitrary phase anisotropy.

Consider first Problem I, Equation (2.4). By linearity, the effect of θ_0 can be determined separately, and is in fact represented by $\mathbf{b}_r(\mathbf{x})$ in (2.6). This tensor can be evaluated from the following decomposition scheme:

(a) The phases are separated from each other and subjected to a uniform temperature rise θ_0 which causes the uniform strains

$$\boldsymbol{\varepsilon}_1 = \mathbf{m}_1\theta_0, \qquad \boldsymbol{\varepsilon}_2 = \mathbf{m}_2\theta_0, \tag{2.8}$$

and zero stresses.

(b) Certain unknown tractions derived from an auxiliary uniform stress field

$$\hat{\boldsymbol{\sigma}}_1(\mathbf{x}) = \hat{\boldsymbol{\sigma}}_2(\mathbf{x}) = \hat{\boldsymbol{\sigma}}, \tag{2.9}$$

are applied to each phase such that the uniform strains caused by (2.8) and (2.9) make the phases compatible. This condition is met by demanding that

$$\mathbf{M}_1\hat{\boldsymbol{\sigma}} + \mathbf{m}_1\theta_0 = \mathbf{M}_2\hat{\boldsymbol{\sigma}} + \mathbf{m}_2\theta_0. \tag{2.10}$$

Therefore,

$$\hat{\boldsymbol{\sigma}} = (\mathbf{M}_1 - \mathbf{M}_2)^{-1}(\mathbf{m}_2 - \mathbf{m}_1)\theta_0, \tag{2.11}$$

providing that the inverse exists. A discussion of this proviso appears in Appendix A.

(c) In the final step of the decomposition procedure, overall tractions $-\hat{\boldsymbol{\sigma}}\mathbf{n}$ are applied at S to cancel the tractions introduced there in step (b). By superposition and with regard to the definition (2.6) of $\mathbf{B}_r(\mathbf{x})$, the tensor $\mathbf{b}_r(\mathbf{x})$ can now be written in the desired form

$$\mathbf{b}_r(\mathbf{x}) = [\mathbf{I} - \mathbf{B}_r(\mathbf{x})](\mathbf{M}_1 - \mathbf{M}_2)^{-1}(\mathbf{m}_2 - \mathbf{m}_1), \tag{2.12}$$

where $\mathbf{I}$ is the fourth-order unit tensor defined by

$$I_{ijkl} = \tfrac{1}{2}(\delta_{ik}\delta_{jl} + \delta_{il}\delta_{jk}), \tag{2.13}$$

with δ_{ik} being the Kronecker delta.

Consider next the thermal loading Problem II, Equation (2.5). The solution follows again from the above decomposition which remains unchanged except

for the conditions (2.9) and (2.10) which are now replaced by the forms

$$\boldsymbol{\varepsilon}_1(\mathbf{x}) = \boldsymbol{\varepsilon}_2(\mathbf{x}) = \boldsymbol{\varepsilon}, \tag{2.14}$$

$$\mathbf{L}_1\boldsymbol{\varepsilon} + \mathbf{l}_1\theta_0 = \mathbf{L}_2\boldsymbol{\varepsilon} + \mathbf{l}_2\theta_0. \tag{2.15}$$

The uniform auxiliary strain field then follows as

$$\boldsymbol{\varepsilon} = (\mathbf{L}_1 - \mathbf{L}_2)^{-1}(\mathbf{l}_2 - \mathbf{l}_1)\theta_0. \tag{2.16}$$

The last step (c) of the procedure is now implemented by applying on S the displacement field

$$u_r(S) = -\boldsymbol{\varepsilon}\mathbf{x}. \tag{2.17}$$

That leads to the final expression for $\mathbf{a}_r(\mathbf{x})$

$$\mathbf{a}_r(\mathbf{x}) = [\mathbf{I} - \mathbf{A}_r(\mathbf{x})](\mathbf{L}_1 - \mathbf{L}_2)^{-1}(\mathbf{l}_2 - \mathbf{l}_1). \tag{2.18}$$

For the special case of a binary composite made of isotropic constituents, (2.12) and (2.18) can be reduced to the expressions for thermal stress and strain concentration factors given, respectively, by Dvorak (1986), equations (38) and (40). For fibrous composites with two transversely isotropic phases, the original decomposition procedure allows the imposition of an additional relation between phase stress or strain averages, such as equation (11) in the 1986 paper. Such additional relations cannot be prescribed in the present case of arbitrary phase geometry. We note, however, that the original and the present procedures coincide if we choose the additional constraint to be in agreement with (2.9) above, i.e., as $d\sigma_1^r = d\sigma_2^r$ (using the notation of the 1986 paper). We also note that (2.12) and (2.18) are analogous to the relations between mechanical and thermal microstress fields in fibrous composites consisting of three cylindrical transversely isotropic phases, which were recently derived by Dvorak and Chen (1988).

3. Effective Thermal Expansion Coefficients

We now utilize the above decomposition procedure in a derivation of the overall thermal expansion coefficients of binary composites with anisotropic phases.

The effective constitutive law of a heterogeneous thermoelastic medium can be written in the form

$$\bar{\boldsymbol{\varepsilon}} = \mathbf{M}\bar{\boldsymbol{\sigma}} + \mathbf{m}\bar{\theta}, \qquad \bar{\boldsymbol{\sigma}} = \mathbf{L}\bar{\boldsymbol{\varepsilon}} + \mathbf{l}\bar{\theta}, \tag{3.1}$$

with

$$\mathbf{l} = -\mathbf{L}\mathbf{m}, \qquad \mathbf{M} = \mathbf{L}^{-1}, \tag{3.2}$$

where the overbars denote representative volume averages of the stress or strain fields, M, L are the effective overall compliance and stiffness tensors

given by Hill (1963) as

$$\mathbf{M} = c_1\mathbf{M}_1\mathbf{B}_1 + c_2\mathbf{M}_2\mathbf{B}_2, \qquad \mathbf{L} = c_1\mathbf{L}_1\mathbf{A}_1 + c_2\mathbf{L}_2\mathbf{A}_2, \tag{3.3}$$

where c_r are the constituent volume fractions, and $\mathbf{m}$ and $\mathbf{l}$ in (3.1) and (3.2) are the overall thermal strain and thermal stress tensors. It is again recalled that $\mathbf{B}_r$ and $\mathbf{A}_r$ are representative phase volume averages of the fields $\mathbf{B}_r(\mathbf{x})$, $\mathbf{A}_r(\mathbf{x})$ defined in (2.6) and (2.7), respectively.

Consider first a special form of Problem I, Equation (2.4), in which $\sigma_0 = \mathbf{0}$. Since in this case $\bar{\sigma} = \mathbf{0}$ and $\bar{\theta} = \theta_0$, we find from (3.1_1) that

$$\mathbf{m}\theta_0 = \bar{\varepsilon} = c_1\varepsilon_1 + c_2\varepsilon_2, \tag{3.4}$$

where ε_1, ε_2 are phase volume averages of local strains $\varepsilon_1(\mathbf{x})$ and $\varepsilon_2(\mathbf{x})$. Substitution of (2.12) into (2.6) with $\sigma_0 = \mathbf{0}$, and the result in (2.2) provides

$$\varepsilon_r = \mathbf{M}_r[\mathbf{I} - \mathbf{B}_r](\mathbf{M}_1 - \mathbf{M}_2)^{-1}(\mathbf{m}_2 - \mathbf{m}_1)\theta_0. \tag{3.5}$$

Equations (3.5), (3.4), and (3.3), finally give the overall thermal strain tensor $\mathbf{m}$

$$\mathbf{m} = c_1\mathbf{m}_1 + c_2\mathbf{m}_2 + (\mathbf{M} - c_1\mathbf{M}_1 - c_2\mathbf{M}_2)(\mathbf{M}_1 - \mathbf{M}_2)^{-1}(\mathbf{m}_1 - \mathbf{m}_2), \tag{3.6}$$

which is precisely equation (2.2) in Rosen and Hashin (1970). It is interesting to observe that in this process of substitution, $\mathbf{B}_1$ and $\mathbf{B}_2$ combine in the manner of (3.3_1) into the overall property $\mathbf{M}$. Equivalent forms of (3.6) which can be arrived at after some manipulation are

$$\mathbf{m} = \mathbf{m}_1 + (\mathbf{M}_1 - \mathbf{M})(\mathbf{M}_2 - \mathbf{M}_1)^{-1}(\mathbf{m}_1 - \mathbf{m}_2), \tag{3.7}$$

and the symmetric form

$$\mathbf{m} = (\mathbf{M} - \mathbf{M}_2)(\mathbf{M}_1 - \mathbf{M}_2)^{-1}\mathbf{m}_1 + (\mathbf{M} - \mathbf{M}_1)(\mathbf{M}_2 - \mathbf{M}_1)^{-1}\mathbf{m}_2. \tag{3.8}$$

We now turn to Problem II, Equation (2.5), and seek the solution for $\varepsilon_0 = \mathbf{0}$. Equation (3.1_2) provides

$$\mathbf{l}\theta_0 = \sigma = c_1\sigma_1 + c_2\sigma_2, \tag{3.9}$$

where σ_1 and σ_2 are phase volume averages of $\sigma_1(\mathbf{x})$ and $\sigma_2(\mathbf{x})$, respectively. This, together with (2.18) and (2.7) at $\varepsilon_0 = \mathbf{0}$, and (2.1) with (3.3_1) yields

$$\mathbf{l} = c_1\mathbf{l}_1 + c_2\mathbf{l}_2 + (\mathbf{L} - c_1\mathbf{L}_1 - c_2\mathbf{L}_2)(\mathbf{L}_1 - \mathbf{L}_2)^{-1}(\mathbf{l}_1 - \mathbf{l}_2). \tag{3.10}$$

The equivalent forms are

$$\mathbf{l} = \mathbf{l}_1 + (\mathbf{L}_1 - \mathbf{L})(\mathbf{L}_2 - \mathbf{L}_1)^{-1}(\mathbf{l}_1 - \mathbf{l}_2), \tag{3.11}$$

$$\mathbf{l} = (\mathbf{L} - \mathbf{L}_2)(\mathbf{L}_1 - \mathbf{L}_2)^{-1}\mathbf{l}_1 + (\mathbf{L} - \mathbf{L}_1)(\mathbf{L}_2 - \mathbf{L}_1)^{-1}\mathbf{l}_2. \tag{3.12}$$

Laws (1973) derived this last formula in a different way.

Using (2.3) and (3.2_2), we can verify that $\mathbf{m}$ and $\mathbf{l}$ as given by (3.6) and (3.10), or by their equivalent forms, satisfy (3.2_1).

Special forms of (3.6) and (3.10) for fibrous and particulate composites were given by equations (26), (29), (37), and (39) in Dvorak's (1986) paper.

The direct derivation of the overall thermal strain and stress tensors $\mathbf{m}$ and $\mathbf{l}$, from the above relations between thermal and mechanical concentration factors, implies that these tensors can be found once the effective mechanical properties have been predicted by a certain micromechanical model. However, a valid question to ask is whether the model, if used to estimate the effective thermal strain and stress tensors directly, would give the predictions that coincide with those found from (3.6) and (3.10). The following section establishes such consistency for the Mori–Tanaka model.

4. Application of the Mori–Tanaka Method to Thermoelastic Problems

4.1. *Review of the Method and Principal Results*

We start by giving a concise summary of this model, in the framework of its application to purely mechanical problems, as presented by Benveniste (1987).

Consider the loading configuration of Problem I, Equation (2.4), with $\theta_0 = 0$. In this case, $\bar{\boldsymbol{\sigma}} = \boldsymbol{\sigma}_0$, hence we have

$$c_1\mathbf{B}_1 + c_2\mathbf{B}_2 = \mathbf{I}, \tag{4.1}$$

which, when combined with (3.3_1), results in

$$\mathbf{M} = \mathbf{M}_1 + c_2(\mathbf{M}_2 - \mathbf{M}_1)\mathbf{B}_2, \tag{4.2}$$

so that we need to know $\mathbf{B}_2$ (or $\mathbf{B}_1$) to determine $\mathbf{M}$.

Similarly, in Problem II, Equation (2.5), with $\theta_0 = 0$ there is $\bar{\boldsymbol{\varepsilon}} = \boldsymbol{\varepsilon}_0$, hence

$$c_1\mathbf{A}_1 + c_2\mathbf{A}_2 = \mathbf{I}, \tag{4.3}$$

with

$$\mathbf{L} = \mathbf{L}_1 + c_2(\mathbf{L}_2 - \mathbf{L}_1)\mathbf{A}_2. \tag{4.4}$$

In all results obtained so far it was possible to regard both phases on equal footing. In contrast, the Mori–Tanaka method makes a clear distinction between the continuous matrix and the discrete fibrous or particulate reinforcement. Therefore, it is necessary to designate the phases by numbers, which we select as 1 for the matrix and 2 for the reinforcement. We furthermore assume here that the particulate phase is represented by ellipsoidal inclusions of similar shape but which can be, however, of different size. The model can be applied to inclusions which are aligned, may have a certain orientation distribution, or are of random orientation. For simplicity of the exposition we chose to deal here with the case of aligned inclusions.

The approximate evaluation of the strain concentration factor $\mathbf{A}_2$ will illustrate the method. Under dilute conditions, $\mathbf{A}_2$ would be found from strains in a single inclusion embedded in an infinite matrix subjected to the uniform boundary strains (2.5) with $\theta = 0$. The solution of this problem is

$$\mathbf{A}_2 = \mathbf{T}, \tag{4.5}$$

where

$$\mathbf{T} = [\mathbf{I} + \mathbf{S}\mathbf{L}_1^{-1}(\mathbf{L}_2 - \mathbf{L}_1)]^{-1}, \tag{4.6}$$

and S is the Eshelby (1957) tensor.

Of course, in the case of a single inclusion the average strain in the infinite matrix is not affected by the presence of the inclusion and is thus equal to ε_0. In contrast, when many inclusions are present, the magnitude of the average strain in the matrix, and in the inclusions, is influenced by their interaction. The Mori–Tanaka method assumes that the average strain ε_r in the interacting inclusions can be approximated by that of a single inclusion embedded in an infinite matrix subjected to the uniform average matrix strain ε_1. This is illustrated in Fig. 1(a) which shows Problem I with $\theta_0 = 0$, which must now be solved for a single inclusion in a certain large volume V' which is enclosed

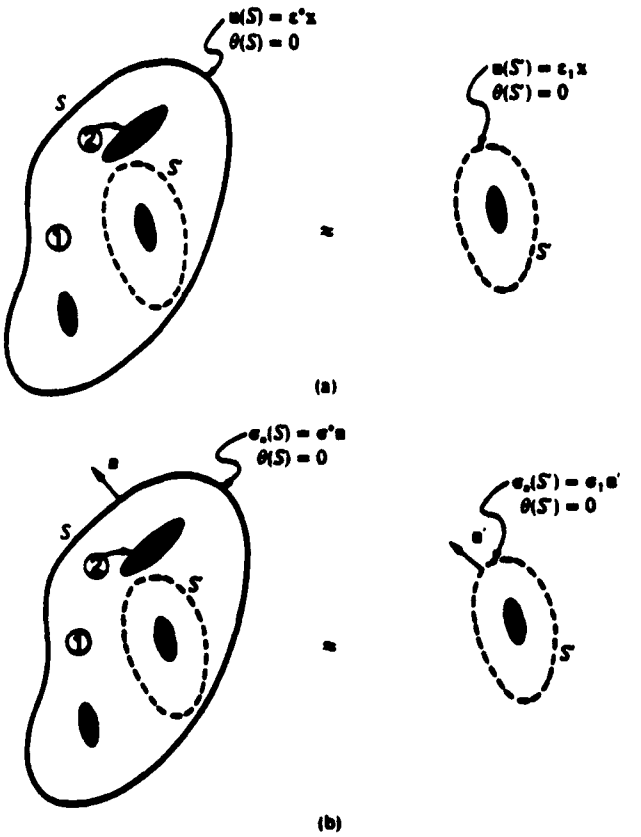

FIG. 1. A schematic representation of the Mori–Tanaka model for the case of mechanical loading.

by a surface S', and subjected to the boundary condition

$$\mathbf{u}(S') = \boldsymbol{\varepsilon}_1 \mathbf{x}. \tag{4.7}$$

The solution is

$$\boldsymbol{\varepsilon}_2 = \mathbf{T}\boldsymbol{\varepsilon}_1, \tag{4.8}$$

and as clarified by Benveniste (1987), it represents the essential assumption of the Mori–Tanaka method. It also implies that

$$\mathbf{A}_2 = \mathbf{T}\mathbf{A}_1. \tag{4.9}$$

Using (4.3), we obtain the estimates of the matrix (1) and reinforcement (2) strain concentration factors

$$\mathbf{A}_1 = (c_1\mathbf{I} + c_2\mathbf{T})^{-1}, \tag{4.10}$$

$$\mathbf{A}_2 = \mathbf{T}(c_1\mathbf{I} + c_2\mathbf{T})^{-1}, \tag{4.11}$$

which can be substituted into (4.4) to provide an estimate of the overall stiffness

$$\mathbf{L} = \mathbf{L}_1 + c_2(\mathbf{L}_2 - \mathbf{L}_1)\mathbf{T}(c_1\mathbf{I} + c_2\mathbf{T})^{-1}. \tag{4.12}$$

A similar procedure with the boundary conditions (2.4) and $\theta_0 = 0$ and (4.1) and (4.2) yields an estimate of the overall compliance

$$\mathbf{M} = \mathbf{M}_1 + c_2(\mathbf{M}_2 - \mathbf{M}_1)\mathbf{W}(c_1\mathbf{I} + c_2\mathbf{W})^{-1}, \tag{4.13}$$

where $\mathbf{W}$ denotes the stress concentration factor tensor of an isolated inclusion and is given by

$$\mathbf{W} = \mathbf{L}_2\mathbf{T}\mathbf{M}_1. \tag{4.14}$$

Benveniste (1987) had shown that the results (4.12) and (4.13) are consistent in the sense that $\mathbf{M} = \mathbf{L}^{-1}$. We note that these equations cannot be reduced to a symmetric form because the two phases do not enter on equal footing.

Turning next to the effective thermal strain and stress tensors, we substitute (4.12) and (4.13) into (3.6) and (3.10), respectively, to obtain

$$\mathbf{m} = \mathbf{m}_1 + c_2(\mathbf{M}_2 - \mathbf{M}_1)\mathbf{W}(c_1\mathbf{I} + c_2\mathbf{W})^{-1}(\mathbf{M}_2 - \mathbf{M}_1)^{-1}(\mathbf{m}_2 - \mathbf{m}_1), \tag{4.15}$$

$$\mathbf{l} = \mathbf{l}_1 + c_2(\mathbf{L}_2 - \mathbf{L}_1)\mathbf{T}(c_1\mathbf{I} + c_2\mathbf{T})^{-1}(\mathbf{L}_2 - \mathbf{L}_1)^{-1}(\mathbf{l}_2 - \mathbf{l}_1). \tag{4.16}$$

Since (3.6) and (3.10) satisfy (3.2_1) and, as we just concluded, $\mathbf{M} = \mathbf{L}^{-1}$, it follows that the $\mathbf{m}$ and $\mathbf{l}$ obey the relation $\mathbf{l} = -\mathbf{L}\mathbf{m}$.

4.2. Proof of Consistency

The Mori–Tanaka method has been used previously to predict the effective thermal expansion coefficients of particulate composites (Wakashima *et al.*, 1974; Takahashi *et al.*, 1980; Takao, 1985; Takao and Taya, 1985). In these works, the method was not implemented through (3.6) and (3.10). Instead, it

was applied directly to the thermal case by using the equivalent inclusion idea of Eshelby (1957) and the eigenstrain concept. In what follows we rederive the Mori–Tanaka results in a different way, and then prove that the results are consistent with (4.15) and (4.16).

Consider first the thermal loading problem (2.4) with $\boldsymbol{\sigma}_0 = \mathbf{0}$. As in Section 4.1, we write the solution of this problem for the single inclusion case in the form

$$\boldsymbol{\sigma}_1' = \mathbf{0}, \qquad \boldsymbol{\sigma}_2' = \mathbf{w}\theta_0, \tag{4.17}$$

where $\mathbf{w}$ is the average stress in a single inclusion embedded in the matrix and subjected to unit temperature and zero traction at the remote boundary S'. From the volume average of (2.12) we find the average stress in the single inclusion as

$$\mathbf{w} = (\mathbf{I} - \mathbf{W})(\mathbf{M}_1 - \mathbf{M}_2)^{-1}(\mathbf{m}_2 - \mathbf{m}_1). \tag{4.18}$$

For a finite concentration of the reinforcement, the solution is obtained again from the Mori–Tanaka assumption that the average stress in each inclusion is equal to that found for the dilute case with the boundary conditions shown in Fig. 2(a)

$$\theta(S') = \theta_0, \qquad \boldsymbol{\sigma}_0(S') = \boldsymbol{\sigma}_1 \mathbf{n}', \tag{4.19}$$

where $\boldsymbol{\sigma}_1$ is the unknown average stress in the matrix at finite concentration and $\mathbf{n}'$ is the outside normal to S'.

To find $\boldsymbol{\sigma}_1$, we note that the boundary conditions (4.19) cause the average stress in each inclusion

$$\boldsymbol{\sigma}_2 = \mathbf{w}\theta_0 + \mathbf{W}\boldsymbol{\sigma}_1, \tag{4.20}$$

where the second term accounts for particle interaction and $\mathbf{W}$ is given by (4.14). Recall now (3.4) and write the strains as in (2.2)

$$\mathbf{m}\theta_0 = c_1(\mathbf{M}_1\boldsymbol{\sigma}_1 + \mathbf{m}_1\theta_0) + c_2(\mathbf{M}_2\boldsymbol{\sigma}_2 + \mathbf{m}_2\theta_0). \tag{4.21}$$

Also recall that for $\boldsymbol{\sigma}_0 = \mathbf{0}$

$$\bar{\boldsymbol{\sigma}} = c_1\boldsymbol{\sigma}_1 + c_2\boldsymbol{\sigma}_2 = \mathbf{0}. \tag{4.22}$$

The last three equations lead to the expressions

$$\mathbf{m}\theta_0 = [\mathbf{m}_1 + c_2(\mathbf{m}_2 - \mathbf{m}_1)]\theta_0 + (\mathbf{M}_1 - \mathbf{M}_2)c_1\boldsymbol{\sigma}_1, \tag{4.23}$$

$$\boldsymbol{\sigma}_1 = -c_2(c_1\mathbf{I} + c_2\mathbf{W})^{-1}\mathbf{w}\theta_0. \tag{4.24}$$

Substitution of (4.18) into (4.24) and then into (4.23) yields

$$\mathbf{m} = \mathbf{m}_1 + c_2[\mathbf{I} - (\mathbf{M}_1 - \mathbf{M}_2)c_1(c_1\mathbf{I} + c_2\mathbf{W})^{-1} \cdot (\mathbf{I} - \mathbf{W})(\mathbf{M}_1 - \mathbf{M}_2)^{-1}](\mathbf{m}_2 - \mathbf{m}_1), \tag{4.25}$$

which can be written as

$$\mathbf{m} = \mathbf{m}_1 + c_2(\mathbf{M}_1 - \mathbf{M}_2)(c_1\mathbf{I} + c_2\mathbf{W})^{-1} \cdot [(c_1\mathbf{I} + c_2\mathbf{W})(\mathbf{M}_1 - \mathbf{M}_2)^{-1} - c_1(\mathbf{I} - \mathbf{W})(\mathbf{M}_1 - \mathbf{M}_2)^{-1}](\mathbf{m}_2 - \mathbf{m}_1). \tag{4.26}$$

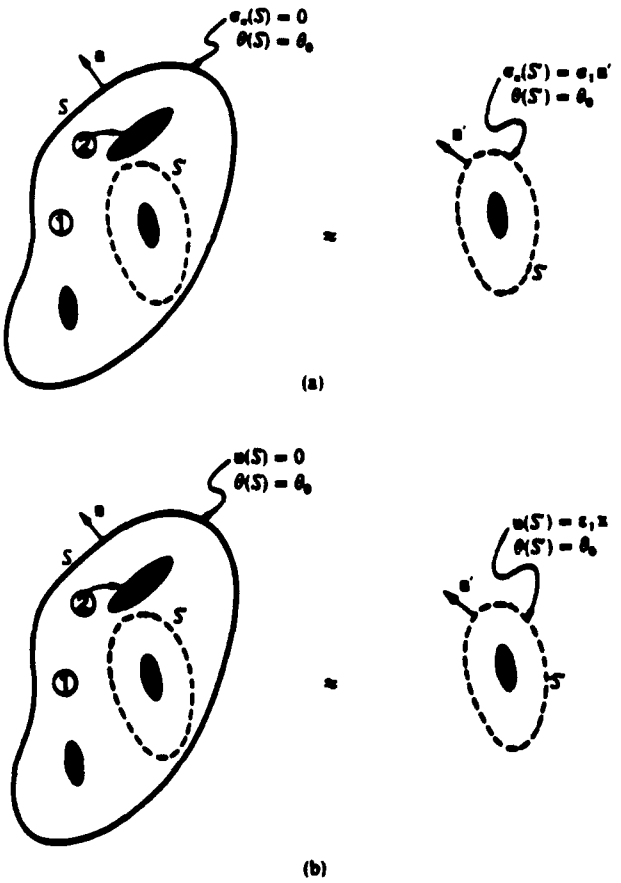

FIG. 2. A schematic representation of the Mori–Tanaka model for the case of thermal loadings.

Factoring out $(\mathbf{M}_1 - \mathbf{M}_2)^{-1}$ in the middle expression provides

$$\mathbf{m}_1 = \mathbf{m}_1 + c_2(\mathbf{M}_2 - \mathbf{M}_1)(c_1\mathbf{I} + c_2\mathbf{W})^{-1}\mathbf{W}(\mathbf{M}_2 - \mathbf{M}_1)^{-1}(\mathbf{m}_2 - \mathbf{m}_1), \quad (4.27)$$

which, together with the identity

$$(c_1\mathbf{I} + c_2\mathbf{W})^{-1}\mathbf{W} = \mathbf{W}(c_1\mathbf{I} + c_2\mathbf{W})^{-1}, \quad (4.28)$$

shows that (4.27) is identical to (4.15). In addition, we demonstrate in Appendix B that the overall $\mathbf{m}$ given by (4.27) is actually identical to that derived in a different way by Takao and Taya (1985).

A similar proof of consistency can be given for the overall thermal stress vector $\mathbf{l}$, (4.16). Here we consider Problem II, with the boundary conditions (2.5) and $\varepsilon_0 = 0$. In the spirit of the Mori–Tanaka method, we first take a

single inclusion in a large matrix volume V' and specify that on S', $u(S') = \varepsilon_1 x$, the average matrix strain at finite concentration, Fig. 2(b). The inclusion strain is given by the counterpart of (4.20)

$$\varepsilon_2 = t\theta_0 + T\varepsilon_1, \tag{4.29}$$

where t follows from the volume average of (2.18) as

$$t = (I - T)(L_1 - L_2)^{-1}(l_2 - l_1). \tag{4.30}$$

Here, the first term denotes the average strain in an isolated particle embedded in an infinite, stress-free matrix medium and subjected to a uniform thermal change θ_0, whereas the second term, with T given by (4.6), accounts for particle interaction. We also write

$$\bar{\varepsilon} = c_1\varepsilon_1 + c_2\varepsilon_2 = 0, \tag{4.31}$$

and substitute from (2.1) and (3.1_1), with $\bar{\varepsilon} = 0$, to find

$$l\theta_0 = c_1(L_1\varepsilon_1 + l_1\theta_0) + c_2(L_2\varepsilon_2 + l_2\theta_0). \tag{4.32}$$

Due to the similar structure of ((4.29), (4.30), (4.3_1), (4.32)) ((4.20), (4.18), (4.22), (4.21)), respectively, it is clear that the former set will result in l given by (4.16), in the same manner that the latter set resulted in (4.15).

5. Temperature-Dependent Material Properties

In many cases of practical interest, and particularly in high-temperature applications of composite materials, the magnitudes of certain material properties such as stiffness and thermal expansion coefficients depend on temperature. Typically, elastic moduli or compliances are experimentally measured at specific temperatures, and the coefficients of thermal expansion are obtained as derivatives of strain–temperature records taken in a certain temperature interval. In any case, the temperature dependence of thermoelastic coefficients can be represented by suitable functions which approximate the experimental data with sufficient accuracy.

We recall that all the results obtained in the preceding sections were derived from solutions of either Problem I or II, Equations (2.4) and (2.5), which were formulated for linear thermoelastic materials with temperature-independent properties. These results certainly remain valid for infinitesimal thermal changes. For example, consider Problem I, and assume that at a given σ_0 and θ_0 the tensors B_r, b_r, M_r, and m_r are known, and are now functions of θ_0. For an increase in temperature and stress denoted by $d\theta_0$ and σ_0, we can now write

$$d\sigma_r = B_r(x; \theta_0)\, d\sigma_0 + b_r(x; \theta_0)\, d\theta_0, \tag{5.1}$$

with

$$b_r(x; \theta_0) = [I - B_r(x; \theta_0)][M_1(\theta_0) - M_2(\theta_0)]^{-1}[m_2(\theta_0) - m_1(\theta_0)]. \tag{5.2}$$

It is therefore clear that with the temperature-dependent properties represented in a step-wise constant manner, an incremental implementation of the results derived in the present paper becomes possible.

Acknowledgments

The first author is indebted to Professor G. J. Dvorak for the visiting appointment at RPI during 1987/1988. Support from the Office of Naval Research and the DARPA-HiTASC program at RPI is gratefully acknowledged.

References

Benveniste, Y. (1987), A new approach to the application of Mori–Tanaka's theory in composite materials, *Mech. Materials*, 6, 147–157.

Dvorak, G. J. (1983), Metal matrix composites: Plasticity and fatigue, in *Mechanics of Composite Materials—Recent Advances*, edited by Z. Hashin and C. T. Herakovich, Pergamon Press, New York, pp. 73–92.

Dvorak, G. J. (1986), Thermal expansion of elastic–plastic composite materials, *J. Appl. Mech.*, 53, 737–743.

Dvorak, G. J. and Chen, T., (1988), Thermal expansion of three-phase composite materials, to be published.

Eshelby, J. D. (1957), The determination of the elastic field of an ellipsoidal inclusion and related problems, *Proc. Roy. Soc. London*, A241, 376–396.

Hill, R. (1963), Elastic properties of reinforced solids: Some theoretical principles, *J. Mech. Phys. Solids*, 11, 357–372.

Laws, N. (1973), On the thermostatics of composite materials, *J. Mech. Phys. Solids*, 21, 9–17.

Laws, N. (1974), The overall thermoelastic moduli of transversely isotropic composites according to the self-consistent method, *Int. J. Engng. Sci.*, 12, 79–87.

Levin, V. M. (1967), Thermal expansion coefficients of heterogeneous materials, *Mekhanika Tverdogo Tela*, 2, 88–94.

Mori, T. and Tanaka, K. (1973), Average stress in matrix and average elastic energy of materials with misfitting inclusions, *Acta Metallurgica*, 21, 571–574.

Rosen, B. W. and Hashin, Z. (1970), Effective thermal expansion coefficients and specific heats of composite materials, *Int. J. Engng. Sci.* 8, 157–173.

Schapery, R. A. (1968), Thermal expansion coefficients of composite materials based on energy principles, *J. Composite Materials*, 2, 380–404.

Takahashi, K., Harakawa, K., and Sakai, T. (1980), Analysis of the thermal expansion coefficients of particle filled polymers, *J. Composite Materials, Suppl.*, 14, 144–159.

Takao, Y. (1985), Thermal expansion coefficients in misoriented short-fiber composites, in *Recent Advances in Composites in the United States and Japan*, ASTM STP 864, 685–689.

Takao, Y. and Taya, M. (1985), Thermal expansion coefficients and thermal stresses in an aligned short fiber composite with application to a short carbon fiber/aluminum, *J. Appl. Mech.*, 52, 806–810.

Wakashima, K., Otsuka, M., and Umekawa, S. (1974), Thermal expansion of heterogeneous solids containing aligned ellipsoidal inclusions, *J. Composite Materials*, 8, 391–404.

Appendix A

This appendix presents a discussion of the decomposition scheme for the degenerate cases in which $(\mathbf{M}_1 - \mathbf{M}_2)^{-1}$ or $(\mathbf{L}_1 - \mathbf{L}_2)^{-1}$ fail to exist. The two important cases of isotropic and transversely isotropic constituents will be analyzed.

Consider first the case of isotropic constituents for which the tensors $\mathbf{M}_i$ and m_i can be written in component form as follows:

$$(M_{pqrs})_i = \frac{1}{9\kappa_i}\delta_{pq}\delta_{rs} + \frac{1}{4\mu_i}(\delta_{pr}\delta_{qs} + \delta_{ps}\delta_{qr} - \tfrac{2}{3}\delta_{pq}\delta_{rs}), \tag{A1.1}$$

$$(m_{rs})_i = \alpha_i\delta_{rs}, \tag{A1.2}$$

where κ_i, μ_i are the bulk and shear moduli of the phases and α_i are the thermal expansion coefficients. For the sake of brevity we limit ourselves to (2.11), a similar discussion applies for (2.16).

The difference $(\mathbf{M}_1 - \mathbf{M}_2)^{-1}$ can now be written in component form

$$[(\mathbf{M}_1 - \mathbf{M}_2)^{-1}]_{pqrs} = \left(\frac{1}{\kappa_1} - \frac{1}{\kappa_2}\right)^{-1}\delta_{pq}\delta_{rs} + \left(\frac{1}{\mu_1} - \frac{1}{\mu_2}\right)^{-1}(\delta_{pr}\delta_{qs} + \delta_{ps}\delta_{qr} - \tfrac{2}{3}\delta_{pq}\delta_{rs}). \tag{A1.3}$$

Use of (A1.2) and (A1.3) in (2.11) yields

$$\delta_{pq} = 3\left(\frac{1}{\kappa_1} - \frac{1}{\kappa_2}\right)^{-1}(\alpha_1 - \alpha_2)\delta_{pq}, \tag{A1.4}$$

which means that even though $(\mathbf{M}_1 - \mathbf{M}_2)^{-1}$ becomes singular for $\mu_1 = \mu_2$, the decomposition scheme continues to be well defined. The decomposition fails, however, if $\kappa_1 = \kappa_2$.

Equation (2.11), and the specific result of (A1.4) in (24), give the well-known Levin's formula

$$\alpha = c_1\alpha_1 + c_2\alpha_2 + (\alpha_1 - \alpha_2)\left(\frac{1}{\kappa_1} - \frac{1}{\kappa_2}\right)^{-1}\left[\frac{1}{\kappa} - \frac{c}{\kappa_1} - \frac{c_2}{\kappa_2}\right], \tag{A1.5}$$

which also becomes singular when $\kappa_1 = \kappa_2$. It should be noted, however, that this difficulty can be circumvented if the more general Levin's result, based on the concentration factors $\mathbf{B}_i$ (see equation (2.17) in Rosen and Hashin (1970)), is used instead of (A1.5). It is of interest to note that these degenerate cases of Levin's result have not been dealt before in the literature.

We consider next the case of transversely isotropic constituents and choose this time to illustrate the analysis with (2.16). The tensors $\mathbf{L}_i$ and $\mathbf{l}$ can now be denoted using the scheme used by Hill (1963), Walpole (1969), and Laws (1974) (see the last reference for a comprehensive exposition of this notation)

$$\mathbf{L}_i = (2k_i, l_i, l_i, n_i, 2m_i, 2p_i), \tag{A1.6}$$

$$\mathbf{l}_i = (\beta_T^{(i)}, \beta_L^{(i)}), \tag{A1.7}$$

where k_i is the plane strain bulk modulus for lateral dilatation without longitudinal extension, n_i is the modulus for longitudinal uniaxial straining, l_i is the associated cross modulus, m_i is the shear modulus for shearing in any transverse direction, and n_i is the modulus for longitudinal shearing; finally $\beta_T^{(i)}$ and $\beta_L^{(i)}$ denote, respectively, the thermal stress coefficients in the transverse and longitudinal direction.

In the notation of (A1.6), $(\mathbf{L}_1 - \mathbf{L}_2)$ becomes

$$(\mathbf{L}_1 - \mathbf{L}_2) = [2(k_1 - k_2), (l_1 - l_2), (l_1 - l_2), (n_1 - n_2), (2m_1 - 2m_2), (2p_1 - 2p_2)], \tag{A1.8}$$

so that $(\mathbf{L}_1 - \mathbf{L}_2)^{-1}$ is given by

$$(\mathbf{L}_1 - \mathbf{L}_2) = \left(\frac{n_1 - n_2}{2\lambda}, -\frac{l_1 - l_2}{2\lambda}, -\frac{l_1 - l_2}{2\lambda}, \frac{k_1 - k_2}{\lambda}, \frac{1}{2m_1 - 2m_2}, \frac{1}{2p_1 - 2p_2}\right), \tag{A1.9}$$

where λ is defined as

$$\lambda = (k_1 - k_2)(n_1 - n_2) - (l_1 - l_2)^2. \tag{A1.10}$$

The product $(\mathbf{L}_1 - \mathbf{L}_2)^{-1}(\mathbf{l}_1 - \mathbf{l}_2)$ therefore becomes

$$(\mathbf{L}_1 - \mathbf{L}_2)^{-1}(\mathbf{l}_1 - \mathbf{l}_2) = (p, q), \tag{A1.11}$$

with p and q given by

$$p = \frac{n_1 - n_2}{2\lambda}(\beta_T^{(1)} - \beta_T^{(2)}) - \frac{l_1 - l_2}{2\lambda}(\beta_L^{(1)} - \beta_L^{(2)}), \tag{A1.12}$$

$$q = -2\frac{l_1 - l_2}{2\lambda}(\beta_T^{(1)} - \beta_T^{(2)}) + \frac{k_1 - k_2}{2\lambda}(\beta_L^{(1)} - \beta_L^{(2)}), \tag{A1.13}$$

so that the product in (A1.11), and thus the decomposition scheme fail to exist when λ, as given by (A1.10), vanishes.

The reduction of the present results to the case of isotropic constituents can be readily carried out by noting that for isotropic phases

$$\mathbf{L}_i = [2(\kappa_i + \tfrac{1}{3}\mu_i), (\kappa_i - \tfrac{2}{3}\mu_i), (\kappa_i - \tfrac{2}{3}\mu_i), \kappa_i + \tfrac{4}{3}\mu_i, 2\mu_i, 2\mu_i], \tag{A1.14}$$

$$\mathbf{l} = [\beta, \beta], \tag{A1.15}$$

thus reducing λ to

$$\lambda = 3(\mu_1 - \mu_2)(\kappa_1 - \kappa_2), \tag{A1.16}$$

and p and q to

$$p = q = \frac{1}{3(\kappa_1 - \kappa_2)}(\beta_1 - \beta_2). \tag{A1.17}$$

Therefore, in the case of isotropic constituents, the decomposition scheme fails only when $\kappa_1 = \kappa_2$.

Appendix B

In this Appendix we will prove the equivalence between our result (4.25) and that obtained by Takao and Taya (1985). The approach used by these authors is based on the eigenstrain concepts and equivalent inclusion formalism. Four equations in Takao and Taya (1985) determine the effective thermal expansion tensor. We will reproduce them here and show that they lead, in fact, to the relatively compact closed form of (4.27).

We first note that the effective thermal expansion tensor is denoted in the Takao and Taya paper by α_c, whereas the symbol α^* is used there to denote the thermal strain due to the difference between $\mathbf{m}_1$ and $\mathbf{m}_2$ under temperature change θ.

Equations (3), (6), (7), and (13) of that work are,

$$\alpha^* = (\mathbf{m}_2 - \mathbf{m}_1)\theta_0, \tag{B1.1}$$

$$\mathbf{L}_1[\bar{\varepsilon} + (\mathbf{S} - \mathbf{I})\alpha^* + (\mathbf{S} - \mathbf{I})\varepsilon^*] = \mathbf{L}_2[\bar{\varepsilon} + (\mathbf{S} - \mathbf{I})\alpha^* + \mathbf{S}\varepsilon^*], \tag{B1.2}$$

$$\bar{\varepsilon} + c_2(\mathbf{S} - \mathbf{I})(\alpha^* + \varepsilon^*) = 0, \tag{B1.3}$$

$$\mathbf{m} = \mathbf{m}_1 + \frac{c_2(\varepsilon^* + \alpha^*)}{\theta_0}. \tag{B1.4}$$

We have also used $\mathbf{m}_1$, $\mathbf{m}_2$ for α_1, α_2; $\mathbf{L}_1$ and $\mathbf{L}_2$ for $\mathbf{C}_m$ and $\mathbf{C}_f$; θ_0 for Δt; and c_2 has been used instead of f in Takao and Taya. In that work ε^* denotes the fictitious strain called "eigenstrain" or "transformation strain" and $\bar{\varepsilon}$ is the volume-averaged disturbance of strain in the matrix. The tensor S stands again for the Eshelby tensor appearing in our equation (4.6).

We start by substituting (B1.1) into (B1.4)

$$\mathbf{m} = c_1\mathbf{m}_1 + c_2\mathbf{m}_2 + \frac{c_2\varepsilon^*}{\theta_0}. \tag{B1.5}$$

Use of (B1.3) and (B1.1) in (B1.2) gives for ε^*

$$\frac{1}{c_1}[c_1(\mathbf{L}_2 - \mathbf{L}_1)\mathbf{S} + c_1\mathbf{L}_1 + c_2\mathbf{L}_2]\varepsilon^* = (\mathbf{L}_1 - \mathbf{L}_2)(\mathbf{S} - \mathbf{I})(\mathbf{m}_2 - \mathbf{m}_1)\theta_0, \tag{B1.6}$$

which, when substituted in (B1.5) provide Takao and Taya's principal result

$$\mathbf{m} = c_1\mathbf{m}_1 + c_2\mathbf{m}_2 + (c_2c_1)[c_1(\mathbf{L}_2 - \mathbf{L}_1)\mathbf{S} + c_1\mathbf{L}_1 + c_2\mathbf{L}_2]^{-1} \cdot (\mathbf{L}_1 - \mathbf{L}_2)(\mathbf{S} - \mathbf{I})(\mathbf{m}_2 - \mathbf{m}_1). \tag{B1.7}$$

We will now show that this last expression is identical to (4.27) or to an equivalent form which is obtained by substituting (4.13) into (3.6).

After some manipulation we obtain

$$\mathbf{m} = c_1\mathbf{m}_1 + c_2\mathbf{m}_2 + c_1c_2(\mathbf{M}_1 - \mathbf{M}_2)(\mathbf{I} - \mathbf{W}) \cdot (c_1\mathbf{I} + c_2\mathbf{W})^{-1}(\mathbf{M}_2 - \mathbf{M}_1)^{-1}(\mathbf{m}_2 - \mathbf{m}_1) \tag{B1.8}$$

this implies that (B1.7) is identical to (B1.8) if the following equality holds:

$$[c_1(\mathbf{L}_2 - \mathbf{L}_1)\mathbf{S} + c_1\mathbf{L}_1 + c_2\mathbf{L}_2]^{-1}(\mathbf{L}_1 - \mathbf{L}_2)(\mathbf{S} - \mathbf{I}) = (\mathbf{M}_1 - \mathbf{M}_2)(\mathbf{I} - \mathbf{W})(c_1\mathbf{I} + c_2\mathbf{W})^{-1}(\mathbf{M}_2 - \mathbf{M}_1)^{-1}. \tag{B1.9}$$

Using (4.6) and (4.14) we note first that

$$\mathbf{I} - \mathbf{W} = [\mathbf{M}_2 + \mathbf{S}(\mathbf{M}_1 - \mathbf{M}_2)]^{-1}(\mathbf{S} - \mathbf{I})(\mathbf{M}_1 - \mathbf{M}_2), \tag{B1.10}$$

$$(c_1\mathbf{I} + c_2\mathbf{W})^{-1} = [c_2\mathbf{M}_1 + c_1\mathbf{M}_2 + c_1\mathbf{S}(\mathbf{M}_1 - \mathbf{M}_2)]^{-1} \cdot [\mathbf{M}_2 + \mathbf{S}(\mathbf{M}_1 - \mathbf{M}_2)]. \tag{B1.11}$$

Next, taking into account the equality

$$(\mathbf{I} - \mathbf{W})(c_1\mathbf{I} + c_2\mathbf{W})^{-1} = (c_1\mathbf{I} + c_2\mathbf{W})^{-1}(\mathbf{I} - \mathbf{W}), \tag{B1.12}$$

it is easy to show that (B1.9) is in fact valid. This proves the equivalence between our relation (B1.8) and that resulting from Takao and Taya's work.

On transformation strains and uniform fields in multiphase elastic media

BY GEORGE J. DVORAK[1] AND YAKOV BENVENISTE[2]

[1] *Civil Engineering Department, Rensselaer Polytechnic Institute, Troy, New York 12180, U.S.A.*

[2] *Department of Solid Mechanics, Materials and Structures, Tel Aviv University, 69978 Ramat-Aviv, Israel*

The effect of local eigenstrain and eigenstress fields, or transformation fields, on the local strains and stresses is explored in multiphase elastic solids of arbitrary geometry and material symmetry. The residual local fields caused by such transformation fields are sought in terms of certain transformation influence functions and transformation concentration factor tensors. General properties of these functions and concentration factors, and their relation to the analogous mechanical influence functions and concentration factors, are established, in part, with the help of uniform strain fields in multiphase media. Specific estimates of the transformation concentration factor tensors are evaluated by the self-consistent and Mori–Tanaka methods. It is found here that although the two methods use different constraint tensors in solutions of the respective dilute problems, their estimates of the mechanical, thermal, and transformation concentration factor tensors, and of the overall stiffness of multiphase media have a similar structure. Proofs that guarantee that these methods comply with the general properties of the transformation influence functions, and provide diagonally symmetric estimates of the overall elastic stiffness, are given for two-phase and multiphase systems consisting of, or reinforced by, inclusions of similar shape and alignment. One of the possible applications of the results, in analysis of overall instantaneous properties and local fields in inelastic composite materials, is described in the following paper.

1. Introduction

Apart from the stress and strain fields induced by mechanical loads, heterogeneous media and composite materials in particular, must often accommodate eigenstrains or transformation strains, and the residual fields that they cause in the phases. Many different physical processes give rise to the eigenstrain fields (e.g. temperature changes, phase transformations and inelastic deformation). The emerging smart materials are expected to provide a desired response to eigenstrains induced by a suitable actuator, such as a piezoceramic or shape memory alloy phase. In contrast to homogeneous solids, complex eigenstrain fields may be generated in heterogeneous media by one or more of these sources even under uniform overall stress, strain, or thermal change. Such fields are of considerable interest in applications, as their influence on the overall behaviour and on structural integrity of composite materials may well exceed that of the mechanical service loads.

Proc. R. Soc. Lond. A (1992) **437**, 291–310
Printed in Great Britain

Inspired by Eshelby (1957), the micromechanics literature abounds with studies of transformation strain problems for solitary homogeneous and inhomogeneous inclusions of ellipsoidal shape in infinite elastic media (Mura 1987). Of course, some of the results are useful in evaluations of estimates of local fields and properties of heterogeneous media. However, except for thermal strains, little attention has been given to the role of transformation strains and the associated residual fields in multiphase solids of arbitrary phase geometry and material symmetry.

A particularly significant application of results of this kind has been identified in evaluation of properties and local fields in inelastic composite materials. For two-phase systems this has been discussed by Dvorak (1991), whereas the following paper (Dvorak 1992) expands this line of inquiry to multiphase media. To introduce this subject we derive here some general properties of the transformation and residual fields in heterogeneous media. The opening §§2 and 3 present some useful forms of the total strains in the presence of local eigenstrains, together with definitions of the transformation influence functions and transformation concentration factor tensors. Then, §4 extends the concept of uniform strain fields in heterogeneous media (Dvorak 1990) to multiphase systems. This provides an insight into the general properties of transformation and residual fields discussed in §5, and simplifies the derivation of the self-consistent and Mori–Tanaka estimates of the local fields in §6. The general properties of the transformation influence functions confirm the conclusion reached by Benveniste *et al.* (1991), that the two methods are admissible in applications to two-phase and multiphase systems where all inclusions have the same shape and alignment. For such systems we establish in §§6 and 7 a hitherto unnoticed connection between the two methods, namely that the estimates they provide of the overall stiffness or compliance, and of the mechanical, thermal, and transformation concentration factor tensors in multiphase media, have a similar structure. Finally, we discuss some aspects of a finite element evaluation of the transformation concentration factor tensors for sub-elements of unit cell models of composite materials.

Throughout the paper we assume that the overall mechanical properties and the local fields caused in the media of interest by application of uniform overall stresses or strains, are known or can be obtained by available procedures. If this is taken for granted, then it is often possible to evaluate the residual fields caused by the transformation strains and stresses in terms of the overall mechanical properties, and the appropriate mechanical influence functions or concentration factor tensors.

The customary notation is used. (6×1) vectors are denoted by boldface lower case Greek or Roman letters, (6×6) matrices by boldface uppercase Roman letters, and $\boldsymbol{A}\boldsymbol{A}^{-1} = \boldsymbol{A}^{-1}\boldsymbol{A} = \boldsymbol{I}$, if the inverse exists. Scalars are denoted by lightface letters. Volume averages of fields such as $\boldsymbol{A}_r(\boldsymbol{x})$, $\boldsymbol{\varepsilon}_r(\boldsymbol{x})$ in V_r, or of $\boldsymbol{\sigma}(\boldsymbol{x})$ in V, are denoted by $\boldsymbol{A}_r$, $\boldsymbol{\varepsilon}_r$ or $\boldsymbol{\sigma}$.

2. Local and overall transformation strains

The composite material under consideration consists of many distinct elastic phases which, unless otherwise stated, are perfectly bonded at their interfaces. No restrictions are imposed on phase elastic symmetry or on the geometry of the microstructure. However, the composite is assumed to be homogeneous on the macroscale, so that a certain representative volume V with surface S can be selected to study both local and overall behaviour. Such representative volume may be defined either in a general sense, as a sufficiently large sample that contains many

phases and reflects typical macroscopic properties of the mixture (Hill 1963), or more specifically, in terms of a representative unit cell of a usually periodic model of the actual material geometry, under prescribed periodic boundary conditions.

The loads that may be applied at the surface S of the representative volume consist of displacements $u_i(S) = \epsilon_{ij}^0 x_j$, or tractions $t_i(S) = \sigma_{ji}^0 n_j$, derived, respectively, from uniform overall strain $\boldsymbol{\epsilon}^0$ or stress $\boldsymbol{\sigma}^0$. The response under such loads defines a unique overall elastic stiffness $\boldsymbol{L}$, or compliance $\boldsymbol{M}$, which are assumed to be known. In addition, an eigenstress field $\boldsymbol{\lambda}(\boldsymbol{x})$ and an eigenstrain field $\boldsymbol{\mu}(\boldsymbol{x})$, collectively called transformation fields, may exist in V. On the macroscale, they cause an overall eigenstress $\boldsymbol{\lambda}$ or eigenstrain $\boldsymbol{\mu}$, which both vanish in the absence of the local transformation fields. Therefore, the overall constitutive relations of the representative volume are written as

$$\boldsymbol{\sigma} = \boldsymbol{L}\boldsymbol{\epsilon} + \boldsymbol{\lambda}, \quad \boldsymbol{\epsilon} = \boldsymbol{M}\boldsymbol{\sigma} + \boldsymbol{\mu}. \tag{1}$$

where $\boldsymbol{M} = \boldsymbol{L}^{-1}$, $\boldsymbol{\lambda} = -\boldsymbol{L}\boldsymbol{\mu}$, $\boldsymbol{\mu} = -\boldsymbol{M}\boldsymbol{\lambda}$.

Since the overall strain and stress in (1) are uniform in any properly defined representative volume V, it follows that the local transformation and residual fields that are admissible in V must create a macroscopically uniform overall stress $\boldsymbol{\lambda}$ or strain $\boldsymbol{\mu}$. Examples of such fields include those due to a uniform change in temperature, or to phase transformation within any one phase, as well as inelastic deformation fields caused in V by uniform thermomechanical loading.

A phase is defined as an elastically homogeneous part of the representative volume: no limitations are placed on phase geometry or elastic symmetry, except that the latter remains fixed in the overall coordinate system. In the description of local fields, the representative volume V is typically divided into sub-volumes or *local volumes* V_r, $r = 1, 2, \ldots, N$, which contain the individual phases, or individual volumes of each phase. Subdivision of phases is preferred in evaluations of estimates of phase volume averages of the local fields (e.g. by the self-consistent or Mori–Tanaka methods). Of course, if a representative unit cell is used in a finite element evaluation of the local fields, then each phase is divided into several sub-elements V_r, with distinct mechanical and transformation fields.

The constitutive relations in each local volume are written in the form

$$\boldsymbol{\sigma}_r(\boldsymbol{x}) = \boldsymbol{L}_r\boldsymbol{\epsilon}_r(\boldsymbol{x}) + \boldsymbol{\lambda}_r(\boldsymbol{x}), \quad \boldsymbol{\epsilon}_r(\boldsymbol{x}) = \boldsymbol{M}_r\boldsymbol{\sigma}_r(\boldsymbol{x}) + \boldsymbol{\mu}_r(\boldsymbol{x}), \tag{2}$$

where $\boldsymbol{L}_r$ and $\boldsymbol{M}_r = \boldsymbol{L}_r^{-1}$ are known phase stiffness and compliance tensors, and $\boldsymbol{\mu}_r(\boldsymbol{x})$ denotes a prescribed distribution of local eigenstrains. The $\boldsymbol{\lambda}_r(\boldsymbol{x}) = -\boldsymbol{L}_r\boldsymbol{\mu}_r(\boldsymbol{x})$ is the corresponding eigenstress field. The local and overall strain and stress fields under superimposed mechanical loads and transformation fields are not yet known. However, the contribution to the local fields (2) by purely mechanical loads is

$$\boldsymbol{\epsilon}_r(\boldsymbol{x}) = \boldsymbol{A}_r(\boldsymbol{x})\boldsymbol{\epsilon}^0, \quad \boldsymbol{\sigma}_r(\boldsymbol{x}) = \boldsymbol{B}_r(\boldsymbol{x})\boldsymbol{\sigma}^0. \tag{3}$$

where, as indicated in §1, the mechanical influence functions are assumed to be known.

Let us now establish a relation between the overall and local transformation fields in (1) and (2) respectively. This can be done by invoking the elastic reciprocal theorem. In particular, consider a representative volume of a composite under zero overall stress, and introduce a single eigenstress $\boldsymbol{\lambda}_p(\boldsymbol{x})$, derived from the eigenstrain $\boldsymbol{\mu}_p(\boldsymbol{x}) = -\boldsymbol{M}_p\boldsymbol{\lambda}_p(\boldsymbol{x})$, in one or more local volumes $V_p \in V$. Denote the overall strain caused by this eigenstrain as $\boldsymbol{\mu}$, and the resulting surface displacements on S by $\boldsymbol{u}$.

Next, remove the above eigenstress and apply at the surface S certain tractions t' which are in equilibrium with a uniform overall stress $\boldsymbol{\sigma}'$. This creates the stress $\boldsymbol{\sigma}'_p(\boldsymbol{x}) = \boldsymbol{B}_p(\boldsymbol{x})\boldsymbol{\sigma}'$, and strain $\boldsymbol{\varepsilon}'_p(\boldsymbol{x}) = \boldsymbol{M}_p\boldsymbol{\sigma}'_p(\boldsymbol{x})$ in V_p. As shown in the Appendix, the elastic reciprocal theorem relates the above fields by the following work equation

$$\int_S \boldsymbol{t}'\cdot\boldsymbol{u}\,\mathrm{d}S = -\int_{V_p}\boldsymbol{\lambda}_p(\boldsymbol{x})\cdot\boldsymbol{\varepsilon}'_p(\boldsymbol{x})\,\mathrm{d}V. \tag{4}$$

where the integration over V_p acknowledges that $\boldsymbol{\lambda}_p(\boldsymbol{x})$ is applied only within V_p.

Since $\boldsymbol{t}' = \boldsymbol{\sigma}'\boldsymbol{n}$, where $\boldsymbol{n}$ is the outside normal to S, one can rewrite (4) in the indicial notation.

$$\sigma'_{ij}\int_S \tfrac{1}{2}(u_i n_j + u_j n_i)\,\mathrm{d}S = -\int_{V_p}\lambda^p_{ij}(\boldsymbol{x})M^p_{ijkl}B^p_{klrs}(\boldsymbol{x})\sigma'_{rs}\,\mathrm{d}V. \tag{5}$$

Note first that the term multiplying σ'_{ij} on the left-hand side is by definition the average overall strain $\boldsymbol{\varepsilon}$, which, under $\boldsymbol{\sigma} = \boldsymbol{0}$, is equal to the overall eigenstrain $\boldsymbol{\mu}$. Next, write the second integrand as

$$\lambda^p_{ij}(\boldsymbol{x})M^p_{ijkl}B^p_{klrs}(\boldsymbol{x})\sigma'_{rs} = \sigma'_{rs}(B^p_{rskl}(\boldsymbol{x}))^{\mathrm{T}}(M^p_{klij})^{\mathrm{T}}\lambda^p_{ij}(\boldsymbol{x}). \tag{6}$$

and observe that the subscripts rs and ij can be exchanged. Of course, $\boldsymbol{M}_p$ is diagonally symmetric, and $\boldsymbol{M}_p\boldsymbol{\lambda}_p(\boldsymbol{x}) = -\boldsymbol{\mu}_p(\boldsymbol{x})$, so (4) can be solved for the overall eigenstrain as

$$\boldsymbol{\mu} = \frac{1}{V}\int_{V_p}\boldsymbol{B}^{\mathrm{T}}_p(\boldsymbol{x})\boldsymbol{\mu}_p(\boldsymbol{x})\,\mathrm{d}V. \tag{7}$$

In an analogous way, one may derive the relation

$$\boldsymbol{\lambda} = \frac{1}{V}\int_{V_p}\boldsymbol{A}^{\mathrm{T}}_p(\boldsymbol{x})\boldsymbol{\lambda}_p(\boldsymbol{x})\,\mathrm{d}V. \tag{8}$$

For the special case of piecewise uniform eigenstrains, (7) and (8) can be evaluated in each local volume V_r and the results added together to provide the following expressions

$$\boldsymbol{\lambda} = \sum_{r=1}^{N} c_r\boldsymbol{A}^{\mathrm{T}}_r\boldsymbol{\lambda}_r, \quad \boldsymbol{\mu} = \sum_{r=1}^{N} c_r\boldsymbol{B}^{\mathrm{T}}_r\boldsymbol{\mu}_r. \tag{9}$$

where $\boldsymbol{A}_r$ and $\boldsymbol{B}_r$ are the mechanical concentration factor tensors, evaluated as volume averages in V_r of the influence functions in (3). For transformation fields associated with a uniform change in temperature, (7)–(9) reduce to the results found by Levin (1967).

3. Transformation influence functions and concentration factors

The transformation fields may represent consequences of several different physical processes. However, if they conform with the additive decomposition suggested by (1) and (2) then, regardless of their origin, they may be considered as additional strains or stresses applied to the elastic composite aggregate, in superposition with the uniform overall stress or strain. The combined effect can be described in several different forms. For example, when the transformation fields are represented by certain functions $\boldsymbol{\mu}(\boldsymbol{x})$, the local strain field follows from

$$\boldsymbol{\varepsilon}(\boldsymbol{x}) = \boldsymbol{\varepsilon}^0(\boldsymbol{x}) - \int_V \boldsymbol{\Gamma}(\boldsymbol{x},\boldsymbol{x}')[(\boldsymbol{L}(\boldsymbol{x}') - \boldsymbol{L}^0)\boldsymbol{\varepsilon}(\boldsymbol{x}') - \boldsymbol{L}(\boldsymbol{x}')\boldsymbol{\mu}(\boldsymbol{x}')]\,\mathrm{d}\boldsymbol{x}'. \tag{10}$$

where $\varepsilon^0(x)$ denotes the strain field that would exist in a comparison homogeneous medium L^0 under the same boundary conditions, and

$$\Gamma_{ijkl}(x, x') = -\tfrac{1}{2}(G_{ik,jl}(x, x') + G_{jk,il}(x, x')), \tag{11}$$

where G_{ik} is the Green's function of the homogeneous medium L^0 that satisfies

$$L^0_{ijkl} G_{kp,lj}(x, x') + \delta_{ip}\delta(x - x') = 0, \quad x, x' \in V. \tag{12}$$

where δ_{ip} is the Kronecker symbol, and $\delta(x - x')$ is the Dirac delta function. Examples of such forms can be found in the papers by Levin (1976), Willis (1978, 1981), Berveiller *et al.* (1987) and Walker *et al.* (1990) where they are typically used in evaluation of overall properties.

In actual solutions, (10) is often simplified such that the actual field $\varepsilon_r(x)$, and the eigenstrain field $\mu_r(x)$, if present, are replaced by piecewise uniform approximations in the phases. Then, (10) is reduced to a system of N linear algebraic equations for the local average strains. When compared with the averages of (3) over V_r at $\mu(x') = 0$, the solution of this system provides expressions for the mechanical concentration factor tensors in terms of integrals of $\Gamma(x, x')$ in (11_1). Benveniste (1990) shows that certain simplified solutions of (10), constructed in this spirit in the above papers by Levin and Willis, coincide with the Mori–Tanaka estimates of the local strains under uniform overall strain or stress.

The approach adopted here starts with the assumption that the transformation fields are represented by distributions which are piecewise uniform, either in the phases, or in local volumes V_s within those phases. The total strain caused in V_s by the uniform overall strain ε or stress σ, and a piecewise uniform eigenstrains μ_s or eigenstress λ_s, is sought in the following form that extends (3) as (Dvorak 1990)

$$\varepsilon_s(x) = A_s(x)\varepsilon + \sum_{r=1}^{N} D_{sr}(x)\mu_r \quad (r, s = 1, 2, \ldots, N). \tag{13}$$

$$\sigma_s(x) = B_s(x)\sigma + \sum_{r=1}^{N} F_{sr}(x)\lambda_r \quad (r, s = 1, 2, \ldots, N). \tag{14}$$

Here, the $D_{ss}(x)$ and $D_{sr}(x)$ are, respectively, the self-induced and transmitted *eigenstrain influence functions*: the $F_{ss}(x)$ and $F_{sr}(x)$ are the corresponding *eigenstress influence functions*. In analogy with the accepted notation for description of the response to mechanical and thermal loads, the local volume averages in V_s of these functions may be referred to as the *eigenstress or eigenstrain concentration factor tensors* D_{ss}, D_{sr}, F_{ss} and F_{sr}. Collectively, these will be called the *transformation influence functions and concentration factors*.

Note that (13) or (14) each represent the contribution of three different fields to the total local strain or stress in V_s. For example, the right-hand side of (13) is the sum of the mechanical field $A_s(x)\varepsilon$, the residual fields $D_{sr}(x)\mu_r$ which reflect the influence of the eigenstrains μ_r in $V_r \neq V_s$ on $\varepsilon_s(x)$, and finally, the residual strain and the eigenstrain μ_s prescribed in V_s itself. The last two contributions are both accounted for by the influence function $D_{ss}(x)$, or by $F_{ss}(x)$ in (14), hence these two functions are different in this regard from the $D_{sr}(x)$ and $F_{sr}(x)$. In contrast to (1) and (2), the definitions combine ε with μ_r, and σ with λ_r, to assure that the coefficients of these tensor functions are dimensionless. As in (1), the transformation fields that may be admitted in (13) and (14) must produce a uniform overall body force λ or eigenstrain μ in the representative volume. This is always the case for each single component of

$\boldsymbol{\mu}_r$ in a sub-element of a properly defined unit cell, and it is also assured in the evaluation of the self-consistent and Mori–Tanaka estimates of the transformation factor tensors discussed in §6 below. However, an eigenstrain distribution corresponding, for example, to a temperature gradient in V would not be admissible.

To connect the transformation influence functions to the integral equation formulation of the problem, one may consider any eigenstrain field $\boldsymbol{\mu}(\boldsymbol{x})$ in a representative volume of a heterogeneous medium under zero overall strain, and define the transformation strain influence function $\boldsymbol{D}(\boldsymbol{x}, \boldsymbol{x}')$ as

$$\boldsymbol{\varepsilon}(\boldsymbol{x}) = \boldsymbol{D}(\boldsymbol{x}, \boldsymbol{x}')\,\boldsymbol{\mu}(\boldsymbol{x}'). \tag{15}$$

Its evaluation then follows from (10) as

$$\boldsymbol{D}(\boldsymbol{x}, \boldsymbol{x}')\,\boldsymbol{\mu}(\boldsymbol{x}') = -\int_V \boldsymbol{\Gamma}(\boldsymbol{x}, \boldsymbol{x}')\,[(\boldsymbol{L}(\boldsymbol{x}') - \boldsymbol{L}^0)\,\boldsymbol{D}(\boldsymbol{x}', \boldsymbol{x}') - \boldsymbol{L}(\boldsymbol{x}')]\,\boldsymbol{\mu}(\boldsymbol{x}')\,\mathrm{d}\boldsymbol{x}'. \tag{16}$$

Note also that in an infinite homogeneous medium loaded only by a single uniform eigenstrain within a homogeneous inclusion of ellipsoidal shape, $\boldsymbol{D}_{rs} = \boldsymbol{S}$, the Eshelby tensor.

The eigenstress and eigenstrain influence functions can be related in the following way. Let the overall eigenstrain in (1_1) be evaluated from (9_2) and the total strain then substituted into (13), where the $\boldsymbol{\varepsilon}_r(\boldsymbol{x})$ is written in terms of the local stresses using (2_1).

$$\boldsymbol{\sigma}_r(\boldsymbol{x}) = \boldsymbol{L}_r\,\boldsymbol{A}_r(\boldsymbol{x})\,\boldsymbol{M}\boldsymbol{\sigma} - \boldsymbol{L}_r \sum_{s=1}^{N} [(c_s\,\boldsymbol{A}_r(\boldsymbol{x})\,\boldsymbol{B}_s^{\mathrm{T}} - \boldsymbol{D}_{rs}(\boldsymbol{x}))\,\boldsymbol{M}_s\,\boldsymbol{\lambda}_s] + \boldsymbol{\lambda}_r. \tag{17}$$

Compare that with (14) to find

$$\boldsymbol{A}_r(\boldsymbol{x})\,\boldsymbol{M} = \boldsymbol{M}_r\,\boldsymbol{B}_r(\boldsymbol{x}). \quad \boldsymbol{F}_{rs}(\boldsymbol{x}) = \boldsymbol{L}_r[\delta_{rs}\,\boldsymbol{I} - c_s\,\boldsymbol{A}_r(\boldsymbol{x})\,\boldsymbol{B}_s^{\mathrm{T}} + \boldsymbol{D}_{rs}(\boldsymbol{x})]\,\boldsymbol{M}_s. \tag{18}$$

where δ_{rs} is the Kronecker symbol, but no summation is indicated by repeated subscripts.

The definition of the transformation concentration factors permits derivation of another pair of expressions for $\boldsymbol{\mu}$ and $\boldsymbol{\lambda}$, which may be used in place of (9). Consider again the loading case $\boldsymbol{\varepsilon} = 0, \boldsymbol{\mu}_r \neq 0$, and note that from (1) and (2) there is

$$\boldsymbol{\sigma} = \boldsymbol{\lambda} = \sum_{r=1}^{N} c_r\,\boldsymbol{\sigma}_r = \sum_{r=1}^{N} c_r(\boldsymbol{L}_r\,\boldsymbol{\varepsilon}_r + \boldsymbol{\lambda}_r). \tag{19}$$

However, under zero overall strain, $c_1\,\boldsymbol{\varepsilon}_1 = -\sum_{r=2}^{N} c_r\,\boldsymbol{\varepsilon}_r$, so that (19) provides

$$\boldsymbol{\lambda} = \sum_{r=1}^{N} c_r\,\boldsymbol{\lambda}_r + \sum_{r=2}^{N} c_r(\boldsymbol{L}_r - \boldsymbol{L}_1)\,\boldsymbol{\varepsilon}_r. \tag{20}$$

Refer now to (13), evaluate the average local strain $\boldsymbol{\varepsilon}_r$ in each volume V_r, and substitute $-\boldsymbol{M}_r\,\boldsymbol{\lambda}_r = \boldsymbol{\mu}_r$. This provides the desired result

$$\boldsymbol{\lambda} = \sum_{r=1}^{N} c_r\,\boldsymbol{\lambda}_r - \sum_{r=1}^{N}\sum_{s=1}^{N} c_r\,\boldsymbol{L}_r\,\boldsymbol{D}_{rs}\,\boldsymbol{M}_s\,\boldsymbol{\lambda}_s. \tag{21}$$

An analogous derivation yields

$$\boldsymbol{\mu} = \sum_{r=1}^{N} c_r\,\boldsymbol{\mu}_r - \sum_{r=1}^{N}\sum_{s=1}^{N} c_r\,\boldsymbol{M}_r\,\boldsymbol{F}_{rs}\,\boldsymbol{L}_s\,\boldsymbol{\mu}_s. \tag{22}$$

The conditions that assure consistency of these results with those found in (9) can be found as follows. Substitute for $\boldsymbol{\lambda}$ from (9_1) into (21), assign the eigenstrain $\boldsymbol{\lambda}_p$ and let all other eigenstresses vanish. Then, recall that $\boldsymbol{\lambda}_r = \delta_{rp}\boldsymbol{\lambda}_p$, and cancel all $\boldsymbol{\lambda}_p$. A similar procedure can be used between (9_2) and (22). After rearrangements, this provides

$$\sum_{r=1}^{N} c_r \boldsymbol{L}_r \boldsymbol{D}_{rs} \boldsymbol{M}_s = c_s(\boldsymbol{I}-\boldsymbol{A}_s^{\mathrm{T}}). \quad \sum_{r=1}^{N} c_r \boldsymbol{M}_r \boldsymbol{F}_{rs} \boldsymbol{L}_s = c_s(\boldsymbol{I}-\boldsymbol{B}_s^{\mathrm{T}}). \tag{23}$$

Summation over s then gives another pair of consistency conditions for $\boldsymbol{D}_{rs}$ and $\boldsymbol{F}_{rs}$

$$\sum_{s=1}^{N}\sum_{r=1}^{N} c_r \boldsymbol{L}_r \boldsymbol{D}_{rs} \boldsymbol{M}_s = 0. \quad \sum_{s=1}^{N}\sum_{r=1}^{N} c_r \boldsymbol{M}_r \boldsymbol{F}_{rs} \boldsymbol{L}_s = 0. \tag{24}$$

4. Uniform fields

Before proceeding with the derivation of specific forms of the transformation concentration factor tensors, it is useful to establish the general properties of these tensors, and of the underlying influence functions, which are implied by uniform strain and stress fields in heterogeneous media.

The existence of a uniform strain field in an inhomogeneous medium is usually associated with Eshelby's (1957) discovery of such fields within ellipsoidal inclusions in infinite solids under overall uniform strain. However, it is not universally appreciated that uniform strain fields may exist in multiphase heterogeneous media of any phase geometry and material symmetry. In uniformly strained two-phase composite media, such fields result from a superposition of the actual mechanical strains with auxiliary eigenstrains in the phases (Dvorak 1990). Similar superposition will now be applied to multiphase systems. (A reviewer brought to our attention the paper by Cribb (1968) which uses a similar procedure to study thermal expansion in a solid with two isotropic phases.) We note that the fields exist not only in the statistically homogeneous media considered above, but also in media of any shape, with cracks and cavities, provided the overall strain is uniform and no substantial geometry changes occur during loading.

The first principal problem of interest can be stated as follows. Suppose that the volume V, which was initially stress free, has been loaded by certain tractions $\boldsymbol{t}^0$ on S which are in equilibrium with a uniform overall stress $\boldsymbol{\sigma} = \boldsymbol{\sigma}^0$. The goal is to modify the non-uniform local fields by superposition with certain auxiliary eigenstrains, introduced in the local volumes such that a uniform stress field $\boldsymbol{\sigma}_r = \boldsymbol{\sigma}^0$, together with a uniform strain field are created everywhere in V.

The problem can be solved in the following way. The uniform stress $\boldsymbol{\sigma}^0$ is prescribed in all local volumes to create a piecewise uniform but incompatible strain field. Compatibility is restored by superposition of a piecewise uniform eigenstrain field $\boldsymbol{\mu}_r$ which makes the strains uniform everywhere in V; stress equilibrium is already guaranteed by the uniform stress $\boldsymbol{\sigma}^0$. The local strains thus become

$$\boldsymbol{\varepsilon} = \boldsymbol{\varepsilon}_r = \boldsymbol{M}_1\boldsymbol{\sigma}^0 + \boldsymbol{\mu}_1 = \ldots = \boldsymbol{M}_p\boldsymbol{\sigma}^0 + \boldsymbol{\mu}_p = \boldsymbol{M}_q\boldsymbol{\sigma}^0 + \boldsymbol{\mu}_q = \ldots = \boldsymbol{M}_N\boldsymbol{\sigma}^0 + \boldsymbol{\mu}_N$$
$$(r = 1, 2, \ldots, N) \tag{25}$$

A dual problem arises when surface displacements $\boldsymbol{u}^0$, derived from a uniform overall strain field $\boldsymbol{\varepsilon}^0$, are prescribed at S. An eigenstress field is sought such that its

superposition with the stress field caused by $\boldsymbol{u}^0$ on S will lead to uniform stress and strain fields in V. The strain $\boldsymbol{\varepsilon}^0$ is applied to all phases, and a piecewise uniform eigenstress field $\hat{\boldsymbol{\lambda}}_r$ is added to make the phase stresses uniform in V

$$\boldsymbol{\sigma} = \boldsymbol{\sigma}_r = \boldsymbol{L}_1\boldsymbol{\varepsilon}^0 + \hat{\boldsymbol{\lambda}} = \ldots = \boldsymbol{L}_p\boldsymbol{\varepsilon}^0 + \hat{\boldsymbol{\lambda}}_p = \boldsymbol{L}_q\boldsymbol{\varepsilon}^0 + \hat{\boldsymbol{\lambda}}_q = \ldots = \boldsymbol{L}_N\boldsymbol{\varepsilon}^0 + \hat{\boldsymbol{\lambda}}_N \quad (r = 1, 2, \ldots, N)$$

Of course, any initial strains or stresses in V must be included in the above $\hat{\boldsymbol{\mu}}_r$ and $\hat{\boldsymbol{\lambda}}_r$.

We examine four specific forms of the above solutions, in terms of the variables which may be prescribed or evaluated in applications. In each case, the prescribed quantities will be denoted as $\boldsymbol{\varepsilon}^0$, $\boldsymbol{\sigma}^0$, $\boldsymbol{\mu}_r^0$, $\hat{\boldsymbol{\lambda}}_r^0$, etc., and the quantities that need to be added to make the internal fields uniform as $\hat{\boldsymbol{\varepsilon}}$, $\hat{\boldsymbol{\sigma}}$, $\hat{\boldsymbol{\mu}}_r$, $\hat{\boldsymbol{\lambda}}_r$, etc.

(*a*) Surface tractions $\boldsymbol{t}^0$, in equilibrium with a uniform overall stress $\boldsymbol{\sigma}^0$, are prescribed on S, and for a chosen $r = q$, a uniform eigenstrain $\boldsymbol{\mu}_q = \boldsymbol{\mu}_q^0$ is introduced in the local volume V_q. A uniform strain field $\boldsymbol{\varepsilon}$ is created in V by addition of the eigenstrains

$$\hat{\boldsymbol{\mu}}_r = \boldsymbol{\mu}_q^0 - (\boldsymbol{M}_r - \boldsymbol{M}_q)\boldsymbol{\sigma}^0. \quad \boldsymbol{\varepsilon} = \boldsymbol{\varepsilon}_r = \boldsymbol{M}_q\boldsymbol{\sigma}^0 + \boldsymbol{\mu}_q^0. \tag{26}$$

(*b*) Surface displacements $\boldsymbol{u}^0$ compatible with a uniform overall strain $\boldsymbol{\varepsilon}^0$ are prescribed on S, together with one uniform eigenstress $\hat{\boldsymbol{\lambda}}_q = \hat{\boldsymbol{\lambda}}_q^0$ in $r = q$. The local eigenstresses which need to be added to produce a uniform stress field $\boldsymbol{\sigma}$ in V are

$$\hat{\boldsymbol{\lambda}}_r = \hat{\boldsymbol{\lambda}}_q^0 - (\boldsymbol{L}_r - \boldsymbol{L}_q)\boldsymbol{\varepsilon}^0. \quad \boldsymbol{\sigma} = \boldsymbol{\sigma}_r = \boldsymbol{L}_q\boldsymbol{\varepsilon}^0 + \hat{\boldsymbol{\lambda}}_q^0. \tag{27}$$

(*c*) The tractions $\boldsymbol{t}^0$, in equilibrium with $\boldsymbol{\sigma}^0$, are prescribed on S, and a piecewise uniform eigenstrain field $\hat{\boldsymbol{\mu}}_r$ is sought to make the strain field uniform and equal to a prescribed magnitude $\boldsymbol{\varepsilon}_r = \boldsymbol{\varepsilon}^0$. An identical field is formed if displacements $\boldsymbol{u}^0$, compatible with a prescribed overall strain $\boldsymbol{\varepsilon}^0$, are applied on S together with an auxiliary eigenstress field $\hat{\boldsymbol{\lambda}}_r$ to create a uniform stress field of prescribed magnitude $\boldsymbol{\sigma}_r = \boldsymbol{\sigma}^0$ in V. The two transformation fields are found as

$$\hat{\boldsymbol{\mu}}_r = \boldsymbol{\varepsilon}^0 - \boldsymbol{M}_r\boldsymbol{\sigma}^0. \quad \hat{\boldsymbol{\lambda}}_r = \boldsymbol{\sigma}^0 - \boldsymbol{L}_r\boldsymbol{\varepsilon}^0. \tag{28}$$

In the special case of a statistically homogeneous medium, which follows the constitutive equations (1), (28) become

$$\hat{\boldsymbol{\mu}}_r = \boldsymbol{\mu} + (\boldsymbol{M} - \boldsymbol{M}_r)\boldsymbol{\sigma}^0. \quad \hat{\boldsymbol{\lambda}}_r = \boldsymbol{\lambda} + (\boldsymbol{L} - \boldsymbol{L}_r)\boldsymbol{\varepsilon}^0. \tag{29}$$

(*d*) The heterogeneous medium is initially stress free. Uniform eigenstrains are introduced in two local volumes $r = p, q$, as $\boldsymbol{\mu}_p = \boldsymbol{\mu}_p^0$, and $\boldsymbol{\mu}_q = \boldsymbol{\mu}_q^0$. Alternately, uniform eigenstresses $\hat{\boldsymbol{\lambda}}_p = \hat{\boldsymbol{\lambda}}_p^0$, and $\hat{\boldsymbol{\lambda}}_q = \hat{\boldsymbol{\lambda}}_q^0$ may be applied. The goal is to find the overall stress $\hat{\boldsymbol{\sigma}}$ or strain $\hat{\boldsymbol{\varepsilon}}$ that need to be imposed via $\hat{\boldsymbol{t}}$ or $\hat{\boldsymbol{u}}$ on S, and the eigenstrains $\hat{\boldsymbol{\mu}}_r$ or eigenstresses $\hat{\boldsymbol{\lambda}}_r$ in the remaining local volumes such that the local fields become uniform. The solution is

$$\left.\begin{aligned} \hat{\boldsymbol{\mu}}_r &= \boldsymbol{\mu}_q^0 - (\boldsymbol{M}_r - \boldsymbol{M}_q)\hat{\boldsymbol{\sigma}} = \boldsymbol{\mu}_p^0 - (\boldsymbol{M}_r - \boldsymbol{M}_p)\hat{\boldsymbol{\sigma}}. \\ \hat{\boldsymbol{\sigma}} &= \boldsymbol{\sigma}_r = -(\boldsymbol{M}_p - \boldsymbol{M}_q)^{-1}(\boldsymbol{\mu}_p^0 - \boldsymbol{\mu}_q^0). \\ \hat{\boldsymbol{\varepsilon}} &= \boldsymbol{\varepsilon}_r = \boldsymbol{M}_r\hat{\boldsymbol{\sigma}} + \hat{\boldsymbol{\mu}}_r = \boldsymbol{M}_p\hat{\boldsymbol{\sigma}} + \boldsymbol{\mu}_p^0 = \boldsymbol{M}_q\hat{\boldsymbol{\sigma}} + \boldsymbol{\mu}_q^0. \end{aligned}\right\} \tag{30}$$

and

$$\left.\begin{aligned} \hat{\boldsymbol{\lambda}}_r &= \hat{\boldsymbol{\lambda}}_q^0 - (\boldsymbol{L}_r - \boldsymbol{L}_q)\hat{\boldsymbol{\varepsilon}} = \hat{\boldsymbol{\lambda}}_p^0 - (\boldsymbol{L}_r - \boldsymbol{L}_p)\hat{\boldsymbol{\varepsilon}}. \\ \hat{\boldsymbol{\varepsilon}} &= \boldsymbol{\varepsilon}_r = -(\boldsymbol{L}_p - \boldsymbol{L}_q)^{-1}(\hat{\boldsymbol{\lambda}}_p^0 - \hat{\boldsymbol{\lambda}}_q^0). \\ \hat{\boldsymbol{\sigma}} &= \boldsymbol{\sigma}_r = \boldsymbol{L}_r\hat{\boldsymbol{\varepsilon}} + \hat{\boldsymbol{\lambda}}_r = \boldsymbol{L}_p\hat{\boldsymbol{\varepsilon}} + \hat{\boldsymbol{\lambda}}_p^0 = \boldsymbol{L}_q\hat{\boldsymbol{\varepsilon}} + \hat{\boldsymbol{\lambda}}_q^0. \end{aligned}\right\} \tag{31}$$

Recall that by their definition, $\hat{\boldsymbol{\lambda}}_p^0 = -\boldsymbol{L}_p\boldsymbol{\mu}_p^0$ and $\hat{\boldsymbol{\lambda}}_q^0 = -\boldsymbol{L}_q\boldsymbol{\mu}_q^0$. Some algebra then shows that the fields (30) and (31) are identical.

It is now possible to see more clearly in which circumstances the uniform fields may and may not be created in a multiphase medium. Also, their structure and relation to the polarization fields becomes more obvious. For example, if in case (*a*) the given eigenstrain is selected as $\boldsymbol{\mu}_q^0 = \mathbf{0}$, or if the entire field is reduced by subtracting the strain $\boldsymbol{\mu}_q^0$ everywhere, then one finds a particularly convenient form of (25) or (26) as

$$\hat{\boldsymbol{\mu}}_r = -(\boldsymbol{M}_r - \boldsymbol{M}_q)\boldsymbol{\sigma}^0, \quad \boldsymbol{\varepsilon} = \boldsymbol{\varepsilon}_r = \boldsymbol{M}_q\boldsymbol{\sigma}^0 = \boldsymbol{M}_r\boldsymbol{\sigma}^0 + \hat{\boldsymbol{\mu}}_r. \tag{32}$$

A similar result follows from case (*b*):

$$\hat{\boldsymbol{\lambda}}_r = -(\boldsymbol{L}_r - \boldsymbol{L}_q)\boldsymbol{\varepsilon}^0, \quad \boldsymbol{\sigma} = \boldsymbol{\sigma}_r = \boldsymbol{L}_q\boldsymbol{\varepsilon}^0 = \boldsymbol{L}_r\boldsymbol{\varepsilon}^0 + \hat{\boldsymbol{\lambda}}_r. \tag{33}$$

If the $\boldsymbol{M}_q$ and $\boldsymbol{L}_q$ were selected as the properties of a homogeneous comparison material, then the $\hat{\boldsymbol{\mu}}_r$ and $\hat{\boldsymbol{\lambda}}_r$ would define in the usual way the polarization strains and stresses.

In case (*c*), the resulting fields (28) reveal that the medium will accommodate a piecewise uniform eigenstrain field that makes the strain field uniform and equal to $\boldsymbol{\varepsilon}^0$ everywhere in V. However, it is not possible to find a non-zero eigenstrain field (28) which, if applied to a stress-free body, would cause the overall strain $\boldsymbol{\varepsilon}^0$ to vanish. Therefore, the transformation fields that appear in (25) and (26) are unique for a given pair of $\boldsymbol{\sigma}^0$ and $\boldsymbol{\varepsilon}$, or $\boldsymbol{\varepsilon}^0$ and $\boldsymbol{\sigma}$.

Case (*d*) confirms that the fields caused in the medium by a uniform change in temperature, or by any other event that creates piecewise uniform eigenstrains in the local volumes, may be adjusted to a uniform field by purely mechanical loads only in two-phase media, but not in a multiphase medium, or in one subdivided into many local volumes with different local eigenstrains. Of course, such adjustment is possible if the initial fields are made part of the local transformation fields (30) or (31).

5. Some properties of the transformation influence functions

The existence of the uniform fields, and the elastic reciprocal theorem provide certain general relations which must be satisfied by the influence functions in multiphase media, regardless of microstructural geometry and phase properties, even in the absence of statistical homogeneity. First, we consider a representative volume V subjected to a uniform state of overall stress $\boldsymbol{\sigma}^0$. As in (26), we select a uniform eigenstrain $\boldsymbol{\mu}_q^0$ in a local volume V_q, and superimpose the eigenstrains (26_1) with the local strain field caused by $\boldsymbol{\sigma}^0$, to create the uniform strain field $\hat{\boldsymbol{\varepsilon}}$ (26_2) everywhere in V. According to (13), this field is

$$\boldsymbol{\varepsilon}_s = \boldsymbol{A}_s(\boldsymbol{x})\boldsymbol{\varepsilon} + \sum_{r=1}^{N} \boldsymbol{D}_{sr}(\boldsymbol{x})\hat{\boldsymbol{\mu}}_r. \tag{34}$$

Next, substitute from (26) to recover the relation

$$\sum_{r=1}^{N} \boldsymbol{D}_{sr}(\boldsymbol{x})(\boldsymbol{M}_r - \boldsymbol{M}_q) = -(\boldsymbol{I} - \boldsymbol{A}_s(\boldsymbol{x}))\boldsymbol{M}_q. \tag{35}$$

Since this must hold for any selected $\boldsymbol{M}_q$, it follows that for each local volume V_s

$$\sum_{r=1}^{N} \boldsymbol{D}_{sr}(\boldsymbol{x}) = \boldsymbol{I} - \boldsymbol{A}_s(\boldsymbol{x}), \quad \sum_{r=1}^{N} \boldsymbol{D}_{sr}(\boldsymbol{x})\boldsymbol{M}_r = \mathbf{0}. \tag{36}$$

For a statistically homogeneous medium, one can convert (36_1) into an expression

for volume averages in V_s, multiply the result by $c_s L_s$ and write the sum of both sides with respect to s. Since $\sum c_s L_s A_s = L$, this leads to an alternative expression for the overall stiffness

$$L = \sum_{s=1}^{N} \left[c_s L_s \left(I - \sum_{r=1}^{N} D_{sr} \right) \right]. \tag{37}$$

Another relation for the transformation concentration factor tensors follows from the familiar condition $\sum c_r \varepsilon_r = \varepsilon$. The averages of strains in the local volumes are obtained by integration of (13), so that the sum becomes

$$\varepsilon = \sum_{r=1}^{N} c_r A_r \varepsilon + \sum_{r=1}^{N} c_r \sum_{s=1}^{N} D_{rs} \mu_s. \tag{38}$$

Since $\sum c_r A_r = I$, the last term in (38) must vanish. Each local eigenstrain can be chosen independently, hence this provides the relation

$$\sum_{r=1}^{N} c_r D_{rs} = \mathbf{0}. \tag{39}$$

In addition to the above connections derived from the uniform fields, there are certain reciprocal relations between the transformation concentration factor tensors. They can be derived from the elastic reciprocal theorem, in a manner that is similar to the derivation of (4)–(7). Consider a volume V of the heterogeneous medium and focus on two specific local volumes V_r and V_s. Prescribe the overall strain as $\varepsilon^0 = \mathbf{0}$, and introduce a uniform eigenstress λ_r into the local volume V_r. Since there are no other loads, the local strain field at V_s is, according to (13),

$$\varepsilon_s(x) = -D_{sr}(x) M_r \lambda_r. \tag{40}$$

Similarly, if a uniform eigenstress λ'_s is introduced in V_s only, the local strain at V_r is

$$\varepsilon'_r(x) = -D_{rs}(x) M_s \lambda'_s. \tag{41}$$

Recall now the *elastic reciprocal theorem* (A 11) in the Appendix, and substitute from the above equations for the work of the primed on unprimed fields, and vice versa. This leads to

$$\frac{1}{V} \int_{V_s} \lambda'_s \cdot D_{sr}(x) M_r \lambda_r \, \mathrm{d}V = \frac{1}{V} \int_{V_r} \lambda_r \cdot D_{rs}(x) M_s \lambda'_s \, \mathrm{d}V, \tag{42}$$

where the integration over the two local volumes was done in recognition of the fact that eigenstresses λ_r and λ'_s were prescribed only in V_r and V_s respectively.

Inasmuch as all local compliance tensors are diagonally symmetric, and the applied eigenstresses are constant, the procedure leading to (7) reduces (42) to the form

$$c_s D_{sr} M_r = c_r M_s D_{rs}^{\mathrm{T}}. \tag{43}$$

This is a general result, valid for any pair of the transmitted eigenstrain influence functions. For the self-induced factors, it reduces to $D_{ss} M_s = M_s D_{ss}^{\mathrm{T}}$.

It is of interest to note that the above relations (23_1) and (39) can also be obtained by an independent procedure that uses (36) and (43). Rewrite (43) as

$$c_r D_{rs} = c_s M_r D_{sr}^{\mathrm{T}} L_s \tag{44}$$

and then evaluate the sum

$$\sum_{r=1}^{N} c_r D_{rs} = c_s \left[\sum_{r=1}^{N} M_r D_{sr}^{\mathrm{T}} \right] L_s. \tag{45}$$

The expression in the parentheses is the transpose of (36_2), and therefore vanishes: (39) is thus recovered. It can also be shown that (36_1) and (44) lead to (23_1). Moreover, (36_1) and (43) give

$$c_s \boldsymbol{I} - \sum_{r=1}^{N} c_r \boldsymbol{L}_r \boldsymbol{D}_{rs} \boldsymbol{M}_s = c_s \boldsymbol{A}_s^{\mathrm{T}}. \quad c_s \boldsymbol{I} - \sum_{r=1}^{N} c_r \boldsymbol{M}_r \boldsymbol{F}_{rs} \boldsymbol{L}_s = c_s \boldsymbol{B}_s^{\mathrm{T}}. \tag{46}$$

For convenience, we summarize the principal results (36), (43) and (39), together with the analogous relations for the eigenstress influence functions

$$\sum_{r=1}^{N} \boldsymbol{D}_{sr}(\boldsymbol{x}) = \boldsymbol{I} - \boldsymbol{A}_s(\boldsymbol{x}). \quad \sum_{r=1}^{N} \boldsymbol{F}_{sr}(\boldsymbol{x}) = \boldsymbol{I} - \boldsymbol{B}_s(\boldsymbol{x}). \tag{47}$$

$$\sum_{r=1}^{N} \boldsymbol{D}_{sr}(\boldsymbol{x}) \boldsymbol{M}_r = \boldsymbol{0}. \quad \sum_{r=1}^{N} \boldsymbol{F}_{sr}(\boldsymbol{x}) \boldsymbol{L}_r = \boldsymbol{0}. \tag{48}$$

$$c_s \boldsymbol{D}_{sr} \boldsymbol{M}_r = c_r \boldsymbol{M}_s \boldsymbol{D}_{rs}^{\mathrm{T}}, \quad c_s \boldsymbol{F}_{sr} \boldsymbol{L}_r = c_r \boldsymbol{L}_s \boldsymbol{F}_{rs}^{\mathrm{T}}, \tag{49}$$

$$\sum_{r=1}^{N} c_r \boldsymbol{D}_{rs} = \boldsymbol{0}. \quad \sum_{r=1}^{N} c_r \boldsymbol{F}_{rs} = \boldsymbol{0}. \tag{50}$$

with $r = 1, 2, \ldots, N$ everywhere. Note that all these relations are exact, but that (48) and (49) provide (50). It turns out that only (47) and (48) or (49) are independent. In other words, there are only $(2 \times N)$ independent relations for the $(N \times N)$ unknown transformation influence functions. Thus one can solve the system and find exact expressions for the transformation functions in terms of their mechanical counterparts only in two-phase materials. Indeed, the two-phase form of (47) and (48) can be readily solved, with the phases denoted as $r = \alpha, \beta$,

$$\boldsymbol{D}_{\alpha\alpha}(\boldsymbol{x}) = -(\boldsymbol{I} - \boldsymbol{A}_\alpha(\boldsymbol{x}))\, \boldsymbol{M}_\beta (\boldsymbol{M}_\alpha - \boldsymbol{M}_\beta)^{-1}, \quad \boldsymbol{D}_{\alpha\beta}(\boldsymbol{x}) = (\boldsymbol{I} - \boldsymbol{A}_\alpha(\boldsymbol{x}))\, \boldsymbol{M}_\alpha (\boldsymbol{M}_\alpha - \boldsymbol{M}_\beta)^{-1}. \tag{51}$$

The identity $(\boldsymbol{L}_\alpha - \boldsymbol{L}_\beta)^{-1} \boldsymbol{L}_\alpha = -\boldsymbol{M}_\beta (\boldsymbol{M}_\alpha - \boldsymbol{M}_\beta)^{-1}$ shows that these coincide with equations (123) to (126) in Dvorak (1990). It can also be verified that these results conform with (47) to (50): the reciprocal relation (43) requires that $(\boldsymbol{L}_\alpha - \boldsymbol{L}_\beta) \boldsymbol{A}_\beta = \boldsymbol{A}_\beta^{\mathrm{T}} (\boldsymbol{L}_\alpha - \boldsymbol{L}_\beta)$, which does hold in two-phase systems. Since $c_\alpha \boldsymbol{A}_\alpha = (\boldsymbol{L}_\alpha - \boldsymbol{L}_\beta)^{-1} (\bar{\boldsymbol{L}} - \boldsymbol{L}_\beta)$, the eigenstrain concentration factor tensors $\boldsymbol{D}_{\alpha\alpha}$ and $\boldsymbol{D}_{\alpha\beta}$, which are the volume averages of (51) in V_α may be expressed in terms of the overall and local stiffnesses and volume fractions. In any case, it is clear that the eigenstrain problem in two-phase media can be converted into a solution of a mechanical loading problem. Of course, no such conversion is possible for $r > 2$. Exact treatment of such multiphase problems must take into consideration phase interaction under eigenstrain loading for each specific geometry of the microstructure.

However, (47) and (48) can be used to derive certain universal relations between the unknown $\boldsymbol{D}_{ij}(\boldsymbol{x})$ or $\boldsymbol{F}_{ij}(\boldsymbol{x})$. For example, for a three-phase medium one can establish the following exact relations between the transmitted and self-induced transformation influence functions and the mechanical influence functions

$$\left.\begin{aligned}
\boldsymbol{D}_{12}(\boldsymbol{x})(\boldsymbol{M}_2 - \boldsymbol{M}_3) &= \boldsymbol{D}_{11}(\boldsymbol{x})(\boldsymbol{M}_3 - \boldsymbol{M}_1) - (\boldsymbol{I} - \boldsymbol{A}_1(\boldsymbol{x}))\, \boldsymbol{M}_3, \\
\boldsymbol{D}_{13}(\boldsymbol{x})(\boldsymbol{M}_3 - \boldsymbol{M}_2) &= \boldsymbol{D}_{11}(\boldsymbol{x})(\boldsymbol{M}_2 - \boldsymbol{M}_1) - (\boldsymbol{I} - \boldsymbol{A}_1(\boldsymbol{x}))\, \boldsymbol{M}_2, \\
\boldsymbol{D}_{21}(\boldsymbol{x})(\boldsymbol{M}_1 - \boldsymbol{M}_3) &= \boldsymbol{D}_{22}(\boldsymbol{x})(\boldsymbol{M}_3 - \boldsymbol{M}_2) - (\boldsymbol{I} - \boldsymbol{A}_2(\boldsymbol{x}))\, \boldsymbol{M}_3, \\
\boldsymbol{D}_{23}(\boldsymbol{x})(\boldsymbol{M}_3 - \boldsymbol{M}_1) &= \boldsymbol{D}_{22}(\boldsymbol{x})(\boldsymbol{M}_1 - \boldsymbol{M}_2) - (\boldsymbol{I} - \boldsymbol{A}_2(\boldsymbol{x}))\, \boldsymbol{M}_1, \\
\boldsymbol{D}_{31}(\boldsymbol{x})(\boldsymbol{M}_1 - \boldsymbol{M}_2) &= \boldsymbol{D}_{33}(\boldsymbol{x})(\boldsymbol{M}_2 - \boldsymbol{M}_3) - (\boldsymbol{I} - \boldsymbol{A}_3(\boldsymbol{x}))\, \boldsymbol{M}_2, \\
\boldsymbol{D}_{32}(\boldsymbol{x})(\boldsymbol{M}_2 - \boldsymbol{M}_1) &= \boldsymbol{D}_{33}(\boldsymbol{x})(\boldsymbol{M}_1 - \boldsymbol{M}_3) - (\boldsymbol{I} - \boldsymbol{A}_3(\boldsymbol{x}))\, \boldsymbol{M}_1.
\end{aligned}\right\} \tag{52}$$

Note that these relations hold for any three local volumes where distinct uniform local eigenstrains have been prescribed. The local properties $\boldsymbol{M}_r$ can be selected as desired, some as equal to each other. Therefore, these relations apply also to two-phase media where two different eigenstrains have been specified in one phase. For a homogeneous medium with three distinct eigenstrains, (52) reduce to identities, but since $\boldsymbol{A}_r(\boldsymbol{x}) = \boldsymbol{I}$ in this case, (47) or (48) provide the connections

$$\sum_{r=1}^{N} \boldsymbol{D}_{sr}(\boldsymbol{x}) = \boldsymbol{0}. \quad \text{for} \quad r, s = 1, 2, 3.$$

6. Self-consistent and Mori–Tanaka estimates

6.1. *Summary of principal results*

As pointed out in a recent paper by Benveniste *et al.* (1991), the two methods provide diagonally symmetric estimates of the overall stiffness tensor in two-phase systems of any phase geometry, and in those multiphase systems which are reinforced by or consist of aligned inclusions of identical shape. In contrast, when these methods are applied to multiphase systems of arbitrary phase geometry, the stiffness estimates are not diagonally symmetric. In addition, under those circumstances that guarantee diagonal symmetry of the overall stiffness, the methods also provide direct estimates of the overall thermal stress tensor that are in agreement with Levin's (1967) exact relations. Moreover, Chen *et al.* (1992) show that the Mori–Tanaka method delivers diagonally symmetric $\boldsymbol{L}$ for systems reinforced by randomly orientated fibres or platelets of the same shape. Related results were found by Ferrari (1991). These restrictions are respected in the derivations that follow, in fact, the admissibility of the two methods is proved only for two-phase and multiphase aggregates containing or consisting of inclusion of similar shape and alignment.

Moreover, we show here that apart from the differences in evaluation of the constraint tensors, the estimates provided by the two methods of the mechanical, thermal, and transformation concentration factor tensors, and of the overall stiffness and compliance tensors of multiphase heterogeneous media, have a similar structure. It appears that this feature has not been noticed in any of the numerous studies of these methods in the technical literature.

In two-phase media the transformation influence functions have already been evaluated, in (51), in terms of their mechanical counterparts. Thus the self-consistent or Mori–Tanaka estimates of the transformation concentration factors can be found from the corresponding estimates of either the overall stiffness, or the mechanical concentration factor for one phase. In multiphase media with aligned inclusions of similar shape, the overall stiffness can be expressed in the general form

$$\boldsymbol{L} = \boldsymbol{L}_1 + \sum_{r=2}^{N} c_r(\boldsymbol{L}_r - \boldsymbol{L}_1)\boldsymbol{A}_r, \quad \boldsymbol{M} = \boldsymbol{M}_1 + \sum_{r=2}^{N} c_r(\boldsymbol{M}_r - \boldsymbol{M}_1)\boldsymbol{B}_r. \tag{53}$$

where $\boldsymbol{L}_1$ usually refers to the matrix, if any, but it can actually represent any phase. We show in the sequel that in the said systems, the mechanical strain concentration factors $\boldsymbol{A}_r$, and the stress concentration factors $\boldsymbol{B}_r$, are estimated both by the self-consistent and Mori–Tanaka methods in the form

$$\boldsymbol{A}_r = (\boldsymbol{L}^* + \boldsymbol{L}_r)^{-1}(\boldsymbol{L}^* + \boldsymbol{L}), \quad \boldsymbol{B}_r = (\boldsymbol{M}^* + \boldsymbol{M}_r)^{-1}(\boldsymbol{M}^* + \boldsymbol{M}), \quad r = 1, 2, \ldots, N. \tag{54}$$

Here, $\boldsymbol{L}^*$ denotes Hill's (1965) constraint tensor of the ellipsoidal transformed homogeneous inclusion; $\boldsymbol{M}^* = (\boldsymbol{L}^*)^{-1}$. For media with aligned inclusions of similar shape there is only a single $\boldsymbol{L}^*$ tensor, hence the relation $\sum c_r \boldsymbol{A}_r = \sum c_r \boldsymbol{B}_r = \boldsymbol{I}$ and (54) render the following symmetric forms of the overall stiffness and compliance

$$\boldsymbol{L} = \left[\sum_{r=1}^{N} c_r(\boldsymbol{L}^* + \boldsymbol{L}_r)^{-1}\right]^{-1} - \boldsymbol{L}^*, \quad \boldsymbol{M} = \left[\sum_{r=1}^{N} c_r(\boldsymbol{M}^* + \boldsymbol{M}_r)^{-1}\right]^{-1} - \boldsymbol{M}^*. \tag{55}$$

The principal distinction between the two approximate procedures is that in the self-consistent method $\boldsymbol{L}^*$ is evaluated for a cavity in the effective homogeneous medium of overall stiffness $\boldsymbol{L}$, whereas in the Mori–Tanaka method $\boldsymbol{L}^*$ is evaluated for a cavity in the matrix, or any phase $r = 1$, of stiffness $\boldsymbol{L}_1$. The constraint tensor is related to the polarization tensors $\boldsymbol{P}$ and $\boldsymbol{P}_r$, which are defined in the self-consistent procedure as

$$\boldsymbol{P} = (\boldsymbol{L}^* + \boldsymbol{L})^{-1}, \quad \boldsymbol{P}_r = (\boldsymbol{L}^* + \boldsymbol{L}_r)^{-1}, \quad \boldsymbol{P} = \boldsymbol{S}\boldsymbol{L}^{-1}, \quad \boldsymbol{L}^*\boldsymbol{S} = \boldsymbol{L}(\boldsymbol{I} - \boldsymbol{S}), \tag{56}$$

and in the Mori–Tanaka procedure as

$$\boldsymbol{P} = (\boldsymbol{L}^* + \boldsymbol{L}_1)^{-1}, \quad \boldsymbol{P}_r(\boldsymbol{L}^* + \boldsymbol{L}_r)^{-1}, \quad \boldsymbol{P} = \boldsymbol{S}\boldsymbol{L}_1^{-1}, \quad \boldsymbol{L}^*\boldsymbol{S} = \boldsymbol{L}_1(\boldsymbol{I} - \boldsymbol{S}); \tag{57}$$

$\boldsymbol{S}$ denotes the Eshelby tensor of a homogeneous ellipsoidal inclusion. In both methods, the above restrictions on inclusion shape and alignment limit the number of allowable constraint tensors $\boldsymbol{L}^*$ in a multiphase medium to one. In what follows, we show that the same restrictions must be respected in using the methods to estimate the transformation concentration factor tensors.

To facilitate the derivation, we first summarize the principal results obtained below. Remarkably enough, the transformation factor tensors derived from the self-consistent and the Mori–Tanaka methods are formally similar, and valid for $r = 1, 2, \ldots, N$:

$$\left.\begin{aligned} \boldsymbol{D}_{sr} &= [\delta_{sr}\boldsymbol{I} - c_r(\boldsymbol{L}^* + \boldsymbol{L}_s)^{-1}(\boldsymbol{L}^* + \boldsymbol{L})](\boldsymbol{L}^* + \boldsymbol{L}_r)^{-1}\boldsymbol{L}_r, \\ \boldsymbol{F}_{sr} &= [\delta_{sr}\boldsymbol{I} - c_r(\boldsymbol{M}^* + \boldsymbol{M}_s)^{-1}(\boldsymbol{M}^* + \boldsymbol{M})](\boldsymbol{M}^* + \boldsymbol{M}_r)^{-1}\boldsymbol{M}_r, \end{aligned}\right\} \tag{58}$$

or, with regard to (54),

$$\left.\begin{aligned} \boldsymbol{D}_{sr} &= (\boldsymbol{I} - \boldsymbol{A}_s)(\boldsymbol{L}_s - \boldsymbol{L})^{-1}(\delta_{sr}\boldsymbol{I} - c_r\boldsymbol{A}_r^{\mathrm{T}})\boldsymbol{L}_r, \\ \boldsymbol{F}_{sr} &= (\boldsymbol{I} - \boldsymbol{B}_s)(\boldsymbol{M}_s - \boldsymbol{M})^{-1}(\delta_{sr}\boldsymbol{I} - c_r\boldsymbol{B}_r^{\mathrm{T}})\boldsymbol{M}_r, \end{aligned}\right\} \tag{59}$$

where δ_{sr} is the Kronecker symbol, and again, no summation is indicated by repeated subscripts.

Some simple algebra shows that the forms (58) and (59) satisfy the general connections (47) to (49), and therefore (50). The proofs are particularly simple if (58_1) is used with a substitution from (54). In the self-consistent method, the similarity in inclusion shape and alignment is enforced by admitting only a single $\boldsymbol{L}^*$ in (58), that restriction is required to satisfy the reciprocal relations (49). In the Mori–Tanaka derivation, the restriction is invoked in the derivation itself, cf. (55_1), in addition to being required by (49). Of course, one can also show that if $r = \alpha, \beta$, the above forms are in agreement with the results (51) for two-phase media.

6.2. *Self-consistent estimates*

We consider a statistically homogeneous medium with perfectly bonded phases, and seek estimates of the transformation concentration factors by the self-consistent

method. In this method, the average local strain or stress in each phase is evaluated from the solution of a dilute problem for a single inclusion of that phase, contained within a large volume of a homogeneous medium which has the effective composite properties $\boldsymbol{L}$. If the dilute problem is solved under uniform overall strain, one finds the strain concentration factor tensor in the form (Hill 1965):

$$\boldsymbol{A}_r = [\boldsymbol{I} + \boldsymbol{P}(\boldsymbol{L}_r - \boldsymbol{L})]^{-1}, \tag{60}$$

where for each particular shape, $\boldsymbol{P}$ is given by (56) and one thus recovers (53). Note that apart from the inclusion shape, $\boldsymbol{P} = \boldsymbol{P}^{\mathrm{T}}$ depends only on the coefficients of $\boldsymbol{L}$, and that the above restrictions admit only a single $\boldsymbol{P}$ in (60) for the strain concentration factors of all phases. The overall stiffness then follows from (55).

The self-consistent estimates of the transformation concentration factor tensors in (13) are derived from the local field $\boldsymbol{\varepsilon}_s$, evaluated in the solution of a dilute problem in which the inclusion $\boldsymbol{L}_s$ is bonded to a large volume of the effective medium $\boldsymbol{L}$. An overall uniform strain $\boldsymbol{\epsilon}$ is prescribed at infinity, together with the uniform eigenstrain $\boldsymbol{\mu}_s$ in V_s, and, according to (9_2), the eigenstrain $\boldsymbol{\mu} = \sum c_r \boldsymbol{B}_r^{\mathrm{T}} \boldsymbol{\mu}_r$ in the effective medium. The corresponding eigenstresses are $\boldsymbol{\lambda}_s = -\boldsymbol{L}_s \boldsymbol{\mu}_s$, and $\boldsymbol{\lambda} = \sum c_r \boldsymbol{A}_r^{\mathrm{T}} \boldsymbol{\lambda}_r = -\boldsymbol{L}\boldsymbol{\mu}$ in V_s and V respectively.

The solution is sought in terms of $\boldsymbol{A}_s$, and is best found by creating first in the entire volume the uniform strain field $\hat{\boldsymbol{\varepsilon}}$ suggested by (31_2),

$$\hat{\boldsymbol{\varepsilon}} = -(\boldsymbol{L}_s - \boldsymbol{L})^{-1}(\boldsymbol{\lambda}_s - \boldsymbol{\lambda}). \tag{61}$$

This is followed by restoring the overall strain from $\hat{\boldsymbol{\varepsilon}}$ to the prescribed magnitude $\boldsymbol{\varepsilon}$, which yields the desired estimate of the local strain as

$$\boldsymbol{\varepsilon}_s = \boldsymbol{A}_s \boldsymbol{\varepsilon} + (\boldsymbol{I} - \boldsymbol{A}_s)(\boldsymbol{L}_s - \boldsymbol{L})^{-1}\left(\boldsymbol{L}_s \boldsymbol{\mu}_s - \sum_{r=1}^{N} c_r \boldsymbol{A}_r^{\mathrm{T}} \boldsymbol{L}_r \boldsymbol{\mu}_r\right). \tag{62}$$

A comparison with (13) then provides the eigenstrain concentration factors

$$\left.\begin{aligned} \boldsymbol{D}_{ss} &= (\boldsymbol{I} - \boldsymbol{A}_s)(\boldsymbol{L}_s - \boldsymbol{L})^{-1}(\boldsymbol{I} - c_s \boldsymbol{A}_s^{\mathrm{T}})\boldsymbol{L}_s, \\ \boldsymbol{D}_{sr} &= -c_r(\boldsymbol{I} - \boldsymbol{A}_s)(\boldsymbol{L}_s - \boldsymbol{L})^{-1}\boldsymbol{A}_r^{\mathrm{T}} \boldsymbol{L}_r. \end{aligned}\right\} \tag{63}$$

which coincide with those in (59).

In an entirely similar way one may find the self-consistent estimates of the transformation stress concentration factor tensors in (14), and find the result in (59).

6.3. *The Mori–Tanaka method*

The method was originally intended for use with matrix-based composites with perfectly bonded interfaces. One of the phases, $r = 1$, is regarded as a matrix, and phase strains are evaluated from solutions of dilute problems for each single phase in an infinite matrix volume under overall strain $\boldsymbol{\varepsilon}_1$ or stress $\boldsymbol{\sigma}_1$, the respective average values in the matrix $\boldsymbol{L}_1$. In the reformulation of the original form (Mori & Tanaka 1973) by Benveniste (1987), this translates into the following relations.

Under uniform overall strain $\boldsymbol{\varepsilon}$, or stress $\boldsymbol{\sigma}$,

$$\boldsymbol{\varepsilon}_r = \boldsymbol{T}_r \boldsymbol{\varepsilon}_1, \quad \boldsymbol{\sigma}_r = \boldsymbol{W}_r \boldsymbol{\sigma}_1, \quad \boldsymbol{T}_1 = \boldsymbol{W}_1 = \boldsymbol{I}, \quad \boldsymbol{W}_r = \boldsymbol{L}_r \boldsymbol{T}_r \boldsymbol{M}_1, \tag{64}$$

where $\boldsymbol{\varepsilon}_1$ and $\boldsymbol{\sigma}_1$ are as yet unknown average matrix strain and stress. The partial concentration factors $\boldsymbol{T}_r$ and $\boldsymbol{W}_r$ are derived from solutions of the dilute problems.

Since $\boldsymbol{\varepsilon} = \sum_r c_r \boldsymbol{\varepsilon}_r$, etc. one can find the average strain and stress in the phases in terms of $\boldsymbol{T}_r$ or $\boldsymbol{W}_r$ as

$$\left.\begin{aligned} \boldsymbol{\varepsilon}_1 &= \left[\sum_{r=1}^{N} c_r \boldsymbol{T}_r\right]^{-1} \boldsymbol{\varepsilon}, \qquad \boldsymbol{\sigma}_1 = \left[\sum_{r=1}^{N} c_r \boldsymbol{W}_r\right]^{-1} \boldsymbol{\sigma}, \\ \boldsymbol{A}_s &= \boldsymbol{T}_s\left[\sum_{r=1}^{N} c_r \boldsymbol{T}_r\right]^{-1}, \qquad \boldsymbol{B}_s = \boldsymbol{W}_s\left[\sum_{r=1}^{N} c_r \boldsymbol{W}_r\right]^{-1}, \quad s = 1, 2, \ldots, N. \end{aligned}\right\} \tag{65}$$

This leads to the following estimate of the overall stiffness:

$$\boldsymbol{L} = \left[\sum_{r=1}^{N} c_r \boldsymbol{L}_r \boldsymbol{T}_r\right]\left[\sum_{r=1}^{N} c_r \boldsymbol{T}_r\right]^{-1}. \tag{66}$$

According to the assumption of the method, the tensor $\boldsymbol{T}_s$ is evaluated in analogy to (54) and (60) as

$$\boldsymbol{T}_r = (\boldsymbol{L}^* + \boldsymbol{L}_r)^{-1}(\boldsymbol{L}^* + \boldsymbol{L}_1) = [\boldsymbol{I} + \boldsymbol{P}(\boldsymbol{L}_r - \boldsymbol{L}_1)]^{-1}. \tag{67}$$

where $\boldsymbol{P} = \boldsymbol{P}^{\mathrm{T}}$ is defined by (57). Again, only a single $\boldsymbol{P}$ is admitted in multiphase systems, and this permits derivation of the symmetric form (55), as also pointed out by Norris (1989). Note that (55) holds for both methods, and that it can be used to recover

$$\sum_{r=1}^{N} c_r (\boldsymbol{L}^* + \boldsymbol{L}_r)^{-1} = (\boldsymbol{L} + \boldsymbol{L}^*)^{-1}. \tag{68}$$

which is particularly useful in evaluation of the sums of (67) in (65), that can be shown to yield the $\boldsymbol{A}_s$ in (54).

Next, consider evaluation of the transformation concentration factors in (13). As in the self-consistent method, we evaluate the average strain in a solitary inclusion $\boldsymbol{L}_s$, but in an infinite matrix medium $\boldsymbol{L}_1$. A uniform strain $\boldsymbol{\varepsilon}_1$ is applied at infinity, and uniform phase eigenstrains $\boldsymbol{\mu}_1$ and $\boldsymbol{\mu}_s$ are prescribed in V_1 and V_s. In analogy with (13), we seek the strain averages in matrix and inclusion in the form

$$\boldsymbol{\varepsilon}_1 = \boldsymbol{T}_1 \boldsymbol{\varepsilon}_1 + \boldsymbol{R}_{11}\boldsymbol{\mu}_1 + \boldsymbol{R}_{1s}\boldsymbol{\mu}_s, \quad \boldsymbol{\varepsilon}_s = \boldsymbol{T}_s \boldsymbol{\varepsilon}_1 + \boldsymbol{R}_{s1}\boldsymbol{\mu}_1 + \boldsymbol{R}_{ss}\boldsymbol{\mu}_s, \tag{69}$$

where we have introduced the partial transformation strain concentration factors $\boldsymbol{R}_{ij}$, which apply to the case of a single inclusion $\boldsymbol{L}_s$ embedded in the matrix $\boldsymbol{L}_1$, and are to be evaluated from the dilute solution. Clearly, in the dilute solution, the contribution of $\boldsymbol{\mu}_s$ to the average strain in the infinite matrix is negligible, and therefore $\boldsymbol{R}_{1s} = \boldsymbol{0}$. Since $\boldsymbol{T}_1 = \boldsymbol{I}$, it also follows that $\boldsymbol{R}_{11} = \boldsymbol{0}$.

Recall first that $\boldsymbol{\varepsilon} = \sum_r c_r \boldsymbol{\varepsilon}_r$, and find the average matrix strain as

$$\boldsymbol{\varepsilon}_1 = \left[\sum_{r=1}^{N} c_r \boldsymbol{T}_r\right]^{-1}\left[\boldsymbol{\varepsilon} - \left(\sum_{r=1}^{N} c_r \boldsymbol{R}_{r1}\right)\boldsymbol{\mu}_1 - \sum_{r=2}^{N} c_r \boldsymbol{R}_{rr}\boldsymbol{\mu}_r\right]. \tag{70}$$

Then, use that in (69_2) to find $\boldsymbol{\varepsilon}_s$ as

$$\boldsymbol{\varepsilon}_s = \boldsymbol{T}_s\left[\sum_{r=1}^{N} c_r \boldsymbol{T}_r\right]^{-1}\left[\boldsymbol{\varepsilon} - \left(\sum_{r=1}^{N} c_r \boldsymbol{R}_{r1}\right)\boldsymbol{\mu}_1 - \sum_{r=2}^{N} c_r \boldsymbol{R}_{rr}\boldsymbol{\mu}_r\right] + \boldsymbol{R}_{s1}\boldsymbol{\mu}_1 + \boldsymbol{R}_{ss}\boldsymbol{\mu}_s. \tag{71}$$

Compare the two results with (13), and recover the following intermediate forms of the eigenstrain concentration factors

$$\left.\begin{aligned} \boldsymbol{D}_{11} &= -\boldsymbol{A}_1 \sum_{r=2}^{N} c_r \boldsymbol{R}_{r1}, \quad \boldsymbol{D}_{s1} = -\boldsymbol{A}_s \sum_{r=2}^{N} c_r \boldsymbol{R}_{r1} + \boldsymbol{R}_{s1}, \\ \boldsymbol{D}_{1s} &= -c_s \boldsymbol{A}_1 \boldsymbol{R}_{ss}, \quad \boldsymbol{D}_{ss} = (\boldsymbol{I} - c_s \boldsymbol{A}_s)\boldsymbol{R}_{ss}, \quad \boldsymbol{D}_{sr} = -c_r \boldsymbol{A}_s \boldsymbol{R}_{rr}. \end{aligned}\right\} \tag{72}$$

where, since $\boldsymbol{R}_{11} = 0$, the sums were truncated so that $s, r > 1$.

It is now clear which auxiliary terms must be evaluated from the solution of the dilute problem. Recall that the overall uniform strain $\boldsymbol{\varepsilon}_1$ is prescribed at infinity, and transformation strains $\boldsymbol{\mu}_1$ and $\boldsymbol{\mu}_s$ are prescribed in the phases. For any inclusion shape, the solution of this dilute problem may be found with the help of the uniform strain field $\hat{\boldsymbol{\varepsilon}}$ in (31_2). First, this field is created both in the entire matrix volume and in the inclusion. Then, the overall strain is reduced from $\hat{\boldsymbol{\varepsilon}}$ to the prescribed value $\boldsymbol{\varepsilon}_1$, and the average strain in the inclusion is found in terms of the mechanical partial strain concentration factor tensor $\boldsymbol{T}_s$ as

$$\boldsymbol{\varepsilon}_s = \boldsymbol{T}_s\boldsymbol{\varepsilon}_1 + (\boldsymbol{I} - \boldsymbol{T}_s)(\boldsymbol{L}_s - \boldsymbol{L}_1)^{-1}(\boldsymbol{L}_s\boldsymbol{\mu}_s - \boldsymbol{L}_1\boldsymbol{\mu}_1). \tag{73}$$

The result is compared with (71_2) and yields the unknown factors in (72) as

$$\boldsymbol{R}_{s1} = -(\boldsymbol{I} - \boldsymbol{T}_s)(\boldsymbol{L}_s - \boldsymbol{L}_1)^{-1}\boldsymbol{L}_1, \quad \boldsymbol{R}_{ss} = (\boldsymbol{I} - \boldsymbol{T}_s)(\boldsymbol{L}_s - \boldsymbol{L}_1)^{-1}\boldsymbol{L}_s. \tag{74}$$

and this also yields $\boldsymbol{R}_{r1}$ and $\boldsymbol{R}_{rr}$ by exchange of subscripts.

After substitution into (72), and some heavy algebra that utilizes (67), (68) and (54), one recovers the results listed in (58_1) and (59_1). An entirely analogous derivation in terms of stresses leads to the estimates of the transformation stress concentration factors in (58_2) and (59_2). For two-phase systems, one can recover the self-consistent and Mori–Tanaka estimates either from (58) and (59), or by a direct substitution of the appropriate mechanical concentration factor tensors (54) into the two-phase expressions for $\boldsymbol{D}_{ij}$ in (51).

7. Closure

Although there is no intent to discuss specific cases of eigenstrain fields, it is appropriate to mention the connection between the present results and those obtained in studies of the thermoelastic response in composite materials subjected to a uniform temperature change θ. The corresponding eigenstrains assume the form $\boldsymbol{\mu}_r = \boldsymbol{m}_r\theta$, where $\boldsymbol{m}_r$ is the tensor of phase thermal expansion coefficients. It is then customary to focus on evaluation of thermal strain and stress influence functions $\boldsymbol{a}_r$ and $\boldsymbol{b}_r$, which provide the contribution $\boldsymbol{a}_r\theta$ and $\boldsymbol{b}_r\theta$ to the local strains and stresses, in lieu of the last terms in (13). In particular, the complete expressions for the total thermomechanical strains and stresses are

$$\boldsymbol{\varepsilon}_s = \boldsymbol{A}_s\boldsymbol{\varepsilon} + \boldsymbol{a}_s\theta, \quad \boldsymbol{\sigma}_s = \boldsymbol{B}_s\boldsymbol{\sigma} + \boldsymbol{b}_s\theta, \tag{75}$$

and by comparison with (13) there is

$$\boldsymbol{a}_s = \sum_{r=1}^{N} \boldsymbol{D}_{sr}\boldsymbol{m}_r, \quad \boldsymbol{b}_s = \sum_{r=1}^{N} \boldsymbol{F}_{sr}\boldsymbol{l}_r. \tag{76}$$

This indicates that available solutions $\boldsymbol{a}_s$ or $\boldsymbol{b}_s$ of thermoelastic inclusion problems are not directly useful in evaluation of $\boldsymbol{D}_{sr}$ or $\boldsymbol{F}_{sr}$, as they do not yield the individual transformation factor tensors entering the sums.

However, it is desirable to verify that the forms (58) and (59) do yield the proper expressions for $\boldsymbol{a}_r$ in a multiphase medium with aligned inclusions of similar shape. To this end, substitute these forms into (76), with $\boldsymbol{\mu}_r = \boldsymbol{m}_r\theta$, and $\boldsymbol{\lambda}_r = \boldsymbol{l}_r\theta = -\boldsymbol{L}_r\boldsymbol{m}_r\theta$. After some rearrangements find the result

$$\boldsymbol{a}_s = \boldsymbol{A}_s \sum_{r=1}^{N} c_r(\boldsymbol{L}^* + \boldsymbol{L}_r)^{-1}\boldsymbol{l}_r - (\boldsymbol{L}^* + \boldsymbol{L}_s)^{-1}\boldsymbol{l}_s. \tag{77}$$

Note also that, (9) provides Levin's (1967) result

$$\boldsymbol{m} = \sum_{r=1}^{N} c_r \boldsymbol{B}_r^{\mathrm{T}} \boldsymbol{m}_r, \quad \boldsymbol{l} = \sum_{r=1}^{N} c_r \boldsymbol{A}_r^{\mathrm{T}} \boldsymbol{l}_r. \tag{78}$$

Recall now (54), substitute into (78_2), and then rewrite (77) as

$$\boldsymbol{a}_s = (\boldsymbol{L}^* + \boldsymbol{L}_s)^{-1}(\boldsymbol{l} - \boldsymbol{l}_s). \tag{79}$$

Both (77) and (79) follow from the summation (76) of the eigenstrain concentration factors. With an appropriate choice of $\boldsymbol{L}^*$, from (56) or (57), they provide the self-consistent or Mori–Tanaka estimates of the thermal strain concentration factors.

It remains to be shown that (77) or (79) can be derived directly from the two methods, without referring to (76). First, we recall the self-consistent result for multiphase systems with inclusions of similar shape and alignment (Benveniste *et al.* 1991, equation 51).

$$\boldsymbol{a}_s = (\boldsymbol{I} - \boldsymbol{A}_s)(\boldsymbol{L}_s - \boldsymbol{L})^{-1}(\boldsymbol{l} - \boldsymbol{l}_s). \tag{80}$$

Then, a substitution for $\boldsymbol{A}_s$ from (54) serves to recover (79); hence there is agreement between (76_1) and (80) for the self-consistent estimates.

The Mori–Tanaka result appears in Benveniste *et al.* (1991, equation 24_3), it can be written as:

$$\boldsymbol{a}_s = -\boldsymbol{A}_s \sum_{r=1}^{N} c_r \boldsymbol{t}_r + \boldsymbol{t}_s, \tag{81}$$

$$\boldsymbol{t}_r = (\boldsymbol{L}^* + \boldsymbol{L}_r)^{-1}(\boldsymbol{l}_1 - \boldsymbol{l}_r), \tag{82}$$

where $\boldsymbol{t}_r$ is the partial thermal strain concentration factor, and $\boldsymbol{t}_1 = \boldsymbol{0}$.

Substitute now (82) into (81), and use (65_3) with (67) to find

$$\boldsymbol{a}_s = (\boldsymbol{L}^* + \boldsymbol{L}_s)^{-1}\left[\left(\sum_{r=1}^{N} c_r(\boldsymbol{L}^* + \boldsymbol{L}_r)^{-1}\right)^{-1}\left(\sum_{r=1}^{N} c_r(\boldsymbol{L}^* + \boldsymbol{L}_r)^{-1}\boldsymbol{l}_r\right) - \boldsymbol{l}_s\right]. \tag{83}$$

Next, recall Levin's relation (78_2) and use it in conjunction with (65_3) and (67) to obtain

$$\boldsymbol{l} = \left(\sum_{r=1}^{N} c_r(\boldsymbol{L}^* + \boldsymbol{L}_r)^{-1}\right)^{-1}\left(\sum_{r=1}^{N} c_r(\boldsymbol{L}^* + \boldsymbol{L}_r)^{-1}\boldsymbol{l}_r\right). \tag{84}$$

Finally, substitute this into (83) to find that the direct Mori–Tanaka result coincides with (79).

This proves that the transformation strain form (76) of $\boldsymbol{a}_s$ conforms with the independently derived self-consistent and Mori–Tanaka results (80) and (81). Moreover, the formal similarity of the self-consistent and Mori–Tanaka expressions in (79) complements the noted property of the expressions (54) for the mechanical concentration factors, (58) and (59) for the transformation concentration factors, and (55) for the overall stiffness.

It is beyond the present scope to discuss in detail the evaluation of the transformation concentration factor tensors in sub-elements of unit cell models of composite materials. Of course, even in two-phase composites, the representative volumes within such cells may consist of many local volumes with different eigenstrains. However, the task is quite simple in principle. If uniform strain elements are selected as the local volumes, which is often advantageous in modelling of inelastic deformation, then each such element s has its own elastic transformation

concentration factor matrix $\boldsymbol{D}_{sr}$. Individual columns of each such matrix are generated by applying, in sequence, a single unit eigenstrain $\boldsymbol{\mu}_1, \boldsymbol{\mu}_2, \ldots, \boldsymbol{\mu}_N$ in each element $r = 1, 2, \ldots, N$, while the overall strain in the unit cell is kept equal to zero. The local strain components evaluated by this process in each element s are equal to the required coefficients of $\boldsymbol{D}_{sr}$.

A very simple example illustrates how this may be accomplished through available routines which evaluate thermal strains. Suppose that the thermal expansion coefficients in all elements, except in one element r, are set equal to zero. Unit local eigenstrains in that element are generated by prescribing a uniform temperature change. Then the total local strains in all elements $s = 1, 2, \ldots, r, \ldots, N$, are found, and finally those are converted into the respective columns of coefficients in the $\boldsymbol{D}_{sr}$ matrices of those elements. Of course, much more efficient procedures for evaluation of $\boldsymbol{D}_{sr}$ may be designed using the stiffness matrix of the unit cell.

This work was supported by the Office of Naval Research, and by the ONR/DARPA-HiTASC project and Rensselaer. Dr Yapa Rajapakse and Dr Steve Fishman served as program monitors. Y. B. is a Visiting Professor at Rensselaer Polytechnic Institute.

Appendix

The elastic reciprocal theorem states that in a linearly elastic body subjected to two systems of body and surface forces, the work of one system on the displacements caused by the other system is related by Sokolnikoff (1956, p. 392)

$$\int_S t_i u_i' \, \mathrm{d}S + \int_V F_i u_i' \, \mathrm{d}V = \int_S t_i' u_i \, \mathrm{d}S + \int_V F_i' u_i \, \mathrm{d}V. \tag{A 1}$$

where u_i are the displacements caused by the system t_i, F_i, and u_i' are the displacements caused by the system t_i', F_i'.

When distributions of eigenstresses λ_{ij} and λ_{ij}' are respectively applied together with the two systems, the local stress field is given by (2_1). In the unprimed system, the stresses are given by

$$\sigma_{ij}(\boldsymbol{x}) = \tilde{\sigma}_{ij}(\boldsymbol{x}) + \lambda_{ij}(\boldsymbol{x}), \tag{A 2}$$

where

$$\tilde{\sigma}_{ij}(\boldsymbol{x}) = L_{ijkl} \epsilon_{kl}(\boldsymbol{x}).$$

The field (A 2) satisfies

$$\tilde{\sigma}_{ij,j} + F_i + \lambda_{ij,j} = 0 \text{ in } V, \quad \tilde{\sigma}_{ij} n_j + \lambda_{ij} n_j = t_i \text{ on } S. \tag{A 3}$$

A similar representation holds for the primed system.

Define new body forces and surface tractions

$$\tilde{F}_i = F_i + \lambda_{ij,j}, \quad \tilde{t}_i = t_i - \lambda_{ij} n_j, \tag{A 4}$$

and rewrite (A 1) to read

$$\int_S \tilde{t}_i u_i' \, \mathrm{d}S + \int_V \tilde{F}_i u_i' \, \mathrm{d}V = \int_S \tilde{t}_i' u_i \, \mathrm{d}S + \int_V \tilde{F}_i' u_i \, \mathrm{d}V. \tag{A 5}$$

Consider first the left-hand side and substitute from (A 3) to find the expression

$$\int_S (t_i - \lambda_{ij} n_j) u_i' \, \mathrm{d}S + \int_V F_i u_i' \, \mathrm{d}V + \int_V \lambda_{ij,j} u_i' \, \mathrm{d}V. \tag{A 6}$$

Note that the last term can be written as

$$\int_V (\lambda_{ij,j} u_i')\,\mathrm{d}V = \int_V (\lambda_{ij} u_i')_{,j}\,\mathrm{d}V - \int_V \lambda_{ij} u_{i,j}'\,\mathrm{d}V. \tag{A 7}$$

whereas the divergence theorem provides

$$\int_V (\lambda_{ij} u_i')_{,j}\,\mathrm{d}V = \int_S \lambda_{ij} u_i' n_j\,\mathrm{d}S. \tag{A 8}$$

Moreover, $u_{i,j}' = \epsilon_{ij}' + \omega_{ij}'$ and $\lambda_{ij} = \lambda_{ji}$, $\omega_{ij}' = -\omega_{ij}'$, hence (A 7) becomes

$$\int_V \lambda_{ij,j} u_i'\,\mathrm{d}V = \int_S \lambda_{ij} u_i' n_j\,\mathrm{d}S - \int_V \lambda_{ij} \epsilon_{ij}'\,\mathrm{d}V. \tag{A 9}$$

Finally, the substitution of (A 9) in (A 6) gives

$$\int_S t_i u_i'\,\mathrm{d}S + \int_V F_i u_i'\,\mathrm{d}V - \int_V \lambda_{ij} \epsilon_{ij}'\,\mathrm{d}V. \tag{A 10}$$

which is the final form of the left-hand side of (A 5). The same procedure can be applied to the right-hand side of (A 5). That finally leads to the following form of the reciprocal theorem, which now accounts for the effect of the applied eigenstress fields:

$$\int_S t_i u_i'\,\mathrm{d}S + \int_V F_i u_i'\,\mathrm{d}V - \int_V \lambda_{ij} \epsilon_{ij}'\,\mathrm{d}V = \int_S t_i' u_i\,\mathrm{d}S + \int_V F_i' u_i\,\mathrm{d}V - \int_V \lambda_{ij}' \epsilon_{ij}\,\mathrm{d}V. \tag{A 11}$$

References

Benveniste, Y. 1987 *Mech. Mater.* **6**, 147–157.

Benveniste, Y. 1990 *J. appl. Mech.* **57**, 474–476.

Benveniste, Y., Dvorak, G. J. & Chen, T. 1991 *J. Mech. Phys. Solids.* **39**, 927–946.

Chen, T., Dvorak, G. J. & Benveniste, Y. 1992 *J. appl. Mech.* (In the press.)

Cribb, J. L. 1968 *Nature, Lond.* **220**, 576–577.

Dvorak, G. J. 1990 *Proc. R. Soc. Lond.* A **431**, 89–110.

Dvorak, G. J. 1991 In *Metal matrix composites: mechanisms and properties* (ed. R. K. Everett & R. J. Arsenault), pp. 1–77. Boston: Academic Press.

Dvorak, G. J. 1992 Transformation field analysis of inelastic composite materials. *Proc. R. Soc. Lond.* A **437**, 311–327. (Following paper.)

Eshelby, J. D. 1957 *Proc. R. Soc. Lond.* A **241**, 376–396.

Ferrari, M. 1991 *Mech. Mater.* **11**, 251–256.

Hill, R. 1963 *J. Mech. Phys. Solids* **11**, 357–372.

Hill, R. 1965 *J. Mech. Phys. Solids* **13**, 213–222.

Levin, V. M. 1967 *Izv. AN SSSR, Mekhanika Tverdogo Tela* **2**, 88–94.

Levin, V. M. 1976 *Izv. AN SSSR, Mekhanika Tverdogo Tela* **11**, 137–145.

Mori, T. & Tanaka, K. 1973 *Acta Metal.* **21**, 571–574.

Mura, T. 1987 *Micromechanics of defects in solids*, 2nd edn. Dordrecht: Martinus Nijhoff.

Norris, A. N. 1989 *J. appl. Mech.* **56**, 83–88.

Sokolnikoff, I. S. 1956 *Mathematical theory of elasticity*, 2nd edn. New York: McGraw-Hill.

Walker, K. P., Jordan, E. H. & Freed, A. 1990 *Micromechanics and inhomogeneity* (ed. G. Weng, M. Taya & H. Abe), pp. 536–558. Berlin: Springer-Verlag.

Willis, J. R. 1978 *Continuum models of discrete systems* (ed. J. W. Provan), pp. 185–215. University of Waterloo Press.

Willis, J. R. 1981 *Advances in applied mechanics* (ed. C. S. Yih), vol. 21, pp. 1–78. New York: Academic Press.

Received 5 August 1991; accepted 5 December 1991

Transformation field analysis of inelastic composite materials

By George J. Dvorak

Civil Engineering Department, Rensselaer Polytechnic Institute, Troy, New York 12180, U.S.A.

A new method is proposed for evaluation of local fields and overall properties of composite materials subjected to incremental thermomechanical loads and to transformation strains in the phases. The composite aggregate may consist of many perfectly bonded inelastic phases of arbitrary geometry and elastic material symmetry. In principle, any inviscid or time-dependent inelastic constitutive relation that complies with the additive decomposition of total strains can be admitted in the analysis. The governing system of equations is derived from the representation of local stress and strain fields by novel transformation influence functions and concentration factor tensors, as discussed in the preceding paper by G. J. Dvorak and Y. Benveniste. The concentration factors depend on local and overall thermoelastic moduli, and can be evaluated with a selected micromechanical model. Applications to elastic–plastic, viscoelastic, and viscoplastic systems are discussed. The new approach is contrasted with some presently accepted procedures based on the self-consistent and Mori–Tanaka approximations, which are shown to violate exact relations between local and overall inelastic strains.

1. Introduction

The purpose of this paper is to introduce a method for incremental micromechanical analysis of local fields and overall properties of inelastic heterogeneous media subjected to uniform thermomechanical loading along a prescribed path. The proposed approach relies on an explicit evaluation of piecewise uniform approximations of the residual fields that are introduced in multiphase solids by a distribution of piecewise uniform eigenstrains or eigenstresses, jointly referred to as transformation fields. As described in the preceding paper (I) by Dvorak & Benveniste (1992), such evaluations are made with the help of novel transformation influence functions, or concentration factor tensors. (References to, say, equation (23) in the companion paper (I) will be denoted here by (I 23), etc.) The treatment is suitable for composite aggregates made of any number of different, perfectly bonded inelastic phases which are represented by constitutive equations that admit the additive decomposition of total strains into elastic and inelastic components. However, any phase geometry and elastic material symmetry can be prescribed, and specific micromechanical models, such as the self-consistent, Mori–Tanaka, or unit cell approximations, are needed only in evaluations of the transformation concentration factor tensors. In any event, since the latter depend on local and overall thermoelastic moduli, only elastic solutions are required.

The elements of the present approach have been outlined by Dvorak (1991) for elastic plastic two-phase composite materials at small strains. The present work goes

Proc. R. Soc. Lond. A (1992) **437**, 311–327
Printed in Great Britain

much farther in that it treats multiphase media and allows for many different types of inelastic behaviour. The opening §2 reviews the connections between the local and overall inelastic and total strains. The essence of the method is described in §3, through the formulation of governing systems of equations for evaluation of the total local strains or stresses, where the coefficients are formed, in part, by the transformation factor tensors. Section 4 is concerned with thermomechanical deformation of elastic–plastic composite systems. Explicit forms of the instantaneous mechanical and thermal concentration factors are found there for two and three-phase solids. Applications to viscoelastic and viscoplastic systems are described in §§5 and 6. Finally, §7 contrasts the new approach with some accepted procedures based on the self-consistent or Mori–Tanaka approximations, which are shown to violate a general connection between the local and overall inelastic strains.

2. Decompositions of local and overall fields

We are concerned with a representative volume V of a composite material that consists of many perfectly bonded phases which may have any physically admissible elastic symmetry and microstructural geometry. The volume V may be subdivided into several local volumes V_r, $r = 1, 2, \ldots, N$, $\sum V_r = V$, such that each contains only one phase material, although any given phase may reside in more than one volume V_r. The boundary conditions imposed on V are limited to displacements compatible with a uniform overall strain $\boldsymbol{\varepsilon}$, or tractions derived from a uniform overall stress $\boldsymbol{\sigma}$, and a uniform temperature change θ; all are expressed in a cartesian coordinate system $\boldsymbol{x}$ defined in V. The strains are assumed to be small, but both elastic and inelastic behaviour of the phases is admitted, providing that at each instant of loading it conforms with the additive decomposition

$$\boldsymbol{\sigma}_r(\boldsymbol{x}) = \boldsymbol{\sigma}_r^{\mathrm{e}}(\boldsymbol{x}) + \boldsymbol{\sigma}_r^{\mathrm{re}}(\boldsymbol{x}), \quad \boldsymbol{\varepsilon}_r(\boldsymbol{x}) = \boldsymbol{\varepsilon}_r^{\mathrm{e}}(\boldsymbol{x}) + \boldsymbol{\varepsilon}_r^{\mathrm{in}}(\boldsymbol{x}), \tag{1}$$

where the inelastic strain $\boldsymbol{\varepsilon}_r^{\mathrm{in}}(\boldsymbol{x})$ accumulates incrementally under applied stress, according to a certain phase constitutive relation which may or may not depend on time and temperature; specific examples of such relations will be discussed later. The $\boldsymbol{\sigma}_r^{\mathrm{re}}(\boldsymbol{x})$ represents a relaxation stress, that develops in a similar way under applied phase strain.

The $\boldsymbol{\sigma}_r^{\mathrm{e}}(\boldsymbol{x})$ and $\boldsymbol{\varepsilon}_r^{\mathrm{e}}(\boldsymbol{x})$ are elastic fields related by the usual constitutive relations, so that (1) can be recast as

$$\boldsymbol{\sigma}_r(\boldsymbol{x}) = \boldsymbol{L}_r \boldsymbol{\varepsilon}_r(\boldsymbol{x}) + \boldsymbol{l}_r \theta + \boldsymbol{\sigma}_r^{\mathrm{re}}(\boldsymbol{x}), \quad \boldsymbol{\varepsilon}_r(\boldsymbol{x}) = \boldsymbol{M}_r \boldsymbol{\sigma}_r(\boldsymbol{x}) + \boldsymbol{m}_r \theta + \boldsymbol{\varepsilon}_r^{\mathrm{in}}(\boldsymbol{x}), \tag{2}$$

in terms of the phase elastic stiffness $\boldsymbol{L}_r$, or compliance $\boldsymbol{M}_r = \boldsymbol{L}_r^{-1}$, and the thermal stress and strain tensors $\boldsymbol{l}_r$ and $\boldsymbol{m}_r = -\boldsymbol{M}_r \boldsymbol{l}_r$. Since θ and one of the inelastic fields are independent, it follows that

$$\boldsymbol{m}_r = -\boldsymbol{M}_r \boldsymbol{l}_r, \quad \boldsymbol{l}_r = -\boldsymbol{L}_r \boldsymbol{m}_r, \quad \boldsymbol{\varepsilon}_r^{\mathrm{in}}(\boldsymbol{x}) = -\boldsymbol{M}_r \boldsymbol{\sigma}_r^{\mathrm{re}}(\boldsymbol{x}), \quad \boldsymbol{\sigma}_r^{\mathrm{re}}(\boldsymbol{x}) = -\boldsymbol{L}_r \boldsymbol{\varepsilon}_r^{\mathrm{in}}(\boldsymbol{x}). \tag{3}$$

In the special case of a purely elastic response of the composite aggregate, the local fields and overall loads are related by the mechanical and thermal elastic influence functions

$$\left.\begin{aligned} \boldsymbol{\varepsilon}_r(\boldsymbol{x}) &= \boldsymbol{A}_r(\boldsymbol{x})\boldsymbol{\varepsilon} + \boldsymbol{a}_r(\boldsymbol{x})\theta \quad \text{if } \boldsymbol{\sigma}_s^{\mathrm{re}}(\boldsymbol{x}) = 0, \\ \boldsymbol{\sigma}_r(\boldsymbol{x}) &= \boldsymbol{B}_r(\boldsymbol{x})\boldsymbol{\sigma} + \boldsymbol{b}_r(\boldsymbol{x})\theta \quad \text{if } \boldsymbol{\varepsilon}_s^{\mathrm{in}}(\boldsymbol{x}) = 0. \end{aligned}\right\} \; s = 1, 2, \ldots, r, \ldots, N. \tag{4}$$

The total overall stress under an applied overall strain $\boldsymbol{\varepsilon} = \boldsymbol{\varepsilon}_0$, or the total overall

strain of the representative volume V under an overall stress $\boldsymbol{\sigma} = \boldsymbol{\sigma}_0$, and the temperature change θ_0, are evaluated by integration of (2) over V. As in (1), one can recover the additive decompositions

$$\boldsymbol{\sigma} = \boldsymbol{\sigma}^{\mathrm{e}} + \boldsymbol{\sigma}^{\mathrm{re}}, \quad \boldsymbol{\varepsilon} = \boldsymbol{\varepsilon}^{\mathrm{e}} + \boldsymbol{\varepsilon}^{\mathrm{in}}, \tag{5}$$

where the individual terms are defined as

$$\left.\begin{aligned} \boldsymbol{\sigma}^{\mathrm{e}} &= \frac{1}{V}\int_V [\boldsymbol{L}_r \boldsymbol{A}_r(\boldsymbol{x})\boldsymbol{\varepsilon}_0 + (\boldsymbol{L}_r \boldsymbol{a}_r(\boldsymbol{x}) + \boldsymbol{l}_r)\theta_0]\,\mathrm{d}V, \\ \boldsymbol{\sigma}^{\mathrm{re}} &= \frac{1}{V}\int_V [\boldsymbol{L}_r(\boldsymbol{\varepsilon}_r(\boldsymbol{x}) - \boldsymbol{A}_r(\boldsymbol{x})\boldsymbol{\varepsilon}_0 - \boldsymbol{a}_r(\boldsymbol{x})\theta_0) + \boldsymbol{\sigma}_r^{\mathrm{re}}(\boldsymbol{x}))\,\mathrm{d}V. \end{aligned}\right\} \tag{6}$$

$$\left.\begin{aligned} \boldsymbol{\varepsilon}^{\mathrm{e}} &= \frac{1}{V}\int_V [\boldsymbol{M}_r \boldsymbol{B}_r(\boldsymbol{x})\boldsymbol{\sigma}_0 + (\boldsymbol{M}_r \boldsymbol{b}_r(\boldsymbol{x}) + \boldsymbol{m}_r)\theta_0]\,\mathrm{d}V, \\ \boldsymbol{\varepsilon}^{\mathrm{in}} &= \frac{1}{V}\int_V [\boldsymbol{M}_r(\boldsymbol{\sigma}_r(\boldsymbol{x}) - \boldsymbol{B}_r(\boldsymbol{x})\boldsymbol{\sigma}_0 - \boldsymbol{b}_r(\boldsymbol{x})\theta_0) + \boldsymbol{\varepsilon}_r^{\mathrm{in}}(\boldsymbol{x})]\,\mathrm{d}V. \end{aligned}\right\} \tag{7}$$

The $\boldsymbol{\sigma}^{\mathrm{e}}$ and $\boldsymbol{\varepsilon}^{\mathrm{e}}$ represents the purely elastic, fully recoverable overall response to the applied loads $\boldsymbol{\varepsilon}_0$ or $\boldsymbol{\sigma}_0$, and θ_0, that follows from (2) to (4); the associated local elastic fields in V are given by (4). The $\boldsymbol{\sigma}^{\mathrm{re}}$ and $\boldsymbol{\varepsilon}^{\mathrm{in}}$ are the overall stress and strain caused by the local inelastic fields which are, in general, independent of the current thermomechanical loads. However, to be admissible in the present analysis, the local inelastic strains and the corresponding residual fields must be associated with inelastic strains that are macroscopically uniform. Note that they are obtained by superposition of the volume averages of the local inelastic fields $\boldsymbol{\sigma}_r^{\mathrm{re}}(\boldsymbol{x})$ or $\boldsymbol{\varepsilon}_r^{\mathrm{in}}(\boldsymbol{x})$ themselves, with the residual elastic fields induced in the aggregate by those local fields, i.e. by $\boldsymbol{\sigma}_r^{\mathrm{re}}(\boldsymbol{x})$ at $\boldsymbol{\varepsilon} = \boldsymbol{0}$ and $\theta = 0$, or by $\boldsymbol{\varepsilon}_r^{\mathrm{in}}(\boldsymbol{x})$ at $\boldsymbol{\sigma} = \boldsymbol{0}$ and $\theta = 0$. The implication is that the inelastic fields, introduced by some thermomechanical loading history leading to the current values of $\boldsymbol{\varepsilon}$, $\boldsymbol{\sigma}$ and θ, cannot be recovered by an instantaneous elastic unloading.

The decomposition (5) of the overall response is consistent with the decomposition (1) of the total local strain or stress fields, in the sense that

$$\boldsymbol{\sigma} = \boldsymbol{\sigma}^{\mathrm{e}} + \boldsymbol{\sigma}^{\mathrm{re}} = \frac{1}{V}\int_V [\boldsymbol{\sigma}_r^{\mathrm{e}}(\boldsymbol{x}) + \boldsymbol{\sigma}_r^{\mathrm{re}}(\boldsymbol{x})]\,\mathrm{d}V. \tag{8}$$

$$\boldsymbol{\varepsilon} = \boldsymbol{\varepsilon}^{\mathrm{e}} + \boldsymbol{\varepsilon}^{\mathrm{in}} = \frac{1}{V}\int_V [\boldsymbol{\varepsilon}_r^{\mathrm{e}}(\boldsymbol{x}) + \boldsymbol{\varepsilon}_r^{\mathrm{in}}(\boldsymbol{x})]\,\mathrm{d}V. \tag{9}$$

However, the individual terms do not correspond to each other. On the local scale, the elastic fields in (1) results from the superposition of the elastic local fields (4) with the local residual elastic fields. On the overall scale, the elastic terms are volume integrals of the elastic fields (4), whereas the inelastic terms are volume integrals of the residual elastic fields superimposed with the inelastic local fields.

Evaluation of the inelastic terms in the above relations is facilitated by the results obtained in (I). In particular, if the local fields in (2) are compared with those in (I 2), and the overall fields in (8) with those in (I 1), the above thermal and inelastic fields are identified as certain local and overall transformation fields,

$$\boldsymbol{\lambda}_r(\boldsymbol{x}) = \boldsymbol{l}_r\theta + \boldsymbol{\sigma}_r^{\mathrm{re}}(\boldsymbol{x}), \quad \boldsymbol{\mu}_r(\boldsymbol{x}) = \boldsymbol{m}_r\theta + \boldsymbol{\varepsilon}_r^{\mathrm{in}}(\boldsymbol{x}), \tag{10}$$

$$\boldsymbol{\lambda} = \boldsymbol{l}\theta + \boldsymbol{\sigma}^{\mathrm{re}}, \quad \boldsymbol{\mu} = \boldsymbol{m}\theta + \boldsymbol{\varepsilon}^{\mathrm{in}}. \tag{11}$$

Since the thermal fields are uniform, one finds from (I 7) to (I 9) that

$$\boldsymbol{l} = \sum_{r=1}^{N} c_r \boldsymbol{A}_r^{\mathrm{T}} \boldsymbol{l}_r, \quad \boldsymbol{\sigma}^{\mathrm{re}} = \frac{1}{V}\int_V \boldsymbol{A}_r^{\mathrm{T}}(\boldsymbol{x})\boldsymbol{\sigma}_r^{\mathrm{re}}(\boldsymbol{x})\,\mathrm{d}V, \tag{12}$$

$$\boldsymbol{m} = \sum_{r=1}^{N} c_r \boldsymbol{B}_r^{\mathrm{T}} \boldsymbol{m}_r, \quad \boldsymbol{\varepsilon}^{\mathrm{in}} = \frac{1}{V}\int_V \boldsymbol{B}_r^{\mathrm{T}}(\boldsymbol{x})\boldsymbol{\varepsilon}_r^{\mathrm{in}}(\boldsymbol{x})\,\mathrm{d}V, \tag{13}$$

where $c_r = V_r/V$.

In the spirit of the approach outlined in §3 of (I), the actual local fields will be approximated below by piecewise uniform distributions. Under such circumstances all local fields and the influence functions in (2)–(7) are replaced by their averages over V_r, and one also recovers

$$\boldsymbol{\sigma}^{\mathrm{re}} = \sum_{r=1}^{N} c_r \boldsymbol{A}_r^{\mathrm{T}} \boldsymbol{\sigma}^{\mathrm{re}}, \quad \boldsymbol{\varepsilon}^{\mathrm{in}} = \sum_{r=1}^{N} c_r \boldsymbol{B}_r^{\mathrm{T}} \boldsymbol{\varepsilon}_r^{\mathrm{in}}. \tag{14}$$

It is then possible to evaluate the total stress and strain in (8) and (9) as

$$\boldsymbol{\sigma} = \boldsymbol{L}\boldsymbol{\varepsilon} + \boldsymbol{l}\theta + \sum_{r=1}^{N} c_r \boldsymbol{A}_r^{\mathrm{T}} \boldsymbol{\sigma}_r^{\mathrm{re}} = \sum_{r=1}^{N} c_r \boldsymbol{\sigma}_r, \tag{15}$$

$$\boldsymbol{\varepsilon} = \boldsymbol{M}\boldsymbol{\sigma} + \boldsymbol{m}\theta + \sum_{r=1}^{N} c_r \boldsymbol{B}_r^{\mathrm{T}} \boldsymbol{\varepsilon}_r^{\mathrm{in}} = \sum_{r=1}^{N} c_r \boldsymbol{\varepsilon}_r, \tag{16}$$

with the usual definitions of the overall elastic stiffness $\boldsymbol{L}$ and compliance $\boldsymbol{M} = \boldsymbol{L}^{-1}$, and the overall elastic thermal stress and strain tensors $\boldsymbol{l}$, $\boldsymbol{m}$,

$$\boldsymbol{M} = \sum_{r=1}^{N} c_r \boldsymbol{M}_r \boldsymbol{B}_r, \quad \boldsymbol{m} = \sum_{r=1}^{N} (\boldsymbol{M}_r \boldsymbol{b}_r + \boldsymbol{m}_r), \tag{17}$$

$$\boldsymbol{L} = \sum_{r=1}^{N} c_r \boldsymbol{L}_r \boldsymbol{A}_r, \quad \boldsymbol{l} = \sum_{r=1}^{N} (\boldsymbol{L}_r \boldsymbol{a}_r + \boldsymbol{l}_r), \tag{18}$$

that follows from (2)–(4), (6_1) and (7_1).

The expressions for overall averages are seen to be analogous to those for the local fields in (2), and one can also establish connections that are analogous to those in (3)

$$\boldsymbol{m} = -\boldsymbol{M}\boldsymbol{l}, \quad \boldsymbol{l} = -\boldsymbol{L}\boldsymbol{m}, \quad \boldsymbol{\varepsilon}^{\mathrm{in}} = -\boldsymbol{M}\boldsymbol{\sigma}^{\mathrm{re}}, \quad \boldsymbol{\sigma}^{\mathrm{re}} = -\boldsymbol{L}\boldsymbol{\varepsilon}^{\mathrm{in}}. \tag{19}$$

Note that in addition to the usual connections (15_2) and (16_2) between the local and overall total strains, there exist additional independent connections (14) between the local and overall inelastic fields. Sections 3–6 below outline the procedure that guarantees their satisfaction in various inelastic heterogeneous solids, while §7 points out that many micromechanical models currently in use violate (14).

Note also that in a homogeneous material ($\boldsymbol{L}_r = \boldsymbol{L}$, $\boldsymbol{l}_r = \boldsymbol{l}$, etc.), there is, according to (4), $\boldsymbol{A}_r(\boldsymbol{x}) = \boldsymbol{B}_r(\boldsymbol{x}) = \boldsymbol{I}$, and $\boldsymbol{a}_r(\boldsymbol{x}) = \boldsymbol{b}_r(\boldsymbol{x}) = \boldsymbol{0}$. Since the volume average of $\boldsymbol{\varepsilon}_r(\boldsymbol{x})$ in V is equal to $\boldsymbol{\varepsilon}_0$, and that of $\boldsymbol{\sigma}_r(\boldsymbol{x})$ to $\boldsymbol{\sigma}_0$, the volume integrals of the residual fields vanish and the overall inelastic terms are equal to the volume averages of the local inelastic fields.

3. Evaluation of the transformation fields

We now recall the representation of the local fields by the transformation concentration factor tensors defined in (I 13) and (I 14). For any representative volume under uniform overall strain $\boldsymbol{\varepsilon} = \boldsymbol{\varepsilon}_0$ or stress $\boldsymbol{\sigma} = \boldsymbol{\sigma}_0$, and a temperature

change $\theta = \theta_0$, which contains a piecewise uniform distribution of the thermal and inelastic fields associated with uniform overall loading and deformation, the averages of the local fields are written as

$$\boldsymbol{\varepsilon}_s = \boldsymbol{A}_s \boldsymbol{\varepsilon}_0 + \sum_{r=1}^{N} \boldsymbol{D}_{sr}(\boldsymbol{m}_r \theta_0 + \boldsymbol{\varepsilon}_r^{\text{in}}), \quad r, s = 1, 2, \ldots, N, \tag{20}$$

$$\boldsymbol{\sigma}_s = \boldsymbol{B}_s \boldsymbol{\sigma}_0 + \sum_{r=1}^{N} \boldsymbol{F}_{sr}(\boldsymbol{l}_r \theta_0 + \boldsymbol{\sigma}_r^{\text{re}}), \quad r, s = 1, 2, \ldots, N. \tag{21}$$

The $\boldsymbol{A}_s$ and $\boldsymbol{B}_s$ are the mechanical concentration factor tensors, and $\boldsymbol{D}_{sr}$, $\boldsymbol{F}_{sr}$ are certain eigenstrain and eigenstress concentration factor tensors. They all depend on the local and overall elastic moduli, and on the shape and volume fraction of the phases, and are therefore constant. The self-induced factors $\boldsymbol{D}_{ss}$ and $\boldsymbol{F}_{ss}$ contribute both the residual field caused in V_s by the transformation fields, and the fields themselves, these two contributions may be separated. Self-consistent and Mori–Tanaka estimates of these tensors were discussed in §6 in (I), the key results are reproduced in (63) and (64) below. Recall also that (I 76) provides the connections

$$\boldsymbol{a}_s = \sum_{r=1}^{N} \boldsymbol{D}_{sr} \boldsymbol{m}_r, \quad \boldsymbol{b}_s = \sum_{r=1}^{N} \boldsymbol{F}_{sr} \boldsymbol{l}_r, \tag{22}$$

hence the thermal terms in (20) and (21) may be eliminated from the sums.

Many inelastic constitutive laws relate either the local relaxation stress $\boldsymbol{\sigma}_r^{\text{re}}$ to the past history of the local strain $\boldsymbol{\varepsilon}_r$, or the strain $\boldsymbol{\varepsilon}_r^{\text{in}}$ to the history of the local stress $\boldsymbol{\sigma}_r$. When these stresses and strains are uniform in V_r, this can be formally written as

$$\boldsymbol{\sigma}_r^{\text{re}} = \boldsymbol{g}(\boldsymbol{\varepsilon}_r), \quad \boldsymbol{\varepsilon}_r^{\text{in}} = \boldsymbol{f}(\boldsymbol{\sigma}_r). \tag{23}$$

In some cases (e.g. in plasticity of metals) such relations exist between the respective increments. In any event, to accommodate (23), the equations (20) and (21) are modified by the identities $\boldsymbol{\varepsilon}_r^{\text{in}} = -\boldsymbol{M}_r \boldsymbol{\sigma}_r^{\text{re}}$ and $\boldsymbol{\sigma}_r^{\text{re}} = -\boldsymbol{L}_r \boldsymbol{\varepsilon}_r^{\text{in}}$, derived from (3), and by the relations (22). This provides the following two systems of governing equations for evaluation of the local strains and stresses

$$\boldsymbol{\varepsilon}_s + \boldsymbol{D}_{ss} \boldsymbol{M}_s \boldsymbol{g}(\boldsymbol{\varepsilon}_s) + \sum_{\substack{r=1 \\ r \neq s}}^{N} \boldsymbol{D}_{sr} \boldsymbol{M}_r \boldsymbol{g}(\boldsymbol{\varepsilon}_r) = \boldsymbol{A}_s \boldsymbol{\varepsilon} + \boldsymbol{a}_s \theta, \quad r, s = 1, 2, \ldots, N, \tag{24}$$

$$\boldsymbol{\sigma}_s + \boldsymbol{F}_{ss} \boldsymbol{L}_s \boldsymbol{f}(\boldsymbol{\sigma}_s) + \sum_{\substack{r=1 \\ r \neq s}}^{N} \boldsymbol{F}_{sr} \boldsymbol{L}_r \boldsymbol{f}(\boldsymbol{\sigma}_r) = \boldsymbol{B}_s \boldsymbol{\sigma} + \boldsymbol{b}_s \theta, \quad r, s = 1, 2, \ldots, N. \tag{25}$$

At any point of the prescribed overall thermomechanical loading path, these equations must be satisfied by the piecewise uniform approximations of the total local fields in the representative volume of an inelastic heterogeneous medium. As long as all the concentration factor tensors are constant, similar equations also hold for local and overall strain and stress increments, and for their time rates of change. If at least one of the above systems can be solved along the prescribed thermomechanical loading path, it yields piecewise uniform approximations to the total local fields in (2).

In this manner, the inelastic deformation problem for a multiphase composite material is reduced to evaluation of the mechanical, thermal and transformation

factor tensors, which depend only on the local and overall thermoelastic moduli, and to integration of one of the systems of the governing equations (24) or (25) along the prescribed loading path.

The concentration factors may be evaluated from a micromechanical model for elastic heterogeneous solids, as discussed in §§6 and 7 of (I). To be admissible, these factors must satisfy the general connections (I 47) to (I 50). This guarantees that the respective local and overall inelastic fields conform with the relations (12) to (14), and that the total local and overall stresses and strains satisfy (15) and (16). Therefore, one can substitute from (15_2) or (16_2) into (25) or (24), respectively, to reduce the number of unknowns in either system from N to $N-1$. Under certain circumstances, one can also use (15_1) or (16_1) to accomplish additional reductions; this is illustrated in §7 below.

In unit-cell models, the concentration factor tensors are usually found from elastic finite element solutions, and integration of (24) or (25) then reproduces the results that would be obtained from a finite element solution of the particular inelastic unit-cell domain during the prescribed loading history. Under certain circumstances, the present approach is more efficient than the finite element method, and in any case, it offers a particularly simple way for introduction of the constitutive relations of the phases.

The method of solution of (24) or (25) depends on the specific form of the inelastic constitutive equations (23), and is best illustrated by the examples that follow.

4. Elastic–plastic composite systems

As one of the possible applications of (24) and (25), we consider a composite aggregate with elastic–plastic phases (Dvorak 1991). No attempt will be made to spell out the details of the various constitutive theories. Instead, we adopt the general incremental form for material points which, subject to certain loading and unloading criteria, undergo plastic straining from some current state

$$\mathrm{d}\boldsymbol{\sigma}_r(\boldsymbol{x}) = \mathscr{L}_r[\boldsymbol{\varepsilon}_r(\boldsymbol{x})-\boldsymbol{\beta}_r(\boldsymbol{x}), H_r(\boldsymbol{x})]\,\mathrm{d}\boldsymbol{\varepsilon}_r(\boldsymbol{x})+\boldsymbol{\ell}_r[H_r(\boldsymbol{x})]\,\mathrm{d}\theta \tag{26}$$

$$\mathrm{d}\boldsymbol{\varepsilon}_r(\boldsymbol{x}) = \mathscr{M}_r[\boldsymbol{\sigma}_r(\boldsymbol{x})-\boldsymbol{\alpha}_r(\boldsymbol{x}), H_r(\boldsymbol{x})]\,\mathrm{d}\boldsymbol{\sigma}_r(\boldsymbol{x})+\boldsymbol{m}_r[H_r(\boldsymbol{x})]\,\mathrm{d}\theta. \tag{27}$$

The $\mathscr{L}_r$ and $\mathscr{M}_r$ are the instantaneous mechanical stiffness and compliance, and $\boldsymbol{\ell}_r$, $\boldsymbol{m}_r$ are the instantaneous thermal stress and strain vectors which usually reflect the variation of yield stress with temperature. The above $\mathscr{L}_r$, $\mathscr{M}_r$ depend on the magnitude of the invariants of the local strain $\boldsymbol{\varepsilon}_r(\boldsymbol{x})-\boldsymbol{\beta}_r(\boldsymbol{x})$, or stress $\boldsymbol{\sigma}_r(\boldsymbol{x})-\boldsymbol{\alpha}_r(\boldsymbol{x})$, where $\boldsymbol{\beta}_r(\boldsymbol{x})$ and $\boldsymbol{\alpha}_r(\boldsymbol{x})$ denote certain back-strain or stress terms, associated with the centres of the current relaxation and yield surface of the material at point $\boldsymbol{x}$ in V_r; $H_r(\boldsymbol{x})$ is a functional of past deformation history.

Volume averages of (26) and (27) can be evaluated only if the actual fields are known. In piecewise uniform approximations of those fields, one may replace (26) and (27) with

$$\mathrm{d}\boldsymbol{\sigma}_r \doteq \mathscr{L}_r(\boldsymbol{\varepsilon}_r-\boldsymbol{\beta}_r, H_r)\,\mathrm{d}\boldsymbol{\varepsilon}_r+\boldsymbol{\ell}_r(H_r)\,\mathrm{d}\theta, \quad \mathrm{d}\boldsymbol{\varepsilon}_r \doteq \mathscr{M}_r(\boldsymbol{\sigma}_r-\boldsymbol{\alpha}_r, H_r)\,\mathrm{d}\boldsymbol{\sigma}_r+\boldsymbol{m}_r(H_r)\,\mathrm{d}\theta. \tag{28}$$

in each local volume V_r. Of course, if the subdivision of the representative volume V into local volumes V_r is such that the actual fields in V_r deviate substantially from their respective averages, this replacement may lead to large errors.

From (26) and (2), the local relaxation stress and plastic strain are,

$$\mathrm{d}\boldsymbol{\sigma}_r^{\mathrm{re}} = (\mathscr{L}_r-\boldsymbol{L}_r)\,\mathrm{d}\boldsymbol{\varepsilon}_r+(\boldsymbol{\ell}_r-\boldsymbol{l}_r)\,\mathrm{d}\theta, \quad \mathrm{d}\boldsymbol{\varepsilon}_r^{\mathrm{in}} = (\mathscr{M}_r-\boldsymbol{M}_r)\,\mathrm{d}\boldsymbol{\sigma}_r+(\boldsymbol{m}_r-\boldsymbol{m}_r)\,\mathrm{d}\theta. \tag{29}$$

or, in a condensed version, with instantaneous plastic stiffness and compliance tensors

$$\mathrm{d}\boldsymbol{\sigma}_r^{\mathrm{re}} = \boldsymbol{\mathscr{L}}_r^{\mathrm{p}}\,\mathrm{d}\boldsymbol{\varepsilon}_r + \boldsymbol{\ell}_r^{\mathrm{p}}\,\mathrm{d}\theta, \quad \mathrm{d}\boldsymbol{\varepsilon}_r^{\mathrm{in}} = \boldsymbol{\mathscr{M}}_r^{\mathrm{p}}\,\mathrm{d}\boldsymbol{\sigma}_r + \boldsymbol{m}_r^{\mathrm{p}}\,\mathrm{d}\theta. \tag{30}$$

When this is substituted into the incremental form of (24) and (25), the governing equations for evaluation of the local strain and stress increments become

$$\mathrm{d}\boldsymbol{\varepsilon}_s + \sum_{r=1}^{N} \boldsymbol{D}_{sr}\boldsymbol{M}_r\boldsymbol{\mathscr{L}}_r^{\mathrm{p}}\,\mathrm{d}\boldsymbol{\varepsilon}_r = \boldsymbol{A}_s\,\mathrm{d}\boldsymbol{\varepsilon} + \left(\boldsymbol{a}_s - \sum_{r=1}^{N} \boldsymbol{D}_{sr}\boldsymbol{M}_r\boldsymbol{\ell}_r^{\mathrm{p}}\right)\mathrm{d}\theta. \tag{31}$$

$$\mathrm{d}\boldsymbol{\sigma}_s + \sum_{r=1}^{N} \boldsymbol{F}_{sr}\boldsymbol{L}_r\boldsymbol{\mathscr{M}}_r^{\mathrm{p}}\,\mathrm{d}\boldsymbol{\sigma}_r = \boldsymbol{B}_s\,\mathrm{d}\boldsymbol{\sigma} + \left(\boldsymbol{b}_s - \sum_{r=1}^{N} \boldsymbol{F}_{sr}\boldsymbol{L}_r\boldsymbol{m}_r^{\mathrm{p}}\right)\mathrm{d}\theta. \tag{32}$$

In multiphase systems, these equations are best solved numerically, but closed-form solutions can be easily obtained, for example, for systems consisting of two or three phases. In any case, it is desirable to write the result in the form that is analogous to (4),

$$\mathrm{d}\boldsymbol{\varepsilon}_r = \boldsymbol{\mathscr{A}}_r\,\mathrm{d}\boldsymbol{\varepsilon} + \boldsymbol{a}_r\,\mathrm{d}\theta, \quad \mathrm{d}\boldsymbol{\sigma}_r = \boldsymbol{\mathscr{B}}_r\,\mathrm{d}\boldsymbol{\sigma} + \boldsymbol{\ell}_r\,\mathrm{d}\theta, \tag{33}$$

where $\boldsymbol{\mathscr{A}}_r$, $\boldsymbol{a}_r$ and $\boldsymbol{\mathscr{B}}_r$, $\boldsymbol{\ell}_r$ are the instantaneous mechanical and thermal strain and stress concentration factor tensors for the local volumes V_r.

Once the instantaneous concentration factor tensors are known, the instantaneous overall stiffness and compliance of the inelastic composite medium can be defined as tensors relating the overall stress and strain at any instant of loading. The derivation and the resulting expressions are entirely analogous to the elastic case cf. (15) to (18),

$$\mathrm{d}\boldsymbol{\sigma} = \boldsymbol{\mathscr{L}}\,\mathrm{d}\boldsymbol{\varepsilon} + \boldsymbol{\ell}\,\mathrm{d}\theta, \quad \mathrm{d}\boldsymbol{\varepsilon} = \boldsymbol{\mathscr{M}}\,\mathrm{d}\boldsymbol{\sigma} + \boldsymbol{m}\,\mathrm{d}\theta, \tag{34}$$

$$\boldsymbol{\mathscr{L}} = \sum_{r=1}^{N} c_r\boldsymbol{\mathscr{L}}_r\boldsymbol{\mathscr{A}}_r, \quad \boldsymbol{\ell} = \sum_{r=1}^{N} c_r(\boldsymbol{\mathscr{L}}_r\boldsymbol{a}_r + \boldsymbol{\ell}_r), \tag{35}$$

$$\boldsymbol{\mathscr{M}} = \sum_{r=1}^{N} c_r\boldsymbol{\mathscr{M}}_r\boldsymbol{\mathscr{B}}_r, \quad \boldsymbol{m} = \sum_{r=1}^{N} c_r(\boldsymbol{\mathscr{M}}_r\boldsymbol{\ell}_r + \boldsymbol{m}_r). \tag{36}$$

As one illustration, we present the closed-form solution for a *two-phase system*, where the phases are denoted as $r = \alpha, \beta$, and $s = \alpha, \beta$. Then, (31) or (32) each provide two equations, which may be supplemented by (15_2) and (16_2), solved in the form (33), and thus give the concentration factor tensors

$$\left.\begin{aligned} \boldsymbol{\mathscr{A}}_\alpha &= [\boldsymbol{I} + \boldsymbol{D}_{\alpha\alpha}\boldsymbol{M}_\alpha\boldsymbol{\mathscr{L}}_\alpha^{\mathrm{p}} - (c_\alpha/c_\beta)\,\boldsymbol{D}_{\alpha\beta}\boldsymbol{M}_\beta\boldsymbol{\mathscr{L}}_\beta^{\mathrm{p}}]^{-1}[\boldsymbol{A}_\alpha - (1/c_\beta)\,\boldsymbol{D}_{\alpha\beta}\boldsymbol{M}_\beta\boldsymbol{\mathscr{L}}_\beta^{\mathrm{p}}], \\ \boldsymbol{a}_\alpha &= [\boldsymbol{I} + \boldsymbol{D}_{\alpha\alpha}\boldsymbol{M}_\alpha\boldsymbol{\mathscr{L}}_\alpha^{\mathrm{p}} - (c_\alpha/c_\beta)\,\boldsymbol{D}_{\alpha\beta}\boldsymbol{M}_\beta\boldsymbol{\mathscr{L}}_\beta^{\mathrm{p}}]^{-1}[\boldsymbol{a}_\alpha - \boldsymbol{D}_{\alpha\alpha}\boldsymbol{M}_\alpha\boldsymbol{\ell}_\alpha^{\mathrm{p}} - \boldsymbol{D}_{\alpha\beta}\boldsymbol{M}_\beta\boldsymbol{\ell}_\beta^{\mathrm{p}}]. \end{aligned}\right\} \tag{37}$$

$$\left.\begin{aligned} \boldsymbol{\mathscr{B}}_\alpha &= [\boldsymbol{I} + \boldsymbol{F}_{\alpha\alpha}\boldsymbol{L}_\alpha\boldsymbol{\mathscr{M}}_\alpha^{\mathrm{p}} - (c_\alpha/c_\beta)\,\boldsymbol{F}_{\alpha\beta}\boldsymbol{L}_\beta\boldsymbol{\mathscr{M}}_\beta^{\mathrm{p}}]^{-1}[\boldsymbol{B}_\alpha - (1/c_\beta)\,\boldsymbol{F}_{\alpha\beta}\boldsymbol{L}_\beta\boldsymbol{\mathscr{M}}_\beta^{\mathrm{p}}], \\ \boldsymbol{\ell}_\alpha &= [\boldsymbol{I} + \boldsymbol{F}_{\alpha\alpha}\boldsymbol{L}_\alpha\boldsymbol{\mathscr{M}}_\alpha^{\mathrm{p}} - (c_\alpha/c_\beta)\,\boldsymbol{F}_{\alpha\beta}\boldsymbol{L}_\beta\boldsymbol{\mathscr{M}}_\beta^{\mathrm{p}}]^{-1}[\boldsymbol{b}_\alpha - \boldsymbol{F}_{\alpha\alpha}\boldsymbol{L}_\alpha\boldsymbol{m}_\alpha^{\mathrm{p}} - \boldsymbol{F}_{\alpha\beta}\boldsymbol{L}_\beta\boldsymbol{m}_\beta^{\mathrm{p}}]. \end{aligned}\right\} \tag{38}$$

The concentration factors for phase β are obtained by exchange of the α and β subscripts.

One may recall here that the transformation concentration factor tensors of two-phase materials are related by exact connections to the elastic mechanical concentration factors (Dvorak 1990, equations (123)–(126))

$$\left.\begin{aligned} \boldsymbol{D}_{r\alpha} &= (\boldsymbol{I} - \boldsymbol{A}_r)(\boldsymbol{L}_\alpha - \boldsymbol{L}_\beta)^{-1}\boldsymbol{L}_\alpha, \quad \boldsymbol{D}_{r\beta} = -(\boldsymbol{I} - \boldsymbol{A}_r)(\boldsymbol{L}_\alpha - \boldsymbol{L}_\beta)^{-1}\boldsymbol{L}_\beta, \\ \boldsymbol{F}_{r\alpha} &= (\boldsymbol{I} - \boldsymbol{B}_r)(\boldsymbol{M}_\alpha - \boldsymbol{M}_\beta)^{-1}\boldsymbol{M}_\alpha, \quad \boldsymbol{F}_{r\beta} = -(\boldsymbol{I} - \boldsymbol{B}_r)(\boldsymbol{M}_\alpha - \boldsymbol{M}_\beta)^{-1}\boldsymbol{M}_\beta. \end{aligned}\right\} \tag{39}$$

These may be substituted into (37) and (38) to derive expressions for the instantaneous concentration factor tensors which depend only on the elastic

mechanical concentration factor tensors, phase volume fractions, and on the instantaneous phase properties. If desired, the dependence of the instantaneous concentration factor tensors on local geometry can be eliminated altogether by appealing to (A 17) in the Appendix, which relates the elastic concentration factor tensors to the overall elastic moduli $\boldsymbol{L}$ or compliances $\boldsymbol{M}$.

Another illustration pertains to a *three-phase* system, $r = 1, 2, 3$, where one may write (31) or (32), together with (15_2) or (16_2), to express one of the unknown strains, say $\mathrm{d}\boldsymbol{\varepsilon}_3$, as

$$\mathrm{d}\boldsymbol{\varepsilon}_3 = (\mathrm{d}\boldsymbol{\varepsilon} - c_1\,\mathrm{d}\boldsymbol{\varepsilon}_1 - c_2\,\mathrm{d}\boldsymbol{\varepsilon}_2)/c_3. \tag{40}$$

This reduces the system (31) to two equations that can be readily solved. With reference to (33_1), one finds the following instantaneous strain concentration factors,

$$\left.\begin{aligned} \boldsymbol{\mathscr{A}}_1 &= [\boldsymbol{Z}_2^{-1}\boldsymbol{Z}_1 - \boldsymbol{Y}_2^{-1}\boldsymbol{Y}_1]^{-1}[\boldsymbol{Z}_2^{-1}\boldsymbol{Z}_3 - \boldsymbol{Y}_2^{-1}\boldsymbol{Y}_3]^{-1}, \\ \boldsymbol{a}_1 &= [\boldsymbol{Z}_2^{-1}\boldsymbol{Z}_1 - \boldsymbol{Y}_2^{-1}\boldsymbol{Y}_1]^{-1}[\boldsymbol{Z}_2^{-1}\boldsymbol{z}_4 - \boldsymbol{Y}_2^{-1}\boldsymbol{y}_4), \end{aligned}\right\} \tag{41}$$

$$\left.\begin{aligned} \boldsymbol{\mathscr{A}}_2 &= [\boldsymbol{Z}_1^{-1}\boldsymbol{Z}_2 - \boldsymbol{Y}_1^{-1}\boldsymbol{Y}_2]^{-1}[\boldsymbol{Z}_1^{-1}\boldsymbol{Z}_3 - \boldsymbol{Y}_1^{-1}\boldsymbol{Y}_3], \\ \boldsymbol{a}_2 &= [\boldsymbol{Z}_2^{-1}\boldsymbol{Z}_1 - \boldsymbol{Y}_2^{-1}\boldsymbol{Y}_1]^{-1}[\boldsymbol{Z}_1^{-1}\boldsymbol{z}_4 - \boldsymbol{Y}_1^{-1}\boldsymbol{y}_4], \end{aligned}\right\} \tag{42}$$

$$\boldsymbol{\mathscr{A}}_3 = (1/c_3)[\boldsymbol{I} - c_1\boldsymbol{\mathscr{A}}_1 - c_2\boldsymbol{\mathscr{A}}_2], \quad \boldsymbol{a}_3 = (1/c_3)[\boldsymbol{I} - c_1\boldsymbol{a}_1 - c_2\boldsymbol{a}_2], \tag{43}$$

where the auxiliary tensors were defined as

$$\left.\begin{aligned} \boldsymbol{Z}_1 &= \boldsymbol{I} + \boldsymbol{D}_{11}\boldsymbol{M}_1\boldsymbol{\mathscr{L}}_1^{\mathrm{p}} - (c_1/c_3)\,\boldsymbol{D}_{13}\boldsymbol{M}_3\boldsymbol{\mathscr{L}}_3^{\mathrm{p}}, \\ \boldsymbol{Z}_2 &= \boldsymbol{D}_{12}\boldsymbol{M}_2\boldsymbol{\mathscr{L}}_2^{\mathrm{p}} - (c_2/c_3)\,\boldsymbol{D}_{13}\boldsymbol{M}_3\boldsymbol{\mathscr{L}}_3^{\mathrm{p}}, \\ \boldsymbol{Z}_3 &= \boldsymbol{A}_1 - (1/c_3)\,\boldsymbol{D}_{13}\boldsymbol{M}_3\boldsymbol{\mathscr{L}}_3^{\mathrm{p}}, \\ \boldsymbol{z}_4 &= \boldsymbol{a}_1 - \boldsymbol{D}_{11}\boldsymbol{M}_1\boldsymbol{\ell}_1^{\mathrm{p}} - \boldsymbol{D}_{12}\boldsymbol{M}_2\boldsymbol{\ell}_2^{\mathrm{p}} - \boldsymbol{D}_{13}\boldsymbol{M}_3\boldsymbol{\ell}_3^{\mathrm{p}}, \\ \boldsymbol{Y}_1 &= \boldsymbol{D}_{21}\boldsymbol{M}_1\boldsymbol{\mathscr{L}}_1^{\mathrm{p}} - (c_1/c_3)\,\boldsymbol{D}_{23}\boldsymbol{M}_3\boldsymbol{\mathscr{L}}_3^{\mathrm{p}}, \\ \boldsymbol{Y}_2 &= \boldsymbol{I} + \boldsymbol{D}_{22}\boldsymbol{M}_2\boldsymbol{\mathscr{L}}_2^{\mathrm{p}} - (c_2/c_3)\,\boldsymbol{D}_{23}\boldsymbol{M}_3\boldsymbol{\mathscr{L}}_3^{\mathrm{p}}, \\ \boldsymbol{Y}_3 &= \boldsymbol{A}_2 - (1/c_3)\,\boldsymbol{D}_{23}\boldsymbol{M}_3\boldsymbol{\mathscr{L}}_3^{\mathrm{p}}, \\ \boldsymbol{y}_4 &= \boldsymbol{a}_2 - \boldsymbol{D}_{21}\boldsymbol{M}_1\boldsymbol{\ell}_1^{\mathrm{p}} - \boldsymbol{D}_{22}\boldsymbol{M}_2\boldsymbol{\ell}_2^{\mathrm{p}} - \boldsymbol{D}_{23}\boldsymbol{M}_3\boldsymbol{\ell}_3^{\mathrm{p}}. \end{aligned}\right\} \tag{44}$$

5. Linearly viscoelastic composite systems

The typical approach to problems of this kind uses the correspondence principle of linear viscoelasticity, to relate the effective viscoelastic properties to the effective elastic properties. In general, an exact analytical solution of an elasticity problem for a given geometry of a heterogeneous medium can be converted into a transform parameter multiplied Laplace or Fourier transform of an analogous viscoelasticity problem. The latter problem is thus reduced to an inversion of the respective transformed solution (Christensen 1971).

The present approach offers an alternative which may be useful when the analytic elasticity solution or the inversion prove difficult to find. As before, we consider a representative volume of the composite aggregate, but allow viscoelastic deformation to take place in one or more phases. The total strain in each local volume is assumed to conform with the additive decomposition (1), where the elastic fields correspond to an instantaneous elastic response and thus depend only on the current local strain or stress according to (2), while the inelastic fields are certain functions of time and of the local strain or stress history. The overall stress or strain and temperature change applied to the representative volume are assumed to be uniform. The

derivation is limited to thermorheologically simple materials, where the effect of a uniform temperature change on the relaxation function is reflected by replacing the time variable in this function by a new variable that depends both on time and on a temperature-dependent shift function. Therefore, it is sufficient to consider isothermal viscoelastic behaviour in the derivations that follow, and allow for the influence of temperature changes on these relations only in actual evaluations.

In linear viscoelastic solids, the total strain caused by a history of applied stress that starts from zero stress at $t = 0$, is usually described by (Christensen 1971)

$$\boldsymbol{\varepsilon}_r(t) = \int_0^t \boldsymbol{J}_r(t-\tau)\frac{\mathrm{d}\boldsymbol{\sigma}_r(\tau)}{\mathrm{d}\tau}\mathrm{d}\tau, \tag{45}$$

where the function $\boldsymbol{J}_r(t-\tau)$ is the creep compliance, assumed to possess the symmetries $J^r_{ijkl} = J^r_{jikl} = J^r_{klij}$. If the strains due to the instantaneous elastic response can be separated from the total strain (45), as in (2_2), the corresponding elastic moduli serve in evaluation of the various concentration factor tensors in (24) and (25), while the inelastic part of (45) is substituted into (23) and then into (24).

In a similar manner, if the local volume V_r is subjected to a certain time history of prescribed deformation starting from $\boldsymbol{\varepsilon}_r = \mathbf{0}$ at $t = 0$, one can write the resulting total stress as

$$\boldsymbol{\sigma}_r(t) = \int_0^t \boldsymbol{G}_r(t-\tau)\frac{\mathrm{d}\boldsymbol{\varepsilon}_r(\tau)}{\mathrm{d}\tau}\mathrm{d}\tau, \tag{46}$$

where $\boldsymbol{G}_r(t-\tau)$ is the local relaxation function which has the same symmetries as the creep compliance, and then call upon (2_1) to separate the instantaneous elastic response. Again, the resulting elastic moduli are used to evaluate the concentration factor tensors that appear in (25), and the relaxation stress component of (46) is substituted into (23) and (25). In either case, one obtains a system of integral equations for evaluation of the total local strains or stresses.

The preferred form of the solution of (24) or (25) for the local stresses and strains at a given time t of the overall loading history is

$$\boldsymbol{\varepsilon}_r(t) = \mathfrak{A}_r(t)\,\boldsymbol{\varepsilon}(t) + \mathfrak{a}_r(t)\,\theta(t), \quad \boldsymbol{\sigma}_r(t) = \mathfrak{B}_r(t)\,\boldsymbol{\sigma}(t) + \mathfrak{b}_r(t)\,\theta(t), \tag{47}$$

where $\mathfrak{A}_r(t)$, $\mathfrak{a}_r(t)$, and $\mathfrak{B}_r(t)$, $\mathfrak{b}_r(t)$ are certain mechanical and thermal influence functions corresponding to the prescribed history of a uniform overall strain or stress. As in (15) and (16), these results may be used to evaluate the total overall stress or strain at time t.

In addition to the total local and overall strains and stresses, it may be necessary to find the corresponding rates at time t. As long as the instantaneous elastic moduli used in evaluation of the concentration factor tensors that enter (24) and (25) remain constant, one can rewrite these equations for the local and overall rates. The corresponding constitutive relations for the rates are the time derivatives of (45) and (46). For example, if one considers a local deformation history starting from $\boldsymbol{\sigma}_r = \mathbf{0}$ at $t = 0$, (45) can be differentiated with respect to time, and the result integrated by parts to yield

$$\dot{\boldsymbol{\varepsilon}}_r(t) = \boldsymbol{M}_r\,\dot{\boldsymbol{\sigma}}_r(t) + \dot{\boldsymbol{J}}_r(0)\,\boldsymbol{\sigma}_r(t) + \int_0^t \ddot{\boldsymbol{J}}_r(t-\tau)\,\boldsymbol{\sigma}_r(\tau)\,\mathrm{d}\tau. \tag{48}$$

The elastic part of the total strain rate, $\dot{\boldsymbol{\varepsilon}}^e_r(t) = \boldsymbol{M}_r\,\dot{\boldsymbol{\sigma}}_r(t)$, replaces here the original term $\boldsymbol{J}_r(0)\,\dot{\boldsymbol{\sigma}}_r(t)$, that reflects the instantaneous elastic response.

Similarly, for a local deformation history that starts from $\boldsymbol{\varepsilon} = \mathbf{0}$ at $t = 0$, (46) can be differentiated and then integrated by parts to establish that the total local stress rate is

$$\dot{\boldsymbol{\sigma}}_r(t) = \boldsymbol{L}_r \dot{\boldsymbol{\varepsilon}}_r(t) + \dot{\boldsymbol{G}}_r(0)\,\boldsymbol{\varepsilon}_r(t) + \int_0^t \ddot{\boldsymbol{G}}_r(t-\tau)\,\boldsymbol{\varepsilon}_r(\tau)\,\mathrm{d}\tau. \tag{49}$$

where the elastic part of the total stress rate, $\dot{\boldsymbol{\sigma}}_r^{\mathrm{e}}(t) = \boldsymbol{L}_r \dot{\boldsymbol{\varepsilon}}_r(t) = \boldsymbol{G}_r(0)\,\dot{\boldsymbol{\varepsilon}}_r(t)$.

If the solution of the equations (24) or (25) for the respective rates is found in the form

$$\dot{\boldsymbol{\varepsilon}}_r(t) = \mathscr{A}_r(t)\,\dot{\boldsymbol{\varepsilon}}(t) + a_r(t)\,\dot{\theta}(t), \quad \dot{\boldsymbol{\sigma}}_r(t) = \mathscr{B}_r(t)\,\dot{\boldsymbol{\sigma}}(t) + \ell_r(t)\,\dot{\theta}(t). \tag{50}$$

one can then define the instantaneous overall stiffness and compliance, and the thermal strain and stress tensors of the composite medium as

$$\dot{\boldsymbol{\sigma}}_r(t) = \mathscr{L}(t)\,\dot{\boldsymbol{\varepsilon}}(t) + \ell(t)\,\dot{\theta}(t), \quad \dot{\boldsymbol{\varepsilon}}(t) = \mathscr{M}(t)\,\dot{\boldsymbol{\sigma}}(t) + m(t)\,\dot{\theta}(t). \tag{51}$$

and evaluate them as suggested by (35) and (36). The $\mathscr{A}_r(t)$ and $\mathscr{B}_r(t)$ in (50) are the instantaneous mechanical concentration factor tensors, and the $a_r(t)$ and $\ell_r(t)$ are the instantaneous thermal concentration factor tensors. The latter may reflect both the elastic response and any contribution that a temperature change may make to the inelastic terms in (45) to (49), under the stated assumption of thermorheologically simple phase materials.

Once again, the problem can be simplified if the composite aggregate under consideration consists of only two phases and local volumes $r = \alpha, \beta$. Then, one can employ (15_2) and (16_2) to write the connections $c_\alpha \boldsymbol{\sigma}_\alpha(t) + c_\beta \boldsymbol{\sigma}_\beta(t) = \boldsymbol{\sigma}(t)$, $c_\alpha \boldsymbol{\varepsilon}_\alpha(t) + c_\beta \boldsymbol{\varepsilon}_\beta(t) = \boldsymbol{\varepsilon}(t)$, and recover separate equations for each of the unknowns.

For example, consider a two-phase composite system subjected to a prescribed history of overall strain $\boldsymbol{\varepsilon}(t)$ and uniform temperature change $\theta(t)$. Let the phase constitutive relations be known in the form (45), or (46). To evaluate the estimates of local strain rates at time t, in terms of a piecewise uniform distribution in the two phases, appeal to the rate form of (24) and write the governing equations for this case as

$$\left.\begin{aligned} \dot{\boldsymbol{\varepsilon}}_\alpha(t) + \boldsymbol{D}_{\alpha\alpha}\boldsymbol{M}_\alpha \dot{\boldsymbol{\sigma}}_\alpha^{\mathrm{re}}(t) + \boldsymbol{D}_{\alpha\beta}\boldsymbol{M}_\beta \dot{\boldsymbol{\sigma}}_\beta^{\mathrm{re}}(t) &= \boldsymbol{A}_\alpha \dot{\boldsymbol{\varepsilon}}(t) + \boldsymbol{a}_\alpha \dot{\theta}(t), \\ \dot{\boldsymbol{\varepsilon}}_\beta(t) + \boldsymbol{D}_{\beta\alpha}\boldsymbol{M}_\alpha \dot{\boldsymbol{\sigma}}_\alpha^{\mathrm{re}}(t) + \boldsymbol{D}_{\beta\beta}\boldsymbol{M}_\beta \dot{\boldsymbol{\sigma}}_\beta^{\mathrm{re}}(t) &= \boldsymbol{A}_\beta \dot{\boldsymbol{\varepsilon}}(t) + \boldsymbol{a}_\beta \dot{\theta}(t). \end{aligned}\right\} \tag{52}$$

Next, let the relaxation stresses be expressed by the last two terms in (49). To separate the variables, substitute in turn for one of the local strain rates from the above connections, to recover two uncoupled equations for the two rates. Only one of them needs to be considered; for example the equation for evaluation of the rate $\dot{\boldsymbol{\varepsilon}}_\beta(t)$ is

$$\begin{aligned} [(c_\beta/c_\alpha)\,\boldsymbol{D}_{\alpha\alpha}^{-1} + \boldsymbol{D}_{\beta\alpha}^{-1}]\,\dot{\boldsymbol{\varepsilon}}_\beta(t) = (\boldsymbol{D}_{\alpha\alpha}^{-1}\boldsymbol{D}_{\alpha\beta} - \boldsymbol{D}_{\beta\alpha}^{-1}\boldsymbol{D}_{\beta\beta})\,\boldsymbol{M}_\beta \left[\dot{\boldsymbol{G}}_\beta(0)\,\boldsymbol{\varepsilon}_\beta(t) + \int_0^t \ddot{\boldsymbol{G}}_\beta(t-\tau)\,\boldsymbol{\varepsilon}_\beta(\tau)\,\mathrm{d}\tau\right] \\ - [\boldsymbol{D}_{\alpha\alpha}^{-1}(\boldsymbol{A}_\alpha - c_\alpha^{-1}\boldsymbol{I}) - \boldsymbol{D}_{\beta\alpha}^{-1}\boldsymbol{A}_\beta]\,\dot{\boldsymbol{\varepsilon}}(t) - (\boldsymbol{D}_{\alpha\alpha}^{-1}\boldsymbol{a}_\alpha - \boldsymbol{D}_{\beta\alpha}^{-1}\boldsymbol{a}_\beta)\,\dot{\theta}(t), \end{aligned} \tag{53}$$

where the concentration factors $\boldsymbol{A}_\alpha$, $\boldsymbol{a}_\alpha$, $\boldsymbol{D}_{\alpha\beta}$, etc., are evaluated from the instantaneous elastic moduli. Once this has been solved, one can find the other rate as $\dot{\boldsymbol{\varepsilon}}_\alpha(t) = (\dot{\boldsymbol{\varepsilon}}(t) - c_\beta \dot{\boldsymbol{\varepsilon}}_\beta(t))/c_\alpha$, and add the resulting increments in total strains to the current values.

A similar procedure can be followed in evaluation of the total local strains. In

particular, for the above two-phase system subjected to the prescribed history of overall strain $\boldsymbol{\varepsilon}(t)$ and uniform temperature change $\theta(t)$. (24) provides two equations for the local strain fields which can be solved for one of the unknowns, say $\boldsymbol{\varepsilon}_\beta(t)$, to yield

$$\begin{aligned}[(c_\beta/c_\alpha)\,\boldsymbol{D}_{\alpha\alpha}^{-1}+\boldsymbol{D}_{\beta\alpha}^{-1}+(\boldsymbol{D}_{\alpha\alpha}^{-1}\boldsymbol{D}_{\alpha\beta}-\boldsymbol{D}_{\beta\alpha}^{-1}\boldsymbol{D}_{\beta\beta})\,\boldsymbol{M}_\beta\boldsymbol{G}_\beta(0)]\,\boldsymbol{\varepsilon}(t)\\ =(\boldsymbol{D}_{\alpha\alpha}^{-1}\boldsymbol{D}_{\alpha\beta}-\boldsymbol{D}_{\beta\alpha}^{-1}\boldsymbol{D}_{\beta\beta})\,\boldsymbol{M}_\beta\int_0^t\boldsymbol{G}_\beta(t-\tau)\,\dot{\boldsymbol{\varepsilon}}_\beta(\tau)\,\mathrm{d}\tau\\ -[\boldsymbol{D}_{\alpha\alpha}^{-1}(\boldsymbol{A}_\alpha-c_\alpha^{-1}\boldsymbol{I})-\boldsymbol{D}_{\beta\alpha}^{-1}\boldsymbol{A}_\beta]\,\boldsymbol{\varepsilon}(t)-(\boldsymbol{D}_{\alpha\alpha}^{-1}\boldsymbol{a}_\alpha-\boldsymbol{D}_{\beta\alpha}^{-1}\boldsymbol{a}_\beta)\,\theta(t).\end{aligned}\tag{54}$$

6. Viscoplastic systems

As pointed out in a recent review by Chaboche (1989), most constitutive theories for viscoplastic deformation of metals conform with the additive decomposition (1), and are of the unified type, i.e. no distinction is made between the inviscid and viscous part of the inelastic strain. The general framework of the unified theories often involves an assumed or implied viscoplastic potential Ω. The inelastic strain rate is then expressed, with reference to a particular homogeneous phase r, as

$$\dot{\boldsymbol{\varepsilon}}_r^{\mathrm{in}}=\partial\Omega_r/\partial\boldsymbol{\sigma}_r=\tfrac{3}{2}\langle\sigma_r^{\mathrm{v}}/K_r^*\rangle^n(\boldsymbol{\sigma}_r'-\boldsymbol{X}_r')/J(\boldsymbol{\sigma}_r-\boldsymbol{X}_r),\tag{55}$$

with the overstress or viscous stress σ_r^{v} and the function $J(\boldsymbol{\sigma}_r-\boldsymbol{X}_r)$ defined by

$$\sigma_r^{\mathrm{v}}=J(\boldsymbol{\sigma}_r-\boldsymbol{X}_r)-R_r^*-k_r^*,\quad J(\boldsymbol{\sigma}_r-\boldsymbol{X}_r)=[3(\boldsymbol{\sigma}_r'-\boldsymbol{X}_r')\,(\boldsymbol{\sigma}_r'-\boldsymbol{X}_r')/2]^{\frac{1}{2}},\tag{56}$$

where $\boldsymbol{X}_r$ is the back stress; $\boldsymbol{\sigma}_r'$, $\boldsymbol{X}_r'$ denote the deviators of $\boldsymbol{\sigma}_r$ and $\boldsymbol{X}_r$. The scalar k_r^* denotes the initial yield stress magnitude and R_r^* its evolution, their sum is the equilibrium stress corresponding to a vanishing strain rate at constant stress; K_r^* is the drag stress; each may be a function of temperature. The bracket $\langle x\rangle=xH(x)$, where $H(x)$ is the Heaviside function.

Several particular forms and variants of (55) are in use, with different time and temperature-dependent evolution rules for the variables $\boldsymbol{X}$, K^*, and R^*, or for analogous variables. Some theories (Krempl & Lu 1984) forego the assumption of a viscoplastic potential, and the associated loading/unloading criteria, and regard the entire deformation process as rate dependent, even at vanishingly small rates. This can be convenient in applications which are likely to lead to complex loading histories with frequent load reversals. In any case, actual evaluations of the inelastic strains for a prescribed stress history tend to be quite involved, and are often predicated on the availability of specific magnitudes of many material parameters. Best agreement between predicted and actual behaviour usually obtains under cyclic loading, where the requisite material parameters appear to have more reproducible magnitudes.

If (55) or its equivalent is taken to represent the response of one or more phases of a composite material, the local inelastic strain is obtained by time integration of (55), under the actual local stress history. The latter is not known *a priori*, but may be evaluated at any time t, from the solution of the system (25), rewritten as

$$\boldsymbol{\sigma}_s(t)+\sum_{r=1}^{N}\boldsymbol{F}_{sr}\boldsymbol{L}_r\int_0^t\dot{\boldsymbol{\varepsilon}}_r^{\mathrm{in}}(\tau)\,\mathrm{d}\tau=\boldsymbol{B}_s\boldsymbol{\sigma}(t)+\boldsymbol{b}_s\theta(t),\quad r,s=1,2,\ldots,N,\tag{57}$$

under the initial conditions $\boldsymbol{\sigma}_r=\boldsymbol{0}$, $\theta=0$ at $t=0$, boundary conditions $\boldsymbol{\sigma}=\boldsymbol{\sigma}(t)$, and

a uniform temperature change $\theta = \theta(t)$ in the representative volume. The preferred form of the solution is formally identical with that given by (47_2). For a two-phase system, one can easily write a governing equation similar to (54).

Equation (57) can also be used to analyse systems where the total strain rate of one or more phases is described by nonlinear functions of the current stress, providing that the total strain can be decomposed according to (1). This may be useful in nonlinear viscous systems with phases undergoing power-law creep.

7. Comparison with related methods

The standard procedure for evaluation of the overall instantaneous properties of inelastic heterogeneous media is based on the early work by Hill (1965, 1966, 1967), and its elaboration by Hutchinson (1970) and by many later writers. The basic idea is to estimate the total strains or stresses in the phases, under an applied history of uniform overall strain or stress, by the self-consistent method. For example, in an elastic–plastic, isothermally deformed composite or polycrystal one can rewrite (33) as

$$\mathrm{d}\boldsymbol{\varepsilon}_r = \boldsymbol{\mathcal{A}}_r \mathrm{d}\boldsymbol{\varepsilon}, \quad \mathrm{d}\boldsymbol{\sigma}_r = \boldsymbol{\mathcal{B}}_r \mathrm{d}\boldsymbol{\sigma}. \tag{58}$$

The self-consistent estimates of the instantaneous concentration factor tensors are found from the solution of an inclusion problem, in which an ellipsoidal volume of each phase is embedded in an elastic homogeneous medium with certain instantaneous stiffness $\mathscr{L}$, or compliance $\mathscr{M}$. The $\mathscr{L}$ and $\mathscr{M}$ are identified with the as yet unknown effective properties of the composite aggregate, and the concentration factor tensors are found from the formula (I 54), written as

$$\boldsymbol{\mathcal{A}}_r = (\mathscr{L}^* + \mathscr{L}_r)^{-1}(\mathscr{L}^* + \mathscr{L}), \quad \boldsymbol{\mathcal{B}}_r = (\mathscr{M}^* + \mathscr{M}_r)^{-1}(\mathscr{M}^* + \mathscr{M}). \tag{59}$$

Here, the $\mathscr{L}_r$ and $\mathscr{M}_r$ are the instantaneous phase stiffness and compliance matrices defined by (28), and the $\mathscr{L}^*$ and $\mathscr{M}^*$ are the instantaneous constraint tensors of the transformed homogeneous inclusion in the effective medium.

The unknown instantaneous overall properties are found from the general connections (15_2) and (16_2), in the form analogous to (34), (35_1), and (36_1),

$$\mathscr{L} = \sum_{r=1}^{N} c_r \mathscr{L}_r \boldsymbol{\mathcal{A}}_r, \quad \mathscr{M} = \sum_{r=1}^{N} c_r \mathscr{M}_r \boldsymbol{\mathcal{B}}_r. \tag{60}$$

In this manner, the incremental solution of an isothermal loading problem for an elastic–plastic composite is reduced to a sequence of elasticity problems for a composite with varying local and overall moduli. We recall from (I 53) to (I 57) that approximate solutions of such elasticity problems by the self-consistent method are formally similar to solutions by the Mori–Tanaka method, providing that the constraint tensors in (59) are evaluated from the instantaneous properties of the matrix. Therefore, with this proviso, the above relations can also be used to construct the Mori–Tanaka estimates of instantaneous overall properties of the inelastic composite. Such results were recently found from a different approach by Tandon & Weng (1988), Gavazzi & Lagoudas (1990) and others. Of course, to assure that these expressions can be reduced to a diagonally symmetric form, cf. (I 55), it is necessary to limit the selection of admissible heterogeneous aggregates either to two-phase composites, or to multiphase systems reinforced by inclusions of the same shape and alignment, or to multiphase systems reinforced by similarly shaped but randomly orientated inclusions (Benveniste *et al.* 1991; Chen *et al.* 1992).

It is clear that the above estimates (60) of the instantaneous $\mathscr{L}$ and $\mathscr{M}$ tensors do comply with the general connections (15_2) and (16_2) between the local and overall total strains and stresses. If the elastic compliance is subtracted from the total, one finds the overall instantaneous inelastic compliance as

$$\mathscr{M} - M = \sum_{r=1}^{N} c_r (\mathscr{M}_r \mathscr{B}_r - M_r B_r). \tag{61}$$

However, if one substitutes into (14_2) the $\mathrm{d}\boldsymbol{\varepsilon}_r^{\mathrm{in}}$ from (29_2) for $\mathrm{d}\theta = 0$, and uses (33) to replace the local stress $\mathrm{d}\boldsymbol{\sigma}_r$ by the overall stress $\mathrm{d}\boldsymbol{\sigma}$, then ($16_1$) can be used to find the overall inelastic compliance as

$$\mathscr{M} - M = \sum_{r=1}^{N} c_r B_r^{\mathrm{T}} (\mathscr{M}_r - M_r) \mathscr{B}_r. \tag{62}$$

These are completely general expressions that follow from the representation of local stresses by (4) and (58), and from the two independent connections between the local and overall inelastic strains (14_2) and total strains (16_2), respectively. It is interesting to note that (61) and (62) may also be derived as two different self-consistent estimates of $\mathscr{M}$. Of course, the first equation (61) is such an estimate for a multiphase solid where the overall total strain complies with the condition $\boldsymbol{\varepsilon} = \Sigma c_r \boldsymbol{\varepsilon}_r$. In contrast, (62) is a similar estimate of $\mathscr{M}$ for the same multiphase solid, where the above condition has been replaced by the relation (14_2) between local and overall inelastic strains.

It is thus apparent that the two expressions are distinct, except perhaps in rigid-plastic solids where $M_r \to \mathbf{0}$ and $B_r \to I$. However, they can be simultaneously satisfied if the instantaneous stress concentration factor tensors $\mathscr{B}_r$ is evaluated in the manner described in §4. In contrast, some simple algebra shows that if the $\mathscr{B}_r$ are found from (59), then (61) and (62) provide entirely different estimates of the instantaneous inelastic compliance. Therefore, one must conclude that regardless of their apparent popularity in the micromechanics literature, the self-consistent, Mori–Tanaka or other procedures based on (59) and (61), or their analogues, are not admissible in inelastic analysis of heterogeneous media.

That is not to say that the methods themselves are without merit. For example, they may serve in the evaluation of the transformation concentration factor tensors $\boldsymbol{D}_{sr}$ and $\boldsymbol{F}_{sr}$ that enter the governing equations (24) and (25), and thus be of use in the analysis outlined in §§4–6. Such evaluation was described in §6 of (I), with the result (I 58) and (I 59) which is reproduced here for completeness:

$$\begin{aligned} \boldsymbol{D}_{sr} &= [\delta_{sr} I - c_r (L^* + L_s)^{-1} (L^* + L)] (L^* + L_r)^{-1} L_r \\ &= (I - A_s)(L_s - L)^{-1} (\delta_{sr} I - c_r A_r^T) L_r, \end{aligned} \tag{63}$$

$$\begin{aligned} \boldsymbol{F}_{sr} &= [\delta_{sr} I - c_r (M^* + M_s)^{-1} (M^* + M)] (M^* + M_r)^{-1} M_r \\ &= (I - B_s)(M_s - M)^{-1} (\delta_{sr} I - c_r B_r^T) M_r, \end{aligned} \tag{64}$$

where δ_{sr} is the Kronecker symbol, but no summation is indicated by repeated subscripts.

These expressions satisfy the conditions (I 47) to (I 50) which guarantee that the solutions of inelastic problems found from (24) or (25) agree with both (14) and (15) or (16). In the particular case of an elastic–plastic composite, such result may be written as (33_2) or (58_2), and the instantaneous stress concentration factors $\mathscr{B}_r$ found

in this particular way then satisfy both (61) and (62). Note that in contrast to (59), the evaluation of (63) or (64) involves only the constraint tensors and/or the mechanical concentration factor tensors of the elastic composite.

To illustrate these aspects of the problem more completely, we focus on a two-phase elastic–plastic system, $r = \alpha, \beta$, where both phases may experience inelastic deformation. In this case, there are two unknown tensors $\mathscr{B}_r$ which must satisfy the additional relation $c_\alpha \mathscr{B}_\alpha + c_\beta \mathscr{B}_\beta = \boldsymbol{I}$, so that only one of the unknowns needs to be found. One possible way is to solve (61) and (62) for a single $\mathscr{B}_r$, as

$$\mathscr{B}_\alpha = (1/c_\alpha)[\boldsymbol{M}_\alpha - \boldsymbol{M}_\beta - (\boldsymbol{B}_\alpha^{\mathrm{T}} - \boldsymbol{I})(\mathscr{M}_\alpha - \boldsymbol{M}_\alpha) + (\boldsymbol{B}_\beta^{\mathrm{T}} - \boldsymbol{I})(\mathscr{M}_\beta - \boldsymbol{M}_\beta)]^{-1} \times [\boldsymbol{M} - \boldsymbol{M}_\beta + (\boldsymbol{B}_\beta^{\mathrm{T}} - \boldsymbol{I})(\mathscr{M}_\beta - \boldsymbol{M}_\beta)]. \quad (65)$$

which may be contrasted with (59_2).

To prove that this result is identical to that derived by the analysis of §4, one may use the notation $\mathscr{M}_r^{\mathrm{p}} = (\mathscr{M}_r - \boldsymbol{M}_r)$ from (30), and then compare (65) with the analogous expression (38_1). First, it is useful to recall that for $r = \alpha, \beta$, the $\boldsymbol{F}_{r\alpha}, \boldsymbol{F}_{r\beta}$ tensors in (38_1) appear in (39), and that their substitution into (38_1) provides

$$\mathscr{B}_\alpha = [\boldsymbol{I} - (c_\beta/c_\alpha)(\boldsymbol{I} - \boldsymbol{B}_\beta)(\boldsymbol{M}_\alpha - \boldsymbol{M}_\beta)^{-1}\mathscr{M}_\alpha^{\mathrm{p}} + (c_\alpha/c_\beta)(\boldsymbol{I} - \boldsymbol{B}_\alpha)(\boldsymbol{M}_\alpha - \boldsymbol{M}_\beta)^{-1}\mathscr{M}_\beta^{\mathrm{p}}]^{-1} \times [\boldsymbol{B}_\alpha + (1/c_\beta)(\boldsymbol{I} - \boldsymbol{B}_\alpha)(\boldsymbol{M}_\alpha - \boldsymbol{M}_\beta)^{-1}\mathscr{M}_\beta^{\mathrm{p}}]. \quad (66)$$

Then, one can proceed as indicated in the Appendix to show that (65) and (66) are indeed identical and satisfy the identity relation preceding (65).

8. Closure

Equations similar to (14) have been known for many years (Levin 1967; Rice 1970; Hill 1971). However, except for the recent papers by Hill (1984, 1985), they have not been widely appreciated in inelastic analysis of heterogeneous solids. One possible reason was the difficulty inherent in evaluation of the residual local fields, which has now been resolved by Dvorak (1990) for two-phase media, and by Dvorak & Benveniste (1992) for multiphase media. This provides a more consistent basis for the theory, but it also modifies certain aspects of the approach that follows (59) and (62). In particular, only elastic solutions of inclusion problems are used in the evaluation of local strains, hence the pronounced directional weakness in constraint of an already yielded aggregate (Hill 1965) is no longer reflected through the solution of an inclusion problem in an elastic homogeneous medium with the instantaneous overall stiffness $\mathscr{L}$, which leads to (59). Instead, this feature is accounted for by solving the inclusion problem in an elastic medium $\boldsymbol{L}$, which contains the eigenstrain equal to the total overall plastic strain, cf. §6 in (I).

Of course, the absence of inelastic inclusion problems in the analysis provides for a much simpler implementation of specific inelastic constitutive relations into the governing equations (34) or (25); this is illustrated for example by the closed-form expressions (37) to (40) for the elastic plastic solids. That may be particularly advantageous in unit-cell models, which have to use specific inelastic finite element routines. It is now sufficient to use only elastic finite element solutions to find the constant transformation factor tensors in (24) and (25), and then solve these equations directly with any chosen constitutive relations. We will show elsewhere that more efficient procedures can result, especially with coarsely subdivided unit cells that are used in analysis and design of composite structures.

It should be noted in passing that the present results may resolve some questions that are discussed from time to time in the technical literature. One pertains to the possibility of separation of the mechanical and thermal load effects in inelastic multiphase media. The results of §§4–6 make it clear that under combined thermomechanical loading of the aggregate, the temperature change may contribute to the current magnitude of $\boldsymbol{\sigma}_r^{re}(\boldsymbol{x})$ and $\boldsymbol{\varepsilon}_r^{in}(\boldsymbol{x})$, where the relative thermal and mechanical contributions to these total local fields depend on the inelastic response of the phases, the microstructural geometry, and on the combined thermomechanical loading path leading to the current overall magnitudes of $\boldsymbol{\sigma}$ or $\boldsymbol{\varepsilon}$, and θ. Therefore, the thermal contributions to the total inelastic fields may not be separated *a posteriori*, and it may not be possible to define the total thermal strain or relaxation stress, either in (1), or in (5). Only if such definitions can be made for the respective increments, e.g. in the elastic–plastic systems in §4, the total thermal strain may be separated in integration along the path. However, even in the elastic–plastic systems one cannot confirm an inelastic analog of the Levin formula (13_1), although it is well known that the thermal response of certain two-phase elastic–plastic composites can be simulated by mechanical loading along a modified path (Dvorak 1986, 1992).

Another observation can be useful in formulation of so-called inverse problems, which attempt to determine the local inelastic strains from observed changes in surface displacements, or in total overall strains. Note that equations (12) to (14) suggest that any number of local inelastic fields may exist in a heterogeneous medium such that the overall inelastic strain or relaxation stress both vanish. Of course, the existence of such fields may bring into question the uniqueness of solutions of the inverse problems.

This work was supported by the Office of Naval Research and by the ONR/DARPA HiTASC program at Rensselaer. Dr Yapa Rajapaske and Dr Steve Fishman served as program monitors.

Appendix

Here we prove that the instantaneous stress concentration factors in (38_1) or (66), and in (65) both satisfy the relation $c_\alpha \mathscr{B}_\alpha + c_\beta \mathscr{B}_\beta = \boldsymbol{I}$, and are identical.

Rewrite the $\mathscr{B}_\alpha$ in (66) as

$$\mathscr{B}_\alpha^{(1)} = [\mathscr{B}_\alpha^{(11)}]^{-1}\mathscr{B}_\alpha^{(12)}, \tag{A 1}$$

where

$$\mathscr{B}_\alpha^{(11)} = \boldsymbol{I} - (c_\beta/c_\alpha)(\boldsymbol{I}-\boldsymbol{B}_\beta)(\boldsymbol{M}_\alpha-\boldsymbol{M}_\beta)^{-1}\mathscr{M}_\alpha^{p} - (c_\alpha/c_\beta)(\boldsymbol{I}-\boldsymbol{B}_\alpha)(\boldsymbol{M}_\alpha-\boldsymbol{M}_\beta)^{-1}\mathscr{M}_\beta^{p}, \tag{A 2}$$

$$\mathscr{B}_\alpha^{(12)} = \boldsymbol{B}_\alpha + (1/c_\beta)(\boldsymbol{I}-\boldsymbol{B}_\alpha)(\boldsymbol{M}_\alpha-\boldsymbol{M}_\beta)^{-1}\mathscr{M}_\beta^{p}. \tag{A 3}$$

Similarly, write the $\mathscr{B}_\alpha$ in (65) as

$$\mathscr{B}_\alpha^{(2)} = [\mathscr{B}_\alpha^{(21)}]^{-1}\mathscr{B}_\alpha^{(22)}, \tag{A 4}$$

where

$$\mathscr{B}_\alpha^{(21)} = \boldsymbol{M}_\alpha - \boldsymbol{M}_\beta - (\boldsymbol{B}_\alpha^{T}-\boldsymbol{I})\mathscr{M}_\alpha^{p} + (\boldsymbol{B}_\beta^{T}-\boldsymbol{I})\mathscr{M}_\beta^{p}, \tag{A 5}$$

$$\mathscr{B}_\alpha^{(22)} = (1/c_\alpha)[\boldsymbol{M}-\boldsymbol{M}_\beta + (\boldsymbol{B}_\beta^{T}-\boldsymbol{I})\mathscr{M}_\beta^{p}]. \tag{A 6}$$

The phase subscripts α, β can be exchanged to obtain

$$\mathscr{B}_\beta^{(1)} = [\mathscr{B}_\beta^{(11)}]^{-1}\mathscr{B}_\beta^{(12)}, \quad \mathscr{B}_\beta^{(2)} = [\mathscr{B}_\beta^{(21)}]^{-1}\mathscr{B}_\beta^{(22)}. \tag{A 7}$$

where $$\mathscr{B}_\beta^{(11)} = \mathscr{B}_\alpha^{(11)}, \quad \mathscr{B}_\beta^{(21)} = -\mathscr{B}_\alpha^{(21)} \tag{A 8}$$

and $$\mathscr{B}_\beta^{(12)} = \boldsymbol{B}_\beta - (1/c_\alpha)(\boldsymbol{I}-\boldsymbol{B}_\beta)(\boldsymbol{M}_\alpha - \boldsymbol{M}_\beta)^{-1}\mathscr{M}_\alpha^{\mathrm{D}}, \tag{A 9}$$

$$\mathscr{B}_\beta^{(22)} = (1/c_\beta)\{\boldsymbol{M}-\boldsymbol{M}_\alpha + (\boldsymbol{B}_\alpha^{\mathrm{T}}-\boldsymbol{I})\mathscr{M}_\alpha^{\mathrm{D}}\}. \tag{A 10}$$

It is now easy to show that

$$c_\alpha \mathscr{B}_\alpha^{(1)} + c_\beta \mathscr{B}_\beta^{(1)} = [\mathscr{B}_\alpha^{(11)}]^{-1}(c_\alpha \mathscr{B}_\alpha^{(12)} + c_\beta \mathscr{B}_\beta^{(12)}) = \boldsymbol{I}. \tag{A 11}$$

$$c_\alpha \mathscr{B}_\alpha^{(2)} + c_\beta \mathscr{B}_\beta^{(2)} = [\mathscr{B}_\alpha^{(21)}]^{-1}(c_\alpha \mathscr{B}_\alpha^{(22)} - c_\beta \mathscr{B}_\beta^{(22)}) = \boldsymbol{I}. \tag{A 12}$$

To prove that

$$\mathscr{B}_\alpha^{(1)} = \mathscr{B}_\alpha^{(2)}, \quad \mathscr{B}_\beta^{(1)} = \mathscr{B}_\beta^{(2)}, \tag{A 13}$$

we focus on the first equality, and write it using (A 1) and (A 4) as

$$[\mathscr{B}_\alpha^{(11)}]^{-1}\mathscr{B}_\alpha^{(12)} = [\mathscr{B}_\alpha^{(21)}]^{-1}\mathscr{B}_\alpha^{(22)}, \tag{A 14}$$

or as $$\mathscr{B}_\alpha^{(12)}[\mathscr{B}_\alpha^{(22)}]^{-1} = \mathscr{B}_\alpha^{(11)}[\mathscr{B}_\alpha^{(21)}]^{-1}, \tag{A 15}$$

under the assumption that the inverses exist.

The relation (A 15) can be proved by verifying that

$$\mathscr{B}_\alpha^{(12)} = (\boldsymbol{M}_\alpha - \boldsymbol{M}_\beta)^{-1}\mathscr{B}_\alpha^{(22)}, \quad \mathscr{B}_\alpha^{(11)} = (\boldsymbol{M}_\alpha - \boldsymbol{M}_\beta)^{-1}\mathscr{B}_\alpha^{(21)}. \tag{A 16}$$

This can be easily shown to be true for any finite $\mathscr{M}_\alpha^{\mathrm{D}}, \mathscr{M}_\beta^{\mathrm{D}}$, if one recalls the identities that holds for two-phase materials,

$$c_\alpha(\boldsymbol{I}-\boldsymbol{B}_\alpha) = -c_\beta(\boldsymbol{I}-\boldsymbol{B}_\beta), \quad c_\alpha \boldsymbol{B}_\alpha = (\boldsymbol{M}_\alpha - \boldsymbol{M}_\beta)^{-1}(\boldsymbol{M}-\boldsymbol{M}_\beta),$$
$$c_\alpha \boldsymbol{B}_\beta = -(\boldsymbol{M}_\alpha - \boldsymbol{M}_\beta)^{-1}(\boldsymbol{M}-\boldsymbol{M}_\alpha), \tag{A 17}$$

and appeals to the symmetry relations

$$\left.\begin{aligned} \boldsymbol{M} = \boldsymbol{M}^{\mathrm{T}}, \quad \boldsymbol{M}_\alpha = \boldsymbol{M}_\alpha^{\mathrm{T}}, \quad \boldsymbol{M}_\beta = \boldsymbol{M}_\beta^{\mathrm{T}}, \\ \boldsymbol{B}_\alpha(\boldsymbol{M}_\alpha - \boldsymbol{M}_\beta)^{-1} = (\boldsymbol{M}_\alpha - \boldsymbol{M}_\beta)^{-1}\boldsymbol{B}_\alpha^{\mathrm{T}}, \quad \boldsymbol{B}_\beta(\boldsymbol{M}_\alpha - \boldsymbol{M}_\beta)^{-1} = (\boldsymbol{M}_\alpha - \boldsymbol{M}_\beta)^{-1}\boldsymbol{B}_\beta^{\mathrm{T}}. \end{aligned}\right\} \tag{A 18}$$

Q.E.D.

References

Benveniste, Y., Dvorak, G. J. & Chen, T. 1991 *J. Mech. Phys. Solids* **39**, 927–946.

Chaboche, J. L. 1989 *Int. J. Plasticity* **5**, 247–302.

Chen, T., Dvorak, G. J. & Benveniste, Y. 1992 *J. appl. Mech.* (In the press.)

Christensen, R. M. 1971 *Theory of viscoelasticity, an introduction*. New York: Academic Press.

Christensen, R. M. 1979 *Mechanics of composite materials*. New York: John Wiley & Sons.

Dvorak, G. J. 1986 *J. appl. Mech.* **53**, 737–742.

Dvorak, G. J. 1990 *Proc. R. Soc. Lond.* A **431**, 89–110.

Dvorak, G. J. 1991 *Metal matrix composites: mechanisms and properties* (ed. R. K. Everett & R. J. Arsenault), pp. 1–77. Boston: Academic Press.

Dvorak, G. J. 1992 *J. Thermal Stresses*. (In the press.)

Dvorak, G. J. & Benveniste, Y. 1992 *Proc. R. Soc. Lond.* A **437**, 291–310. (Preceding paper).

Gavazzi, A. C. & Lagoudas, D. C. 1990 *Computational Mech.* **7**, 13–19.

Hill, R. 1965 *J. Mech. Phys. Solids* **13**, 89–101.

Hill, R. 1966 *J. Mech. Phys. Solids* **14**, 95–102.

Hill, R. 1967 *J. Mech. Phys. Solids* **15**, 79–95.

Hill, R. 1971 *Prikl. Mat. Mekh. (PMM)* **35**, 31–39.

Hill, R. 1984 *Math. Proc. Camb. phil. Soc.* **95**, 481–494.

Hill, R. 1985 *Math. Proc. Camb. phil. Soc.* **98**, 579–590.
Hutchinson, J. W. 1970 *Proc. R. Soc. Lond.* A **319**, 247–272.
Krempl, E. & Lu, H. 1984 *ASME J. Engng Mater. Technol.* **106**, 376–382.
Levin, V. M 1967 *Izv. ANSSSR, Mekhanika Tverdogo Telc* **2**, 88–94.
Mori, T. & Tanaka, K. 1973 *Acta metal.* **21**, 571–574.
Rice, J. R. 1970 *J. appl. Mech.* **37**, 728.
Tandon, G. P. & Weng, G. J. 1988 *J. appl. Mech.* **55**, 126–135.

Received 5 August 1991; accepted 5 December 1991

Tungyang Chen[1]

George J. Dvorak
Fellow ASME.

Department of Civil Engineering,
Rensselaer Polytechnic Institute,
Troy, NY 12180-3590

Yakov Benveniste

Department of Solid Mechanics,
Materials and Structures,
Tel-Aviv University,
Tel-Aviv, Israel

Mori-Tanaka Estimates of the Overall Elastic Moduli of Certain Composite Materials

Simple, explicit formulae are derived for estimates of the effective elastic moduli of several multiphase composite materials with the Mori-Tanaka method. Specific results are given for composites reinforced by aligned or randomly oriented, transversely isotropic fibers or platelets, and for fibrous systems reinforced by aligned, cylindrically orthotropic fibers.

1 Introduction

Estimates of overall elastic moduli of composite materials, in terms of phase geometry and moduli, can be obtained by several well-known methods. For example, the Hashin-Shtrikman bounds which bracket the actual magnitudes of the moduli are available for many two-phase and multiphase systems (Hashin and Shtrikman 1963, Walpole 1969, 1981, 1984). Also, self-consistent estimates have been available for many years for such systems as aligned fiber composites (Hill 1965a), two-phase media reinforced by spherical particles (Budiansky 1965), or by randomly orientated inclusions of various shapes (Walpole 1969), and for multiphase aggregates with fibrous and penny-shaped (platelet) inclusions (Laws, 1974). Other such estimates were found by Christensen and Waals (1972), Boucher (1974), Berryman (1980), Cleary, Chen, and Lee (1980), and Willis (1981). The conditions which guarantee that the self-consistent estimates lie within the bounds were established by Hill (1965b) and Walpole (1969, 1981).

In its recent reformulation by Benveniste (1987), the Mori-Tanaka (1973) method offers another alternative to finding estimates of elastic moduli and local fields in composite materials. Recent applications include the work of Weng (1984) who found the effective bulk and shear moduli of two and three-phase composites with spherical isotropic inclusions in an isotropic matrix. Benveniste, Dvorak, and Chen (1989) applied this method to coated fiber composites. Zhao, Tandon, and Weng (1989) derived the effective moduli for a class of porous materials with various distributions. Norris (1989) examined many aspects of the method and its relation to the Hashin-Shtrikman bounds.

The present paper is concerned with evaluation of estimates of overall elastic moduli of certain composite materials by the Mori-Tanaka method. In particular, we consider multiphase composites reinforced either by aligned fibers or platelets, and similar systems with randomly oriented reinforcement. In either case, the reinforcement may be isotropic or transversely isotropic. Moreover, we examine fibrous composites reinforced by cylindrically orthotropic fibers. As Benveniste, Dvorak, and Chen (1991a) have shown, both the Mori-Tanaka and the self-consistent methods deliver diagonally symmetric estimates of overall stiffness in the selected systems. However, such symmetry does not obtain in estimates of overall stiffness for multiphase systems with inclusions of different shapes or orientation.

We start with a summary of most of the present results. This is followed by an outline of the method and its application to the selected systems. For the most part, the derivation is relatively straightforward. However, the cylindrically orthotropic fibers call for a special treatment. Some of the moduli are found by replacement of the actual fiber by an equivalent transversely isotropic fiber, but this approach does not extend to the shear modulus in the transverse plane. That particular result can be extracted only from a numerical evaluation of the overall stiffness tensor.

2 Phase and Overall Properties

Fibers and platelets used as composite reinforcements are often transversely isotropic. The same is true for composite aggregates reinforced by aligned fibers or platelets. If the axis of symmetry is chosen as parallel to the x_1-axis of a Cartesian coordinate system, then the elastic response of a transversely isotropic solid may be described in the form:

$$\begin{bmatrix} s \\ \sigma \end{bmatrix} = \begin{bmatrix} k & l \\ l & n \end{bmatrix} \begin{bmatrix} e \\ \epsilon \end{bmatrix} \tag{1}$$

$$\tau_{23} = 2m\epsilon_{23},\ \tau_{12} = 2p\epsilon_{12},\ \tau_{13} = 2p\epsilon_{13}$$

where

$$s = \frac{1}{2}(\sigma_{22} + \sigma_{33}),\ \sigma = \sigma_{11},\ e = \epsilon_{22} + \epsilon_{33},\ \epsilon = \epsilon_{11}, \tag{2}$$

and k, l, m, n, and p are Hill's elastic moduli (1964). In particular, k is the plane-strain bulk modulus for lateral dil-

Contributed by the Applied Mechanics Division of THE AMERICAN SOCIETY OF MECHANICAL ENGINEERS for publication in the ASME JOURNAL OF APPLIED MECHANICS.

Discussion on this paper should be addressed to the Technical Editor, Professor Leon M. Keer, The Technological Institute, Northwestern University, Evanston, IL 60208, and will be accepted until four months after final publication of the paper itself in the JOURNAL OF APPLIED MECHANICS.

Manuscript received by the ASME Applied Mechanics Division, Nov. 28, 1990; final revision, Aug. 1, 1991. Associate Technical Editor: L. M. Keer.

atation without longitudinal extension, n is the modulus for longitudinal uniaxial straining, l is the associated cross modulus, m is the shear modulus in any transverse direction, and p is the shear modulus for longitudinal shearing.

For an isotropic material, these moduli are related to the bulk and shear moduli K and G as:

$$k = K + \frac{1}{3}G,\ l = K - \frac{2}{3}G,\ n = K + \frac{4}{3}G,\ m = p = G. \tag{3}$$

In what follows, the above notation will be used both for the phase and overall moduli. The phase properties will have a subscript $r = 1, 2, \ldots N$, while the overall quantities will appear without a subscript.

Some fibers, particularly carbon fibers, are cylindrically orthotropic. Their elastic moduli in the tangential, radial, and axial directions are distinct. Nine stiffness coefficients describe this kind of anisotropy. In a cylindrical coordinate system, the stress-strain relation of a cylindrically orthotropic solid is usually written as:

$$\begin{Bmatrix} \sigma_r \\ \sigma_\theta \\ \sigma_z \\ \sigma_{r\theta} \\ \sigma_{z\theta} \\ \sigma_{rz} \end{Bmatrix} = \begin{bmatrix} C_{rr} & C_{r\theta} & C_{rz} & 0 & 0 & 0 \\ C_{\theta r} & C_{\theta\theta} & C_{\theta z} & 0 & 0 & 0 \\ C_{zr} & C_{z\theta} & C_{zz} & 0 & 0 & 0 \\ 0 & 0 & 0 & G_{r\theta} & 0 & 0 \\ 0 & 0 & 0 & 0 & G_{z\theta} & 0 \\ 0 & 0 & 0 & 0 & 0 & G_{rz} \end{bmatrix} \begin{Bmatrix} \epsilon_r \\ \epsilon_\theta \\ \epsilon_z \\ 2\epsilon_{r\theta} \\ 2\epsilon_{z\theta} \\ 2\epsilon_{rz} \end{Bmatrix} \tag{4}$$

where z is the axis of rotational symmetry, and C_{ij}, $G_{r\theta}$, $G_{z\theta}$, and G_{rz} are stiffness coefficients.

3 Summary of Present Results

For convenience, we first summarize the main results for several systems of practical interest: composites reinforced by aligned, transversely isotropic fibers or platelets, systems with randomly oriented, transversely isotropic fiber or platelet reinforcement, and unidirectionally reinforced materials with cylindrically orthotropic fibers. Derivation of the results appear in Sections 5, 6, and 7.

3.1 Unidirectional Fibrous Composites. We consider a system reinforced by aligned, transversely isotropic fibers ($r = 2, 3, \ldots N$) in a transversely isotropic matrix ($r = 1$). Many different fiber materials may be admitted at the same time. The overall elastic moduli of such a fiber system are:

$$p = \frac{\sum_{r=1}^{N} \frac{c_r p_r}{p_1 + p_r}}{\sum_{r=1}^{N} \frac{c_r}{p_1 + p_r}},\quad m = \frac{\sum_{r=1}^{N} \frac{c_r m_r}{m_r + \gamma_1}}{\sum_{r=1}^{N} \frac{c_r}{m_r + \gamma_1}},\quad \gamma_1 = \left(\frac{1}{m_1} + \frac{2}{k_1}\right)^{-1} \tag{5}$$

$$k = \frac{\sum_{r=1}^{N} \frac{c_r k_r}{k_r + m_1}}{\sum_{r=1}^{N} \frac{c_r}{k_r + m_1}},\quad l = \frac{\sum_{r=1}^{N} \frac{c_r l_r}{k_r + m_1}}{\sum_{r=1}^{N} \frac{c_r}{k_r + m_1}}, \tag{6}$$

$$n = \sum_{r=1}^{N} c_r n_r - \sum_{r=1}^{N} c_r \frac{(l_r - l_1)^2}{k_r + m_1} + \frac{\left[\sum_{r=1}^{N} \frac{c_r (l_r - l_1)}{k_r + m_1}\right]^2}{\sum_{r=1}^{N} \frac{c_r}{k_r + m_1}}. \tag{7}$$

We now list the results for two-phase systems of technological interest; the subscripts f and m represent the fiber and matrix, respectively:

$$p = \frac{2c_f p_m p_f + c_m p_m p_f + p_m^2)}{2c_f p_m + c_m (p_f + p_m)} \tag{8}$$

$$m = \frac{m_m m_f (k_m + 2m_m) + k_m m_m (c_f m_f + c_m m_m)}{k_m m_m + (k_m + 2m_m)(c_f m_m + c_m m_f)} \tag{9}$$

$$k = \frac{c_f k_f (k_m + m_m) + c_m k_m (k_f + m_m)}{c_f (k_m + m_m) - c_m (k_f + m_m)} \tag{10}$$

$$l = \frac{c_f l_f (k_m + m_m) + c_m l_m (k_f - m_m)}{c_f (k_m + m_m) + c_m (k_f + m_m)} \tag{11}$$

$$n = c_m n_m + c_f n_f + (l - c_f l_f - c_m l_m)\frac{l_f - l_m}{k_f - k_m}. \tag{12}$$

It should be mentioned that the effective plane-strain bulk modulus k and cross modulus l in (10) and (11), predicted by the Mori-Tanaka method, coincide with those derived by Hill (1964, Eq. (3.6)) for the cylindrical composite element. In two-phase fibrous media, the effective modulus n obeys the universal connections, hence all the moduli k, l, n have the same values as those derived by Hill (1964). Therefore, for axisymmetric loading situations, the Mori-Tanaka predictions coincide with those suggested by the composite cylinder model.

Furthermore, Norris (1989) has shown that the Mori-Tanaka approximation for multiphase composites, where all particles have the same shape and alignment, satisfies the appropriate Hashin-Shtrikman or Hill-Hashin bounds.

3.2 Unidirectional Platelet-Reinforced Composites. As above, we denote the matrix as $r = 1$, and the platelets as $r = 2, 3, \ldots N$. Transverse isotropy or isotropy via (3) is assumed in all phases, together with alignment of the phase symmetry axes with x_1. The overall elastic moduli of such composite are

$$p^{-1} = \sum_{r=1}^{N} c_r p_r^{-1},\ m = \sum_{r=1}^{N} c_r m_r,\ n^{-1} = \sum_{r=1}^{N} c_r n_r^{-1},$$

$$\frac{l}{n} = \sum_{r=1}^{N} c_r \frac{l_r}{n_r},\ k = \sum_{r=1}^{N} c_r k_r + \frac{l^2}{n} - \sum_{r=1}^{N} c_r \frac{l_r^2}{n_r}. \tag{13}$$

Surprisingly, the effective Mori-Tanaka moduli k, l, m, n, p of composites with aligned platelet reinforcement are identical with those derived from the self-consistent model by Laws (1974, Eqs. (42)–(46)). Moreover, we note that they also coincide with the effective moduli of a laminated plate (Postma, 1955).

3.3 Composites With Randomly Oriented Fibers or Platelets. We assume that both the matrix ($r = 1$) and the composite are isotropic and characterized by the bulk and shear moduli K_1, K, and G_1, G. The elastic moduli of the reinforcing phases $r = 2, 3, \ldots N$ are defined in the local coordinates of each phase r, and in those coordinates each phase may be transversely isotropic or isotropic. The overall moduli of composites with such random reinforcements are

$$K = K_1 + \frac{1}{3}\sum_{r=2}^{N} c_r \frac{(\delta_r - 3K_1\alpha_r)}{\left[c_1 + \sum_{r=2}^{N} c_r \alpha_r\right]},$$

$$G = G_1 + \frac{1}{2}\sum_{r=2}^{N} c_r \frac{(\eta_r - 2G_1\beta_r)}{\left[c_1 + \sum_{r=2}^{N} c_r \beta_r\right]}, \tag{14}$$

where the parameters α_r, β_r, δ_r, η_r depend on the moduli and geometry of the phases.

For fibrous systems, these parameters are given as in terms of phase moduli of the phases as

$$\alpha_r=\frac{3K_1+3G_1+k_r-l_r}{3G_1+3k_r} \tag{15}$$

$$\beta_r=\frac{1}{5}\left[\frac{4G_1+(2k_r+l_r)}{3G_1+3k_r}+\frac{4G_1}{p_r+G_1}+\frac{2(\gamma_1+G_1)}{\gamma_1+m_r}\right] \tag{16}$$

$$\delta_r=\frac{1}{3}\left[n_r+2l_r+\frac{(2k_r+l_r)(3K_1+2G_1-l_r)}{k_r+G_1}\right] \tag{17}$$

$$\eta_r=\frac{1}{5}\left[\frac{2}{3}(n_r-l_r)+\frac{8m_rG_1(3K_1+4G_1)}{m_r(3K_1+4G_1)+G_1(3K_1+3m_r+G_1)}+\frac{8p_rG_1}{p_r+G_1}+\frac{4k_rG_1-4l_rG_1-2l_r^2+2k_rl_r}{3k_r+3G_1}\right] \tag{18}$$

where in this case (isotropic matrix) γ_1 in (5) reduces to

$$\gamma_1=\frac{3G_1K_1+G_1^2}{3K_1+7G_1}. \tag{19}$$

For penny-shaped, randomly oriented inclusions, the above parameters assume the values

$$\alpha_r=\frac{K_1}{n_r}+\frac{2}{3}\frac{n_r-l_r}{n_r},\quad \beta_r=\frac{1}{5}\left[\frac{7n_r+2l_r+4G_1}{3n_r}+\frac{2G_1}{p_r}\right]$$

$$\delta_r=K_1+2K_1\frac{l_r}{n_r}+\frac{4}{3}\left[k_r-\frac{l_r^2}{n_r}\right],$$

$$\eta_r=\frac{1}{5}\left[4m_r+\frac{2}{3}\left(k_r-\frac{l_r^2}{n_r}\right)+\frac{16}{3}G_1-\frac{4}{3}G_1\frac{l_r}{n_r}\right]. \tag{20}$$

If the fibers or penny-shaped inclusions are *isotropic*, then one can verify that

$$\delta_r=3K_r\alpha_r,\ \eta_r=2G_r\beta_r, \tag{21}$$

and for composites with reinforcements of these two kinds, the bulk and shear moduli in (14) can be simplified as

$$K=K_1+\sum_{r=2}^{N}c_r(K_r-K_1)\frac{\alpha_r}{\left[c_1+\sum_{r=2}^{N}c_r\alpha_r\right]}$$

$$G=G_1+\sum_{r=2}^{N}c_r(G_r-G_1)\frac{\beta_r}{\left[c_1+\sum_{r=2}^{N}c_r\beta_r\right]}. \tag{22}$$

For such isotropic fibers or needle-shaped inclusions, (15) and (16) reduce to

$$\alpha_r=\frac{3K_1+3G_1+G_r}{3K_r+3G_1+G_r} \tag{23}$$

$$\beta_r=\frac{1}{5}\left[\frac{4G_1+3K_r}{3K_r+3G_1+G_r}+\frac{4G_1}{G_1+G_r}+\frac{2(\gamma_1+G_1)}{\gamma_1+G_r}\right]. \tag{24}$$

Therefore, for two-phase media with randomly oriented fibrous reinforcements, the effective bulk modulus K and shear modulus G become

$$K=K_2-c_1(K_2-K_1)\left[1-c_2\frac{3K_2-3K_1}{3K_2+G_2+3G_1}\right]^{-1} \tag{25}$$

$$G=G_2-c_1(G_2-G_1)\left[1-\frac{1}{5}\frac{G_2-G_1}{3K_2+3G_1+G_2}-\frac{2}{5}c_2\frac{G_2-G_1}{G_2+\gamma_1}-\frac{2}{5}c_2\frac{G_2-G_1}{G_2+G_1}\right]^{-1}. \tag{26}$$

Equations (25) and (26) can be compared with similar but not identical results found from the self-consistent method by Walpole (1969, Eq. (60)).

For randomly oriented, isotropic, penny-shaped inclusions, (20_1) reduces to

$$\alpha_r=\frac{3K_1+4G_r}{3K_r+4G_r},\quad \beta_r=\frac{2}{5}\frac{G_1}{G_r}+\frac{1}{5}\frac{9K_r+8G_r+4G_1}{3K_r+4G_r} \tag{27}$$

and the overall bulk and shear moduli of two-phase media can be obtained as

$$K=K_2-c_1(K_2-K_1)\left[1-c_2\frac{3(K_2-K_1)}{3K_2+4G_2}\right]^{-1} \tag{28}$$

$$G=G_2-c_1(G_2-G_1)\left[1-\frac{4}{5}c_2\frac{G_2-G_1}{3K_2+4G_2}-\frac{2}{5}c_2\frac{G_2-G_1}{G_2}\right]^{-1}. \tag{29}$$

It is interesting to note that (28) and (29) are exactly the same expressions as those derived with the self-consistent method by Walpole (1969, Eq. (61)).

Also, it should be mentioned that Benveniste (1987) has recently proved that the bulk and shear moduli predicted by the Mori-Tanaka method for a two-phase composite with randomly oriented ellipsoidal particles will lie within the Hashin-Shtrikman bounds.

3.4 Composites Reinforced by Cylindrically Orthotropic Fibers. The constitutive Eq. (4) suggests that cylindrically orthotropic fibers have constant moduli in the cylindrical coordinate system. However, most overall moduli must be evaluated in a Cartesian system, where the fiber properties are no longer constant. The effective moduli of unidirectional composites of this kind are still those of a transversely isotropic solid, and can be obtained from the Mori-Tanaka procedure, but at least one of the overall moduli, the transverse shear modulus m, may not be found in closed form. Except for m, evaluation of the moduli is best accomplished by introduction of a *replacement fiber* which, under certain overall stress states has the same effective properties as the cylindrically orthotropic fiber described by (4). In particular, in their recent study of thermomechanical behavior of composite systems reinforced by coated cylindrically orthotropic fibers, Chen, Dvorak, and Benveniste (1990) and Hashin (1990) observed that *in axisymmetric loading situations* the cylindrically orthotropic fiber can be replaced by an equivalent *transversely isotropic* fiber without changing the fields of outer phases and the overall behavior of the composite. Moreover, we show in Section 7 that a replacement fiber with an effective modulus p_f can also be found for the longitudinal shear loading case. No such replacement seems possible for transverse normal or shear loading.

The effective moduli of the replacement fiber are recorded here as

$$k_f=(C_{rr}\eta+C_{r\theta})/2,\quad l_f=\frac{C_{rz}\eta+C_{\theta z}}{\eta+1},\quad p_f=\sqrt{G_{\theta z}G_{rz}} \tag{30}$$

$$n_f=\frac{l^2}{k}+[(C_{rz}H_1+C_{\theta z}H_1+C_{zz})-\frac{2}{1+\eta}\frac{C_{rz}\eta+C_{\theta z}}{C_{rr}\eta+C_{r\theta}}(C_{rr}H_1+C_{r\theta}H_1+C_{rz})],$$

where the C_{ij} were defined in (4), p_f is derived in Section 7, and

$$\eta=(C_{\theta\theta}/C_{rr})^{\frac{1}{2}},\quad H_1=\frac{C_{\theta z}-C_{rz}}{C_{rr}-C_{r\theta}}. \tag{31}$$

These effective fiber moduli can be employed in (8), and (10) to (12), to find the corresponding overall moduli of the unidirectional composite reinforced by the cylindrically orthotropic fibers. The overall transverse shear modulus m must be extracted from the overall stiffness derived in Section 7.

4 The Mori-Tanaka Method

To introduce the derivation of the above results we summarize here the essence of this method, in the form which was recently suggested by Benveniste (1987). A representative volume element V of the composite is chosen such that under homogeneous boundary conditions it represents the macroscopic response of the composite. The volume is filled with a certain number of homogeneous phases which are perfectly bonded to a common matrix. The phase volume fractions c_r satisfy $\Sigma\, c_r = 1$; $r = 1, 2, .. N$. In the sequel, $r = 1$ denotes the *matrix* phase. The volume V is subjected to uniform displacement or traction boundary conditions

$$\mathbf{u}(S) = \epsilon^0\mathbf{x}, \quad \mathbf{t}(S) = \sigma^0\mathbf{n} \tag{32}$$

where $\mathbf{u}$ and $\mathbf{t}$ denote the applied displacement and traction; ϵ^0, σ^0 are constant strain and stress tensors, and $\mathbf{n}$ is the outside normal to S.

The objective is to evaluate the overall elastic stiffness $\mathbf{L}$ and its inverse, the compliance $\mathbf{M}$, of the composite aggregate, defined by

$$\bar{\sigma} = \mathbf{L}\epsilon^0, \ \bar{\epsilon} = \mathbf{M}\sigma^0, \tag{33}$$

where $\bar{\sigma}$ and $\bar{\epsilon}$ denote the volume average stresses and strains in V. An intermediate step is evaluation of the elastic fields in the phases. Those are found in terms of phase volume averages (Hill 1963)

$$\epsilon_r = \mathbf{A}_r\epsilon^0, \quad \sigma_r = \mathbf{B}_r\sigma^0, \tag{34}$$

where $\mathbf{A}_r$ and $\mathbf{B}_r$ are referred to as mechanical concentration factors. Under the boundary conditions (32_1) and (32_2), the local and overall field averages in V are respectively related by

$$\epsilon^0 = \sum_{r=1}^{N} c_r\epsilon_r, \quad \sigma^0 = \sum_{r=1}^{N} c_r\sigma_r. \tag{35}$$

Then, the overall elastic moduli $\mathbf{L}$ and compliance $\mathbf{M}$ follow as

$$\mathbf{L} = \sum_{r=1}^{N} c_r\mathbf{L}_r\mathbf{A}_r, \quad \mathbf{M} = \sum_{r=1}^{N} c_r\mathbf{M}_r\mathbf{B}_r. \tag{36}$$

In the evaluation of the concentration factors by the Mori-Tanaka method, each inclusion is regarded as a solitary inhomogeneity embedded in an infinite matrix material under a remotely applied strain or stress equal to the matrix average ϵ_1 or σ_1. For ellipsoidal inclusions, the local fields in such solitary inhomogeneities are uniform, and can be evaluated in terms of partial concentration factors $\mathbf{T}_r$, $\mathbf{W}_r$:

$$\epsilon_r = \mathbf{T}_r\epsilon_1, \quad \sigma_r = \mathbf{W}_r\sigma_1. \tag{37}$$

Once the $\mathbf{T}_r$ and $\mathbf{W}_r$ are known, one can utilize (35) to establish that

$$\epsilon_1 = \left[\sum_{r=1}^{N} c_r\mathbf{T}_r\right]^{-1}\epsilon^0, \quad \sigma_1 = \left[\sum_{r=1}^{N} c_r\mathbf{W}_r\right]^{-1}\sigma^0, \tag{38}$$

and derive the mechanical concentration factors in (34) as

$$\mathbf{A}_r = \mathbf{T}_r\left[\sum_r c_r\mathbf{T}_r\right]^{-1}, \quad \mathbf{B}_r = \mathbf{W}_r\left[\sum_r c_r\mathbf{W}_r\right]^{-1}. \tag{39}$$

The effective stiffness and compliance tensors $\mathbf{L}$ and $\mathbf{M}$ then follow from (36) and (39):

$$\mathbf{L} = \left[\Sigma\, c_r\mathbf{L}_r\mathbf{T}_r\right]\left[\Sigma\, c_r\mathbf{T}_r\right]^{-1},$$

$$\mathbf{M} = \left[\Sigma\, c_r\mathbf{M}_r\mathbf{W}_r\right]\left[\Sigma\, c_r\mathbf{W}_r\right]^{-1}. \tag{40}$$

The partial concentration factors in (37) are conveniently expressed in the form

$$\mathbf{T}_r = [\mathbf{I} + \mathbf{P}(\mathbf{L}_r - \mathbf{L}_1)]^{-1}, \ \mathbf{W}_r = [\mathbf{I} + \mathbf{Q}(\mathbf{M}_r - \mathbf{M}_1)]^{-1} \tag{41}$$

where the tensors of $\mathbf{P}$ and $\mathbf{Q}$ depend only on the shape of the inclusion, and on the elastic moduli of the surrounding matrix. For example, for an inclusion in the shape of a circular cylinder in a transversely isotropic matrix, the nonvanishing terms of $\mathbf{P}$, written in a (6×6) array are (Walpole, 1969),

$$P_{22} = P_{33} = \frac{k_1 + 4m_1}{8m_1(k_1 + m_1)}, \quad P_{23} = P_{32} = \frac{-k_1}{8m_1(k_1 + m_1)},$$

$$P_{55} = P_{66} = \frac{1}{2p_1}, \quad P_{44} = \frac{k_1 + 2m_1}{2m_1(k_1 + m_1)} \tag{42}$$

in terms of the elastic moduli (1) or (3) of the matrix ($r = 1$). Similarly, for a circular disk in a plane normal to the direction of x_1,

$$P_{11} = \frac{1}{n_1}, \quad P_{55} = P_{66} = \frac{1}{p_1}. \tag{43}$$

Alternatively, (41) can be written in terms of the overall constraint tensors $\mathbf{L}_1^*$, $\mathbf{M}_1^*$ (Hill, 1965b) which relate the uniform fields in the inclusion r to the uniform applied fields σ^0 and ϵ^0 as

$$\sigma_r - \sigma^0 = \mathbf{L}_1^*(\epsilon^0 - \epsilon_r), \quad \epsilon_r - \epsilon^0 = \mathbf{M}_1^*(\sigma^0 - \sigma_r). \tag{44}$$

Those are connected to the partial concentration factors by

$$\mathbf{T}_r = (\mathbf{L}_1^* + \mathbf{L}_r)^{-1}(\mathbf{L}_1^* + \mathbf{L}_1), \ \mathbf{W}_r = (\mathbf{M}_1^* + \mathbf{M}_r)^{-1}(\mathbf{M}_1^* + \mathbf{M}_1). \tag{45}$$

The determination of $\mathbf{L}^*$ and $\mathbf{M}^*$ relies on solutions of boundary value problems for a uniformly stressed or strained cavity in the infinite matrix medium. For example, the nonvanishing terms of the overall constraint compliance $\mathbf{M}_1^*$ of a circular cylindrical cavity are (Walpole, 1969; Laws, 1974):

$$(M_1^*)_{22} = (M_1^*)_{33} = \frac{1}{2}\left(\frac{1}{m_1} + \frac{1}{k_1}\right), \quad (M_1^*)_{23} = (M_1^*)_{32} = -\frac{1}{2k_1}$$

$$(M_1^*)_{55} = (M_1^*)_{66} = \frac{1}{p_1}, \quad (M_1^*)_{44} = \frac{1}{m_1} + \frac{2}{k_1}. \tag{46}$$

5 Composites Reinforced by Aligned Inclusions

5.1 Aligned Fiber or Needle-Shaped Inclusions. We now proceed to derive the results which were summarized in Section 3.1. First, consider a single fiber in an infinite matrix ($r = 1$) subjected to a longitudinal shear strain $2\epsilon_1$ on its outside boundary. In this dilute configuration, $2\epsilon_1$ is equal to the average matrix strain, and the overall stress is a pure shear $\tau_1 = 2p_1\epsilon_1$. This is an antiplane problem, hence the stress and strain in the fiber r have only the longitudinal shear components $\tau_r = 2p_r\epsilon_r$. These local and overall quantities are related, according to (44_1) and (46_3), as

$$\tau_r - \tau_1 = 2p_1(\epsilon_1 - \epsilon_r). \tag{47}$$

From the phase constitutive relations and (47), one finds that $\tau_r/\tau_1 = 2p_r/(p_r + p_1)$, and the average matrix longitudinal shear stress follows from (35_2) as

$$\tau_1 = \left[\sum_{r=1}^{N} c_r \frac{2p_r}{p_r + p_1}\right]^{-1} \tau^0, \tag{48}$$

where τ^0 is the overall longitudinal shear stress that is actually applied to the composite. The average phase strains in (35_1) can be written here as

$$\sum_{r=1}^{N} c_r \frac{\tau_r}{p_r} = \frac{\tau^0}{p}. \tag{49}$$

Finally, a substitution of (47) and (48) in (49) leads to the expression for the effective longitudinal shear modulus p in (5_1).

A similar procedure can be extended to the transverse shear loading case. The constraint tensor in (46_4), (44_1) reduces to $\gamma_1 = (1/m_1 + 2/k_1)^{-1}$, hence $\tau_r - \tau_1 = 2\gamma_1(\epsilon_1 - \epsilon_r)$, where τ_r and ϵ_r represent the corresponding transverse shear stress and shear strain in the phase r, respectively. As in the derivation of the longitudinal shear loading case, the average stress in the matrix is

$$\tau_1 = \left[\sum_{r=1}^{N} c_r \frac{m_r(m_1+\gamma_1)}{m_1(m_r+\gamma_1)}\right]^{-1} \tau^0, \tag{50}$$

and the effective transverse shear modulus m can then be derived in the form given by (5_2).

Next, a pure lateral dilatation is applied without longitudinal straining; i.e., $e^0 \neq 0$, $\epsilon^0 = 0$ in (1). The local stress and strain relation is thus reduced to $s_r = k_r e_r$, and from (46_1) and (46_2) the corresponding equation for the constraint modulus is $(s_r - s_1) = m_1(e_1 - e_r)$. This and (35_2) imply that

$$\frac{s_r}{s_1} = \frac{k_r(k_1+m_1)}{k_1(k_r+m_1)}, \quad s_1 = \left[\sum_{r=1}^{N} c_r \frac{k_r(k_1+m_1)}{k_1(k_r+m_1)}\right]^{-1} s^0. \tag{51}$$

Then, the effective plane-strain bulk modulus k given by (6_1) can be derived from (35_1).

In the same loading situation as above, $\epsilon^0 = 0$ suggests that

$$\bar{s} = ke^0, \ \bar{\sigma} = le^0. \tag{52}$$

From (35_2) and (52), one can write the average longitudinal stress as

$$\sum_{r=1}^{N} c_r \frac{l_r}{k_r} s_r = \frac{l}{k} s^0. \tag{53}$$

Then, (51), and (6_1) lead to the expression for the effective cross modulus l in (6_2).

For evaluation of the modulus n, consider overall uniaxial straining without lateral contraction, i.e., $\epsilon^0 \neq 0$, $e^0 = 0$ in (1). The phase averages in the transverse plane and in the longitudinal direction are

$$\Sigma c_r e_r = 0, \ \Sigma c_r s_r = l\epsilon^0, \ \Sigma c_r \sigma_r = n\epsilon^0, \ \epsilon_r = \epsilon^0, \qquad r = 1,2..,N. \tag{54}$$

Using (54_1), Eqs. (54_2) and (54_3) can be recast as:

$$\sum_{r=1}^{N} c_r(k_r - k_1)e_r = \left[l - \sum_{r=1}^{N} c_r l_r\right]\epsilon^0,$$

$$\sum_{r=1}^{N} c_r(l_r - l_1)e_r = \left(n - \sum_{r=1}^{N} c_r n_r\right)\epsilon^0. \tag{55}$$

In two-phase media, n follows from (55) and from the universal connections for two-phase fibrous media with transversely isotropic constituents (Hill 1964):

$$\frac{n - c_1 n_1 - c_2 n_2}{l - c_1 l_1 - c_2 l_2} = \frac{l_1 - l_2}{k_1 - k_2}. \tag{56}$$

In multiphase systems, one additional condition is needed for evaluation of n, namely the magnitude of e_r/ϵ^0. In the Mori-Tanaka method, one can use (41_1) and (39_1), with the $\mathbf{P}$ tensor given in (42) to obtain the necessary components:

$$\frac{e_r}{\epsilon} = \frac{l_1 - l_r}{k_r + m_1} - \frac{\dfrac{1}{k_r + m_1}\displaystyle\sum_{r=1}^{N} \frac{c_r(l_r - l_1)}{k_r + m_1}}{\displaystyle\sum_{r=1}^{N} \frac{c_r}{k_r + m_1}}. \tag{57}$$

Then, the effective modulus n in (7) for longitudinal uniaxial straining can be obtained from (55_2) and (57).

5.2 Aligned Penny-Shaped Inclusions. Consider penny-shaped or disk-shaped reinforcement with the normal to the plane face of the platelet in the x_1-direction. Due to the simple form of the $\mathbf{P}$ tensor in (43), the partial strain concentration factor can be derived from (41_1). The nonvanishing components are:

$$T'_{11} = \frac{n_1}{n_r}, \ T'_{12} = T'_{13} = \frac{l_1 - l_r}{n_r},$$

$$T'_{22} = T'_{33} = T'_{44} = 1, \ T'_{55} = T'_{66} = \frac{p_1}{p_r}. \tag{58}$$

The effective moduli can be derived as in Section 5.1 or by applying (58) directly in (40). In either case, the results obtained appear in (13).

6 Randomly Oriented Inclusions

In this section, the matrix is assumed to be isotropic and the inclusions at most transversely isotropic in their respective local coordinate systems. The effective properties predicted by the Mori-Tanaka method follow from a modification of (40_1) and have the form (Benveniste 1987),

$$\mathbf{L} = \mathbf{L}_1 + \sum_{r=2}^{N} c_r\{(\mathbf{L}_r - \mathbf{L}_1)\mathbf{T}_r\}\left[\sum_{r=1}^{N} c_r\{\mathbf{T}_r\}\right]^{-1}. \tag{59}$$

Curly brackets $\{\Delta\}$ denote the average of Δ over all possible orientations. Note that all such averaged quantities in (59) are isotropic fourth-order tensors, even though the underlying tensor quantities, such as $\mathbf{T}_r$, need not be isotropic. Hill (1965c) and Walpole (1981) pointed out that any general isotropic tensor Λ is subject to the spectral decomposition

$$\Lambda = a\mathbf{J} + b\mathbf{K} \tag{60}$$

where a and b are certain scalars, and

$$J_{ijkl} = \frac{1}{3}\delta_{ij}\delta_{kl}, \ K_{ijkl} = \frac{1}{2}(\delta_{ik}\delta_{jl} + \delta_{il}\delta_{jk} - \frac{2}{3}\delta_{ij}\delta_{kl})$$
$$\mathbf{JJ} = \mathbf{J}, \ \mathbf{KK} = \mathbf{K}, \ \mathbf{JK} = \mathbf{KJ} = \mathbf{0}. \tag{61}$$

This invites the notation $\Lambda = (a, b)$, $\Lambda^{-1} = (1/a, 1/b)$ in lieu of that in (60).

To evaluate the overall elastic moduli (59), we recall the following result of Kröner (1958). For any fourth-order tensor Δ_{ijkl}, the orientation averaged quantity $\{\Delta\}$ can be expressed as

$$\{\Delta\} = (\alpha, \beta), \ \{\Delta\}^{-1} = \left(\frac{1}{\alpha}, \frac{1}{\beta}\right) \tag{62}$$

where the scalars α, β are given as

$$\alpha = \frac{1}{3}\Delta_{iijj}, \ \beta = \frac{1}{5}\Delta_{ijij} - \frac{1}{15}\Delta_{iijj}. \tag{63}$$

To apply this result to the $\mathbf{L}_r$ and $\mathbf{T}_r$ tensors we write

$$\{\mathbf{T}_r\} = (\alpha_r, \beta_r), \quad \{\mathbf{L}_r\mathbf{T}_r\} = (\delta_r, \eta_r) \tag{64}$$

and utilize it in (59) to arrive at the expressions for the effective bulk and shear moduli that appear in (14).

Certain simplifications are possible for two-phase media with isotropic constituents, where one can rewrite (59) as

$$\mathbf{L} = \mathbf{L}_2 + c_1\{\mathbf{L}_1 - \mathbf{L}_2\}[c_1\mathbf{I} + c_2\{\mathbf{t}_r\}]^{-1}. \tag{65}$$

Since both phases are isotropic then the first orientation average term in (65) becomes

$$\{\mathbf{L}_1 - \mathbf{L}_2\} = (3K_1 - 3K_2,\ 2G_1 - 2G_2) \tag{66}$$

where K_1, G_1 are matrix moduli.

7 Cylindrically Orthotropic Fibers

7.1 Replacement Fiber. With reference to the discussion in Section 3.4, we present the derivation of the effective longitudinal shear modulus p_f of a replacement fiber. Under remotely applied stress σ^0_{yz}, the admissible displacement field selected in the fiber, and the nonvanishing components of stress are (Chen, Dvorak, and Benveniste, 1990):

$$u_z^f = A^f r^q \sin\phi,\ \sigma_{rz}^f = G_{rz}A^f q r^{q-1}\sin\phi,\ \sigma_{\phi z}^f = G_{\phi z}A^f r^{q-1}\cos\phi, \tag{67}$$

where $q = \sqrt{G_{\phi z}/G_{rz}}$ for the original fiber, and $q = 1$ for the transversely isotropic replacement fiber. To insure that the local field in the outer phase does not change after replacement of the fiber, the interfacial quantities, u_z^f and σ_{rz}^f, must both be identical in the replacement fiber and in the original, cylindrically orthotropic fiber. Evaluation of this requirement leads to the equivalent longitudinal shear modulus of transversely isotropic fiber in the form listed in (30_3).

Moreover, the average stress $\bar{\sigma}_{yz}^f$ must have the same magnitude in both fibers. Evaluation of this condition provides the following expression for the effective longitudinal shear modulus of the replacement fiber:

$$p_f = \frac{G_{rz}q + G_{\phi z}}{q+1}. \tag{68}$$

It can be shown that (30_3) and (68) are identical, hence either represents the unique longitudinal shear modulus of the replacement fiber.

7.2 Evaluation of the Overall Transverse Shear Modulus m. In a homogeneous elastic medium subjected to a uniform field of simple shear deformation in the transverse xy-plane, the displacement components are defined by:

$$u_x = cx,\ u_y = -cy,\ u_z = 0, \tag{69}$$

where c is a constant. In cylindrical coordinates this becomes

$$u_r = cr\cos 2\phi,\ u_\phi = -cr\sin 2\phi,\ u_z = 0. \tag{70}$$

In analogy with (70), we assume that the displacement field in a cylindrically orthotropic medium under transverse shear has the general form:

$$u_r = U_r(r)\cos 2\phi,\ u_\phi = U_\phi(r)\sin 2\phi,\ u_z = 0, \tag{71}$$

where $U_r(r)$, $U_\phi(r)$ are unknown functions of r, which need to be determined from the equations of equilibrium in cylindrical coordinates. The requisite substitution provides the following equations for evaluation of $U_r(r)$, $U_\phi(r)$:

$$C_{rr}\frac{d^2U_r}{dr^2} + \frac{C_{rr}}{r}\frac{dU_r}{dr} - \left(\frac{4}{r^2}G_{r\theta} + \frac{1}{r^2}C_{\theta\theta}\right)U_r + \frac{2(C_{r\theta}+G_{r\theta})}{r}\frac{dU_\theta}{dr} - \frac{2}{r^2}(G_{r\theta}+C_{\theta\theta})U_\theta = 0 \tag{72}$$

$$-\frac{2(G_{r\theta}+C_{r\theta})}{r}\frac{dU_r}{dr} - \frac{2(G_{r\theta}+C_{\theta\theta})}{r^2}U_r + G_{r\theta}\frac{d^2U_\theta}{dr^2} + \frac{G_{r\theta}}{r}\frac{dU_\theta}{dr} - \frac{G_{r\theta}+4C_{\theta\theta}}{r^2}U_\theta = 0. \tag{73}$$

These can be solved analytically, the result is:

$$U_r(r) = 2[(G_{r\theta}+C_{\theta\theta}) - \eta_1(C_{r\theta}+G_{r\theta})]Ar^{\eta_1} + 2[(G_{r\theta}+C_{\theta\theta}) + \eta_1(C_{r\theta}+G_{r\theta})]Br^{\eta_1} + 2[(G_{r\theta}+C_{\theta\theta}) - \eta_2(C_{r\theta}+G_{r\theta})]Cr^{\eta_2} + 2[(G_{r\theta}+C_{\theta\theta}) + \eta_2(C_{r\theta}+G_{r\theta})]Dr^{-\eta_2} \tag{74}$$

$$U_\theta(r) = [C_{rr}\eta_1^2 - (4G_{r\theta}+C_{\theta\theta})]Ar^{\eta_1} + [C_{rr}\eta_1^2 - (4G_{r\theta}+C_{\theta\theta})]Br^{-\eta_1} + [C_{rr}\eta_2^2 - (4G_{r\theta}+C_{\theta\theta})]Cr^{\eta_2} + [C_{rr}\eta_2^2 - (4G_{r\theta}+C_{\theta\theta})]Dr^{-\eta_2} \tag{75}$$

where η_1^2 and η_2^2 are the roots of

$$C_{rr}G_{r\theta}\eta^4 + [4C_{r\theta}^2 + 8C_{r\theta}G_{r\theta} - 4C_{rr}C_{\theta\theta} - G_{r\theta}(C_{rr}+C_{\theta\theta})]\eta^2 + 9G_{r\theta}C_{\theta\theta} = 0,$$

and A, B, C, and D are certain constants.

In the Mori-Tanaka procedure, one must first solve an auxiliary problem for a single fiber in an infinite matrix volume. The displacements (71), (74), and (75) are admitted in the fiber domain, while the displacements in the matrix are special forms of (74) and (75) for a transversely isotropic or isotropic medium. In any event, to assure boundedness of the displacements at the origin, the terms which contain the negative powers of η_1 and η_2 must be excluded. The resulting admissible displacement field are best written in terms of the transverse normal stress σ^0 as

$$u_r^f = \frac{b\sigma^0}{4G_{r\theta}}\left\{2[(G_{r\theta}+C_{\theta\theta}) - \eta_1(C_{r\theta}+G_{r\theta})]a_1\left(\frac{r}{b}\right)^{\eta_1} + 2[(G_{r\theta}+C_{\theta\theta}) - \eta_2(C_{r\theta}+G_{r\theta})]c_1\left(\frac{r}{b}\right)^{\eta_2}\right\}\cos 2\phi \tag{76}$$

$$u_\phi^f = \frac{b\sigma^0}{4G_{r\theta}}\left\{[C_{rr}\eta_1^2 - (4G_{r\theta}+C_{\theta\theta})]a_1\left(\frac{r}{b}\right)^{\eta_1} + [C_{rr}\eta_2^2 - (4G_{r\theta}+C_{\theta\theta})]c_1\left(\frac{r}{b}\right)^{\eta_2}\right\}\sin 2\phi$$

$$u_z^f = 0$$

$$u_r^m = \frac{b\sigma^0}{4m^m}\left[\frac{2}{b}r + (\xi_m+1)\frac{b}{r}a_2 + \left(\frac{b}{r}\right)^3 c_2\right]\cos 2\phi$$

$$u_\phi^m = \frac{b\sigma^0}{4m^m}\left[-\frac{2}{b}r - (\xi_m-1)\frac{b}{r}a_2 + \left(\frac{b}{r}\right)^3 c_2\right]\sin 2\phi \tag{77}$$

$$u_z^m = 0,$$

where

$$\xi_m = (2m^m + k^m)/k^m,$$

and σ^0 is the normal transverse stress applied at infinity. As yet unknown constants a_1, a_2, c_1, and c_2 have been introduced to replace the A, B, C, D constants in (74) and (75). Since the matrix is regarded as transversely isotropic, we have used the connections between elastic constants to introduce the Hill's moduli k^m and m^m.

To complete the solution of the auxiliary problem, the four unknown constants must be evaluated from the usual continuity requirements for the stresses σ_{rr}, $\sigma_{r\phi}$ and the displacements u_r, u_ϕ at the interface $r = a$. However, the resulting equations are coupled, and are best solved numerically. Once the constants are known, the phase stress fields under overall transverse shear loading can be derived from the displacement fields (76) to (77), and the appropriate constitutive relations (1) or (4).

This completes the solution of the auxiliary problem, and opens the way to evaluation of the Mori-Tanaka estimate of the overall stiffness which contains the unknown transverse shear modulus m. Of course, the above solution delivers the auxiliary stress and strain fields in the phases in the cylindrical coordinate system, and both the fields and the phase moduli must be first transformed into the Cartesian system. As in Chen et al. (1990, Section 3), we denote the cylindrical system by the vector ξ, the fields themselves by primed letters $\sigma'(\xi)$ and $\epsilon'(\xi)$, and the phase properties in the ξ system by $\mathbf{L}'$, $\mathbf{M}'$. Note that the factor 2 must appear in the shear terms of the 6×1 strain vector. In the Cartesian coordinates, these quantities are denoted by similar but unprimed letters.

At any point in a given phase r, the transformation of the stress and strain fields between the current, cylindrical, and the Cartesian components is written as

$$\sigma_r(\mathbf{x}) = \mathbf{R}\sigma_r'(\epsilon), \qquad \epsilon_r(\mathbf{x}) = \mathbf{S}\epsilon_r'(\xi), \tag{78}$$

where, the transformation matrices $\mathbf{R}$ and $\mathbf{S}$ are related by $\mathbf{R}^T = \mathbf{S}^{-1}$. Of course, in a transformation between the cylindrical and Cartesian systems, $\mathbf{R}$ and $\mathbf{S}$ are functions of the angle ϕ. Next, write the phase constitutive relations, such as (4), in the symbolic form:

$$\sigma_r'(\xi) = \mathbf{L}_r'(\xi)\epsilon_r'(\xi), \ \epsilon_r'(\xi) = \mathbf{M}_r'(\xi)\sigma_r'(\xi). \tag{79}$$

Equations (78) and (79) provide the relations

$$\sigma_r(\mathbf{x}) = \mathbf{R}\mathbf{L}_r'\mathbf{S}^{-1}\epsilon_r(\mathbf{x}), \ \epsilon_r(\mathbf{x}) = \mathbf{S}\mathbf{M}_r'\mathbf{R}^{-1}\sigma_r(\mathbf{x}) \tag{80}$$

at each point $\mathbf{x}$. Note that $\mathbf{S}$, $\mathbf{R}$, $\mathbf{L}_r'$, $\mathbf{M}_r'$ may now be functions of $\mathbf{x}$, but for brevity in notation the argument will be omitted in the sequel.

The local fields in (80) are related to the uniform, remotely applied fields ϵ^0 and σ^0 through certain influence functions $\mathbf{A}_r(\mathbf{x})$, $\mathbf{B}_r(\mathbf{x})$; their volume averages, the mechanical concentration factors, appear in (34). Thus, under overall applied strain, (32_1), the local strain field in (80_2) may be replaced by the term $\mathbf{A}_r(\mathbf{x})\,\epsilon^0$, and the result substituted into the formal phase constitutive relation $\sigma_r = \mathbf{L}_r\epsilon_r$. When solved for r, the relation yields the result

$$\mathbf{L}_r = \left[\frac{1}{V_r}\int_{V_r} \mathbf{R}\mathbf{L}_r'\mathbf{S}^{-1}\mathbf{A}_r(\mathbf{x})dV_r\right]\mathbf{A}_r^{-1}. \tag{81}$$

A similar operation on the local stress field in (80_1), but under boundary conditions (32_2), leads to

$$\mathbf{M}_r = \left[\frac{1}{V_r}\int_{V_r} \mathbf{S}\mathbf{M}_r'\mathbf{R}^{-1}\mathbf{B}_r(\mathbf{x})dV_r\right]\mathbf{B}_r^{-1}. \tag{83}$$

The above transformation relations are valid for any actual composite material or its model. Of course, in the Mori-Tanaka model one can employ the expressions (39) for $\mathbf{A}_r$ and $\mathbf{B}_r$ to find

$$\mathbf{L}_r = \left[\frac{1}{V_r}\int_{V_r} \mathbf{R}\mathbf{L}_r'\mathbf{S}^{-1}\mathbf{T}_r(\mathbf{x})dV_r\right]\mathbf{T}_r^{-1},$$

$$\mathbf{M}_r = \left[\frac{1}{V_r}\int_{V_r} \mathbf{S}\mathbf{M}_r'\mathbf{R}^{-1}\mathbf{W}_r(\mathbf{x})dV_r\right]\mathbf{W}_r^{-1}. \tag{83}$$

Recall that the partial concentration factors and the underlying influence functions follow from the solution (77) of the auxiliary problem, and the transformation relations (78). When substituted into (83), they provide the necessary phase stiffnesses and concentration factors for evaluation of the overall stiffness and compliance in (40). Of course, the procedure yields all components of $\mathbf{L}$ and $\mathbf{M}$. However, the magnitudes of the moduli k, l, n, and p for the present system are already known from (30) and (8), (10), (11), and (12), and only the magnitude of m represents new information.

We note in passing that in a transversely isotropic solid with the x_1-axis of symmetry, the Hill's elastic moduli and the stiffness coefficients are related as follows:

$$L_{11} = n, \ L_{12} = L_{13} = l, \ L_{22} = L_{33} = k + m, \tag{84}$$
$$L_{23} = k - m, \ L_{44} = m, \ L_{55} = L_{66} = p.$$

8 Closure

The formulation of the Mori-Tanaka method does not guarantee diagonal symmetry of the estimated overall stiffness tensor. Indeed, it is easy to construct systems for which the predicted stiffness is not diagonally symmetric. However, Benveniste, Dvorak, and Chen (1991a,b) prove that the Mori-Tanaka estimates are symmetric in all two-phase systems of any geometry, and in those multiphase systems where all inclusions have the same shape and orientation, or the P tensor. Such proof was also constructed for the unidirectional composite reinforced by coated, cylindrically orthotropic fibers. This suggests that the present estimates of overall stiffness for all systems with aligned fibers or inclusions are diagonally symmetric. An analogous conclusion for the randomly orientated reinforcement is indicated by (65).

Both the Mori-Tanaka and the self-consistent methods provide approximations which are admissible only if they are bracketed by available Hashin-Shtrikman bounds. For the Mori-Tanaka method, this question was recently explored by Norris (1989), who shows that the effective moduli estimated by the Mori-Tanaka approximation for two-phase composites always satisfy the Hashin-Shtrikman and Hill-Hashin bounds. However, this property does not generalize to general multiphase composites. The status of the estimates for aligned platelet reinforced systems, and for multiphase random reinforcement, remains to be established.

Acknowledgment

This work has been supported by the ONR/DARPA-HiTASC program at Rensselaer.

Note: For more discussion of the Mori-Tanaka method, the reader is referred to the recent papers by Weng (1990) and Ferrari (1991).

References

Benveniste, Y., 1987, "A New Approach to the Application of Mori-Tanaka's Theory in Composite Materials," *Mech. Mat.*, Vol. 6, pp. 147–15[illegible].

Benveniste, Y., Dvorak, G. J., and Chen, T., 1989, "Stress Fields in Composites with Coated Inclusions," *Mech. Mat.*, Vol. 7, pp. 305–317.

Benveniste, Y., Dvorak, G. J., and Chen, T., 1991a, "On Diagonal and

Elastic Symmetry of the Approximate Effective Stiffness Tensor of Heterogeneous Media," *J. Mech. Phys. Solids*, Vol. 39, pp. 927-946.

Benveniste, Y., Dvorak, G. J., and Chen, T., 1991b, "On Effective Properties of Composites with Coated Cylindrically Orthotropic Fibers," *Mech. Mat.*, Vol. 12, pp. 289-297.

Berryman, J. G., 1980, "Long-Wavelength Propagation in Composite Elastic Media. II. Ellipsoidal Inclusions," *J. Acoust. Soc. Amer.*, Vol. 68, pp. 1820-1831.

Boucher, S., 1974, "On the Effective Moduli of Isotropic Two-Phase Elastic Composites," *J. Comp. Mat.*, Vol. 8, pp. 82-89.

Budiansky, B., 1965, "On the Elastic Moduli of Some Heterogeneous Materials," *J. Mech. Phys. Solids*, Vol. 13, pp. 223-227.

Chen, T., Dvorak, G. J., and Benveniste, Y., 1990, "Stress Fields in Composites Reinforced by Coated Cylindrically Orthotropic Fibers," *Mech. Mat.*, Vol. 9, pp. 17-32.

Christensen, R. M., and Waals, F. M., 1972, "Effective Stiffness of Randomly Oriented Fiber Composites," *J. Comp. Mat.*, Vol. 6, pp. 518-532.

Cleary, M. P., Chen, I. W., and Lee, S. M., 1980, "Self-Consistent Techniques for Heterogeneous Solids," *J. Engng. Mech.*, Vol. 106, pp. 861-887.

Eshelby, J. D., 1957, "The Determination of the Elastic Field of an Ellipsoidal Inclusion and Related Problems," *Proc. Roy. Soc. London*, Vol. A241, pp. 376-396.

Ferrair, M., 1991, "Asymmetry of the High Concentration Limit of the Mori-Tanaka Effective Medium Theory," *Mech. Mat.*, Vol. 11, pp. 251-256.

Hashin, Z., and Shtrikman, S., 1963, "A Variational Approach to the Theory of the Behavior of Multiphase Materials," *J. Mech. Phys. Solids*, Vol. 11, pp. 127-140.

Hashin, Z., 1990, "Thermoelastic Properties and Conductivity of Carbon/Carbon Fiber Composites," *Mech. Mat.*, Vol. 8, pp. 293-308.

Hill, R., 1963, "Elastic Properties of Reinforced Solids: Some Theoretical Principles," *J. Mech. Phys. Solids*, Vol. 11, pp. 357-372.

Hill, R., 1964, "Theory of Mechanical Properties of Fiber-Strengthened Materials: I. Elastic Behavior," *J. Mech. Phys. Solids*, Vol. 12, pp. 199-212.

Hill, R., 1965a, "Theory of Mechanical Properties of the Fibre-Strengthened Materials—III Self-Consistent Model," *J. Mech. Phys. Solids*, Vol. 13, pp. 189-198.

Hill, R., 1965b, "A Self-Consistent Mechanics of Composite Materials," *J. Mech. Phys. Solids*, Vol. 12, pp. 213-222.

Hill, R., 1965c, "Continuum Micro-Mechanics of Elastoplastic Polycrystals," *J. Mech. Phys. Solids*, Vol. 13, pp. 89-101.

Kröner, E., 1958, "Berechnung der elastischen Konstanten des Vielkristalls aus Konstanten des Einkristalls," *Z. Phys.*, Vol. 136, pp. 504-518.

Laws, N., 1974, "The Overall Thermoelastic Moduli of Transversely Isotropic Composites According to the Self-Consistent Method," *Int. J. Engng. Sci.*, Vol. 12, pp. 79-87.

Mori, T., and Tanaka, K., 1973, "Average Stress in Matrix and Average Elastic Energy of Materials with Misfitting Inclusions," *Acta Metal.* Vol. 21, pp. 571-574.

Norris, A. N., 1989, "An Examination of the Mori-Tanaka Effective Medium Approximation for Multiphase Composites," ASME JOURNAL OF APPLIED MECHANICS, Vol. 56, pp. 83-88.

Postma, G. W., 1955, "Wave Propagation in a Stratified Medium," *Geophysics*, Vol. 20, pp. 780-806.

Walpole, L. J., 1969, "On the Overall Elastic Moduli of Composite Materials," *J. Mech. Phys. Solids*, Vol. 17, pp. 235-251.

Walpole, L. J., 1981, "Elastic Behavior of Composite Material: Theoretical Foundations," *Advances in Applied Mechanics*, Vol. 21, C. S. Yih, ed., Academic Press, New York, pp. 170-242.

Walpole, L. J., 1984, "The Analysis of the Overall Elastic Properties of Composite Materials," *Fundamentals of Deformation and Fracture*, B. A. Bilby, K. J. Miller and J. R. Willis, eds., pp. 91-107.

Weng, G. J., 1984, "Some Elastic Properties of Reinforced Solids, with Special Reference to Isotropic Ones Containing Spherical Inclusions," *Int. J. Engng. Sci.*, Vol. 22, pp. 845-856.

Weng, G. J., 1990, "The Theoretical Connection Between Mori-Tanaka's Theory and the Hashin-Shtrikman-Walpole Bounds," *Int. J. Eng. Sci.*, Vol. 28, pp. 1111-1120.

Willis, J. R., 1981, "Variational and Related Methods for the Overall Properties of Composites," *Advances in Applied Mechanics*, Vol. 21, C. S. Yih, ed., Academic Press, New York, pp. 1-78.

Zhao, Y. H., Tandon, G. P., and Weng, G. J., 1989, "Elastic Moduli for a Class of Porous Materials," *Acta Mechanica*, Vol. 76, pp. 105-130.

Some Remarks on a Class of Uniform Fields in Fibrous Composites

Y. Benveniste[4] and G. J. Dvorak[5]

1 Introduction

In a series of recent papers, Dvorak (1983, 1986) pointed out that a one-parameter uniform strain field can be created in certain fibrous composite media of any transverse geometry by a superposition of a uniform overall stress with a uniform change in temperature. Moreover, under such superimposed loads, Dvorak and Chen (1989) found a uniform strain field in a three-phase fibrous composite, and Benveniste and Dvorak (1990a, 1990b) constructed uniform stress and strain fields in two-phase media of any geometry and phase material symmetry. Finally, Dvorak (1990a) identified uniform strain fields in both fibrous and general two-phase media of any phase material symmetry in the presence of arbitrary but uniform eigenstrains in the phases.

The existence of uniform strain fields is useful in solution of problems which involve phase eigenstrains, e.g., thermal, swelling, or plastic strains. If such eigenstrains are or are taken as uniform, then it is possible to evaluate an auxiliary uniform overall stress state which will change the initial strain field into a uniform strain field in the entire volume. Of course, the auxiliary stress needs to be removed, but that can be accomplished in a purely mechanical loading step. In this way, eigenstrain problems may be converted into much simpler mechanical loading problems. For example, thermoplasticity problems in composite media can be solved as mechanical problems along a modified loading path. Many other applications of the technique can be found in Dvorak (1990a, 1990b).

This Note is concerned with Dvorak's (1986) paper, where a one-parameter family of uniform strain fields was created in a binary fibrous composite through a uniform temperature change and proportional mechanical loading. The parameter can be selected in many different ways, the actual choice in Dvorak (1986) related the longitudinal normal stress and the transverse hydrostatic stress in the matrix through a scalar parameter ρ. The results included a derivation of the instantaneous effective thermal expansion coefficients of two-phase composite aggregates with plastically deforming matrices. Even though the derivation utilized an arbitrary parameter, it was expected that the resulting effective thermal expansion coefficients would be independent of that parameter. This was verified in Dvorak (1986) by numerical examples, but not established analytically. Moreover, since the overall expansion coefficients depend on some overall moduli, the examples had to make recourse to approximate micromechanical models for evaluation of such moduli.

The present Note gives an analytical proof of the independence of Dvorak's (1986) final result for the overall thermal expansion coefficients on the free parameter ρ. Although Dvorak's analysis applies to fibrous systems with transversely isotropic phases, we restrict ourselves to the simpler case of isotropic phases. First, the Note presents a simplified derivation of the relevant results of the (1986) paper. Then, an analytical proof shows that these results are independent of the parameter ρ. The proof is completely general and does not rely on any micromechanical model. Finally, it is shown that the thermal expansion coefficients found with the uniform fields technique coincide with those derived by Levin (1967) from the virtual work theorem. This supplements a similar conclusion reached by a different route in Dvorak (1990a), and confirms that the uniform field technique, while offering a much more extensive scope in applications, gives results in agreement with those that follow from Levin's approach.

2 Analysis

Let us consider a binary composite consisting of an isotropic matrix reinforced by perfectly bonded, aligned, isotropic cylindrical fibers of arbitrary cross-section. A Cartesian coordinate system is chosen with the x_3-axis aligned with the direction of the fibers. As pointed out by Dvorak (1986), a uniform strain field and a piecewise uniform stress field can be created in this binary composite by superposition of a uniform temperature change with certain auxiliary tractions on the external boundary. Let the desired uniform fields be denoted by $\hat{\sigma}_{ij}^s$ and $\hat{\epsilon}_{ij}^s$ with $s = f, m$ for the fiber and matrix, respectively. They must satisfy the traction and displacement continuity at the cylindrical fiber-matrix interfaces. Since the fields are uniform, the continuity requirements are met if the fields conform to the following conditions:

$$\hat{\sigma}_{11}^f = \hat{\sigma}_{11}^m = \hat{\sigma}_{22}^m = \hat{\sigma}_{22}^f = \hat{\sigma} \tag{1}$$

$$\hat{\epsilon}_{33}^f = \hat{\epsilon}_{33}^m, \quad \hat{\epsilon}_{11}^f = \hat{\epsilon}_{11}^m, \quad \hat{\epsilon}_{22}^f = \hat{\epsilon}_{22}^m. \tag{2}$$

The shear strain and stress components of the auxiliary fields vanish in the present situation. The $\hat{\sigma}_{33}^f$ and $\hat{\sigma}_{33}^m$ need not be equal to each other, but are also uniform within each phase. In other words, the $\hat{\sigma}_{33}$ stresses are piecewise constant in the fibrous composite, while all the other strains and stresses are uniform throughout.

We now appeal to the familiar thermoelastic constitutive relations, and express the phase strains in (2) under the constraints indicated by (1). Thus, Eq. $(2)_1$ results in

$$(\hat{\sigma}_{33}^f/E_f) - (2\nu_f/E_f)\hat{\sigma} + \alpha_f\theta_0 = (\hat{\sigma}_{33}^m/E_m) - (2\nu_m/E_m)\hat{\sigma} + \alpha_m\theta_0 \tag{3}$$

where E_s, ν_s, α_s with $s = f, m$ denote, respectively, the Young's modulus, Poisson's ratio, and the thermal expansion coeffi-

[4]Department of Solid Mechanics, Materials and Structures, Faculty of Engineering, Tel-Aviv University, Ramat-Aviv 69978, Israel. Also, Visiting Professor, Rensellaer Polytechnic Institute, Troy, NY 12180.

[5]Institute Center for Composite Materials and Structures, Rensselaer Polytechnic Institute, Troy, NY 12180. Fellow ASME.

Manuscript received by the ASME Applied Mechanics Division, Oct. 5, 1990; final revision, Aug. 6, 1991. Associate Technical Editor: L. M. Keer.

cient of the matrix and fiber, respectively; θ_0 is the uniform temperature change. Similarly, under (1), Eqs. $(2)_2$ and $(2)_3$ become

$$\left(\frac{1-\nu_f}{E_f}\right)\hat{\sigma}-\frac{\nu_f}{E_f}\hat{\sigma}^f_{33}+\alpha_f\theta_0=\left(\frac{1-\nu_m}{E_m}\right)\hat{\sigma}-\frac{\nu_m}{E_m}\hat{\sigma}^m_{33}+\alpha_m\theta_0. \quad (4)$$

For a given temperature change, (3) and (4) provide two equations for the three unknown components $\hat{\sigma}$, $\hat{\sigma}^f_{33}$, $\hat{\sigma}^m_{33}$ of the piecewise uniform stress field. This suggests that an additional relation may be prescribed between these unknowns. In accordance with Dvorak (1986), we chose

$$\hat{\sigma}^m_{33}=\rho\hat{\sigma}, \quad (5)$$

where ρ is an arbitrary parameter. From (3), (4), and (5) one readily obtains

$$\hat{\sigma}^f_{33}=\hat{\sigma}\{1+[(1+\nu_m)E_f(\rho-1)/(1+\nu_f)E_m]\} \quad (6)$$

$$\hat{\sigma}=\frac{(1+\nu_f)(\alpha_f-\alpha_m)\theta_0}{[1-\nu_m-2\nu_m\nu_f+\rho(\nu_f-\nu_m)]/E_m+(1+\nu_f)(2\nu_f-1)/E_f}. \quad (7)$$

Therefore, for any finite value of ρ, uniform fields can be created in the fibrous composite by application of the stresses (5) and (6) on planes x_3 = constant, together with tractions resulting from $\hat{\sigma}$ on the lateral surface, and by a uniform temperature change θ_0 throughout. These uniform fields can be used to derive the effective thermoelastic constants of the composite.

At this stage we focus our attention on a fibrous composite which is transversely isotropic on the macroscale and is subjected to a uniform temperature change, while its external surface is kept traction-free. By definition, the longitudinal and transverse thermal expansion coefficients of the composite are given by

$$\alpha_L\theta_0=c_f\bar{\epsilon}^f_{33}+c_m\bar{\epsilon}^m_{33} \quad (8)$$

$$\alpha_T\theta_0=c_f\bar{\epsilon}^f_{11}+c_m\bar{\epsilon}^m_{11}=c_f\bar{\epsilon}^f_{22}+c_m\bar{\epsilon}^m_{22} \quad (9)$$

where an overbar denotes an average over the volume of respective phases and c_s, $s = f, m$ are the volume fractions.

The thermal strains on the left-hand side of (8) and (9) can be derived from the uniform strain field. This is accomplished by an application of a loading/unloading sequence where the loading consists of θ_0 and $\hat{\sigma}_{ij}$, and the unloading is a subtraction of the average surface tractions, which have been induced by $\hat{\sigma}_{ij}$. Then, (8) and (9) may be rewritten as

$$\alpha_L\theta_0=\hat{\epsilon}_{33}-(c_f\hat{\sigma}^f_{33}+c_m\rho\hat{\sigma})/E_L+(2\nu_L/E_L)\hat{\sigma} \quad (10)$$

$$\alpha_T\theta_0=\hat{\epsilon}_{11}-[(1-\nu_T)/E_T]\hat{\sigma}+(\nu_L/E_L)(c_m\rho\hat{\sigma}+c_f\hat{\sigma}^f_{33}), \quad (11)$$

where E_L, E_T, ν_L, and ν_T are, respectively, the effective longitudinal and transverse Young's moduli and longitudinal and transverse Poisson's ratios of the transversely isotropic fibrous composite.

The expressions for $\hat{\sigma}$, $\hat{\sigma}^f_{33}$ and $\hat{\epsilon}^f_{33}$, $\hat{\epsilon}^f_{11}$ obtained in (6), (7), (3), and (4), render Eqs. (10) and (11) in the form

$$\alpha_L=\alpha_m+(\alpha_f-\alpha_m)(1+\nu_f)(A_L+B_L\rho)/(C_L+D_L\rho) \quad (12)$$

$$\alpha_T=\alpha_m+(\alpha_f-\alpha_m)(1+\nu_f)(A_T+B_T\rho)/(C_T+D_T\rho), \quad (13)$$

where

$$A_L=-\left[\frac{2\nu_m}{E_m}-\frac{2\nu_L}{E_L}\right]-\frac{c_f}{E_L}\left[1-\frac{(1+\nu_m)E_f}{(1+\nu_f)E_m}\right],$$

$$B_L=\frac{1}{E_m}-\frac{1}{E_L}\left[c_m+c_f\frac{(1+\nu_m)E_f}{(1+\nu_f)E_m}\right],$$

$$C_L=\left[\frac{1}{E_m}(1-\nu_m-2\nu_m\nu_f)+\frac{1}{E_f}(1+\nu_f)(2\nu_f-1)\right],$$

$$D_L=(\nu_f-\nu_m)/E_m \quad (14)$$

$$A_T=\frac{1-\nu_m}{E_m}-\frac{1-\nu_T}{E_T}+\frac{\nu_L}{E_L}c_f\left[1-\frac{(1+\nu_m)E_f}{(1+\nu_f)E_m}\right]$$

$$B_T=-\frac{\nu_m}{E_m}+\frac{\nu_L}{E_L}\left[c_m+c_f\frac{(1+\nu_m)E_f}{(1+\nu_f)E_m}\right],$$

$$C_T=C_L, \quad D_T=D_L. \quad (15)$$

At this stage we ask whether the results (12) and (13) are independent of the arbitrary parameter ρ, and whether these expressions can be reduced to the following well-known formulae, originally derived by a different approach by Levin (1967)

$$\alpha_L=\alpha_m+\frac{\alpha_f-\alpha_m}{\left[\frac{1}{K_f}-\frac{1}{K_m}\right]}\left[\frac{3(1-2\nu_L)}{E_L}-\frac{1}{K_m}\right] \quad (16)$$

$$\alpha_T=\alpha_m+\frac{\alpha_f-\alpha_m}{\left[\frac{1}{K_f}-\frac{1}{K_m}\right]}\left[\frac{3}{2k}-\frac{3(1-2\nu_L)\nu_L}{E_L}-\frac{1}{K_m}\right], \quad (17)$$

where

$$K_s=E_s/[3(1-2\nu_s)] \text{ with } s=f,m, \quad (18)$$

and k denotes the effective plane-strain bulk modulus for lateral dilatation without axial extension.

In what follows, the equivalence between (12)–(13) and (16)–(17), respectively, is established by recalling first Hill's (1964) universal relations between the effective moduli of a binary, transversely isotropic fibrous composite with cylindrical, transversely isotropic phases. Two of these relations which will be needed here are (see, for example, Hashin, 1983):

$$E_L=(c_fE_f+c_mE_m)+\left(4(\nu_f-\nu_m)^2\left(\frac{c_f}{k_f}+\frac{c_m}{k_m}-\frac{1}{k}\right)\Big/\left(\frac{1}{k_f}-\frac{1}{k_m}\right)^2\right) \quad (19)$$

$$\nu_L=(c_f\nu_f+c_m\nu_m)-\left((\nu_f-\nu_m)\left(\frac{c_f}{k_f}+\frac{c_m}{k_m}-\frac{1}{k}\right)\Big/\left(\frac{1}{k_f}-\frac{1}{k_m}\right)\right) \quad (20)$$

where

$$k_s^{-1}=2(1+\nu_s)(1-2\nu_s)E_s^{-1} \text{ with } s=f,m, \quad (21)$$

and k is the same effective modulus appearing in (17). Equations (19) and (20) allow one to write

$$E_L=a+b\nu_L, \quad \frac{1}{k}=c+d\nu_L \quad (22)$$

with

$$a=(c_fE_f+c_mE_m)+\left\{[4(\nu_f-\nu_m)(c_f\nu_f+c_m\nu_m)]/\left(\frac{1}{k_f}-\frac{1}{k_m}\right)\right\}$$

$$b=\frac{4(\nu_m-\nu_f)}{\left[\frac{1}{k_f}-\frac{1}{k_m}\right]}, \quad c=\left(\frac{\nu_f}{k_m}-\frac{\nu_m}{k_f}\right)/(\nu_f-\nu_m),$$

$$d=-4/b. \quad (23)$$

Let us now show the equivalence of (12) and (16). To this end we first express ν_L in terms of E_L and the constituent properties through $(22)_1$. Then, (18) allows one to cast (16) into the form

$$\alpha_L = \alpha_m + \left[\frac{1+\nu_f}{\nu_f-\nu_m} - \frac{1}{E_L}\left(\frac{c_f(1+\nu_m)E_f}{\nu_f-\nu_m} + \frac{c_m(1+\nu_f)E_m}{\nu_f-\nu_m}\right)\right](\alpha_f-\alpha_m) \quad (24)$$

which involves only E_L as the single effective elastic modulus.

Application of the same procedure to (14_1) makes it possible to express the constant A_L in terms of constituents properties and E_L only. It is now clear that for the parameter ρ to disappear altogether from (12), the following relation must hold between A_L, B_L, C_L, and D_L:

$$A_L/C_L = B_L/D_L, \quad (25)$$

which results in

$$(A_L + B_L\rho)/(C_L + D_L\rho) = B_L/D_L. \quad (26)$$

Some algebra shows that (25) is indeed fulfilled, and it becomes then an easy matter to verify that one can use (26), together with $(14)_2$ and $(14)_4$ to reduce Eq. (12) identically to (24).

Establishing the equivalence between (13) and (17) is similar in principle to the procedure described previously. We start by using (22) in conjunction with (18) and (21) and choose this time to cast (17) in terms of the constituent properties and ν_L only. After considerable manipulation, (17) can be written in the form

$$\alpha_T = \alpha_m + (\alpha_f-\alpha_m)(e+f\nu_L)/(a+b\nu_L) \quad (27)$$

where a and b are given by (23) and

$$e = a[-\nu_m(1+\nu_f)/(\nu_f-\nu_m)], \quad f = f_1 + c_f f_2 \quad (28)$$

with

$$f_1 = \frac{2(1+\nu_f)k_m[2k_f\nu_m(\nu_f-\nu_m) - (1+\nu_m)(2\nu_m-1)(k_m-k_f)]}{(k_m-k_f)(\nu_f-\nu_m)} \quad (29)$$

$$f_2 = -(1+\nu_f)(1+\nu_m)[2k_m^2(1+\nu_m)(1-2\nu_m) + 2k_f^2(1+\nu_f)(1-2\nu_f) + k_mk_f(8\nu_m\nu_f - 4 + 2\nu_m + 2\nu_f)] / \{(\nu_f-\nu_m)[(1+\nu_m)k_m - k_f(1+\nu_f)]\}. \quad (30)$$

Next we turn to Eq. (13). In analogy to (25) and (26), what now needs to be established is that

$$A_T/C_T = B_T/D_T \quad \text{or} \quad A_T/B_T = C_T/D_T \quad (31)$$

or

$$(A_T + B_T\rho)/(C_T + D_T\rho) = B_T/D_T \quad (32)$$

so that ρ disappears from (13). Furthermore, it needs to be shown that

$$(1+\nu_f)(B_T/D_T) = (e+f\nu_L)/(a+b\nu_L). \quad (33)$$

The ratio C_T/D_T in $(31)_2$ easily follows from (15_1), (15_2), $(14)_3$, $(14)_4$ as

$$C_T/D_T = [E_m(1+\nu_f)(2\nu_f-1) + E_f(1-\nu_m-2\nu_m\nu_f)]/[E_f(\nu_f-\nu_m)] \quad (34)$$

which is seen not to contain any effective moduli. On the other hand, the expression A_T/B_T in $(31)_2$ does contain the effective constants ν_T, E_T, ν_L, and E_L as seen from $(14)_5$ and $(16)_6$.

At this stage, we recall the identity (see, for example, Hashin, 1983, Eq. 3.2.4)

$$(1-\nu_T)/E_T = [E_L + 4k\nu_L^2]/(2kE_L), \quad (35)$$

and make use of $(22)_1$ and (22) to express all the effective moduli in $(15)_1$ and $(15)_2$ in terms of ν_L only. The ratio A_T/B_T can eventually be written as

$$A_T/B_T = [(1+\nu_L h)/(1+\nu_L j)](C_T/D_T) \quad (36)$$

where

$$h = b/a - (E_m d - 2c_f g/a)[2(1-\nu_m) - cE_m]^{-1}$$
$$g = E_m\left[1 - \frac{(1+\nu_m)E_f}{(1+\nu_f)E_m}\right] \quad (37)$$
$$j = -(E_m - \nu_m b - c_f g)/(\nu_m a),$$

and a, b, c, d, are given by (23).

To establish the validity of $(31)_2$, it needs to be shown that $h = j$; this follows after some algebra from (23) and (37).

Finally, to prove the validity of (33), B_T in $(14)_6$ needs to be expressed in terms of ν_L and the constituents properties from $(22)_1$. Then, the expressions for a, b, e, f which were derived in (23) and (28) lead, after considerable manipulation, to Eq. (33). This shows that (33) is indeed valid.

3 Conclusion

In summary, we have shown that Eqs. (12) and (13) derived by the procedure described in Dvorak's (1986) paper are indeed independent of the free parameter ρ, and that they reduce properly to the forms (16) and (17) originally derived by Levin (1967). Of course, the proof has been constructed only for the case of isotropic constituents, whereas Dvorak's results also apply to transversely isotropic phases. Extension of the proof to such systems should be possible, but it if beyond our present scope.

Acknowledgment

This work was supported by the DARPA-HiTASC program at Rensselaer Polytechnic Institute.

References

Benveniste, Y., and Dvorak, G. J., 1990a, "On a Correspondence Between Mechanical and Thermal Effects in Two-Phase Composites," *Micromechanics and Inhomogeneity*, (Toshio Mura Anniversary Volume), G. J. Weng, M. Taya, and H. Abe, eds., Springer-Verlag, New York, pp. 65–81.

Benveniste, Y., and Dvorak, G. J., 1990b, "On a Correspondence Between Mechanical and Thermal Fields in Composites with Slipping Interfaces," *Inelastic Deformation of Composite Materials*, G. J. Dvorak, ed., IUTAM Symposium, Troy, NY, May 29–June 1, 1990, Springer-Verlag, New York, pp. 77–98.

Dvorak, G. J., 1983, "Metal Matrix Composites: Plasticity and Fatigue," *Mechanics of Composite Materials: Recent Advances*, Z. Hashin and C. Herakovich, eds., Pergamon Press, New York, pp. 73–92.

Dvorak, G. J., 1986, "Thermal Expansion of Elastic-Plastic Composite Materials," ASME JOURNAL OF APPLIED MECHANICS, Vol. 53, pp. 737–743.

Dvorak, G. J., 1986, "Thermomechanical Deformation and Coupling in Elastic-Plastic Composite Materials," *Thermomechanical Couplings in Solids*, H. D. Bui and Q.S. Nguyen, North-Holland, Amsterdam, pp. 43–54.

Dvorak, G. J., and Chen, T., 1989, "Thermal Expansion of Three-Phase Composite Materials," ASME JOURNAL OF APPLIED MECHANICS, Vol. 56, pp. 418–422.

Dvorak, G. J., 1990a, "On Uniform Fields in Heterogeneous Media," *Proceedings of the Royal Society, London*, Vol. A431, pp. 89–110.

Dvorak, G. J., 1990b, "Plasticity Theories for Fibrous Composite Materials," *Metal Matrix Composites*, R. J. Arsenault and R. K. Everett, eds., Academic Press, Boston, MA.

Hashin, Z., 1983, "Analysis of Composite Materials," ASME JOURNAL OF APPLIED MECHANICS, Vol. 50, pp. 481–505.

Hill, R., 1964, "Theory of the Mechanical Properties of Fiber-Strengthened Materials—1. Elastic Behavior," *Journal of the Mechanics and Physics of Solids*, Vol. 12, pp. 199–212.

Levin, V. M., 1967, "Thermal Expansion Coefficients of Heterogeneous Materials," *Mekhanika Tverdogo Tela*, Vol. 2, pp. 88–94, (English translation: *Mechanics of Solids*, Vol. 11, pp. 58–61).

The American Society of Mechanical Engineers

Reprinted From
AD – Vol. 25 – 2, Damage and Oxidation Protection in High Temperature Composites
Editors: G. K. Haritos, and O. O. Ochoa
Book No. H0692B – 1991

LOCAL FIELDS IN UNCOATED AND COATED HIGH TEMPERATURE FIBROUS COMPOSITE SYSTEMS

Yehia A Bahei-El-Din and George J. Dvorak
Department of Civil Engineering
Institute Center for Composite Materials and Structures
Rensselaer Polytechnic Institute
Troy, New York

ABSTRACT

Local stresses caused by mechanical and thermal loads in high temperature intermetallic matrix composites are evaluated using a finite element solution for a periodic hexagonal array microstructure. Both uncoated and coated elastic fibers are considered. The matrix is assumed to be elastic–plastic and insensitive to loading rates. Mechanical properties of the phases are function of temperature. It was found that a CVD deposited carbon coating can be quite effective in reducing thermal stresses at the matrix/coating interface. Certain mechanical stress concentration factors, however, may be aggravated by the compliant coating. In composite systems with a ductile matrix, plastic deformations reduce stress concentration and lead to stress redistribution. In such systems, thermomechanical loading regimes can be designed to reduce adverse local stresses introduced during fabrication, for example, by hot isostatic pressing.

INTRODUCTION

It is well known that the overall behavior of fibrous composites is directly affected by the local phenomena. For example, the overall performance of a composite may be impaired if damage or instability is initiated in the phases or at their interfaces. On the other hand, the overall strength may be enhanced by plastic flow of the matrix. Therefore, evaluation of local stresses in fibrous composites is important in material selection, evaluation and design under both thermal and mechanical loads.

The present paper is concerned with evaluation of the local stresses in high temperature fibrous composites under thermomechanical loads. Specifically, the stresses in uncoated and coated fiber reinforced intermetallic matrix composites are examined. For unidirectional composites, the analysis was performed for an idealised geometry of the microstructure using the Periodic Hexagonal Array (PHA) model (Dvorak and Teply, 1985; Teply and Dvorak, 1988). This geometry permits selection of a representative unit cell, the response of which is identical with the response of the composite aggregate under overall uniform stress or strain fields. The overall response and local fields are then found in the unit cell using the finite element method.

The results reported in this paper focus on the effect of fiber coating on the local thermal and mechanical stress concentration factors in elastic as well as elastic–plastic matrices. Thermal residual stresses generated by cooldown of unidirectional composites from fabrication temperatures are also evaluated. The present study examines various thermomechanical loading regimes that may be applied during the fabrication process to reduce the tensile stresses in the matrix.

The paper begins with a brief description of the PHA model for unidirectionally reinforced composites. Next, material properties for the composite system examined in this study are given. Two principal results obtained with the PHA model for intermetallic matrix composites reinforced by uncoated and coated fibers are then presented and discussed. One is concerned with the effect of fiber coating on thermal and mechanical stresses, the other examines the effect of the thermomechanical loading regime applied during fabrication of composites by hot isostatic pressing on the local stresses.

THE COMPOSITE MODEL

Several material models have been developed for elastic–plastic fibrous composites under various approximations of the microgeometry. While averaging models, such as the self–consistent model (Hill, 1965) and the Mori–Tanaka (1973) method, approximate the microgeometry by a single inclusion embedded in an infinite mass of a different material, periodic models (Aboudi, 1986; Dvorak and Teply, 1985; Nemat–Nasser et al., 1982) consider actual details of the microstructure. The latter class of models assumes certain periodic arrangements of the fiber in the transverse plane of the composite and performs the analysis on a unit representative cell of the periodic microstructure. Other models which are phenomenological in nature have been also developed (see for example the Vanishing Fiber Diameter (VFD) model by Dvorak and Bahei–El–Din, 1982; and the Bimodal Plasticity Theory (BPT) by Dvorak and Bahei–El–Din, 1987) but are more suitable for prediction of the overall response of composites. A survey of the above models can be found in the reviews by Bahei–El–Din and Dvorak (1989) and Dvorak (1991).

An essential requirement in the theoretical model used in the present study is the ability to represent details of the local stress and strain fields in the phases of a unidirectionally reinforced composite subjected to uniform overall stress and thermal change. This narrows down our choices to the periodic models. In particular, we employed the PHA model developed by Dvorak and Teply (1985) and Teply and Dvorak (1988) which we have verified experimentally (Dvorak et al., 1988; Dvorak et al., 1990). In this model, the microstructural geometry in the transverse plane of a unidirectionally reinforced fibrous composite is represented by a periodic distribution of the fibers in a hexagonal array. Cross section of the fibers is approximated by a nx6–sided polygon. An example of the PHA microgeometry with dodecagonal fiber cross section is shown in Fig. 1a. The hexagonal array shown in Fig. 1a is divided into two unit cells, as indicated by the shaded and unshaded triangles. Under overall uniform stresses or strains, the two sets of unit cells have related internal fields. Accordingly, under properly prescribed periodic boundary conditions, only one unit cell from either set needs to be analyzed. Figure 1b shows a three dimensional view of one of the unit cells.

The actual analysis is performed by the finite element method. The unit cell is subdivided into a selected number of subelements in the matrix, fiber, and coating subdomains. A fairly refined subdivision is required for evaluation of the local fields. Figure 2 shows two examples of such a finite element mesh. The results reported here were found with the ABAQUS finite element program. Resident constitutive relations were used for the homogeneous phases. The fiber and the coating were assumed elastic, whereas the matrix was assumed elastic–plastic, inviscid, and follows the Mises yield criterion. Stress–plastic strain response of the matrix was assumed to follow a linear strain hardening behavior, and the matrix yield surface to follow the Prager–Ziegler kinematic hardening rule. Thermoelastic properties of the phases as well as the matrix yield stress and plastic tangent modulus are piecewise linear functions of temperature.

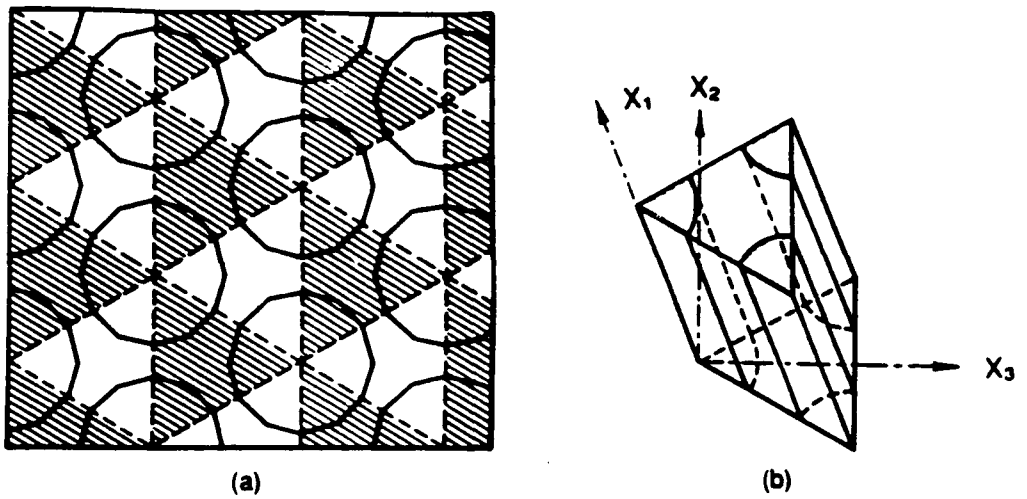

Fig. 1 Microgeometry of the Periodic Hexagonal Array (PHA) model, (a) Transverse plane, (b) Unit cell.

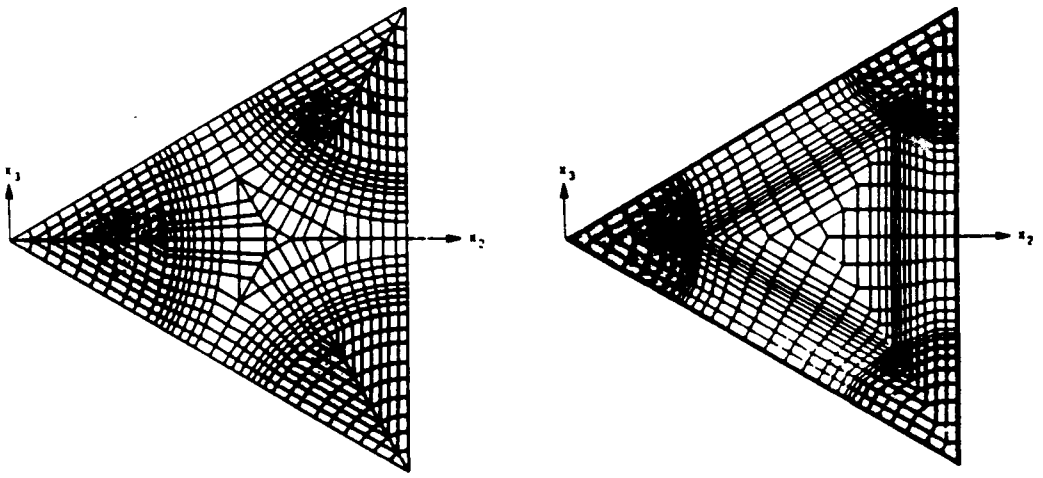

Fig. 2 Two refined meshes of the PHA unit cell.

THE COMPOSITE SYSTEM

An intermetallic matrix composite system reinforced by aligned continuous fibers is considered. The matrix is a nickel–aluminide compound ($Ni_3A\ell$), and the reinforcement is a carbon–coated or uncoated silicon–carbide fiber (SCS6) at 25% volume fraction. The carbon coating thickness is 10 μm. Tables 1 and 2 show material properties of the phases. Thermoelastic constants of the silicon–carbide fiber and the carbon coating are not function of temperature, while those of the nickel–aluminide matrix vary with temperature. Also, the yield stress and the plastic tangent modulus of the $Ni_3A\ell$ compound vary with temperature. Figure 3 shows variation of the tensile yield stress with temperature for the $Ni_3A\ell$ matrix. Unlike other aluminide compounds, for example $Ti_3A\ell$, for which the yield stress increases monotonically with decreasing temperature (see Fig. 3), the yield stress of the nickel–aluminide compound decreases with decreasing temperature if the latter is below 600°C. This causes plastic deformation of the matrix during cooldown of $Ni_3A\ell$–based system which may help in reducing the adverse thermal residual stresses.

RESULTS

Effect of Fiber Coating on Local Stresses

To examine the effect of fiber coating on the local thermal and mechanical stresses, we plotted stress contours in the unit cell for the transverse local stress σ_{22}. Figures 4 and 5 show the results for the SCS6/$Ni_3A\ell$ composite in the elastic range under thermal loading and overall transverse tension, respectively. It was assumed that the composite is stress free at the fabrication temperature of 1200°C, and small increments of a temperature decrease and transverse tensile stress were applied separately. The local stress σ_{22} found from finite element solution of the unit cell was then normalized by the applied load and plotted in the transverse plane. The unit cell is indicated in Figs. 4 and 5 by the dashed triangular boundary. The contours outside the unit cell were generated using the periodic properties of the local stress field.

It is seen from Fig. 4a that tensile hoop stresses, and compressive radial stresses develop in the matrix if the temperature is decreased, whereas compressive hoop stresses develop in the fiber. These stresses are caused by the mismatch between the thermal strains generated in the fiber and the matrix. At the fiber/matrix interface in the system under consideration, the matrix tends to move in the volume occupied by the fiber when the temperature is decreased, but is prevented by the stiff fiber which deforms at a much smaller temperature rate. Consequently, radial cracks may develop in the matrix under cooling from the fabrication temperature. If, on the other hand, the coefficient of thermal expansion of the fiber was larger than that of the matrix, local damage under temperature reduction would take the form of disbonds at the fiber/matrix interface, and radial cracks in the fibers.

Applying a carbon coat to the fiber causes significant reductions in the local thermal stresses, particularly at the fiber/matrix interface, Fig. 4b. Compared to the matrix and the fiber, the carbon coating has a much smaller elastic stiffness in the transverse plane, and as such it can accommodate the thermal strains developed in the phases. Conversely, the coating enhances sharply the mechanical transverse stresses as seen in Fig. 5. This tradeoff must be carefully considered in design of composites.

If the matrix deforms plastically, the local stresses are reduced substantially, particularly under thermal loads. This is seen in the contours plotted in Figs. 6 and 7 after loading the composite well into the plastic region so that the matrix subdomain is fully plastic. In this case, the matrix is very much compliant compared to the fiber and therefore can deform without developing large stresses. In fact, the stiffness of the matrix in the plastic range is comparable to the stiffness of the carbon coating so that the differences in the stresses developing in the coated and the uncoated systems are not significant.

These results indicate that material selection may favor uncoated fibrous systems with ductile matrices over coated elastic systems. Under repeated loads, however, low cycle fatigue may develop in the matrix under cyclic plastic straining leading to nucleation of small cracks. Certain tradeoffs therefore exist and must be applied in material selection and evaluation.

Table 1 Material properties of SCS6 fiber and carbon coating

	E_L[1] GPa	E_T[2] GPa	G_L[3] GPa	G_T[4] GPa	ν_L[5]	α_L[6]	α_T[7]
						$(10^{-6}/°C)$	
SCS6 fiber	413.6	413.6	159.1	159.1	0.3	4.6	4.6
Carbon coating	172.4	6.9	14.5	3.8	0.3	1.8	28

[1]Longitudinal Young's modulus
[2]Transverse Young's modulus
[3]Longitudinal shear modulus
[4]Transverse shear modulus
[5]Longitudinal Poisson's ratio
[6]Longitudinal coefficient of thermal expansion
[7]Transverse coefficient of thermal expansion

Table 2 Material properties of $Ni_3A\ell$ matrix (Stoloff, 1989)

T[1] °C	E[2] GPa	ν[3]	α[4] $10^{-6}/°C$	Y[5] MPa	H[6] GPa
1200	134	0.32	20.6	137	6.70
994	142	0.32	19.0	279	7.10
776	150	0.32	17.2	459	7.50
673	154	0.32	16.4	557	7.70
642	155	0.32	16.1	564	7.75
578	158	0.32	15.6	535	7.90
376	165	0.32	14.3	356	8.25
327	167	0.32	14.0	279	8.35
206	172	0.32	13.4	156	8.60
127	175	0.32	13.0	110	8.75
21	179	0.32	12.5	79	8.95

[1]Temperature
[2]Young's modulus
[3]Poisson's ratio
[4]Coefficient of thermal expansion
[5]Tensile yield stress
[6]Tensile plastic tangent modulus

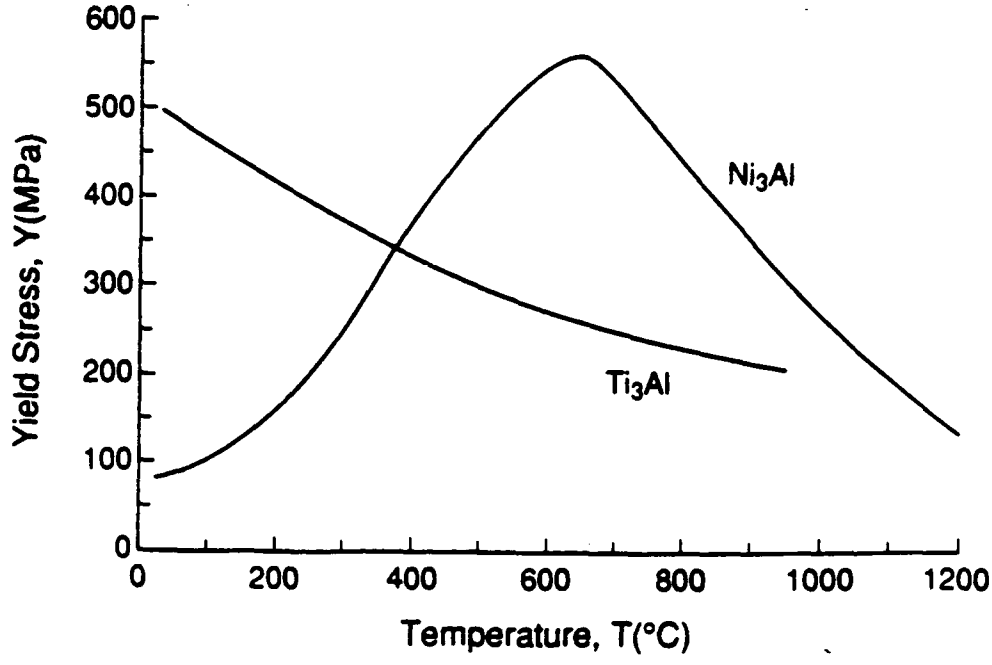

Fig. 3 Yield stress–temperature curve for $Ni_3A\ell$ and $Ti_3A\ell$ compounds.

Effect of Fabrication Parameters on Residual Stresses

This part of our study of local stresses in fibrous system is concerned with evaluation of the thermal residual stresses generated during fabrication and examination of possible thermomechanical loading regimes that can be applied during cooldown to room temperature so that high tensile thermal stresses in the matrix can be reduced. The results presented in the preceding section indicate that plastic flow of the matrix causes redistribution of the local stresses and reduction of the interfacial stresses in the matrix. Consequently, in fabrication of intermetallic matrix composites by hot isostatic pressing (HIP), one can select the optimum temperature/pressure path to follow so as to minimize the adverse local stresses in the phases, particularly the matrix. This, of course, can be accomplished only for composites with a ductile matrix.

Considering the SCS6/$Ni_3A\ell$ composite, we first examined the local stresses retained in the system at room temperature after exposure to HIP temperature of 1200°C and hydrostatic pressure, σ_o, of 200 MPa when the room temperature/zero pressure condition is reached through the various unloading options shown in Fig. 8. In particular, we compared the magnitude of the local interfacial stresses in the phases of uncoated and coated systems for the various cases listed in Fig. 8. In each case, the composite was assumed to be free of internal stresses at the fabrication temperature (1200°C), and the hydrostatic pressure σ_o was applied in small increments up to 200 MPa. Although the overall load applied in this segment of the loading path is isotropic, the matrix stress is not necessarily isotropic. Nonetheless, the matrix isotropic stress was dominant so that the matrix phase, which was assumed to be plastically incompressible, remained elastic under 200 MPa hydrostatic pressure and 1200°C. In a typical HIP process, the composite is treated at the HIP condition for a specific duration. In our simulation, however, we assumed that the matrix is inviscid, and continued to unload the composite from the HIP conditions to the room temperature and atmospheric pressure. Plastic flow of the nickel–aluminide matrix occurred in all the cases shown in Fig. 8 but the onset of yielding varied among these cases. The local stresses retained in the composite at room temperature are, therefore, expected to vary as well among the loading cases shown in Fig. 8.

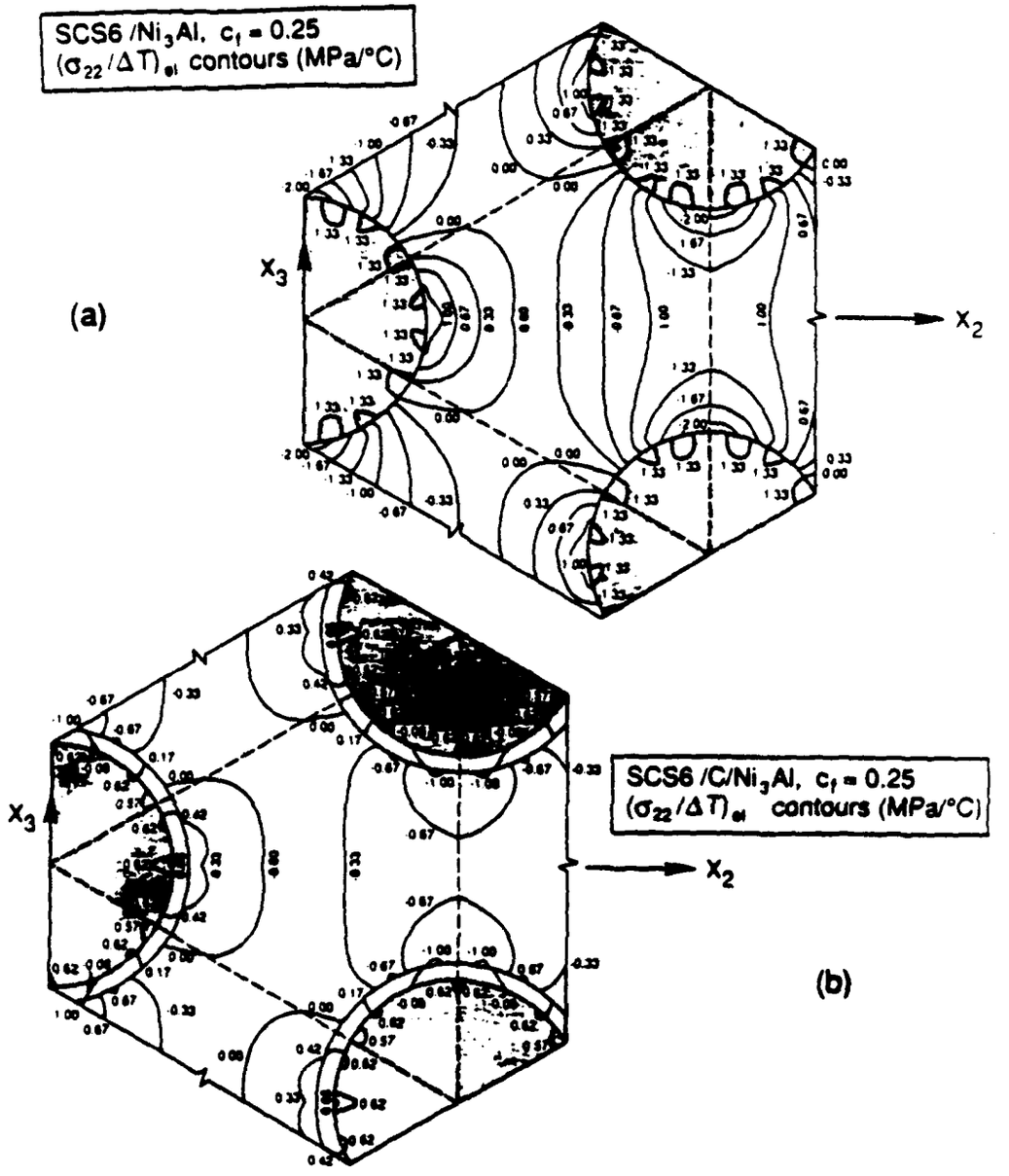

Fig. 4 Transverse thermal stress concentration factors computed in a *SCS6/Ni₃Al* composite in the elastic range, (a) uncoated fiber, (b) carbon–coated fiber.

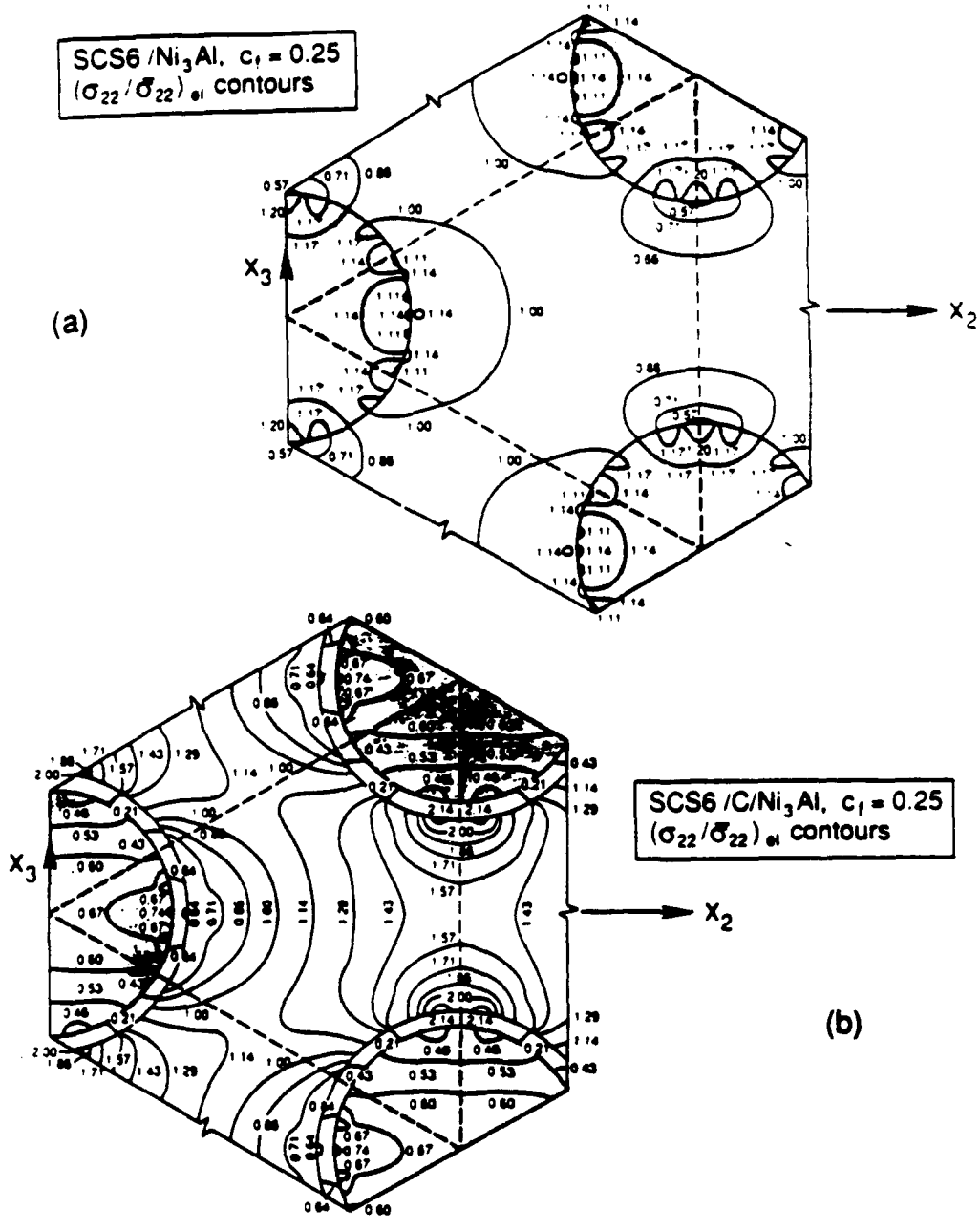

Fig. 5 Transverse mechanical stress concentration factors computed in a SCS6/Ni_3Al composite in the elastic range under overall transverse tension, (a) uncoated fiber, (b) carbon–coated fiber.

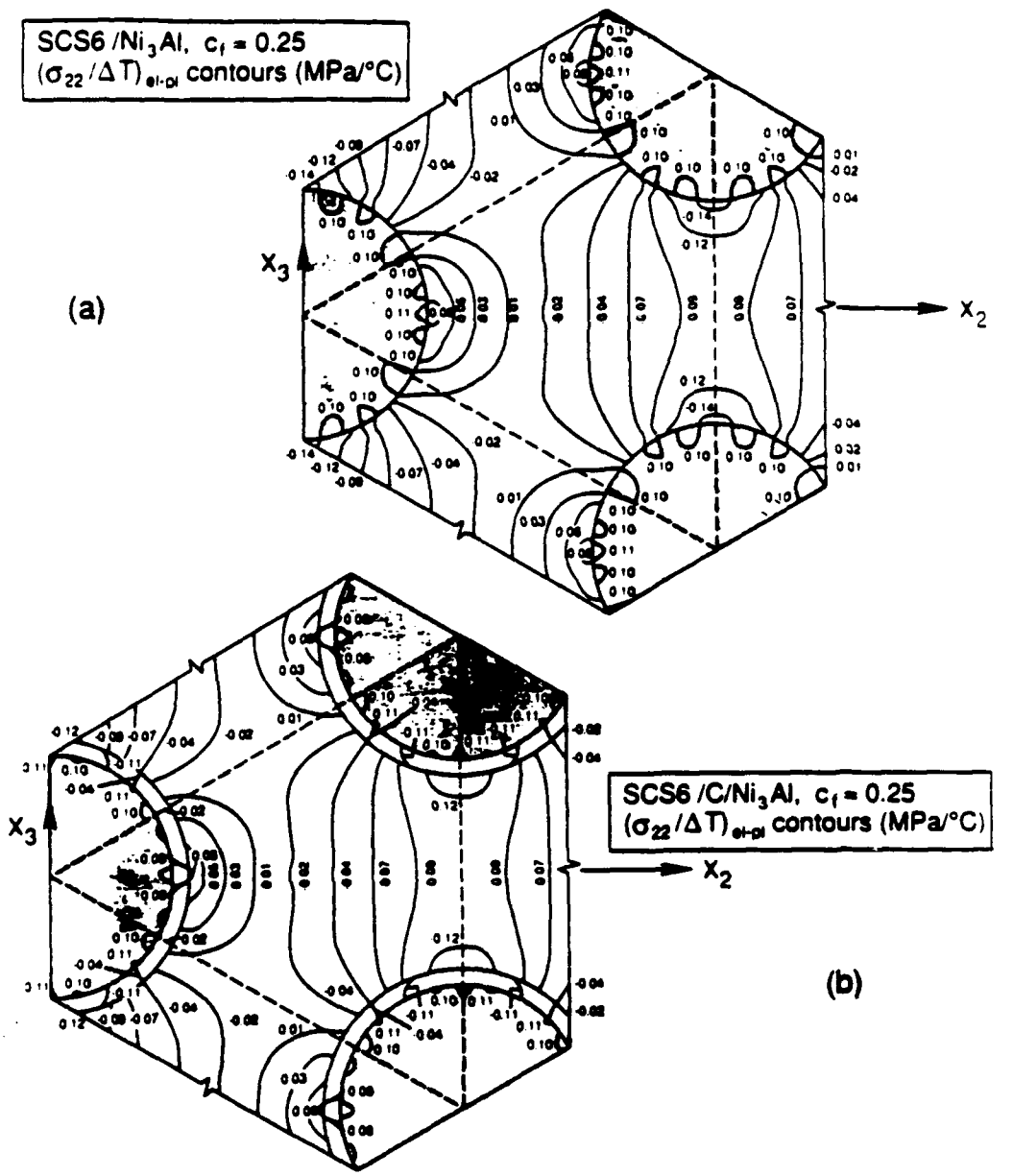

Fig. 6 Transverse thermal stress concentration factors computed in a SCS6/Ni_3Al composite in the elastic–plastic range, (a) uncoated fiber, (b) carbon–coated fiber.

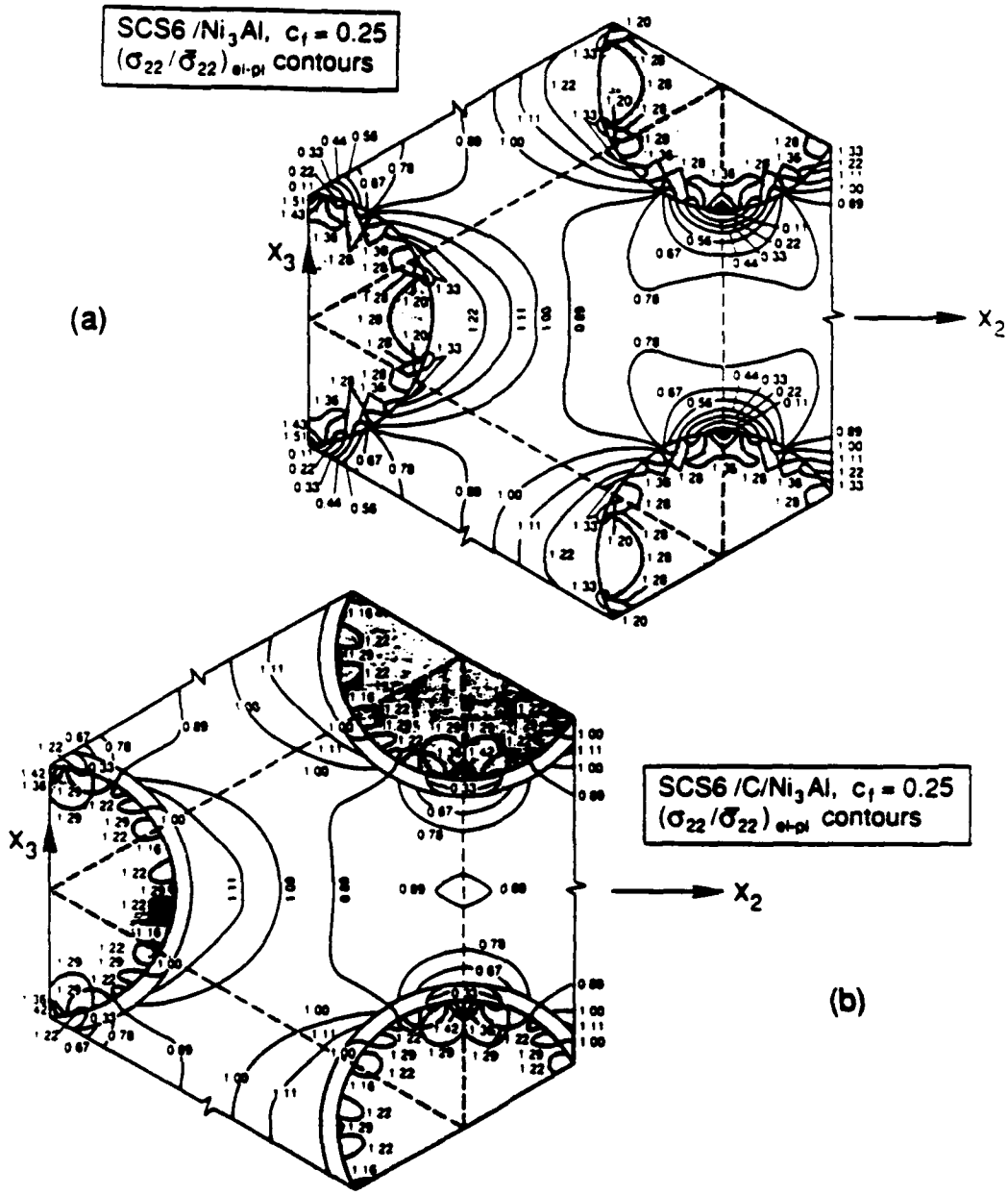

Fig. 7 Transverse mechanical stress concentration factors computed in a SCS6/Ni_3Al composite in the elastic–plastic range under overall transverse tension, (a) uncoated fiber, (b) carbon–coated fiber.

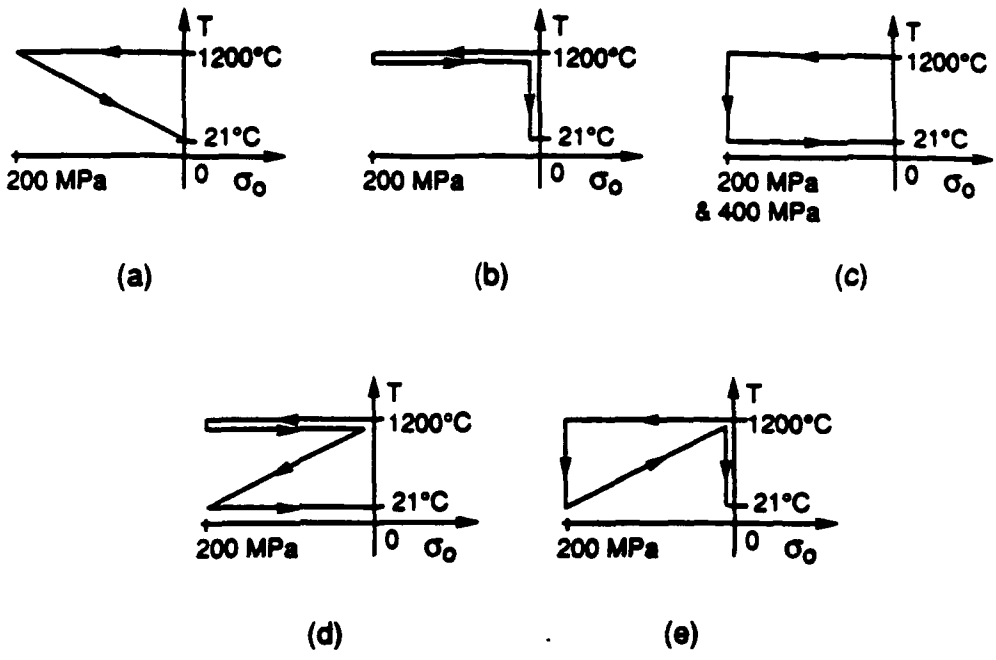

Fig. 8 Possible variations of the temperature/hydrostatic pressure loading path applied to unidirectional composites during hot isostatic pressing.

Comparing the magnitude of the local interfacial stresses in the phases of the uncoated and the coated SCS6/$Ni_3A\ell$ composite, we found that the stresses computed in cases (a), (b), (d)–(e), Fig. 8, are very similar. On the other hand, the adverse stresses were substantially reduced when the hydrostatic pressure, σ_o, was sustained during cooldown of the composite, Fig. 8c. Moreover, the stresses benefit from increasing the magnitude of the hydrostatic pressure applied during the HIP process. Specifically, the tensile stresses found in the phases were reduced substantially when σ_o was increased from 200 MPa to 400 MPa.

Table 3 compares the interfacial stresses computed in uncoated and coated SCS6/$Ni_3A\ell$ composites when the thermomechanical loading paths shown in Figs. 8a,c were applied. The stresses found in case (c) under hydrostatic pressure of 200 MPa and 400 MPa are shown. The table lists the radial stress, σ_{rr}, tangential stress, σ_{tt}, and axial stress, σ_{ll}, found at the interface at either point 'a' or point 'b' indicated on the unit cell shown in the inset in Table 3. The isotropic stress in the matrix, $(\sigma_o)_m$, found in each case is also indicated. It is seen that the tensile stresses at the fiber/matrix interface have been reduced in the uncoated composite by maintaining the hydrostatic pressure while cooling the composite down to room temperature. More reductions in the tensile stresses are achieved by elevating the hydrostatic stress to 400 MPa. For example, the matrix hoop stress is reduced by 18% when the pressure is 200 MPa, and by 37% when the pressure is 400 MPa. It appears that the tensile stresses can be reduced further by increasing the hydrostatic pressure during the HIP process. However, the magnitude of the pressure that can be applied during fabrication is usually limited by the equipment used in the HIP process.

The matrix interfacial tensile stresses in the coated system have been also reduced, but to a lesser extent, by following the loading path indicated in Fig. 8c, Table 3. The hoop stress in the coating, however, is not affected by the thermomechanical path applied during fabrication. Except for the axial stress, elevating the pressure applied during the

Table 3 Maximum interfacial stresses found in a SCS6/$Ni_3A\ell$ composite at room temperature following hot isostatic pressing

Interfacial Stress (MPa)	Uncoated Fiber	Coated Fiber	Uncoated Fiber	Coated Fiber	Uncoated Fiber	Coated Fiber
$(\sigma_{rr})_m$	–98●b	–84●b	–79●b	–94●b	–60●b	–91●b
$(\sigma_{tt})_m$	190●b	158●b	155●b	152●b	120●b	152●b
$(\sigma_{ll})_m$	198●b	186●b	179●b	143●b	161●b	141●b
$(\sigma_{tt})_c$	–	185●a	–	188●a	–	188●a
$(\sigma_{ll})_c$	–	–668●b	–	–633●b	–	–624●b
$(\sigma_{rr})_f$	–98●b	–110●b	–79●b	–122●b	–60●b	–121●b
$(\sigma_{tt})_f$	–94●a	–108●a	–76●a	–117●a	–59●a	–116●a
$(\sigma_{ll})_f$	–605●b	–364●b	–552●b	–280●b	–500●b	–261●b
$(\sigma_o)_m$	97●b	87●b	85●b	67●b	74●b	67●b

Table 4 Matrix internal stresses found in a SCS6/$Ni_3A\ell$ composite at room temperature following hot isostatic pressing

Stress at 'c' (MPa)	Uncoated Fiber	Coated Fiber	Uncoated Fiber	Coated Fiber	Uncoated Fiber	Coated Fiber
$(\sigma_{ll})_m$	213	213	195	179	177	177
$(\sigma_2)_m$	115	128	96	162	76	164
$(\sigma_o)_m$	101	105	90	106	79	106

HIP process does not affect the stresses in the coated system. In any case, the matrix isotropic stress, and consequently damage initiation, is affected by the thermomechanical loading path followed during the HIP run.

Table 4 lists the local stresses found in the matrix internal point 'c' (see inset of unit cell). The axial stress, $(\sigma_{11})_m$, the transverse stress, $(\sigma_{22})_m$, and the isotropic stress, $(\sigma_o)_m$, are shown for three thermomechanical loading regimes applied during the HIP process. It is seen that the stresses in the uncoated system are affected by the HIP regime. Substantial reductions in the matrix stresses are achieved by cooling down the composite under constant pressure, and by elevating the hydrostatic pressure applied during the HIP run. While these factors reduce the matrix axial stress in the coated system, the transverse stress is increased and the isotropic stress is unchanged.

The stresses found in the phases after the composite was reheated to 1200°C were not affected by the loading path, or the magnitude of the hydrostatic pressure, σ_o, applied during the HIP process.

DISCUSSION

A particular CVD deposited carbon coating can be quite effective in reducing the adverse thermal residual stresses generated during fabrication of fibrous composites. The fiber coating, however, enhances certain local mechanical stresses. In any case, the significance of these effects depends on the relative stiffness of the matrix, the fiber, and the coating. In particular, plastic flow of the matrix causes substantial reductions in the tensile interfacial stresses in the phases. The implication is that mechanical compatibility in fibrous composites is not only a function of the thermal properties of the phases, but also depends on the constitutive behavior of the phases. Accurate evaluation of thermal residual stresses, therefore, can be only performed with appropriate micromechanical models.

Plastic flow of the matrix can be utilized to reduce the tensile local stresses generated during hot isostatic pressing (HIP) of fibrous composites. Selection of the temperature/pressure path as well as the magnitude of the hydrostatic pressure applied during the HIP treatment should focus on inducing plastic deformation in the matrix early during the cooldown cycle. In our study of the local stresses in a unidirectional SCS6/$Ni_3A\ell$ composite we found that the matrix interfacial tensile stresses are lowest when the isotropic pressure applied during the HIP process was maintained during cooling to room temperature. Also the local stresses can be reduced by increasing the HIP isotropic pressure. Our yet unpublished results indicate that more reductions in the thermal residual stresses can be achieved through plastic deformation of the matrix if the hydrostatic pressure applied during the HIP process is confined to the composite's transverse plane. The results which qualify this proposition are published elsewhere (Bahei–EL–Din et al., 1991).

ACKNOWLEDGEMENT

This work was supported, in part, by the Air Force Office of Scientific Research, the Office of Naval Research, and the DARPA–HiTASC program at RPI. Dr. J.F. Wu assisted in the finite element calculations using the ABAQUS program.

REFERENCES

Aboudi, J., 1986, "Elastoplasticity Theory for Composite Materials," *Solid Mech. Archives*, Vol. 11, pp. 141–183.

Bahei–El–Din, Y.A., and Dvorak, G.J., 1989, "A Review of Plasticity Theory of Fibrous Composite Materials," *Metal Matrix Composites: Testing, Analysis, and Failure Modes*, ASTM STP 1032, W.S. Johnson, ed., American Society for Testing and Materials, Philadelphia, pp. 103–129.

Bahei–El–Din, Y.A., Dvorak, G.J., and Wu, J.F., 1991, "Fabrication Stresses in High Temperature Fibrous Composites with Ductile Matrices," to be published.

Dvorak, G.J., 1991 "Plasticity Theories for Fibrous Composite Materials," *Metal Matrix Composites, Vol. 2, Mechanisms and Properties*, R.K. Everett and R.J. Arsenault, eds., Academic Press, Boston, pp. 1–77.

Dvorak, G.J., and Bahei–El–Din, Y.A., 1982, "Plasticity Analysis of Fibrous Composites," *J. Appl. Mech.*, Vol. 49, pp. 327–335.

Dvorak, G.J., and Bahei–El–Din, Y.A., 1987, "A Bimodal Plasticity Theory of Fibrous Composite Material," *Acta Mechanica*, Vol. 69, pp. 219–241.

Dvorak, G.J., Bahei–El–Din, Y.A., Macheret, Y., and Liu, C.H., 1988, "An Experimental Study of Elastic–Plastic Behavior of a Fibrous Boron–Aluminum Composite," *J. Mech. Phys. Solids*, Vol. 36, pp. 655–687.

Dvorak, G.J., Bahei–El–Din, Y.A., Shah, R.S., and Nigam, H., 1990, "Experiments and Modeling in Plasticity of Fibrous Composites," *Inelastic Deformation of Composite Materials*, G.J. Dvorak, editor, Springer–Verlag, New York, Inc., pp. 270–293.

Dvorak, G.J., and Teply, J.L., 1985, "Periodic Hexagonal Array Models for Plasticity of Composite Materials," *Plasticity Today: Modeling, Methods and Applications*, A. Sawczuk and V. Bianchi, eds., Elsevier, Amsterdam, pp. 623–642.

Hill, R., 1965, "Theory of Mechanical Properties of Fiber–Strengthened Materials–III, Self–Consistent Model," *J. Mech. Phys. Solids*, Vol. 13, pp. 189–198.

Mori, T., and Tanak, K., 1973, "Average Stress in Matrix and Average Elastic Energy of Materials with Misfitting Inclusions," *Acta Metal.*, Vol. 21, pp. 571–574.

Nemat–Nasser, S., Iwakuma, T., and Hejazi, M., 1982, "On Composites with Periodic Structure," *Mech. of Materials*, Vol. 1, pp. 239–267.

Stoloff, N.S., 1989, "The Physical and Mechanical Metallurgy of Ni_3Al and its Alloys," *Intl. Materials Reviews*, Vol. 34.

Teply, J.L., and Dvorak, G.J., 1988, "Bounds on Overall Instantaneous Properties of Elastic–Plastic Composites," *J. Mech. Phys. Solids*, Vol. 36, pp. 29–58.

International Journal of Plasticity, Vol. 8, pp. 867-892, 1992
Printed in the USA

0749-6419/92 $5.00 + .00

UNIFORM FIELDS, YIELDING, AND THERMAL HARDENING IN FIBROUS COMPOSITE LAMINATES

YEHIA A. BAHEI-EL-DIN[1]

Cairo University

Abstract—A uniform strain field is found in fibrous composite laminates with isotropic matrix and transversely isotropic fiber under uniform phase thermal strains and overall uniform stresses which are functions of thermoelastic properties of the phases. The only restriction on the structure of the laminate is that the plies be identical except for the fiber orientation. Thermoelastic properties of the phases are functions of temperature. The resulting uniform strain field in the laminate is isotropic. The corresponding stress field is uniform and isotropic in the transverse plane of each lamina and piecewise uniform in the longitudinal direction. In any case, the matrix stress is isotropic which causes no plastic deformation in plastically incompressible materials. The solution leads to a correspondence between thermal and mechanical loads in laminates which converts, in an exact way, any thermomechanical loading path to an equivalent mechanical path. Application of the thermomechanical uniform fields to initial yielding of composites identifies thermal hardening of the overall yield surface with translation along a stress vector that is a function of the phase thermal strains. Examples of thermal hardening in intermetallic matrix composite laminates are shown.

1. INTRODUCTION

It is well known that the stress and strain fields in heterogeneous media subjected to uniform boundary conditions are, in general, not uniform. The existence of uniform fields in heterogeneous media, particularly two-phase fibrous composites, under overall uniform fields and phase thermal strains has been shown in many publications (DVORAK [1983,1986,1987]; DVORAK & CHEN [1989]; BENVENISTE & DVORAK [1990]). A general evaluation of uniform fields in two-phase media of arbitrary geometry has been worked out recently by DVORAK [1990a]. It was shown that local uniform stress or strain fields can be created by uniform phase eigenstrains and certain uniform overall stress or strain fields which are functions of the eigenstrains. Moreover, DVORAK [1990a] found that a uniform strain field can be created by overall stress or strain fields that have one free parameter that can be selected at will. These uniform fields have several applications in fibrous composite media. A particularly useful result, which was found by DVORAK [1983,1990a] and BENVENISTE and DVORAK [1990] for two-phase media, is the correspondence between thermal and mechanical loads.

The present study is concerned with evaluation of uniform fields in fibrous composite laminates and their application to thermomechanical loading and yielding problems. The problem can be stated as follows: if the phases of several identical laminae, which are bonded together with variable fiber orientation to form a symmetric laminate, are subjected to uniform thermal strains, we wish to find a strain state that is spatially uniform in the plane of the laminate. Since the laminae have different fiber orientations, the requirement of uniform in-plane strains implies that the strains must be isotropic in the plane of the laminate.

[1]Formerly research associate professor, Department of Civil and Environmental Engineering, Rensselaer Polytechnic Institute, Troy, NY, USA.

The solution to this problem can be found by a decomposition procedure that utilizes the uniform fields found by BENVENISTE and DVORAK [1990] and DVORAK [1990a] for unidirectional composites. The procedure consists of decomposition of the laminate into separate plies and application of the temperature change to each individual ply. Existing solutions for uniform strains in unidirectional composites under phase eigenstrains are then used to reassemble the laminate maintaining a uniform strain field in each ply. In certain cases, the strain fields found in the different plies are not compatible due to the variation in fiber orientation. In these cases, another uniform strain field is created by mechanical loads applied to the individual layers and superimposed on the strain field created by the phase thermal strains. The lamina stresses are found from compatibility of the total strain field in the plane of the laminate. Finally, the laminate overall stress is determined from equilibrium with the lamina stresses.

Section II evaluates uniform strain fields in unidirectional fibrous composites and laminates under phase thermal strains. The solution leads to a correspondence between thermal and mechanical loads in laminates which is introduced in section III. Section IV is devoted to evaluation of overall yielding in laminates where a general description of the overall yield surface is given and followed by a specific evaluation using the bimodal theory (DVORAK & BAHEI-EL-DIN [1987]). Using the uniform fields constructed in laminates, the effect of temperature variations on the overall yield surface is determined in section V. Finally, examples showing the effect of cool-down from fabrication temperatures on the bimodal yield surfaces of specific intermetallic matrix composites are given in section VI.

Throughout this study, (6×1) vectors are denoted by boldface, lowercase Greek or Latin letters. A superimposed prime on a boldface, lowercase Greek or Latin letter denotes a (3×1) vector, whereas unprimed boldface, uppercase Latin letters denote (3×3) matrices, unless otherwise indicated. The transpose of a matrix $\mathbf{A}$ is denoted $\mathbf{A}^T$, and the inverse is denoted $\mathbf{A}^{-1}$. Scalars are denoted by lightface letters. The customary indicial and contracted notations are interchangeably used for stress and strain components.

II. UNIFORM FIELDS IN FIBROUS MEDIA

II.1. *Unidirectional composites*

Consider a unidirectionally reinforced lamina consisting of an elastic cylindrical fiber aligned parallel to the $\tilde{x}_1$-axis of a Cartesian coordinate system, and embedded in an elastic matrix. The $\tilde{x}_2\tilde{x}_3$-plane coincides with the transverse plane of the fibrous lamina. The two phases are assumed to be homogeneous and perfectly bonded. A transversely isotropic fiber and an isotropic matrix with thermoelastic constants that vary with temperature are considered. The total phase strain $\boldsymbol{\epsilon}_r$ caused by a uniform stress $\boldsymbol{\sigma}_r$ and a temperature change θ from a reference temperature θ_0 is given by

$$\boldsymbol{\epsilon}_r = \mathbf{M}_r(\theta)\boldsymbol{\sigma}_r + \int_{\theta_0}^{\theta} \mathbf{m}'_r(\theta)\, d\theta, \tag{1}$$

where $\mathbf{M}_r$ is the elastic compliance matrix corresponding to the current temperature and $\mathbf{m}'_r$ is a list of the coefficients of thermal expansion of the phase. The incremental form of (1) is found as

$$d\boldsymbol{\epsilon}_r = \mathbf{M}_r(\theta)\, d\boldsymbol{\sigma}_r + \mathbf{m}_r(\boldsymbol{\sigma}_r, \theta)\, d\theta, \tag{2}$$

$$\mathbf{m}_r(\sigma_r, \theta) = \frac{d\mathbf{M}_r(\theta)}{d\theta}\,\sigma_r + \mathbf{m}_r'(\theta). \tag{3}$$

The thermomechanical coupling implied by the first term in (3) is due to variation of the elastic compliance with temperature during application of the thermal change $d\theta$. This, however, does not suggest that the response is path dependent. On the contrary, the accumulated mechanical and thermal strains found by integration of (2) and (3) over a specified thermomechanical loading path are uncoupled and independent of the thermomechanical loading sequence, eqn (1). To avoid this kind of ambiguity, our derivation of the uniform fields will, in some instances, start with evaluation of cumulative fields and then derive the incremental form of the solution.

Assuming the unidirectional lamina to be free of internal stresses, we first consider a temperature change $(\theta - \theta_0)$, and find a uniform strain field in the entire composite. This can be achieved by the following decomposition sequence, which was outlined by BENVENISTE and DVORAK [1990] and DVORAK [1990a]. Separate the fiber and matrix phases from each other and apply the uniform thermal strain given by the second term of (1). To reassemble the composite, the phases must be compatible. This is achieved by applying to each phase unknown tractions derived from the auxiliary uniform stress field

$$\hat{\boldsymbol{\sigma}}_f^a(\bar{\mathbf{x}}) = \hat{\boldsymbol{\sigma}}_m^a(\bar{\mathbf{x}}) = \hat{\boldsymbol{\sigma}}^a, \tag{4}$$

such that the total strain is uniform. Hence,

$$\hat{\boldsymbol{\epsilon}}_f^a(\bar{\mathbf{x}}) = \hat{\boldsymbol{\epsilon}}_m^a(\bar{\mathbf{x}}) = \hat{\boldsymbol{\epsilon}}^a. \tag{5}$$

From (1), (4), and (5_1), the overall stress $\hat{\boldsymbol{\sigma}}^a$ is found as

$$\hat{\boldsymbol{\sigma}}^a = [\mathbf{M}_f(\theta) - \mathbf{M}_m(\theta)]^{-1} \int_{\theta_0}^{\theta} [\mathbf{m}_m'(\theta) - \mathbf{m}_f'(\theta)]\, d\theta. \tag{6}$$

The increment of the auxiliary stress can be found by differentiating (6) after premultiplying both sides of the equation by the matrix $[\mathbf{M}_f(\theta) - \mathbf{M}_m(\theta)]$. Hence,

$$d\hat{\boldsymbol{\sigma}}^a = [\mathbf{M}_f(\theta) - \mathbf{M}_m(\theta)]^{-1} [\mathbf{m}_m(\hat{\boldsymbol{\sigma}}^a, \theta) - \mathbf{m}_f(\hat{\boldsymbol{\sigma}}^a, \theta)]\, d\theta, \tag{7}$$

where $\mathbf{m}_r$, $r = f, m$, is given by (3). Using the explicit form of the elastic compliance matrices $\mathbf{M}_f$ and $\mathbf{M}_m$ and the coefficients of thermal expansion $\mathbf{m}_f'$, $\mathbf{m}_m'$ for transversely isotropic fiber and isotropic matrix, we find that the auxiliary stress in (6) is axisymmetric and vector $\mathbf{m}_r$, eqn (3), has a transversely isotropic form. Hence, the incremental auxiliary stress field given by (7) is also axisymmetric:

$$d\hat{\sigma}_1^a = dS_A^a = s_A^a\, d\theta, \qquad d\hat{\sigma}_2^a = d\hat{\sigma}_3^a = dS_T^a = s_T^a\, d\theta, \qquad d\hat{\sigma}_j^a = 0, \quad j = 4,5,6. \tag{8}$$

The coefficients s_A^a and s_T^a are found from (3), (7) as

$$s_A^a = \frac{a\Delta m_L - 2b\Delta m_T}{(ac - 2b^2)}, \qquad s_T^a = \frac{-b\Delta m_L + c\Delta m_T}{(ac - 2b^2)}, \tag{9}$$

$$a = \frac{n_f}{2k_f E_L^f} - \frac{(1 - \nu_m)}{E_m}, \qquad b = \frac{-\nu_L^f}{E_L^f} + \frac{\nu_m}{E_m}, \qquad c = \frac{1}{E_L^f} - \frac{1}{E_m}, \tag{10}$$

$$\Delta m_L = m_L^f - m_L^m = \frac{dc}{d\theta} S_A^a + 2\frac{db}{d\theta} S_T^a + \beta_L^f - \beta_m, \tag{11}$$

$$\Delta m_T = m_T^f - m_T^m = \frac{db}{d\theta} S_A^a + \frac{da}{d\theta} S_T^a + \beta_T^f - \beta_m. \tag{12}$$

Young's modulus and Poisson's ratio of the matrix are denoted E_m, ν_m, and those of the fiber associated with loading in the longitudinal direction $\bar{x}_1$ are denoted E_L^f, ν_L^f. The constants n_f, k_f denote Hill's moduli for the fiber (HILL [1964]). The symbols m_L^r and m_T^r, $r = f, m$, denote the components of the thermal strain vector $\mathbf{m}_r$, eqn (3), in the axial direction and transverse plane, respectively, whereas β_L^f, β_T^f denote axial and transverse coefficients of thermal expansion of the fiber, and β_m denote coefficient of thermal expansion of the isotropic matrix.

According to (5), the strains are uniform in the composite aggregate. From (2), (5_2), and (8) we find

$$d\hat{\epsilon}_1^a = \frac{1}{E_m}\left[s_A^a - 2\nu_m s_T^a + E_m m_L^m\right] d\theta, \tag{13}$$

$$d\hat{\epsilon}_2^a = d\hat{\epsilon}_3^a = \frac{1}{E_m}\left[s_T^a(1 - \nu_m) - \nu_m s_A^a + E_m m_T^m\right] d\theta, \tag{14}$$

$$d\hat{\epsilon}_j^a = 0, \quad j = 4,5,6. \tag{15}$$

If both the matrix and fiber are isotropic, the above solution reduces to

$$d\hat{\sigma}_1^a = d\hat{\sigma}_2^a = d\hat{\sigma}_3^a = s_T\, d\theta, \qquad d\hat{\sigma}_j^a = 0, \quad j = 4,5,6, \tag{16}$$

$$d\hat{\epsilon}_1^a = d\hat{\epsilon}_2^a = d\hat{\epsilon}_3^a = h\, d\theta, \quad d\hat{\epsilon}_j^a = 0, \quad j = 4,5,6, \tag{17}$$

$$s_T = -3(m_f - m_m)/(1/K_f - 1/K_m), \tag{18}$$

$$h = s_T^a/3K_m + m_m = (K_m m_m - K_f m_f)/(K_m - K_f), \tag{19}$$

where $K_r, r = f, m$, is the bulk modulus and m_r denotes the component of the isotropic thermal strain vector $\mathbf{m}_r$, eqn (3). In this case, the stress and strain fields are isotropic and spatially uniform in the entire composite lamina.

If thermoelastic properties of the phases are functions of temperature, the solution at a given temperature θ is found by integrating (8)–(15), or (16)–(19). However, since the phases are elastic and their thermomechanical response is path independent, the solution can be easily found at the current temperature by reducing eqns (8)–(15) or (16)–(19) to the temperature-independent form, in which the temperature derivatives in (11) and (12) vanish, and the coefficients of thermal expansion of the phases, $\beta_m, \beta_L^f, \beta_T^f$, are replaced by the average thermal strain per unit temperature computed over the tem-

perature range $(\theta - \theta_0)$. For example, β_m is replaced by $\bar{\beta}_m = [\int_{\theta_0}^{\theta} \beta_m(\theta)\, d\theta]/(\theta - \theta_0)$. Similar expressions define the average thermal strains $\bar{\beta}_L^f, \bar{\beta}_T^f$ for the fiber.

In this way, uniform strain and stress fields can be created in unidirectional composites under a thermal change $d\theta$ if the composite is simultaneously subjected to mechanical load $d\hat{\boldsymbol{\sigma}}^a$, which is a function of the thermoelastic constants of the phases. Since the fields are uniform, the solution is exact regardless of microstructural details of the composite. If one phase is at most transversely isotropic, the overall stress and strain fields are axisymmetric. On the other hand, the overall fields are isotropic if both phases are isotropic. In the latter case, the strains in any longitudinal plane are independent of the fiber orientation in that plane. This feature is useful in analysis of laminates as discussed in the sequel.

Uniform strain fields can also be created by mechanical loads. Considering an overall uniform stress $d\hat{\boldsymbol{\sigma}}^b$ applied to a stress-free unidirectional composite, while the current temperature is held constant, we wish to find the magnitude of $d\hat{\boldsymbol{\sigma}}^b$ which causes a uniform strain field in the entire composite. This is the homogeneous part of a more general problem considered by DVORAK [1990a]. The solution is again obtained with a decomposition sequence in which the phases are separated and subjected to certain surface tractions of unknown magnitude, which cause uniform stresses $d\hat{\boldsymbol{\sigma}}_r^b$ in the phases. The composite is then reassembled satisfying the constraint equation

$$d\hat{\boldsymbol{\epsilon}}_f^b(\bar{\mathbf{x}}) = d\hat{\boldsymbol{\epsilon}}_m^b(\bar{\mathbf{x}}) = d\hat{\boldsymbol{\epsilon}}^b, \tag{20}$$

as well as the traction equilibrium condition at the cylindrical interfaces between the fiber and the matrix. Since the local stresses are uniform, then

$$d\hat{\sigma}_1^b = c_f\, d\hat{\sigma}_1^{bf} + c_m\, d\hat{\sigma}_1^{bm}, \tag{21}$$

$$d\hat{\sigma}_j^b = d\hat{\sigma}_j^{bf} = d\hat{\sigma}_j^{bm}, \quad j = 2,3,\ldots 6, \tag{22}$$

where c_f and c_m are volume fractions of the phases such that $c_f + c_m = 1$.

Equations (21) and (22) contain seven unknown stresses. From (20_1), we obtain the following system of six equations for the unknown stresses $d\hat{\sigma}_1^{bf}, d\hat{\sigma}_1^{bm}, d\hat{\sigma}_j^b, j = 2,3,\ldots 6$ (DVORAK [1990a]):

$$M_{i1}^f\, d\hat{\sigma}_1^{bf} - M_{i1}^m\, d\hat{\sigma}_1^{bm} + \sum_{j=2}^{6} (M_{ij}^f - M_{ij}^m)\, d\hat{\sigma}_j^b = 0; \quad i = 1,2,\ldots 6. \tag{23}$$

One of the unknown stresses may be selected as a free parameter, the remaining stresses are found by solving the above system of equations.

For isotropic matrix and transversely isotropic fiber, the solution of (23) is found, after some algebra, as:

$$d\hat{\sigma}_1^{bf} = \gamma_f\, dS_T^b, \qquad d\hat{\sigma}_1^{bm} = \gamma_m\, dS_T^b, \tag{24}$$

$$d\hat{\sigma}_2^b = d\hat{\sigma}_3^b = dS_T^b, \qquad d\hat{\sigma}_j^b = 0, \quad j = 4,5,6, \tag{25}$$

$$\gamma_f = [E_L^f/2k_f - (1 + \nu_m)E_L^f/3K_m + 2\nu_L^f(\nu_L^f - \nu_m)]/(\nu_L^f - \nu_m), \tag{26}$$

$$\gamma_m = [E_m/2k_f + \nu_m(2\nu_L^f + 1) - 1]/(\nu_L^f - \nu_m). \tag{27}$$

Note that the solution in (24)–(27) exists only if $\nu_L^f \neq \nu_m$. The solution for the general case where this condition is violated is given by DVORAK [1990a].

The overall axial stress is then found from (21) and (24) as:

$$d\hat{\sigma}_1^b = dS_A^b = \bar{\gamma}\, dS_T^b, \qquad \bar{\gamma} = c_f\gamma_f + c_m\gamma_m. \tag{28}$$

The overall strain $d\hat{\epsilon}^b$ is found from (20). Considering (20_2), we find

$$d\hat{\epsilon}_1^b = h_1\, dS_T^b, \qquad d\hat{\epsilon}_2^b = d\hat{\epsilon}_3^b = h_2\, dS_T^b, \qquad d\hat{\epsilon}_j^b = 0, \quad j = 4,5,6, \tag{29}$$

$$h_1 = \frac{1/2k_f - (1+\nu_m)/3K_m}{(\nu_L^f - \nu_m)}, \qquad h_2 = \frac{-\nu_m/2k_f + \nu_L^f(1+\nu_m)/3K_m}{(\nu_L^f - \nu_m)}. \tag{30}$$

It is seen that application of an overall axisymmetric stress dS_A^b in the axial direction and dS_T^b in the transverse plane causes a spatially uniform strain field in the composite and a uniform local stress field in the phases. The magnitudes of dS_A^b and dS_T^b are related by eqn (28). Either dS_A^b or dS_T^b may be selected as a free parameter in the solution which depends on the elastic properties of the phases and their volume fractions.

II.2. *Laminates*

Consider a symmetric laminate consisting of $2n$ identical unidirectionally reinforced thin laminae in which the matrix is isotropic and the fiber is transversely isotropic, and whose thermomechanical properties vary with temperature. Fiber volume fraction is equal in all plies, but ply thickness can be different. The ply volume fraction is defined as $c_i = t_i/t$, where t_i is the ply thickness and $2t$ is the laminate thickness. The plane of the laminate coincides with the x_1x_2-plane of a Cartesian coordinate system (Fig. 1), and is parallel to the $\bar{x}_1\bar{x}_2$-planes associated with the laminae. Fiber orientation of lamina i is specified with the angle φ_i between the $\bar{x}_1$-axis and the x_1-axis. The plies are assumed to be perfectly bonded together such that they deform equally in the x_1x_2-plane. If the phases of all the laminae deform with the uniform thermal strain $\int_{\theta_0}^{\theta} \mathbf{m}_r'(\theta)\, d\theta$, we wish to find a strain field which is spatially uniform in the entire laminate.

This problem can be solved by applying a decomposition approach similar to that employed for unidirectional composites and utilizing the uniform fields found in the preceding section. Specifically, we first decompose the laminate into separate plies, apply the temperature change $(\theta - \theta_0)$ to each lamina, and recall the uniform fields found in section II.1. The next step is to reassemble the laminate maintaining strain compatibility among the layers in the x_1x_2-plane. Since the plies have different fiber orientations, strain compatibility among the plies in the x_1x_2-plane can be achieved if we require the uniform strain field $\hat{\epsilon}$ in each lamina to be isotropic in the x_1x_2-plane:

$$d\hat{\epsilon}_1 = d\hat{\epsilon}_2. \tag{31}$$

In what follows, we find the solution for two cases: a composite laminate with transversely isotropic fiber and isotropic matrix, and a composite laminate with isotropic phases. The solution is found in incremental form for temperature-dependent phase properties. As indicated in section II.1, the solution at the current temperature θ can be obtained either by integrating the resulting equations, or by evaluating the solution using

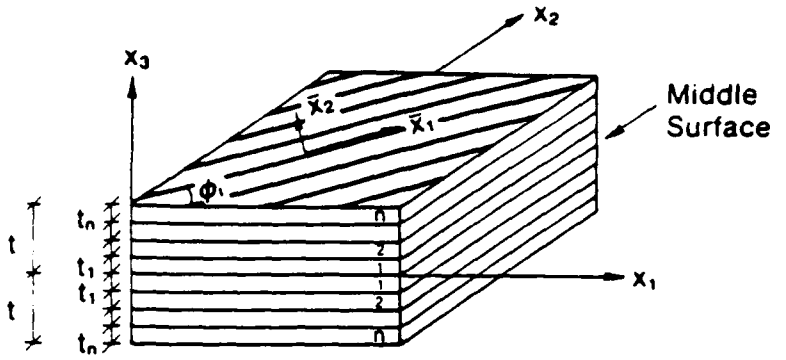

Fig. 1. Geometry of a fibrous composite laminate.

the elastic constants given at θ and replacing the coefficients of thermal expansion of the phases by their average over the temperature range $(\theta - \theta_0)$.

Consider first the case of transversely isotropic fiber and isotropic matrix. In this case, the uniform strain field, $d\hat{\epsilon}^a$, found in each unidirectional lamina under the uniform temperature increment $d\theta$ and the auxiliary stress field $d\hat{\sigma}^a$, eqns (13)–(15), does not satisfy (31). The required field can be found by superposition of $d\hat{\epsilon}^a$ and the uniform strains $d\hat{\epsilon}^b$, eqns (29) and (30), caused by the unknown overall axisymmetric stresses dS_A^b and dS_T^b. Satisfying (31) with the total strain $(d\hat{\epsilon}^a + d\hat{\epsilon}^b)$ and using (28_2), the magnitudes of dS_A^b and dS_T^b can be found. The local and overall fields are then obtained by superposition of the two solutions. The resulting lamina stresses in the $\bar{x}_j$ coordinate system are given by

$$d\hat{\sigma}_1 = s_A\, d\theta, \qquad d\hat{\sigma}_2 = d\hat{\sigma}_3 = s_T\, d\theta, \qquad d\hat{\sigma}_j = 0, \quad j = 4,5,6, \tag{32}$$

$$s_A = \frac{[a(1-\gamma_m) + (a+b)\bar{\gamma}]\Delta m_L - [2b(1-\gamma_m) + (c+2b)\bar{\gamma}]\Delta m_T}{(ac - 2b^2)(1-\gamma_m)}, \tag{33}$$

$$s_T = \frac{(a + b\gamma_m)\Delta m_L - (2b + c\gamma_m)\Delta m_T}{(ac - 2b^2)(1-\gamma_m)}. \tag{34}$$

The total matrix stress is isotropic, whereas the fiber stress is axisymmetric:

$$d\hat{\sigma}_1^m = d\hat{\sigma}_2^m = d\hat{\sigma}_3^m = d\hat{\sigma}_2^f = d\hat{\sigma}_3^f = s_T\, d\theta, \qquad d\hat{\sigma}_j^m = d\hat{\sigma}_j^f = d\hat{\sigma}_j = 0, \quad j = 4,5,6, \tag{35}$$

$$d\hat{\sigma}_1^f = \frac{1}{c_f}(s_A - c_m s_T)\, d\theta. \tag{36}$$

The strains are uniform in the composite aggregate, the magnitude of which can be found from the matrix strains:

$$d\hat{\epsilon}_j = d\hat{\epsilon}_j^f = d\hat{\epsilon}_j^m = h\, d\theta, \quad j = 1,2,3, \tag{37}$$

$$d\hat{\epsilon}_j = d\hat{\epsilon}_j^f = d\hat{\epsilon}_j^m = 0, \quad j = 4,5,6, \tag{38}$$

$$h = s_T/3K_m + m_m. \tag{39}$$

Using a different approach, and assuming temperature-independent phase properties, DVORAK [1986] found equations analogous to the above solution.

Next, we consider the case of isotropic phases. In this case, the strains $d\hat{\epsilon}^a$, eqn (17), are isotropic and satisfy (31), which permits the laminate to be reassembled from the individual plies. The required solution is given by eqns (16)–(19).

The above solutions result in lamina stresses $s_A\, d\theta$ in the axial direction and $s_T\, d\theta$ in the transverse plane in the $\bar{x}_j$ coordinate system. The corresponding laminate stresses, denoted $d\hat{\boldsymbol{\sigma}}^L$, are found by transformation of the lamina stresses to the x_j coordinates, and satisfying the overall force equilibrium conditions. The result is

$$d\hat{\sigma}_1^L = s_1\, d\theta, \qquad d\hat{\sigma}_2^L = s_2\, d\theta, \qquad d\hat{\sigma}_3^L = s_T\, d\theta, \tag{40}$$

$$d\hat{\sigma}_4^L = d\hat{\sigma}_5^L = 0, \qquad d\hat{\sigma}_6^L = s_3\, d\theta. \tag{41}$$

$$s_1 = s_A C_1 + s_T C_2, \qquad s_2 = s_A C_2 + s_T C_1, \qquad s_3 = \tfrac{1}{2}(s_A - s_T) C_3, \tag{42}$$

$$C_1 = \sum_{i=1}^{n} c_i \cos^2 \varphi_i, \qquad C_2 = \sum_{i=1}^{n} c_i \sin^2 \varphi_i, \qquad C_3 = \sum_{i=1}^{n} c_i \sin 2\varphi_i, \tag{43}$$

where c_i is the volume fraction of a ply and φ_i is the angle between the local $\bar{x}_1$-axis and the overall x_1-axis, Fig. 1. For balanced layups, the in-plane shear stress $d\hat{\sigma}_6^L$ vanishes. If both phases are isotropic, there is $s_A = s_T$, where s_T is given by eqn (18) and the stress field given by (40),(41) is spatially uniform and isotropic. Since the solution in this case is independent of the fiber volume fraction, c_f, the plies can have different fiber concentrations.

III. THERMOMECHANICAL CORRESPONDENCE

Assuming the matrix to be plastically incompressible, the fields found in the preceding section are unaffected by plastic deformations induced by any loading regime prior to application of the temperature increment $d\theta$ and the auxiliary overall stress $d\hat{\boldsymbol{\sigma}}^L$. This becomes clear if we view the matrix phase during the decomposition procedure as an elastic material that has been subjected to eigenstrains caused by prior thermomechanical loading histories. Since application of $d\theta$ and the auxiliary fields required to reassemble the laminate causes isotropic stresses in the matrix [see eqn (35)], only elastic strains are produced in the matrix and the current plastic strains are unaltered. The composite laminate is now left with the overall stress $d\hat{\boldsymbol{\sigma}}^L$ which must be removed. This loading step, together with the overall in-plane stress increments $d\sigma_1, d\sigma_2, d\sigma_6$, which may be applied simultaneously with the temperature increment, can cause plastic deformation in the matrix. The total fields are then found by superposition of the solutions of the thermal problem and the mechanical one. The result is equivalent to application of the mechanical load

$$d\boldsymbol{\sigma}^* = [(d\sigma_1 - s_1\, d\theta) \quad (d\sigma_2 - s_2\, d\theta) \quad -s_T\, d\theta \quad 0 \quad 0 \quad (d\sigma_6 - s_3\, d\theta)]^T. \tag{44}$$

Let superimposed prime on the stress or strain vectors indicate (3 × 1) arrays listing the components associated with the x_1x_2-plane of the laminate, e.g. $d\boldsymbol{\sigma}' = [d\sigma_1 \quad d\sigma_2 \quad d\sigma_6]^T$, $d\boldsymbol{\epsilon}' = [d\epsilon_1 \quad d\epsilon_2 \quad 2d\epsilon_6]^T$. The overall in-plane strains caused by simultaneous application of $d\boldsymbol{\sigma}'$ and $d\theta$ are then found as

$$d\boldsymbol{\epsilon}' = h \quad \mathbf{1} \quad d\theta + \mathcal{M}[d\boldsymbol{\sigma}' - (\mathbf{s} + \mathcal{L}s_T)\, d\theta], \tag{45}$$

$$\mathbf{s} = [s_1 \quad s_2 \quad s_3]^T, \qquad \mathbf{1} = [1 \quad 1 \quad 0]^T. \tag{46}$$

Matrix $\mathcal{M}$ is the instantaneous compliance of the laminate associated with in-plane loads, and $\mathcal{L}$ defines in-plane stresses caused by unit out-of-plane normal stress when the in-plane strain $d\boldsymbol{\epsilon}'$ equals zero. Expressions for $\mathcal{M}$ and $\mathcal{L}$ are derived in the Appendix. The first term in (45) is the uniform strain generated by the phase thermal strains in each ply of the decomposed laminate, eqns (37),(38). The second term is the in-plane strain caused by application of the equivalent stress $d\boldsymbol{\sigma}^*$, eqn (44), to the laminate.

The nonzero phase stresses in the plies are the in-plane stress $d\boldsymbol{\sigma}_r^i = [d\sigma_1^r \quad d\sigma_2^r \quad d\sigma_6^r]^T$, $r = f, m$, and the out-of-plane component $d\sigma_3^r$. The local stresses are nonuniform in reality. Let $\mathcal{G}_r^i(\bar{\mathbf{x}})$ and $\boldsymbol{g}_r^i(\bar{\mathbf{x}})$ define phase instantaneous stress concentrations for the in-plane stress $d\boldsymbol{\sigma}_r^i$ caused in the ith ply under overall in-plane stresses and out-of-plane normal stress, respectively. The first column of $\mathcal{G}$ is the stress $d\boldsymbol{\sigma}_r^i$ caused by overall stress $d\sigma_1 = 1$ applied to the laminate, the second column corresponds to $d\sigma_2 = 1$, etc. Similarly, $\boldsymbol{g}$ is the stress $d\boldsymbol{\sigma}_r^i$ caused by $d\sigma_3 = 1$. Also, let $\boldsymbol{j}_r^{iT}(\bar{\mathbf{x}})$ and e_r^i define stress concentration factors for out-of-plane normal stress in the phases corresponding to overall in-plane stresses and out-of-plane normal stress, respectively. The phase stresses caused in lamina i by $d\boldsymbol{\sigma}'$ and $d\theta$ can be written as

$$d\boldsymbol{\sigma}_r^i(\bar{\mathbf{x}}) = s_T\boldsymbol{\xi}_r\, d\theta + \mathcal{G}_r^i(\bar{\mathbf{x}})(d\boldsymbol{\sigma}' - \mathbf{s}\, d\theta) - \boldsymbol{g}_r^i(\bar{\mathbf{x}})s_T\, d\theta, \tag{47}$$

$$d\sigma_3^{ri}(\bar{\mathbf{x}}) = s_T\, d\theta + \boldsymbol{j}_r^{iT}(\bar{\mathbf{x}})(d\boldsymbol{\sigma}' - \mathbf{s}\, d\theta) - e_r^i(\bar{\mathbf{x}})s_T\, d\theta, \tag{48}$$

$$\boldsymbol{\xi}_r = [\zeta_r \quad 1 \quad 0]^T, \quad \zeta_m = 1, \quad \zeta_f = (s_A/s_T - c_m)/c_f. \tag{49}$$

The concentration factors $\mathcal{G}$, $\boldsymbol{g}$, $\boldsymbol{j}^T$, and e are given in the Appendix. The first term in (47) and (48) is the uniform stress caused in the phases by the local thermal strains in the decomposed laminate, eqns (35),(36). As noted previously, this stress is isotropic in the matrix and does not cause plastic deformation in plastically incompressible materials. The second term is the stress caused by the in-plane mechanical load $(d\boldsymbol{\sigma}' - \mathbf{s}\, d\theta)$, and the third term is the stress caused by removing the out-of-plane normal stress $s_T\, d\theta$.

In this way, any thermomechanical loading path applied to symmetric laminates with identical plies and variable fiber orientation can be converted in an exact way to a mechanical path. The magnitude of the equivalent mechanical load depends on the volume fraction of the phases, the laminate layup, and the elastic thermomechanical properties of the phases. The overall strain and local fields caused by the actual thermomechanical loads are found by superposition of the uniform fields caused by the phase thermal strains and the auxiliary stress field, and the field caused by the equivalent mechanical load (44).

The laminate in-plane stress–strain relations can be written in the alternate form

$$d\boldsymbol{\epsilon}' = \mathcal{M}\, d\boldsymbol{\sigma}' + \mathbf{m}'\, d\theta, \tag{50}$$

where $\mathbf{m}'$ is a (3×1) thermal strain vector which lists the in-plane coefficients of thermal expansion of the laminate. Comparing eqns (45) and (50), we find

$$\mathbf{m}' = h\mathbf{1} - \mathcal{M}(\mathbf{s} + \mathbf{f}s_T), \tag{51}$$

which defines the overall thermal strain in terms of the mechanical properties. Similarly, the phase stresses can be written as

$$d\sigma_r^i(\bar{\mathbf{x}}) = \mathbf{g}_r^i(\bar{\mathbf{x}})\, d\boldsymbol{\varepsilon}' + \mathbf{g}_r^i(\bar{\mathbf{x}})\, d\theta, \tag{52}$$

$$d\sigma_3^{ri}(\bar{\mathbf{x}}) = \mathbf{j}_r^{iT}(\bar{\mathbf{x}})\, d\boldsymbol{\varepsilon}' + e_r^i(\bar{\mathbf{x}})\, d\theta, \tag{53}$$

where $\mathbf{g}_r^i$ and e_r^i are thermal stress concentration factors. From eqns (47), (48), (52), and (53), we find

$$\mathbf{g}_r^i(\bar{\mathbf{x}}) = s_T\boldsymbol{\xi}_r - (\mathbf{G}_r^i(\bar{\mathbf{x}})\mathbf{s} + \mathbf{g}_r^i(\bar{\mathbf{x}})s_T), \tag{54}$$

$$e_r^i(\bar{\mathbf{x}}) = s_T - (\mathbf{j}_r^{iT}(\bar{\mathbf{x}})\mathbf{s} + e_r^i(\bar{\mathbf{x}})s_T). \tag{55}$$

Equations (54) and (55) define the thermal stress concentration factors for the matrix and fiber, $r = f, m$, in terms of their mechanical counterparts. Alternate expressions for the thermal concentration factors have been derived by BAHEI-EL-DIN [1990] using the laminate theory of symmetric plates.

IV. OVERALL YIELD SURFACE

IV.1. *General description*

Assume the existence of a matrix yield surface which encompasses all stress states that can be reached from the current state by purely elastic deformation. The onset of yielding begins when the stress point is on the yield surface. Plastic deformation develops only when the loading point traverses the yield surface. In this case, and assuming that the load is quasistatic, the yield surface translates in the stress space to contain the loading point. This is known as kinematic hardening of the yield surface. Translation of the yield surface may be accompanied by isotropic deformation of the surface which is caused, in part, by variation of the yield stress with temperature. In the subsequent discussion, we will assume that the matrix yield surface hardens kinematically, and that any isotropic change will be caused only by variation of the matrix yield stress with temperature. Hence, the current yield surface of the matrix is defined by the function

$$f[(\boldsymbol{\sigma}_m - \boldsymbol{\alpha}_m), \theta] = 0, \tag{56}$$

where $\boldsymbol{\alpha}_m$ is the center of the yield surface or back stress. If $\boldsymbol{\alpha}_m = 0$, eqn (56) represents the initial yield surface. Considering stress states in which the σ_{32} and σ_{31} stresses vanish, we list the in-plane stress components $\sigma_1, \sigma_2, \sigma_6$, followed by the out-of-plane stress σ_3 in the stress vectors, which now represent (4×1) arrays. In this case, eqn (56) is written for elastically isotropic Mises-type matrix material as

$$f[(\boldsymbol{\sigma}_m - \boldsymbol{\alpha}_m), \theta] \equiv \tfrac{1}{2}(\boldsymbol{\sigma}_m - \boldsymbol{\alpha}_m)^T\mathbf{C}(\boldsymbol{\sigma}_m - \boldsymbol{\alpha}_m) - \tau_0^2(\theta) = 0, \tag{57}$$

where $\mathbf{C}$ is a (4×4) symmetric matrix with nonzero coefficients $c_{11} = c_{22} = c_{44} = \frac{2}{3}$, $c_{33} = 2$, $c_{12} = c_{14} = c_{24} = -\frac{1}{3}$, and τ_0 is the matrix initial yield stress in shear. Under a multiaxial stress state, the onset of initial yielding in the Mises matrix occurs when the effective stress given by $\sqrt{3}J_2$, where J_2 is the second invariant of the deviatoric stress tensor of the matrix, equals the tension yield stress given by $\sqrt{3}\tau_0$.

Corresponding to the matrix yield surface (56), there exists a yield surface in the $\bar{\sigma}_i$ lamina stress space. We assume that at a temperature θ, the lamina yield surface is located at $\bar{\alpha}_i$. If in addition the lamina yield stress is a function of temperature, then its yield surface is defined by the function

$$\bar{g}_i[(\bar{\sigma}_i - \bar{\alpha}_i), \theta] = 0. \tag{58}$$

Similarly, there exists a lamina yield surface g_i in the overall stress space with center at α_i such that

$$g_i[(\sigma - \alpha_i), \theta] = 0. \tag{59}$$

Since the stress states within the yield surface correspond to purely elastic deformation, the "radii" of the yield surfaces f, $\bar{g}_i$, and g_i are related (BAHEI-EL-DIN & DVORAK [1982]; BAHEI-EL-DIN [1990]):

$$(\bar{\sigma}_i - \bar{\alpha}_i) = \mathbf{W}_i(\sigma - \alpha_i), \tag{60}$$

$$[\sigma'_m(\bar{\mathbf{x}}) - \alpha'_m(\bar{\mathbf{x}})] = \mathbf{B}_m(\bar{\mathbf{x}})(\bar{\sigma}_i - \bar{\alpha}_i) = \mathbf{G}'_m(\bar{\mathbf{x}})(\sigma - \alpha_i). \tag{61}$$

Matrix $\mathbf{W}_i$ relates the lamina stresses in the $\bar{x}_j$ coordinates to the laminate stresses, whereas $\mathbf{B}_m$ and $\mathbf{G}'_m = \mathbf{B}_m\mathbf{W}_i$ relate the matrix local stresses to the lamina stresses and the laminate stresses, respectively. Here, we assume identical plies, in which case $\mathbf{B}_m$ does not vary among the plies. Expressions for the elastic "concentration" factors $\mathbf{W}_i, \mathbf{B}_m, \mathbf{G}'_m$ are given in terms of the overall properties in the Appendix. As indicated in (61), the matrix stress is not uniform in reality. In actual calculations, however, the stress concentration factor $\mathbf{B}_m$ is found for a piecewise uniform matrix stress field. For example, in the Periodic Hexagonal Array model (DVORAK & TEPLY [1985]; TEPLY & DVORAK [1988]), the matrix domain is subdivided into a number of finite elements in which the stresses are uniform. On the other hand, averaging models such as the self-consistent method (HILL [1965]), the Mori-Tanaka method (MORI & TANAKA [1973]), and the Vanishing Fiber Diameter model (DVORAK & BAHEI-EL-DIN [1982]) compute an average stress concentration factor $\mathbf{B}_m$ for the matrix phase. In any case, eqn (61) is replaced by

$$(\sigma_m^{ik} - \alpha_m^{ik}) = \mathbf{B}_m^k(\bar{\sigma}_i - \bar{\alpha}_{ik}) = \mathbf{G}_m^{ik}(\sigma - \alpha_{ik}), \quad i = 1, n; \quad k = 1, N, \tag{62}$$

where N is the number of matrix subelements.

Considering the averaging models for which $N = 1$, the yield functions g_i and $\bar{g}_i$, $i = 1, n$, can be written from (56) and (58)–(61) as

$$g_i[(\sigma - \alpha_i), \theta] \equiv \bar{g}_i[\mathbf{W}_i(\sigma - \alpha_i), \theta] \equiv f[\mathbf{G}'_m(\sigma - \alpha_i), \theta] = 0. \tag{63}$$

If f is given by (57), then

$$g_i[(\sigma - \alpha_i), A] \equiv \tfrac{1}{2}(\sigma - \alpha_i)^T \bar{\mathbf{C}}_i (\sigma - \alpha_i) - \tau_0^2(\theta) = 0, \tag{64}$$

$$\bar{\mathbf{C}}_i = \mathbf{G}_m'^T \mathbf{C}_i \mathbf{G}_m'. \tag{65}$$

Equation (63) or (64) represents n yield surfaces in the laminate stress space σ. At the current temperature θ, the centers of the yield surfaces are located at the stress point given by the vectors α_i, $i = 1, n$. The laminate yield surface is then the inner envelope of the surfaces $g_1, g_2, \ldots g_n$. Specific forms of the overall yield functions, g_i, are found next using the bimodal theory.

IV.2. *Bimodal yield surfaces*

The laminate yield surface defined above is obtained here using a specific material model. Namely, we find the yield surface (58) of a unidirectional lamina using the bimodal plasticity theory of DVORAK and BAHEI-EL-DIN [1987]. The theory, which was verified experimentally (DVORAK *et al.* [1988]), admits two distinct overall deformation modes, the matrix-dominated mode (MDM) and fiber-dominated mode (FDM), that may exist in binary elastic-plastic fibrous composite systems under certain loading conditions. To each mode, there corresponds a segment of the overall yield surface that reflects the onset of yielding of the matrix phase in that mode. The inner envelope of these two segments is the overall surface of the composite lamina. In its application to laminates, the yield surface (58) corresponding to each mode must be separately transformed to the laminate stress space for each lamina according to (63_1). This results in $2n$ yield surfaces of the type (59), the inner envelope of which constitutes the laminate yield surface.

Matrix-dominated mode (MDM): This deformation mechanism is characterized by plastic shear deformation in the matrix on certain hypothetical slip planes that are parallel to the fiber axis, and in certain preferred slip directions on these planes. Apart from specifying the orientation of the slip planes, the fiber does not participate in this mode. Hence, the composite is treated as a macroscopically homogeneous medium with known slip systems, which are, of course, in the matrix constituent. Under the normal stresses $\bar{\sigma}_1'$, $\bar{\sigma}_2'$, and $\bar{\sigma}_3'$ and the longitudinal shear stress $\bar{\sigma}_6'$, the lamina yield surface $\bar{g}_i$ in this mode has two branches (DVORAK & BAHEI-EL-DIN [1987]; BAHEI-EL-DIN & DVORAK [1989]):

$$\bar{g}_i \equiv \tfrac{1}{4}\left((\bar{\sigma}_2' - \bar{\alpha}_2') - (\bar{\sigma}_3' - \bar{\alpha}_3')\right)^2 (1 + \bar{q}_i^2)^2 - \tau_0^2(\theta) = 0, \quad |\bar{q}_i| \le 1, \tag{66}$$

$$\bar{g}_i \equiv (\bar{\sigma}_6' - \bar{\alpha}_6')^2 - \tau_0^2(\theta) = 0, \quad |\bar{q}_i| \ge 1, \tag{67}$$

where

$$\bar{q}_i = (\bar{\sigma}_6' - \bar{\alpha}_6')/\left((\bar{\sigma}_2' - \bar{\alpha}_2') - (\bar{\sigma}_3' - \bar{\alpha}_3')\right). \tag{68}$$

The first term in (66) and (67) is the resolved shear stress on a specific slip plane and slip direction which depend on the lamina stresses. Hence, plastic flow occurs in the matrix-dominated mode when the maximum resolved shear stress reaches the initial yield stress τ_0. Since the slip planes are parallel to the fiber longitudinal axis, the axial stress

$\bar{\sigma}_4^i$ does not contribute to the resolved shear stress on these planes and, therefore, does not appear in eqns (66) or (67).

The lamina stresses are given in terms of the overall stress by eqn (60). Substituting (60) into (66) and (67), and noting the structure of matrix $\mathbf{W}$ found in eqns (A-27) and (A-28) in the Appendix, the lamina yield surface g_i described in the overall stress space is found as

$$g_i \equiv \tfrac{1}{4}(\mathbf{y}_i^T(\boldsymbol{\sigma} - \boldsymbol{\alpha}_i))^2(1 + q_i^2)^2 - \tau_0^2(\theta) = 0, \quad |q_i| \le 1, \tag{69}$$

$$g_i \equiv (\mathbf{z}_i^T(\boldsymbol{\sigma} - \boldsymbol{\alpha}_i))^2 - \tau_0^2(\theta) = 0, \quad |q_i| \ge 1, \tag{70}$$

where

$$q_i = \tilde{q}_i = (\mathbf{z}_i^T(\boldsymbol{\sigma} - \boldsymbol{\alpha}_i))/(\mathbf{y}_i^T(\boldsymbol{\sigma} - \boldsymbol{\alpha}_i)) \tag{71}$$

$$\mathbf{y}_i^T = [\mathbf{W}_{21}^i\, \mathbf{W}_{22}^i\, \mathbf{W}_{23}^i\, (\mathbf{W}_{24}^i - 1)], \tag{72}$$

$$\mathbf{z}_i^T = [\mathbf{W}_{31}^i\, \mathbf{W}_{32}^i\, \mathbf{W}_{33}^i\, \mathbf{W}_{34}^i], \tag{73}$$

where $\mathbf{W}_{ij}$ is the (i, j)th entry of matrix $\mathbf{W}$.

Fiber-dominated mode (FDM): In this mode the matrix and fiber phases deform together in the elastic as well as the plastic ranges. In contrast to the matrix-dominated mode, no specific deformation mechanism is suggested. Instead, the fiber-dominated mode is treated as a general case of plastic deformation of a heterogeneous medium. The overall yield surface in this case is the envelope of all stress states which can be reached by pure elastic deformation in the matrix phase. Hence, the FDM yield surfaces g_i of the plies described in the overall stress space are defined by eqn (63). An example is given in (64) for a Mises matrix. Averaging models such as the self-consistent method or the Mori–Tanaka method can be used to determine the stress concentration factors required in this deformation mode. Our unpublished calculations of FDM yield surfaces using the Vanishing Fiber Diameter (VFD) model indicate that, contrary to experimental observations, this model predicts fiber-dominated yielding, which always supersedes matrix-dominated yielding. In composite systems where MDM deformation may be present, as in boron- or silicon–carbide-reinforced metals, the VFD model should be avoided.

V. THERMAL HARDENING

In contrast to homogeneous materials, uniform temperature changes cause internal stresses in heterogeneous media when the phases have distinct coefficients of thermal expansion. The thermal stress field affects the overall mechanical behavior of the material and alters the overall yield stress. This effect causes hardening of the overall yield surface which appears in the stress space as a translation and deformation of the yield surface. In this section, we consider fibrous composites subjected to pure thermal loading and evaluate hardening of the overall yield surface with the help of the uniform fields constructed in section II.

First, consider elastic phases with temperature-independent thermoelastic constants. In this case, the concentration factors $\mathbf{G}_m^r$ [eqn (61)], which define the local stresses in the matrix subelements in terms of the overall stress, are not functions of temperature.

Consequently, the change in the "radius" of the matrix yield surface can be evaluated by writing (62) in the incremental form

$$[d\sigma_m^{ik} - d\alpha_m^{ik}] = \mathbf{G}_m^{ik}(d\sigma - d\alpha_{ik}), \quad i = 1, n; \quad k = 1, N. \tag{74}$$

Considering the auxiliary stress field found in section II for isotropic matrix and transversely isotropic fiber, we find that the matrix stress is uniform and isotropic, eqn (35). Since only the deviatoric stress causes plastic deformation in plastically incompressible materials, then $d\alpha_m^{ik} = 0$. Substituting $d\sigma_m^{ik}$ from (35) and $d\sigma$ from (40), (41), into (74), the increment $d\alpha_{ik}$, $i = 1, n$, $k = 1, N$ is found from (74) as

$$d\alpha_{ik} = \left([s_1 \quad s_2 \quad s_3 \quad s_T]^T - s_T[\mathbf{G}_m^{ik}]^{-1}[1 \quad 1 \quad 0 \quad 1]^T \right) d\theta, \tag{75}$$

where the stresses s_j, $j = 1,2,3$, are given by (42) and (43). Since the matrix is plastically incompressible, the matrix yield surface (56) represents an open cylinder with generators parallel to the hydrostatic stress direction $\sigma_1^m = \sigma_2^m = \sigma_3^m$ [see e.g. the Mises yield surface (57)]. In this case, the lamina yield surface g_i in (59) is also an open cylinder with generators parallel to the stress vector given by the second term in (75), which is the projection of the matrix hydrostatic stress axis in the overall stress space. Therefore, the second term in (75) does not affect yielding of the composite laminate, and the yield surfaces of all matrix subelements in the entire laminate translate together in the overall stress space according to the following rule:

$$d\alpha_{ik} = \mathbf{s}\, d\theta, \quad i = 1, n; \quad k = 1, N, \tag{76}$$

$$\mathbf{s} = [s_1 \quad s_2 \quad s_3 \quad s_T]^T. \tag{77}$$

The actual translation of the yield surfaces due to the temperature increment $d\theta$ is found by superposition of the translation given by (76) and that found during removal of the overall auxiliary stress $\mathbf{s}\, d\theta$. The latter causes hardening of the overall yield surfaces only if plastic deformations take place in the matrix phase. Description of hardening in laminates caused by plastic deformation of the matrix can be found in BAHEI-EL-DIN and DVORAK [1982] and BAHEI-EL-DIN [1990].

The hardening rule (76) is general, independent of the form of g_i. We recall, however, that all plies must be identical except for the fiber orientation and lamina thickness. Also, the translation of the yield surfaces specified in (76) is unaffected by previous loading histories, since the auxiliary stresses used in deriving (76) are unaffected by previous loading histories as discussed in section II.

Consider now local thermoelastic properties which vary with temperature and apply a temperature change θ from a reference temperature θ_0. Noting that the "radius" of the matrix yield surface at a given temperature θ is related to the "radius" of the overall yield surface by (61) and (62), a similar derivation leads to the following equation for the center of the yield surface of a matrix subelement:

$$\alpha_{ik}(\theta) = \mathbf{s}(\theta)(\theta - \theta_0). \tag{78}$$

From (78), the following incremental form replaces (76) when the local properties vary with temperature:

$$d\alpha_{ik} = \left[\mathbf{s} + \frac{d\mathbf{s}}{d\theta}(\theta - \theta_0)\right] d\theta, \quad i = 1, n; \quad k = 1, N. \tag{79}$$

The center of the laminate yield surfaces can be found by integration of (79). Alternately, the center can be found from (78), provided that the average coefficients of thermal expansion of the phases over the temperature range $(\theta - \theta_0)$ are used in evaluation of the stress s, as indicated in section II.

Equations (76) and (79) indicate that the configuration of the initial cluster of the laminae yield surfaces g_i, eqn (59), found at a given temperature θ, does not change when the temperature increment $d\theta$ is applied. However, since the laminae yield surfaces are oriented differently in the overall stress space, the translation given by (76) or (79) may affect their projections on a specific overall stress plane. This is illustrated next for selected composite laminates.

VI. APPLICATIONS

To illustrate the analysis described above, we present results for two aluminide intermetallic matrix composite laminates. For each system, the laminate yield surface at the processing temperature and at a subsequent temperature during cooling are found.

VI.1. *SCS6/Ti_3Al-$(0 \pm 45)_s$ laminate*

The properties of the silicon-carbide fiber and the titanium-aluminide matrix are shown in Tables 1 and 2, respectively, as function of temperature (Dvorak [1990a]). The fiber volume fraction, c_f, is 0.35. The composite laminate was cooled down from the processing temperature $\theta_0 = 950°C$ to room temperature ($\theta = 21°C$). Figures 2 and 3 show the bimodal yield surfaces of the laminae in the overall $\sigma_{11}\sigma_{21}$-plane and $\sigma_{11}\sigma_{22}$-plane, respectively, at 950°C. Two yield surfaces are plotted for each lamina, a matrix-dominated mode (MDM) yield surface and a fiber-dominated mode (FDM) yield surface. In evaluating the FDM yield surface, we used the self-consistent method (SCM) to determine the matrix stress concentration factor $\mathbf{B}_m$. Since the lamina is stress free at 950°C, the centers of all yield surfaces are located at the stress origin. We note here the flat branches found in the MDM yield surfaces in contrast to the ellipsoidal shapes of the FDM yield surfaces. We also note that the laminate yield surface represented by the inner envelope of the six yield surfaces in Figs. 2 and 3 consists of MDM branches only.

Table 1. Material properties of SCS6 fiber

θ (°C)	E_f (GPa)	ν_f	β_f (10^{-6}/°C)
982	413	0.25	6.30
871	413	0.25	5.50
760	413	0.25	5.30
649	413	0.25	4.50
538	413	0.25	4.40
24	413	0.25	4.15

Table 2. Material properties of the Ti_3Al matrix

θ (°C)	E_m (GPa)	ν_m	β_m (10^{-6}/°C)	$Y = \sqrt{3}\,\tau_0$ (MPa)
950	46	0.3	18.0	200
760	72	0.3	15.8	237
649	87	0.3	13.6	302
427	91	0.3	12.6	418
260	93	0.3	12.0	505
21	97	0.3	9.6	624

Hence, plastic yielding in the stress planes shown in Figs. 2 and 3 is dominated by the slip mechanism assumed in the matrix-dominated deformation mode.

Temperature changes from the reference temperature $\theta_0 = 950°C$ cause translation of the yield surfaces of all laminae as given by eqn (78). Also, since the matrix yield stress is a function of temperature, the yield surfaces will experience isotropic deformation. At a specific temperature $\theta \neq \theta_0$, one or more of the yield branches shown in Figs. 2 and 3 comes in contact with the stress origin, which indicates initial yielding of the composite laminate. In order to evaluate the yield temperature for the laminate considered here during cooling from the processing temperature, the matrix effective stress and maximum resolved shear stress in all plies of the laminate were computed as functions of

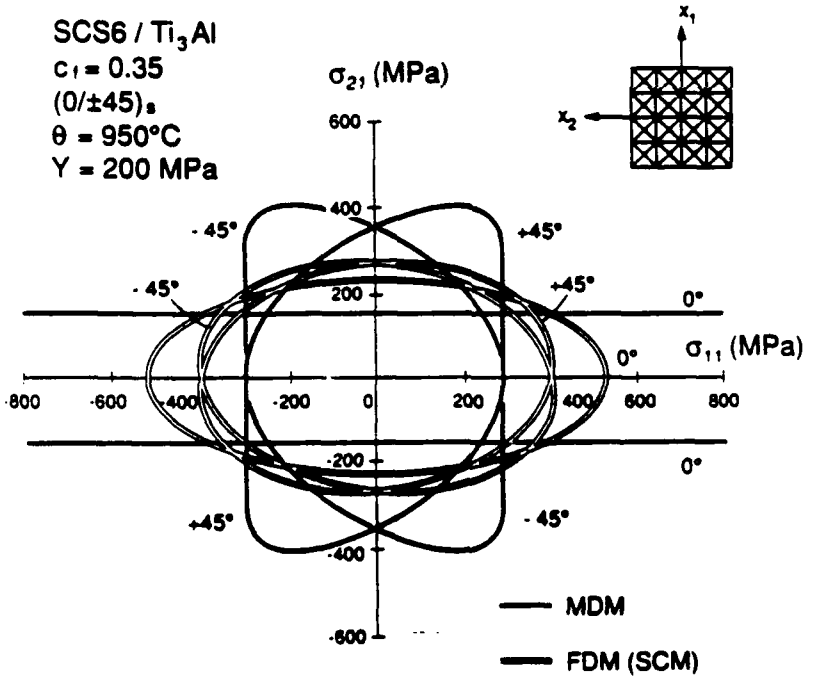

Fig. 2. Bimodal initial yield surfaces of a SCS6/Ti_3Al, $(0/\pm45)_s$ laminate in the $\sigma_{11}\sigma_{21}$-plane at 950°C.

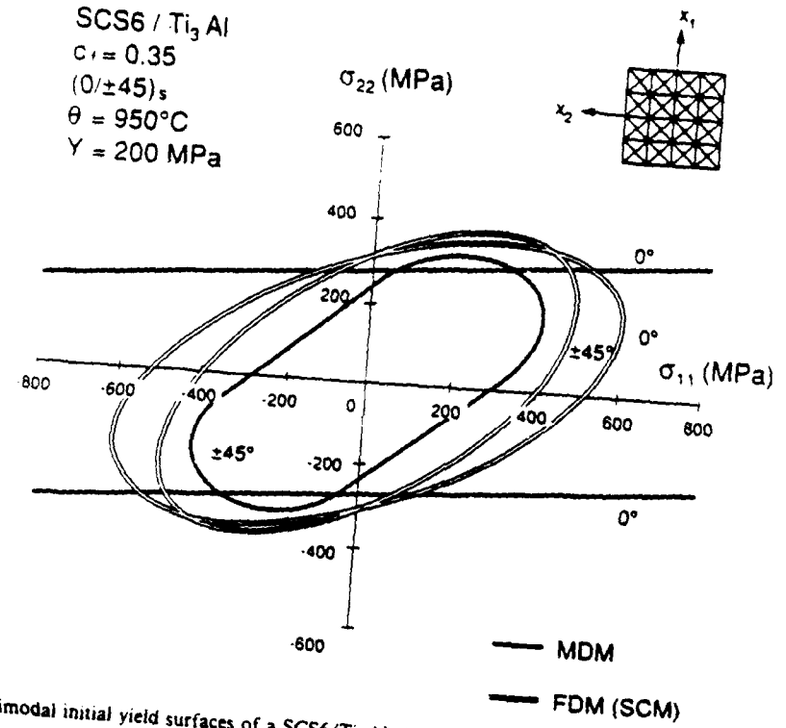

Fig. 3. Bimodal initial yield surfaces of a SCS6/Ti_3Al, $(0/\pm45)_s$ laminate in the $\sigma_{11}\sigma_{22}$-plane at 950°C.

the temperature. The result is shown in Fig. 4 together with the variation of the matrix yield stress with temperature. Note that the resolved shear stress was magnified by a factor of $\sqrt{3}$ in order to plot the shear stress and tension stress on the same scale. At 950°C, the laminate is stress free and all local stresses vanish. The stresses build up in the plies and the phases as the laminate is cooled down from the processing temperature. As seen in Fig. 4, both the matrix effective stress and the maximum resolved shear stress in all plies are lower than the matrix yield stress in the entire temperature range from 950°C to room temperature (21°C). Hence, neither the fiber-dominated mode nor the matrix-dominated mode become active, and the laminate remains elastic. The nonlinear variation of the stresses found in Fig. 4 is caused by variation of the thermoelastic constants of the phases with temperature (Tables 1 and 2).

Figures 5 and 6 show the laminae yield surfaces after cooling to 21°C. Although the yield surfaces translate with the same vector in the overall stress space, eqn (78), their sections in the $\sigma_{11}\sigma_{21}$- and $\sigma_{11}\sigma_{22}$-planes assume positions different from those found at the reference temperature. In contrast to the behavior at 950°C, the laminate yielding mode at room temperature could be of either the MDM- or FDM-type depending on the direction of the mechanical load. This is clearly shown in Figs. 7 and 8, where the inner envelope of the laminae yield surfaces at 950°C and 21°C are compared. Subsequent heating from room temperature may lead to an overall yield surface which consists of a different cluster of MDM and FDM branches. In any case, the dominant deformation mode can be detected with the method presented here.

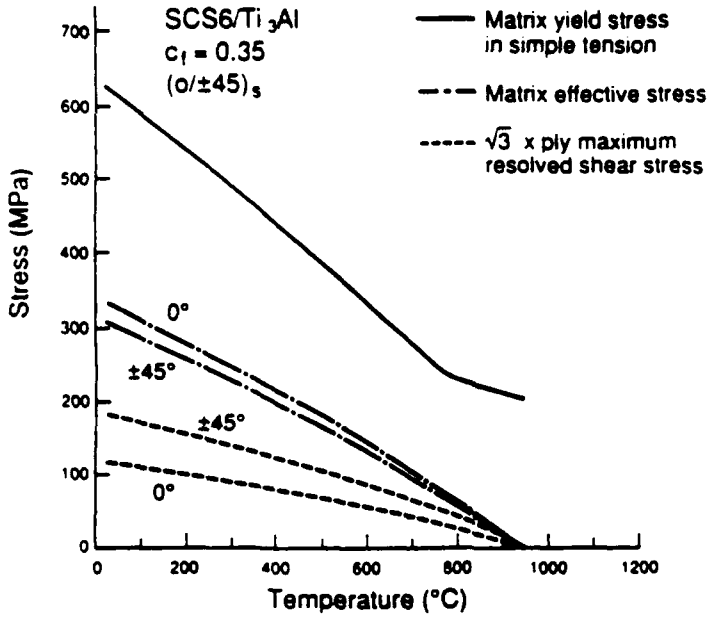

Fig. 4. Variation of matrix yield stress, matrix effective stress, ply maximum resolved shear stress, with temperature found in a SCS6/Ti_3Al, $(0/\pm45)_s$ laminate.

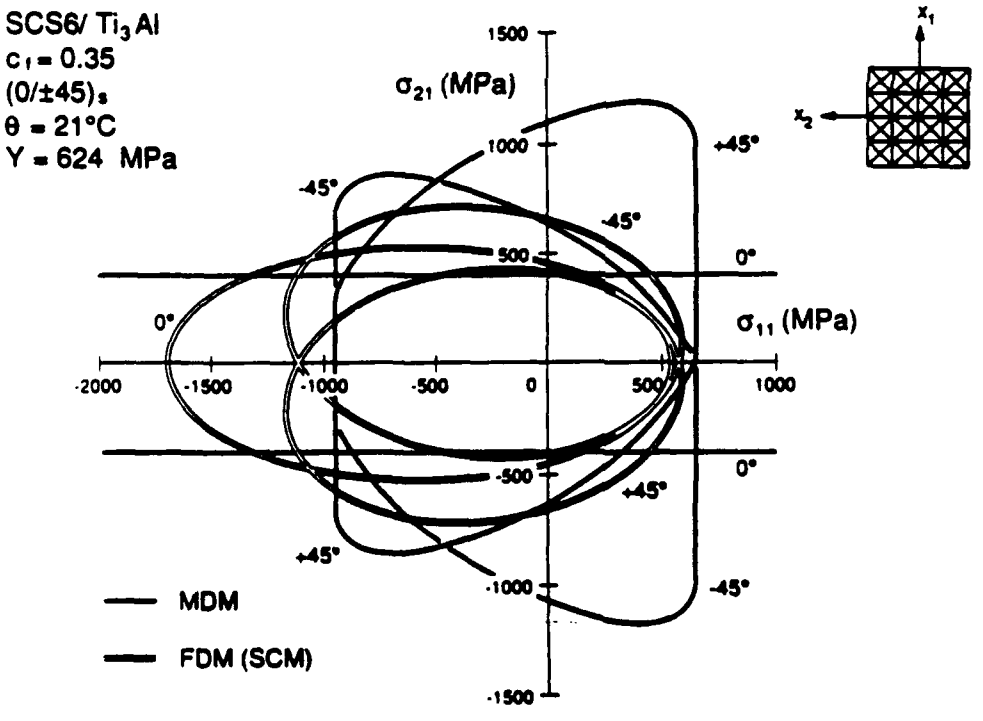

Fig. 5. Bimodal yield surfaces of a SCS6/Ti_3Al, $(0/\pm45)_s$ laminate in the $\sigma_{11}\sigma_{21}$-plane at 21°C after cooling from 950°C.

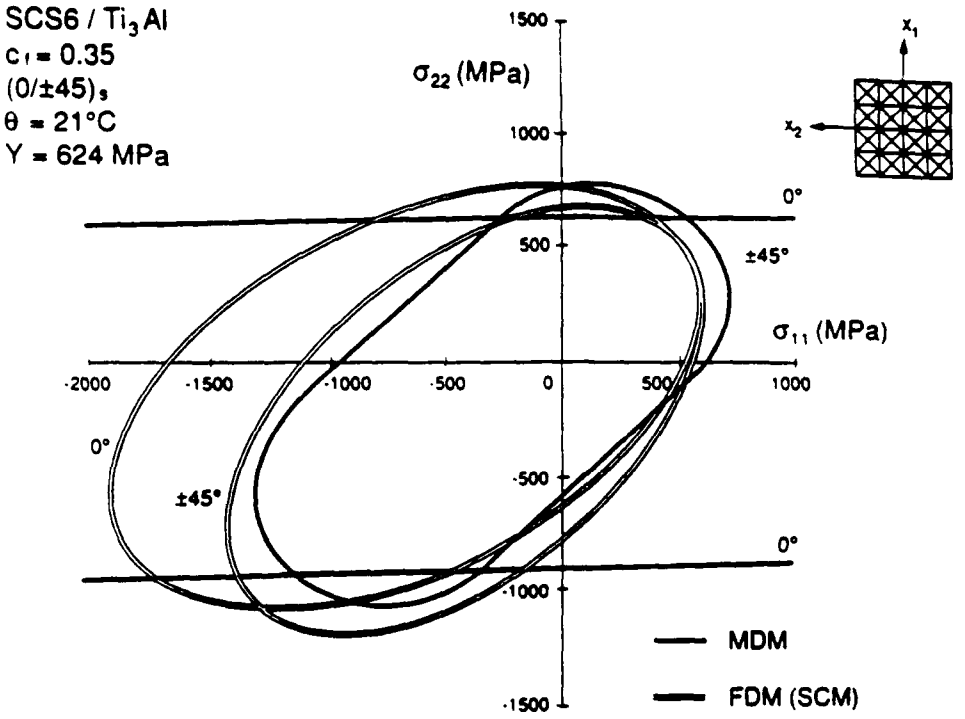

Fig. 6. Bimodal yield surfaces of a SCS6/Ti_3Al, $(0/\pm45)_s$ laminate in the $\sigma_{11}\sigma_{22}$-plane at 21°C after cooling from 950°C.

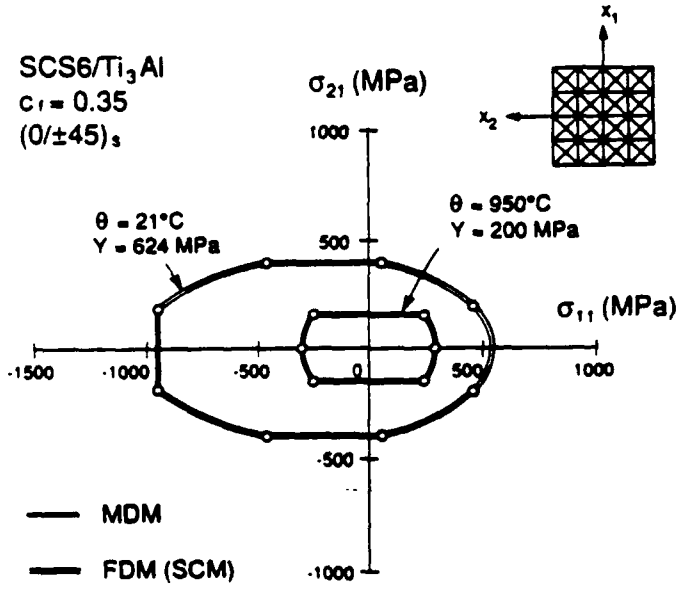

Fig. 7. Bimodal overall yield surfaces of a SCS6/Ti_3Al, $(0/\pm45)_s$ laminate in the $\sigma_{11}\sigma_{21}$-plane at 950°C and 21°C.

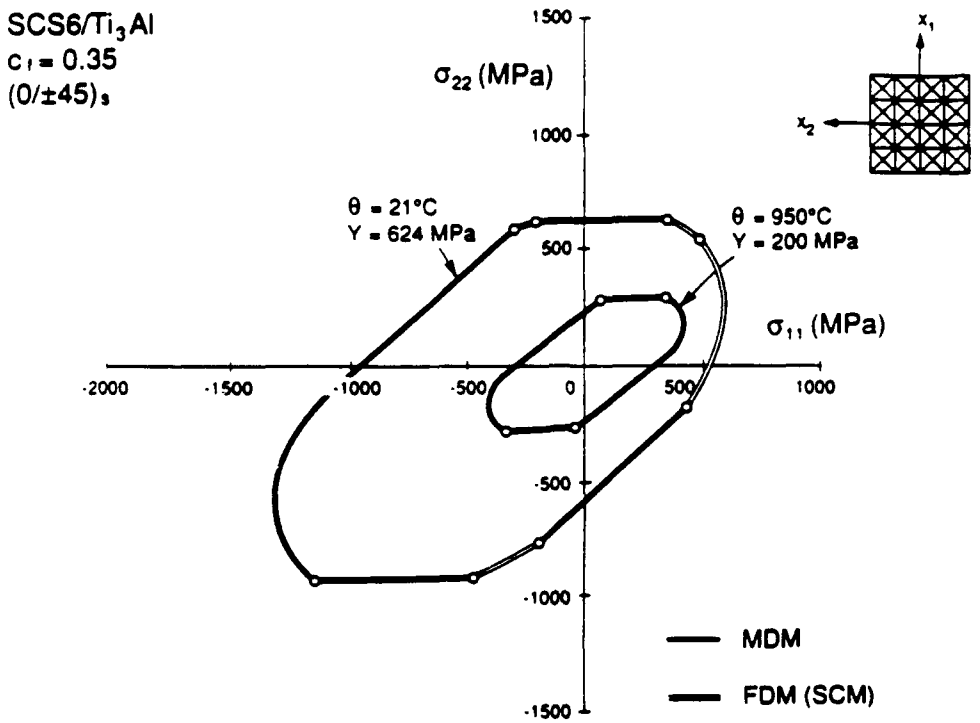

Fig. 8. Bimodal overall yield surfaces of a SCS6/Ti_3Al, $(0/\pm45)_s$ laminate in the $\sigma_{11}\sigma_{22}$-plane at 950°C and 21°C.

VI.2. *SCS6/Ni_3Al-(0/±45)$_s$ laminate*

The properties of the nickel-aluminide matrix are shown in Table 3 (STOLOFF [1989]). Fiber volume fraction is 0.35. In contrast to the titanium-aluminide matrix, the magnitude of the yield stress of the Ni_3Al matrix increases with increasing temperature up to 650°C, then decreases rapidly. The processing temperature for this composite is about

Table 3. Material properties of Ni_3Al matrix

θ (°C)	E_m (GPa)	ν_m	β_m (10^{-6}/°C)	$Y = \sqrt{3}\,\tau_0$ (MPa)
1200	134	0.32	20.6	137
994	142	0.32	19.0	279
776	150	0.32	17.2	459
673	154	0.32	16.4	557
642	155	0.32	16.1	564
578	158	0.32	15.6	535
376	165	0.32	14.3	356
327	167	0.32	14.0	279
206	172	0.32	13.4	156
127	175	0.32	13.1	110
21	179	0.32	12.5	79

1200°C. Figure 9 shows the variation of the matrix effective stress and the maximum resolved shear stress in all plies with temperature. At about 505°C, the matrix effective stress in the 0° lamina approximately equals the matrix yield stress in tension. Figures 10 and 11 show the laminate yield surfaces in the $\sigma_{11}\sigma_{21}$- and $\sigma_{11}\sigma_{22}$-plane, respectively, at the reference temperature $\theta_0 = 1200°C$, and after cooling to 505°C. Details of the laminae yield surfaces have been omitted; only the inner envelope of the yield surfaces is shown. It is seen that this cooling path causes initial yielding in the 0° lamina. At 1200°C, yielding is mainly dominated by the slip mechanism of the matrix-dominated mode, whereas, at 505°C, the deformation is controlled by the fiber-dominated mode.

VII. CONCLUSION

Uniform strain fields found in unidirectional fibrous composites have been used to construct spatially uniform and isotropic strain fields in composite laminates under phase thermal strains. The solution was found for identical plies with variable fiber orientation, isotropic matrix, and transversely isotropic fiber. In this case, the matrix stress is isotropic, the fiber stress is axisymmetric, and the laminate stress which supports the local fields consists of in-plane normal and shear stresses and out-of-plane normal stress. For balanced layups, the overall in-plane shear stress vanishes. If both the fiber and matrix are isotropic, the solution leads to spatially uniform stress and strain fields which are also isotropic. In this case, the solution is not a function of the fiber volume fraction which can vary among the plies.

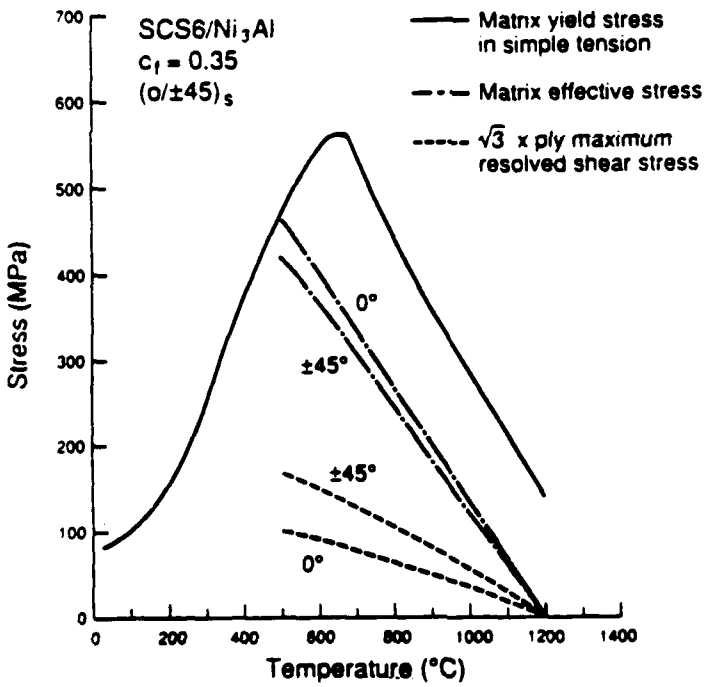

Fig. 9. Variation of matrix yield stress, matrix effective stress, ply maximum resolved shear stress, with temperature found in a SCS6/Ni_3Al, $(0/\pm45)_s$ laminate.

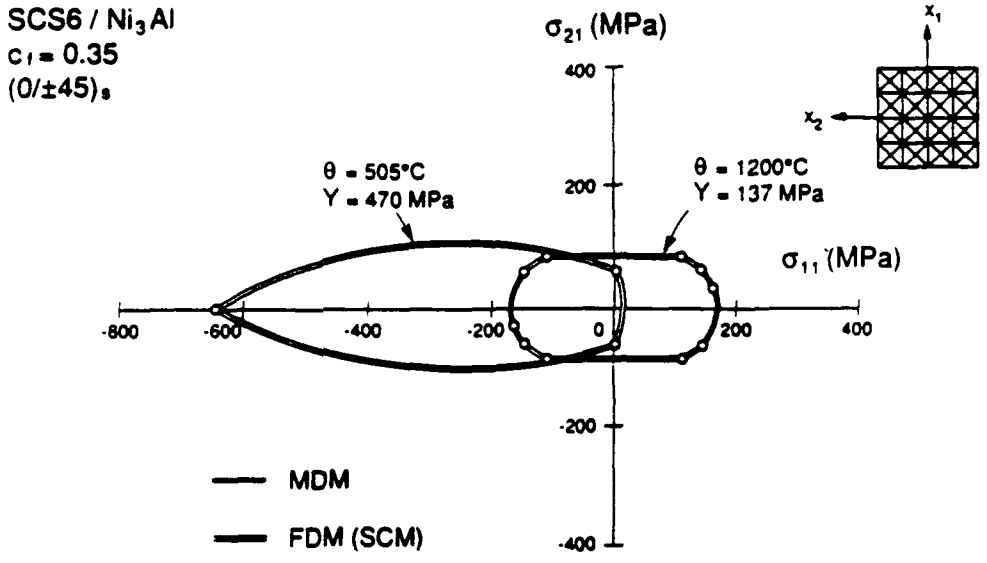

Fig. 10. Bimodal overall yield surfaces of a SCS6/Ni_3Al, $(0/\pm45)_s$ laminate in the $\sigma_{11}\sigma_{21}$-plane at 1200°C and 505°C.

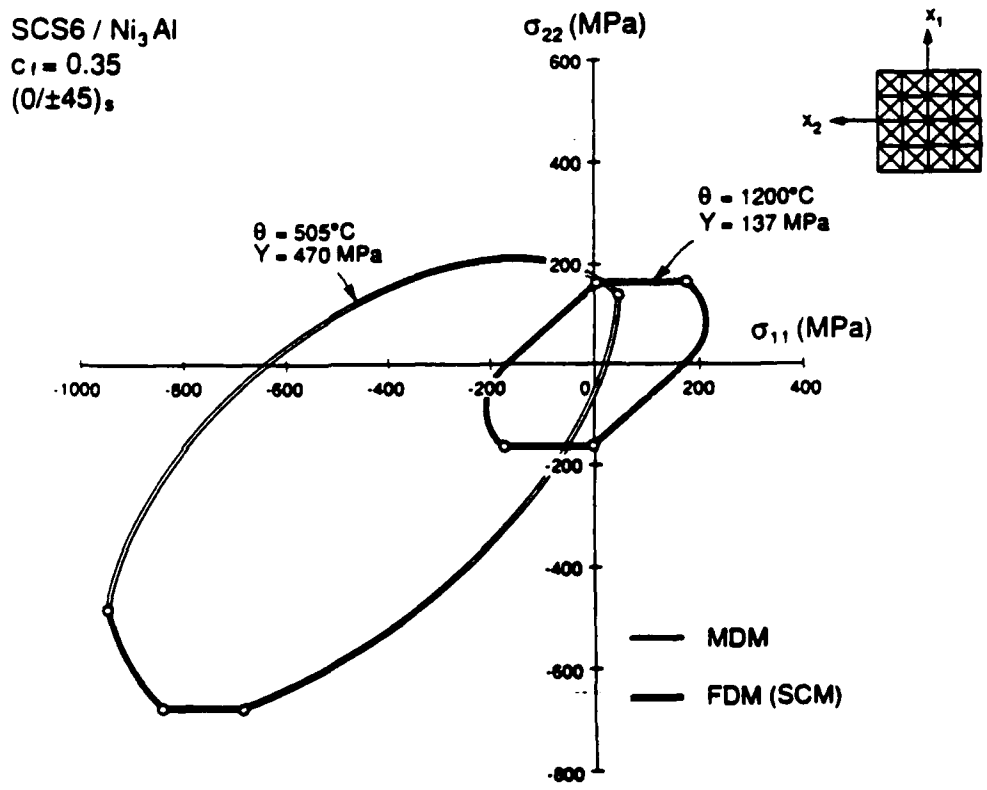

Fig. 11. Bimodal overall yield surfaces of a SCS6/Ni_3Al, $(0/\pm45)_s$ laminate in the $\sigma_{11}\sigma_{22}$-plane at 1200°C and 505°C.

A useful result of the fields found here is the existence of a correspondence between thermal and mechanical loads applied to composite laminates. This permits replacement of any thermomechanical loading path by an equivalent mechanical path in composite systems with a plastically incompressible matrix. In this case, the system remains elastic under deformation caused by the phase thermal strains which produce an isotropic stress field in the matrix. Laminate analysis methods, derived mainly for mechanical loads, can be applied to thermomechanical loading problems by simply modifying the loading path.

The effect of a temperature change on yielding of a fibrous composite laminate was evaluated with the help of the uniform fields. This thermal effect was found to be a universal rigid body translation applied to the yield surface in the overall stress space. The magnitude and direction of hardening depend on thermoelastic properties and volume fractions of the phases, and the laminate layup. When both the fiber and matrix phase are isotropic, the translation is independent of the fiber volume fraction. The translation vector is applied to all yield branches associated with the individual plies regardless of the fiber orientation. Consequently, the configuration of the initial cluster of the yield surfaces of the laminae that defines the overall yield surface is unaffected by temperature variations. The projection of the yield surface on the plane stress subspace, however, will be very different from the initial configuration, since the lamina yield surfaces are oriented differently in the overall stress space. In addition, isotropic hardening may be present if the matrix yield stress is a function of temperature.

Examples of thermal hardening caused by cool-down of intermetallic matrix composites showed significant changes in the geometry of the yield surface and the deformation modes available in the plane stress space.

Acknowledgements—This work was supported, in part, by the Air Force Office of Scientific Research, the Office of Naval Research, and the DARPA-HiTASC program at Rensselaer Polytechnic Institute. Drs. George Haritos of the AFOSR and Yapa Rajapakse of the ONR served as contract monitors. The author is indebted to Professor George Dvorak for useful suggestions.

REFERENCES

1963 Hill, R., "Elastic Properties of Reinforced Solids: Some Theoretical Principles," J. Mech. Phys. Solids, 11, 357.
1964 Hill, R., "Theory of Mechanical Properties of Fibre-Strengthened Materials: I. Elastic Behaviour," J. Mech. Phys. Solids, 12, 199.
1965 Hill, R., "Theory of Mechanical Properties of Fiber-Strengthened Materials: III. Self-Consistent Model," J. Mech. Phys. Solids, 13, 189.
1973 Mori, T., and Tanaka, K., "Average Stress in Matrix and Average Elastic Energy of Materials with Misfitting Inclusion," Acta Metall., 21, 571.
1982 Bahei-El-Din, Y.A., and Dvorak, G.J., "Plasticity Analysis of Laminated Composite Plates," J. Appl. Mech., 49, 740.
1982 Dvorak, G.J., and Bahei-El-Din, Y.A., "Plasticity Analysis of Fibrous Composites," J. Appl. Mech., 49, 327.
1983 Dvorak, G.J., "Metal Matrix Composites: Plasticity and Fatigue," in Hashin, Z. and Herakovich, C.T. (eds.), Mechanics of Composite Materials: Recent Advances, Pergamon Press, Oxford, p. 73.
1985 Dvorak, G.J., and Teply, J.L., "Periodic Hexagonal Array Models for Plasticity Analysis of Composite Materials," in Sawczuk, A. and Bianchi, V. (eds.), Plasticity Today: Modeling, Methods and Applications, W. Olszak Memorial Volume, p. 623, Elsevier, Amsterdam.
1986 Dvorak, G.J., "Thermal Expansion of Elastic-Plastic Composite Materials," J. Appl. Mech., 53, 737.
1987 Dvorak, G.J., "Thermomechanical Deformation and Coupling in Elastic-Plastic Composite Materials," in Bin, H.D. and Nguyen, Q.S. (eds.), Thermomechanical Couplings in Solids, p. 43, North-Holland, Amsterdam.
1987 Dvorak, G.J., and Bahei-El-Din, Y.A., "A Bimodal Plasticity Theory of Fibrous Composite Materials," Acta Mech., 69, 219.

1988 DVORAK, G.J., BAHEI-EL-DIN, Y.A., MACHERET, Y., and LIU, C.H., "An Experimental Study of Elastic-Plastic Behavior of a Fibrous Boron-Aluminum Composite," J. Mech. Phys. Solids, 36, 655.
1988 TEPLY, J.L., and DVORAK, G.J., "Bounds on Overall Instantaneous Properties of Elastic-Plastic Composites," J. Mech. Phys. Solids, 36, 29.
1989 BAHEI-EL-DIN, Y.A., and DVORAK, G.J., "New Results in Bimodal Plasticity of Fibrous Composite Materials," in Khan, A.S. and Tokuda, M. (eds.), Advances in Plasticity 1989, p. 121, Pergamon Press, Oxford.
1989 DVORAK, G.J., and CHEN, T., "Thermal Expansion of Three-Phase Composite Materials," J. Appl. Mech., 56, 418.
1989 STOLOFF, N.S., "The Physical and Mechanical Metallurgy of Ni_3Al and its Alloys," Int. Mater. Rev., 34.
1990 BAHEI-EL-DIN, Y.A., "Plasticity Analysis of Fibrous Composite Laminates Under Thermomechanical Loads," in Kennedy, J.M., Moeller, H.H., and Johnson, W.S. (eds.), Thermal and Mechanical Behavior of Ceramic and Metal Matrix Composites, ASTM STP 1080, American Society for Testing and Materials, p. 20. Philadelphia.
1990 BENVENISTE, Y., and DVORAK, G.J., "On a Correspondence Between Mechanical and Thermal Effects in Two-Phase Composites," in Weng, G.J., Taya, M., and Abe, H. (eds.), Micromechanics and Inhomogeneity, The Toshio Mura 65th Anniversary Volume, p. 65, Springer-Verlag, Berlin.
1990a DVORAK, G.J., "On Uniform Fields in Heterogeneous Media," Proc. R. Soc., London, A431, 89.
1990b DVORAK, G.J., private communication.

Structural Engineering Department
Cairo University
Giza, Egypt

(*Received* 26 *October* 1990; *in final revised form* 29 *January* 1992)

APPENDIX

Here we derive expressions for the overall compliance $\mathcal{M}$, the stress vector $\mathfrak{L}$, and the mechanical stress concentration factors $\mathfrak{S}_r^i, \mathfrak{g}_r^i, \mathfrak{z}_r^{iT}, \mathfrak{e}_r^i$ of the phases which appeared in section III, and the distribution factors W_i of the plies which appeared in section IV. Considering the in-plane stresses $d\boldsymbol{\sigma}'$ and the out-of-plane normal stress $d\sigma_3$, the stress-strain relations of lamina i, $i = 1, n$, can be written in the laminate x_j coordinates as

$$d\boldsymbol{\epsilon}_i' = \mathcal{M}_i\, d\boldsymbol{\sigma}_i' + \mathfrak{m}_i\, d\sigma_3^i, \tag{A-1}$$

$$d\boldsymbol{\sigma}_i' = \mathfrak{L}_i\, d\boldsymbol{\epsilon}_i' + \mathfrak{k}_i\, d\sigma_3^i, \tag{A-2}$$

where $\mathcal{M}_i$ and $\mathfrak{L}_i$ are overall instantaneous compliance and stiffness matrices for in-plane mechanical loading, $\mathfrak{m}_i$ is the in-plane strain caused by unit out-of-plane normal stress, and $\mathfrak{k}_i$ is the lamina in-plane stress caused by unit out-of-plane normal stress when the lamina in-plane strains vanish. From (A-1) and (A-2), we find

$$\mathfrak{L}_i = \mathcal{M}_i^{-1}, \quad \mathfrak{k}_i = -\mathfrak{L}_i \mathfrak{m}_i. \tag{A-3}$$

The lamina stress and strain vectors transform to the $\bar{x}_j$ axes (BAHEI-EL-DIN [1990])

$$d\bar{\boldsymbol{\sigma}}_i' = \mathfrak{R}_i\, d\boldsymbol{\sigma}_i, \quad d\bar{\sigma}_3^i = d\sigma_3^i, \tag{A-4}$$

$$d\bar{\boldsymbol{\epsilon}}_i' = \mathbf{Q}_i\, d\boldsymbol{\epsilon}_i, \quad d\bar{\epsilon}_3^i = d\epsilon_3^i, \tag{A-5}$$

where

$$\mathfrak{R}_i = \begin{bmatrix} \cos^2\varphi_i & \sin^2\varphi_i & \sin 2\varphi_i \\ \sin^2\varphi_i & \cos^2\varphi_i & -\sin 2\varphi_i \\ -\tfrac{1}{2}\sin 2\varphi_i & \tfrac{1}{2}\sin 2\varphi_i & \cos 2\varphi_i \end{bmatrix}, \quad \mathbf{Q}_i^T = \mathfrak{R}_i^{-1}. \tag{A-6}$$

This suggests the following transformations for the lamina properties:

$$\mathcal{M}_i = \mathfrak{R}_i^T \bar{\mathcal{M}} \mathfrak{R}_i, \quad \mathfrak{m}_i = \mathfrak{R}_i^T \bar{\mathfrak{m}}, \tag{A-7}$$

$$\mathfrak{L}_i = \mathbf{Q}_i^T \bar{\mathfrak{L}} \mathbf{Q}_i, \quad \mathfrak{k}_i = \mathbf{Q}_i^T \bar{\mathfrak{k}}, \tag{A-8}$$

where $\bar{\mathcal{M}}$, $\bar{\mathfrak{L}}$, $\bar{\mathfrak{m}}$, and $\bar{\mathfrak{k}}$ are lamina properties referred to the local coordinates $\bar{x}_j$. Since the plies are identical, the lamina properties in the $\bar{x}_j$ coordinates are also identical among all plies.

The overall properties of a lamina in the $\bar{x}_j$ coordinate system can be found from a material model which specifies phase stresses in terms of the overall stresses in the form

$$d\sigma_r'(\bar{\mathbf{x}}) = \mathfrak{B}_r(\bar{\mathbf{x}})\, d\bar{\sigma}_i' + \mathfrak{b}_r(\bar{\mathbf{x}})\, d\bar{\sigma}_3', \tag{A-9}$$

$$d\sigma_3^r(\bar{\mathbf{x}}) = \mathfrak{c}_r^T(\bar{\mathbf{x}})\, d\bar{\sigma}_i' + \eta_r(\bar{\mathbf{x}})\, d\bar{\sigma}_3', \tag{A-10}$$

where $\mathfrak{B}$, $\mathfrak{b}$, $\mathfrak{c}^T$, and η are phase stress concentration factors. The stress concentration factors, or their averages, can be evaluated using available micromechanical material models such as the Periodic Hexagonal Array model (DVORAK & TEPLY [1985]; TEPLY & DVORAK [1988]), the self-consistent model (HILL [1965]), and the Mori–Tanaka model (MORI & TANAKA [1973]). Following the derivation given by HILL [1963] which approximates the local fields by certain phase uniform fields, the overall compliance $\bar{\mathcal{M}}$ and $\bar{\mathfrak{m}}$ of a lamina are found in the notation used here as

$$\bar{\mathcal{M}} = \mathcal{M}_f + c_m[(\mathcal{M}_m - \mathcal{M}_f)\mathfrak{B}_m + (\mathfrak{m}_m - \mathfrak{m}_f)\mathfrak{c}_m^T], \tag{A-11}$$

$$\bar{\mathfrak{m}} = \mathfrak{m}_f + c_m[(\mathcal{M}_m - \mathcal{M}_f)\mathfrak{b}_m + (\mathfrak{m}_m - \mathfrak{m}_f)\eta_m], \tag{A-12}$$

where $\mathcal{M}_r$, $\mathfrak{m}_r$, $r = f, m$, are phase in-plane compliance associated with loading in the $\bar{x}_1\bar{x}_2$-plane, and with the out-of-plane normal stress, respectively.

The in-plane lamina stresses are related to the overall stresses applied to the laminate by

$$d\sigma_i' = \mathfrak{K}_i\, d\sigma' + \mathfrak{k}_i\, d\sigma_3, \quad d\sigma_3^i = d\sigma_3, \tag{A-13}$$

where $\mathfrak{K}_i$ and $\mathfrak{k}_i$ are stress distribution factors. Since the plies deform together in the x_1x_2-plane, then

$$d\epsilon' = d\epsilon_i'. \tag{A-14}$$

In analogy with (A-1) and (A-2), the laminate stress–strain relations can be written as

$$d\epsilon' = \mathcal{M}\, d\sigma' + \mathfrak{m}\, d\sigma_3, \tag{A-15}$$

$$d\sigma' = \mathfrak{L}\, d\epsilon' + \mathfrak{k}\, d\sigma_3, \tag{A-16}$$

where the overall compliance $\mathcal{M}$, $\mathcal{m}$ and stiffness $\mathcal{L}$, $\mathcal{k}$ are yet to be determined. From (A-1) and (A-13)–(A-15), we obtain

$$\mathcal{K}_i = \mathcal{L}_i \mathcal{M}, \qquad \mathcal{k}_i = \mathcal{L}_i(\mathcal{m} - \mathcal{m}_i). \tag{A-17}$$

From force equilibrium in the x_1x_2-plane, the distribution factors must satisfy

$$\sum_{i=1}^{n} c_i \mathcal{K}_i = \mathbf{I}, \qquad \sum_{i=1}^{n} c_i \mathcal{k}_i = \mathbf{0}, \tag{A-18}$$

where $\mathbf{I}$ is a (3×3) identity matrix and $\mathbf{0}$ is a (3×1) null vector. The overall compliance and stiffness matrices can now be found by substituting (A-17) into (A-18):

$$\mathcal{L} = \sum_{i=1}^{n} c_i \mathcal{L}_i, \qquad \mathcal{k} = \sum_{i=1}^{n} c_i \mathcal{k}_i, \tag{A-19}$$

$$\mathcal{M} = \mathcal{L}^{-1}, \qquad \mathcal{m} = -\mathcal{M}\mathcal{k}. \tag{A-20}$$

From (A-4), (A-9), (A-10), and (A-13), the phase stresses can be expressed in terms of the laminate applied stresses as

$$d\boldsymbol{\sigma}_r^i(\bar{\mathbf{x}}) = \mathcal{G}_r^i(\bar{\mathbf{x}})\, d\boldsymbol{\sigma}' + \mathcal{g}_r^i(\bar{\mathbf{x}})\, d\sigma_3, \tag{A-21}$$

$$d\sigma_3^n(\bar{\mathbf{x}}) = \mathcal{j}_r^{iT}(\bar{\mathbf{x}})\, d\boldsymbol{\sigma}' + \mathcal{c}_r^i(\bar{\mathbf{x}})\, d\sigma_3, \tag{A-22}$$

$$\mathcal{G}_r^i(\bar{\mathbf{x}}) = \mathcal{B}_r(\bar{\mathbf{x}})\mathcal{R}_i\mathcal{K}_i, \qquad \mathcal{g}_r^i(\bar{\mathbf{x}}) = \mathcal{B}_r(\bar{\mathbf{x}})\mathcal{R}_i\mathcal{k}_i + \mathcal{k}_r(\bar{\mathbf{x}}), \tag{A-23}$$

$$\mathcal{j}_r^{iT}(\bar{\mathbf{x}}) = \mathcal{c}_r^{iT}(\bar{\mathbf{x}})\mathcal{R}_i\mathcal{K}_i, \qquad \mathcal{c}_r^i(\bar{\mathbf{x}}) = \mathcal{c}_r^{iT}(\bar{\mathbf{x}})\mathcal{R}_i\mathcal{k}_i + \eta_r(\bar{\mathbf{x}}). \tag{A-24}$$

Finally, if $\boldsymbol{\sigma}_m^i$ denote matrix stress, $\bar{\boldsymbol{\sigma}}^i$ and $\boldsymbol{\sigma}^i$ denote lamina stresses in $\bar{x}_j$ and x_j coordinate systems, respectively, and $\boldsymbol{\sigma}$ denote laminate overall stress, such that each vector is (4×1) listing the in-plane stresses $\sigma_1, \sigma_2, \sigma_6$, followed by the out-of-plane stress σ_3, then we can write

$$\boldsymbol{\sigma}_m^i = \mathbf{B}_m \bar{\boldsymbol{\sigma}}^i, \qquad \bar{\boldsymbol{\sigma}}^i = \mathbf{R}_i \boldsymbol{\sigma}^i, \qquad \boldsymbol{\sigma}^i = \mathbf{H}_i \boldsymbol{\sigma}. \tag{A-25}$$

$$\boldsymbol{\sigma}_m^i = \mathbf{G}_i \boldsymbol{\sigma}, \qquad \bar{\boldsymbol{\sigma}}^i = \mathbf{W}_i \boldsymbol{\sigma}, \tag{A-26}$$

$$\mathbf{G}_i = \mathbf{B}_m \mathbf{R}_i \mathbf{H}_i, \qquad \mathbf{W}_i = \mathbf{R}_i \mathbf{H}_i, \tag{A-27}$$

where

$$\mathbf{B}_m = \begin{bmatrix} \mathcal{B}_m & \mathcal{k}_m \\ \mathcal{c}_m^T & \eta_m \end{bmatrix}, \qquad \mathbf{H}_i = \begin{bmatrix} \mathcal{K}_i & \mathcal{k}_i \\ \mathbf{0}^T & 1 \end{bmatrix}, \qquad \mathbf{R}_i = \begin{bmatrix} \mathcal{R}_i & \mathbf{0} \\ \mathbf{0}^T & 1 \end{bmatrix}. \tag{A-28}$$

As discussed above, the stress concentration factors $\mathcal{B}_m$, $\mathcal{k}_m$, $\mathcal{c}_m^T$, and η_m are evaluated using appropriate micromechanical models. The transformation factors $\mathcal{R}_i$, and the stress distribution factors $\mathcal{K}_i$, and $\mathcal{k}_i$ are given by eqns (A-6) and (A-17), respectively.

International Union of Theoretical
and Applied Mechanics

George J. Dvorak (Ed.)

Inelastic Deformation of Composite Materials

IUTAM Symposium, Troy, New York
May 29–June 1, 1990

With 101 Illustrations

Springer-Verlag
New York Berlin Heidelberg London
Paris Tokyo Hong Kong Barcelona

On a Correspondence Between Mechanical and Thermal Fields in Composites with Slipping Interfaces

Y. Benveniste and G. J. Dvorak

Department of Solid Mechanics, Material and Structures
Faculty of Engineering, Tel–Aviv University
Ramat Aviv, 69978
Israel

Department of Civil Engineering
Rensselaer Polytechnic Institute
Troy, New York 12180–3590
USA

Abstract

The present paper is concerned with composites in which the constituent interfaces are weak in shear and therefore exhibit shear deformation associated with sliding. Thermomechanical loadings of such systems are considered which consist of homogeneous traction or displacement boundary conditions and a uniform temperature change on the outside surface of the composite. For binary systems with isotropic constituents, it is shown that the actual fields in the purely thermal problem can be uniquely determined from the solution of the purely mechanical problem. This correspondence relation is used to determine the effective thermal strain and stress tensors on the basis of the effective mechanical properties. For multi–phase systems with anisotropic constituents undergoing interface slip and separation, the theorem of virtual work is used to establish a similar relation between the effective thermal tensors and the mechanical concentration factors and constituent properties of the composite.

Introduction

Thermal problems in heterogeneous media have drawn much interest in the last years due to the increasing importance of high temperature composites. Several fundamental aspects in the micromechanics of composites in the context of thermomechanical problems have recently been investigated by the authors, Dvorak (1986), Dvorak and Chen (1989), Benveniste and Dvorak (1989) where the reader can find a list of references in the field.

Most of the work dealing with composites assumes perfect bonding between the constituents. However, due to poor bonding between the phases, a jump in the displacement field may occur at internal boundaries, and it is of interest to study thermomechanical problems in composites under such circumstances. Determination of the effective properties requires special attention in the presence of imperfect bonding, and a proper framework for the investigation of such problems has been laid down by Benveniste (1985). Interfaces which are weak in shear may be modeled by demanding that the normal displacements are continuous, but the tangential displacements exhibit a jump which is proportional to the shear tractions. For limiting values of the constant of proportionality, the special cases of perfect bonding and lubricated contact are obtained. Such models of a flexible interface which may also include imperfect bonding in the normal direction have been previously used in the literature, see for example Lené and Leguillon (1982), Benveniste and Aboudi (1984), Aboudi (1987), Benveniste and Miloh (1986), Jasiuk and Tong (1989), Achenbach and Zhu (1989), and Hashin (1990). The reader is referred to these works for a further list of references on imperfect interfaces. Recently, several problems of inclusions which undergo pure slip at interfaces have been considered by Mura et al. (1985), Tsuchida et al. (1986), and Jasiuk et al. (1988).

The present paper is concerned with binary systems with flexible interfaces in shear, and isotropic constituents. It starts by establishing a correspondence relation between local fields induced in such two–phase composites by purely mechanical and purely thermal problems. These relations are obtained by using a decomposition scheme originally proposed by Dvorak (1983, 1986), and further employed by Benveniste and Dvorak (1989) in binary composites with anisotropic constituents, arbitrary phase geometry, but perfect bonding

between the phases. Recently, Dvorak (1990) has thoroughly explored the implications of this concept in regard to the existence of uniform fields in heterogeneous media. We show here that this decomposition scheme can be generalized to the case of two–phase media undergoing slip at interphase boundaries, but with isotropic constituents. The implementation of the scheme shows that local fields in such composites which are induced by a uniform temperature change at external boundaries can be uniquely determined from the solution of the same system subjected to uniform overall mechanical loading. In the second part of the first section of the paper, the established correspondence principle is used to derive the effective thermal strain and stress tensors on the basis of the effective mechanical properties of the composite. The second section of the paper is concerned with multiphase composites with anisotropic constituents undergoing slip of the above described nature at interphase boundaries. Only effective properties are considered in this section, and a generalization of Levin's (1967) and Rosen and Hashin's (1970) result is derived using the theorem of virtual work. The obtained results reduce correctly to those obtained in the previous section for the case of binary composites with isotropic constituents.

1. Correspondence Between Purely Mechanical and Purely Thermal Problems in Binary Composites with Interfaces Weak in Shear

1a. General Theory

Consider a two–phase composite with isotropic constituents, but arbitrary phase geometry. Let the thermoelastic constitutive relations of the homogeneous phases $r = 1,2$ be given by:

$$\underline{\sigma}_r = \underline{L}_r\,\underline{\epsilon}_r + \underline{\ell}_r\theta \qquad , \qquad r = 1, 2$$

$$\underline{\epsilon}_r = \underline{M}_r\,\underline{\sigma}_r + \underline{m}_r\theta \qquad , \tag{1}$$

where $\underline{\sigma}_r$, $\underline{\epsilon}_r$ and θ denote respectively the stress, strain tensors and temperature field, $\underline{L}_r$ and $\underline{M}_r = \underline{L}_r^{-1}$ are the phase stiffness and compliance tensors, $\underline{m}_r$ is the thermal strain tensor (of

expansion coefficients), and $\underset{\sim}{\ell}_r$ is the thermal stress tensor such that $\underset{\sim}{\ell}_r = -\underset{\sim}{L}_r \, \underset{\sim}{m}_r$. In this paper we will denote the matrix phase by the index $r = 1$ and the inclusion phase by index $r = 2$.

The two–phase composite is assumed to have constituents interfaces which are weak in shear and are modeled by a jump in the tangential displacement which is prescribed as proportional to the shear traction there. Perfect bonding in the normal direction is assumed in this part of the work; however, in the second part open cracks at interfaces are allowed. Let $\underset{\sim}{p}$ denote the unit normal vector at S_{12} pointing from phase $r = 2$ to phase $r = 1$, and let $\underset{\sim}{u}$ and $\underset{\sim}{t}$ denote respectively the displacement and traction vectors. The interface conditions at S_{12} may be expressed in the following manner. Let $(\underset{\sim}{p}, \underset{\sim}{q}, \underset{\sim}{s})$ be an orthogonal set of unit vectors at S_{12} where $\underset{\sim}{p}$ denotes the unit normal vector. The components of the traction and displacements vectors in this coordinate system are respectively expressed as $\underset{\sim}{t} = \underset{\sim}{t}_p + \underset{\sim}{t}_q + \underset{\sim}{t}_s$, $\underset{\sim}{u} = \underset{\sim}{u}_p + \underset{\sim}{u}_q + \underset{\sim}{u}_s$. The interface is then modeled by the following set of equations:

$$
\begin{aligned}
&[\underset{\sim}{u}_p]_{S_{12}} = 0 \quad , \quad [\underset{\sim}{t}]_{S_{12}} = 0 \\
&[\underset{\sim}{u}_q]_{S_{12}} = R \, \underset{\sim}{t}_q \qquad\qquad [\underset{\sim}{u}_s]_{S_{12}} = Q \, \underset{\sim}{t}_s
\end{aligned}
\tag{2}
$$

where R and Q are constants of proportionality for the interface which is flexible in shear and a square bracket [ ] on a quantity $\underset{\sim}{\psi}$ denotes the jump in that quantity across S_{12}, that is

$$
\left[\underset{\sim}{\psi}\right] = \underset{\sim}{\psi}^{(2)}\Big|_{S_{12}} - \underset{\sim}{\psi}^{(1)}\Big|_{S_{12}} \quad , \tag{3}
$$

It is noted that for $R \to 0$, $Q \to 0$, perfect bonding in shear is obtained, and that $R \to \infty$, $Q \to \infty$ yield the case of lubricated contact. The analysis which follows in this section

is also valid if at part of the interfaces there exists imperfect bonding ($R \neq 0$, $Q \neq 0$), and at other parts perfect bonding prevails ($R = 0$, $Q = 0$); in fact different values of R and Q may exist at different points in the interface.

Consider now purely mechanical problems in which the outside surface of the composite is subjected to homogeneous displacement or traction boundary conditions described by:

$$\begin{aligned} \underset{\sim}{u}(S) &= \underset{\sim}{\epsilon}_0 \underset{\sim}{x} \quad , \qquad \theta(S) = 0 \quad , \\ \underset{\sim}{t}(S) &= \underset{\sim}{\sigma}_0 \underset{\sim}{n} \quad , \qquad \theta(S) = 0 \quad , \end{aligned} \tag{4}$$

where $\underset{\sim}{u}(S)$ and $\underset{\sim}{t}(S)$ denote the displacement and traction vector at S, $\underset{\sim}{n}$ is the outside normal to S, $\underset{\sim}{\epsilon}_0$ and $\underset{\sim}{\sigma}_0$ are constant strain and stress tensors, and finally $\underset{\sim}{x}$ denotes the components of a Cartesian system.

Let the local strain and stress fields induced in the phases by these boundary conditions be denoted by

$$\underset{\sim}{\epsilon}_r(\underset{\sim}{x}) = \underset{\sim}{A}_r(\underset{\sim}{x})\underset{\sim}{\epsilon}_0 \, , \qquad \underset{\sim}{\sigma}_r(\underset{\sim}{x}) = \underset{\sim}{L}_r \underset{\sim}{A}_r(\underset{\sim}{x})\underset{\sim}{\epsilon}_0 \, , \tag{5}$$

$$\underset{\sim}{\sigma}_r(\underset{\sim}{x}) = \underset{\sim}{B}_r(\underset{\sim}{x})\underset{\sim}{\sigma}_0 \, , \qquad \underset{\sim}{\epsilon}_r(\underset{\sim}{x}) = \underset{\sim}{M}_r \underset{\sim}{B}_r(\underset{\sim}{x})\underset{\sim}{\sigma}_0 \, , \tag{6}$$

with (5) and (6) corresponding to $(4)_1$ and $(4)_2$ respectively. Furthermore, let us denote the jump in the displacement vector at S_{12} by

$$\begin{aligned} \left[\underset{\sim}{u}(\underset{\sim}{x})\right]_{S_{12}} &= \underset{\sim}{D}(\underset{\sim}{x})\,\underset{\sim}{\epsilon}_0 \quad , \\ \left[\underset{\sim}{u}(\underset{\sim}{x})\right]_{S_{12}} &= \underset{\sim}{F}(\underset{\sim}{x})\,\underset{\sim}{\sigma}_0 \, , \end{aligned} \tag{7}$$

again, under $(4)_1$ and $(4)_2$ respectively. Of course, the fields (5), (6), and (7) satisfy the interface conditions in (2). Local fields are denoted in this paper by the argument $(\underset{\sim}{x})$, whereas expressions without such an argument will refer to average quantities.

Next, consider thermal loading problems in which the surface of the composite is subjected to a uniform temperature rise and to zero displacement or traction boundary conditions.

$$\theta(S) = \theta_0 \qquad \underset{\sim}{u}(S) = \underset{\sim}{0} \quad , \tag{8}$$

$$\theta(S) = \theta_0 \qquad \underset{\sim}{t}(S) = \underset{\sim}{0} \quad . \tag{9}$$

The local fields under (8) and (9) will respectively be denoted by:

$$\begin{aligned} &\underset{\sim}{\epsilon}_r(\underset{\sim}{x}) = \underset{\sim}{a}_r(\underset{\sim}{x})\theta_0 \quad , \\ &\underset{\sim}{\sigma}_r(\underset{\sim}{x}) = (\underset{\sim}{L}_r\underset{\sim}{a}_r(\underset{\sim}{x}) + \underset{\sim}{\ell}_r)\theta_0 \quad , \end{aligned} \tag{10}$$

$$\begin{aligned} &\left[\underset{\sim}{u}(\underset{\sim}{x})\right]_{S_{12}} = \underset{\sim}{d}(\underset{\sim}{x})\theta_0 \\ &\underset{\sim}{\sigma}_r(\underset{\sim}{x}) = \underset{\sim}{b}_r(\underset{\sim}{x})\,\theta_0 \quad , \\ &\underset{\sim}{\epsilon}_r(\underset{\sim}{x}) = (\underset{\sim}{M}_r\,\underset{\sim}{b}_r(\underset{\sim}{x}) + \underset{\sim}{m}_r)\theta_0 \quad , \end{aligned} \tag{11}$$

$$\left[\underset{\sim}{u}(\underset{\sim}{x})\right]_{S_{12}} = \underset{\sim}{f}(\underset{\sim}{x})\theta_0 \quad ,$$

where the vectors $\underset{\sim}{d}(\underset{\sim}{x})$ and $\underset{\sim}{f}(\underset{\sim}{x})$ satisfy the interface conditions in (2). We also note that a uniform temperature field will prevail in the composite under (8) and (9).

It will be shown now that in the two–phase composite with isotropic constituents characterized by the constitutive relations (1) and the interface conditions (2), knowledge of the tensors $\underset{\sim}{A}_r(\underset{\sim}{x})$, $\underset{\sim}{D}(\underset{\sim}{x})$ uniquely determines $\underset{\sim}{a}_r(\underset{\sim}{x})$, $\underset{\sim}{d}(\underset{\sim}{x})$, and $\underset{\sim}{B}_r(\underset{\sim}{x})$, $\underset{\sim}{F}(\underset{\sim}{x})$ determine $\underset{\sim}{b}_r(\underset{\sim}{x})$, $\underset{\sim}{f}(\underset{\sim}{x})$.

Let us first establish the correspondence between the fields induced by $(4)_1$ and (8). This is achieved by using the decomposition scheme described by Dvorak (1986), and Benveniste and Dvorak (1989) for the case of perfectly bonded composites. We will see here that this procedure can be used to establish the desired correspondence relations in the case of interface conditions (2) for two–phase composites with

isotropic phases. In the first stage of this decomposition scheme we seek a strain field $\hat{\underline{\epsilon}}$ which is uniform in V under a uniform temperature change θ_0. This can be achieved by demanding that $\hat{\underline{\epsilon}}$ and θ_0 result in a uniform stress field:

$$\underline{L}_1 \hat{\underline{\epsilon}} + \underline{\ell}_1 \theta_0 = \underline{L}_2 \hat{\underline{\epsilon}} + \underline{\ell}_2 \theta_0 \quad , \tag{12}$$

so that the tractions at S_{12} are continuous. Equation (12) yields for $\hat{\underline{\epsilon}}$:

$$\hat{\underline{\epsilon}} = (\underline{L}_1 - \underline{L}_2)^{-1} (\underline{\ell}_2 - \underline{\ell}_1) \theta_0 \quad . \tag{13}$$

At this stage of the procedure, uniform strain and stress fields prevail in the composite, and both the displacements and tractions are continuous at S_{12}. Also, it turns out that for the isotropic constituents, the created uniform stresses are hydrostatic, and shear tractions at S_{12} vanish. Therefore, the interface conditions at S_{12} described in (2) are automatically satisfied. At the outside boundary S, displacements arising from (13) have been now induced and, as demanded by (8) they need to be reduced to zero. To accomplish this, we apply the following displacements on S:

$$\underline{u}(S) = -\hat{\underline{\epsilon}}\, \underline{x} \quad , \tag{14}$$

and obtain

$$\begin{aligned} &\underline{\epsilon}_r(\underline{x}) = -\underline{A}_r(\underline{x}) \hat{\underline{\epsilon}} \quad , \\ &\left[\underline{u}(\underline{x})\right]_{S_{12}} = -\underline{D}(\underline{x}) \hat{\underline{\epsilon}} \quad . \end{aligned} \tag{15}$$

By superposition with the uniform fields, the resulting fields at the end of the decomposition scheme are therefore:

$$\underset{\sim}{\epsilon}_r(\underset{\sim}{x}) = (\underset{\sim}{I} - \underset{\sim}{A}_r(\underset{\sim}{x}))(\underset{\sim}{L}_1 - \underset{\sim}{L}_2)^{-1}(\underset{\sim}{\ell}_2 - \underset{\sim}{\ell}_1)\theta_0 \quad , \tag{16}$$

$$\left[\underset{\sim}{u}(\underset{\sim}{x})\right]_{S_{12}} = -\underset{\sim}{D}(\underset{\sim}{x})(\underset{\sim}{L}_1 - \underset{\sim}{L}_2)^{-1}(\underset{\sim}{\ell}_2 - \underset{\sim}{\ell}_1)\theta_0 \quad . \tag{17}$$

with $\underset{\sim}{I}$ being the fourth order identity tensor. The concentration factors $\underset{\sim}{a}_r(\underset{\sim}{x})$ and $\underset{\sim}{d}(\underset{\sim}{x})$ can be therefore read out as:

$$\underset{\sim}{a}_r(\underset{\sim}{x}) = (\underset{\sim}{I} - \underset{\sim}{A}_r(\underset{\sim}{x}))\,(\underset{\sim}{L}_1 - \underset{\sim}{L}_2)^{-1}(\underset{\sim}{\ell}_2 - \underset{\sim}{\ell}_1) \quad , \tag{18}$$

$$\underset{\sim}{d}(\underset{\sim}{x}) = -\underset{\sim}{D}(\underset{\sim}{x})\,(\underset{\sim}{L}_1 - \underset{\sim}{L}_2)^{-1}(\underset{\sim}{\ell}_2 - \underset{\sim}{\ell}_1) \quad . \tag{19}$$

The difficulty of extending the above procedure to anisotropic constituents becomes now apparent. For such constituents, shear tractions at S_{12} would exist after the reassembly of the aggregate. To remove these shear tractions, one would have to solve a boundary value problem in which the S_{12} interfaces are loaded by the negative of the shear tractions induced therein. Even though the solution of such a boundary value problem can be formulated in principle, it is not clear at this time that such a solution can be related to a purely mechanical problem with prescribed overall strain.

The correspondence between the fields resulting from $(4)_2$ and (9) can be similarly established. In the first step, a uniform stress field $\hat{\underset{\sim}{\sigma}}$ is sought which together with a temperature change θ_0 causes a in uniform strain field, and therefore continuous displacements throughout. The condition is

$$\underset{\sim}{M}_1\,\hat{\underset{\sim}{\sigma}} + \underset{\sim}{m}_1\,\theta_0 = \underset{\sim}{M}_2\,\hat{\underset{\sim}{\sigma}} + \underset{\sim}{m}_2\,\theta_0 \quad ; \tag{20}$$

it yields

$$\hat{\underset{\sim}{\sigma}} = (\underset{\sim}{M}_1 - \underset{\sim}{M}_2)^{-1}(\underset{\sim}{m}_2 - \underset{\sim}{m}_1)\theta_0 \quad . \tag{21}$$

Since some the constituents are isotropic, these stresses do not result in shear tractions or displacement jumps at S_{12}. To comply with (9), we now remove the tractions induced on the outside surface by (21), by application of:

$$\underline{t}\,(S) = -\hat{\underline{\sigma}}\,\underline{n} \quad , \tag{22}$$

which by themselves cause the local effects

$$\begin{aligned} \underline{\sigma}_r(\underline{x}) &= -\underline{B}_r(\underline{x})\hat{\underline{\sigma}} \quad , \\ [\underline{u}(\underline{x})]_{S_{12}} &= -\underline{F}(\underline{x})\hat{\underline{\sigma}} \quad . \end{aligned} \tag{23}$$

This is superimposed with the uniform field $\hat{\sigma}$ to yield:

$$\underline{\sigma}_r(\underline{x}) = (\underline{I} - \underline{B}_r(\underline{x}))\,(\underline{M}_1 - \underline{M}_2)^{-1}(\underline{m}_2 - \underline{m}_1)\,\theta_0 \quad , \tag{24}$$

$$\left[\underline{u}(\underline{x})\right]_{S_{12}} = -\underline{F}(\underline{x})\,(\underline{M}_1 - \underline{M}_2)^{-1}(\underline{m}_2 - \underline{m}_1)\,\theta_0 \quad , \tag{25}$$

The concentration factors thus are

$$\underline{b}_r(\underline{x}) = (\underline{I} - \underline{B}_r(\underline{x}))\,(\underline{M}_1 - \underline{M}_2)^{-1}(\underline{m}_2 - \underline{m}_1) \tag{26}$$

$$\underline{f}(\underline{x}) = -\underline{F}(\underline{x})\,(\underline{M}_1 - \underline{M}_2)^{-1}(\underline{m}_2 - \underline{m}_1)\,. \tag{27}$$

We have therefore established the desired correspondence relations. It is of interest to note here that the structure of (18) and (26), is similar to that given in Benveniste and Dvorak (1989) for perfect bonding between the constituents.

1b. Application: Effective Thermal Stress and Strain Tensors

One of the applications of the correspondence principle described in the previous section is the determination of the effective thermal tensors of the composite based solely on the information obtained from the mechanical problem. Suppose therefore that the effective constitutive law of the composite is described by

$$\begin{aligned} \underset{\sim}{\sigma} &= \underset{\sim}{L}\,\underset{\sim}{\epsilon} + \underset{\sim}{\ell}\,\theta \quad , \\ \underset{\sim}{\epsilon} &= \underset{\sim}{M}\,\underset{\sim}{\sigma} + \underset{\sim}{m}\,\theta \quad , \end{aligned} \tag{28}$$

where $\underset{\sim}{L}$ and $\underset{\sim}{M}$ with $\underset{\sim}{M} = \underset{\sim}{L}^{-1}$ denote respectively the effective stiffness and compliance tensors, $\underset{\sim}{\ell}$ and $\underset{\sim}{m}$ with $\underset{\sim}{\ell} = -\underset{\sim}{L}\,\underset{\sim}{m}$ are the effective thermal strain and stress tensors. The tensors $\underset{\sim}{\sigma}$ and $\underset{\sim}{\epsilon}$, and the temperature θ refer to average quantities.

The tensors $\underset{\sim}{\ell}$ and $\underset{\sim}{m}$ are determined in principle by subjecting the composite to boundary conditions (8) and (9) respectively. Let us first consider the determination of $\underset{\sim}{\ell}$. It is important to note here that since displacement jumps occur at constituent interfaces, special care should be taken in defining average quantities in the composite, and the reader is referred to Benveniste (1985) for a proper framework for the computation of effective properties in these situations. Under (8), the average strain in the composite vanishes, therefore in accordance with the quoted paper

$$\underset{\sim}{\epsilon} = c_1\,\underset{\sim}{\epsilon}_1 + c_2\,\underset{\sim}{\epsilon}_2 - c_2\,\underset{\sim}{J} = 0 \quad , \tag{29}$$

where $\underset{\sim}{J}$ is a second order tensor representing the deformation at internal boundaries, and is given by:

$$J_{ij} = \frac{1}{2V}\int_{S_{12}} ([u_i]\,p_j + [u_j]\,p_i)\,dS_{12} \quad , \tag{30}$$

where p_j was defined in (2); c_r and $\underset{\sim}{\epsilon}_r$ with $r = 1, 2$ denote the phase volume fractions and phase strain averages respectively, and V is the volume of the composite. The average stress in the composite, in view of $(1)_1$, $(28)_1$, and (29) is given by

$$\underset{\sim}{\sigma} = c_1\underset{\sim}{\sigma}_1 + c_2\underset{\sim}{\sigma}_2 =$$
$$= c_1(\underset{\sim}{L}_1\underset{\sim}{\epsilon}_1+\underset{\sim}{\ell}_1\theta_0) + c_2(\underset{\sim}{L}_2\underset{\sim}{\epsilon}_2+\underset{\sim}{\ell}_2\theta_0) = \underset{\sim}{\ell}\,\theta_0 \quad , \qquad (31)$$

where we have used the fact that a uniform temperature prevails throughout. Elimination of $\underset{\sim}{\epsilon}_2$ from (29) and substitution into (31) provides:

$$\underset{\sim}{\ell} = c_1\underset{\sim}{\ell}_1 + c_2\underset{\sim}{\ell}_2 + c_2\,(\underset{\sim}{L}_2 - \underset{\sim}{L}_1)\,\underset{\sim}{a}_2 + c_2\,\underset{\sim}{L}_1\,\underset{\sim}{a} \quad , \qquad (32)$$

where the concentration factors are defined as in (10):

$$\underset{\sim}{\epsilon}_2 = \underset{\sim}{a}_2\,\theta_0 \quad , \quad \underset{\sim}{J} = \underset{\sim}{a}\,\theta_0 \quad . \qquad (33)$$

The tensor $\underset{\sim}{a}_2$ is simply the average of $\underset{\sim}{a}_2(\underset{\sim}{x})$ in (18), and is given by

$$\underset{\sim}{a}_2 = (\underset{\sim}{I} - \underset{\sim}{A}_2)(\underset{\sim}{L}_1 - \underset{\sim}{L}_2)^{-1}(\underset{\sim}{\ell}_2 - \underset{\sim}{\ell}_1) \quad , \qquad (34)$$

where $\underset{\sim}{A}_2$ is again the phase volume average of $\underset{\sim}{A}_2\,(\underset{\sim}{x})$. The tensor $\underset{\sim}{a}$ is obtained by substituting $(10)_3$ and (19) into (30):

$$\underset{\sim}{a} = -\underset{\sim}{A}\,(\underset{\sim}{L}_1 - \underset{\sim}{L}_2)^{-1}\,(\underset{\sim}{\ell}_2 - \underset{\sim}{\ell}_1) \quad , \qquad (35)$$

with the concentration factor $\underset{\sim}{J} = \underset{\sim}{A}\,\underset{\sim}{\epsilon}^{\circ}$ defined as:

$$A_{ijkl} = \frac{1}{2V}\int_{S_{12}} (D_{ikl}\,(\underset{\sim}{x})\,p_j + D_{jkl}\,(\underset{\sim}{x})\,p_i)\,dS_{12} \quad . \qquad (36)$$

Substitution of (34) and (35) into (32) provides

$$\underline{\ell} = c_1\underline{\ell}_1 + c_2\underline{\ell}_2 + \\ + c_2(\underline{L}_2 - \underline{L}_1)(\underline{I} - \underline{A}_2)(\underline{L}_1 - \underline{L}_2)^{-1}(\underline{\ell}_2 - \underline{\ell}_1) \\ - c_2\,\underline{L}_1\,\underline{A}\,(\underline{L}_1 - \underline{L}_2)^{-1}(\underline{\ell}_2 - \underline{\ell}_1) \quad , \tag{37}$$

hence $\underline{\ell}$ has been determined in terms of the constituent phase properties and the mechanical concentration factors $\underline{A}_2$ and $\underline{A}$.

Equation (37) can be further simplified. To this end, recall that the effective stiffness $\underline{L}$ of the composite is obtained by subjecting the external surface S to $(4)_1$ and using the fact that

$$\underline{\epsilon} = c_1\underline{\epsilon}_1 + c_2\underline{\epsilon}_2 - c_2\underline{J} = \underline{\epsilon}_0 \quad . \tag{38}$$

After some manipulations this leads to (Benveniste (1985)):

$$\underline{L} = \underline{L}_1 + c_2\,(\underline{L}_2 - \underline{L}_1)\,\underline{A}_2 + c_2\underline{L}_1\underline{A} \quad . \tag{39}$$

Solving for $\underline{A}_2$ in (39), and substituting into (37), we obtain:

$$\underline{\ell} = \underline{\ell}_1 + (\underline{L} - \underline{L}_1)(\underline{L}_2 - \underline{L}_1)^{-1}(\underline{\ell}_2 - \underline{\ell}_1) \tag{40}$$

Equation (40), interestingly enough, is the same as equation (3.11) in Benveniste and Dvorak (1989). Note however that imperfect bonding at S_{12} as described in equation (2) still affects the effective thermal tensor $\underline{\ell}$, since $\underline{L}$ itself is affected, as in (39).

The determination of $\underline{m}$ follows similar steps, this time under the stress boundary conditions (9). It leads to a set of equations which are counterparts to (29), (31) and (32):

$$\underline{\sigma} = c_1\underline{\sigma}_1 + c_2\underline{\sigma}_2 = 0 \quad , \tag{41}$$

$$\underline{\epsilon} = c_1\underline{\epsilon}_1 + c_2\underline{\epsilon}_2 - c_2\underline{J} = c_1(\underline{M}_1\underline{\sigma}_1 + \underline{m}_1\theta_0) + \\ + c_2(\underline{M}_2\underline{\sigma}_2 + \underline{m}_2\theta_0) = \underline{m}\theta_0 \quad , \tag{42}$$

$$\underset{\sim}{m} = c_1\underset{\sim}{m}_1 + c_2\underset{\sim}{m}_2 + c_2(\underset{\sim}{M}_2 - \underset{\sim}{M}_1)\underset{\sim}{b}_2 - c_2\underset{\sim}{b} \quad , \tag{43}$$

where we have defined the concentration factors $\underset{\sim}{b}_2$ and $\underset{\sim}{b}$ as follows:

$$\underset{\sim}{\sigma}_2 = \underset{\sim}{b}_2\theta_0 \qquad \underset{\sim}{J} = \underset{\sim}{b}\theta_0 \quad . \tag{44}$$

In analogy to (34) and (35), these tensors can be written in the form:

$$\underset{\sim}{b}_2 = (\underset{\sim}{I} - \underset{\sim}{B}_2)\,(\underset{\sim}{M}_1 - \underset{\sim}{M}_2)^{-1}\,(\underset{\sim}{m}_2 - \underset{\sim}{m}_1) \quad , \tag{45}$$

$$\underset{\sim}{b} = -\,\underset{\sim}{B}\,(\underset{\sim}{M}_1 - \underset{\sim}{M}_2)^{-1}\,(\underset{\sim}{m}_2 - \underset{\sim}{m}_1) \quad , \tag{46}$$

with

$$B_{ijkl} = \frac{1}{2V}\int_{S_{12}} (F_{ikl}(x)p_j + F_{jkl}(x)p_i)\,dS_{12} \quad . \tag{47}$$

The equation for $\underset{\sim}{m}$, finally becomes:

$$\begin{aligned}\underset{\sim}{m} = {} & c_1\underset{\sim}{m}_1 + c_2\underset{\sim}{m}_2 + \\ & + c_2(\underset{\sim}{M}_2 - \underset{\sim}{M}_1)(\underset{\sim}{I} - \underset{\sim}{B}_2)(\underset{\sim}{M}_1 - \underset{\sim}{M}_2)^{-1}(\underset{\sim}{m}_2 - \underset{\sim}{m}_1) \\ & + c_2\underset{\sim}{B}(\underset{\sim}{M}_1 - \underset{\sim}{M}_2)^{-1}(\underset{\sim}{m}_2 - \underset{\sim}{m}_1) \quad .\end{aligned} \tag{48}$$

The expression for the effective compliance tensor (Benveniste (1985)),

$$\underset{\sim}{M} = \underset{\sim}{M}_1 + c_2\,(\underset{\sim}{M}_2 - \underset{\sim}{M}_1)\underset{\sim}{B}_2 - c_2\,\underset{\sim}{B} \quad , \tag{49}$$

helps to reduce equation (48) to the form

$$\underset{\sim}{m} = \underset{\sim}{m}_1 + (\underset{\sim}{M} - \underset{\sim}{M}_1)\,(\underset{\sim}{M}_2 - \underset{\sim}{M}_1)^{-1}\,(\underset{\sim}{m}_2 - \underset{\sim}{m}_1) \quad , \tag{50}$$

which is the counterpart of (40). Using $\underset{\sim}{\ell}_r = -\,\underset{\sim}{L}_r\,\underset{\sim}{m}_r$ and the

fact that $\underset{\sim}{L} = \underset{\sim}{M}^{-1}$, one can verify that $\underset{\sim}{\ell}$ and $\underset{\sim}{m}$ as given by (40) and (50) fulfill the relation $\underset{\sim}{\ell} = -\underset{\sim}{L}\underset{\sim}{m}$.

We have utilized here the correspondence relations established in the previous section to derive expressions for the effective thermal tensors $\underset{\sim}{\ell}$ and $\underset{\sim}{m}$ in terms of effective mechanical properties of the composite. The correspondence relations are limited to isotropic constituents, and therefore, the derived equations (40) and (50) apply also to such systems only.

Expressions for the effective thermal tensors in terms of effective mechanical properties have been given before in the literature for the case of composites with perfectly bonded anisotropic phases. The basic idea was due to Levin (1967) which used the principle of virtual work to this end. Levin's paper was extended to anisotropic constituents by Rosen and Hashin (1970), see also Laws (1973) and Schulgasser (1989) for an alternative derivation of these relations. We will show in the next section that the virtual work theorem can again lead to equations similar to (40) and (50) for the case of multiphase materials with anisotropic phases and imperfect interfaces of the type described in (2). It should be of course made clear that in spite of its limitation to isotropic constituents in the present case, the decomposition scheme is in a sense more general than the results provided by the virtual work theorem since it provides results *on fields* and not only on average properties.

2. Effective Thermal and Stress Tensors in Multiphase Composites with Anisotropic Constituents and Interfaces Weak In Shear

We consider now multiphase composites described by (1) and (2), but allow this time for general anisotropic behavior in for the phases. As in Section 1, different parts of the interfaces may possess different values of $0 \leq R \leq \infty$ and $0 \leq Q \leq \infty$. An expression for the effective thermal stress tensor $\underset{\sim}{\ell}$ in terms of purely mechanical properties will be first derived by considering the boundary conditions $(4)_1$ and (8). For convenience, we let the fields induced by $(4)_1$ be denoted by primed quantities and those resulting from (8) by unprimed

quantities. The principle of virtual work for composites with imperfect interfaces can be found in Benveniste (1985). When applied to the boundary value problems $(4)_1$ and (8), it can be written as:

$$\int_V \sigma_{ij}(\underset{\sim}{x})\epsilon'_{ij}(\underset{\sim}{x})dV$$

$$= \int_S t_i(\underset{\sim}{x})u'_i(\underset{\sim}{x})dS + \sum_{r=2}^{N}\int_{S_{1r}} t_i(\underset{\sim}{x})[u'_i(\underset{\sim}{x})]dS_{1r} \ , \qquad (51)$$

where t_i and u_i denote the traction and displacement vector, $r = 1$ stands for the matrix, and S_{1r} denotes the boundaries of the inclusion phases with the matrix.

Substitution of σ_{ij} from (1) into (51) yields:

$$\int_V L_{ijkl}\,\epsilon_{kl}(\underset{\sim}{x})\,\epsilon'_{ij}(\underset{\sim}{x})\,dV + \int_V \ell_{ij}\,\epsilon'_{ij}(\underset{\sim}{x})\,\theta_0 dV$$

$$= \int_S t_i(\underset{\sim}{x})u'_i(\underset{\sim}{x})dS + \sum_{r=2}^{N}\int_{S_{1r}} t_i(\underset{\sim}{x})[u'_i(\underset{\sim}{x})]dS_{1r}\,, \quad (52)$$

with the material properties assuming the index $r = 1, 2, \ldots N$ depending on the position of the point $\underset{\sim}{x}$ in the composite. For the boundary condition $(4)_1$, the first integral on the right hand side of (52) can be simplified as:

$$\int_S t_i(\underset{\sim}{x})u'_i(\underset{\sim}{x})dS = \int_S t_i(\underset{\sim}{x})\epsilon^0_{ij}x_j dS$$

$$= \epsilon^0_{ij}\int_S \sigma_{ik}(\underset{\sim}{x})n_k x_j dS$$

$$= \epsilon^0_{ij}\, \sigma_{ij}\, V = \epsilon^0_{ij}\, \ell_{ij}\, \theta_0 V \quad , \tag{53}$$

where, σ_{ij} denotes the overall average stress, and the fact that the average strain vanishes under (8) has been used. Substitution of (53) into (52) gives:

$$\int_V L_{ijkl}\, \epsilon_{kl}(\underset{\sim}{x}) \epsilon'_{ij}(\underset{\sim}{x}) dV + \int_V \ell_{ij}\, \epsilon'_{ij}(\underset{\sim}{x}) \theta_0\, dV$$

$$= \sum_{r=2}^{N} \int_{S_{1r}} t_i(\underset{\sim}{x})[u'_i(\underset{\sim}{x})]\, dS_{1r} + \epsilon^0_{ij}\, \ell_{ij}\, \theta_0\, V \quad . \tag{54}$$

The virtual work theorem is now applied to the boundary value problems $(4)_1$ and (8) with the alternative choice of admissible displacement and stress fields; the fields in $(4)_1$ are denoted by primed quantities and those in (8) by unprimed ones. The result is:

$$\int_V \sigma'_{ij}(\underset{\sim}{x})\, \epsilon_{ij}(\underset{\sim}{x}) dV$$

$$= \int_S t'_i(\underset{\sim}{x}) u_i(\underset{\sim}{x}) dS + \sum_{r=2}^{N} \int t'_i(\underset{\sim}{x})[u_i(\underset{\sim}{x})] dS_{1r}, \tag{55}$$

$$\int_V L_{ijkl}\, \epsilon'_{kl}(\underset{\sim}{x})\, \epsilon_{ij}(\underset{\sim}{x}) dV$$

$$= \sum_{r=2}^{N} \int t'_i(\underset{\sim}{x})[u_i(\underset{\sim}{x})] dS_{1r} \quad , \tag{56}$$

where we used the condition $u_i(S) = 0$. Subtraction of (56) from (54) yields

$$\sum_{r=1}^{N} c_r \ell_{ij}^{(r)} \epsilon_{ij}^{(r)} \theta_0$$

$$= \frac{1}{V} \sum_{r=2}^{N} \int_{S_{1r}} \left\{ t_i(\underset{\sim}{x})[u_i'(\underset{\sim}{x})] - t_i'(\underset{\sim}{x})[u_i(\underset{\sim}{x})] \right\} dS_{1r}$$

$$+ \ell_{ij} \overset{0}{\epsilon}_{ij} \theta_0 \quad . \tag{57}$$

The integral on the right hand side involves the scalar product between the traction vector in one loading system and the displacement jump vector in the second system. The interface conditions described in (2) make this term vanish. Equation (57) therefore yields:

$$\underset{\sim}{\ell} = \sum_{r=1}^{N} c_r \underset{\sim}{A}_r^T \underset{\sim}{\ell}_r \quad , \tag{58}$$

where we have invoked the definition of the concentration factors $\underset{\sim}{A}_r$ and reverted again to the bold face tensorial notation. The transpose sign in (58) denotes:

$$(\underset{\sim}{A}_r^T)_{ijkl} = (\underset{\sim}{A}_r)_{klij} \quad . \tag{59}$$

It is somewhat surprising to see that equation (58) is the same as Rosen and Hashin's (1970) result for perfect bonding between the phases. Note however that due to interface slip, the tensors $\underset{\sim}{A}_r^T$ are not equal to those which would be obtained under perfect bonding conditions. We finally mention that if part of the interfaces at S_{12} contain open cracks,(58) remains valid since the tractions at these boundaries vanish identically if all crack closure effects are neglected.

For the case of binary composites equation (58) can also be written in other equivalent forms with one among them making contact with the results obtained in the previous section. Under $(4)_1$, note that

$$c_1\underset{\sim}{A}_1 + c_2\underset{\sim}{A}_2 - c_2\underset{\sim}{A} = \underset{\sim}{I} \quad , \tag{60}$$

where $\underset{\sim}{A}$ was defined in (36). Solving for $c_1\underset{\sim}{A}_1^T$ in (60) and substituting in (58) provides:

$$\underset{\sim}{\ell} = \underset{\sim}{\ell}_1 + c_2\,\underset{\sim}{A}_2^T(\underset{\sim}{\ell}_2 - \underset{\sim}{\ell}_1) + c_2\,\underset{\sim}{A}^T\underset{\sim}{\ell}_1 \quad . \tag{61}$$

Another form can be obtained by writing first (39) as:

$$\underset{\sim}{L} = \underset{\sim}{L}_1 + c_2\underset{\sim}{A}_2^T(\underset{\sim}{L}_2 - \underset{\sim}{L}_1) + c_2\,\underset{\sim}{A}^T\,\underset{\sim}{L}_1 \quad , \tag{62}$$

where the diagonal symmetry of the stiffness tensors has been invoked. Solving for $\underset{\sim}{A}_2^T$ in (62) and substituting into (61) provides:

$$\begin{aligned}\underset{\sim}{\ell} = \underset{\sim}{\ell}_1 &+ (\underset{\sim}{L} - \underset{\sim}{L}_1)(\underset{\sim}{L}_2 - \underset{\sim}{L}_1)^{-1}(\underset{\sim}{\ell}_2 - \underset{\sim}{\ell}_1) + \\ &+ c_2\,\underset{\sim}{A}^T\left\{\underset{\sim}{\ell}_1 - \underset{\sim}{L}_1(\underset{\sim}{L}_2 - \underset{\sim}{L}_1)^{-1}(\underset{\sim}{\ell}_2 - \underset{\sim}{\ell}_1)\right\} \quad .\end{aligned} \tag{63}$$

Equation (63) is the counterpart of (40) of the previous section for the case of anisotropic constituents. Let us next prove that in the special of isotropic phases the last term in (63) vanishes.

For isotropic phases let,

$$(\underset{\sim}{\ell}_1)_{ij} = \alpha\,\delta_{ij} \quad ,$$

$$(\underset{\sim}{L}_1)_{ijrs} = \beta\,\delta_{ij}\,\delta_{rs} + \gamma(\delta_{ir}\,\delta_{js} + \delta_{is}\,\delta_{jr} - \frac{2}{3}\,\delta_{ij}\,\delta_{rs}) \quad ,$$

$$(\underset{\sim}{L}_2 - \underset{\sim}{L}_1)^{-1}_{rsmn} = \xi\delta_{rs}\delta_{mn} + \zeta(\delta_{rm}\delta_{sn} + \delta_{rn}\delta_{sm} - \tfrac{2}{3}\delta_{rs}\delta_{mn}) \quad ,$$

$$(\underset{\sim}{\ell}_2 - \underset{\sim}{\ell}_1)_{mn} = \lambda\,\delta_{mn} \quad , \tag{64}$$

where α, β, γ, ξ, ζ, λ are constants. Writing $\underset{\sim}{A}^T$ in indicial notation and carrying out the summation in (63) according to

(64) shows that the tensor $\underset{\sim}{A}^T$ enters only as $(\underset{\sim}{A}^T)_{pqii}$. However, since according to the interface conditions (2) the normal displacements are continuous at S_{12} it follows from (36) that $A_{iikl} \equiv 0$ or, in fact, $(\underset{\sim}{A}^T)_{pqii} \equiv 0$. We have therefore shown that for the case of isotropic constituents (63) reduce to (40).

A similar implementation of the virtual work theorem (51) to the boundary value problems $(4)_2$ and (9) yields equations for the thermal strain tensor $\underset{\sim}{m}$. For the sake of brevity we will give only the final results, counterparts to equations (58), (61) and (63). These are:

$$\underset{\sim}{m} = \sum_{r=1}^{N} c_r \underset{\sim}{B}_r^T \underset{\sim}{m}_r \tag{65}$$

$$\underset{\sim}{m} = \underset{\sim}{m}_1 + c_2 \underset{\sim}{B}_2^T (\underset{\sim}{m}_2 - \underset{\sim}{m}_1) \tag{66}$$

$$\underset{\sim}{m} = \underset{\sim}{m}_1 + (\underset{\sim}{M} - \underset{\sim}{M}_1)(\underset{\sim}{M}_2 - \underset{\sim}{M}_1)^{-1}(\underset{\sim}{m}_2 - \underset{\sim}{m}_1) + \\ + c_2 \underset{\sim}{B}^T (\underset{\sim}{M}_2 - \underset{\sim}{M}_1)^{-1}(\underset{\sim}{m}_2 - \underset{\sim}{m}_1) \tag{67}$$

where the last two equations refer to binary systems only. It is noted that the structure of (66) and (67) are not exactly similar to (61) and (63) respectively. This is due to the fact that $\underset{\sim}{\epsilon}$ and $\underset{\sim}{\sigma}$ in (29) and (31) and also (39) and (49) have a different structure. For the same reasons mentioned above equation (67) reduces to (50) for the case of isotropic constituents.

Finally, it is easy to show that $\underset{\sim}{\ell}$ and $\underset{\sim}{m}$, as given by (58) and (65) for example, satisfy $\underset{\sim}{\ell} = -\underset{\sim}{L}\underset{\sim}{m}$. From the definitions of the $\underset{\sim}{A}_r$ and $\underset{\sim}{B}_r$ tensors and also due to $\underset{\sim}{L} = \underset{\sim}{M}^{-1}$, it results that

$$\underset{\sim}{B}_r = \underset{\sim}{L}_r \underset{\sim}{A}_r \underset{\sim}{L}^{-1} \qquad r = 1, \ldots N \tag{68}$$

which provides

$$\underset{\sim}{L}\,\underset{\sim}{B}_r^T = \underset{\sim}{A}_r^T\,\underset{\sim}{L}_r \qquad r = 1,\ldots N \tag{69}$$

Multiplying (65) by $(-\underset{\sim}{L})$ from the left, using (69) and $\underset{\sim}{\ell}_r = -\underset{\sim}{L}_r\underset{\sim}{m}_r$ shows readily that (58) is in fact recovered.

Acknowledgement

Funding for this work was provided, in part, by the ONR/DARPA–HiTASC composites program at Rensselaer, and by the Air Force Office of Scientific Research.

References

Aboudi, J., 1987, "Damage in Composites — Modeling of Imperfect Bonding," *Comp. Sci. and Tech.* **28**, pp. 103–128.

Achenbach, J.D. and Zhu, H., 1989, "Effect of Interfacial Zone on Mechanical Behavior and Failure of Fiber–Reinforced Composites," *J. Mech. Phys. Solids*, 37, pp. 381–393.

Benveniste, Y., 1985, "The Effective Mechanical Behaviour of Composite Materials with Imperfect Contact Between the Constituents," *Mechanics of Materials*, 4, pp. 197–208.

Benveniste, Y. and Aboudi, J., 1984 "A Continuum Model for Fiber Reinforced Materials with Debonding," *Int. J. Solids Structures*, 20, 11/12, pp. 935–951.

Benveniste, Y. and Dvorak, G. J., 1990, "On a Correspondence Between Mechanical and Thermal Effects in Two–Phase Composites," in Toshio Mura Anniversary Volume *Micromechanics and Inhomogeneity*, Editors: Weng, G.J., Taya, M., and Abe, H, Springer Verlag, pp. 65–81.

Benveniste, Y. and Miloh, T., 1986, "The Effective Conductivity of Composites with Imperfect Thermal Contact at Constituent Interfaces," *Int. J. Eng. Sci.* 24, pp. 1537–1552.

Dvorak, G.J., 1983, "Metal Matrix Composites: Plasticity and Fatigue," in *Mechanics of Composite Materials -- Recent Advances*, edited by Z. Hashin and C.T. Herakovich, Pergamon Press, New York, pp. 73–92.

Dvorak, G.J., 1986, "Thermal Expansion of Elastic–Plastic Composite Materials," *J. Appl. Mech.* 53, pp. 737–743.

Dvorak, G.J. and Chen, T., 1989, "Thermal Expansion of Three–Phase Composite Materials" *J. Appl. Mech.* 56, pp. 418–422.

Dvorak, G.J., 1990, "On Uniform Fields in Heterogeneous Media," to appear in *Proceedings A of the Royal Society.*

Hashin, Z., 1990, "Thermoelastic Properties of Fiber Composites with Imperfect Interface," *Mechanics of Materials* 8, pp. 333–348.

Jasiuk, I., Mura, T., and Tsuchida, E., 1988, "Thermal Stresses and Thermal Expansion Coefficients of Short Fiber Composites with Sliding Interfaces," *J. of Engng. Mat. and Tech.*, 110, pp. 96–100.

Jasiuk, I. and Tong, Y., 1989, "The Effect of Interface on the Elastic Stiffness of Composites," in *Mechanics of Composite Materials and Structures*, edited by J.N. Reddy and J.L. Teply, AMD–Vol. 100, pp. 49–54.

Laws, N., 1973, "On the Thermostatics of Composite Materials," *J. Mech. Phys. Solids* 21, pp. 9–17.

Lene, F. and Leguillon, D., 1982, "Homogeneized Constitutive Law for a Partially Cohesive Composite Material," *Int. J. Solids Structures* 18, pp. 443–458.

Levin, V.M., 1967, "Thermal Expansion Coefficients of Heterogeneous Materials", *Mekhanika Tverdago Tela*, 2, pp. 88 – 94. English Translation *Mechanics of Solids*, 11, pp. 58 – 61.

Mura, T., Jasiuk, I. and Tsuchida, E. 1985, "The Stress Field of a Sliding Inclusion," *Int. J. Solids and Struct.*, 12, pp. 1165–1179.

Rosen, B.W. and Hashin Z., 1970, "Effective Thermal Expansion Coefficients and Specific Heats of Composite Materials", *Int. J. Engng. Sci.* 8, pp. 157–173.

Schulgasser, K., 1989, "Environmentally–Induced Expansion of Heterogeneous Media," *J. Appl. Mech.* 56, pp. 546–549.

Tsuchida, E., Mura, T. and Dundurs, J., 1986 "The Elastic Field of an Elliptic Inclusion with a Slipping Interface," *J. Appl. Mech.* 53, pp. 103–107.

Int. J. Solids Structures Vol. 29, No. 23, pp. 2907–2919, 1992
Printed in Great Britain.

0020–7683/92 $5.00 + .00

ON THE THERMOMECHANICS OF COMPOSITES WITH IMPERFECTLY BONDED INTERFACES AND DAMAGE

G. J. DVORAK
Institute Center for Composite Materials and Structures, Rensselaer Polytechnic Institute, Troy, NY 12180, U.S.A.

and

Y. BENVENISTE†
Department of Solid Mechanics, Materials and Structures, Faculty of Engineering, Tel-Aviv University, Ramat-Aviv, 69978, Israel

(*Received* 29 *July* 1991; *in revised form* 19 *March* 1992)

Abstract—General connections are established between the mechanical and thermal responses of composite materials with debonded or imperfectly bonded interfaces, and with internal cracks or cavities. In particular, such results are found for multiphase composites or polycrystals in which normal and/or shear displacement jumps may exist at interfaces or cracks, consistent with complete debonding or with the presence of a nonlinearly elastic interphase layer. In two-phase systems with isotropic phases and sliding interfaces, we also recover exact connections between the mechanical and thermal stress or strain fields in the phases.

1. INTRODUCTION

Evaluation of thermoelastic properties of composite materials is of considerable interest, particularly in high-temperature ceramic systems. Although perfect bonding between the phases may be desirable, various types of imperfect bonding at interfaces, as well as internal cracking may exist in actual systems. Any such damage mode will cause a change in overall stiffness, in local mechanical fields, and also in the overall thermal expansion coefficients and in the thermal stress and strain fields. It is well known that in perfectly bonded systems, the overall thermal properties can be evaluated in terms of phase properties and mechanical concentration factors (Levin, 1967). More general relations involving local fields also exist for certain perfectly bonded two-phase systems (Dvorak, 1983, 1986, 1990; Dvorak and Chen, 1989; Benveniste and Dvorak, 1990a), and also for two-phase composites with isotropic constituents and slipping interfaces (Benveniste and Dvorak, 1990b).

The present paper extends this line of inquiry, and establishes such connections for many other damaged composite materials. In particular, we show in the first part of the paper that the Levin-type connections are recovered in multiphase composite systems of arbitrary phase geometry and material symmetry, even if the interfaces, or their parts, undergo debonding which is either complete, or consistent with the presence of a very thin nonlinearly elastic interphase layer which permits both normal and shear displacement jumps at interfaces. In the second part, special forms of these results are found for two-phase composites. Moreover, in two-phase systems with isotropic constituents and slipping interfaces, exact relationships are found between mechanical and thermal stress or strain fields in the phases. This is accomplished with the help of uniform strain and stress fields in heterogeneous media (Dvorak, 1990; Benveniste and Dvorak, 1990a).

The emphasis is on evaluation of general thermomechanical connections rather than the formulation of micromechanical models. Examples of the latter may be found in other recent references, e.g. Chen and Argon (1979a, b); Lené and Leguillon (1982); Benveniste and Aboudi (1984); Mura *et al.* (1985); Benveniste and Miloh (1986); Tsuchida *et al.* (1986); Jasiuk *et al.* (1988); Achenbach and Zhu (1989); Jasiuk and Tong (1989); Hashin (1990). Therefore, throughout the paper we assume that the local fields caused by

† Also Visiting Professor at RPI.

mechanical loads can be evaluated by an independent analysis. Our purpose is to provide a general methodology for evaluation of the thermal response of damaged composites from the various solutions of mechanical loading problems.

2. MULTIPHASE COMPOSITES

2.1. *Phase and interface properties*

We first consider multiphase media with N constituent phases, which may represent such actual systems as matrix-based composites or polycrystals, and focus our attention at a sufficiently large representative volume which has the same effective properties as any other volume of such or larger size. If a matrix is present, then it will be denoted by $r = 1$, and $r = 2, 3, \ldots, N$ will represent the reinforcing phases. All phases are linear thermoelastic solids, their constitutive relations are

$$\boldsymbol{\sigma}_r = \mathbf{L}_r\boldsymbol{\varepsilon}_r + \mathbf{l}_r\theta_0, \quad \boldsymbol{\varepsilon}_r = \mathbf{M}_r\boldsymbol{\sigma}_r + \mathbf{m}_r\theta_0, \quad r = 1, 2, \ldots, N, \tag{1}$$

where $\boldsymbol{\sigma}_r$, $\boldsymbol{\varepsilon}_r$, $\mathbf{L}_r$, $\mathbf{l}_r$, θ_0 denote, respectively, the stress, strain, stiffness, thermal stress tensors and a uniform temperature change. $\mathbf{M}_r = \mathbf{L}_r^{-1}$ and $\mathbf{m}_r = -\mathbf{M}_r\mathbf{l}_r$ are the compliance and thermal strain tensors.

Damage in composites may be due to internal cavities or cracks, and imperfect bonding between the phases. Imperfect bonding may be regarded in terms of a thin interphase region of certain stiffness, or as interface cracks and cavities. The interface between phases r and s will be represented in this paper by an idealized geometrical surface of zero thickness. Nevertheless, it will be convenient to think of these interfaces as two-sided surfaces S_{rs} and S_{sr} adjacent to phases r and s respectively; such a notation will also help symmetrize many expressions in the paper. The displacement field may or may not be discontinuous across such interfaces. Should a cavity or a crack develop between the phases r and s, the surface of that vacuous zone will be denoted by S_{rr} and S_{ss}. The surface S_{rr} will be that in contact with phase r, and S_{ss} that in contact with phase s, (see Fig. 1a). The phases may also contain internal cracks or cavities. The surface of such a defect which is internal to phase r will be

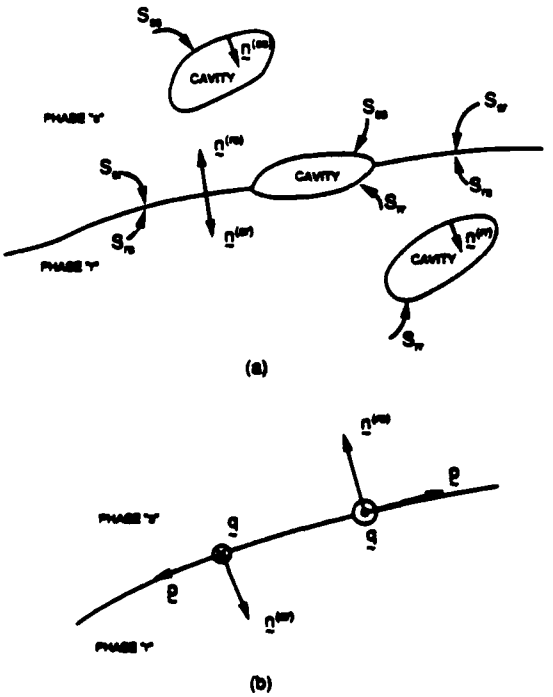

Fig. 1. (a) Interface between two phases r and s. (b) Possible choice of coordinate systems at interfaces.

denoted by S_{rr}. In the case of a thin crack in phase r, it may be convenient, though not necessary, to consider the decomposition $S_{rr} = S_{rr}^{+} \cup S_{rr}^{-}$ where S_{rr}^{+} and S_{rr}^{-} denote the upper and lower surfaces of the crack.

At any point on the interfacial surface between phase r and phase s, it will be convenient to define the unit normals $\mathbf{n}^{(sr)} = -\mathbf{n}^{(rs)}$ from phase s to phase r. At the surface of a cavity or crack which is in contact with phase r we will define the normal $\mathbf{n}^{(rr)}$ from phase r into the vacuous zone.

The displacements and tractions, together with the unit normals described above at any point $\mathbf{x}$ of the interfacial surface, will be described in a *single* Cartesian coordinate system. This Cartesian system can in principle be fixed in space, but can also be conveniently chosen at the generic point $\mathbf{x}$ on the interface. In the latter alternative, we may choose either $(\mathbf{n}^{(rs)}, \mathbf{p}, \mathbf{q})$ *or* $(\mathbf{n}^{(sr)}, \mathbf{p}, \mathbf{q})$ where $\mathbf{p}$ and $\mathbf{q}$ describe the tangential unit vectors at the interface (see Fig. 1b). For a cavity or a crack, we will choose $(\mathbf{n}^{(rr)}, \mathbf{p}, \mathbf{q})$. With no loss of generality, we thus adopt the coordinate system $(\mathbf{n}^{(rs)}, \mathbf{p}, \mathbf{q})$, where in the case of a pore or a crack there is $r = s$.

At any generic point $\mathbf{x}$ of the interface, let us define the traction vector exerted from phase r to phase s as $\mathbf{t}^{(rs)}$, and from s to r as $\mathbf{t}^{(sr)}$:

$$\mathbf{t}^{(rs)} = (t_n^{(rs)}, t_p^{(rs)}, t_q^{(rs)})^{\mathrm{T}}, \quad \mathbf{t}^{(sr)} = (t_n^{(sr)}, t_p^{(sr)}, t_q^{(sr)})^{\mathrm{T}}. \tag{2}$$

We note that both are expressed in the coordinate system $(\mathbf{n}^{(rs)}, \mathbf{p}, \mathbf{q})$. Regardless of the nature of the bond, $\mathbf{t}^{(rs)}$ must be in equilibrium with $\mathbf{t}^{(sr)}$, thus

$$\mathbf{t}^{(rs)} + \mathbf{t}^{(sr)} = 0. \tag{3}$$

For a generic point $\mathbf{x}$, at a surface S_{rr} of a cavity or crack adjacent to phase r, it follows that

$$\mathbf{t}^{(rr)} = (t_n^{(rr)}, t_p^{(rr)}, t_q^{(rr)})^{\mathrm{T}} = 0, \tag{4}$$

where the quantities are described in the coordinate system $(\mathbf{n}^{(rr)}, \mathbf{p}, \mathbf{q})$ defined above.

Displacement vectors at any point $\mathbf{x}$ of the interface are defined at each side and expressed in the coordinate system $(\mathbf{n}^{(rs)}, \mathbf{p}, \mathbf{q})$ as:

$$\mathbf{u}^{(r)} = (u_n^{(r)}, u_p^{(r)}, u_q^{(r)})^{\mathrm{T}}, \quad \mathbf{u}^{(s)} = (u_n^{(s)}, u_p^{(s)}, u_q^{(s)})^{\mathrm{T}}, \tag{5}$$

the difference or jump in those displacements across the interface will be denoted by

$$[\mathbf{u}] = \mathbf{u}^{(r)} - \mathbf{u}^{(s)}. \tag{6}$$

These conventions permit us to define the following types of interface bonding that will be of interest in the sequel. A *perfectly bonded* interface which does not contain any interphase layer is characterized by the relations

$$\mathbf{t}^{(rs)} = -\mathbf{t}^{(sr)} \neq \mathbf{0}, \quad [\mathbf{u}] = \mathbf{0}. \tag{7}$$

At a *debonded interface* which is actually considered a cavity or a crack,

$$\mathbf{t}^{(rr)} = \mathbf{0}. \tag{8}$$

Our interest will frequently focus on *imperfectly bonded interfaces*, which allow non-vanishing relative displacements to exist together with nonzero tractions. The implication is that the displacements and tractions are related in a certain way at each instant of loading, as if the interfaces were connected by a very thin layer of interphase material. We limit our

attention to systems where such relationships, or the properties of the interphase, are described by the incremental form

$$\begin{aligned} \mathrm{d}[u_n] &= M_{nn}(\mathbf{t}^0)\,\mathrm{d}t_n, \\ \mathrm{d}[u_p] &= M_{pp}(\mathbf{t}^0)\mathrm{d}t_p + M_{pq}(\mathbf{t}^0)\mathrm{d}t_q, \\ \mathrm{d}[u_q] &= M_{qp}(\mathbf{t}^0)\mathrm{d}t_p + M_{qq}(\mathbf{t}^0)\mathrm{d}t_q, \end{aligned} \tag{9}$$

at each current magnitude $\mathbf{t}^{(sr)} = -\mathbf{t}^{(rs)} = \mathbf{t}^0$ of the interface traction; for simplicity we have denoted $(\mathrm{d}t_n, \mathrm{d}t_p, \mathrm{d}t_q) = (\mathrm{d}t_n^{(sr)}, \mathrm{d}t_p^{(sr)}, \mathrm{d}t_q^{(sr)})$. The $M_{\alpha\beta}$, with $\alpha, \beta = \mathrm{n}, \mathrm{p}, \mathrm{q}$, are the instantaneous "compliances" of the interface, or interphase layer, and are assumed to be represented by smooth, continuous functions, that satisfy the symmetry condition $M_{\alpha\beta} = M_{\beta\alpha}$. Since the interphase is assumed to be very thin, the contributions of the terms $M_{np}\mathrm{d}t_p$, $M_{nq}\mathrm{d}t_q$, etc., to $\mathrm{d}[\mathbf{u}]$ are considered to be insignificant and are neglected.

The imperfectly bonded interface that can be represented by (9) includes nonlinearly elastic coatings, and also interfaces which are weak in shear but perfectly bonded in the normal direction, in which case $M_{nn}(\mathbf{t}^0) = 0$, and $[u_n] = 0$. The representation (9) may imply an interpenetration in the normal displacement components u_n across the idealized interface in the case of a normal compressive traction. However, since we limit ourselves to small strains, and since these interfaces do in fact represent interphase regions with a certain thickness, such interpenetration can be accommodated by compression of the interphase. Interfaces that exhibit frictional contact, perfect bonding, or complete debonding are not represented by (9). Indeed, interface friction would relate the tangential components of the traction to the compressive normal component when $[u_n] = 0$, but without reference to the magnitude of $[\mathbf{u}]$, although the ratio of $t_p^{(rs)}$ to $t_q^{(rs)}$ may determine the direction of $[\mathbf{u}]$.

2.2. *Local fields*

Let a representative volume of a composite material be subjected to an overall uniform stress $\bar{\boldsymbol{\sigma}}$, or strain $\bar{\boldsymbol{\varepsilon}}$, and to a uniform temperature change θ_0. In particular, we select the overall thermomechanical loading on external surface S as

$$\mathbf{u}(S) = \boldsymbol{\varepsilon}_0\mathbf{x}, \quad \theta(S) = \theta_0, \tag{10}$$

so that $\bar{\boldsymbol{\varepsilon}} = \boldsymbol{\varepsilon}_0$, and examine its effect on local strain and displacement fields in the phase.

We assume that the local fields can be evaluated by an independent analysis of each specific system. Examples can be found in the references listed in the Introduction. In systems which undergo progressive debonding, i.e. involving changes in the size or location of the interfaces (8), and progressive deformation induced at the imperfectly bonded interfaces (9), such analysis may need to be performed at many different points of the prescribed loading path leading to the current state (10). In any event, the current local strain and displacement fields can be denoted by

$$\boldsymbol{\varepsilon}_r(\mathbf{x}) = \boldsymbol{\varepsilon}_r^0(\mathbf{x}; \boldsymbol{\varepsilon}_0, \theta_0), \quad \mathbf{u}_r(\mathbf{x}) = \mathbf{u}_r^0(\mathbf{x}; \boldsymbol{\varepsilon}_0, \theta_0), \quad \theta(\mathbf{x}) = \theta_0. \tag{11}$$

The displacement and temperature increments on the outer surface S of the representative volume are incrementally specified for a change in the temperature or strain, as

$$\mathbf{u}(S) = \boldsymbol{\varepsilon}_0\mathbf{x}, \quad \theta(S) = \theta_0 + \mathrm{d}\theta_0 \tag{12}$$

or

$$\mathbf{u}(S) = (\boldsymbol{\varepsilon}_0 + \mathrm{d}\boldsymbol{\varepsilon}_0)\mathbf{x}, \quad \theta(S) = \theta_0. \tag{13}$$

The resulting incremental strain and displacement fields to be superimposed on (11) are:

$$d\boldsymbol{\varepsilon}_r(\mathbf{x}) = \mathbf{a}_r(\mathbf{x}; \boldsymbol{\varepsilon}_0, \theta_0)\, d\theta_0, \quad d\mathbf{u}_r = \mathbf{d}_r(\mathbf{x}; \boldsymbol{\varepsilon}_0, \theta_0)\, d\theta_0 \tag{14}$$

or

$$d\boldsymbol{\varepsilon}_r(\mathbf{x}) = \mathbf{A}_r(\mathbf{x}; \boldsymbol{\varepsilon}_0, \theta_0) d\boldsymbol{\varepsilon}_0, \quad d\mathbf{u}_r = \mathbf{D}_r(\mathbf{x}; \boldsymbol{\varepsilon}_0, \theta_0)\, d\boldsymbol{\varepsilon}_0, \tag{15}$$

where $\mathbf{a}_r(\mathbf{x}; \boldsymbol{\varepsilon}_0, \theta_0)$, $\mathbf{d}_r(\mathbf{x}; \boldsymbol{\varepsilon}_0, \theta_0)$ are certain thermal influence functions, and $\mathbf{A}_r(\mathbf{x}; \boldsymbol{\varepsilon}_0, \theta_0)$, $\mathbf{D}_r(\mathbf{x}; \boldsymbol{\varepsilon}_0, \theta_0)$ are the mechanical influence functions. Their dependence on $\boldsymbol{\varepsilon}_0$ and θ_0 is the consequence of possible progressive debonding and/or nonlinear behavior of the interfaces.

2.3. *Overall properties*

The overall average strain in the presence of imperfect bonding is the sum of average phase strains, and strains that may be contributed by the relative displacement at the interfaces as well as by the presence of cavities and cracks. A derivation for two-phase, matrix-based composites has been given by Benveniste (1985). Here we present a more general result that applies to multiphase composites, not necessarily matrix-based, which may contain cracks and cavities.

Using the notation introduced in Section 2.1, we show in Appendix A that the average strain in such a composite is given by

$$\bar{\boldsymbol{\varepsilon}} = \sum_{r=1}^{N} c_r \bar{\boldsymbol{\varepsilon}}^{(r)} - \sum_{r=1}^{N} \sum_{s=1}^{N} \mathbf{J}_{rs}, \tag{16}$$

where c_r denotes the volume fraction of phase r, N is the number of phases, $\bar{\boldsymbol{\varepsilon}}^{(r)}$ is the average strain within that phase, and the second order tensors $\mathbf{J}_{rs}$ are given by:

$$J_{ij}^{(rs)} = \frac{1}{2V} \int_{S_{rs}} (u_i^{(r)} n_j^{(rs)} + u_j^{(r)} n_i^{(rs)})\, dS_{rs}, \quad J_{ij}^{(sr)} = \frac{1}{2V} \int_{S_{sr}} (u_i^{(s)} n_j^{(sr)} + u_j^{(r)} n_i^{(sr)})\, dS_{sr}. \tag{17}$$

It is noted here that thinking of the interface surface between the phases r and s as two-sided surfaces S_{rs} and S_{sr} allows a symmetrical representation of eqns $(17)_1$ and $(17)_2$.

It is often convenient to introduce concentration factors that reflect the presence of damage. In particular, under the load increments prescribed in (12) and (13), one finds from (14), (15) and (17):

$$d\mathbf{J}_{rs} = \mathbf{F}_{rs}(\boldsymbol{\varepsilon}_0, \theta_0) d\boldsymbol{\varepsilon}_0 + \mathbf{f}_{rs}(\boldsymbol{\varepsilon}_0, \theta_0)\, d\theta_0, \quad r, s = 1, 2, \ldots, N, \tag{18}$$

where the concentration factor tensors $\mathbf{F}_{rs}$ and $\mathbf{f}_{rs}$ are related to the $\mathbf{D}_r$ and $\mathbf{d}_r$ influence functions in $(14)_2$ and $(15)_2$ as:

$$F_{ijkl}^{rs} = \frac{1}{2V} \int_{S_{rs}} (D_{ikl}^{(r)}(\mathbf{x}) n_j^{(rs)} + D_{jkl}^{(r)}(\mathbf{x}) n_i^{(rs)})\, dS_{rs},$$

$$f_{ij}^{rs} = \frac{1}{2V} \int_{S_{rs}} (\mathbf{d}_i^{(r)}(\mathbf{x}) n_j^{(rs)} + d_j^{(r)}(\mathbf{x}) n_i^{(rs)})\, dS_{rs}. \tag{19}$$

The concentration factors $\mathbf{F}_{sr}$ and $\mathbf{f}_{sr}$ related to $d\mathbf{J}_{sr}$ are described simply by interchanging r and s in (18) and (19). Together with the related factors defined in (14) and (15), they facilitate the description of overall properties of the damaged composite materials. We refer again to the representative volume of a composite material which is subjected to overall uniform stress $\bar{\boldsymbol{\sigma}}$, or strain $\bar{\boldsymbol{\varepsilon}}$ and to a uniform temperature change θ_0. Since the overall response is not necessarily linear, it is sought in the incremental form

$$d\bar{\boldsymbol{\sigma}} = \mathbf{L}(\bar{\boldsymbol{\varepsilon}}, \theta_0)d\bar{\boldsymbol{\varepsilon}} + \mathbf{l}(\bar{\boldsymbol{\varepsilon}}, \theta_0)\, d\theta_0,$$
$$d\bar{\boldsymbol{\varepsilon}} = \mathbf{M}(\bar{\boldsymbol{\varepsilon}}, \theta_0)d\bar{\boldsymbol{\sigma}} + \mathbf{m}(\bar{\boldsymbol{\varepsilon}}, \theta_0)\, d\theta_0, \tag{20}$$

where $\mathbf{L}(\bar{\boldsymbol{\varepsilon}}, \theta_0)$ and $\mathbf{l}(\bar{\boldsymbol{\varepsilon}}, \theta_0)$ are the instantaneous stiffness and thermal stress tensors which depend on the current overall strain and temperature. The $\mathbf{M}(\bar{\boldsymbol{\varepsilon}}, \theta_0)$ and $\mathbf{m}(\bar{\boldsymbol{\varepsilon}}, \theta_0)$ are the corresponding compliance and thermal strain tensors.

These effective properties can be determined once the concentration factors $\mathbf{a}_r$, $\mathbf{A}_r$, the volume averages of the influence functions $\mathbf{a}_r(\mathbf{x}; \boldsymbol{\varepsilon}_0, \theta_0)$, $\mathbf{A}_r(\mathbf{x}; \boldsymbol{\varepsilon}_0, \theta_0)$ introduced in (14) and (15), and the tensors $\mathbf{F}_{rs}$, $\mathbf{f}_{rs}$ defined in (19) are known. Equations $(14)_1$, $(15)_1$, (16), (18) and $(20)_2$ readily provide the following expressions for $\mathbf{L}$ and $\mathbf{l}$:

$$\mathbf{L}(\boldsymbol{\varepsilon}_0, \theta_0) = \mathbf{L}_1 + \sum_{r=2}^{N} c_r(\mathbf{L}_r - \mathbf{L}_1)\mathbf{A}_r(\boldsymbol{\varepsilon}_0, \theta_0) + \mathbf{L}_1 \sum_{r=1}^{N}\sum_{s=1}^{N} \mathbf{F}_{rs}(\boldsymbol{\varepsilon}_0, \theta_0)$$
$$\mathbf{l}(\boldsymbol{\varepsilon}_0, \theta_0) = \sum_{r=1}^{N} c_r\mathbf{l}_r + \sum_{r=2}^{N} c_r(\mathbf{L}_r - \mathbf{L}_1)\mathbf{a}_r(\boldsymbol{\varepsilon}_0, \theta_0) + \mathbf{L}_1 \sum_{r=1}^{N}\sum_{s=1}^{N} \mathbf{f}_{rs}(\boldsymbol{\varepsilon}_0, \theta_0). \tag{21}$$

Similar equations can be obtained for $\mathbf{M}$ and $\mathbf{m}$.

2.4. *Evaluation of* $\mathbf{l}$ *and* $\mathbf{m}$

In his (1967) paper, Levin found an expression which relates the thermal stress tensor $\mathbf{l}$ to the mechanical concentration factors $\mathbf{A}_r$ of the phases and to phase thermal vectors $\mathbf{l}_r$ in an undamaged composite with perfectly bonded interfaces. An analogous relation exists between the overall thermal strain tensor $\mathbf{m}$ and the stress concentration factor $\mathbf{B}_r$ and phase thermal strain tensors $\mathbf{m}_r$. Under certain conditions, a similar formula can be derived for composites with imperfectly bonded or partially debonded interfaces defined in (7)–(9). The derivation presented here will use the reciprocal theorem, although a similar result follows from a modified principle of virtual work for composites of this type (Benveniste, 1985). For completeness, we present in Appendix B a derivation of the reciprocal theorem which accounts for the effect of applied eigenstrain fields and imperfect interfaces.

Suppose that the composite has been loaded to some current known state $(\boldsymbol{\varepsilon}_0, \boldsymbol{\sigma}_0, \theta_0)$, where the extent of partial and/or complete interface debonding has been evaluated such that all coefficients in (9) and the mechanical influence functions $\mathbf{A}_r(\mathbf{x}; \boldsymbol{\varepsilon}_0, \theta_0)$, $\mathbf{B}_r(\mathbf{x}; \boldsymbol{\varepsilon}_0, \theta_0)$† and $\mathbf{D}_r(\mathbf{x}; \boldsymbol{\varepsilon}_0, \theta_0)$ in (15) are known together with the instantaneous overall stiffness $\mathbf{L}$ and compliance $\mathbf{M} = \mathbf{L}^{-1}$. In this current state, we apply two separate load increments (′) and (″) such that there is no change in the type of interface bonding (7)–(9) on S_{rs}. First, an overall uniform stress increment $d\boldsymbol{\sigma}_0$ is applied at the current temperature $\theta(S) = \theta_0$. According to (15), this will cause the strain and displacement fields in the phases

$$d\boldsymbol{\varepsilon}_r'(\mathbf{x}) = \mathbf{M}_r\mathbf{B}_r(\mathbf{x}; \boldsymbol{\varepsilon}_0, \theta_0) \quad d\boldsymbol{\sigma}_0' = \mathbf{A}_r(\mathbf{x}; \boldsymbol{\varepsilon}_0, \theta_0)\mathbf{M}\, d\boldsymbol{\sigma}_0'. \tag{22}$$

$$d\mathbf{u}_r'(\mathbf{x}) = \mathbf{D}_r(\mathbf{x}; \boldsymbol{\varepsilon}_0, \theta_0)\mathbf{M}\, d\boldsymbol{\sigma}_0'. \tag{23}$$

Next, the overall temperature is changed from θ_0 to θ_0'' at fixed overall stress $\boldsymbol{\sigma}_0$. This will cause the local thermal strains $\mathbf{m}_r\, d\theta''$ which can be expressed as

$$d\boldsymbol{\lambda}_r'' = -\mathbf{L}_r\mathbf{m}_r\, d\theta_0'' = \mathbf{l}_r\, d\theta_0'', \tag{24}$$

as well as the displacement fields denoted by

† The influence function $\mathbf{B}_r(\mathbf{x}; \boldsymbol{\varepsilon}_0, \theta_0)$ relates the stress increment $d\boldsymbol{\sigma}_0$ to the local field $d\boldsymbol{\sigma}_r$ in the same way as the function $\mathbf{A}_r$ relates the strains in (15).

$$d\mathbf{u}_r'' = \mathbf{d}_r(\mathbf{x}; \boldsymbol{\varepsilon}_0, \theta_0)\, d\theta_0''. \tag{25}$$

Let us now use the reciprocal theorem given in (B8) in its incremental form. Note that $dF_i' = dF_i'' = d\lambda_{ij}' = dt_i'' = 0$, and write

$$\int_S d\boldsymbol{\sigma}_0' \mathbf{n} \cdot d\mathbf{u}''\, dS + \int_{S_{int}} dt_{int}' \cdot [d\mathbf{u}'']\, dS_{int} = \sum_{r=1}^{N} \int_{V_r} -d\lambda_r''\, d\boldsymbol{\varepsilon}_r'\, dV + \int_{S_{int}} dt_{int}'' \cdot [d\mathbf{u}']\, dS_{int}. \tag{26}$$

where we have used the notation S_{int} to denote *all* interfaces between the phases r in volumes V_r. Of course, at surfaces in contact with vacuous zones, the tractions and thus these integrals vanish.

The first integral on the left-hand side is, by definition, the scalar product of the overall stress increment with the strain increment $d\sigma_{ij}^{0'}\, d\bar{\varepsilon}_{ij}''$. A substitution from (9) reveals that the two integrals over S_{int} contain terms $dt'\, \mathbf{M}_{int}\, dt''$ and $dt''\, \mathbf{M}_{int}^{T}\, dt' = dt'\, \mathbf{M}_{int}^{T}\, dt''$, respectively. Since (9) was assumed to admit only interfaces where $\mathbf{M}_{int} = \mathbf{M}_{int}^{T}$, those integrals are equal and cancel each other. At locations where the interface is perfectly bonded ($[d\mathbf{u}] = \mathbf{0}$), or completely debonded ($dt = \mathbf{0}$), both integrals vanish.

The remaining two integrals over V are rewritten with the help of (22)–(24). One form is

$$\int_V d\boldsymbol{\sigma}_0' \mathbf{m}\, d\theta_0''\, dV = \sum_{r=1}^{N} \left\{ \int_{V_r} \mathbf{L}_r \mathbf{m}_r \mathbf{M}_r \mathbf{B}_r(\mathbf{x}; \boldsymbol{\sigma}_0, \theta_0)\, d\boldsymbol{\sigma}_0'\, d\theta_0''\, dV \right\}. \tag{27}$$

Since $\mathbf{M}_r = \mathbf{M}_r^{T} = \mathbf{L}_r^{-1}$, the right-hand side integrand can be shown to be rewritten as $d\boldsymbol{\sigma}_0' \mathbf{B}_r^{T} \mathbf{m}_r\, d\theta_0''$. Thus (27) can be solved for the overall thermal strain tensor $\mathbf{m}$ as

$$\mathbf{m}(\boldsymbol{\sigma}_0, \theta_0) = \sum_{r=1}^{N} \left\{ \int_{V_r} \mathbf{B}_r^{T}(\mathbf{x}; \boldsymbol{\sigma}_0, \theta_0) \mathbf{m}_r\, dV \right\}. \tag{28}$$

An analogous analysis yields the expression for the overall thermal stress vector

$$\mathbf{l}(\boldsymbol{\varepsilon}_0, \theta_0) = \sum_{r=1}^{N} \left\{ \int_{V_r} \mathbf{A}_r^{T}(\mathbf{x}; \boldsymbol{\varepsilon}_0, \theta_0) \mathbf{l}_r\, dV \right\}. \tag{29}$$

Taking the phase volume averages of the influence functions over V_r gives

$$\mathbf{m}(\boldsymbol{\sigma}_0, \theta_0) = \sum_{r=1}^{N} c_r \mathbf{B}_r^{T}(\boldsymbol{\sigma}_0, \theta_0) \mathbf{m}_r, \quad \mathbf{l}(\boldsymbol{\sigma}_0, \theta_0) = \sum_{r=1}^{N} c_r \mathbf{A}_r^{T}(\boldsymbol{\varepsilon}_0, \theta_0) \mathbf{l}_r. \tag{30}$$

This result is formally identical to that found by Levin (1967), however, the mechanical concentration factors entering here are those of the damaged composite, and as such they depend on the current geometry of the imperfectly bonded or debonded interfaces. Therefore, (28)–(30) should be utilized in conjunction with an incremental solution of a thermomechanical loading problem for the damaged composite material. Of course, such a solution may provide the overall strains, and (30) can then identify the purely thermal contribution. *However, if the geometry changes cease at a certain load level, e.g.* because the imperfectly bonded interfaces have separated, then the mechanical concentration factors remain independent of further load or temperature changes. Once these become known from the solution of a mechanical loading problem for the damaged composite, the above relations can be used to find the overall thermal properties.

3. TWO-PHASE COMPOSITES

3.1. *Overall properties*

First, consider some specific forms of the above results which apply to two-phase composite systems. Suppose that $r = 1$ denotes the matrix and $r = 2$ a reinforcing phase. Then the general expressions (21) for the overall stiffness $\mathbf{L}$ can be rearranged as:

$$\mathbf{L}(\boldsymbol{\varepsilon}^0, \theta_0) = \mathbf{L}_1 + c_2(\mathbf{L}_2 - \mathbf{L}_1)\mathbf{A}_2(\boldsymbol{\varepsilon}_0, \theta_0) + \mathbf{L}_1\mathbf{A}(\boldsymbol{\varepsilon}_0, \theta_0),$$
$$\mathbf{l}(\boldsymbol{\varepsilon}^0, \theta_0) = c_1\mathbf{l}_1 + c_2\mathbf{l}_2 + c_2(\mathbf{L}_2 - \mathbf{L}_1)\mathbf{a}_2(\boldsymbol{\varepsilon}_0, \theta_0) + \mathbf{L}_1\mathbf{a}(\boldsymbol{\varepsilon}_0, \theta_0), \tag{31}$$

where the $\mathbf{A}$ and $\mathbf{a}$ tensors reflect the effect of damage, and the $\mathbf{A}_2$, $\mathbf{a}_2$ are the mechanical concentration factor tensors of the damaged composite. The overall average strain (16) now becomes

$$\bar{\boldsymbol{\varepsilon}} = c_1\bar{\boldsymbol{\varepsilon}}_1 + c_2\bar{\boldsymbol{\varepsilon}}_2 - \mathbf{J}, \tag{32}$$

where $\bar{\boldsymbol{\varepsilon}}_r$ are the average strains in the constituents, and $\mathbf{J}$ is given by the double sum in (16) taken over $r, s = 1, 2$. From the above representation, it is seen that

$$\mathrm{d}\mathbf{J} = \mathbf{A}(\boldsymbol{\varepsilon}_0, \theta_0)\,\mathrm{d}\boldsymbol{\varepsilon}_0 + \mathbf{a}(\boldsymbol{\varepsilon}_0, \theta_0)\,\mathrm{d}\theta_0. \tag{33}$$

For two-phase composites, an alternative expression for the $\mathbf{l}(\boldsymbol{\varepsilon}_0, \theta_0)$ in $(31)_2$ can be obtained as follows. First write (32) in incremental form, and recall that under (12) and (13) $\mathrm{d}\bar{\boldsymbol{\varepsilon}} = \mathrm{d}\boldsymbol{\varepsilon}^0$. Next, make use of $(14)_1$, $(15)_1$ and (33) to obtain

$$c_1\mathbf{A}_1(\boldsymbol{\varepsilon}_0, \theta_0) + c_2\mathbf{A}_2(\boldsymbol{\varepsilon}_0, \theta_0) - \mathbf{A}(\boldsymbol{\varepsilon}_0, \theta_0) = \mathbf{I}, \quad c_1\mathbf{a}_1(\boldsymbol{\varepsilon}_0, \theta_0) + c_2\mathbf{a}_2(\boldsymbol{\varepsilon}_0, \theta_0) - \mathbf{a}(\boldsymbol{\varepsilon}_0, \theta_0) = \mathbf{0}, \tag{34}$$

where $\mathbf{I}$ is the fourth order unit tensor. Finally, write $(30)_2$ for two-phase media as

$$\mathbf{l}(\boldsymbol{\varepsilon}_0, \theta_0) = c_1\mathbf{A}_1^{\mathrm{T}}(\boldsymbol{\varepsilon}_0, \theta_0)\mathbf{l}_1 + c_2\mathbf{A}_2^{\mathrm{T}}(\boldsymbol{\varepsilon}_0, \theta_0)\mathbf{l}_2. \tag{35}$$

One can now solve for $\mathbf{A}_1^{\mathrm{T}}(\boldsymbol{\varepsilon}_0, \theta_0)$ and $\mathbf{A}_2^{\mathrm{T}}(\boldsymbol{\varepsilon}_0, \theta_0)$ from $(31)_1$ and $(34)_1$, and substitute them into (35) to find

$$\mathbf{l}(\boldsymbol{\varepsilon}_0, \theta_0) = \{\mathbf{L}(\boldsymbol{\varepsilon}_0, \theta_0) - \mathbf{L}_1\}(\mathbf{L}_2 - \mathbf{L}_1)^{-1}(\mathbf{l}_2 - \mathbf{l}_1)$$
$$+ \mathbf{l}_1 + \mathbf{A}^{\mathrm{T}}(\boldsymbol{\varepsilon}_0, \theta_0)\{\mathbf{l}_1 - \mathbf{L}_1(\mathbf{L}_2 - \mathbf{L}_1)^{-1}(\mathbf{l}_2 - \mathbf{l}_1)\}. \tag{36}$$

The diagonal symmetry of the $\mathbf{L}$ tensor has been invoked in the above derivation.

3.2. *Isotropic constituents with slipping interfaces*

We now consider a two-phase system which admits connections between mechanically and thermally induced pointwise fields that are not available in multiphase composites. The constituents are both isotropic, and the displacements of the interfaces are limited to nonlinear slip, i.e. $M_{rr} = 0$ in (9). Furthermore, the individual phases are assumed to contain no cracks or pores. In this particular system, the influence functions $\mathbf{a}_r(\mathbf{x}; \boldsymbol{\varepsilon}_0, \theta_0)$ and $\mathbf{d}_r(\mathbf{x}; \boldsymbol{\varepsilon}_0, \theta_0)$ are uniquely determined by their mechanical counterparts $\mathbf{A}_r(\mathbf{x}; \boldsymbol{\varepsilon}_0, \theta_0)$ and $\mathbf{D}_r(\mathbf{x}; \boldsymbol{\varepsilon}_0, \theta_0)$, respectively. Also, the general formula (36) can be reduced to a particularly convenient form. The specific results are:

$$\mathbf{a}_r(\mathbf{x}; \boldsymbol{\varepsilon}_0, \theta_0) = \{\mathbf{I} - \mathbf{A}_r(\mathbf{x}; \boldsymbol{\varepsilon}_0, \theta_0)\}(\mathbf{L}_1 - \mathbf{L}_2)^{-1}(\mathbf{l}_2 - \mathbf{l}_1),$$
$$\mathbf{d}_r(\mathbf{x}; \boldsymbol{\varepsilon}_0, \theta_0) = \{\mathbf{x} - \mathbf{D}_r(\mathbf{x}; \boldsymbol{\varepsilon}_0, \theta_0)\}(\mathbf{L}_1 - \mathbf{L}_2)^{-1}(\mathbf{l}_2 - \mathbf{l}_1),$$
$$\mathbf{a} = -\mathbf{A}(\mathbf{L}_1 - \mathbf{L}_2)^{-1}(\mathbf{l}_2 - \mathbf{l}_1), \quad \mathbf{l} = \mathbf{l}_1 + (\mathbf{L} - \mathbf{L}_1)(\mathbf{L}_2 - \mathbf{L}_1)^{-1}(\mathbf{l}_2 - \mathbf{l}_1). \tag{37}$$

The validity of these relations will now be proved using the concept of incremental uniform fields in heterogeneous media introduced by Dvorak (1986). The composite is subjected to the boundary conditions (10), has the local fields (11), and the goal is to evaluate its response under a temperature increment $d\theta_0$ from the current state, as in (14).

Superimpose on (10) the incremental loads $d\hat{\boldsymbol{\varepsilon}}$ and $d\theta_0$:

$$\mathbf{u}(S) = \boldsymbol{\varepsilon}_0\mathbf{x} + d\hat{\boldsymbol{\varepsilon}}\mathbf{x}, \quad \theta(S) = \theta_0 + d\theta_0. \tag{38}$$

The $d\theta_0$ is given but $d\hat{\boldsymbol{\varepsilon}}$ is not known; it is to be determined such that together with $d\theta_0$ it creates a strain field $d\hat{\boldsymbol{\varepsilon}}$, and a stress field $d\hat{\boldsymbol{\sigma}}$ which are both uniform in the entire representative volume. The desired magnitudes of $d\hat{\boldsymbol{\varepsilon}}$ and $d\hat{\boldsymbol{\sigma}}$ can be readily determined from (1). Write the local incremental fields in both phases, make them equal, and evaluate the desired strain

$$d\hat{\boldsymbol{\varepsilon}} = (\mathbf{L}_1 - \mathbf{L}_2)^{-1}(\mathbf{l}_2 - \mathbf{l}_1)\, d\theta_0. \tag{39}$$

An analogous derivation (Dvorak, 1990) for a composite under overall uniform stress shows that a uniform stress field $d\hat{\boldsymbol{\sigma}}$ can coexist with a temperature change $d\theta_0$ if

$$d\hat{\boldsymbol{\sigma}} = (\mathbf{M}_1 - \mathbf{M}_2)^{-1}(\mathbf{m}_2 - \mathbf{m}_1)\, d\theta_0.$$

In the present system with isotropic constituents, both $d\hat{\boldsymbol{\varepsilon}}$ and $d\hat{\boldsymbol{\sigma}}$ are hydrostatic, therefore, in the absence of normal interface displacements, the above increments cause only normal and continuous tractions at all interfaces. Of course, this also prevents interface slip, and the composite responds to the incremental loading (38) as if the interfaces were perfectly bonded.

To restore the original boundary conditions (12), the auxiliary strain $d\hat{\boldsymbol{\varepsilon}}$ must be removed. This is accomplished by changing (38) to

$$\mathbf{u}(S) = \boldsymbol{\varepsilon}^0\mathbf{x} + d\hat{\boldsymbol{\varepsilon}}\mathbf{x} - d\hat{\boldsymbol{\varepsilon}}\mathbf{x}, \quad \theta(S) = \theta_0 + d\theta_0. \tag{40}$$

The incremental fields produced by the loading/unloading sequence (38) and (40) are

$$d\boldsymbol{\varepsilon}_r(\mathbf{x}) = d\hat{\boldsymbol{\varepsilon}} - \mathbf{A}_r(\mathbf{x}; \boldsymbol{\varepsilon}_0, \theta_0)\, d\hat{\boldsymbol{\varepsilon}}, \quad d\mathbf{u}_r(\mathbf{x}) = d\hat{\boldsymbol{\varepsilon}}\mathbf{x} - \mathbf{D}_r(\mathbf{x}; \boldsymbol{\varepsilon}_0, \theta_0)\, d\hat{\boldsymbol{\varepsilon}}, \tag{41}$$

where $d\hat{\boldsymbol{\varepsilon}}$ is to be substituted from (39). Note that (40) and (12) are identical, hence $\mathbf{a}_r(\mathbf{x}; \boldsymbol{\varepsilon}_0, \theta_0)$ and $\mathbf{d}_r(\mathbf{x}; \boldsymbol{\varepsilon}_0, \theta_0)$ can be extracted by comparing (14) with (41). This leads to the expressions $(37)_1$ and $(37)_2$.

To recover $(37)_3$, recall that in the present derivation we rule out vacuous zones, hence

$$\mathbf{A} = \mathbf{F}_{12} + \mathbf{F}_{21}, \quad \mathbf{a} = \mathbf{f}_{12} + \mathbf{f}_{21}, \tag{42}$$

with $\mathbf{F}_{rs}$ and $\mathbf{f}_{rs}$ being given in (19). A substitution from $(37)_2$ to $(19)_2$, together with $(19)_1$ and (42), readily provides $(37)_3$.

Finally, a substitution of $(37)_1$ with $r = 2$, and of $(37)_3$ into $(31)_2$ gives

$$\mathbf{l}(\boldsymbol{\varepsilon}^0, \theta_0) = c_1\mathbf{l}_1 + c_2\mathbf{l}_2 + c_2(\mathbf{L}_2 - \mathbf{L}_1)(\mathbf{I} - \mathbf{A}_2)(\mathbf{L}_1 - \mathbf{L}_2)^{-1}(\mathbf{l}_2 - \mathbf{l}_1) - \mathbf{L}_1\mathbf{A}(\mathbf{L}_1 - \mathbf{L}_2)^{-1}(\mathbf{l}_2 - \mathbf{l}_1). \tag{43}$$

Solving for $\mathbf{A}_2$ in $(31)_1$ and substituting into (42) then provides $(37)_4$.

Recall that the thermal stress tensor $\mathbf{l}$ for two-phase composites with anisotropic constituents is given by $(31)_2$ or (36), and for systems with isotropic phases and slipping interfaces by $(37)_4$. These relations were arrived at by two entirely different approaches, hence it remains to be shown that they are equivalent under similar circumstances.

For isotropic constituents there is:

$$
\begin{aligned}
(l_1)_{ij} &= \alpha\delta_{ij},\\
(L_1)_{ijrs} &= \beta\delta_{ij}\delta_{rs} + \gamma(\delta_{ir}\delta_{rs} + \delta_{is}\delta_{jr} - \tfrac{2}{3}\delta_{ij}\delta_{rs}),\\
(L_2 - L_1)^{-1}_{rsmn} &= \xi\delta_{rs}\delta_{mn} + \zeta(\delta_{rm}\delta_{sn} + \delta_{rn}\delta_{sm} - \tfrac{2}{3}\delta_{rs}\delta_{mn}),\\
(l_2 - l_1)_{mn} &= \lambda\delta_{mn}.
\end{aligned}
\tag{44}
$$

where α, β, δ, ξ, ζ, λ are constants. Writing $\mathbf{A}^T$ in indicial notation and carrying out the summation in (36) according to (44) shows that the tensor $\mathbf{A}^T$ enters only as $(\mathbf{A}^T)_{pqii}$. Moreover, the continuity of normal displacements at S_{21}, which was assumed in the above derivation of $(37)_4$, implies that according to the definition of the $\mathbf{A}$ tensor, in (31)–(33), $A_{ijkl} = 0$, or in fact $(\mathbf{A}^T)_{pqii} = 0$. This leads to the conclusion that (36) indeed reduces to the form $(37)_4$ when the phases are isotropic and the interfaces may experience only shear displacements.

Acknowledgements—Funding for this work was provided, in part, by the DARPA/ONR-HiTASC composites program at Rensselaer and by the Air Force Office of Scientific Research.

REFERENCES

Achenbach, J. D. and Zhu, H. (1989). Effect of interfacial zone on mechanical behavior and failure of fiber-reinforced composites. *J. Mech. Phys. Solids* **37**, 381–393.

Benveniste, Y. (1985). The effective mechanical behaviour of composite materials with imperfect contact between the constituents. *Mech. Mater.* **4**, 197–208.

Benveniste, Y. and Aboudi, J. (1984). A continuum model for fiber reinforced materials with debonding. *Int. J. Solids Structures* **20** (11/12), 935–951.

Benveniste, Y. and Dvorak, G. J. (1990a). On a correspondence between mechanical and thermal effects in two-phase composites. In Toshio Mura Anniversary Volume *Micromechanics and Inhomogeneity* (Edited by G. J. Weng, M. Taya and H. Abe), pp. 65–81. Springer, Berlin.

Benveniste, Y. and Dvorak, G. J. (1990b). On a correspondence between mechanical and thermal fields in composites with slipping interfaces. In *Inelastic Deformation of Composite Materials* (Edited by George J. Dvorak). IUTAM Symposium, Troy, NY, 29 May–1 June, 1990, pp. 77–98. Springer, Berlin.

Benveniste, Y. and Miloh, T. (1986). The effective conductivity of composites with imperfect thermal contact at constituent interfaces. *Int. J. Engng Sci.* **24**, 1537–1552.

Chen, I. W. and Argon, A. S. (1979a). Grain boundary and interphase boundary sliding in power law creep. *Acta Met.* **27**, 749–754.

Chen, I. W. and Argon, A. S. (1979b). Steady state power-law creep in heterogeneous alloys with coarse microstructures. *Acta Met.* **27**, 785–791.

Dvorak, G. J. (1983). Metal matrix composites: plasticity and fatigue. In *Mechanics of Composite Materials—Recent Advances* (Edited by Z. Hashin and C. T. Herakovich), pp. 73–92. Pergamon Press, New York.

Dvorak, G. J. (1986). Thermal expansion of elastic-plastic composite materials. *J. Appl. Mech.* **53**, 737–743.

Dvorak, G. J. (1990). On uniform fields in heterogeneous media. *Proc. R. Soc. London* **A431**, 89–110.

Dvorak, G. J. and Chen, T. (1989). Thermal expansion of three-phase composite materials. *J. Appl. Mech.* **56**, 418–422.

Hashin, Z., (1990). Thermoelastic properties of fiber composites with imperfect interface. *Mech. Mater.* **8**, 333–348.

Jasiuk, I., Mura, T. and Tsuchida, E. (1988). Thermal stresses and thermal expansion coefficients of short fiber composites with sliding interfaces. *J. Engng Mat. Tech.* **110**, 96–100.

Jasiuk, I. and Tong, Y. (1989). The effect of interface on the elastic stiffness of composites. In *Mechanics of Composite Materials and Structures* (Edited by J. N. Reddy and J. L. Teply), AMD-Vol. 100, pp. 49–54.

Lené, F. and Leguillon, D. (1982). Homogenized constitutive law for a partially cohesive composite material. *Int. J. Solids Structures* **18**, 443–458.

Levin, V. M. (1967). Thermal expansion coefficients of heterogeneous materials. *Mekhanika Tverdago Tela*, **2**, 88–94. (English Translation *Mechanics of Solids*, **11**, 58–61.)

Mura, T., Jasiuk, I. and Tsuchida, E. (1985). The stress field of a sliding inclusion. *Int. J. Solids Structures* **12**, 1165–1179.

Tsuchida, E., Mura, T. and Dundurs, J. (1986). The elastic field of an elliptic inclusion with a slipping interface. *J. Appl. Mech.* **53**, pp. 103–107.

APPENDIX A

Equation (16) will be derived in this appendix. The considered multiphase composite may contain pores and cracks at arbitrary locations, but need not be matrix based, see Fig. A1 for a typical volume of such a composite. To derive eqn (16) it is sufficient to consider a three-phase composite as in Fig. A2. Note that phase "s" is in contact both with phases "r" and "p", a situation which would occur in non-matrix based composites. The notation in this figure is that described in Section 2.1. The derived average strain for the configuration of Fig. A2 can be readily generalized to multiphase composites of the type described in Fig. A1.

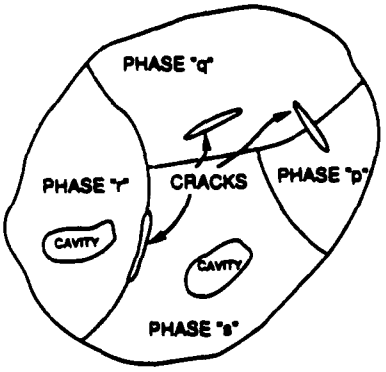

Fig. A1. A multiphase nonmatrix-based composite with defects.

We start by writing the average overall strain for the composite (Benveniste, 1985)

$$\bar{\varepsilon}_{ij} = \frac{1}{2V}\int_S (u_i n_j + u_j n_i)\,\mathrm{d}S, \tag{A1}$$

where S denotes the outside surface and $\mathbf{n}$ the outward normal to S. The average strain in phase r can be written as

$$\bar{\varepsilon}_{ij}^{(r)} = \frac{1}{2V_r}\int_{V_r}\left(\frac{\partial u_i^{(r)}}{\partial x_j} + \frac{\partial u_j^{(r)}}{\partial x_i}\right)\mathrm{d}V_r = \frac{1}{2V_r}\int_S (u_i^{(r)} n_j + u_j^{(r)} n_i)\,\mathrm{d}S + \frac{1}{2V_r}\int_{S_{rs}} (u_i^{(r)} n_j^{(rs)} + u_j^{(r)} n_i^{(rs)})\,\mathrm{d}S_{rs} + \frac{1}{2V_r}\int_{S_{rp}} (u_i^{(r)} n_j^{(rp)} + u_j^{(r)} n_i^{(rp)})\,\mathrm{d}S_{rp} + \frac{1}{2V_r}\int_{S_{rr}} (u_i^{(r)} n_j^{(rr)} + u_j^{(r)} n_i^{(rr)})\,\mathrm{d}S_{rr}, \tag{A2}$$

where Gauss's divergence theorem has been used.

Similarly, we can write the average strain in phases s and p as follows:

$$\bar{\varepsilon}_{ij}^{(s)} = \frac{1}{2V_s}\int_{S_{sr}} (u_i^{(s)} n_j^{(sr)} + u_j^{(s)} n_i^{(sr)})\,\mathrm{d}S_{sr} + \frac{1}{2V_s}\int_{S_{sp}} (u_i^{(s)} n_j^{(sp)} + u_j^{(s)} n_i^{(sp)})\,\mathrm{d}S_{sp},$$

$$\bar{\varepsilon}_{ij}^{(p)} = \frac{1}{2V_p}\int_{S_{pr}} (u_i^{(p)} n_j^{(pr)} + u_j^{(p)} n_i^{(pr)})\,\mathrm{d}S_{pr} + \frac{1}{2V_p}\int_{S_{ps}} (u_i^{(p)} n_j^{(ps)} + u_j^{(p)} n_i^{(ps)})\,\mathrm{d}S_{ps} \tag{A3}$$

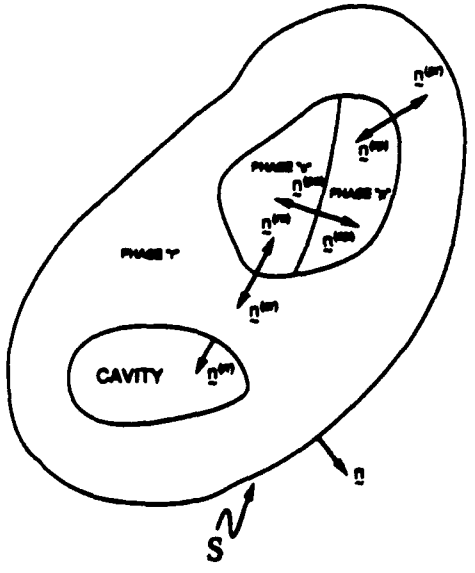

Fig. A2. A three-phase composite used in the derivation of the average strain.

where V_r and V_p denote the volumes of phases s and p, respectively. The total volume $V = V_r + V_s + V_p$. Multiplying eqn (A2) by $c_r = V_r/V$, and equation $(A3)_1$ and $(A3)_2$ by $c_s = V_s/V$ and $c_p = V_p/V$, respectively, and adding, results in

$$\bar{\boldsymbol{\varepsilon}} = c_r\bar{\boldsymbol{\varepsilon}}^{(r)} + c_s\bar{\boldsymbol{\varepsilon}}^{(s)} + c_p\bar{\boldsymbol{\varepsilon}}^{(p)} - \mathbf{J}^{(rr)} - \mathbf{J}^{(rs)} - \mathbf{J}^{(rp)} - \mathbf{J}^{(sr)} - \mathbf{J}^{(ss)} - \mathbf{J}^{(sp)} - \mathbf{J}^{(pr)} - \mathbf{J}^{(ps)} - \mathbf{J}^{(pp)}, \tag{A4}$$

where we used the definitions in (17). A generalization of (A4) to multiphase composites provides eqn (16). Equation (A4) or (16) reduces correctly to eqn (3) in Benveniste (1985) and (29) in Benveniste and Dvorak (1990b) which were written for two-phase matrix-based composites†. To draw a parallel with eqn (3) in Benveniste (1985), we simply note that $\mathbf{n}$ in that equation is given in the present notation by

$$\mathbf{n} = \mathbf{n}^{(21)} = -\mathbf{n}^{(12)}, \tag{A5}$$

where "1" denotes the matrix and "2" the inclusion and $[u_i]$ was defined as

$$[u_i]_{S_{12}} = u_i^{(2)} - u^{(1)} \quad \text{at } S_{12}, \tag{A6}$$

so that

$$\frac{1}{2V}\int_{S_{12}} ([u_i]n_j + [u_j]n_i)\,\mathrm{d}S_{12} = (\mathbf{J}_{21} + \mathbf{J}_{12})_{ij}. \tag{A7}$$

Recalling that no vacuous zones were present in the phases in these previous works, $\mathbf{J}_{11} = \mathbf{J}_{22} = \mathbf{0}$, and it is seen that eqn (3) in Benveniste (1985), and (29) in Benveniste and Dvorak (1990) are simply special cases of (A4).

APPENDIX B

An extension of the elastic reciprocal theorem to the situations in which the linearly elastic body contains interfaces of the type described in Section 2.1 can be written as

$$\int_V F_i'u_i''\,\mathrm{d}V + \int_S t_i'u_i''\,\mathrm{d}S + \int_{S_m} t_i^{(mr)'}u_i^{(r)''}\,\mathrm{d}S_m + \int_{S_w} t_i^{(wr)'}u_i^{(r)''}\,\mathrm{d}S_w$$
$$= \int_V F_i''u_i'\,\mathrm{d}V + \int_S t_i''u_i'\,\mathrm{d}S + \int_{S_m} t_i^{(mr)''}u_i^{(r)'}\,\mathrm{d}S_m + \int_{S_w} t_i^{(wr)''}u_i^{(r)'}\,\mathrm{d}S_w, \tag{B1}$$

where u_i'' are the displacements caused by the system t_i'', F_i'', and u_i' are the displacements caused by the system t_i', F_i'.

When distributions of eigenstresses $\lambda_{ij}' = l_{ij}\theta'$ and $\lambda_{ij}'' = l_{ij}\theta''$ are respectively applied to the two systems, the local stress field is given by

$$\sigma_{ij}'(\mathbf{x}) = \partial_{ij}'(\mathbf{x}) + \lambda_{ij}', \tag{B2}$$

where

$$\partial_{ij}'(\mathbf{x}) = L_{ijkl}(\mathbf{x})e_{kl}'(\mathbf{x}). \tag{B3}$$

The field (B2) satisfies

$$\begin{aligned}
\partial_{ij,j}' + F_i' + \lambda_{ij,j}' &= 0 \quad \text{in } V,\\
\partial_{ij}'n_j + \lambda_{ij}'n_j &= t_i' \quad \text{on } S,\\
\partial_{ij}'n_j^{(mr)} + \lambda_{ij}'n_j^{(mr)} &= t_i^{(mr)} \quad \text{on } S_m,\\
\partial_{ij}'n_j^{(wr)} + \lambda_{ij}'n_j^{(wr)} &= t_i^{(wr)} \quad \text{on } S_w.
\end{aligned} \tag{B4}$$

A similar representation holds for the double-primed system.

Define new body forces and surface tractions

$$\begin{aligned}
\tilde{F}_i &= F_i + \lambda_{ij,j}, \qquad & \tilde{t}_i &= t_i - \lambda_{ij}n_j,\\
\tilde{t}_i^{(mr)} &= t_i^{(mr)} - \lambda_{ij}n_j^{(mr)}, \qquad & \tilde{t}_i^{(wr)} &= t_i^{(wr)} - \lambda_{ij}n_j^{(wr)}
\end{aligned} \tag{B5}$$

and rewrite (B1) with F_i', F_i'' replaced by $\tilde{F}_i'$, $\tilde{F}_i''$, t_i', t_i'' by $\tilde{t}_i'$, $\tilde{t}_i''$ etc.

Consider first the right-hand side of (B1) rewritten as described above and substitute from (B4) to find

† Note that there is a misprint in the definition of J in eqn (30) in Benveniste and Dvorak (1990). The term V should be replaced by V_2 in that equation, as well as in eqns (36) and (47) of that work. Therefore, as we show in (A7), the correspondence between the J term in Benveniste and Dvorak (1990), and the $\mathbf{J}_{12}$, $\mathbf{J}_{21}$ terms in the present paper is: $c_2\mathbf{J} = (\mathbf{J}_{21} + \mathbf{J}_{12})$.

$$\int_V F_i'' u_i' \, dV + \int_V \lambda_{ij}'' \, u_i' \, dV + \int_S (t_i'' - \lambda_{ij}'' n_j) u_i' \, dS + \int_{S_{\sigma\sigma}} (t_i^{(\sigma\sigma)'} - \lambda_{ij}'' n_j^{(\sigma\sigma)}) u_i^{(\sigma)} \, dS_{\sigma\sigma} + \int_{S_{uu}} (t_i^{(uu)'} - \lambda_{ij}'' n_j^{(uu)}) u_i^{(u)} \, dS_{uu}. \quad \text{(B6)}$$

Manipulating the second term in (B6) through the divergence theorem, one finds

$$\int_V \lambda_{ij}'' \, u_i' \, dV = \int_S \lambda_{ij}'' u_i' n_j \, dS + \int_{S_{\sigma\sigma}} \lambda_{ij}'' u_i^{(\sigma)} n_j^{(\sigma\sigma)} \, dS_{\sigma\sigma} + \int_{S_{uu}} \lambda_{ij}'' u_i^{(u)} n_j^{(uu)} \, dS_{uu} - \int_V \lambda_{ij}'' u_{i,j}' \, dV. \quad \text{(B7)}$$

Moreover, $u_{i,j}' = \varepsilon_{ij}' - \omega_{ij}'$, and since $\lambda_{ij}'' = \lambda_{ji}''$, $\omega_{ij}' = -\omega_{ji}'$, it follows that when (B7) is substituted into (B6), some of the integrals on S and $S_{\sigma\sigma}$ cancel out.

A similar procedure applied to the left-hand side of (B1) yields the form of the reciprocal theorem which is valid under internal defects at $S_{\sigma\sigma}$ and in the presence of eigenstrains $\lambda_{ij} = l_{ij}\theta$:

$$\int_V F_i' u_i'' \, dV + \int_S t_i' u_i'' \, dS - \int_V \lambda_{ij}' \varepsilon_{ij}'' \, dV + \int_{S_{\sigma\sigma}} t_i^{(\sigma\sigma)'} u_i^{(\sigma)''} \, dS_{\sigma\sigma} + \int_{S_{uu}} t_i^{(uu)'} u_i^{(u)''} \, dS_{uu}$$

$$= \int_V F_i'' u_i' \, dV + \int_S t_i'' u_i' \, dS - \int_V \lambda_{ij}'' \varepsilon_{ij}' \, dV + \int_{S_{\sigma\sigma}} t_i^{(\sigma\sigma)''} u_i^{(\sigma)'} \, dS_{\sigma\sigma} + \int_{S_{uu}} t_i^{(uu)''} u_i^{(u)'} \, dS_{uu}. \quad \text{(B8)}$$

It is interesting to note that although the linearity of the constitutive law in the phases has been assumed in (B1) and (B8), the constitutive law of the interfaces does not explicitly enter in these equations. In other words the relation between the interface tractions and the resulting interface displacements have not explicitly been used in (B8). We finally mention that eqn (B8) can also be used for an incremental set of loads (dF_i', dt_i', $d\lambda_{ij}'$) and (dF_i'', dt_i'', $d\lambda_{ij}''$) which are superimposed on an existing equilibrium state of deformation.

Eur. J. Mech., A/Solids, 9, n° 6, 517-535, 1990

A variational approximation of stress intensity factors in cracked laminates

G. PIJAUDIER-CABOT * and G. J. DVORAK **

ABSTRACT. – A variational method for solution of plane crack problems in anisotropic layers of laminated plates is presented. The method is developed for a single slit crack which spans the middle layer of a symmetric three-layer laminate, and is loaded by internal pressure. The actual stress field is approximated by a superposition of an asymptotic expansion of the exact singular field at the crack terminating at the interface between two orthotropic layers, with a statically admissible stress field which approximates the stresses at locations far from the crack. The singular field is made to vanish outside a cylindrical region surrounding the crack tip, called the K-zone. Evaluation and minimization of the complementary energy of the admissible field provides an estimate of the stress intensity factors and crack energies. The exact order of singularity is introduced with the singular field. Comparisons with exact analytical solutions show good accuracy. The method offers approximate but simple closed-form solutions to crack problems in layered media, and it can be readily extended to situations involving many similar slit cracks which interact with each other.

1. Introduction

Damage development in fibrous composite laminates is often dominated by growth of transverse cracks in individual layers. Figure 1 shows a typical example of a model of a transverse crack in a single ply of material 1, bonded to adjacent plies of material 2. In actual systems, all plies are usually made of the same unidirectional fiber composite, but the orientation of the fiber is different in each ply or group of plies. The matrix and the fiber – matrix interfaces provide a convenient path for crack growth, hence it tends to take place on planes and in the direction parallel to the fiber axis in each ply. The fibers may be bypassed by the crack in the broken layer, but as their orientation changes at layer interfaces, they produce barriers to crack growth, and confine the crack within the thickness of a single layer. Consequently, the morphology of the crack surface is rather complex. In particular, the geometry of crack tips at ply interfaces is not well defined, as the crack may either break some of the fibers in the next layer, or be briefly deflected along the interface.

* Now at Laboratoire de Mécanique et Technologie, E.N.S. Cachan/C.N.R.S./Université Paris-VI, 61, av. du Président-Wilson, 94230 Cachan, France

** Department of Civil Engineering, Rensselaer Polytechnic Institute, Troy, New York 12180-3590, U.S.A.

EUROPEAN JOURNAL OF MECHANICS, A/SOLIDS, VOL. 9, N° 6, 1990
0997-7538/90/06 517 19/$ 3.90/

Damage affects laminate stiffness and strength, hence prediction of these effects is of interest in design. Models of the damage process can incorporate only a limited amount of microstructural detail. The fibrous layers are usually represented by orthotropic or transversely isotropic homogeneous elastic solids which are assigned some effective elastic properties. The uncertain details of crack zone configuration are ignored on the grounds that the stresses and strains away from the tip zone, and the energy released by the crack, are still governed by the elastic singularity. The crack energy is of particular interest, as its magnitude controls both the crack growth and the resulting stiffness loss.

Interaction between the crack and the adjacent layers, and between several similar cracks in the same layer are among the essential features of such problems. These interactions have an influence not only on the magnitude of the stress intensity factor, but also on the order of singularity at the crack tip. Some exact solutions for cracks in layered media appeared in the literature, [Ashbaugh 1973]; [Cook & Erdogan 1972]; [Delale & Erdogan 1979]; [Gupta 1973], but they seem to be available only for certain mutual orientations and material symmetries of the layers. On the other hand, the structure of singular fields of cracks terminating at interfaces between anisotropic half-planes of any orientation has been brought to light in the work of Ting *et al.* [1981, 1984], but it appears that these results have not yet been utilized in solutions of cracks in layered media.

The purpose of the present paper is to present a variational procedure for solution of crack problems of this kind. The general approach is similar to the recent work by Hashin [1985]. An admissible stress field is selected for evaluation of the complementary energy of the cracked laminate; this energy is minimized, and the resulting admissible field is then used as an approximation to the actual field. The accuracy of the result depends in a large measure on the selected admissible field. In what follows we construct this field by superposition of a nonsingular far field, and a singular field which is exact at the crack tip, but is made to vanish within a certain distance. Section 2 outlines the superposition procedure. The singular field is constructed in Section 3, and constrained to a certain region at the crack tip, the K-zone, in Section 4. The nonsingular far field is derived in Section 5, and the complementary energy is evaluated and minimized in Section 6. Although the procedure may be extended to laminates of many different layups, we focus our attention at the symmetric 0/90 layup, and at comparisons of the resulting crack and complementary energies, and stress intensity factors, with many available exact solutions. The agreement between the exact and approximate results is satisfactory.

2. The superposition scheme

Consider a three-layer composite laminate, in the configuration indicated in Figure 1. The in-plane dimensions of the laminate are much larger than the total thickness 2h. A slit crack has been introduced into the middle layer which is made of some homogeneous material 1. The crack terminates at interfaces between the middle layer and the adjacent layers made of another homogeneous material 2. In the present solution of this problem,

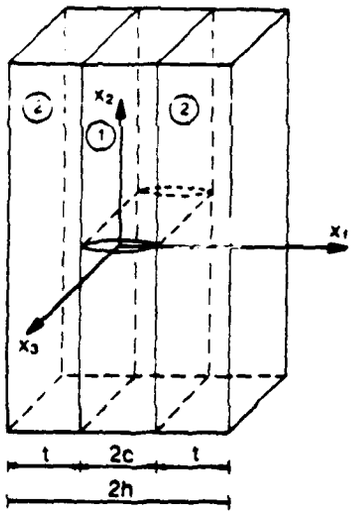

Fig. 1. – Slit crack in a composite laminate.

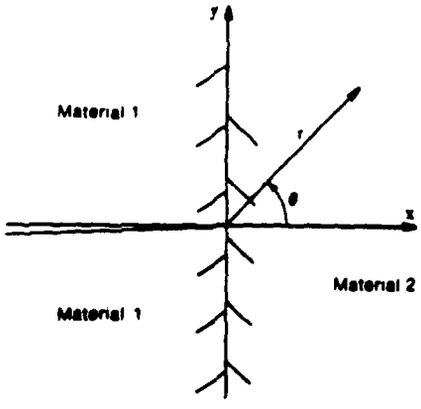

Fig. 3. – Crack which is normal to and ends at the interface between two materials.

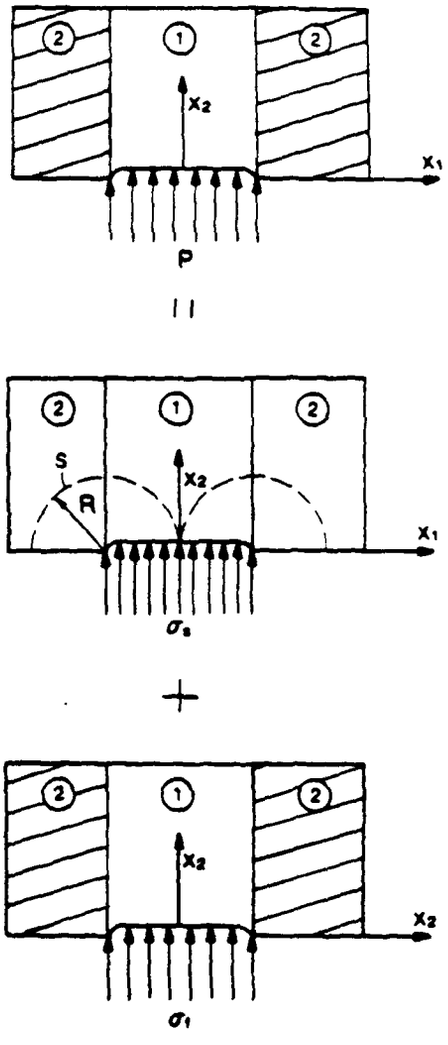

Fig. 2. – Superposition scheme: crack loaded by an internal uniform pressure.

both materials are at most orthotropic, their planes of elastic symmetry coincide with the coordinate planes, but the respective elastic constants assume different magnitudes. The laminate is subjected to a remotely applied uniform normal stress in the longitudinal direction. Our goal is to find an admissible stress field in the x_1, x_2-plane of the laminate, such that it satisfies the prescribed boundary conditions and incorporates known singular terms at the two crack tips. A state of plane strain is assumed.

The superposition procedure we propose to follow is outlined in Figure 2. First, stresses are evaluated in the uncracked laminate under the remotely applied tension load. Those found in the middle layer must be canceled by the stress applied at the surface of the crack. In the present case, the stress $\sigma_{22} = -P$ is the sole surviving component, hence we seek the solution for the cracked laminate loaded by this stress only. The desired admissible field is decomposed into a singular field $\boldsymbol{\sigma}^S(x_1, x_2)$, and a far field $\boldsymbol{\sigma}^F(x_1, x_2)$. Each of these fields will be associated with a normal stress σ_{22} applied at the surface of the crack, these surface stresses are denoted by σ_s and σ_f, respectively. The superposition suggests that the following condition must be met at the crack surface:

$$P = \sigma_s + \sigma_f. \tag{1}$$

The singular field will incorporate the stresses derived from the known elasticity solution for a single crack perpendicular to the interface of materials 1 and 2, Figure 3. However, to assure boundedness of the contribution to the total complementary energy by the singular field, and to avoid additional stresses at the outer boundaries of the adjacent layers, the singular field will be limited to a cylindrical region at each crack tip. These regions will be referred to as the K-zones. In Figure 2, their radius R is selected as equal to the half-thickness of the middle layer, $R = c$; if $t < c$, then $R = t$. This choice avoids direct interaction between the singular fields, but indirect interaction is expected to appear, especially in nonsymmetric laminates, through the far field. In any event, at the boundary $S(r = R)$ of the K-zones, we require that

$$\boldsymbol{\sigma}^S . \mathbf{n} = \mathbf{0} \quad \text{on S} \tag{2}$$

where $\mathbf{n}$ is an outward normal to S. In general, the stress field derived from the solution of the crack problem in Figure 3 will not satisfy this requirement. Therefore, we introduce within the K-zones an additional field $\boldsymbol{\sigma}^D(x_1, x_2)$ such that

$$(\boldsymbol{\sigma}^S - \boldsymbol{\sigma}^D) . \mathbf{n} = 0 \quad \text{on S.} \tag{3}$$

The derivation of the field $\boldsymbol{\sigma}^D$ follows the separate superposition scheme indicated schematically in Figure 4. The singular field $\boldsymbol{\sigma}^S$ from the problem in Figure 3 is found, and the resulting tractions $T_x(\alpha)$, $T_y(\alpha)$ at S are evaluated. An admissible singular field which satisfies (2) is constructed by superposition of the actual singular field with an elastic field $\boldsymbol{\sigma}^D$ within S. In the present approximation, the latter will be found for an isotropic elastic cylinder of radius R, loaded by surface tractions T_x, T_y. Of course, this will create additional stresses on the crack surface which need to be removed. In the present analysis, we accomplish this only in the average sense, *i.e.* we apply at the crack

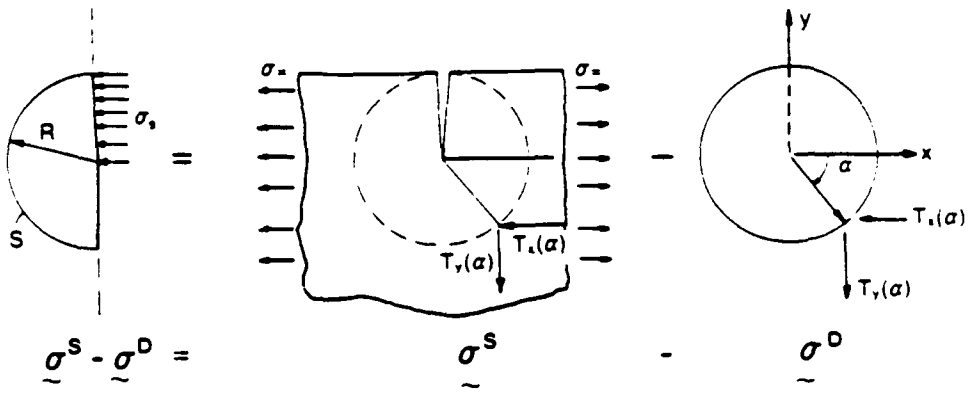

Fig. 4. – Superposition of the local stresses near the crack tip.

surface $(-c < x_1 < c,\ x_2 = 0)$ the uniform normal stress

$$\sigma_s = -\frac{1}{c}\int_0^R \sigma_{22}^D(x_1, 0)\,dx_1. \tag{4}$$

The form of the singular solution assures that σ^D does not create any shear tractions on the surface of the crack.

From the original superposition Eq. (1) we now evaluate the stress

$$\sigma_f = P - \sigma_s \quad \text{for} \quad (-c < x_1 < c,\ x_2 = 0), \tag{5}$$

which remains on the crack surface, and which needs to be accommodated in the nonsingular far field solution of the problem.

In what follows, we first construct the singular field σ^S, then the admissible field σ^D of Figure 4, and finally the admissible far stress field σ^F.

3. Stresses at the crack tip

Elasticity problems in composite laminates with broken plies are usually reduced to a system of integral equations which may not have known closed-form solutions. However, analytic forms of the singular fields at crack tips residing at interfaces between dissimilar anisotropic materials are available. Ting *et al.* [1981, 1984], using the method of Stroh [1962], found such forms for plane problems of this kind. For our present purpose, we recall and specialize these results for a mode I crack.

Consider again the crack configuration in the coordinate system of Figure 3. Denote the respective stiffness tensors of the two materials by $L^{(1)}_{ijkm}$ and $L^{(2)}_{ijkm}$. Attention is restricted to two-dimensional stress and strain fields σ^S and ε^S. The relevant compatibility, constitutive, and equilibrium equations are:

$$\varepsilon^{Sk}_{ij} = (u^{Sk}_{i,j} + u^{Sk}_{j,i})/2 \tag{6}$$

$$\sigma_{ij}^{Sk} = L_{ijkm}^{k} \varepsilon_{km}^{Sk} \tag{7}$$

$$\sigma_{i1,1}^{Sk} + \sigma_{i2,2}^{Sk} = 0 \tag{8}$$

where the superscript $k = 1, 2$, denotes the material, and the subscripts assume values 1, 2 for x, y. At first we are concerned with a general solution of Eqs. (6-8). The transformation [Stroh 1962]

$$u_i^S = V_i f(z) \tag{9}$$

$$z = x + py \tag{10}$$

where p and V_i are constants and f is an arbitrary function, converts (6) and (7) into

$$\sigma_{ij}^{S} = \tau_{ij} \frac{df}{dz} \tag{11}$$

$$\tau_{ij} = (L_{ijk2} + p L_{ijk1}) V_k. \tag{12}$$

In (9), the superscript k has been omitted to simplify the notation, but two different solutions are anticipated for the two materials.

The differential equations of equilibrium become:

$$H_{ij} V_j = 0 \qquad \text{with} \quad H_{ij} = L_{i1j1} + p(L_{i1j2} + L_{i2j1}) + p^2 L_{i2j2}. \tag{13}$$

We seek a nontrivial solution of these equations, *i.e.*, a homogeneous system (8) such that:

$$\| H_{ij} \| = 0. \tag{14}$$

This is a sextic equation in p. Stroh [1962] shows that p is not real and that (14) admits three complex conjugate roots $(p_L, \bar{p}_L)$, $L = 1, 2, 3$. Accordingly, there are six eigenvectors $(V_i^L, \bar{V}_i^L)$. At this point, we can remark that these equations hold both for plane strain and generalized plane stress; only the stiffness L_{ijkm} needs to be modified for each specific case.

For the present case of orthotropic materials with the principal symmetry planes coinciding with the coordinate planes, we use the customary contracted notation $\sigma_{11} = \sigma_1, \ldots \sigma_{23} = \sigma_4, \ldots \varepsilon_{22} = \varepsilon_2, \ldots 2\varepsilon_{13} = \varepsilon_5$, etc., and write the constitutive equations as:

$$\sigma_i = L_{ij} \varepsilon_j. \tag{15}$$

The matrix H_{ij} then becomes:

$$H_{ij} = \begin{bmatrix} L_{11} + p^2 L_{66} & p(L_{12} + L_{66}) & 0 \\ p(L_{12} + L_{66}) & L_{66} + p^2 L_{11} & 0 \\ 0 & 0 & L_{55} + p^2 L_{44} \end{bmatrix}$$

and Eq. (14) reduces to

$$L_{55} + p^2 L_{44} = 0 \tag{16}$$

or to

$$(L_{66}-p^2L_{11})(L_{11}-p^2L_{66})-p^2(L_{12}+L_{66})^2=0. \tag{17}$$

Ting & Hoang [1984] explain that (16) pertains to the out-of-plane motion of the crack surface, and (17) to motion in the xy-plane. In our application, the chosen material geometry, and loading symmetries allow only the latter motion. In general, modes I and II cannot be separated, but are independent of mode III. Then, (14) is a quartic equation. We assume that p_L are single roots; this is not true when the material 1 or 2 are isotropic, that solution calls for a special treatment which was given by Ting & Chow [1981].

The general expressions for displacement and stress field follows from (13) as:

$$u_i^S=\sum_{L=1}^{2}\left(V_i^L f_L(z_L)+\bar{V}_i^L g_L(\bar{z}_L)\right) \tag{18}$$

$$\sigma_{ij}^S=\sum_{L=1}^{2}\left(\tau_{ij}^L\frac{df_L}{dz_L}+\bar{\tau}_{ij}^L\frac{dg_L}{d\bar{z}_L}\right) \tag{19}$$

where

$$\begin{aligned} z_L&=x+p_L y\\ \bar{z}_L&=x+\bar{p}_L y. \end{aligned} \tag{20}$$

This solution is expressed in terms of four arbitrary functions (f_L, g_L), $L=1,2$. Since we wish to find a singular stress field, we choose

$$\begin{aligned} f_L(z_L)&=A_L z_L^{1-\kappa}/(1-\kappa)\\ g_L(\bar{z}_L)&=B_L\bar{z}_L^{1-\kappa}/(1-\kappa) \end{aligned} \tag{21}$$

in which A_L and B_L are complex constants, $\kappa\in[0,1]$ is the order of singularity and is equal to 0.5 when the materials 1 and 2 have identical properties. Otherwise, κ is not immediately known.

Eqs. (18) and (19) may be rewritten in polar coordinates (r,θ) as

$$u_i^S=\frac{r^{1-\kappa}}{(1-\kappa)}\sum_{L=1}^{2}\left\{a_L\,Re(V_i^L\xi_L^{1-\kappa})+\tilde{a}_L\,\mathrm{Im}(V_i^L\xi_L^{1-\kappa})\right\} \tag{22}$$

$$\sigma_{ij}^S=r^{-\kappa}\sum_{L=1}^{2}\left\{a_L\,Re(\tau_{ij}^L\xi_L^{-\kappa})+\tilde{a}_L\,\mathrm{Im}(\tau_{ij}^L\xi_L^{-\kappa})\right\} \tag{23}$$

where

$$\begin{aligned} \xi_L&=\cos\theta+p_L\sin\theta\\ B_L&=A_L=a_L+i\tilde{a}_L. \end{aligned} \tag{24}$$

In each of the two materials, this solution depends on four real constants a_L, $\tilde{a}_L$ and on the order of singularity κ. These constants can be determined from the boundary conditions. Since we have restricted ourselves to the opening mode I, we also restrict the boundary conditions to those existing in the quadrant $x_1>0$, $x_2>0$. The conditions on the crack surface are:

$$\sigma_{12}^{S(1)}=0, \qquad \sigma_{22}^{S(1)}=0 \quad \text{at } \theta=\pi \tag{25}$$

for remotely applied load. The interface conditions are:

$$\begin{aligned} &\sigma_{11}^{S(1)}=\sigma_{11}^{S(2)}, \qquad \sigma_{12}^{S(1)}=\sigma_{12}^{S(2)} \\ &u_1^{S(1)}=u_1^{S(2)}, \qquad u_2^{S(1)}=u_2^{S(2)} \end{aligned} \quad \text{at } \theta=\pi, 2 \tag{26}$$

In addition, the stress components satisfy the symmetry relations:

$$\begin{aligned} &\sigma_{11}^{S(2)}(x, y)=\sigma_{11}^{S(2)}(x, -y) \\ &\sigma_{22}^{S(2)}(x, y)=\sigma_{22}^{S(2)}(x, -y) \\ &\sigma_{12}^{S(2)}(x, y)=-\sigma_{12}^{S(2)}(x, -y). \end{aligned} \tag{27}$$

These relations also hold for material 1, but the stresses need not be expressed in terms of the same constants a_L, $\tilde{a}_L$, because of the discontinuity created by the crack. In other terms, symmetry reduces the number of unknown constants to two in material 2, but four constants remain in material 1 because modes I and II remain coupled.

Eqs. (25) and (26) may be written in the form

$$\mathbf{K}\,\mathbf{g}=\mathbf{0} \tag{28}$$

where

$$\mathbf{g}=[a_1^{(1)}, \tilde{a}_1^{(1)}, a_2^{(1)}, \tilde{a}_2^{(1)}, a_1^{(2)}, \tilde{a}_2^{(2)}]^T$$

and $\mathbf{K}$ is a (6×6) nonsymmetric matrix, a function of κ. Again (28) is a homogeneous system of algebraic equations, a nontrivial solution exists only for $\|\mathbf{K}\|=0$. In the general case there exist three real roots for $\mathbf{K}$, associated respectively with the antisymmetric out-of-plane motion and with the in-plane motion of the crack surface. Therefore, the condition (27) provides only a single root κ in the present case, and (28) is then solved for the eigenvector $\mathbf{g}=[1, \tilde{a}_1^{(1)}, a_2^{(1)}, \tilde{a}_2^{(1)}, a_1^{(2)}, \tilde{a}_2^{(2)}]^T$. The stress fields in materials 1 and 2 are proportional to a single constant, say $a_1^{(1)}$, and so is the stress intensity factor K_I, defined as:

$$K_I=\lim_{r\to 0}\sigma_{22}^{S(2)}(r, 0)\,r^{\kappa}\sqrt{2}. \tag{29}$$

From (23) it follows that

$$K_I=a_1^{(1)}\sqrt{2}\sum_{L=1}^{2}(\tau_{22}^{L(2)}\tilde{a}_L^{(2)}). \tag{30}$$

The obtained solution is an asymptotic expansion of the exact solution near the crack tip. Although this solution may be viewed as a possible statically admissible field in the composite laminate, it turns out that the complementary energy found from this field is infinite when material 2 is unbounded.

4. Stresses in the K-zone

To assure boundedness of the complementary energy term derived from the singular field in section 3, it is necessary to confine the volume affected by this field. As suggested by (2) to (4), the field is admitted only within a cylindrical domain of radius R surrounding the crack tip, which is referred to as the K-zone. This constraint is enforced by an auxiliary stress field $\boldsymbol{\sigma}^D$ which remains to be found. Figure 4 indicates the boundary tractions which are in equilibrium with $\boldsymbol{\sigma}^D$ on $r = R$. Eq. (3) guarantees that the total stresses due to the singular field vanish at $r = R$, while (4) assures that the resultant of the normal stress caused by $\boldsymbol{\sigma}^D$ on the crack surface is equal to zero. Due to the symmetry of the applied tractions about $x_2 = 0$, the same is true for the shear resultant. The field $\boldsymbol{\sigma}^D$ needs to be admissible rather than exact, hence it may be represented by a stress distribution which would exist in a homogeneous and isotropic elastic solid under the prescribed boundary conditions.

We now proceed to derive the stress field $\boldsymbol{\sigma}^D$ from Mukhelishvili potentials. The coordinate system of Fig. 3 is adopted. A homogeneous, isotropic cylinder of radius R and unit thickness $0 < z < 1$ is subjected to tractions $T_x(\alpha)$ and $T_y(\alpha)$ on S, as required by (3):

$$\mathbf{T}(\alpha) = (\boldsymbol{\sigma}^S \cdot \mathbf{n}(\alpha))\, ds \tag{31}$$

or

$$\begin{aligned} T_x(\alpha) &= [\sigma^{Sk}_{xx}(R\cos(\alpha), R\sin(\alpha))\cos(\alpha) \\ &\quad + \sigma^{Sk}_{xy}(R\cos(\alpha), R\sin(\alpha))\sin(\alpha)]\, R\, d\alpha \\ T_y(\alpha) &= [\sigma^{Sk}_{xy}(R\cos(\alpha), R\sin(\alpha))\cos(\alpha) \\ &\quad + \sigma^{Sk}_{yy}(R\cos(\alpha), R\sin(\alpha))\sin(\alpha)]\, R\, d\alpha \end{aligned}$$

$\boldsymbol{\sigma}^{Sk}$ is the singular stress field in Section 3 (*Eq.* 23), with $k = 2$ for $\alpha \in [-\pi/2, \pi/2]$ (material 2) and $k = 1$ for $\alpha \in [\pi/2, 3\pi/2]$ (material 1). These boundary tractions satisfy the overall equilibrium condition

$$\int_0^{2\pi} \mathbf{T}(\alpha)\, d\alpha = \mathbf{0}. \tag{32}$$

It can be verified that the moment equilibrium is also satisfied.

The stress potentials for a disk subjected to the point loads are (Mukhelishvili 1953):

$$\Phi(z)=\frac{1}{2\pi}\left\{(T_x(\alpha)+iT_y(\alpha))\frac{1}{z_j-z}-\frac{\bar{z}_j}{2}\right\}$$
$$\Psi(z)=-\frac{1}{2\pi}\left\{(T_x(\alpha)+iT_y(\alpha))\frac{1}{z_j-z}+\frac{\bar{z}_j}{(z_j-z)^2}\right\} \tag{33}$$

with the notation

$$\begin{cases} z_j=Re^{i\alpha} \\ z_j-z=re^{-i\theta}. \end{cases} \tag{34}$$

In the complex plane, z_j denotes the location of the point loads and z denotes the points at which stress is evaluated. The field σ^D then follows from the relations

$$\begin{cases} \sigma^D_{xx}(\alpha)+\sigma^D_{yy}(\alpha)=4\,\mathrm{Re}(\Phi(z)) \\ \sigma^D_{yy}(\alpha)-\sigma^D_{xx}(\alpha)+2i\sigma_{xy}(\alpha)=2[\bar{z}\Phi'(z)+\Psi(z)] \end{cases} \tag{35}$$

which leads to the final result

$$\sigma^D_{xx}(\alpha)=\frac{T_x(\alpha)}{2\pi}\left\{\frac{\cos 3\theta+3\cos\theta}{r}-\frac{\cos\alpha}{R}\right\}-\frac{T_y(\alpha)}{2\pi}\left\{\frac{\sin 3\theta+\sin\theta}{r}+\frac{\sin\alpha}{R}\right\}$$
$$\sigma^D_{yy}(\alpha)=\frac{T_x(\alpha)}{2\pi}\left\{\frac{\cos\theta-\cos 3\theta}{r}-\frac{\cos\alpha}{R}\right\}+\frac{T_y(\alpha)}{2\pi}\left\{\frac{\sin 3\theta-3\sin\theta}{r}-\frac{\sin\alpha}{R}\right\} \tag{36}$$
$$\sigma^D_{xy}(\alpha)=-\frac{T_x(\alpha)}{2\pi}\left\{\frac{\sin 3\theta+\sin\theta}{r}\right\}-\frac{T_y(\alpha)}{2\pi}\left\{\frac{\cos 3\theta+\cos\theta}{r}\right\}.$$

Integration with respect to α, and transformation from the local (x, y) to the global coordinates (x_1, x_2) coordinates gives:

$$\sigma^D_{11}=\int_0^{2\pi}\sigma^D_{xx}(\alpha)\,d\alpha$$
$$\sigma^D_{22}=\int_0^{2\pi}\sigma^D_{yy}(\alpha)\,d\alpha \tag{37}$$
$$\sigma^D_{12}=\int_0^{2\pi}\sigma^D_{xy}(\alpha)\,d\alpha.$$

The average stresses on the crack face are found as in (4):

$$\sigma_s=-\frac{1}{c}\int_0^R\int_0^{2\pi}\sigma^D_{22}(\alpha)\,d\alpha\,dx_1, \qquad \sigma_t=-\frac{1}{c}\int_0^R\int_0^{2\pi}\sigma^D_{12}(\alpha)\,d\alpha\,dx_1. \tag{38}$$

Due to the symetry with respect to the y axis, σ_t cancels over the total crack length.

As suggested by (31), the tractions are proportional to the factor $a_1^{(1)}$ in σ^S, or to the stress intensity field K_I. Therefore, the traction σ_s on the crack surface is also proportional

to K_I. If δ is defined as a coefficient of proportionality, the superposition Eq. (1) becomes

$$P = \sigma_f + \delta K_I. \tag{39}$$

Of course, the actual magnitude of the stress intensity factor is not yet known. It will be obtained later, from minimization of the complementary energy of the total admissible stress field.

5. The far field

Up to this point, we have derived admissible fields at the tip of the crack. To complete the derivation in the entire solution domain suggested in Figure 1, we now proceed to find an admissible field in the entire laminate. This is a nonsingular field σ^F which satisfies the traction boundary conditions on the crack surface suggested by the superposition Eqs. (1) and (39), *i.e.*, $\sigma^F_{22} = \sigma_f$, and which vanishes at infinity.

The geometry of the domain under consideration appears in Figure 1. The inner and outer layers are made of two different orthotropic materials denoted by the index $k = 1, 2$. The elastic constants are denoted by E^k_{11}, E^k_{22}, G^k_{12}, ν^k_{12}, etc. Stress fields in materials 1 and 2 are denoted by $\sigma^{F(1)}$, and $\sigma^{F(2)}$. A plane strain solution is sought in a domain of unit thickness in the x_3 direction.

The boundary conditions are defined as

$$\begin{cases} \sigma^{F(1)}_{22} = \sigma^{F(1)}_{12} = \sigma^{F(2)}_{22} = \sigma^{F(2)}_{12} = 0 & \text{at } |x_2| \to \infty \\ \sigma^{F(2)}_{12} = \sigma^{F(2)}_{11} = 0 & \text{at } |x_1| = h = c + t \end{cases} \tag{40}$$

on the external surfaces of the domain, and as

$$\begin{cases} \sigma^{F(1)}_{22} = \sigma_f & \text{at } x_2 = 0 \\ \sigma^{F(1)}_{12} = 0 & x_1 \in [-c, c] \end{cases} \tag{41}$$

on the crack faces. In addition, the following interface conditions need to be satisfied at $|x_1| = c$

$$\begin{aligned} \sigma^{F(1)}_{11}(\pm c, x_2) &= \sigma^{F(2)}_{11}(\pm c, x_2), \\ \sigma^{F(1)}_{12}(\pm c, x_2) &= \sigma^{F(2)}_{12}(\pm c, x_2). \end{aligned} \tag{42}$$

Overall equilibrium in the x_2 direction requires that

$$\int_{-h}^{+h} \sigma^F_{22}\, dx_1 = 0, \qquad \int_{-h}^{+h} \sigma^F_{12}\, dx_1 = 0. \tag{43}$$

At this point, various expressions may be proposed for σ^F. For example, Hashin [1985, 1987] used a piecewise uniform distribution of σ^F_{22}. This approximation is acceptable when the thickness $t < c$. However, for $t > c$, which is the most common case in actual

laminates, we select the following distribution of σ_{22}^{F}.

$$\begin{aligned}\sigma_{22}^{F(1)} &= \sigma_f \varphi_1(x_2)\\ \sigma_{22}^{F(2)} &= \sigma_f \exp(-(x_1 - t)/t)\,\varphi_2(x_2).\end{aligned} \tag{44}$$

In the outer plies, the stresses decay exponentially, this will be seen to improve substantially the accuracy of the subsequent estimates of the energy released by the crack in laminates where $t \gg c$. From these assumed forms we derive the following stress components, still in terms of the as yet unknown functions

$$\begin{aligned}
&\sigma_{22}^{F(1)}(x_1, x_2) = \sigma_f \varphi_1(x_2)\\
&\sigma_{12}^{F(1)}(x_1, x_2) = -\sigma_f \dot{\varphi}_1(x_2)\, x_1\\
&\sigma_{11}^{F(1)}(x_1, x_2) = +\sigma_f \ddot{\varphi}_1(x_2)\left\{\frac{x_1^2}{2} - \frac{c^2}{2} + ct\right\}\\
&\sigma_{33}^{F(1)} = -\nu_{31}^{(1)}\sigma_{11}^{F(1)} - \nu_{32}^{(1)}\sigma_{22}^{F(1)}\\
&\sigma_{22}^{F(2)}(x_1, x_2) = \frac{-\sigma_f c}{t(e^{-c/t} - e^{-h/t})}\varphi_1(x_2)e^{-x_1/t}\\
&\sigma_{12}^{F(2)}(x_1, x_2) = \frac{-\sigma_f c}{(e^{-c/t} - e^{-h/t})}\dot{\varphi}_1(x_2)(e^{-x_1/t} - e^{-h/t})\\
&\sigma_{11}^{F(2)}(x_1, x_2) = \frac{-\sigma_f ct}{(e^{-c/t} - e^{-h/t})}\ddot{\varphi}_1(x_2)(e^{-x_1/t} - e^{-h/t}).\\
&\sigma_{33}^{F(2)} = -\nu_{31}^{(2)}\sigma_{11}^{F(2)} - \nu_{32}^{(2)}\sigma_{22}^{F(2)}
\end{aligned} \tag{45}$$

These expressions are valid for $x_1 > 0$, the forms for $x_1 < 0$ follow from symmetry conditions. Note that $\varphi_1(x_2)$ is the only unknown function to appear in (45), because the overall equilibrium conditions (43) provide a relation between $\varphi_1(x_2)$ and $\varphi_2(x_2)$.

The boundary conditions (40) and (41) impose the following requirements on $\varphi_1(x_2)$:

$$\begin{aligned}\varphi_1(0) &= 1\\ \dot{\varphi}_1(0) &= 0\\ \lim_{x_2 \to \infty} \varphi_1(x_2) &= \lim_{x_2 \to \infty} \dot{\varphi}_1(x_2) = 0.\end{aligned} \tag{46}$$

This completes the evaluation of the far field in terms of $\varphi_1(x_2)$ and σ_f, which remain to be found.

6. The complementary energy

Now that the forms of the various components of the admissible stress field in the solution domain in Figure 1 are known, we proceed to evaluate and then to minimize the complementary energy U of the field:

$$U = \frac{1}{2}\int_V (\boldsymbol{\sigma}^S - \boldsymbol{\sigma}^D + \boldsymbol{\sigma}^F)\,\mathbf{M}\,(\boldsymbol{\sigma}^S - \boldsymbol{\sigma}^D + \boldsymbol{\sigma}^F)\,dV \tag{47}$$

where $\mathbf{M}$ is the compliance matrix of the layer materials. The expression is further developed as:

$$(48)\quad U = \frac{1}{2}\int_0^R \int_0^{2\pi} (\sigma^S - \sigma^D)\,\mathbf{M}\,(\sigma^S - \sigma^D)\,dr\,d\theta + \int_0^R \int_0^{2\pi} (\sigma^S - \sigma^D)\,\mathbf{M}\,\sigma^F\,dr\,d\theta + \frac{1}{2}\int_V \sigma^F\,\mathbf{M}\,\sigma^F\,dV$$

The last integral is further expanded into [Hashin 1985]:

$$(49)\quad \frac{1}{2}\int_V \sigma^F\,\mathbf{M}\,\sigma^F\,dV = 4\,\sigma_f^2\,c\int_0^{\infty} (D_{00}(\varphi_1(x_2))^2 + D_{11}(\dot{\varphi}_1(x_2))^2 + D_{02}\,\varphi_1(x_2)\,\ddot{\varphi}_1(x_2) + D_{22}(\ddot{\varphi}_1(x_2))^2\,dx_2$$

where D_{ij} are constants which depend on the dimensions c and t in Figure 1, and on the elastic constants of the layers.

Unfortunately, the second integral or cross-term in (48) gives an expression in $d\varphi_1(x_2)$, its derivatives and non-constant coefficients. The equation

$$U(\varphi_1(x_2) + d\varphi_1(x_2)) - U(\varphi_1(x_2)) = 0$$

can be solved only numerically, which requires a large amount of computation. To avoid this difficulty, we choose to perform a successive minimization. First, the contribution of σ^F to U is minimized and $\varphi_1(x_2)$ is found. Then, the complementary energy is minimized with respect to K_I and an optimum value of K_I, subject to the restrictions imposed by our procedure is established. While the solution is not the best possible approximation, numerical implementations show that the cross-term is small, typically not exceeding 0.1-0.15 U.

The successive minimization is thus performed in two steps. First we find the best statically admissible far field σ^F. Next, this field is superimposed with the singular field in the K-zone, the complementary energy is minimized, and the corresponding magnitude of K_I is evaluated. In the first step, minimization of U with respect to $\varphi_1(x_2)$ yields the fourth-order differential equation

$$(50)\qquad D_{00}\,\varphi_1(x_2) + (D_{02} - D_{11})\,\ddot{\varphi}_1(x_2) + D_{22}\,\varphi_1^{IV}(x_2) = 0$$

in which

$$
\begin{aligned}
D_{00} &= \frac{1}{E_{22}^{(1)}(1-\nu_{32}^{(1)}\nu_{23}^{(1)})} + \frac{1}{E_{22}^{(2)}(1-\nu_{32}^{(2)}\nu_{23}^{(2)})}\,\frac{c}{2t}\left\{\frac{(e^{-2ct}-e^{-2ht})}{(e^{-ct}-e^{-ht})^2}\right\}\\
D_{11} &= \frac{c^2}{3G_{12}^{(1)}} + \frac{c}{G_{12}^{(2)}(e^{-ct}-e^{-ht})^2}\left\{\frac{t}{2}(e^{-2ct}-e^{-2ht}) + 2t(e^{-2ht}-e^{-(h+c)t}+te^{-2ht})\right\}\\
D_{22} &= \frac{1}{E_{11}^{(1)}(1-\nu_{31}^{(1)}\nu_{13}^{(1)})}\left\{\frac{c^4}{20}+\frac{Ac^2}{3}+A^2\right\}\\
&\quad + \frac{c}{E_{11}^{(2)}(1-\nu_{31}^{(2)}\nu_{13}^{(2)})\,t^2(e^{-ct}-e^{-ht})^2}\left\{\frac{t^5}{2}(e^{-2ct}-e^{-2ht}) + 2Bt^3(e^{-ct}-e^{-ht}) + B^2c\right\}\\
D_{02} &= -\left[\frac{\nu_{12}^{(1)}+\nu_{13}^{(1)}\nu_{32}^{(1)}}{2E_{11}^{(1)}} + \frac{\nu_{21}^{(1)}+\nu_{23}^{(1)}\nu_{31}^{(1)}}{2E_{22}^{(1)}}\right]\left(\frac{c^2}{3}+2A\right)\\
&\quad -\left[\frac{\nu_{12}^{(2)}+\nu_{13}^{(2)}\nu_{32}^{(2)}}{2E_{11}^{(2)}} + \frac{\nu_{21}^{(2)}+\nu_{23}^{(2)}\nu_{31}^{(2)}}{2E_{22}^{(2)}}\right]\left\{\frac{e^{-2ct}-e^{-2ht}}{(e^{-ct}-e^{-ht})^2} + \frac{2Bct}{(e^{-ct}-e^{-ht})}\right\}
\end{aligned}
\tag{51}
$$

where

$$
\begin{aligned}
A &= -\frac{c^2}{2} + ct\\
B &= -t^2 e^{-ht}
\end{aligned}
\tag{52}
$$

For $\Delta = 4D_{00}D_{22} - (D_{02}-D_{11})^2 > 0$, the general solution of (50) is:

$$
\varphi_1(x_2) = A_1 e^{-ax_2}\cos bx_2 + A_2 e^{-ax_2}\sin bx_2 + A_3 e^{ax_2}\cos bx_2 + A_4 e^{ax_2}\sin bx_2 \tag{53}
$$

with

$$
a = \left[\frac{D_{00}}{D_{22}}\right]^{1/4}\cos\frac{d}{2},\quad b = \left[\frac{D_{00}}{D_{22}}\right]^{1/4}\sin\frac{d}{2};\qquad d = \operatorname{Arctang}(\sqrt{\Delta}). \tag{54}
$$

The coefficients A_i are computed from the boundary conditions (46):

$$
A_1 = 1,\qquad A_2 = a/b,\qquad A_3 = A_4 = 0. \tag{55}
$$

After some algebra, which follows Hashin's [1985] work, we have:

$$
\frac{1}{2}\int_V \sigma^F M \sigma^F dV = 4D_{22}c\sigma_f^2 a(a^2+b^2). \tag{56}
$$

Substitute now (56) into (48) and minimize U with respect to K_1. Eq. (48) is first rewritten as:

$$
2U = I_1 K_1^2 + 2K_1\sigma_f I_2 + 8D_{22}c\sigma_f^2 a(a^2+b^2) \tag{57}
$$

where I_1 and I_2 are known integrals that can be evaluated numerically. With regard to the superposition relations (39), minimization of (57) yields the desired value of the stress

intensity factor as:

$$K_I = P\frac{8\delta D_{22} ca(a^2+b^2) - I_2}{I_1 - 2\delta I_2 + 8\delta^2 D_{22} ca(a^2+b^2)} \tag{58}$$

The modified procedure which was followed in evaluation of K_I may not identify the minimum value of U for the selected admissible field. However, the estimates of K_I which are derived in the sequel are very close to the available exact results.

Some of the comparisons with related results that follow involve plane stress solutions of crack problems. The plane strain solutions developed so far can be modified for this purpose. In particular, both σ_{33} components in (45) vanish and that affects the terms in (48) and (57). The D_{00}, D_{22}, and D_{02}, in (51) then become:

$$\begin{aligned}
D_{00} &= \frac{1}{E_{22}^{(1)}} + \frac{1}{E_{22}^{(2)}}\frac{c}{2t}\left\{\frac{(e^{-2c/t} - e^{-2h/t})}{(e^{-c/t} - e^{-h/t})^2}\right\} \\
D_{22} &= \frac{1}{E_{11}^{(1)}}\left\{\frac{c^4}{20} + \frac{Ac^2}{3} + A^2\right\} + \left\{\frac{c}{E_{11}^{(2)} t^2 (e^{-c/t} - e^{-h/t})^2}\right\}\left[\frac{t^5}{2}(e^{-2c/t} - e^{-2h/t}) + 2Bt^3(e^{-c/t} - e^{-h/t}) + B^2 c\right] \\
D_{02} &= -\frac{\nu_{12}^{(1)}}{E_{11}^{(1)}}\left(\frac{c^2}{3} + 2A\right) - \frac{ct\,\nu_{12}^{(2)}}{E_{11}^{(2)}}\left[\frac{e^{-2c/t} - e^{-2h/t}}{(e^{-c/t} - e^{-h/t})^2} + \frac{2Bct}{(e^{-c/t} - e^{-h/t})}\right]
\end{aligned} \tag{59}$$

The coefficient D_{11}, and the constraints A and B in (52) remain unchanged. However, Ting's work indicates that the order of singularity does change.

7. Results and discussion

The technique will now be applied to several cracked laminates which have been analyzed by other methods in the literature. Of course, we first consider the case when both layers are made of the same isotropic material. The elastic constants were selected as E = 13 GPa, and ν = 0.3. The c/t ratio in Figure 1 was selected as indicated in Table I.

TABLE I. — Stress intensity factors in an isotropic cracked strip of finite width.

c/t	$K_I/P\sqrt{c}$	$K_{I\,exact}/P\sqrt{c}$	K_I/K_{exact}
0	1.011543	1.00	1.011543
0.1	1.011546	1.0055	1.006
0.2	1.01197	1.02	0.992
0.5	1.0401	1.07	0.972
1	1.1876	1.1867	1.0007

The table shows the approximate and exact values [Tada *et al.* 1985] of the plane strain stress intensity factor K_I. The observed error is between 1 and 3%. For this configuration,

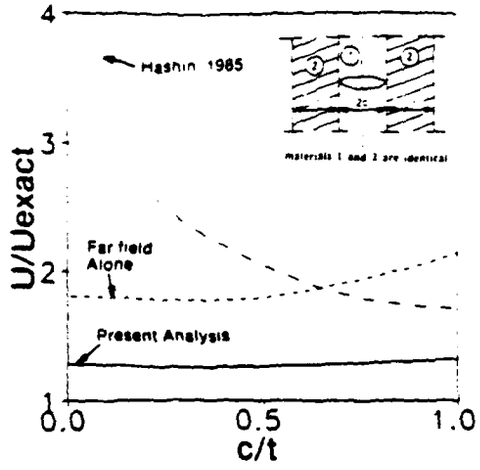

Fig. 5. – Complementary energy in an isotropic cracked strip.

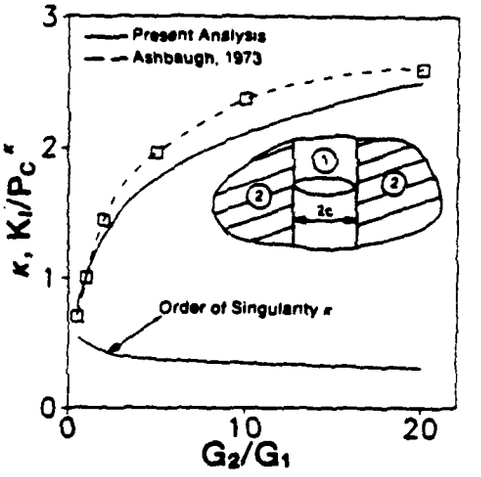

Fig. 6. – The stress intensity factor and order of singularity for a cracked isotropic layer embedded into another isotropic infinite medium.

our estimate of the complementary energy U is compared on Figure 5 with the exact solution by Sneddon and Srivastav, and Sneddon & Lowengrub [1969]. For comparison, we also plot the result that follows from Hashin's (1985) model. Note that Hashin's variational solution for the configuration in Fig. 1 is a plane stress field ($\sigma_{33}=0$), even though the in-plane dimensions of the plate are much larger than its thickness. The latter result indicates an unbounded value for U when $c/t \to 0$; this serves to confirm our assertion that a piecewise linear admissible field σ_{22}^{F} is unsuitable in geometries where $t > c$. In contrast, the exponentially decaying distribution of the far field in the outer plies leads to a finite value of U, but if the far field alone is used in the evaluation of U,

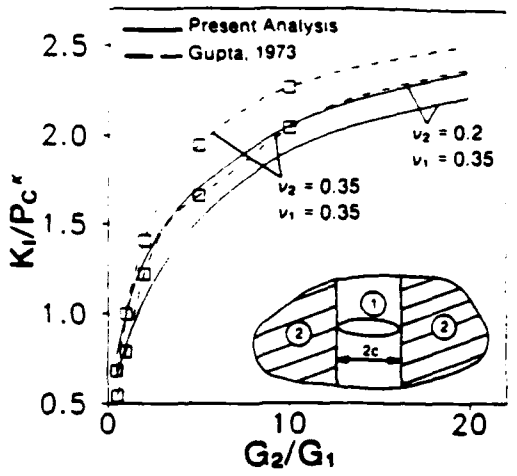

Fig. 7. – Evolution of the stress intensity factor: two isotropic media with various Poisson's ratio.

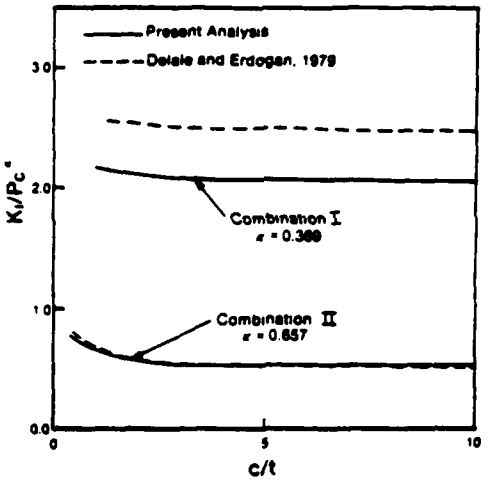

Fig. 8. – Evolution of the stress intensity factor: two orthotropic materials.

the resulting value is about twice as high as the exact one. The addition of the singular field improves the estimate to an acceptable agreement with the exact solution.

In Figure 6 we show results for a laminate made of two isotropic layers with elastic constants G_1 ν_1 and G_2, ν_2, the dimension $t \to \infty$. The exact plane strain solution was found by Ashbaugh (1973) for the case of $\nu_1 = \nu_2 = 0.33$. The graph shows how the order of singularity κ of the stresses at the crack tip changes with the ratio G_2/G_1. The order decreases from 0.5 to about 0.3, and our estimate agrees with the exact solution. The prediction of the magnitude of K_1 is within 12% of the exact solution.

A similar comparison is made in Figure 7 with Gupta's (1973) plane strain results. The results indicate the effect of different Poisson's ratios on κ and K_1. A good agreement

TABLE II. — Comparison of approximate and exact results for a composite laminate made of two isotropic materials.

	κ	$K_I P c^*$	$K_{I\,exact} P c^*$	W (N m)	W_{exact} (N m)
1. Epoxy 2. Aluminum	0.3381	2.281	2.784	4.9×10^{-7}	4.3×10^{-7}
1. Aluminum 2. Steel	0.4125	1.476	-	2.9×10^{-8}	2.5×10^{-8}

Elastic constants:	E (GPa)	ν
Epoxy	3.5	0.35
Aluminum	68.9	0.3
Steel	213.7	0.2

TABLE III. — Elastic constants for the orthotropic laminates

	1	2
E_{11}	134.45 GPa	154.77 GPa
E_{22}	31.03 GPa	155.83 GPa
G_{12}	24.15 GPa	59.68 GPa
ν_{12}	0.65	0.3

exists between the exact and approximate solutions. Another comparison with Gupta's results appears in Table II. The energy W released by the crack is evaluated for two material combinations. Also, the stress intensity factors found from the present solution are compared with those computed by Cook & Erdogan [1972] for a two-layer laminate in which one crack tip touches the interface. In the comparison, a long crack was used in our solution to eliminate the interaction between the two singular fields.

Finally, Figure 8 indicates how K_I varies in laminates made of two different orthotropic materials. In this example plane stress is assumed and various c/t ratios are considered. Table III presents the elastic constants of the layers, those agree with some of those used by Delale & Erdogan [1979]. In Combination I (*Fig.* 8) the crack is located in material 1; in Combination II, the materials are exchanged so that the crack resides in a middle layer made of material 2 indicated in Table III. Delale and Erdogan's results were found for a periodic arrangement of layers, with a periodic distribution of collinear cracks. However, our results were found for the laminate of Figure 1, without any stress at $|x| = h$. The agreement is very good for Combination II, but less satisfactory for Combination I. This is probably caused by our approximation of the far field. We have also used the form $\exp(-qx/t)$ instead of that chosen in (44); this improved the agreement in Combination I by about 50% when q was selected as $q = 0.6$.

In conclusion, the proposed superposition scheme indicates how the available singular solutions for cracks at interfaces can be utilized in analysis of cracked laminates. Of course, the singular solutions may be introduced directly into a finite element program. However, the proposed method is much more efficient. It can be readily extended to the case of many interacting cracks in a layer [Benveniste *et al.* 1989].

Moreover, the technique may be modified and applied to laminates made of three different materials, and also to laminate geometries in which the principal material axes are not aligned.

Acknowledgement

This work was supported in part by the DARPA-HiTASC program at RPI and by the Office of Naval Research.

REFERENCES

ASHBALGH N. E., 1973, Stresses in laminated composites containing a Broken layer. *J. Appl. Mech.*, **40**, 535-540.

BENVENISTE Y., DVORAK G. J., ZARZOUR J., 1989, On interacting cracks and complex crack configurations in linear elastic media. *Int. J. Solids Struct.*, **25**, 1279-1293.

COOK T. S., ERDOGAN F., 1972, Stresses in bonded materials with a crack perpendicular to the interface. *Int. J. Engng. Sci.*, **10**, 677-697.

DELALE F., ERDOGAN F., 1979, Bonded orthotropic strips with cracks. *Int. J. Fract.*, **15**, 343-364.

GUPTA G. D., 1973, A layered composite with a Broken laminate. *Int. J. Solids Struct.*, **9**, 1141-1154.

HASHIN Z., 1985, Analysis of cracked laminates: A variational approach. *Mech. Mat.*, **4**, 121-136.

HASHIN Z., 1987, Analysis of orthogonally cracked laminates under tension. *J. Appl. Mech.*, **54**, 872-879.

MUKHELISHVILI N. I., 1953, *Some basic problems of the mathematical theory of elasticity*, P. Noordhoff pub., 3rd Edition.

SNEDDON I. N., LOWENGRUB N., 1969, *Cracks Problems in Classical Theory of Elasticity*, J. Wiley, p. 221.

STROH A. N., 1962, Steady state problems in anisotropic elasticity. *J. Math. Phys.*, **41**, 77-103.

TADA H., PARIS P. C., IRWIN J. K., 1985, *The Stress Analysis of Cracks Handbook*, 2nd ed., Paris Prod. Inc., St.-Louis, Mo.

TING T. C. T., HOANG P. H., 1984, Singularities at the tip of a crack normal to an interface of an anisotropic layered composite. *Int. J. Solids Struct.*, **20**, 439-454.

TING T. C. T., CHOU S. C., 1981, Edge singularities in anisotropic composites, *Int. J. Solids Struct.*, **17**, 1057-1068.

(Manuscript received March 15, 1989.)

MECHANICS

THERMOVISCOPLASTICITY OF METAL MATRIX LAMINATES

THERMAL, VISCOPLASTIC ANALYSIS OF COMPOSITE LAMINATES

E. KREMPL and K.D. LEE
Rensselaer Polytechnic Institute, Mechanics of Materials Laboratory, Troy, NY 12180-3590

ABSTRACT

For the modeling of ply deformation behavior the orthotropic, thermal viscoplasticity theory based on overstress is used. It can represent creep, relaxation and rate sensitivity as well as monotonic and cyclic loadings. The theory is "unified" since creep and plasticity are not separately modeled. No yield surfaces and loading/unloading conditions are employed. The laminate theory for in-plane loading maintains the geometric assumptions of classical laminate theory. The elasticity law, however, is replaced by the thermal, orthotropic viscoplasticity law. Numerical experiments illustrate the predictions of the theory for an angle-ply and a cross-ply laminate subjected to a temperature increase, temperature hold and subsequent return to the original temperature. The ply and laminate stresses are calculated as a function of time for unconstrained and constrained conditions using postulated properties close to a real metal matrix composite. Redistribution of ply stresses and relaxation are found. In some cases, nearly permanent residual ply stresses are present after completion of the temperature cycle.

INTRODUCTION

Metal matrix composites are increasingly used in primary structures which are subjected to severe conditions of loading and environment. Included are variable temperature services such as occur in a satellite in orbit or during flight of the space plane. Other examples are components in propulsion systems, jet engines and rockets. To ensure safe operation, stress and life-time analyses must be performed long before the part is built.

The high degree of anisotropy present in composite structures requires the development of new analysis techniques which account for the variation of the material properties with direction. When metal matrix composites are used, inelastic deformation cannot be ruled out even if the service is at low homologous temperature and if the overall loads are within the nominal elastic limit [1]. For high homologous temperature service, inelasticity is found in the form of time-dependent deformation, even in monolythic materials.

Traditionally high temperature stress analysis is performed by combining elasticity with time-independent plasticity and creep theories. For each element, a separate constitutive equation is postulated. Except for initial conditions, creep and plasticity are treated as separate phenomena with no interaction between them.

With this approach, the exact identification in experiments of creep and plastic strains is problematic, see [2]. Further, material science shows that dislocations and other changes in the defect structure are responsible for inelastic deformation which is considered to be time dependent. As a consequence, several new constitutive equations have been

Mat. Res. Soc. Symp. Proc. Vol. 120. ©1988 Materials Research Society

proposed during the last two decades which do not separate creep and plastic deformation. They are called "unified" constitutive equations; a recent review of some of these is given in [3].

The viscoplasticity theory based on overstress (VBO) is one of the unified theories. It was developed in response to the observed time-dependence of engineering alloys at ambient temperature [4-7]. Subsequently, an orthotropic version of the theory was formulated [8,9] and applied to the modeling of the in-plane deformation of metal matrix composite laminates [10].

The purpose of this paper is to introduce and to apply a thermal version of the orthotropic VBO to metal matrix composite laminates subjected to thermal and mechanical loadings. Nurerical examples are given for constrained and unconstrained, angle-ply and cross-ply laminates subjected to a temperature increase followed by a temperature hold and subsequent return to the original temperature. Laminate and ply stress components are calculated as a function of time in a simple theory which is patterned after the classical laminate theory (CLT), see [11]. The geometric assumptions of CLT are maintained such as constant strain through the laminate and satisfaction of the stress boundary condition for the whole laminate only. The linear orthotropic elasticity law of CLT is, however, replaced by the thermal, orthotropic viscoplasticity theory based on overstress. It is now possible to model hysteresis, creep, relaxation and rate sensitivity as well as time dependent stress redistributions between plies due to thermal and/or mechanical loadings. The present theory assumes the ply to be an orthotropic continuum with its properties represented by the thermal VBO. No interactions between fiber and matrix are modeled. However, this can be done without any difficulty and will be pursued in the future.

PLY CONSTITUTIVE EQUATIONS

An orthotropic version of the viscoplasticity theory based on overstress (VBO) is used. In this theory, the total small strain rate is the sum of the elastic, inelastic and thermal strain rates. For the elastic strain rates, the rate form of Hooke's law in orthotropic form is employed , i.e. the time derivative of the product of the orthotropic compliance with the stress. The inelastic strain rate is only a function of overstress, which is the difference between the current stress and the equilibrium stress, the state variable of the theory. The equilibrium stress is the stress which can be indefinitely sustained after deformation when all rates have returned to zero. Initially, the equilibrium stress is zero but evolves with deformation according to a separately postulated orthotropic growth law. It is responsible for modeling almost linear elastic regions and hysteresis. In the present theory, no recovery terms are included. An extension of the theory to recovery is under development. The thermal strain rate is the time derivative of the product of the orthotropic coefficient of thermal expansion with the temperature difference reckoned from a reference temperature. All material properties of the theory can be functions of temperature and must be determined from suitable experiments on a ply. This includes tests in the fiber and transverse directions. Rate change tests are essential in determining the viscous (time-dependent) properties of the theory.

The VBO assumes that inelastic deformation is basically rate dependent. Rate dependence is always present and can change with temperature. Normally, it increases with rising temperature. This property can be modeled by making certain constants in the repository for rate dependence a function of temperature. The normally encountered decrease in the flow

stress with increasing temperature is also modeled easily. In fact, since no trend of the temperature dependence is presumed by the theory, even anomalous trends such as an increase in strength with increasing temperature can be represented by this VBO.

The theory does not use a yield surface and loading/unloading conditions. Inelastic strain rates are always present but are extremely small in the elastic regions. On a stress-strain graph, the linear elastic region predicted by the theory can be a perfect straight line. This is accomplished by the growth law for the equilibrium stress.

The equations of the theory need detailed explanations which cannot be included in this paper because of space limitations. The theory is presented in [12].

IN-PLANE LAMINATE BEHAVIOR

The orthotropic VBO described above is now specialized for the case of plane stress and used as a constitutive equation for a particular ply in a simple theory of in-plane laminate behavior. The theory retains all the geometric assumptions of CLT, see [11]. In this paper, the orthotropic, linear elasticity law used in CLT is replaced by the thermal, orthotropic VBO. As a consequence, rate dependence, creep, relaxation and hysteresis can be modeled, in addition to the effects of changing temperature. The theory includes the modeling of stress redistributions between plies during deformation.

This theory has been developed for angle-ply laminates and a computer program has been written for the numerical integration of the resulting simultaneous nonlinear, ordinary differential equations, see [12]. Once the material constants and functions of the theory are known, the program can be used for any thermal and/or mechanical history imposed on the laminate. Included are uniform temperature changes for a constrained or an unconstrained laminate, as well as simultaneous thermal and mechanical loadings.

For the sake of brevity, these equations are not given here. They can be found in [13].

NUMERICAL SIMULATION OF LAMINATE BEHAVIOR UNDER A TEMPERATURE CHANGE

To illustrate some aspects of the capability of the theory without listing the governing equations, the following procedure is adopted. Hypothetical but realistic material properties are assumed in the thermal, orthotropic VBO. These properties result in a certain stress-strain behavior in the fiber and in the transverse directions. These diagrams are taken to be an indication of the material properties of each ply. Then a $[+45/-45]_s$ angle-ply and a $[0/90]_s$ cross-ply laminate are "built theoretically" and their responses to a temperature history with and without mechanical constraints are computed. The uniform temperature excursion (every part of the laminate sees the same temperature) is a 200°C increase followed by a temperature hold and a subsequent decrease to the reference temperature as depicted in Fig.1a. In the first case, the laminates are free to expand and only thermal stresses between the plies develop due to the differences in the orientation and the coefficients of thermal expansion. The laminate boundaries are stress free. In the second case, the laminates are constrained in the one-direction but are free to expand in the two-direction, see Fig.1b. Thermal stresses are now due to

constraint and due to the differences in orientation of the plies. This exercise is to demonstrate the capabilities of the theory under small temperature changes. Of course, larger temperature changes can be simulated, as long as the material data are known. Examples are the computation of the residual stresses that may develop during manufacturing when the laminate cools down from the working temperature.

The stress-strain diagrams of a ply in the fiber and the transverse directions at the reference temperature and at the maximum temperature of the cycle are shown in Figs. 2a and 2b, respectively. The difference in the strengths of the matrix and the fibers is obvious as is the increased rate sensitivity of the matrix as compared to the fibers. Overall, the rate sensitivity modeled by this hypothetical material is not very pronounced. Other stress-strain relations and rate sensitivities can be modeled easily by adjusting the material constants, see [10].

For the simulation of the temperature cycles imposed on the laminate, it is assumed that the positive coefficient of thermal expansion in the fiber direction is about one sixtieth of that of the transverse direction. Such relations are found in some metal matrix plies.

Case 1: Unconstrained Laminates

In this case, no external stresses act on the laminate. Owing to the assumptions of CLT, stresses can act at the boundary of individual lamina as long as their sum is zero.

Fig. 3 shows the computed results for both the angle-ply and the cross-ply laminates. Owing to the small temperature change, the stresses are modest and are within the elastic behavior of the fibers, see Fig. 2a. Due to symmetry, only ply shear stresses exist in the $[+45/-45]_s$ laminate. The stresses in the two plies have opposite signs. In the cross-ply laminate, no shear stresses are found and the ply stresses in the one- and the two-directions are equal. Equilibrium requires that the stresses in the zero and ninety degree ply add up to zero. For these reasons, only one curve is shown in Fig. 3. It is seen that relaxation occurs during the temperature hold and that residual stresses exist when the temperature returns to its original value. They decrease slightly in magnitude with time.

Case 2: Constrained Laminates

Due to the constraint, see Fig. 1b, laminate stresses exist in the one-direction. In the two-direction, the laminate stresses are zero.

The results for the angle-ply laminate are depicted in Fig. 4. Compared to Fig. 3, compressive stresses in the one-direction develop upon heating which are almost zero when the temperature excursion is finished. Due to symmetry, the ply stresses in the one-direction are equal to each other and equal to the laminate stress. Shear ply stresses develop also in the constrained case and their magnitude is smaller than in Fig. 3 due to the presence of the normal stresses and the nonlinearity of the theory. At first glance, it is surprising that the shear stress magnitude is higher than the stress in the one-direction due to constraint. This outcome is largely due to the coefficients of thermal expansion chosen in this case. As mentioned above, the coefficient of thermal expansion is sixty times higher in the two-direction than in the one-direction.

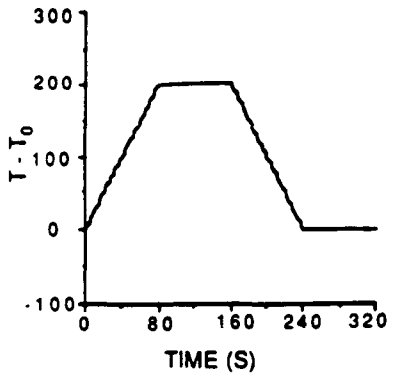

Fig. 1a. Temperature history imposed uniformly on the laminates.

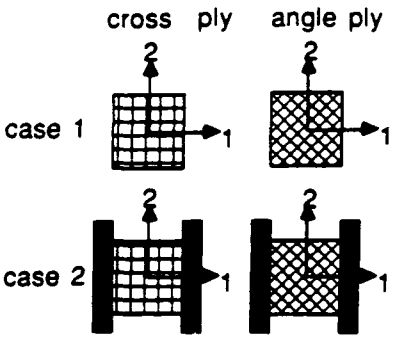

Fig. 1b. Schematic showing the loading conditions. In Case 1, the laminates are free to expand but are fixed in the one-direction in Case 2. A $[0/90]_s$ cross-ply and a $[+45/-45]_s$ angly-ply are considered.

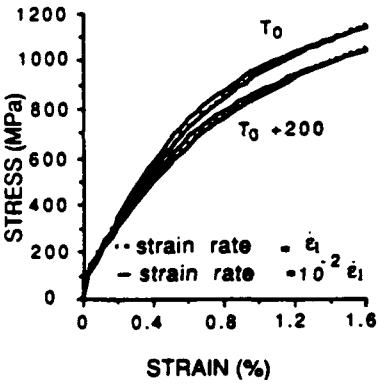

Fig. 2a. Stress-strain diagrams in the fiber direction at the reference temperature T_0 and at T_0 + 200°C for two strain rates differing by two orders of magnitude. $\dot{\varepsilon}_1 = 4\times10^{-4}$ 1/s.

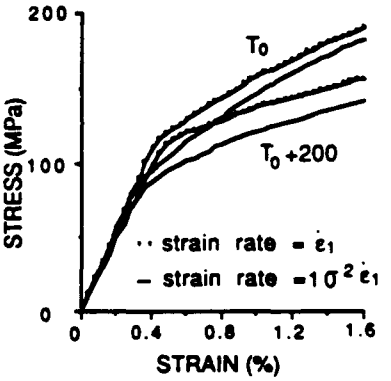

Fig. 2b. Same as Fig. 2a except that the direction of straining is perpendicular to the fibers. In essence, these stress-strain diagrams represent matrix behavior.

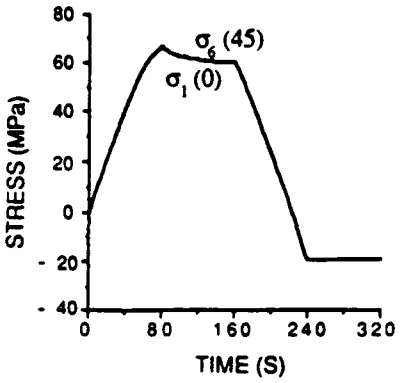

Fig. 3. Stresses in the laminates which are free to expand, see Case 1 in Fig. 1b. In the $[+45/-45]_s$ laminate only the shear stresses σ_6 exist and $\sigma_6[45] = -\sigma_6[-45]$. All other stresses are zero. For the cross-ply laminate, $\sigma_1[0] = \sigma_2[90] = -\sigma_1[90] = -\sigma_2[0]$. The variation of $\sigma_1[0]$ in the cross- ply is equal to the variation of the shear stress $\sigma_6[45]$ in the angle-ply due to symmetry.

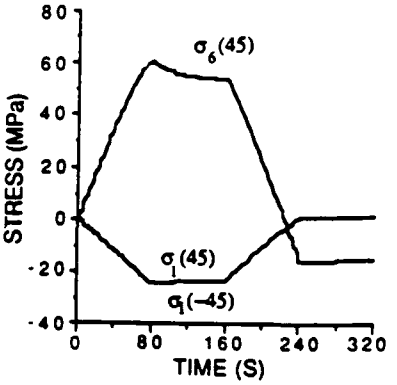

Fig. 4. Stresses in the constrained angle-ply laminate, Case 2 in Fig. 1b. In addition to the self equilibrating shear stress ($\sigma_6[45] = -\sigma_6[-45]$), stresses in the one-direction are induced. The ply stresses are equal to the laminate stress in the one-direction. All other stress components are zero.

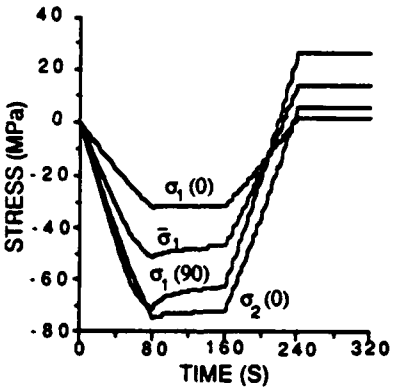

Fig. 5. Stresses in the constrained cross-ply laminate, Case 2 in Fig. 1b. The stresses in the one-direction are shown ($\bar{\sigma}_1$ is the laminate stress). Self equilibrating stresses in the two-direction are induced, $\sigma_2[0] = -\sigma_2[90]$. All other stress components are zero.

The variation of the stress components with time is plotted in Fig. 5 for the cross-ply laminate. The shapes of the curves are very similar to each other and to those of Figs. 3 and 4. It is clearly seen that the laminate stress in the one-direction is the sum of the corresponding ply stresses. Due to the differences in the coefficient of thermal expansion, the stress in the one-direction of the 90-degree ply is higher than the stress in the one-direction of the zero-degree ply. For the same reason, the stress in the one-direction of the 90-degree ply is a little higher than the stress in the two-direction of the zero-degree ply in the elastic region. When inelasticity sets in, this trend is reversed. After the temperature excursion is over, tensile stresses are present in the laminate which, on the graph, do not appear to relax with time. A check of the numerical data, however, reveals a slight decrease in time.

DISCUSSION

The above examples have shown that the theory can model simple cases of thermal stresses in laminates. This includes relaxation and the development of residual stresses. The theory predicts smooth variation of the stresses with temperature history. (The ragged appearance of some of the curves is due to the PC graphics package employed in making the figures.)

This paper uses fictitious material properties to illustrate, in principle, the capability of the theory on some simple examples. For a practical application, the material functions and constants of the theory must be determined by suitable experiments as a function of temperature, see [4,5]. In addition, off-angle tests are necessary, see [10], where some of the pertinent literature is cited. The theory has many flexibilities, such as almost linear elastic behavior in the fiber direction but viscoplastic behavior transverse to it. However, the major question is, what are the minimum number of constants and functions necessary to model a given behavior? This aspect has been considered in [9,10]. There, a "minimal" theory for isothermal deformation is shown which can reproduce the behavior of Borsic/Al metal matrix composites. Similar studies must be performed with the present thermal VBO and additional experience must be gained through further theoretical and experimental research.

The geometric limitations of CLT carry over to the present theory. From Figs. 3-5, it is seen that the ply stresses at free edges are not always zero, only the laminate stresses must vanish there. These ply stresses can be rather large. In Case 2, they are higher than the stresses caused by the constraint. When different sets of thermal expansion coefficients are used, this trend can be altered and the constraint stress magnitude can become the largest. This has been verified by separate computations.

The small temperature excursion and the small coefficient of thermal expansion in the fiber direction are responsible for the small thermal stresses found in the laminate. They are within the elastic region of the stress-strain diagram in the fiber direction. The redistribution of the stresses with time is thought to be due to the chosen "soft" matrix properties. By selecting different "viscous" properties in the material model, the redistributions can be enhanced or retarded. These properties will have to be explored by future numerical experiments.

ACKNOWLEDGEMENT

This research was supported by DARPA/ONR Contract N 00014-86-K0700 to Rensselaer Polytechnic Institute.

REFERENCES

1. G. J. Dvorak, in Mechanics of Composite Materials: Recent Advances (Proc. IUTAM Symposium on Mechanics of Composite Materials, Pergamon Press, Inc., New York, NY, 1982).

2. E. Krempl, Welding Research Council Bulletin No. 195 (Welding Research Council, New York, NY, 1974).

3. A. K. Miller, editor, Unified Constitutive Equations for Creep and Plasticity (Elsevier Applied Science, London and New York, 1987).

4. D. Kujawski and E. Krempl, J. Appl. Mech. 48, 55 (1981).

5. D. Kujawski, V. Kallianpur and E. Krempl, J. Mech. Phys. Solids 28, 129 (1980).

6. D. Yao and E. Krempl, Int. J. of Plasticity 1, 259 (1985).

7. E. Krempl, J. J. McMahon and D. Yao, Mech. of Materials 5, 35 (1986).

8. M. Sutcu, PhD Thesis (Rensselaer Polytechnic Institute, Troy, NY, December 1985).

9. M. Sutcu and E. Krempl, Rensselaer Polytechnic Institute Report MML87-8, September 1987, submitted for publication.

10. E. Krempl and B.-Z. Hong, Rensselaer Polytechnic Institute Report MML87-9, September 1987, submitted for publication.

11. S. W. Tsai and H. T. Hahn, Introduction to Composite Materials (Technomic Publishing Co., Westport, CT, 1980).

12. K. D. Lee and E. Krempl, Rensselaer Polytechnic Institute Report MML 88-1, April 1988.

13. K. D. Lee and E. Krempl, Rensselaer Polytechnic Institute Report MML 88-2, May 1988.

Reprinted from

George J. Dvorak (Ed.)

Inelastic Deformation of Composite Materials

IUTAM Symposium, Troy, New York
May 29-June 1, 1990

Springer-Verlag
New York Berlin Heidelberg London
Paris Tokyo Hong Kong Barcelona

Residual Stresses in Fibrous Metal Matrix Composites: A Thermoviscoplastic Analysis

Erhard Krempl and Nan–Ming Yeh
Mechanics of Materials Laboratory
Rensselaer Polytechnic Institute
Troy, N. Y. 12180–3590

ABSTRACT

The vanishing fiber diameter model together with the thermo-viscoplasticity theory based on overstress are used to analyze the thermomechanical rate (time)–dependent behavior of unidirectional fibrous metal–matrix composites. For the present analysis the fibers are assumed to be transversely isotropic thermoelastic and the matrix constitutive equation is isotropic thermoviscoplastic. All material functions and constants can depend on current temperature. Yield surfaces and loading/unloading conditions are not used in the theory in which the inelastic strain rate is solely a function of the overstress, the difference between stress and the equilibrium stress, a state variable of the theory. Assumed but realistic material elastic and viscoplastic properties as a function of temperature which are close to Gr/Al and B/Al composites permit the computation of residual stresses arising during cool down from the fabrication. These residual stresses influence the subsequent mechanical behavior in fiber and transverse directions. Due to the viscoplasticity of the matrix time–dependent effects such as creep and change of residual stresses with time are depicted. For Gr/Al residual stresses

are affecting the free thermal expansion behavior of the composite under temperature cycling. The computational results agree qualitatively with scarce experimental results.

INTRODUCTION

Metal matrix composites consist of a ductile, usually low strength matrix reinforced with elastic, brittle and strong fibers. Ideally, the strength of the fiber and the ductility of the matrix combine to provide a new material with superior properties. Selecting the best combinations of fiber and matrix materials is a difficult task which involves conflicting demands and many compromises. To prevent self stresses from developing during cool down from the manufacturing temperature it is desirable to have the same coefficient of thermal expansion for fiber and matrix. This ideal, however, is seldom achieved as other considerations but the coefficient of thermal expansion have priority in selecting the constituent materials.

It is known that the residual stresses have an influence on the mechanical behavior, Cheskis and Heckel [1970], Dvorak and Rao [1976], Min and Crossman [1982]. Moreover, the thermal expansion behavior of metal matrix composites is shown to be influenced by the residual stresses, Garmong [1973], Kural and Min [1984] and Tompkins and Dries [1988]. In precision applications the exact thermal expansion behavior is of great interest as it influences the performance.

It is the purpose of this paper to provide a comparatively simple and approximate means of calculating the residual

stresses in a unidirectional metal matrix composite during cool down from the manufacturing temperature and to assess their influence on subsequent mechanical behavior as well as on the thermal expansion of the composite under uniform temperature changes. To accomplish this task the vanishing fiber diameter model of Dvorak and Bahei–El–Din [1982] is combined with the thermoviscoplasticity theory based on overstress (TVBO) of Lee and Krempl [1990]. TVBO is a "unified" theory which does not separately postulate constitutive laws for creep and plasticity but models all inelastic deformation as rate dependent. Experiments with modern servocontrolled testing machines have shown rate dependence even at room temperature for engineering alloys, e.g stainless steels, Krempl [1979], 6061–T6 Al alloy, Krempl and Lu [1983], and Titanium alloys, Kujawski and Krempl [1981]. The transition from low to high homologous temperature behavior is usually characterized by a decrease in strength and an increase in rate dependence with an increase in temperature. This behavior can be modeled easily by TVBO by making certain constants depend on temperature. *It is not* necessary to postulate different laws in different temperature regimes.

First the governing equations are stated. They are represented by a system of first order, nonlinear, coupled differential equations which must be solved for a given boundary condition and loading/temperature history. Base data for 6061–T6 Al alloy for which viscoplastic material properties were determined by Yao and Krempl [1985]. Plausible changes of these properties with temperature were postulated and the system of differential equations was integrated to depict the

properties of the model. Of special interest is the influence of the residual stresses set up during cooling from the manufacturing temperature of 660 °C. Owing to the viscoplastic nature of the matrix constitutive model the residual stresses redistribute while the composite is at ambient temperature. For the material properties chosen in the numerical experiment this redistribution slows down rapidly with time at ambient temperature and after 30 days a nearly constant residual stress state is reached. Since the subsequent response of the composite is affected by the residual stresses an influence of time spent at room temperature on the subsequent behavior is predicted by this analysis. The influence of residual stresses on the subsequent isothermal mechanical behavior and on the thermal expansion behavior of a composite subjected to thermal cycling is investigated by numerical experiments. The computations agree qualitatively with scarce experimental results reported by others.

THE COMPOSITE MODEL. THERMOVISCOPLASTICITY THEORY BASED ON OVERSTRESS (TVBO) AND THE VANISHING FIBER DIAMETER MODEL (VFD)

For the representation of the equations, the usual vector notation for the stress tensor components σ and the small strain tensor components ϵ are used. Boldface capital letters denote 6x6 matrices.

Stresses and strains without a superscript designate quantities imposed on the composite as a whole. Superscripts ^{f} and ^{m} denote fiber and matrix, respectively. The fiber volume

fraction is c^f and c^m denotes the matrix volume fraction with $c^f + c^m = 1$.

A unidirectional fibrous composite element is assumed where the fiber is transversely isotropic thermoelastic, the matrix is isotropic and thermoviscoplastic and represented by TVBO. Fiber orientation in the 3–direction is postulated.

For the VFD model, Dvorak and Bahei–El–Din [1982], the following constraint equations hold

$$\begin{aligned} \dot{\sigma}_i &= \dot{\sigma}_i^f = \dot{\sigma}_i^m \quad \text{for } i \neq 3 \\ \dot{\sigma}_3 &= c^f \dot{\sigma}_3^f + c^m \dot{\sigma}_3^m \\ \dot{\epsilon}_i &= c^f \dot{\epsilon}_i^f + c^m \dot{\epsilon}_i^m \quad \text{for } i \neq 3 \\ \dot{\epsilon}_3 &= \dot{\epsilon}_3^f = \dot{\epsilon}_3^m. \end{aligned}$$

When they are combined with the TVBO equations by Lee and Krempl [1990] the composite is characterized by the following set of equations: (details can be found in Yeh and Krempl [1990])

$$\dot{\epsilon} = \overline{C}^{-1}\dot{\sigma} + (K^m)^{-1}X^m + (\dot{R}^f)^{-1}\sigma^f + (\dot{R}^m)^{-1}\sigma^m + \overline{\alpha}\dot{T} \tag{1}$$

together with a separate growth law for the σ_3^m component of the matrix

$$\dot{\sigma}_3^m = \frac{E^m}{E_{33}}\dot{\sigma}_3 - \frac{c^f}{E_{33}} L(\dot{\sigma}_1 + \dot{\sigma}_2) - \frac{c^f E_{33}^f E^m}{E_{33}} \left\{ \frac{1}{K^m k^m[\Gamma^m]} \left[X_3^m - 0.5(X_1^m + X_2^m) \right] \right\}$$

$$- \frac{c^f E_{33}^f E^m}{E_{33}} \left\{ \left[\frac{1}{(E_{33}^f)^2} (\nu_{31}^f E_{33}^f - \nu_{31}^f \dot{E}_{33}^f) \right.\right.$$

$$\left.\left. - \frac{1}{(E^m)^2} (\nu^m E^m - \nu^m \dot{E}^m) \right] (\sigma_1 + \sigma_2) + \frac{\dot{E}_{33}^f}{(E_{33}^f)^2} \sigma_3^f - \frac{\dot{E}^m}{(E^m)^2} \sigma_3^m \right\}$$

$$- \frac{c^f E_{33}^f E^m}{E_{33}} (\alpha^m - \alpha_3^f)\dot{T}. \qquad (2)$$

In addition growth laws for the two state variables of TVBO, the matrix equilibrium stress g^m and the kinematic stress f^m, are given as

$$\dot{g}^m = q^m[\Gamma^m]\dot{\sigma}^m + \dot{T} \frac{\partial q^m[\Gamma^m]}{\partial T} \sigma^m + \left\{ q^m[\Gamma^m] - \theta^m \left[q^m[\Gamma^m] - p^m(1-q^m[\Gamma^m]) \right] \right\} \frac{X^m}{k^m[\Gamma^m]} \qquad (3)$$

$$\dot{f}^m = \frac{p^m}{k^m[\Gamma^m]} X^m. \qquad (4)$$

with

$$(\Gamma^m)^2 = (X^m)^t H (X^m)$$
$$(\theta^m)^2 = \frac{1}{(A^m)^2}(Z^m)^t H (Z^m)$$
$$X^m = \sigma^m - g^m$$
$$Z^m = g^m - f^m \qquad (5)$$

In the above $\bar{C}^{-1}$ is the symmetric overall compliance matrix whose components are functions of the elastic properties of fiber and matrix. The viscosity matrix $(K^m)^{-1}$ is not symmetric and its components together with those of $\bar{C}^{-1}$ are listed in Appendix I. The matrices $(\dot{R}^f)^{-1}$ and $(\dot{R}^m)^{-1}$ contain time derivatives of the elastic constants of the fiber and the matrix, respectively. Both matrices are not symmetric. Their components are listed in Appendix I. These matrices represent the "additional" terms which can play a significant role in modeling thermomechanical behavior, see [Lee and Krempl 1990a]. The viscosity function $k^m[\Gamma^m]$ and the dimensionless shape function $q^m[\Gamma^m]$ are decreasing ($q^m[0] < 1$ is required) and control the rate dependence and the shape of the stress–strain diagram, respectively. (Square brackets following a symbol denote "function of".) The quantity p^m represents the ratio of the tangent modulus E_t^m at the maximum inelastic strain of interest to the viscosity factor K^m. It sets the slope of stress–inelastic strain diagram at the maximum strain of interest. $\bar{E}_{33}$, L, $\bar{\alpha}$ together with the components of the dimensionless matrix H and other material properties are

defined in Appendix I. An explanation of TVBO is given by Lee and Krempl [1990] and the derivation of the above equations can be found in Yeh and Krempl [1990].

Eq. (1) shows that the overall strain rate is the sum of the overall elastic strain rate, the inelastic strain rate of the matrix and the overall thermal strain rate in the case of constant elastic properties. If temperature dependent elastic properties are assumed then two additional terms contribute to the overall strain rate. They insure that the elastic behavior is path independent, see Lee and Krempl [1990, 1990a].

Eq. (2) is used to calculate the instantaneous axial matrix stress which can not be obtained from the overall boundary conditions directly. σ_3^m is affected by mechanical and thermal loadings and their loading paths. For instance for the isothermal case when $\dot{T} = 0$, matrix stresses in the fiber direction (σ_3^m, g_3^m, f_3^m) can evolve in unidirectional transverse loading, or may evolve in unidirectional shear loading provided the initial value of X_3^m is nonzero. For pure thermal loading (overall stresses are zero), σ_3^m together with g_3^m, f_3^m will develop due to the difference in the coefficients of thermal expansion of fiber and matrix; these matrix stresses in the fiber direction cause coupling between the mechanical and thermal loading in the inelastic range.

NUMERICAL SIMULATION

Eqs. (1) – (5) constitute the model which must now be applied. The boundary conditions must be specified in

addition to the uniform temperature history. Also material properties must be known as a function of temperature. For the purposes of this paper two metal matrix systems, Gr/Al and B/Al are simulated. The matrix viscoplastic properties for 6061–T6 Al alloy are known at room temperature from experiments reported by Yao and Krempl [1985]. Since no experiments were available at other temperatures a plausible temperature dependence was postulated. The elastic properties and the coefficient of thermal expansion for the Gr and B fibers are listed in Table 1. They are assumed to be independent of temperature for simplicity. The matrix properties which are close to 6061–T6 Al alloy are listed in Table 2. They yield the matrix stress–strain diagrams at a strain rate of 10^{-4} s^{-1} depicted in Fig. 1. A decrease in modulus, flow stress and the asymptotic tangent modulus with increasing temperature is modeled.

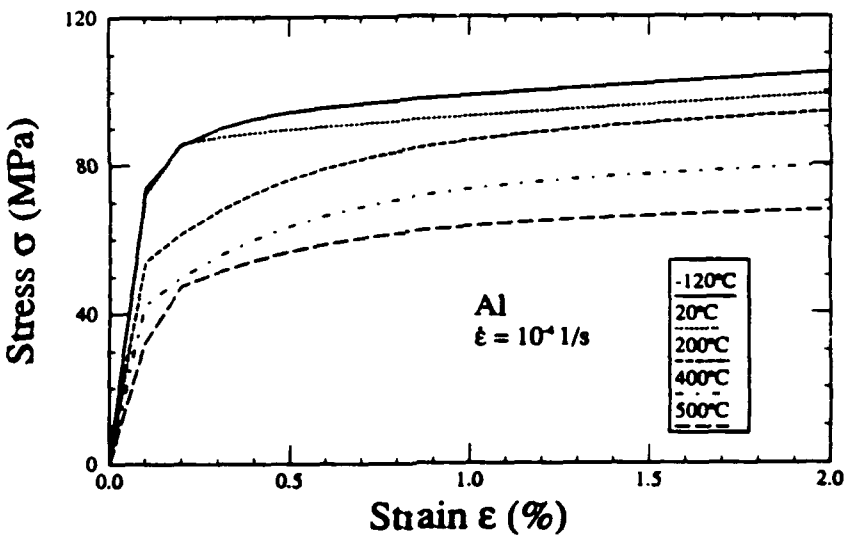

Fig. 1. *Stress–strain diagrams of matrix material at various temperatures.*

Table 1.

Elastic Properties for Boron and Graphite Fibers

Properties	B		Gr (****)
E^f_{33} (MPa)	413400	(*)	689650
ν^f_{31}	0.21	(*)	0.41
G^f_{44} (MPa)	170830	(**)	15517
α^f_3 (m/m/°C)	6.3E–6	(***)	–1.62E–6
E^f_{11} (MPa)	413400	(*)	6069
G^f_{66} (MPa)	170830	(**)	2069
α^f_1 (m/m/°C)	6.3E–6	(***)	1.08E–5

* Kreider and Prewo [1974]

** Estimate

*** Tsirlin [1985]

**** Wu, et al [1989]

Table 2.
Thermoelastic and Thermoviscoplastic Properties of the Matrix

---

$E^m = 74657[1 - (\frac{T}{933})^3]$ (MPa) (*)

$\nu^m = 0.33$ (**)

$G^m = 28066[1 - (\frac{T}{933})^3]$ (MPa) (*)

$\alpha^m = 2.35E{-}5 + 2.476E{-}8(T - 273)$ (m/m/°C) (**)

$q^m[\Gamma^m] = \Psi^m[\Gamma^m]/E^m$, $p^m = E_t^m/K^m$

Viscosity function $k^m[\Gamma^m] = k_1(1 + \frac{\Gamma^m}{k_2})^{-k_3}$

$k_1 = 314200$ (s), $k_2 = 71.38$ (MPa) (***)

$k_3 = 53 - 0.05(T{-}273)$ (**)(***)

Viscosity Factor $K^m = E^m$

$E_t^m = 619[1 - (\frac{T}{933})^3]$ (MPa) (**)

$A^m = 72.24[1 - (\frac{T}{933})^3]$ (MPa) (**)

Shape function $\Psi^m[\Gamma^m] = c_1 + (c_2{-}c_1)\exp(-c_3\Gamma^m)$

$c_1 = 16511[1 - (\frac{T}{933})^3]$ (MPa) (**)

$c_2 = 73910[1 - (\frac{T}{933})^3]$ (MPa) (**)

$c_3 = 8.43E{-}2 + 1.06E{-}4(T{-}273) + 1.914E{-}6(T{-}273)^2$
$+5.304E{-}9(T{-}273)^3$ (MPa^{-1}) (**)

Inelastic Poisson's Ratio: 0.5

$T = °K$, $153°K < T < 933°K$

(*) Estimate. Temperature dependence due to Hillig [1985]

(**) Estimate

(***) Yao and Krempl [1985]

For the integration of the coupled set of differential equations the IMSL routine DGEAR is used.

Residual Stresses upon Cool–Down from Manufacturing Temperature

Overall stresses are assumed to be zero and the temperature is decreased at a constant rate of 0.033 ^{0}C/s. It is assumed that the composite is stress free at 660 ^{0}C and that perfect bonding starts at that temperature. Since the coefficient of thermal expansion is larger for the matrix than for the fibers tensile matrix stresses develop as shown in Fig. 2a for B/Al and in Fig. 2b for Gr/Al. Owing to the assumed fiber volume fraction

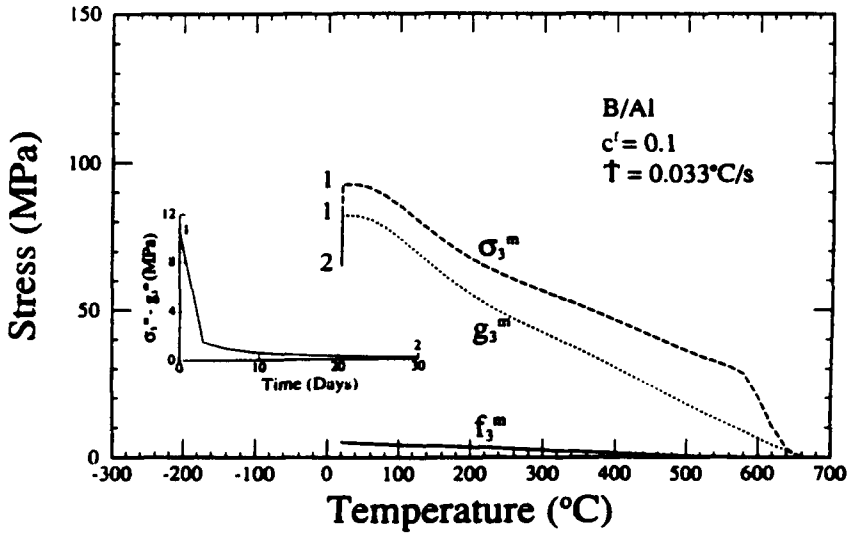

Fig. 2a. *Development of matrix stress σ_3^m, matrix equilibrium g_3^m and kinematic stress f_3^m during cool down from manufacturing temperature. The inset shows the decrease of the overstress during the room temperature hold 1 – 2. Boron/Aluminum.*

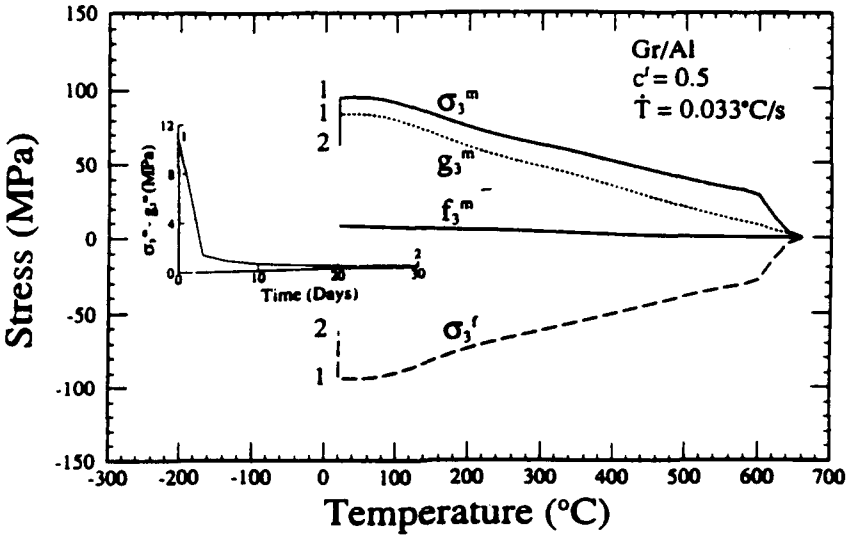

Fig. 2b. *Same as Fig. 2a except that material is Graphite/ Aluminum. The fiber stress σ_3^f is also shown.*

of 0.5 the fiber stresses are equal and opposite in Fig. 2b. They are not shown in Fig. 2a where the fiber volume fraction is 0.1. The VFD assumption listed previously yields $\sigma_3^f = -9\sigma_3^m$. At point 1 room temperature is reached. Due to the viscoplastic nature of the matrix the stresses relax to point 2 with time. The inset shows the overstress $\sigma_3^m - g_3^m$, which "drives" the inelastic deformation, rapidly decreasing with time. All residual stresses enter as initial conditions for simulations of subsequent tests. They can affect the modeled behavior and therefore time appears to influence it. After 30 days the residual stress state is nearly constant. Then the model predicts that the subsequent response becomes independent of the rest time at room temperature. On the scale of this graph the kinematic variable f_3^m does not appear to change with time. However, the digital output confirms the

slight increase predicted by Eq (4).

Influence of Residual Stresses on Room Temperature Mechanical Behavior

In this case a B/Al composite with $c^f = 0.1$ is considered and uniaxial tensile tests in the fiber and the transverse directions are performed at a strain rate of 10^{-4} s^{-1}. When a strain of 0.5% is reached the overall stress is kept constant to allow creep deformation to evolve during a short period of 300 s.

Fig. 3 shows the mechanical behavior for tests in the fiber (3) – direction. The overall stress, the matrix stress and equilibrium stress are plotted vs. overall strain for 3 cases. Fig. 3a shows the behavior without residual stresses, Fig. 3b has the residual stress state at point 1 in Fig. 2 as initial conditions. This is called Case 1 and simulates a tensile test performed immediately after the composite reached room temperature. The relaxed residual state of stress represented by point 2 in Fig. 2 forms the set of initial condition for Case 2. The mechanical behavior with this set of initial conditions is given in Fig. 3c.

By comparing the figures the significant influence of residual stresses on the overall stress–strain diagram can be clearly ascertained. It can be seen that the initial slope, the stress level at which the transition to another slope takes place and the overall appearance of the composite stress–strain diagram are significantly affected by the residual stresses. Owing to a nearly zero overstress in Case 2 the initial slope seems to be

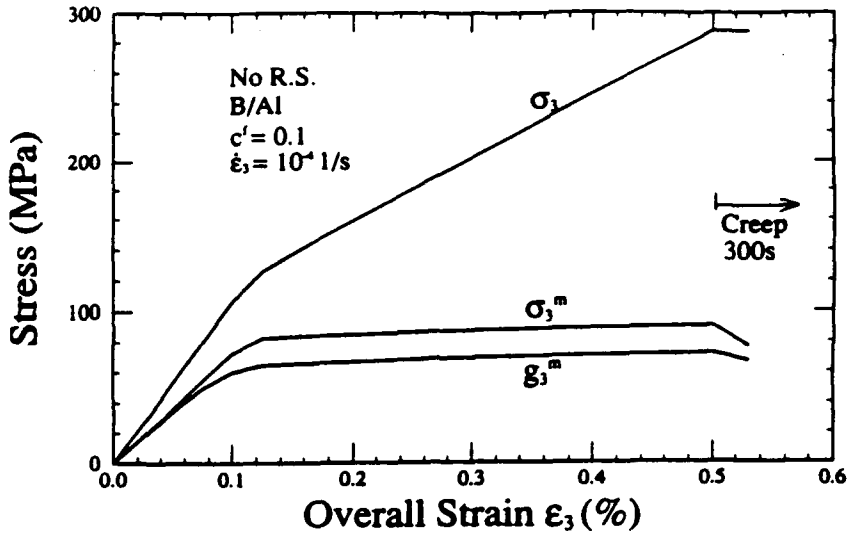

Fig. 3a. *Stresses vs strain in fiber direction at room temperature with a 300 s creep period at the maximum stress.*

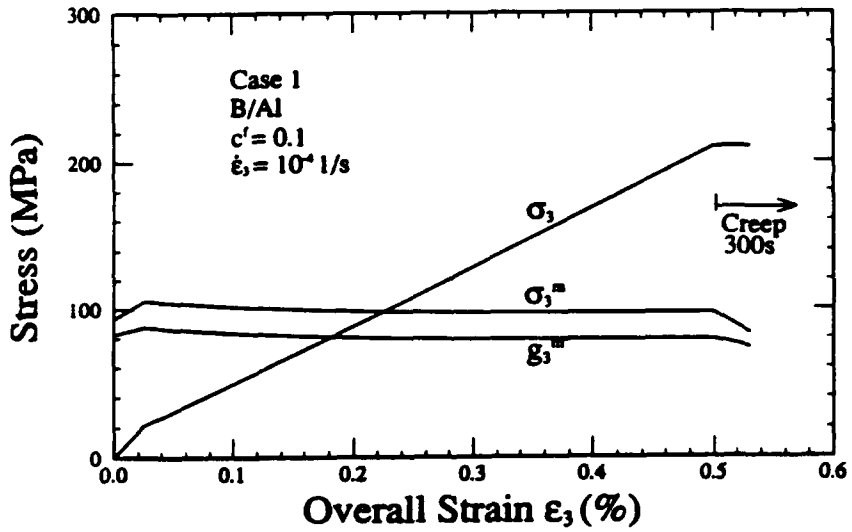

Fig. 3b. *Same as Fig. 3a for Case 1.*

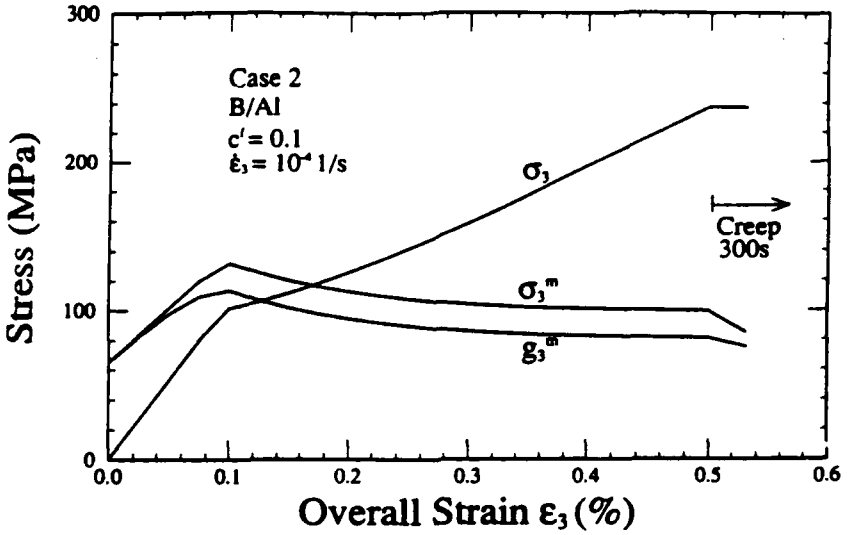

Fig. 3c. *Same as Fig. 3a for Case 2.*

identical to the stress–strain diagram with no residual stresses. The level of the overall stress is considerably lower for Case 2 than for the case without residual stresses. Since it is unlikely that a tensile test will be performed right after reaching room temperature and since the overstress decreases rapidly with time, see inset in Fig.2, an experiment would yield the results of Case 2. The residual stress state has an influence on the relation between the strain in the fiber direction and the transverse strain as shown in Fig. 4. From these curves the actual Poisson's ratio based on total strain could be calculated. The simulation of a tensile test in the transverse direction is shown in Fig. 5a and the relation between the transverse strain ϵ_1 and the two perpendicular strains ϵ_2 and ϵ_3 are shown in Fig. 5b and Fig. 5c, respectively. A significant influence of the residual stress state is evident, especially in Figs. 5a and 5b.

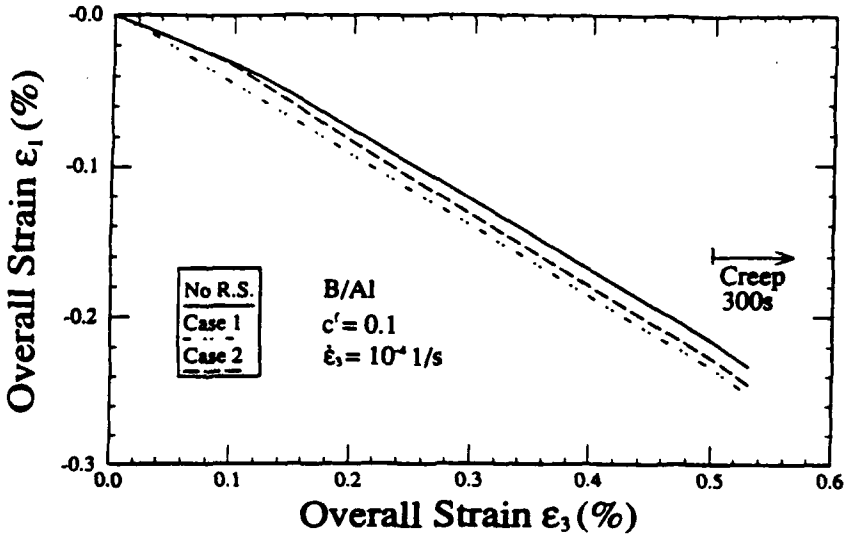

Fig. 4. *The development of the transverse strain during the tests shown in Fig. 3.*

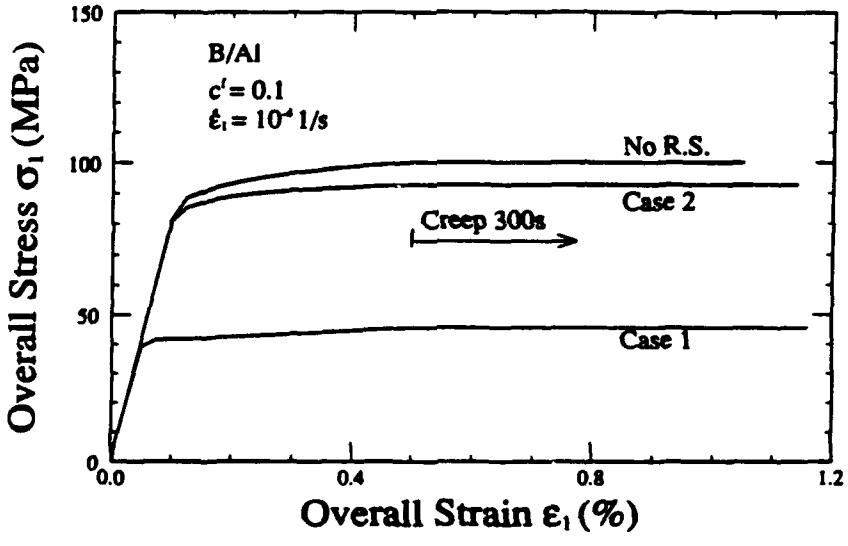

Fig. 5a. *Simulation of a transverse tensile test at room temperature as a function of the residual stresses; transverse stress–strain diagram.*

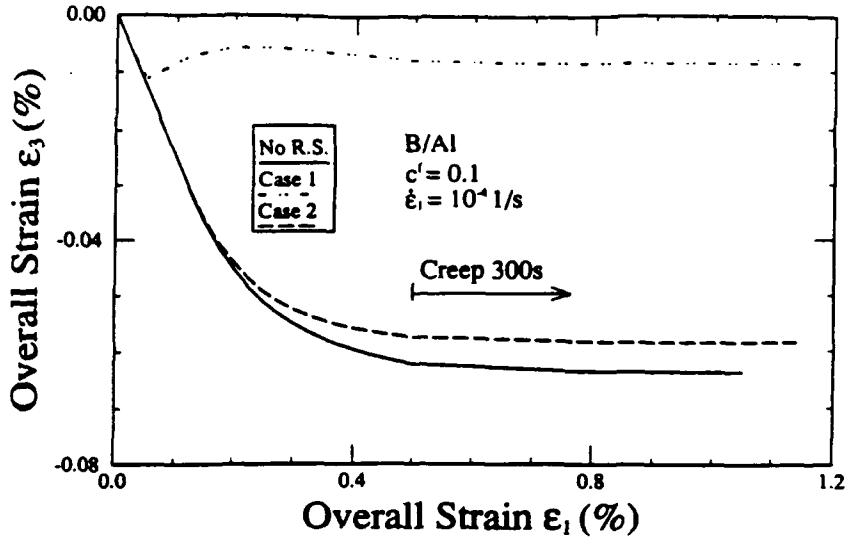

Fig. 5b. *The development of the transverse strain in the 3–direction.*

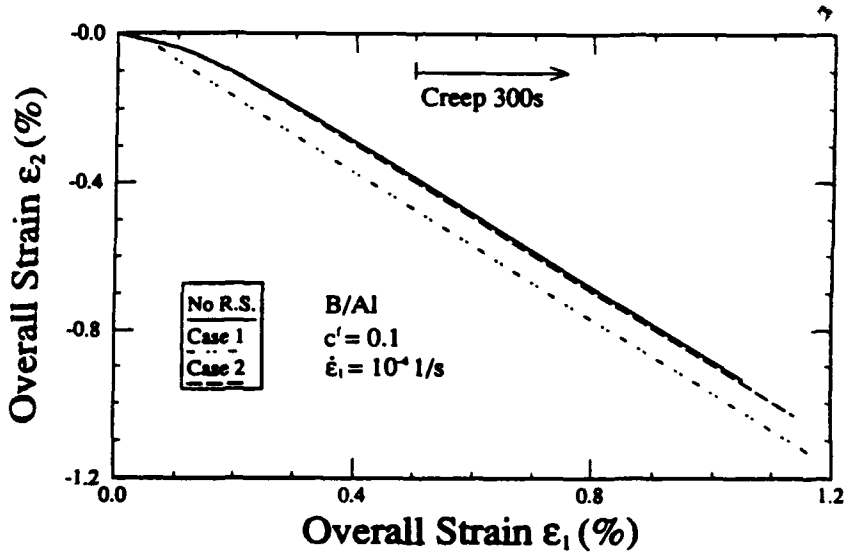

Fig. 5c. *The development of the transverse strain in the 2–direction.*

In Figs. 3 through 5 the behavior during the 300 s creep period is specially marked. As expected the total creep strain accumulated is very significant in the matrix dominated transverse mode, see Fig. 5a. It is small for the fiber direction as shown in Figs. 3. In each case primary creep is modeled with a rapidly decreasing rate. This is shown in Fig. 5d for the transverse case. This corresponds to the so–called "cold creep" phenomenon found at room temperature for ductile engineering alloys. For the strain vs. strain curves , Figs. 4, 5b and 5c, the creep periods do not differ significantly from the periods under increasing stress. Only a slight break in slope is noticeable at the outset of the creep period.

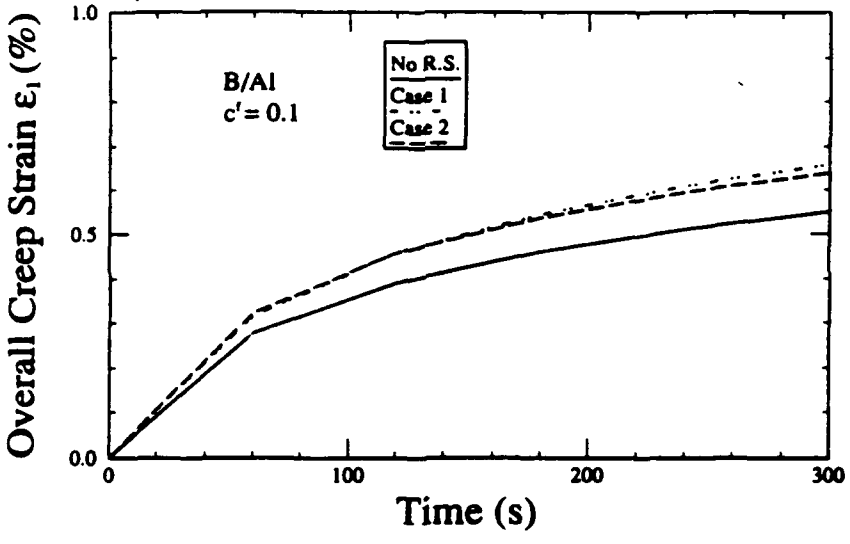

Fig. 5d. *Transverse creep strain during the 300s creep period.*

The Influence of Residual Stresses on the Thermal Cycling Behavior of Gr/Al Composite.

The thermal cycling behavior of Gr/Al is of special interest due to the negative axial CTE of Graphite, see Table 1. It gives rise to some unusual expansion behavior, see Wu et al [1989] and Tompkins and Dries [1988]. In this paper we simulate that the composite is free to expand (overall stresses are zero) and is subjected to a temperature cycle starting from room temperature to ± 120 ^{0}C at a rate of 0.033 ^{0}C/s.

The resulting strain in the fiber direction – temperature hysteresis loop is depicted in Fig. 6a. It is seen that the composite expands on the segment 0–1 but then contracts with increasing temperature, segment 1–2. Upon decrease of temperature from 120^{0}C the composite shrinks as expècted but

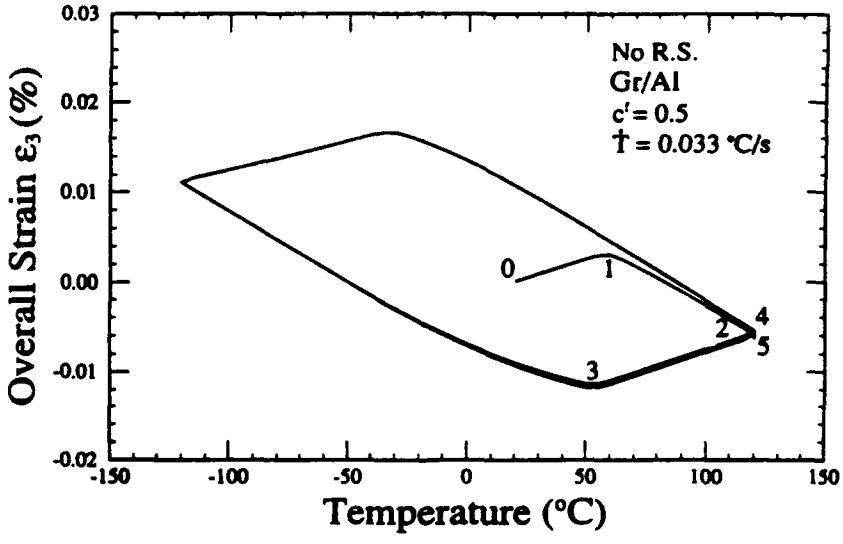

Fig. 6a. *Temperature–strain in the fiber direction loop during temperature cycling of Gr/Al composite.*

expands at point 3 although the temperature continues to decrease. This pattern continues in the subsequent reversals. At point 4 a 600 s temperature hold is introduced and the strain decreases by a small amount, the composite "creeps" under zero external load and the creep curve is shown in Fig. 6b. To demonstrate that the temperature rate has an influence the calculation was repeated with a rate of 0.1 ^{0}C/s. There is very little influence on the temperature/strain curve, but creep during the temperature hold period is accelerated as shown in Fig. 6b.

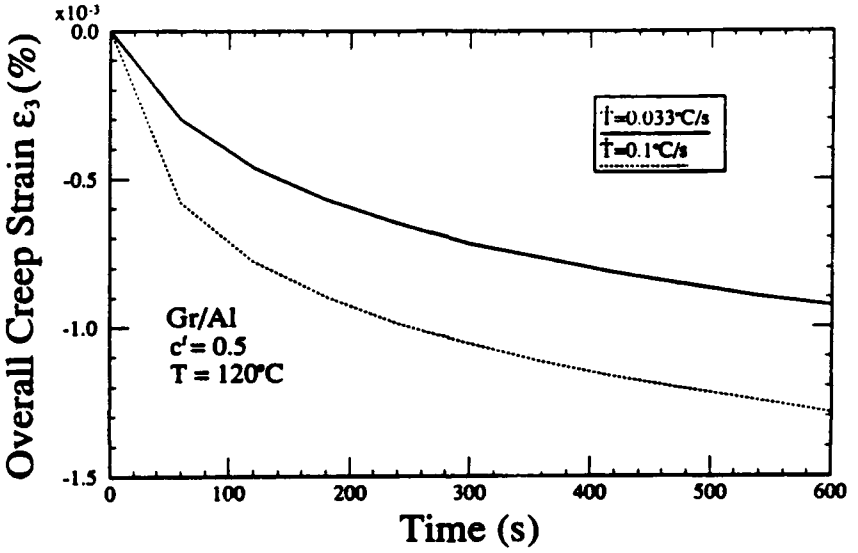

Fig. 6b. *Creep curves during temperature hold at 120° C, see points 4, 5 in Fig. 6a.*

The explanation of this unusual behavior can be found in the development of the fiber and matrix stresses during cycling as shown in Fig. 6c. It is seen that a temperature–stress hysteresis loop develops and that the matrix starts yielding at

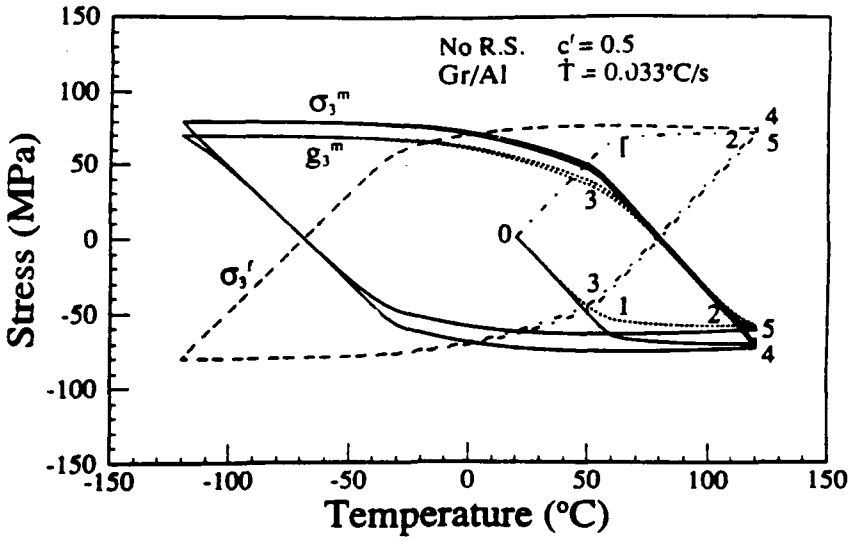

Fig. 6c. *"Internal stresses" which develop during temperature cycling shown in Fig. 6a.*

points 1 and 3 where the breaks in Fig. 6a occur. The unusual behavior is due to the matrix yielding. In the inelastic range the stiffness of the matrix is low and the overall behavior is dominated by the fiber which has a negative axial CTE.

To show the influence of residual stresses Cases 1 and 2 are simulated in Fig. 7a. and Fig. 7b, respectively. Cooling down takes place on 0–1. While the composite rests free of overall stresses at room temperature, see Fig. 2b, the overall strain increases on path 1–2, see Fig. 7b (this portion is absent in Fig. 7a which depicts Case 1). At 2 temperature cycling begins, the composite expands first, 2–3, but starts to shrink, 3–4 and then the pattern of Fig. 6a continues. However, this time the first part of the first cycle 2–5 is not inside the

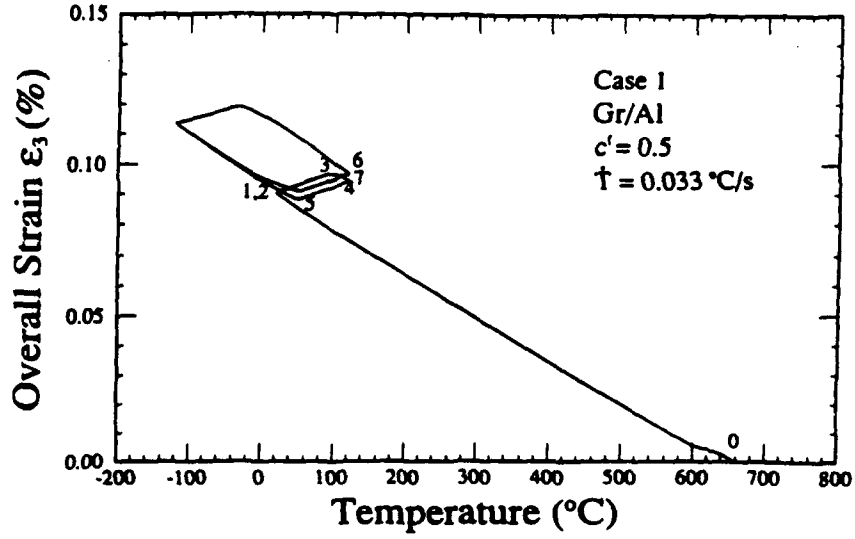

Fig. 7a. *Temperature–strain graph during cool down from 660° C and subsequent cycling as in Fig. 6a. Case 1.*

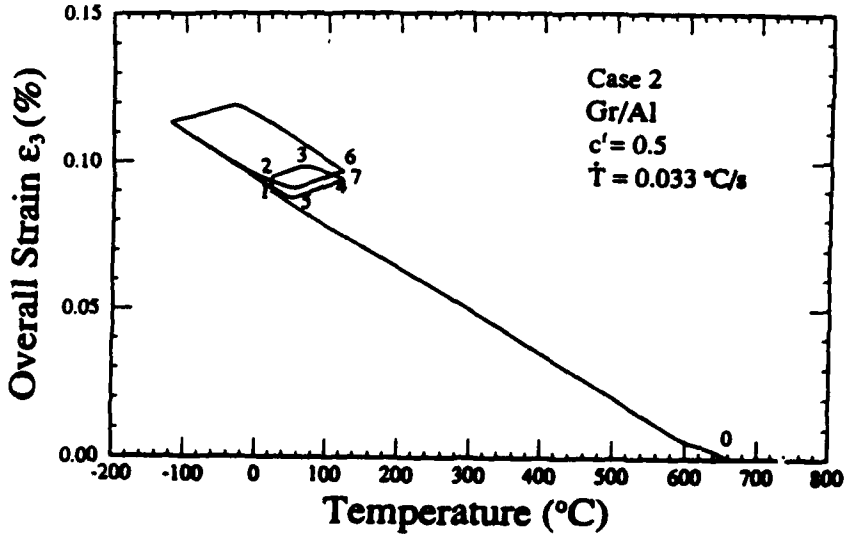

Fig. 7b. *Same as Fig. 7a for Case 2.*

subsequent loop as it was the case for Fig. 6a, see segment 0–3. Rather the first segment is shifted and the shift depends on the case considered. The residual matrix and fiber stresses have altered the cycle pattern. Their development during cycling (the cool–down portion 0–2 is omitted) is depicted in Fig. 7c for Case 2. For the identification the same numbering scheme has been used as in Fig. 7a and in Fig. 7b. It can again be ascertained that the "breaks" in the expansion behavior are coinciding with the onset of inelastic deformation of the matrix.

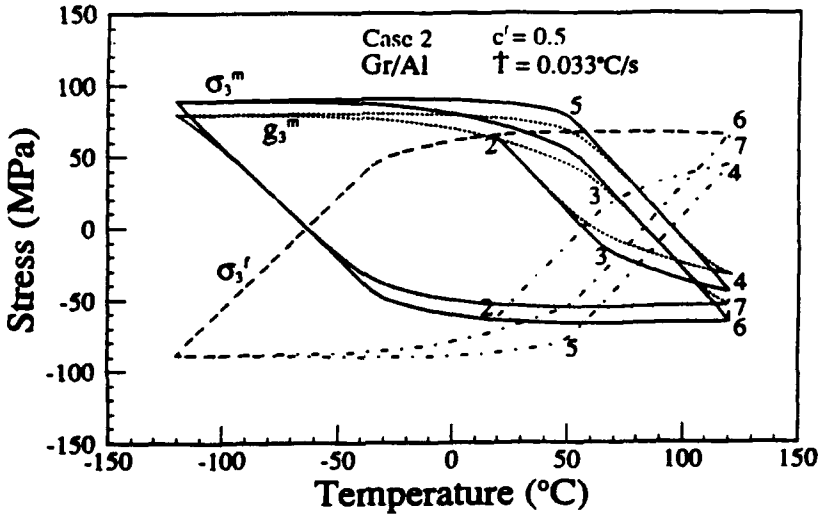

Fig. 7c. *The "internal stresses" developed during temperature cycling for Case 2. Curves start at room temperature, point 2 in Fig. 7b.*

DISCUSSION

A "unified" viscoplastic constitutive model for composite analysis, the thermoviscoplasticity theory based on overstress, was used in conjunction with the vanishing fiber diameter model in a simple analysis of the influence of fiber/matrix residual stresses on the mechanical and thermal cycling behavior. Realistic but assumed material properties permitted the execution of numerical experiments. The stress–strain diagrams reported in Figs. 3a–3c correspond qualitatively with those reported by Cheskis and Heckel [1970]. In both cases a break in the slope of the overall stress–strain diagram is observed when the matrix starts to deform inelastically in an appreciable manner. The presence of residual stresses shift the location of this break point, see Figs. 3a–3b.

Another feature exhibited by the present theory is the manifestation of the influence of rate dependence on the behavior. The first example was the redistribution of the residual stresses while the composite element was sitting stress free at room temperature after cool–down from manufacturing temperature. The theory predicts that this redistribution will nearly come to an end after some time which depends on material constants, especially the viscosity function used. In the present application the redistribution is almost finished after 30 days. While the stresses redistribute the time at room temperature appears to have an influence on the subsequent behavior.

For Gr/Al the residual stresses were shown to affect the free thermal expansion of the composite. The results of Figs. 7a and 7b suggest that residual stresses are responsible for the special shape of the first part of the first cycle of Figs. 6 and 7 of Tompkins and Dries [1988]. In comparing their figures with Figs. 7a and 7b it has to be kept in mind that the presently used theory models only cyclic neutral behavior whereas real matrix alloys may exhibit cyclic hardening or softening. These aspects could be added to the present theory in a refined approach.

The present paper intends to show the capabilities in principle. For the exact modeling of a metal matrix composite various refinements are possible. Included are the determination of matrix and fiber properties as a function of temperature and the use of other micromechanical models.

Acknowledgment

This research was supported by DARPA/ONR Contract N00014–86–K0770 with Rensselaer Polytechnic Institute. Discussions with Dr. Y. A. Bahei–El–Din are acknowledged with thanks.

REFERENCES:

Cheskis, H. P. and Heckel, R. W., 1970, "Deformation Behavior of Continuous–Fiber Metal–Matrix Composite Materials," Metallurgical Transactions, Vol 1, pp. 1931–1942.

Dvorak, G. J. and Rao, M. S. M., 1976, "Thermal Stresses in Heat–Treated Fibrous Composites," ASME Journal of Applied Mechanics, pp. 619–624.

Dvorak, G. J. and Bahei–EL–Din, Y. A., 1982, "Plasticity Analysis of Fibrous Composites," ASME Journal of Applied Mechanics, Vol. 49, pp. 327–335.

Garmong, G., 1974, "Elastic–Plastic Analysis of Deformation Induced by Thermal Stress in Eutectic Composites:1 Theory," Metallurgical Transactions, Vol. 5, pp. 2183–2190.

Hillig, W. B., 1985, "Prospects for Ultra–High–Temperature Ceramic Composites," Report No. 85CRD152, General Electric Research and Development Center.

Krempl, E.,1979, "An Experimental Study of Room–Temperature Rate Sensitivity, Creep and Relaxation of Type 304 Stainless Steel," Journal of the Mechanics and Physics of Solids, Vol. 27, pp. 363–375.

Krempl, E. and Lu, H., 1983, "Comparison of the Stress Responses of an Aluminum Alloy Tube to Proportional and Alternate Axial and Shear Strain Paths at Room Temperature," Mechanics of Materials, Vol. 2, pp. 183–192.

Kreider, K. G. and Prewo, K. M., 1974, "Boron–Reinforced Aluminum," Composite Materials, Vol. 4, Metallic Matrix Composites, Edited by Kenneth G. Kreider, Academic Press.

Kujawski, D., Krempl, E., 1981, "The Rate (Time)–Dependent Behavior of Ti–7Al–2Cb–1Ta Titanium Alloy at Room Temperature Under Quasi–Static Monotonic and Cyclic Loading," ASME Journal of Applied Mechanics, Vol. 48, pp. 55–63.

Kural, M. K. and Min, B. K., 1984, "The Effects of Matrix Plasticity on the Thermal Deformation of Continuous Fiber Graphite/Metal Composites," Journal of Composite Materials, Vol. 18, pp. 519–535.

Lee, K. D. and Krempl, E., 1990, "An Orthotropic Theory of Viscoplasticity Based on Overstress for Thermomechanical Deformations," to appear in International Journal of Solids and Structures.

Lee, K. D. and Krempl, E., 1990a, "Uniaxial thermo–mechanical loading. Numerical experiments using the thermal viscoplasticity theory based on overstress," MML Report 90–1, Rensselaer Polytechnic Institute, March.

Min, B. K. and Crossman, F. W. ,1982, "History–Dependent Thermo–mechanical Properties of Graphite/Aluminum Unidirectional Composites," Composite Materials: Testing and Design (Sixth Conference), ASTM STP 787, I. M. Daniel, Ed, American Society for Testing and Materials, pp. 371–392.

Tompkins, S. S. and Dries, G. A., 1988, "Thermal Expansion Measurement of Metal Matrix Composites," ASTM STP 964, P. R. DiGiovanni and N. R. Adsit, Editors, American Society for Testing and Materials, Philadelphia, pp. 248–258.

Tsirlin, A. M., 1985, "Boron Filaments," Handbook of Composites, Volume 1, "Strong Fibers," Editors: Watt, W. and Perov, B. V., North–Holland.

Wu, J. F., Shephard, M. S., Dvorak, G. J. and Bahei–EL–Din, Y. A., 1989, "A Material Model for the Finite Element Analysis of Metal–Matrix Composites," Composites Science and Technology, Vol. 35, pp. 347–366.

Yao, D. and Krempl, E., 1985, "Viscoplasticity Theory Based on Overstress. The Prediction of Monotonic and Cyclic Proportional and Nonproportional Loading Paths of an Aluminum Alloy," Int. Journal of Plasticity, Vol. 1, pp. 259–274.

Yeh, N. M. and Krempl, E., 1990, " Thermoviscoplastic Analysis of Fibrous Metal–Matrix Composites," MML Report 90–2, Rensselaer Polytechnic Institute, March.

APPENDIX I

For the transversely isotropic (fiber) and the isotropic (matrix) elastic properties the usual designations are employed. For convenience the following quantities are defined and used

$$E_{33} = c^f E^f_{33} + c^m E^m$$
$$L = \nu^f_{31} E^m - \nu^m E^f_{33}$$
$$\bar{\nu}_{31} = c^f \nu^f_{31} + c^m \nu^m .$$

The components of the overall elastic compliance matrix $\bar{C}^{-1}$ are

$$(\bar{C}^{-1})_{11} = \frac{c^f}{E^f_{11}} + \frac{c^m}{E^m} - \frac{c^f c^m L^2}{E^f_{33} E^m E_{33}} = (\bar{C}^{-1})_{22}$$

$$(\bar{C}^{-1})_{12} = -\left(c^f \frac{\nu^f_{12}}{E^f_{11}} + c^m \frac{\nu^m}{E^m} + \frac{c^f c^m L^2}{E^f_{33} E^m E_{33}}\right) = (\bar{C}^{-1})_{21}$$

$$(\bar{C}^{-1})_{13} = \frac{-\bar{\nu}_{31}}{E_{33}} = (\bar{C}^{-1})_{23} = (\bar{C}^{-1})_{31} = (\bar{C}^{-1})_{32}$$

$$(\bar{C}^{-1})_{33} = \frac{1}{E_{33}}$$

$$(\bar{C}^{-1})_{44} = \frac{c^f}{G^f_{44}} + \frac{c^m}{G^m} = (\bar{C}^{-1})_{55}$$

$$(\bar{C}^{-1})_{66} = \frac{c^f}{G^f_{66}} + \frac{c^m}{G^m}$$

with all other $(\bar{C}^{-1})_{ij} = 0$.

The viscosity matrix $(K^m)^{-1}$ is given by the components (the argument of the viscosity function k^m is omitted)

$$(K^{\blacksquare})_{\bar{1}\bar{1}}^{j} = \frac{c^{\blacksquare}}{K^{\blacksquare}k^{\blacksquare}}(1 + 0.5\frac{c^{f}L}{E_{33}}) = (K^{\blacksquare})_{\bar{2}\bar{2}}^{j}$$

$$(K^{\blacksquare})_{\bar{1}\bar{2}}^{j} = \frac{-c^{\blacksquare}}{2K^{\blacksquare}k^{\blacksquare}}(1 - \frac{c^{f}L}{E_{33}}) = (K^{\blacksquare})_{\bar{2}\bar{1}}^{j}$$

$$(K^{\blacksquare})_{\bar{1}\bar{3}}^{j} = \frac{-c^{\blacksquare}}{K^{\blacksquare}k^{\blacksquare}}(0.5 + \frac{c^{f}L}{E_{33}}) = (K^{\blacksquare})_{\bar{2}\bar{3}}^{j}$$

$$(K^{\blacksquare})_{\bar{3}\bar{1}}^{j} = \frac{-c^{\blacksquare}E^{\blacksquare}}{2E_{33}K^{\blacksquare}k^{\blacksquare}} = (K^{\blacksquare})_{\bar{3}\bar{2}}^{j}$$

$$(K^{\blacksquare})_{\bar{3}\bar{3}}^{j} = \frac{c^{\blacksquare}E^{\blacksquare}}{E_{33}K^{\blacksquare}k^{\blacksquare}}$$

$$(K^{\blacksquare})_{\bar{6}\bar{6}}^{j} = \frac{3c^{\blacksquare}}{K^{\blacksquare}k^{\blacksquare}} = (K^{\blacksquare})_{\bar{4}\bar{4}}^{j} = (K^{\blacksquare})_{\bar{5}\bar{5}}^{j}.$$

All other $(K^{\blacksquare})_{\bar{i}\bar{j}}^{j} = 0$.

The components of the "extra terms" $(\dot{R}^f)^{-1}$ and $(\dot{R}^m)^{-1}$ are

$$(\dot{R}^f)^{\bar{1}}_{\bar{1}} = -c^f \frac{\dot{E}^{\S}_{1}}{(E^{\S}_{1})^2} - \frac{c^f c^m L}{(E^{\S}_{3})^2 E_{33}} (\dot{\nu}^{\S}_{31} E^{\S}_{3} - \nu^{\S}_{31} \dot{E}^{\S}_{3})$$

$$= (\dot{R}^f)^{\bar{2}}_{\bar{2}}$$

$$(\dot{R}^f)^{\bar{1}}_{\bar{2}} = -\left[\frac{c^f}{(E^{\S}_{1})^2} (\dot{\nu}^{\S}_{12} E^{\S}_{1} - \nu^{\S}_{12} \dot{E}^{\S}_{1}) + \frac{c^f c^m L}{(E^{\S}_{3})^2 E_{33}} \right.$$

$$\left. (\dot{\nu}^{\S}_{31} E^{\S}_{3} - \nu^{\S}_{31} \dot{E}^{\S}_{3}) \right] = (\dot{R}^f)^{\bar{2}}_{\bar{1}}$$

$$(\dot{R}^f)^{\bar{1}}_{\bar{3}} = \frac{c^f}{E^{\S}_{3} E_{33}} (\bar{\nu}_{31} \dot{E}^{\S}_{3} - \dot{\nu}^{\S}_{31} E_{33}) = (\dot{R}^f)^{\bar{3}}_{\bar{2}}$$

$$(\dot{R}^f)^{\bar{3}}_{\bar{1}} = \frac{c^f}{E^{\S}_{3} E_{33}} (\nu^{\S}_{31} \dot{E}^{\S}_{3} - \dot{\nu}^{\S}_{31} E^{\S}_{3}) = (\dot{R}^f)^{\bar{3}}_{\bar{2}}$$

$$(\dot{R}^f)^{\bar{3}}_{\bar{3}} = -\frac{c^f \dot{E}^{\S}_{3}}{E^{\S}_{3} E_{33}}$$

$$(\dot{R}^f)^{\bar{4}}_{\bar{4}} = -c^f \frac{\dot{G}^{\S}_{44}}{(G^{\S}_{44})^2} = (\dot{R}^f)^{\bar{5}}_{\bar{5}}$$

$$(\dot{R}^f)^{\bar{6}}_{\bar{6}} = -c^f \frac{\dot{G}^{\S}_{66}}{(G^{\S}_{66})^2}$$

with all other $(\dot{R}^f)^{\bar{i}}_{\bar{j}} = 0$.

$$(\dot{R}^m)_{11}^1 = -c^m\frac{\dot{E}^m}{(E^m)^2} + \frac{c^f c^m L}{(E^m)^2 E_{33}}(\nu^m E^m - \nu^m \dot{E}^m) = (\dot{R}^m)_{22}^1$$

$$(\dot{R}^m)_{12}^1 = \frac{c_m}{(E^m)^2}(\nu^m \dot{E}^m - \nu^m E^m)\left(1 - \frac{c^f L}{E_{33}}\right) = (\dot{R}^m)_{21}^1$$

$$(\dot{R}^m)_{13}^1 = \frac{c^m}{E^m E_{33}}(\bar{\nu}_{31}\dot{E}^m - \nu^m E_{33}) = (\dot{R}^m)_{23}^1$$

$$(\dot{R}^m)_{31}^1 = \frac{c^m}{E^m E_{33}}(\nu^m \dot{E}^m - \nu^m E^m) = (\dot{R}^m)_{32}^1$$

$$(\dot{R}^m)_{33}^1 = -\frac{c^m \dot{E}^m}{E^m E_{33}}$$

$$(\dot{R}^m)_{66}^1 = -c^m\frac{\dot{G}^m}{(G^m)^2} = (\dot{R}^m)_{44}^1 = (\dot{R}^m)_{55}^1.$$

All other $(\dot{R}^m)_{ij}^1 = 0$.

The overall coefficient of thermal expansion vector $\bar{\alpha}$ is represented by

$$(\bar{\alpha})_1 = c^f \alpha_1^f + c^m \alpha^m - \frac{c^f c^m L}{E_{33}}(\alpha^m - \alpha_3^f) = (\bar{\alpha})_2$$

$$(\bar{\alpha})_3 = (c^f \alpha_3^f E_{33}^f + c^m \alpha^m E^m)/E_{33}$$

$$(\bar{\alpha})_4 = (\bar{\alpha})_5 = (\bar{\alpha})_6 = 0.$$

Finally

$$H = \begin{bmatrix} 1 & -0.5 & -0.5 & 0 & 0 & 0 \\ & 1 & -0.5 & 0 & 0 & 0 \\ & & 1 & 0 & 0 & 0 \\ \text{sym} & & & 3 & 0 & 0 \\ & & & & 3 & 0 \\ & & & & & 3 \end{bmatrix}.$$

Kyoung-Don Lee[1] *and Erhard Krempl*[1]

Thermomechanical, Time-Dependent Analysis of Layered Metal Matrix Composites

REFERENCE: Lee, K.-D. and Krempl, E., "**Thermomechanical, Time-Dependent Analysis of Layered Metal Matrix Composites,**" *Thermal and Mechanical Behavior of Metal Matrix and Ceramic Matrix Composites, ASTM STP 1080*, J. M. Kennedy, H. H. Moeller, and W. S. Johnson, Eds., American Society for Testing and Materials, Philadelphia, 1990, pp. 40–55.

ABSTRACT: The orthotropic, thermal viscoplasticity theory based on overstress (TVBO) is specialized for plane stress in a simple laminate theory. It maintains the same geometric assumptions as the classical laminate theory except that the orthotropic linear elasticity law is replaced by TVBO. In this way, rate sensitivity, creep, and relaxation can be modeled without the use of a yield surface and loading/unloading conditions. The laminate theory is intended for thermal analysis of metal matrix composites operating at high temperature under simultaneous mechanical and thermal loadings.

The rate-dependent laminate behavior is described by a set of coupled, first order, nonlinear *differential* equations that must be numerically integrated for a given mechanical and thermal history to yield the laminate and ply stresses as well as the laminate total strain as a function of time. To describe the behavior, the elastic constants and the coefficients of thermal expansion need to be known in addition to two material functions and six constants that describe the inelastic deformation behavior. Two metal matrix composites, MMC1 and MMC2, are constructed theoretically. For MMC1, the strength in the fiber and the transverse directions decrease with temperature. The strength in the transverse direction of MMC2, patterned after Ni_3Al/Al_2O_3, increases with temperature before it decreases and the strength in the fiber direction is nearly constant. First, the ply behavior is simulated by off-axis in-phase and out-of-phase thermomechanical numerical tests. Then the behavior of a $[\pm 45]_s$ laminate under a temperature excursion is computed both when it is free to expand and when the laminate is clamped in one direction. After the temperature returns to the datum point, residual stresses are shown to redistribute in time. They are induced by prior inelastic deformation.

KEY WORDS: metal matrix composites, laminates, thermal cycling, residual stresses, analysis, viscoplasticity, creep, relaxation, nickel aluminides, composite materials, thermal properties, mechanical properties

Load carrying parts of hypervelocity vehicles and other aircraft may be made of metal matrix composites and may be subjected to simultaneous thermal and mechanical loading. At high temperatures, inelastic deformations such as creep, relaxation, and rate sensitivity can not be neglected. To model these phenomena, the thermal viscoplasticity theory based on overstress (TVBO) was developed [*1*]. In this paper TVBO is used for the analysis of layered metal matrix composites subjected to in-plane deformation. The formulation follows the assumptions of classical laminate theory (CLT) but the linear elasticity theory is replaced by the orthotropic TVBO.

[1]Graduate student and Professor of Mechanics, respectively, Mechanics of Materials Laboratory, Rensselaer Polytechnic Institute, Troy, NY 12180-3590.

In classical laminate theory, plane stress for each ply and constant total strain for the laminate are assumed. Since stresses are different from one ply to another, only the average stress is expected to satisfy the imposed boundary conditions. In addition, for thermal analysis, it is assumed that the temperature is uniform through the laminate. In keeping with CLT, material idealizations are made at the ply level and the interactions between fibers and matrix are not considered here.

Orthotropic, Thermal Viscoplasticity Theory Based on Overstress

The TVBO developed in Ref *1* is for infinitesimal strain and orthotropic material symmetry. It is of unified type and does not need a yield criterion and loading/unloading conditions. The elastic strain is formulated to be independent of thermomechanical path, and the inelastic strain rate is a function of overstress, the difference between stress, σ, and the equilibrium stress, g; it is a state variable of the theory.

The long-term asymptotic values of stress, equilibrium stress, and kinematic stress rates, which can be obtained for a constant mechanical strain rate at constant temperature, are assumed to be independent of thermal history as are the ultimate levels of the rate-dependent overstress and of the rate-independent contribution to the stress, see Ref *2*. Therefore the material functions and constants can be obtained in principle from isothermal tests within the temperature range of interest.

The model can predict not only the time-dependent phenomena such as creep, relaxation, and rate sensitivity but includes inelastic incompressibility, tension/compression asymmetry, and invariance of the inelastic properties under superposed pressure as special cases [*1*]. Recovery of state, aging, and temperature history dependence are not included in this paper.

Constant elastic and inelastic Poisson's ratios are defined for the uniaxial loading case. The theory permits the computation of the actual Poisson's ratio that depends on the loading history as well as elastic and inelastic Poisson's ratios, see Ref *1*.

All material constants can be functions of temperature. This dependence is not explicitly displayed. The temperature dependence can be the usual Arrhenius relationship or can deviate from that model.

Plane Stress Formulation

For application to the laminate theory the orthotropic TVBO of Ref *1* is reduced to the plane stress case. Bold face capital and small letters denote the material property matrices and vectors, repectively. The reference and preferred material coordinate axes are denoted by 1,2,6 and x,y,s, respectively. Components of vectors and material property matrices are accordingly subscripted. For convenience of writing, the components of the primed vectors and matrices are defined to be referred to the reference coordinate system hereafter. The strain, $\boldsymbol{\varepsilon}'$, stress, $\boldsymbol{\sigma}'$, and the state variable vector, $\mathbf{g}'$, are given by

$$\begin{aligned} \boldsymbol{\varepsilon}'^{t} &= \{\varepsilon_1\ \varepsilon_2\ \varepsilon_6\} \\ \boldsymbol{\sigma}'^{t} &= \{\sigma_1\ \sigma_2\ \sigma_6\} \\ \mathbf{g}'^{t} &= \{g_1\ g_2\ g_6\} \end{aligned} \tag{1}$$

with the overstress defined as $\mathbf{x}' = \boldsymbol{\sigma}' - \mathbf{g}'$

Transformation of strain, stress, and the state variable vector are defined by

$$\boldsymbol{\varepsilon} = \mathbf{N}\boldsymbol{\varepsilon}' \qquad \boldsymbol{\sigma} = \mathbf{M}\boldsymbol{\sigma}' \qquad \mathbf{g} = \mathbf{M}\mathbf{g}' \tag{2}$$

The transformation matrices N and M are, (see Ref *3*)

$$\mathbf{N} = \begin{bmatrix} m^2 & n^2 & mn \\ n^2 & m^2 & -mn \\ -2mn & 2mn & m^2 - n^2 \end{bmatrix} \tag{3}$$

$$\mathbf{M} = \begin{bmatrix} m^2 & n^2 & 2mn \\ n^2 & m^2 & -2mn \\ -mn & mn & m^2 - n^2 \end{bmatrix} \tag{4}$$

where $m = \cos\theta$ and $n = \sin\theta$, and θ is the angle from the 1-axis to the x-axis measured counterclockwise, see Fig. 2.2 in Ref *3*.

In accordance with the assumptions of a unified theory, and total small strain rate, $d\boldsymbol{\varepsilon}/dt$, is the sum of the elastic, $d\boldsymbol{\varepsilon}^{el}/dt$, inelastic, $d\boldsymbol{\varepsilon}^{in}/dt$, and thermal strain rates, $d\boldsymbol{\varepsilon}^{th}/dt$,

$$\dot{\boldsymbol{\varepsilon}}' = \dot{\boldsymbol{\varepsilon}}'^{el} + \dot{\boldsymbol{\varepsilon}}'^{in} + \dot{\boldsymbol{\varepsilon}}'^{th} \tag{5}$$

(Hereafter the superposed dot denotes a total derivative with respect to time.) The temperature path independent elastic strain rate is given by

$$\dot{\boldsymbol{\varepsilon}}'^{el} = \frac{d}{dt}\left(\mathbf{N}^{-1}\mathbf{R}_c^{-1}\mathbf{C}_d^{-1}\mathbf{M}\,\boldsymbol{\sigma}'\right) \tag{6}$$

The inelastic strain rate is solely a function of the overstress

$$\dot{\boldsymbol{\varepsilon}}'^{in} = \mathbf{N}^{-1}\mathbf{R}_c^{-1}\mathbf{K}_d^{-1}[\Gamma]\,\mathbf{M}\,\mathbf{x}' \tag{7}$$

and the thermal strain rate is

$$\dot{\boldsymbol{\varepsilon}}'^{th} = \mathbf{N}^{-1}\boldsymbol{\alpha}\,\dot{T} \tag{8}$$

where T is the absolute temperature and $\boldsymbol{\alpha}$ is the coefficient of thermal expansion vector

$$\boldsymbol{\alpha}' = \{\alpha,\ \alpha,\ 0\}$$

Square brackets following a symbol denote "function of." The growth law for the equilibrium stress is

$$\dot{\mathbf{g}}' = q[\Gamma]\dot{\boldsymbol{\sigma}}' + \dot{T}\frac{\partial q}{\partial T}[\Gamma]\boldsymbol{\alpha}' + q[\Gamma](1-\Theta)\frac{\mathbf{x}'}{k[\Gamma]} \tag{9}$$

The overstress invariant is defined as

$$\Gamma^2 = \mathbf{x}'\mathbf{H}\,\mathbf{x} \tag{10}$$

and the invariant that measures the ultimately rate-independent contribution to the stress, see Ref *1*, as

$$\Theta^2 = \mathbf{g}'\mathbf{P}\,\mathbf{g} \tag{11}$$

The matrices $\mathbf{H}_\sigma$ (dimensionless) and $\mathbf{P}_\sigma$ (dimension reciprocal stress) are repositories for the anisotropy of the viscous and rate-independent contributions to the long-term asymptotic stress [*1–3*]. They are given as

$$\mathbf{H} = \begin{bmatrix} H_{xx} & H_{xy} & \\ H_{xy} & H_{yy} & \\ & & H_{ss} \end{bmatrix} \tag{12}$$

and

$$\mathbf{P} = \begin{bmatrix} P_{xx} & P_{xy} & \\ P_{xy} & P_{yy} & \\ & & P_{ss} \end{bmatrix} \tag{13}$$

The elastic compliance and the constant elastic Poisson's ratio matrices are, respectively,

$$\mathbf{C}_d^{-1} = \begin{bmatrix} \frac{1}{E_{xx}} & & \\ & \frac{1}{E_{yy}} & \\ & & \frac{1}{E_{ss}} \end{bmatrix} \tag{14}$$

and

$$\mathbf{R}_c^{-1} = \begin{bmatrix} 1 & -\nu_{xy} & \\ -\nu_{yx} & 1 & \\ & & 1 \end{bmatrix} \tag{15}$$

The viscosity matrix

$$\mathbf{K}_d^{-1} = \begin{bmatrix} \frac{1}{K_{xx}k[\Gamma]} & & \\ & \frac{1}{K_{yy}k[\Gamma]} & \\ & & \frac{1}{K_{ss}k[\Gamma]} \end{bmatrix} \tag{16}$$

and the inelastic Poisson's ratio matrix

$$\mathbf{R}_k^{-1} = \begin{bmatrix} 1 & -\eta_{xy} & \\ -\eta_{yx} & 1 & \\ & & 1 \end{bmatrix} \tag{17}$$

govern the evolution of the inelastic strain rate. The positive decreasing viscosity function, $k[\Gamma]$, controls the rate sensitivity [*1,2,4*]; the viscosity factors, K_{ij} (dimension of stress) are direction-dependent multipliers.

The positive, non-increasing function, $q[\Gamma]$, is dimensionless and determines the shape of the stress-strain diagram [*1,2,4*]; it is called the modified shape function.

Finally, the elastic and the inelastic Poisson's ratios are defined by

$$\nu_{ij} = -\frac{\dot{\varepsilon}_j^{el}}{\dot{\varepsilon}_i^{el}} \qquad (i,j = x,y,\ i \neq j) \tag{18}$$

and

$$\eta_{ij} = -\frac{\dot{\varepsilon}_j^{in}}{\dot{\varepsilon}_i^{in}} \qquad (i,j = x,y,\ i \neq j) \tag{19}$$

respectively, for uniaxial loading in the j-direction. They are constant for constant temperature.

The preceding theory is a special form of the one presented in Ref *1*. It will reproduce only tension/compression symmetry and all stress-strain curves for constant temperature will ultimately become horizontal. The growth law, Eq 9, contains a term multiplied by dT/dt. It is introduced to ensure temperature path independence when the growth of the equilibrium stress is nearly elastic. Other unified, isotropic theories include an additional term multiplied by dT/dt in the inelastic growth law for the back stress [*5,6*]. An equivalent additional term could be introduced in the growth law for the equilibrium stress, see Eq 9, to affect the inelastic response under variable temperature. It has only an influence on the transient behavior and its importance will be investigated in the future in the context of TVBO.

Although not explicitly displayed, all constants can depend on temperature. No specific temperature dependence is assumed *a priori*. The theory permits the usual Arrhenius temperature dependence or any other. The exact dependence has to be determined for a given ply from tests performed at several constant temperatures.

Application to In-Plane Deformation of a Single Ply

The plane stress formulation just mentioned can be directly used for simulation of ply behavior in stress and total strain control with or without temperature change. For strain control in Directions 1, 2, and 6, Eqs 5 through 8, are rewritten as

$$\dot{\sigma}' = \mathbf{M}^{-1}\mathbf{C}_d\mathbf{R}_c\mathbf{N}\dot{\varepsilon}' - \mathbf{M}^{-1}\mathbf{C}_d\mathbf{R}_c\mathbf{R}_k^{-1}\mathbf{K}_d^{-1}\mathbf{M}\,x' + \left(\mathbf{M}^{-1}\frac{\partial \mathbf{C}_d}{\partial T}\mathbf{C}_d^{-1}\mathbf{M}\sigma' - \mathbf{M}^{-1}\mathbf{C}_d\mathbf{R}_c\alpha\right)\dot{T} \tag{20}$$

For stress control in Directions 1, 2, and 6, inversion of Eq 20 yields

$$\dot{\varepsilon}' = \mathbf{N}^{-1}\mathbf{R}_c^{-1}\mathbf{C}_d^{-1}\mathbf{M}\dot{\sigma}' + \mathbf{N}^{-1}\mathbf{R}_k^{-1}\mathbf{K}_d^{-1}\mathbf{M}\,x' - \left(\mathbf{N}^{-1}\mathbf{R}_c^{-1}\mathbf{C}_d^{-1}\frac{\partial \mathbf{C}_d}{\partial T}\mathbf{C}_d^{-1}\mathbf{M}\sigma' - \mathbf{N}^{-1}\alpha\right)\dot{T} \tag{21}$$

Here, it was assumed that the temperature dependence of the Poisson's ratio is negligible. Equation 20 or 21 is solved together with Eqs 9 through 11 for strain or stress boundary conditions. It is seen that the temperature rate can be specified independently in each case. If loading in only one direction is to be simulated, the appropriate boundary conditions must be specified and incorporated into the equations.

Application to In-Plane Deformation of a Laminate

For description of laminates, the laminate code of Ref *3* is adopted. The average stress is defined as

$$\bar{\sigma} = \frac{1}{h}\sum_{i=1}^{n}\sigma_i h_i \tag{22}$$

where h is the laminate thickness, h_i is the ply thickness of the ith ply, and n denotes the number of plies. According to CLT (see Ref *3*), the strain is constant through the laminate thickness and is given by

$$\dot{\varepsilon}_i = \bar{\varepsilon} \cdot (i = 1, \ldots, n) \tag{23}$$

Strain and Temperature Control

For strain and temperature control in Directions 1, 2, and 6, the strain rates are given and the initial values of the stress, the equilibrium stress, and the strain vectors of each ply are needed. The strain rate of each ply is uniform, see Ref *23*. Then the stress and the equilibrium stress of each ply can be separately calculated by solving the set of equations (Eqs 9–11 and 20); of course, the material functions and constants must be known. The average stress is obtained simply from Eq 22 after obtaining the stress of each ply. Similarly, an average equilibrium stress can be calculated.

Average Stress and Temperature or Mixed Strain and Average Stress and Temperature Control

For the control of the average stress in at least one direction and of the temperature, the average stress rate is obtained from Eqs 20 and 22 using the inverted form of

$$\dot{\bar{\sigma}}' = \left[\sum_{i=1}^{n}\left(\mathbf{M}^{-1}\mathbf{C}_d\mathbf{R}_c\mathbf{N}\right)_i\frac{h_i}{h}\right]\dot{\bar{\varepsilon}}' - \sum_{i=1}^{n}\left\{\mathbf{M}^{-1}\mathbf{C}_d\mathbf{R}_c\mathbf{R}_k^{-1}\mathbf{K}_d^{-1}\mathbf{M}\,x' - \left(\mathbf{M}^{-1}\frac{\partial \mathbf{C}_d}{\partial T}\mathbf{C}_d^{-1}\mathbf{M}\sigma' - \mathbf{M}^{-1}\mathbf{C}_d\mathbf{R}_c\alpha\right)I\right\}\frac{h_i}{h} \tag{24}$$

For average stress-temperature control, the average stress rates in all directions and the temperature rate must be specified. In addition, the initial values of the stress, the equilibrium stress, and the strain are needed. Then the stresses and the equilibrium stresses of all plies can be simultaneously calculated from n sets of equations (Eqs 9–11 and 20) in addition to Eq 24.

Mixed boundary conditions can also be simulated by introducing them into Eq 24. Again, n sets of equations (Eqs 9–11 and 20) must be solved simultaneously with Eq 24. In both cases, the temperature rate can be specified independently.

Stress free boundaries of the laminates are to be incorporated in Eq 24 as a special case. Because of the assumptions of CLT, nonzero ply stresses are possible and only their sum has to be equal to zero.

For each boundary condition, the mechanical strain (defined as the total strain minus the thermal strain) can be calculated for each ply. While it is possible to control the mechanical strain in a single ply, mechanical strains for the laminate are not uniform and can therefore not be controlled.

If $dT/dt = 0$, this theory reduces to a laminate theory similar to the one presented in Ref 4. In contrast to Ref 4 where Poisson's ratio was assumed to be constant, a variable Poisson's ratio is modeled in this paper.

Determination of the Material Functions and Constants

The material constants and functions must be determined from tests performed with specimens cut from plies. The present theory assumes that a temperature history does not affect the ultimate rates of the stress and the equilibrium stress under constant temperature. Therefore, isothermal tests at different temperatures suffice to characterize the response of the material. Although we have had experiences in determining the constants for isotropic alloys [2,7,8] by relaxation and rate change tests, no such an experience has so far been gained for metal matrix composites. In addition to the elastic constants (E_{11}, E_{22}, E_{33}, ν_{12}) and the coefficients of thermal expansion (α_1, α_2), the inelastic deformations need to be described by the viscosity function $k[T]$, the viscosity factors (K_{11}, K_{22}, K_{33}), and the matrices **H** and **P**. The **H** controls the anisotropy of the viscous contribution to the stress [4] and it may be possible to assume that this contribution is isotropic. The **P** controls the anisotropy of the rate-independent contribution to the stress [1]. Strain rate change tests and other tests with on-axis specimens are necessary to determine these matrices. The matrices, $\mathbf{K}_\sigma\mathbf{R}_\varepsilon$ and $\mathbf{C}_\varepsilon\mathbf{R}_\sigma$, are symmetric. With the viscosity factors, K_{ii}, known, only one Poisson's ratio (η_{12}) needs to be determined and the other (η_{21}) is obtained from the symmetry relationship. (CLT ignores the thickness changes of a ply. Modeling of inelastic incompressibility is, therefore, not a condition that can be implemented in CLT since the thickness strain does not enter into the theory.) The viscosity factors, K_{ii}, are set equal to the elastic moduli, E_{ii}, in this paper. (For different choices see Refs 1 and 7.) In this case, the present theory needs two functions (the viscosity and the modified shape functions) and six constants (η_{12}, H_{11}, H_{22}, P_{11}, P_{12}, P_{33}) to describe the inelastic behavior of a ply. Of course, the four elastic constants and the two coefficients of thermal expansion are required as they are in the elastic case.

At each temperature of interest, this determination of the material constants has to be repeated. After this is done, an interpolation is necessary to obtain the temperature dependence of the constants.

At the present time, test data sufficient for determining the material constants of TVBO do not appear to be available either from the literature or from tests in the Mechanics of Materials Laboratory of Rensselear Polytechnic Institute (RPI). For the isothermal case, literature data were sufficient to estimate the constants and they permitted simulations of in-plane loading behavior of several metal matrix composite laminates [4]. Of course, the theory has undergone verification for the isotropic case [2,8].

Numerical Integration

Once the constants and functions are known, the model is ready for performing laminate analyses. To this end, a numerical integration of the set of differential equations becomes necessary. The IMSL routine, DGEAR, that had been used previously for the isotropic case can also be used for this in-plane laminate analysis. A FORTRAN computer program was written for in-plane loading of symmetric laminates that has been used in the simulations to be described below. All computations were performed on the IBM 3081 D mainframe computer of RPI.

Simulation of Ply and Laminate Behaviors

For the demonstration of the capabilities of the theory, two metal matrix composites were "theoretically constructed" by postulating elastic and inelastic properties. For the first metal matrix composite, MMC1, it was assumed that strength decreases in both fiber and transverse directions with a temperature increase. This is the usual behavior. For the second metal matrix composite, MMC2, the strength in the transverse direction is initially increasing with temperature before it decreases; the strength in the fiber direction is assumed to be nearly constant. The relationships are depicted in Fig. 1. The increase in strength with temperature

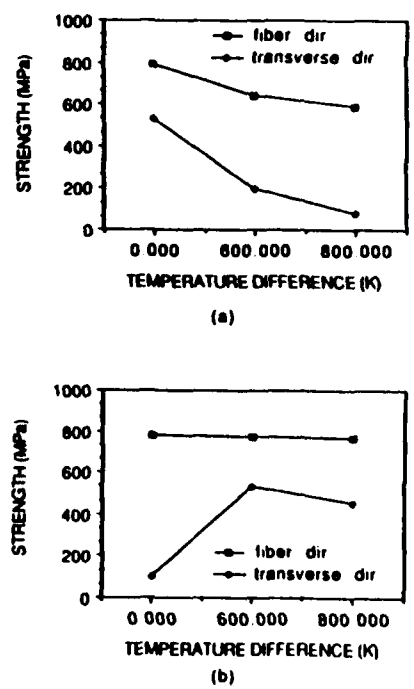

FIG. 1—*Strength properties of MMC1 (a) and MMC2 (b) as a function of temperature*

TABLE 1—*Material properties for MMC2.*

Temperature (K)	RT[a]	RT + 200	RT + 400	RT + 600	RT + 800
		Al_2O_3 FROM REFS 9 AND *10*			
Tensile strength (GPa)	1.8	...	...	...	1.3
Young's modulus, E_f (GPa)	400.0	...	...	...	360.0
Poisson's ratio, ν_f	0.25	...	...	...	0.25
Shear modulus, G_f	$G_f = E_f/(2(1 + \nu_f))$	...	...	...	...
CTE, α_f $(1/K)$ 10^6	7.0	...	...	...	10.0
		Ni_3Al FROM REF *11*			
0.2% flow stress (MPa)	100	210	420	550	460
Young's modulus, E_m (GPa)	180	...	...	...	140
Shear modulus, G_m (GPa)	130	...	...	...	(101)[b]
Poisson's ratio, ν_m	0.384	...	...	...	(0.384)
CTE, α_m $(1/K)$ 10^6	12.5	...	...	...	17.4
		Al_2O_3/Ni_3Al (ν_f = 0.4)[c]			
Strength (MPa)					
σ_x	780[d]	...	...	...	780
σ_y	(100)	(210)	(420)	(550)	(460)
Elastic modulus (GPa)					
E_x	268[d]	...	...	...	228
E_y	231[d]	...	...	...	185
$E_z = 2G$	141[d]	...	...	...	115
Elastic Poisson's ratio					
ν_z	0.33[d]	...	...	...	0.33
CTE $(1/K)$ 10^6					
α_x	9.2[d]	...	...	...	12.5
α_y	10.3[d]	...	...	...	14.1
Overstress[e] (MPa)					
x_x	(10)	(10)	(10)	(10)	(10)
x_y	(10)	(20)	(40)	(65)	(80)

[a]Room temperature.
[b]The values in parentheses are assumed.
[c]The elastic properties of the Al_2O_3/Ni_3Al composite are calculated by using the formula of Ref *12*.
[d]Linear interpolation between values at RT and RT + 800.
[e]The asymptotic overstress at a strain rate, $d\varepsilon/dt = 10^{-4}$, is assumed. It is further assumed that the asymptotic overstress at a strain rate $d\varepsilon/dt = 10^{-6}$ is one hundredth of the one at $d\varepsilon/dt = 10^{-4}$.

increase can be found in nickel aluminides [*11*] and MMC2 is patterned after an Al_2O_3/Ni_3Al composite. MMC1 has the same properties as MMC2 except that the strengths in both directions decrease with a temperature increase.

In finding the constants of the TVBO, it was assumed that the asymptotic stress in the x and the y directions at a strain rate of 10^{-4} s^{-1} is set equal to the strength in the fiber and the transverse directions, respectively. The elastic properties were determined by the rule of mixtures [*12*] from the properties of the fiber and the matrix as shown in Table 1. The viscous properties given in Table 1 were assumed. They determine the rate sensitivity, the creep, and the relaxation behavior. These assumptions yield the material constants as a function of temperature as listed in Table 2 by interpolations.

When these properties are used to simulate tension tests in the fiber and the transverse

TABLE 2—*Material constants as a function of temperature for MMC1 and MMC2* [a]

Young's Modulus:
$E_{xx} = 268\,000 - 50(T - RT)^2$ (MPa)
$E_{yy} = 231\,000 - 57.5(T - RT)$ (MPa)
$E_{zz} = 141\,000 - 32.5(T - RT)$ (MPa)
Elastic Poisson's Ratio:
$\nu_{xz} = 0.33$
Viscosity Function: $k[\Gamma] = K_1(1 + \Gamma/K_2)^{K_3}$
$K_1 = 39.5 - 0.00865(T - RT)(s)$
$K_2 = 38.1$ (MPa)
$K_3 = 20$
Viscosity Factors:
$K_{ii} = E_{ii}$, no sum on i, $i = x, y, s$
Inelastic Poisson's Ratio:
$\eta_{yz} = 0.5$
Modified Shape Function: $q[\Gamma] = C_1 + (C_2 - C_1)\mathrm{EXP}(-C_3\Gamma)$
$C_1 = 0.68 - 0.00035(T - RT)$
$C_2 = 0.9 - 0.0000375(T - RT)$
$C_3 = 0.007$ (1/MPa)
Coefficient of Thermal Expansion:
$\alpha_x = 0.922\mathrm{E} - 5 + 0.41\mathrm{E} - 8(T - RT)$ $(1/K)$
$\alpha_y = 0.103\mathrm{E} - 4 + 0.475\mathrm{E} - 8(T - RT)$ $(1/K)$
Overstress Invariant: $\Gamma^2 = x^t H x$
$H_{xx} = 1.0$
$H_{yy} = (1.0 - 0.002(T - RT) + 0.125\mathrm{E} - 5(T - RT)^2)^2$ for MMC1
$= (1.0 - 0.002344(T - RT) + 0.1465\mathrm{E} - 5(T - RT)^2)^2$ for MMC2
$H_{zz} = H_{yy}$
$H_{xy} = -0.5\,\mathrm{SQRT}(H_{yy})\mathrm{SQRT}(H_{yy})$
Invariant of g: $\Theta^2 = g^t P g$
$P_{xx} = (1/A_{xx})^2$
$P_{yy} = (1/A_{yy})^2$
$P_{xy} = -0.5/(A_{xx}A_{yy})$
$P_{zz} = (1/A_{zz})^2$
For MMC1
$A_{xx} = 780.0 - 0.25(T - RT)^2$ (MPa)
$A_{yy} = 520.0 - 0.5875(T - RT)^2$ (MPa)
$A_{zz} = A_{yy}$ (MPa)
For MMC2
$A_{xx} = 770.0$ (MPa)
$A_{yy} = 90.0 + 0.275(T - RT) + 0.1125\mathrm{E} - 2(T - RT)^2$ (MPa) $0\,K \le T - RT \le 400\,K$
$= -460 + 3.15(T - RT) - 0.2625\mathrm{E} - 2(T - RT)^2$ (MPa) $400\,K \le T - RT \le 800\,K$
$A_{zz} = A_{yy}$ (MPa)

[a]Unless specified, the properties are same for both MMC1 and MMC2.
[b]RT = room temperature.

directions at different constant temperatures, the graphs of Figs. 2 and 3 result. The curves are all reaching the asymptotic stress level at a strain of 1% and this stress level corresponds to the strength of the material depicted in Fig. 1. This property can be adjusted by the constants of the theory. In Ref *4*, it was assumed that the fiber stress-strain diagram was almost linear elastic.

The fiber direction shows very little rate sensitivity and a modest influence of temperature on strength for MMC1, see Fig. 2*a*. For the transverse direction, Fig. 2*b*, the rate sensitivity is small at room temperature and increases with increasing temperature as the strength decreases considerably. In Fig. 3*a*, the asymptotic stress changes very little with temperature but the transient behavior is strongly affected. In the transient region from initially elastic behavior to inelastic behavior, inverse rate sensitivity is reproduced by the model. When

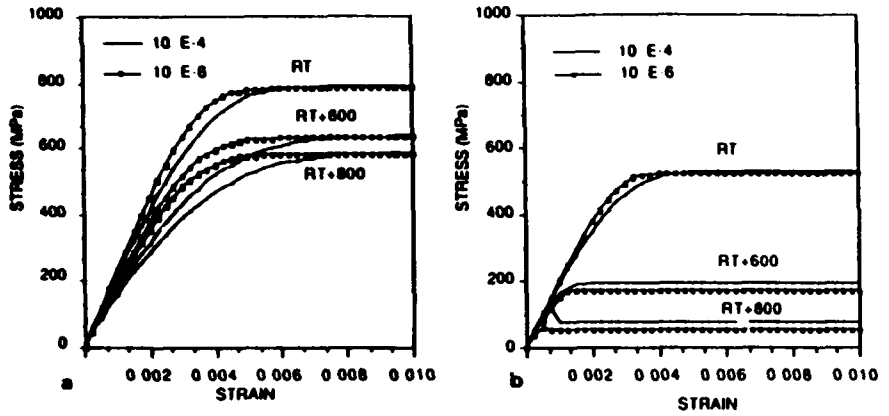

FIG. 2—*Stress-strain curves for MMC1 in the fiber direction (a) and in the transverse direction (b) at room temperature (RT), at RT + 600 K, and at RT + 800 K for two different strain rates 10 $^{-4}$ and 10 $^{-6}$ s $^{-1}$.*

the asymptotic stress is reached, normal rate sensitivity is recovered. (The stress increases with an increase in strain rate.) The increase in strength with a temperature increase is pronounced in Fig. 3*b*. Also the rate sensitivity is made to increase with temperature increase. All these relationships were built into the model and can be changed as the material requires. It would, for example, be possible to model a decrease in rate sensitivity with increasing temperature to stimulate behavior found when strain aging is present.

Thermal Cycling of a Ply

The theory can be applied to any strain- or stress-temperature history for on-axis or off-axis loading. As an example, the response of a uniaxial strain-controlled test is computed for a 45° off-axis specimen under simultaneous strain and temperature cycling. Two cases are considered. In the first, the temperature increases with an increase in strain; for the

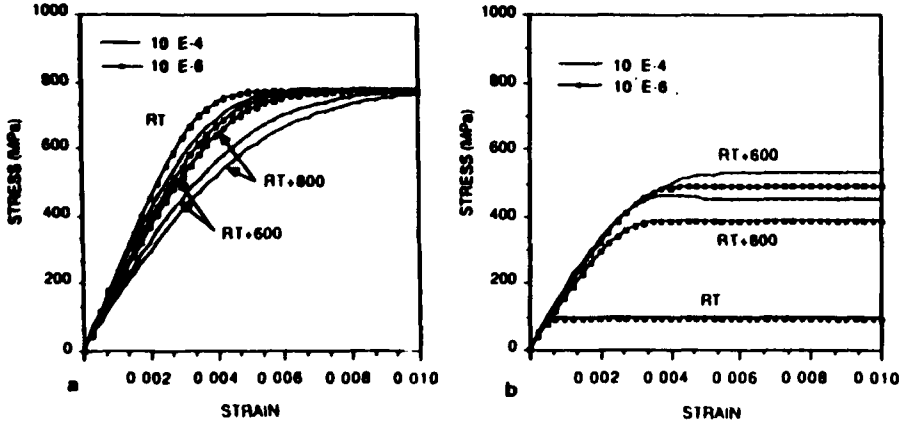

FIG. 3—*Same as Fig. 2 but results are for MMC2.*

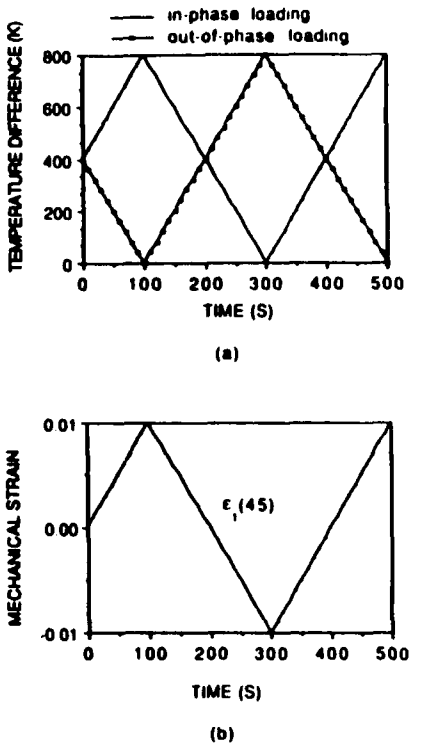

FIG. 4—*Temperature cycles (a) and strain cycle (b) used in the simulations of Figs. 5 and 6.*

second, the temperature decreases with strain increase. These loading cases are called in-phase and out-of-phase, respectively. The temperature and strain cycles are shown in Fig. 4. At 400 K above room temperature, the specimen is assumed to be stress free in both cases of loading.

Figure 5 exhibits the hysteresis loops for MMC1 and MMC2 for one complete cycle. Since the theory represents cyclic neutral behavior, the hysteretic loops close. For MMC1, whose strength decreases with temperature increase, initial elastic loading is followed by yielding and a further decrease in the stress as temperature and strain increase. Unloading at the maximum strain is initially elastic followed by a nearly linear workhardening curve as temperature decreases up to the maximum compressive strain. As strain and temperature increase, unloading is initially elastic, but yielding sets in again before zero strain is reached and the loop joins up with the initial loading curve as temperature increases further. Since the strength increases initially with a temperature increase for MMC2, the stress rises more in this case but also decreases as the maximum strain is approached. Unloading exhibits a rather large linear region followed by plastic flow. The maximum compressive stress is reached close to zero strain followed by a decrease in magnitude as the temperature decreases together with the strain. Unloading from compression is initially linear followed by an increase in the flow stress as the temperature increases together with the strain. Again, the loop closes after one cycle.

The results for the out-of-phase are shown in Fig. 6. Here the temperature decreases with increasing strain and [illegible] MMC1 develops higher stresses than MMC2. The

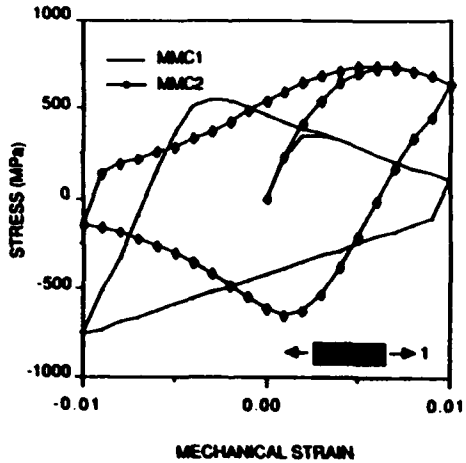

FIG. 5—*Hysteresis loops for an in-phase loading cycle (see Fig. 4) imposed on a 45° off-axis specimen of MMC1 and MMC2.*

opposite is true for unloading from the maximum strain as the temperature increases. Comparison of Figs. 5 and 6 shows that the upper and lower portions of the hysteresis loops appear to be interchanged and the plastic strain range (the width of the hysteresis loop at zero stress) is almost the same in the four cases. These results were unexpected and may be due to the chosen material properties. In any event, the results show the basic capabilities in simulating ply behavior.

Thermal Cycling of a Laminate

The temperature cycle shown in Fig. 7 includes a fast up-ramp followed by a short hold and a slow return of the temperature to the datum point. As in the previous cases, the maximum temperature is 800 K above room temperature. This temperature cycle is imposed

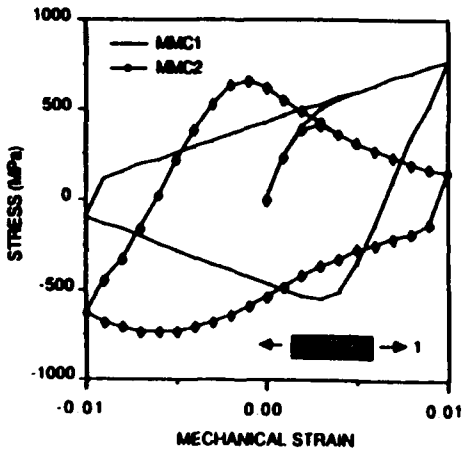

FIG. 6—*Same as Fig. 5 except that the loading is out-of-phase.*

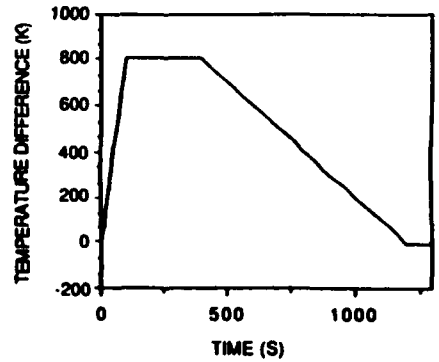

FIG. 7—*Temperature history imposed on the [±45]$_s$ laminate.*

on a [±45]$_s$ laminate that is either expanding freely, Fig. 8, or is rigidly restrained in the one-direction as shown in Fig. 9. In both cases, the stress history is shown versus time.

Overall, the constrained case, Fig. 9, produces much higher stresses than the unconstrained case, Fig. 8. Also, the residual stresses found when the temperature returns to the data point and that are induced by the prior plastic flow follow this pattern. The magnitude of the residual stresses are always higher for MMC1 than for MMC2.

For MMC1 the stress drop during the maximum temperature hold is more pronounced than for MMC2. In both cases, the stress drop is largest initially and subsides rather quickly. Figure 9 shows that the stress is very low during the high temperature hold for MMC1. This fact can be explained by the assumed low strength of this material at the maximum temperature as shown in Fig. 2*b*. When the temperature returns to room temperature, additional relaxation takes place due to the rate dependence of the ply material. The amount of relaxation is small for the unconstrained case but noticeable for the constrained case. A comparison of the computed data during relaxation at the maximum temperature hold and

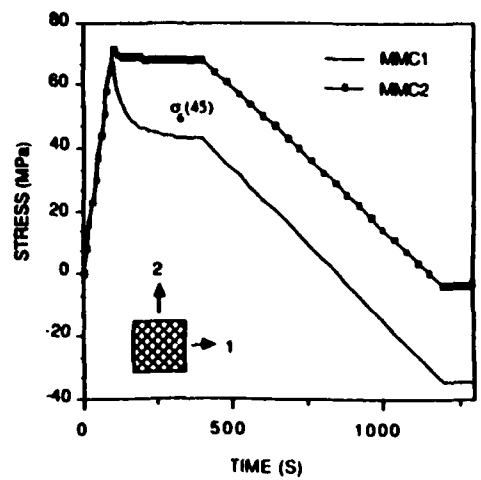

FIG. 8—*Stress response of a [±45]$_s$ laminate subjected to the temperature cycle of Fig. 7. The laminate is free to expand; all normal stresses are zero and $\sigma_x(-45) = -\sigma_x(45)$. The difference in the behavior of MMC1 and MMC2 is noteworthy.*

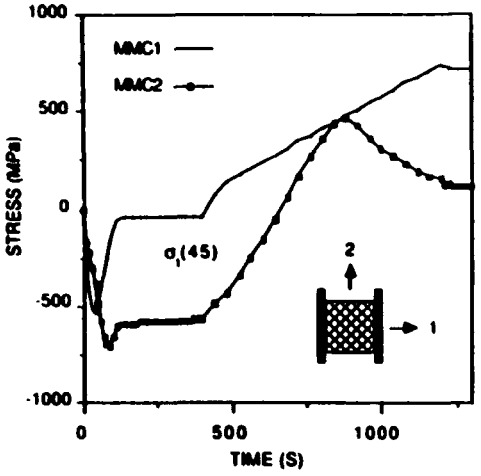

FIG. 9—*Same as Fig. 8 except that the laminate is rigidly constrained in Direction 1,* $\sigma_1(45) = \sigma_1(-45)$; *all other stress components are negligible or zero.*

after the laminate has returned to room temperature is given in Table 3. The computation shows clearly that the theory is capable of reproducing stress redistributions in the laminate.

Discussion

The present paper extends the classical laminate theory to rate dependent material behavior that includes rate sensitivity, creep, and relaxation. In addition, temperature changes are included. The geometric assumptions of classical laminate theory are retained. The strains and the temperature are assumed to be uniform throughout the laminate. Also, only average stress boundary conditions can be satisfied. The equations are in incremental form and their use in the thermomechanical analysis of laminates requires numerical integration of stiff differential equations. To this end, a FORTRAN computer program was written that can handle symmetric laminates for strain or average stress boundary conditions and variable temperature.

The use of the present theory requires that the anisotropic properties of a ply be determined

TABLE 3—*Stress relaxation during constant temperature holds in Figs. 8 and 9.*

	$\sigma_x[45]$ MPa		$\sigma_1[45]$ MPa	
TIME, *s*	MMC1	MMC2	MMC1	MMC2
(*a*) Hold at *RT* + 800° *K*				
100	67.81	71.30	−95.30	−662.5
400	42.78	68.49	−44.83	−574.3
$\lvert\Delta\sigma\rvert$ from 100 to 400 s	25.03	2.81	50.47	88.2
(*b*) Hold at *RT K*				
1200	−34.69	−3.88	737.8	143.8
1300	−34.29	−3.52	710.1	111.8
$\lvert\Delta\sigma\rvert$ from 1200 to 1300 s	0.40	0.36	27.7	32.0

°*RT = room temperature.*

by experiments. They include on-axis tension tests at various strain rates as well as strain rate cycling tests. Longitudinal as well as transverse strains should be measured to determine the elastic constants, the coefficients of thermal expansion and the two material functions and the six constants that characterize the inelasticity.

Although the elastic properties and the coefficients of thermal expansion of a ply can be determined from the fiber and the matrix properties using averaging methods such as the rule of mixtures or the self-consistent methods, no such procedures are available for the viscoplastic properties. Research aimed at providing these tools is beginning.

For the demonstration of the capabilities of the theory, hypothetical metal matrix composites were created that were patterned after two real systems. This approach was pursued since no suitable experimental data were found for the thermal case. For the isothermal case, a theory similar to the present one was shown to reproduce off-axis and on-axis behavior of FP/Al and other materials [*4*]. It is hoped that thermomechanical data for plies will become available in the future so that the theory can be checked against experimental results.

Acknowledgment

This research was supported by DARPA/ONR Contract N00014-86-K0770 with Rensselaer Polytechnic Institute.

References

[*1*] Lee, K.-D. and Krempl, E., "An Orthotropic Theory of Viscoplasticity on Overstress for Thermomechanical Deformations," *International Journal of Solids and Structures*, in press.

[*2*] Yao, D. and Krempl, E., "Viscoplasticity Theory Based on Overstress. The Prediction of Monotonic and Cyclic Proportional and Nonproportional Loading Paths of an Aluminum Alloy," International Journal of Plasticity, Vol. 1, 1985, pp. 259–274.

[*3*] Tsai, S. W. and Hahn, H. T., *Introduction to Composite Materials*, Technomic Publishing Company, Westport, CT, 1980, p. 116.

[*4*] Krempl, E. and Hong, B. Z., "A Simple Laminate Theory Using the Orthotropic Viscoplasticity Theory Based on Overstress. Part I: In Plane Stress-Strain Relations for Metal Matrix Composites," Rensselaer Polytechnic Institute Report MML87-9, *Composites Science and Technology*, Vol. 35, 1989, pp. 53–74.

[*5*] Chaboche, J. L., "Modeling of Cyclic Viscoplasticity in Finite Element Codes," *Constitutive Laws for Engineering Materials. Theory and Applications*, C. S. Desai, E. Krempl, P. D. Kiousis and T. Kundu, Eds., Elsevier, New York, Amsterdam, London, 1987, pp. 1165–1172.

[*6*] Moreno, V. and Jordan, E. H., "Prediction of Material Thermomechanical Response with a Unified Viscoplastic Constitutive Model," *International Journal of Plasticity*, Vol. 2, 1986, pp. 223–245.

[*7*] Choi, S. H. and Krempl, E., "Viscoplasticity Theory Based on Overstress Applied to the Modeling of Cubic Single Crystals," Rensselaer Polytechnic Institute, *European Journal of Mechanics A/ Solids*, Vol. 8, 1989, pp. 219–233.

[*8*] Krempl, E., "The Role of Servocontrolled Testing in the Development of the Theory of Viscoplasticity Based on Total Strain and Overstress," *Mechanical Testing for Deformation Model Development, ASTM STP 765*, R. W. Rhode and J. C. Swearengen, Eds., American Society for Testing and Materials, Philadelphia, 1982, pp. 5–28.

[*9*] "Engineering Properties of selected Ceramic Materials," MCIC Report, MCIC-HB-07, Metals and Ceramics Information Center, Vol. 2, Aug. 1979.

[*10*] Taylor, D., "Thermal Expansion Data," *British Ceramic Transactions and Journal*, Vol. 83, 1984, pp. 92–98.

[*11*] Stoloff, N. S., "Physical and Mechanical Metallurgy of Ni_3Al and its Alloys," *International Material Reviews*, Vol. 34, No. 4, 1989, pp. 153–183.

[*12*] Min, B. K. and Flaggs, D. L., "A Thermomechanical Elastoplastic Analysis of Fibrous Composite Laminates," *Pressure Vessel Components Design and Analysis*, S. J. Brown, Ed., PVP-Vol. 98-2, American Society of Mechanical Engineers, New York, 1985, pp. 265–276.

Eur. J. Mech., A/Solids, **10**, n° 2, 173-192, 1991

Uniaxial thermomechanical loading. Numerical experiments using the thermal viscoplasticity theory based on overstress

K. D. LEE ** and E. KREMPL *

ABSTRACT. – A previously formulated orthotropic thermal viscoplasticity theory based on overstress (OTVBO) is specialized for the uniaxial state of stress (TVBO). In this theory the assumption of path independence of elastic behavior leads to additional terms which are multiplied by the time rate of change of temperature. The influence of these terms is investigated by numerical experiments on three different hypothetical materials which exhibit different temperature dependence of mechanical properties which are patterned after real materials.

The additional terms assure a stiff response and show their influence on the "elastic" behavior as expected as well as on the transition to inelastic flow. The long term asymptotic behavior at constant mechanical strain rate and ultimately constant temperature is, however, unaffected. The magnitude of the influence of these terms is controlled by the temperature dependence of the constants with a dominant effect of the elastic modulus. A definition of 'temperature history effect' is given. Its absence implies that the material properties can be determined from isothermal tests at various temperatures alone. If the asymptotic tangent modulus is zero (the stress-strain curves are horizontal at the maximum strain of interest), then TVBO cannot represent a 'temperature history effect'.

Introduction

The analysis of the inelastic deformation behavior is an important ingredient in the life prediction of components subjected to severe mechanical loading and thermal cycling. Presently the life of components in gas and steam turbines, processing plants, nuclear reactors, and jet and rocket engines must frequently be determined long before the component is being built. Inelastic finite element analyses calculate the state of stress (strain) as a function of location and time in a component. The stresses and strains are then used as inputs for the life prediction.

In the finite element analysis constitutive equations are needed which describe the deformation behavior of the material to be analyzed under constant and variable temperature. Modern constitutive equations based on state variables with no separate repositories for creep and plasticity, the so-called unified theories, are increasingly used. In these theories the equivalents of the classical kinematic and isotropic hardening variables are employed frequently. They have been successful in describing inelastic isothermal

* Mechanics of Materials Laboratory, Rensselaer Polytechnic Institute, Troy, N.Y. 12180-3590, U.S.A.
** Now with Lucky LTD, Dae-deog Danji, Dae-jeon, Korea.

EUROPEAN JOURNAL OF MECHANICS, A/SOLIDS, VOL. 10, N° 2, 1991
0997-7538/91/02 173 20/$ 4.00/

Chan & Lindholm [1990] and by Niitsu & Ikegami [1988], although the latter results could be interpreted to contain some temperature history effect, especially when the additional results which are quoted by Ohno *et al.* [1988] are taken into consideration. A clear case of a temperature history effect and associated microstructural changes in a IN 100 superalloy is reported by Cailletaud & Chaboche [1979].

Although the origin of any temperature history effect may be due to chemical reactions of the microstructure (precipitation reaction such as carbide formation is just one example) it can be identified macroscopically by suitable experiments. Two identical specimens with different prior thermomechanical histories are subjected to the same loading rate and ultimately constant and equal temperature. If the stress-mechanical strain diagrams are ultimately different then history dependence in the sense of plasticity is observed, *see* Krempl [1981] where only isothermal cases are considered. If the prior mechanical history is identical but the temperature history is different for the two specimens, (history 1-7 and history 1-8), as is the case in the example of Figure 1 *b*, then a history effect is found. These definitions can also be applied to the examination of the capabilities of constitutive equations.

The uniaxial version of TVBO

The present uniaxial formulation is an outgrowth of an orthotropic formulation (OTVBO) given previously, *see* Lee & Krempl [1988]. It differs slightly from the formulation given by Krempl *et al.* [1986] and these differences are delineated in the Appendix and in the Appendix of Lee & Krempl [1988].

The stress and the strain are designated by σ and ε, respectively. When only uniaxial states of stress are considered, they can be interpreted as engineering stress and strain or as true (Cauchy) stress and true strain as the need arises. A superposed dot denotes the total time derivative and a square bracket following a symbol denotes "function of". With these preliminaries we list the first assumption of TVBO, total strain rate is the sum of elastic, inelastic and thermal strain rates,

$$\dot{\varepsilon} = \dot{\varepsilon}^{el} + \dot{\varepsilon}^{in} + \dot{\varepsilon}^{th}. \tag{1}$$

Further, the elastic strain is assumed to be independent of thermomechanical path,

$$\dot{\varepsilon}^{el} = \frac{d}{dt}\left(\frac{\sigma}{E[T]}\right) = \frac{\dot{\sigma}}{E[T]} - \dot{T}\frac{\partial}{\partial T}(E[T])\frac{\sigma}{E[T]^2}, \tag{2}$$

where $T = \theta - \theta_0$ is a variable temperature, θ is current temperature, θ_0 is reference temperature (room temperature), and $E[T]$ is the temperature dependent elastic modulus. The inelastic strain rate is a function of overstress, $x = \sigma - g$, the difference between the stress and the equilibrium stress (a state variable),

$$\dot{\varepsilon}^{in} = \frac{x}{\kappa[x, T]}, \tag{3}$$

where $\kappa[x, T] = K[T]k[x, T]$; $K[T]$ is the viscosity factor with the dimension of stress and $k[x, T]$, dimension of time, is the viscosity function employed by Krempl *et al.* [1986]. In that paper the viscosity factor K was set equal to the elastic modulus which is not necessary here and in Lee & Krempl [1988]. The thermal strain rate is

$$\dot{\varepsilon}^{th} = \alpha[T]\dot{T}, \tag{4}$$

where $\alpha[T]$ is a coefficient of thermal expansion, defined as the tangent of the thermal strain-temperature curve. The sum of the elastic and inelastic strain rates is called the mechanical strain rate and is denoted by $\dot{\varepsilon}^{me}$.

The growth law for the equilibrium stress is

$$\dot{g} = \frac{\psi[x, T]}{E[T]}\dot{\sigma} + \dot{T}\frac{\partial}{\partial T}\left(\frac{\psi[x, T]}{E[T]}\right)\sigma + \left(\varphi[x, T] - \frac{|g-f|}{A[T]}\left(\varphi[x, T] - E_t[T]\left(1 - \frac{\psi[x, T]}{E[T]}\right)\right)\right)\frac{\dot{x}}{\kappa[x, T]}, \tag{5}$$

where $\psi[x, T]$ and $\varphi[x, T]$ are shape functions and $\partial/\partial T$ denotes partial temperature derivative. The shape functions ψ and φ, dimension of stress, are not increasing with overstress but their dependence on temperature is not restricted; $\psi[0, T] < E[T]$ and is chosen close to $E[T]$. Further it is required that $\varphi[T] > E_t[T]$. Lee & Krempl [1988] assumed that the elastic growth of the equilibrium stress is path independent and can be approximated by

$$\begin{cases} \dot{g}^{el} \approx \dfrac{d}{dt}\left(\dfrac{\psi[O, T]}{E[T]}\sigma\right) \\ \quad = \dfrac{\psi[0, T]}{E[T]}\dot{\sigma} + \dot{T}\dfrac{\partial}{\partial T}\left(\dfrac{\psi[0, T]}{E[T]}\right)\sigma \end{cases} \tag{6}$$

which explains the formulation given in (5).

The kinematic stress, f, is another state variable. Its evolution equation is

$$\dot{f} = E_t[T]\frac{\dot{x}}{\kappa[x, T]}, \tag{7}$$

where $E_t[T]$ is the tangent modulus of the stress-inelastic strain diagram at the maximum strain of interest.

Properties of the constitutive equation

Eq. (2) and the first two terms on the right hand side of (5) together with (6) ensure the path independence of the elastic deformation and the modeling of elastic regions. Since the latter are important for TVBO the terms containing $\dot{T}$ must appear in (2) and (5). Use of $\dot{T}$ in only one the equations would not allow for the modeling of elastic regions.

The "extra terms" for the present theory are the terms multiplied with $\dot{T}$. They stem from the assumption of path independence of elastic thermomechanical deformation. While this assumption does not appear to be important to others, it leads, within the context of TVBO at least, to terms which are equivalent to the "extra terms" used by others.

For constant strain rate and ultimately constant temperature TVBO admits asymptotic solutions, *see* Cernocky & Krempl [1979] and Sutcu & Krempl [1989] where the isothermal cases are treated. When the asymptotic solution is reached which can happen at small strains, the following relations hold ({ } denotes asymptotic value),

$$\{\dot{\sigma}\} = \{\dot{g}\} = \{\dot{f}\} = E_t[\bar{T}]\{\dot{\varepsilon}^{in}\} \tag{8}$$

where $\bar{T}$ is the ultimately constant temperature. We see that the kinematic variable (7) controls the ultimate slope which can be positive, zero or negative. It can further be shown that

$$\{\sigma - f\} = \{x\} + A[\bar{T}], \tag{9}$$

where

$$\{x\} = \kappa[\{x\}]\dot{\varepsilon}^{me}/(1 + E_t[\bar{T}]/[\bar{T}]) \tag{10}$$

is the asymptotic overstress which is independent of the initial condition and where $A[\bar{T}] = \{g - f\}$ is the rate-independant or plastic contribution to the stress. Examination of (9) and (10) shows that $\{\sigma - f\}$ is independent of temperature history and mechanical history. At a given plastic or total strain when the asymptotic solution (8) holds, the value of the stress σ at the same mechanical strain rate $\dot{\varepsilon}^{me}$ and the same temperature $\bar{T}$ may depend on the temperature history through the temperature dependence of E_t in (7). Since (8) holds always the slopes of the stress-mechanical strain curves are equal and independent of thermomechanical history. The present theory can at most predict a temperature history effect which manifests itself by parallel curves as indicated in Figure 1 *b*. When the tangent modulus E_t is zero no history dependence will be predicted by the present theory.

The formulation given above models cyclic neutral behavior and recovery of state is not included. A cyclic hardening formulation of VBO has been given by Krempl & Yao [1987] and the inclusion of recovery was proposed in the context of an orthotropic theory of VBO by Choi & Krempl [1988]. While these phenomena are important for modeling some elevated temperature properties they are not included in the present paper which is mainly intended to elucidate the role the "extra terms". This can best be achieved with the present version of TVBO. Although we cannot prove that this is the case, the effects of these "extra terms" are expected to be similar when cyclic hardening and/or recovery of state are modeled.

The asymptotic relations do not depend on $\psi[x, T]/E[T]$ or any partial temperature derivatives. The "extra terms" have therefore no bearing on the asymptotic solution. They will affect the nearly elastic behavior and the transition from nearly elastic to the inelastic behavior. Numerical experiments are necessary to eludicate their effect. No analytical representation is possible in the transition region.

Material properties used in the simulations

In the application of TVBO the material functions and constants have to be determined from suitable experiments at constant temperature. The present theory implies that all the properties can be determined from isothermal tests and that the thermal behavior can be obtained by interpolation. There are at the present not enough material data available to check this hypothesis.

TABLE I. — Qualitative properties of the three materials used in the numerical experiments.

Material property	MTL1	MTL2	MTL3
Elastic modulus. E	small (d)	high (d)	same as MTL2
Tangent modulus E_t	small (i)	0	same as MTL2
coef. of thermal exp. α	small (c)	high (i)	same as MTL2
Strength*	high (d)	high (d)	small (i/d)
Rate dependence**	high (i)	small (o)	same as MTL2
$\frac{\partial E}{\partial T}/E^2$	A*	B*	same as MTL2
$\frac{\partial}{\partial T}\left(\frac{\Psi}{E}\right)10^3$	C*	D*	same as MTL2

( ) Indicates variation with increasing temperature; d-decreasing, i-increasing, c-constant.

* As measured by flow stress at a given strain.

** As measured by the asymptotic value of the overstress for $\dot{\varepsilon}_{ss} = 10^{-4}\,s^{-1}$, *see* Eq. (10).

* $A = -75/(10^5 - 75T)^2$. $B = -57.5/(2.31 \times 10^5 - 57.5T)^2$. $C \approx -0.15 + 0.050 \exp(-C_3|x|)$ $(0 \leq T \leq 400$ K); $-0.625 + 0.125 \exp(-C_3|x|)$ $(400 \leq T \leq 800$ K). $D \approx -0.350 + 0.313 \exp(-C_3|x|)$.

The influence of the extra terms on the behavior predicted by TVBO can, however, be ascertained by postulating the material properties.

Some qualitative properties of these hypothetical materials which are close to real materials are listed in Table I. It can be seen that the strength (as measured by the stress level of the stress-strain diagram) decreases for MTL1 and MTL2 with temperature. Such a behavior is usually observed. There are cases where the strength increases with temperature before it decreases. The Nickel Aluminides are one such example, see Lee & Krempl [1989], and MTL3 represents this behavior. As indicated in Table I the three materials differ also by their elastic modulus, their coefficient of thermal expansion and their rate-dependence as measured by the asymptotic overstress at a fixed strain rate and at constant temperature. As the overstress increases the rate-dependence increases also. The properties of the three materials are completely determined by the constants listed in Tables II-IV. These properties manifest themselves in stress-strain diagrams when the set of differential equations is integrated for a given stress or strain or thermal history. In the following stress-strain diagrams are displayed to give an indication of the properties of the three materials.

Numerical experiments

All numerical experiments were performed on personal computers using the IMSL routine DGEAR.

TABLE II. — Material constants as a function of temperature for MTL1.

Young's modulus, $E[T]$ (MPa)

$0 \leq T^{*1} \leq 400$ K	$400 \leq T \leq 800$ K
$E = 100{,}000 - 75\ T$	$E = 100{,}000 - 75\ T$

Viscosity function, $\kappa[x, T] = K_1 (1 + |x| K_2)^{-K_3}$

$0 \leq T \leq 400$ K	$400 \leq T \leq 800$ K
$K_1 = 1.0 \times 10^9 - 0.75 \times 10^6\ T$ (MPa's)	$K_1 = 1.0 \times 10^9 - 0.75 \times 10^6\ T$ (MPa's)
$K_2 = 50 + 0.05\ T$ (MPa)	$K_2 = -10 + 0.2\ T$ (MPa)
$K_3 = 15$	$K_3 = 15$

Modified shape function, $\psi[x, T]/E[T] = C_1 + (C_2 - C_1)\ \mathrm{EXP}\ (-C_3 |x|)$

$0 \leq T \leq 400$ K	$400 \leq T \leq 800$ K
$C_1 = 0.8 - 0.125 \times 10^{-3}\ T$	$C_1 = 1.0 - 0.625 \times 10^{-3}\ T$
$C_2 = 0.18 - 0.75 \times 10^{-4}\ T$	$C_2 = 1.15 - 0.5 \times 10^{-3}\ T$
$C_3 = 0.07 - 0.25 \times 10^{-4}\ T$ (MPa^{-1})	$C_3 = 0.092 - 0.8 \times 10^{-4}\ T$ (MPa^{-1})

Shape function, $\varphi[T]$ (MPa)

$0 \leq T \leq 400$ K	$400 \leq T \leq 800$ K
$\varphi = 0.8 \times 10^5 - 75\ T$	$\varphi = 0.75 \times 10^5 - 62.5\ T$

Rate independent contribution to the stress, $A[T]$ (MPa)

$0 \leq T \leq 400$ K	$400 \leq T \leq 800$ K
$A = 500 - 0.5\ T$	$A = 500 - 0.5\ T$

Tangent modulus, $E_t[T]$ (MPa)

$0 \leq T \leq 400$ K	$400 \leq T \leq 800$ K
$E_t = 2{,}500 + 1.25\ T$	$E_t = 2{,}500 + 1.25\ T$

Coefficient of thermal expansion, $\alpha(K^{-1})$

$0 \leq T \leq 400$ K	$400 \leq T \leq 800$ K
$\alpha = 0.2 \times 10^{-5}$	$\alpha = 0.2 \times 10^{-5}$

*1 $T = \theta - \theta_0$, where θ is current temperature and θ_0 is room temperature.

ELASTIC BEHAVIOR

To illustrate the "path-independence" of elastic behavior, the mechanical strain and the temperature histories shown in Figure 2 are used. The responses of MTL1 with additional terms and without additional terms are depicted in Figure 3*a* and Figure 3*b* respectively. [The additional terms are those multiplied by $\dot{T}$ in (2) and (5).] The stress-strain curves at RT (room temperature) and at RT + 800 are also shown. It is clear from a comparison of Figures 3*a* and 3*b* that the additional terms ensure the stress response to reach the RT + 800 isothermal curve as soon as the temperature reaches that value. The ratio of σ/ε follows the temperature dependent elastic modulus. This is not the case in Figure 3*b*, where a delay is observed. Here, the slope of the stress-strain curves follow the temperature variation of the elastic modulus.

Although inelastic strain rates are always present in TVBO, they are extremely small in the quasi-elastic regions. For negligible overstress and therefore inelastic strain rate

TABLE III. — Material constants as a function of temperature for MTL2.

Young's modulus, $E[T]$ (MPa)

$0 \leqq T^{*1} \leqq 600$ K	$600 \leqq T \leqq 800$ K
$E = 231.000 - 57.5\ T$	$E = 231.000 - 57.5\ T$

Viscosity function, $\kappa[x, T] = K_1 (1 + |x|/K_2)^{-K_3}$; $K_1 = E[T] \times K_1^*$

$0 \leqq T \leqq 600$ K	$600 \leqq T \leqq 800$ K
$K_1^* = 39.47 - 0.865 \times 10^{-2}\ T$ (s)	$K_1^* = 39.47 - 0.865 \times 10^{-2}\ T$ (s)
$K_2 = 38.1 + 0.119\ T$ (MPa)	$K_2 = -19.2 + 0.2145\ T$ (MPa)
$K_3 = 20$	$K_3 = 20$

Modified shap function, $\psi[x, T]/E[T] = C_1 + (C_2 - C_1)\ EXP\ (-C_3 |x|)$

$0 \leqq T \leqq 600$ K	$600 \leqq T \leqq 800$ K
$C_1 = 0.68 - 0.35 \times 10^{-3}\ T$	$C_1 = 0.68 - 0.35 \times 10^{-3}\ T$
$C_2 = 0.9 - 0.375 \times 10^{-3}\ T$	$C_2 = 0.9 - 0.375 \times 10^{-4}\ T$
$C_3 = 0.07$ (MPa^{-1})	$C_3 = 0.07$ (MPa^{-1})

Shape function, $\varphi[T]$ (MPa)

$0 \leqq T \leqq 600$ K	$600 \leqq T \leqq 800$ K
$\varphi = 157.080 - 107.875\ T$	$\varphi = 147.420 - 91.775\ T$

Rate independent contribution to the stress, $A[T]$ (MPa)

$0 \leqq T \leqq 600$ K	$600 \leqq T \leqq 800$ K
$A = 520 - 0.587\,5\ T$	$A = 520 - 0.587\,5\ T$

Tangent modulus, $E_t[T]$ (MPa)

$0 \leqq T \leqq 400$ K	$400 \leqq T \leqq 800$ K
$E_t = 0$	$E_t = 0$

Coefficient of thermal expansion, α (K^{-1})

$0 \leqq T \leqq 600$ K	$600 \leqq T \leqq 800$ K
$\alpha = 0.103 \times 10^{-4} + 0.475 \times 10^{-8}\ T$	$\alpha = 0.103 \times 10^{-4} + 0.475 \times 10^{-8}\ T$

*1 $T = \theta - \theta_0$, where is current temperature and θ_0 is room temperature.

the response of TVBO can be approximated by

$$\dot{\varepsilon}^{el} = \frac{d}{dt}\left(\frac{\sigma}{E[T]}\right) \approx \frac{d}{dt}\left(\frac{g}{\psi[0, T]}\right).$$

and this response is verified by Figures 3*a* and 3*b*

The behaviors of MTL2 and MTL3 are similar. However, their elastic regions are small compared to MTL1, and are therefore not graphed.

INELASTIC BEHAVIOR

Although the additional terms are introduced to insure the path-independence of the elastic behavior their influence reaches into the inelastic region as will be demonstrated by examining the response at various temperature rates and strain rates. The responses are dependent on the material properties.

TABLE IV. — Material constants as a function of temperature for MTL3.

Young's modulus, $E[T]$ (MPa)

$0 \leqq T^{*1} \leqq 600$ K	$600 \leqq T \leqq 800$ K
$E = 231{,}000 - 57.5\,T$	$E = 231{,}000 - 57.5\,T$

Viscosity function, $\kappa[x, T] = K_1 (1 + |x|/K_2)^{-K_3}$; $K_1 = E[T] \times K_1^*$

$0 \leqq T \leqq 600$ K	$600 \leqq T \leqq 800$ K
$K_1^* = 39.47 - 0.865 \times 10^{-2}\,T$ (s)	$K_1^* = 39.47 - 0.865 \times 10^{-2}\,T$ (s)
$K_2 = 38.1 + 0.119\,T$ (MPa)	$K_2 = -19.2 + 0.2145\,T$ (MPa)
$K_3 = 20$	$K_3 = 20$

Modified shape function, $\psi[x, T]/E[T] = C_1 + (C_2 - C_1)\,\mathrm{EXP}\,(-C_3|x|)$

$0 \leqq T \leqq 600$ K	$600 \leqq T \leqq 800$ K
$C_1 = 0.68\text{-}0.35 \times 10^{-3}\,T$	$C_1 = 0.68 - 0.35 \times 10^{-3}\,T$
$C_2 = 0.9 - 0.375 \times 10^{-4}\,T$	$C_2 = 0.9 - 0.375 \times 10^{-4}\,T$
$C_3 = 0.07$ (MPa^{-1})	$C_3 = 0.007$ (MPa^{-1})

Shape function, $\varphi[T]$ (MPa)

$0 \leqq T \leqq 600$ K	$600 \leqq T \leqq 800$ K
$\varphi = 157{,}080 - 107.875\,T$	$\varphi = 147{,}420 - 91.775\,T$

Rate independent contribution to the stress, $A[T]$ (MPa)

$0 \leqq T \leqq 600$ K	$600 \leqq T \leqq 800$ K
$A = 90 + 0.658\,T$	$A = 800 - 0.525\,T$

Tangent modulus, $E_t[T]$ (MPa)

$0 \leqq T \leqq 400$ K	$400 \leqq T \leqq 800$ K
$E_t = 0$	$E_t = 0$

Coefficient of thermal expansion, α (K^{-1})

$0 \leqq T \leqq 600$ K	$600 \leqq T \leqq 800$ K
$\alpha = 0.103 \times 10^{-4} + 0.475 \times 10^{-8}\,T$	$\alpha = 0.103 \times 10^{-4} + 0.475 \times 10^{-8}\,T$

*1 $T = \theta - \theta_0$, where θ is current temperature and θ_0 is room temperature.

(i) *Monotonic straining and temperature cycling*

The imposed history consists of monotonic straining at a constant mechanical strain rate of $10^{-5}\,s^{-1}$ and temperature cycling at a rate of ± 8 K/s as depicted in Figure 4.

The responses of the three materials with additional terms and without additional terms are given in Figures 5A-5C together with the isothermal stress-strain curves performed at the strain rate of $10^{-5}\,s^{-1}$. Since the temperature dependence is monotone for MTL1 and MTL2, the stress-strain curves at the temperature extremes are shown. The highest strengh is reached at RT + 600 for MTL3 and this isothermal stress-strain diagram is graphed in addition to those at the minimum and maximum temperature for MTL3 in Figure 5C.

Comparing the isothermal curves it is evident that the tangent modulus E_t is zero for MTL2 and MTL3 whereas it is positive for MTL1. This observation is also an indication that the asymptotic solutions have been reached on the graphs.

The additional terms have a significant effect on the response of MTL1 but their influence on the behavior of MTL2 and MTL3 is surprisingly small. In none of the cases

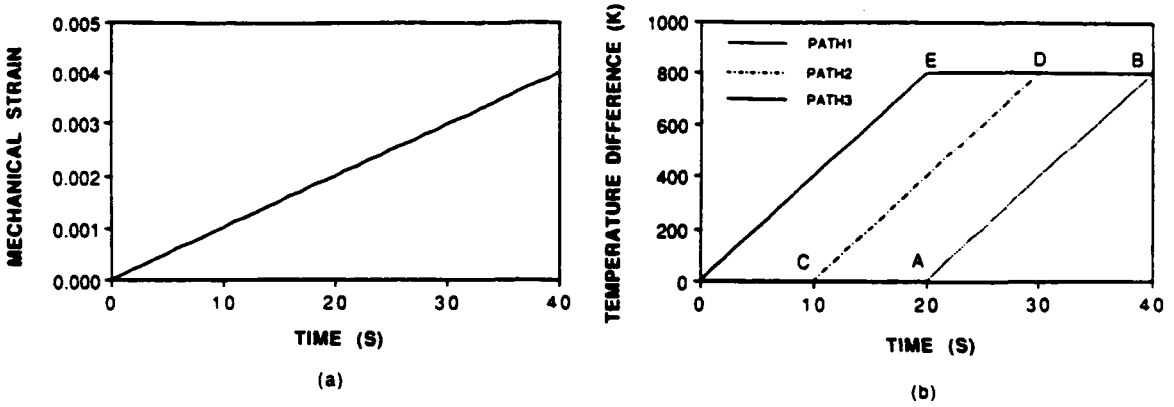

Fig. 2. Imposed mechanical strain (*a*) and temperature (*b*) histories. OAB – PATH 1. OCDB – PATH 2. OEB – PATH 3.

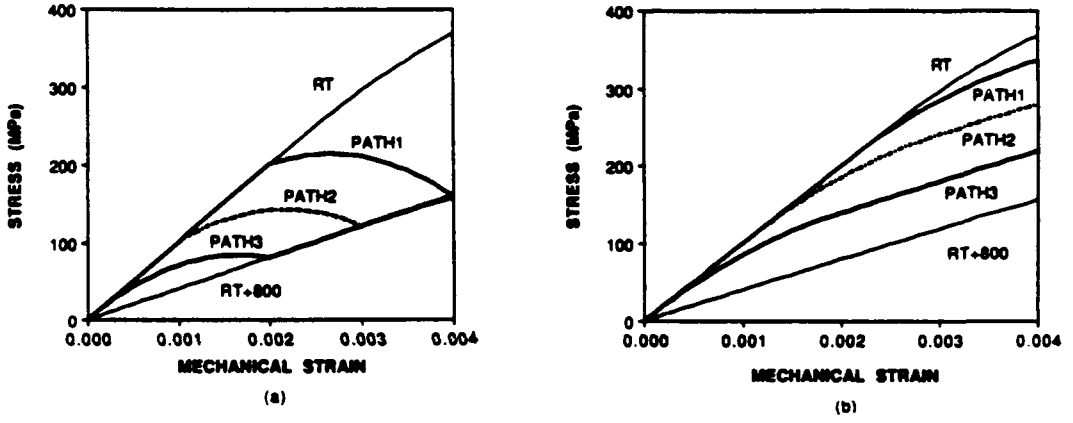

Fig. 3. – Nearly elastic behavior for constant temperature (RT and RT + 800) and responses to the temperature paths of Figure 2*b*. Figure 3*a* shows the responses with additional terms. In Figure 3*b* the additional terms are omitted which results in a considerable delay in reaching the isothermal curve RT + 800.

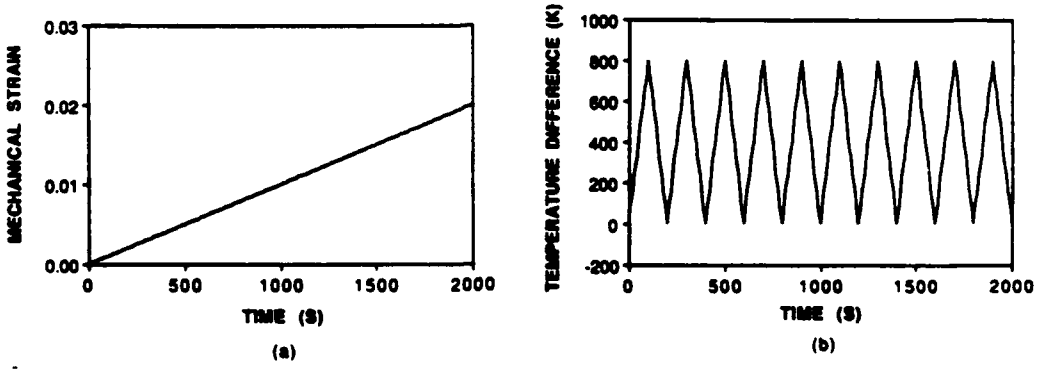

Fig. 4. – Imposed mechanical strain (*a*) and temperature (*b*) histories.

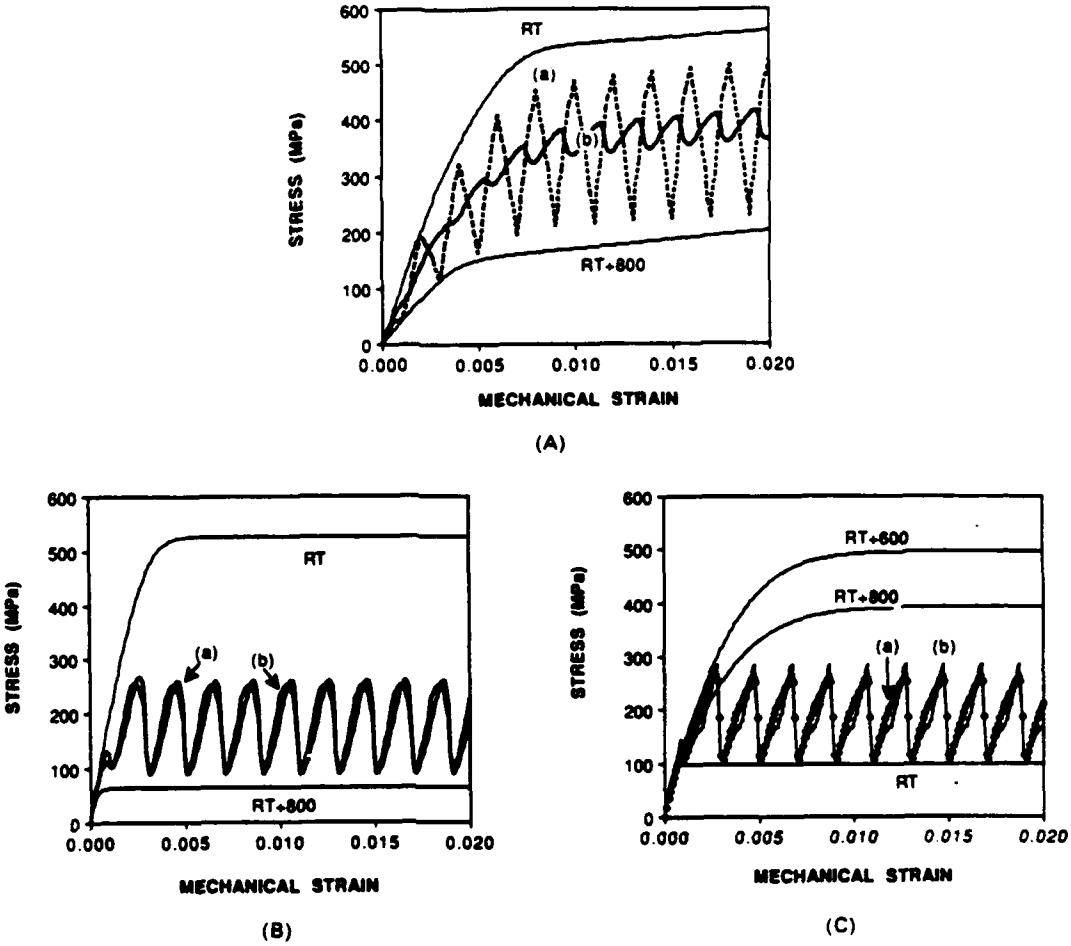

Fig. 5. – Isothermal responses at RT and at RT + 800 and response to the thermomechanical history of Figure 4. Curve *a* depicts the response with additional terms. The response without additional terms is designated by *b*. MTL1 (A); MTL2 (B); MTL3 (C).

the stress-strain curves at the temperature extremes are exactly reached. The variable temperature curve (*a*) in Figure 5A, however, comes close to them.

When the temperature cycle is altered to include 400 s hold times at either extremes, the curves with and without the additional terms reach the stress-strain curves at the temperature extremes for the three materials. These observations show that there is a time delay built into the constitutive equations and that sufficient time must be allowed for the attainment of the asymptotic response. Details are to be found in Lee [1989]. Again the response of MTL1 is sensitive to the additional terms but this is not true for the responses of MTL2 and MTL3.

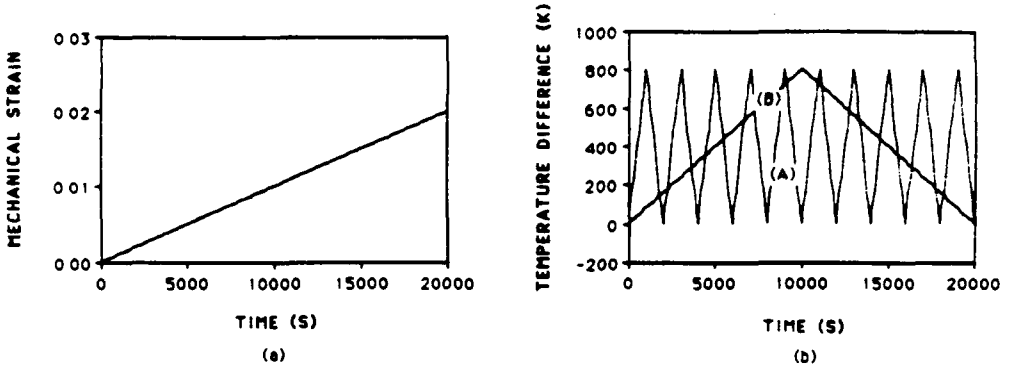

Fig. 6. – Imposed mechanical strain (*a*) and temperature (*b*) histories.

(ii) *Effect of strain and temperature rate*

For the next set of experiments the strain rate was reduced by one order of magnitude to $10^{-6}s^{-1}$. The temperature rate which is now set to 0.8 K/s (A) or to 0.08 K/s (B) is depicted in Figure 6.

The responses of the three materials are graphed in Figures 7*a* through 7*c*. Since the effect of the omission of the additional terms has been shown already in Figures 5*a* through 5*b* only the responses with the additional terms are shown.

By comparing the respective isothermal curves in Figures 5 and 7 the influence of rate can be ascertained. It differs from material to material.

Since the ratio of strain rate to temperature rate remains constant and equals that of Figure 5 for the fast temperature rate (A), no basic difference in the response curves was expected and the numerical experiments bear out this expectation. When the temperature rate is reduced, temperature history B in Figure 6, more time is available to approach the asymptotic solution and the isothermal stress-strain curves are nearly reached for the three materials. The wavy behavior of curve B in Figure 7*c* is due to the unusual temperature dependence of the strength.

Omitting the additional terms would not change the observation of the frequency effect but would maintain the differences between MTL1 and MTL2 on the one hand and MTL3 on the other as shown in Figure 5.

The numerical experiments demonstrate that the solutions tend to approach the asymptotic solutions but sufficient time is needed so this can happen. The additional terms have no influence on the asymptotic solution but can strongly influence the transient behavior.

(iii) *Cyclic loading*

The theory presented here models cyclic neutral behavior and a closure of the hysteresis loop is expected for the isothermal case. In thermal cycling the situation may be different and consequently some numerical experiments are performed using the loading conditions

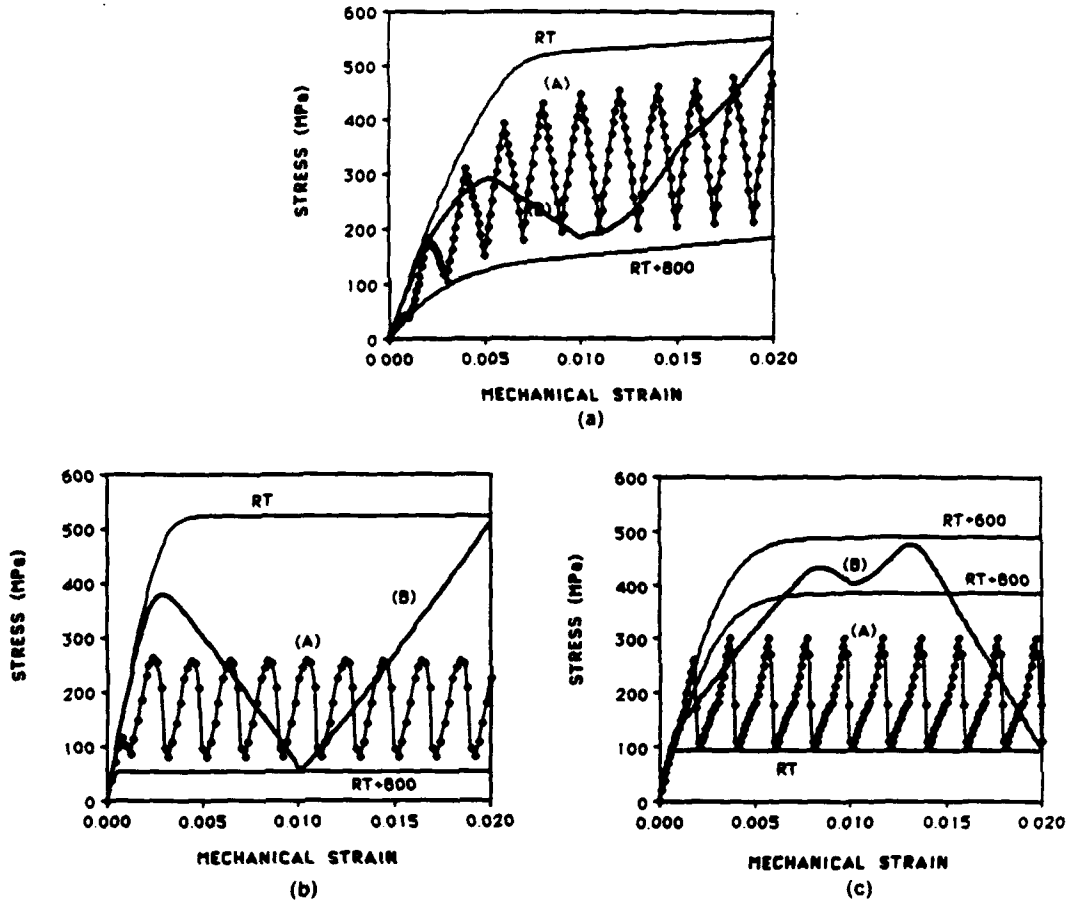

Fig. 7. – Isothermal responses at RT and at RT + 800 and response to the thermomechanical history of Figure 6. Curves A and B show the response to the respective temperature history of Figure 6*b*. MTL1 Figure 7*a*; MTL2 Figure 7*b*; MTL3 Figure 7*c*.

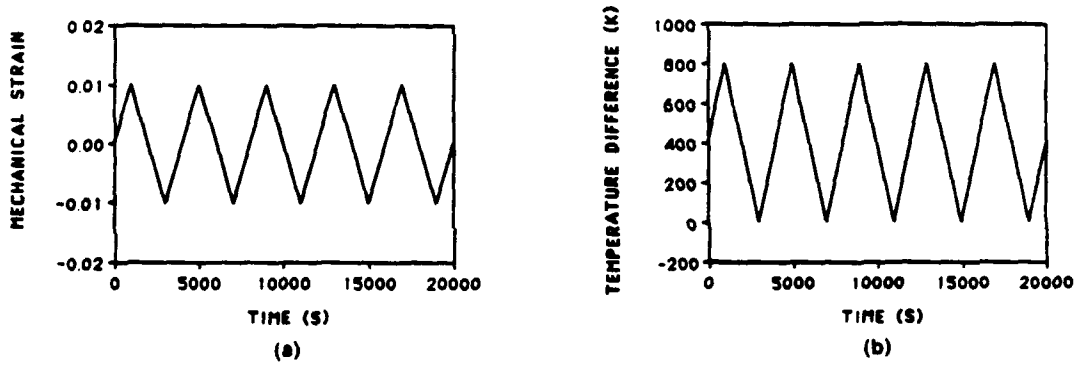

Fig. 8. – Imposed mechanical strain (*a*) and temperature (*b*) histories (In-phase thermal cycling).

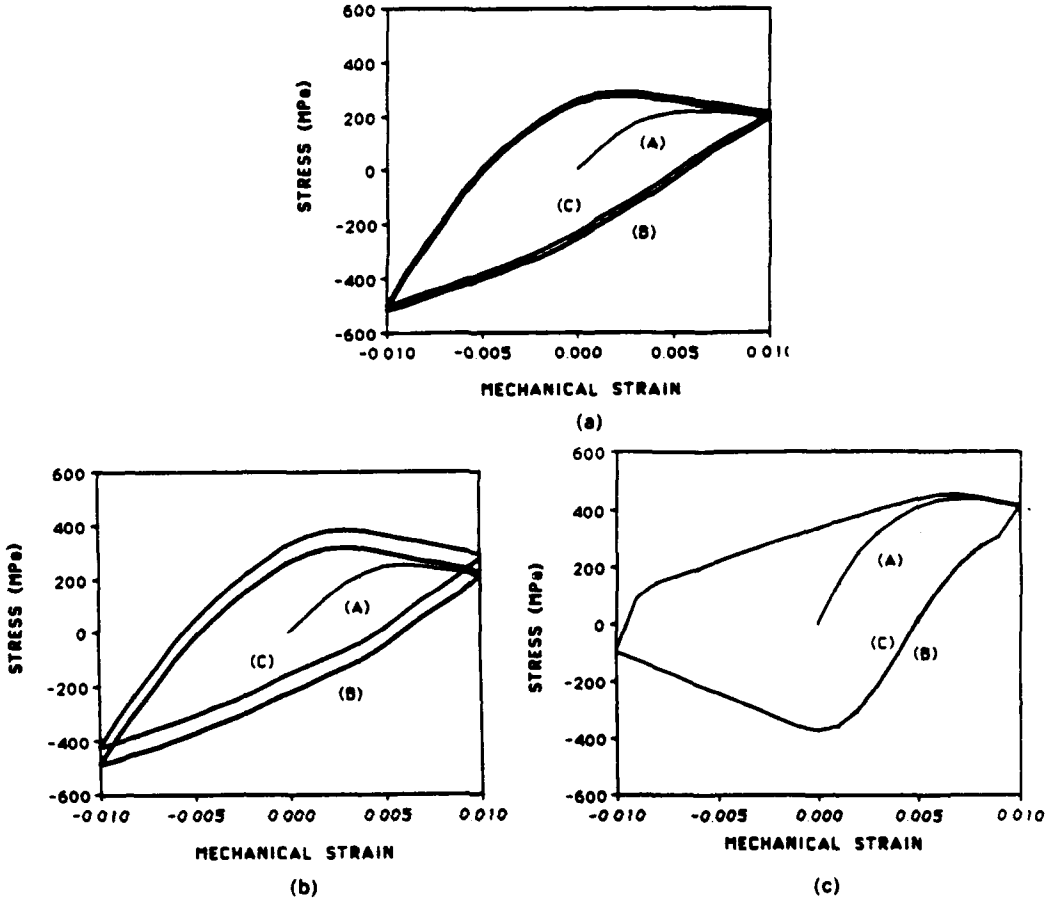

Fig. 9. – Response to thermomechanical history of Figure 8. First quarter cycle A; first cycle B; fifth cycle C. MTL1 with additional terms (*a*); MTL1 without additional terms (*b*); MTL3 with additional terms (*c*).

depicted in Figure 8. Since temperature and strain increase simultaneously the loading corresponds to in-phase cycling.

The response of MTL1 with and without additional terms is depicted in Figures 9*a* and 9*b*, respectively for the first five cycles. It is seen that the loops do not close and that the shift of the loops is larger without the additional terms than with them. Surprisingly no such shift is observed for MTL2 and MTL3. For these materials the loop closes after the first cycle. The hysteresis loop for MTL3 is depicted in Figure 9*c*.

Discussion

General

The numerical experiments confirm the theoretical predictions regarding the behavior in the quasi-elastic region. With the path-independent formulation of the elastic strain rates the response curves follow the temperature path immediately. Stress and strain

reach their respective values as soon as the temperature does. This is clearly demonstrated in Figure 3 *a*.

The asymptotic behavior is independent of the extra terms and can be independent of the temperature history. This property becomes only apparent when there is sufficient time for the asymptotic solution to develop. The temperature rate is too fast in relation to the mechanical strain rate in Figure 5 and the asymptotic solution is not reached. It is almost reached for the slow temperature change, curve B in Figure 7. When 400 s temperature holds are included at the temperature extremes in Figure 4 *b*, as it was done by Lee [1989], the absence of a temperature history effect is clearly demonstrated for MTL2 and MTL3, *see* Figures 4.16 and 4.17 of Lee [1989], respectively. For MTL1 the 400 s hold-time is not enough to react on the asymptotic solutions. Moreover, since $E_t \neq 0$ for this material a temperature history effect equivalent to that shown in Figure 1 *b* could be modeled.

The influence of additional terms vanishes if either the temperature rate is zero or if all the relevant constants do not depend on temperature. These terms were shown to be essential for modeling path independence in the quasi elastic regions and to influence the transition from this region to fully inelastic behavior. The asymptotic behavior is, however, not affected by these terms. At a constant mechanical strain rate and an ultimately constant temperature the asymptotic slope of the stress-mechanical strain curve will be independent of prior history.

The numerical experiments also show that the TVBO is capable of modeling very complex temperature dependence such as that of MTL3. At the same time general features of the equations are maintained. The existence of asymptotic solutions is one example.

With different constants and different material functions $k[x]$, $\psi[x]$ and $\varphi[x]$ different shapes of the stress-strain curves and different temperature dependencies can be modeled. In an application the material constants and functions must be determined from isothermal experiments at different temperatures. This presupposes that the real material does not exhibit a temperature history effect. The data reported by Chan & Lindholm [1990] seem to exhibit this property.

The additional terms have a significant effect on the transition from quasi elastic to inelastic behavior for MTL1 but their influence for MTL2 and MTL3 is small, see Figure 5. The reason for this difference seems to lie in the different temperature dependence of the elastic modulus and of the ψ-function. It can be seen from Table I that the extra terms $(\partial E/\partial T)/E^2$ and $(\partial/\partial T)(\psi/E)$ are smaller for MTL2 than for MTL1 for small overstress x. If it is assumed that the most significant effects are in the elastic region (when x is small), the absence of a major influence of the extra terms for MTL2 and MTL3 is explained.

It is of interest to ascertain under what conditions the extra terms will have an influence. While it is difficult to make a precise statement the relevant equations can be

obtained easily as

$$\dot{\varepsilon}^{el} = \left(\dot{\sigma} - \dot{T}\sigma \frac{\partial E}{\partial T} \Big/ E\right) \Big/ E \quad \text{and} \tag{11}$$

$$\dot{g}^{el} \approx \frac{\psi}{E}\left(\dot{\sigma} + \dot{T}\sigma\left(\frac{\partial \psi}{\partial T} \Big/ \psi - \frac{\partial E}{\partial T} \Big/ E\right)\right) \tag{12}$$

where ψ has to evaluated at negligible overstress. It can be seen that the product of temperature rate time stress times the temperature derivatives of the material properties over the respective properties has to be significant relative to the stress rate for the extra terms to be influential. It is also of interest to note that the major influence of the terms comes through Eq. (11). Usually the temperature dependences of E and ψ have the same trend and the contributions of E and ψ in Eq. (12) tend to compensate each other. (To ensure the existence of the quasi elastic regions $\psi[0, T]$ should be less than but close to the elastic modulus $E[T]$.) On the basis of these expressions it is possible to get an estimate of the significance of the extra terms. For a material which has a strong temperature dependence of elastic modulus the effect is most likely to be significant.

It is also evident that the extra terms make the response stiff, especially the transition from the elastic to the inelastic region. This property was deemed desirable, Walker [1981] and NASA [1984]. A comparison of the prediction of the theory with thermomechanical tests is necessary to ascertain the modeling capabilities of VBO.

Cyclic mechanical strain and temperature

Under isothermal conditions the present theory represents cyclic neutral behavior and the hysteresis loop closes after one cycle. Suprisingly a shift of the in-phase thermomechanical hysteresis loop is observed for MTL1 in Figures 9*a* and 9*b*. The shift is more pronounced when the additional terms are absent (*Fig.* 9*b*) than when they are present (*Fig.* 9*a*). In Figure 9*a* the shift is most likely produced by a net contribution per cycle of the kinematic variable f when (7) is integrated. This hypothesis seems to be confirmed when Figure 9*a* is compared with Figure 9*c* where no shift is observed for MTL3 for which $E_t = 0$. The strain range in the cyclic test is such that the asymptotic solution is not reached for MTL1 at RT and for MTL3 at the maximum temperature (see the stress-strain diagrams in *Figs.* 5*a* and 5*c*). As a consequence the cycle loading takes place within the transient region and a net contribution can remain after a cycle which then accumulates from cycle to cycle. It is not expected that a stable hysteresis loop will be reached for MTL1.

It has been shown that the additional terms make the response of TVBO stiff. This fact may explain the larger shift observed in Figure 9*b* compared to Figure 9*a*. The shift consists only of the E_t contribution of Figure 9*a* (the additional terms are absent.). Since the additional terms where shown to be unimportant for MTL3 their omission is not expected to produce a significant shift of the hysteresis loop in Figure 9*c*.

It should be mentioned that the shift does not necessarily have to be in the direction of positive stress as is the case in Figures 9*a* and 9*b*. A different set of material constants could conceivably cause a shift in the direction of negative stress.

The effect of strength increases with temperature is clearly evident from the shape of the hysterexis lop in Figure 9*c*. A considerably higher stress level is reached upon heating with MTL3 than with MTL1. On the other hand MTL3 yields upon cooling down whereas almost linear behavior is shown for MTL1.

Acknowledgement

This research was supported by DARPA/ONR Contract N000014-86-K0770 with Rensselaer Polytechnic Institute. Mr. S. H. Choi helped in the preparation of the manuscript.

APPENDIX

To compare the growth law for the equilibrium stress in the present theory with one in [Krempl *et al.*, 1986], the isothermal uniaxial equation in (5) is reduced to the isothermal one,

$$\dot{g} = \frac{\psi[x]}{E}\dot{\sigma} + \left(\varphi[x] - \frac{|g-f|}{A}\left(\varphi[x] - E_t\left(1 - \frac{\psi[x]}{E}\right)\right)\right)\frac{x}{\kappa[x]}. \tag{A-1}$$

The isothermal growth law for the equilibrium stress obtained after same algebra from [Krempl *et al.*, 1986] is

$$\dot{g} = \frac{2(1+\nu)}{3}\frac{\psi[x]}{E}\dot{\sigma} + \psi[x]\frac{x}{\kappa[x]} - \frac{(g-f)}{A^*}(\psi[x] - E_t^*)\frac{|x|}{\kappa[x]}. \tag{A-2}$$

In the present paper the tangent modulus E_t is defined with respect to the inelastic strain and A is defined as the asymptotic value of $\{g-f\}$. These quantities are related to E_t^* and A^* defined on the basis of total strain by $E_t^* = E_t/B$ and $A^* = A/B$, respectively, with $B = (1 + E_t/E)$.

Once substitution is made (A − 1) and (A-2) are similar except for the following. $\varphi[x]$ and $|g-f|$ and x are used in (A-1) whereas $|x|$ and $(g-f)$ are employed in (A-2). The function $\varphi[x]$ can be set equal to $\psi[x]$ without changing the initial elastic and the asymptotic properties; it was necessary because of invariance requirements in the orthotropic formulation (*see* [Lee, 1989]. Switching the absolute signs from x to $g-f$ was initially proposed by Sutcu [1985] to facilitate the orthotropic formulation. He showed that there was no essential change in the uniaxial modeling capabilities. A similar change has been implemented in the context of rate independent plasticity by Burlet & Cailletaud [1987].

In [Yao & Krempl, 1985] no distinction was made between elastic and inelastic Poisson's ratio. The new theory considers separate constant elastic and inelastic Poisson's ratios. Setting $\nu = 1/2$ reduces the first factor in (A-2) equal to unity.

The purpose of f, the kinematic variable, is to set the asymptotic tangent modulus. Yao & Krempl [1985] and Krempl *et al.* [1986] used a algebraic expression based on

total strain. Here, (7) is incremental on the basis of inelastic strain rate. This formulation is advantageous for the thermal case. For the isothermal case both formulations are equivalent.

REFERENCES

BURLET H., CAILLETAUD G., 1987, Modeling of cyclic plasticity in finite element codes, *Constitutive Laws for Engineering Materials: Theory and Applications*, C. S. Dsai *et al.* Eds., Elsevier Applied Science, New York, NY, 1157.

CAILLETAUD G., CHABOCHE J. L., 1979, Macroscopic description of the microstructural changes induced by varying temperature, Example of IN 100 Behavior, T. P. ONERA No. 1979-112.

CERNOCKY E. P., KREMPL E., 1979, A non-linear uniaxial integral constitutive equation incorporating rates effects, creep and relaxation, *Int. J. Non-Linear Mech.*, **14**, 183-203.

CERNOCKY E. P., KREMPL E., 1980, A theory of thermoviscoplasticity based on infinitesimal total strain, *Int. J. Sol. Str.*, **16**, 723-741.

CHABOCHE J. L., 1986, Time-independent constitutive theories for cyclic plasticity, *Int. J. Plastic.*, **2**, 149-188.

CHABOCHE J. L., 1989, Constitutive equations for cyclic plasticity and cyclic viscoplasticity, *Int. J. Plastic.*, **5**, 247-302.

CHAN K. S., LINDHOLM U. S., 1990, Inelastic deformation under non-isothermal loading, *J. Engng. Mtls Tech.*, **112**, 15-25.

CHOI S. H., KREMPL E., 1988, Modeling of short-term time-dependent deformation behavior of a nickel based single crystal at high temperature using the orthotropic viscoplasticity theory based on overstress, *Rensselaer Polytechnic Institute Report MML* 88-10.

FREED A. D., 1988, A thermoviscoplastic model with application to copper, *NASA TP*-2845.

KREMPL E., 1981, Plasticity and variable heredity, *Arch. Mech.*, **33**, 289-306.

KREMPL E., MCMAHON J. J., YAO D., 1986, Viscoplasticity based on overstress with a differential growth law for the equilibrium stress, *Mech. Mater.*, **5**, 35-48.

KREMPL E., YAO D., 1987, The viscoplasticity theory based on overstress applied to ratchetting and cyclic hardening, *Low-Cycle Fatigue and Elasto-Plastic Behavior of Materials*, K. T. Rie Ed., Elsevier Applied Science Publishers, 137-148.

LEE K. D., KREMPL E., 1988, An orthotropic theory of viscoplasticity based on overstress for thermomechanical deformations, *Rensselaer Polytechnic Institute Report MML* 88-2, to appear *Int. J. Solids Struct.*

LEE K. D., KREMPL E., 1990, Thermomechanical, time-dependent analysis of layered metal matrix composites, *Thermal and Mechanical Behavior of Ceramic and Metal Matrix Composites, ASTM STP* 1080, J. M. Kennedy and W. S. Johnson Eds., American Society of Testing and Materials, Philadelphia, 40-55.

LEE K. D., 1989, *An orthotropic theory of viscoplasticity based on overstress for thermomechanical deformation and its application to laminated metal matrix composites, Ph. D. Dissertation*, Rensselaer Polytechnic Institute, Troy, NY.

MORENO V. and JORDAN E. H., 1986, Prediction of material thermomechanical response with a unified viscoplastic model, *Int. J. Plastic.*, **2**, 223-245.

NASA, 1986, Nonlinear constitutive relations for high temperature applications, *Proceedings. NASA Conference Publication* 10010.

NIITSU Y., IKEGAMI K., 1988, *Effect of temperature variation on cyclic elastic-plastic behavior of* 304 *stainless steel*, in PVP-Vol 141, D. Hui and T. J. Kozik Eds., American society of Mechanical Engineers, New York, NY, 49-54.

NISHIGUCHI I., SHAM T. L., KREMPL E., 1989, A finite deformation theory of viscoplasticity based on overstress, *J. Appl. Mech.*, **57**, 548-561.

OHNO N., TAKAHASHI Y., KUWABARA K., 1988, Constitutive modeling of cyclic plasticity of 304 stainless steel under temperature variation, Proc. of Mecamat, Conference held at Besançon, France, August 30-September 1, 1988, Oytana C. *et al.* Eds., V303-V317.

SUTCU M., 1985, An orthotropic formulation of the viscoplasticity theory based on overstress, *Ph. D. Dissertation*, Rensselaer Polytechnic Institute, Troy, NY.

SUTCU M., KREMPL E., 1989. A stability analysis of the uniaxial viscoplasticity theory based on overstress. *Comp. Mech.*, **4**, 401-408.

YAO D., KREMPL E., 1985. Viscoplasticity theory based on overstress. The prediction of monotonic and cyclic proportional and nonproportional loading paths of an aluminium alloy. *Int. J. Plastic.*, **1**, 259-274.

WALKER K. P., 1981. Research and development program for nonlinear structural modeling using advanced time-temperature dependent constitutive relations. *NASA Reort CR*-165533.

(Manuscript received April 2, 1990;
accepted July 11, 1990.)

A Numerical Simulation of the Effects of Volume Fraction, Creep and Thermal Cycling on the Behavior of Fibrous Metal-Matrix Composites

NAN-MING YEH AND ERHARD KREMPL
Mechanics of Materials Laboratory
Rensselaer Polytechnic Institute
Troy, NY 12180-3590

(Received September 10, 1990)
(Revised May 14, 1991)

ABSTRACT: A previously derived cyclic neutral thermoviscoplasticity theory for fibrous metal-matrix composites (Yeh and Krempl [1]), which combines the vanishing fiber diameter (VFD) model with the thermoviscoplasticity theory based on overstress (TVBO) is specialized for transversely isotropic, thermoelastic fibers and an isotropic, thermoviscoplastic matrix. Numerical experiments are used to illustrate the predictive capability of the theory. Simulations include the influence of volume fraction on the monotonic and cyclic loading behavior in the fiber and transverse directions with creep holds for B/Al and B/Ti unidirectional composites and thermal cycling of B/Al. The three-dimensional theory permits the calculation of the actual Poisson's ratio in the tests. The results compare favorably with sparsely available experimental results.

INTRODUCTION

METAL-MATRIX COMPOSITES are intended for use in structural applications under constant and variable temperature. In applications the deformation behavior must be known so that the lifetime of a component can be calculated before it is being built. To this end various theoretical and experimental investigations have been performed which are referred to by Yeh and Krempl [1,2].

Unified theories of time (rate)-dependent material deformation behavior have been proposed recently. In these theories creep and plasticity are not separately accounted for. The thermoviscoplasticity theory based on overstress (TVBO) derived by Lee and Krempl [3] offers the advantages of a unified theory. It has been combined with a simple composite model, the vanishing fiber diameter model (VFD) by Yeh and Krempl [1,2] and permits the simulation of observed rate dependence in metals and alloys which includes strain rate effects and hold-times with creep and relaxation. It is simple to use and can be exercised on a PC since

Reprinted from *Journal of* COMPOSITE MATERIALS, *Vol. 26, No. 6/1992*

it only requires the integration of ordinary differential equations. In this way general features can be explored with ease. If needed more sophisticated micromechanics models can be employed to increase the accuracy of the composite analysis.

The purpose of this paper is to perform numerical experiments using a previously developed composite model [1]. The experiments explore the influence of fiber volume fraction c^f on monotonic and cyclic behavior, the effect of creep hold-periods in the fiber and transverse directions and the behavior of B/Al under thermal cycling without constraint. Actual Poisson's ratios are derived and shown to be influenced by the change from monotonic to creep loading.

MATERIAL AND COMPOSITE MODEL

The composite model developed by Yeh and Krempl [1] which combines the TVBO [3] and the VFD of Reference [4] is used in the numerical experiments of this paper. The fiber is transversely isotropic thermoelastic with the matrix idealized by the isotropic, incompressible, cyclic neutral TVBO. Following Reference [1] the fiber direction is the 3-direction with the 1- and 2-axes denoting the transverse directions. The volume fractions of fiber and matrix are c^f and c^m, respectively. As usua. σ and ϵ denote the stress and small strain vectors, respectively. Quantities with no superscript denote stresses or strains applied to the composite. Matrix and fiber quantities are identified by the appropriate superscripts. Details of the theory and its derivation can be found in Reference [1].

To perform numerical calculation the material constants of Equations (11)–(14) in Reference [1] must be known. For specific B/Al and B/Ti composites a complete set of data are not available. Consequently "plausible" properties were postulated. Literature data for the thermoelastic boron fiber were used or assumed (see Table 1). The data for Al and the Ti matrices are from tests on related monolithic materials by Yao and Krempl [5] and Krempl et al. [6], respectively. The material constants listed in Tables 2 and 3 give rise to the mechanical properties which resemble typical matrix properties. However, they are not the exact

Table 1. Elastic properties for boron fibers.

Properties	B	
E'_{33} (MPa)	413,400	*
ν'_{31}	0.21	*
G'_{44} (MPa)	170,830	**
α'_3 (m/m/°C)	6.3E – 6	†
α'_1 (m/m/°C)	6.3E – 6	†
E'_{11} (MPa)	413,400	*
G'_{66} (MPa)	170,830	**

*Kreider and Prewo [12].
**Estimate.
†Tsirlin [13].

Table 2. Thermoelastic and thermoviscoplastic properties of the Al matrix.

$E^m = 74{,}657[1 - (T/933)^3]$ (MPa)*

$\nu^m = 0.33$**

$G^m = 28{,}066[1 - (T/933)^3]$ (MPa)*

$\alpha^m = 2.35\text{E-}5 + 2.476\text{E-}8(T - 273)$ (m/m/°C)**

$q^m[\Gamma^m] = \Psi^m[\Gamma^m]/E^m \qquad p^m = E_t^m/K^m$

Viscosity Function: $k^m[\Gamma^m] = k_1[1 + (\Gamma^m/k_2)]^{-k_3}$

$k_1 = 314{,}200$ (s) $\qquad k_2 = 71.38$ (MPa)†
$k_3 = 53 - 0.05(T - 273)$**†

Viscosity Factor: $K^m = E^m$

$E_t^m = 619[1 - (T/933)^3]$ (MPa)**

$A^m = 72.24[1 - (T/933)^3]$ (MPa)**

Shape Function: $\Psi^m[\Gamma^m] = c_1 + (c_2 - c_1)\exp(-c_3\Gamma^m)$

$c_1 = 16{,}511[1 - (T/933)^3]$ (MPa)**

$c_2 = 73{,}910[1 - (T/933)^3]$ (MPa)**

$c_3 = 8.43\text{E-}2 + 1.06\text{E-}4(T - 273) + 1.914\text{E-}6(T - 273)^2$

$+ 5.304\text{E-}9(T - 273)^3$ (MPa^{-1})**

Inelastic Poisson's Ratio: 0.5

T = K $\qquad 153\text{ K} < T < 933\text{ K}$

*Estimate. Temperature dependence due to Hillig [14].
**Estimate.
†Yao and Krempl [5].

Table 3. Thermoelastic and thermoviscoplastic properties of the Ti alloy matrix.

$E^m = 132{,}848.4 - 38.96T$ (MPa)*,**

$\nu^m = 0.31$**

$G^m = 50{,}705.5 - 14.87T$ (MPa)*,**

$\alpha^m = 8.4\text{E-}6$ (m/m/°C)**

$q^m[\Gamma^m] = \Psi^m[\Gamma^m]/E^m \qquad p^m = E_t^m/K^m$

Viscosity Function: $k^m[\Gamma^m] = k_1[1 + (\Gamma^m/k_2)]^{-k_3}$

$k_1 = 314{,}200$ (s)* $\qquad k_2 = 117$ (MPa)*

$k_3 = 18.646 - 0.0073(T - 273)$*,**

Viscosity Factor: $K^m = E^m$

$E_t^m = 1270.4 - 0.4792T$ (MPa)*,**

$A^m = 856.55 - 0.591T$ (MPa)*,**

Shape Function: $\Psi^m[\Gamma^m] = c_1 + (c_2 - c_1)\exp(-c_3\Gamma^m)$

$c_1 = 88{,}987.5 - 37.5T$ (MPa)*,**

$c_2 = 131{,}438 - 38.546T$ (MPa)*,**

$c_3 = 0.0205 + 4.59\text{E-}4(T - 273)$ (MPa^{-1})*,**

Inelastic Poisson's Ratio: 0.5

T = K $\qquad 293$ K $< T <$ 773 K

*Krempl et al. [6].
**Estimate.

model of a specific composite. The temperature dependence of the inelastic stress-strain behavior of Al was assumed and is illustrated in Figure 1 of Reference [2]. The results presented hereafter are believed to represent typical general behavior of B/Al and B/Ti composites.

NUMERICAL EXPERIMENTS

The IMSL routine DGEAR is used to integrate the set of nonlinear coupled, first order differential equations under appropriate initial and boundary conditions.

Volume Fraction and Rate Effects in B/Al and B/Ti

Although generally not appreciated, inelastic deformation behavior of metals and alloys can be rate dependent at room temperature. This fact has been considered in the TVBO model which is based on observed behavior. As a consequence rate effects, creep and relaxation are predicted in the inelastic range at room temperature.

Uniaxial tests are simulated where the overall strain rate is kept constant except for a 300 s creep period with constant stress introduced at the maximum strain of 0.5%. Tests in the fiber and transverse directions are performed to study the influence of strain rate and volume fraction on the behavior in the straining directions and Poisson's effects.

For a constant strain rate the influence of fiber volume fraction on the stress-strain behavior in the fiber direction and the development of the transverse strain ϵ_1 are depicted in Figures 1 and 2, respectively. As expected the B/Ti composite is, at a given volume fraction, stronger than the B/Al. It is also observed that the creep strain accumulated during 300 s increases with decreasing fiber volume fraction and is larger for B/Ti than for B/Al. For most of the straining B/Al develops a larger absolute value of the transverse strain than B/Ti. As the fiber volume fraction becomes smaller the Poisson's effect increases for both composites. The actual Poisson's ratio which is the slope of the curves in Figure 2 changes at the transition to the creep period.

The curves in Figure 1 are somewhat nonlinear and their nonlinearity increases with decreasing fiber volume fraction. They are affected by the load transfer between matrix and fiber and the yielding behavior of the matrix. The curve for $c^f = 0.1$, B/Al in Figure 1 shows initial yielding around 0.1%. At this strain the matrix starts to yield as shown in Figure 3 and this yielding causes the overall stress-strain curve to bend over. Figure 3 also reveals that the matrix stress and equilibrium stress decrease during creep. Since the matrix overstress $\sigma_3^m - g_3^m$ decreases also transient or primary creep is modeled. This matrix overstress is the driving force of the rate dependence within TVBO.

Due to the matrix dominated behavior, the rate effects are most pronounced in the transverse direction. Results are shown in Figures 4–6. As expected the B/Ti composite shows higher strength and a greater rate sensitivity than B/Al. But the B/Al composite exhibits a greater creep strain accumulation than the B/Ti. As the prior strain rate increases the accumulated creep strain in 300 s increases also for

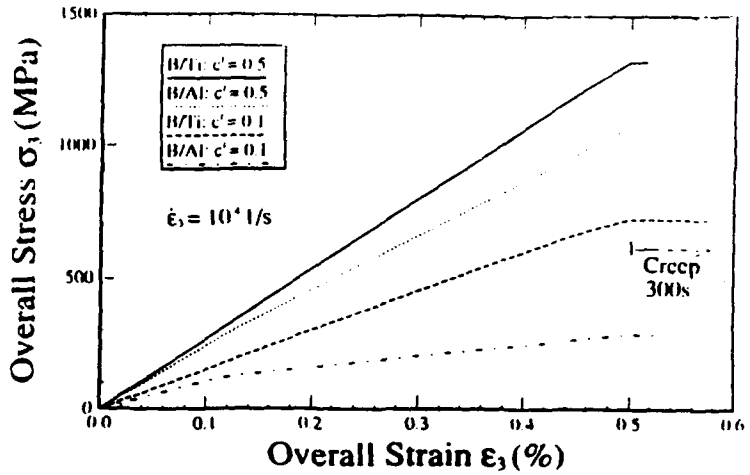

Figure 1. Overall stress-strain curves in the fiber direction of B/Al and B/Ti with different volume fractions. A 300 s creep period is performed at the maximum stress.

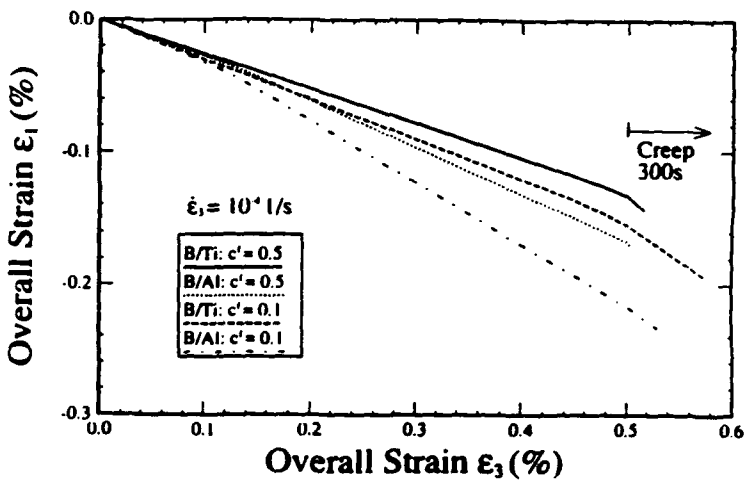

Figure 2. The development of the transverse strain during the tests shown in Figure 1.

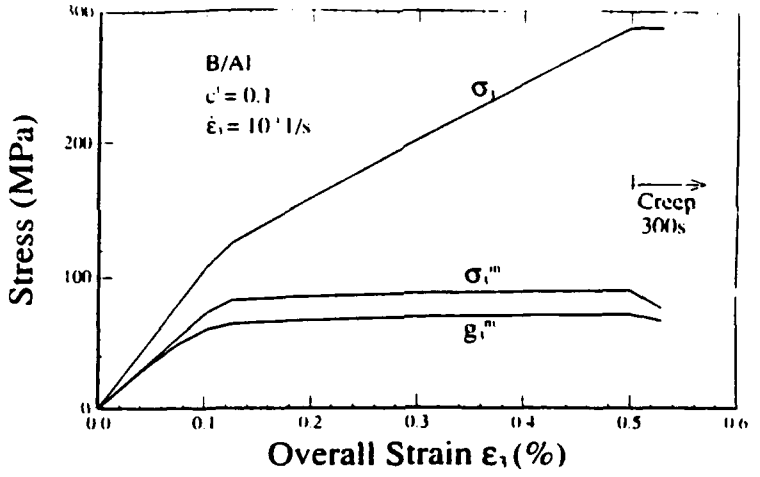

Figure 3. Overall stress σ_3, matrix stress σ_3^m and matrix equilibrium stress g_3^m vs. overall strain ϵ_3 in fiber direction at room temperature with a 300 s creep period at the maximum stress. A uniaxial test in the fiber direction with c' = 0.1 is simulated.

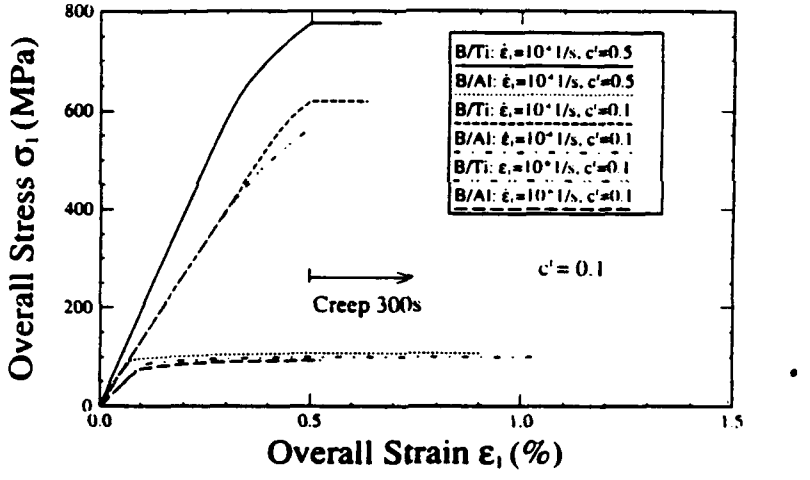

Figure 4. Transverse stress-strain curves of B/Al and B/Ti with different volume fractions and different strain rates. A 300 s creep period starts at 0.5% strain.

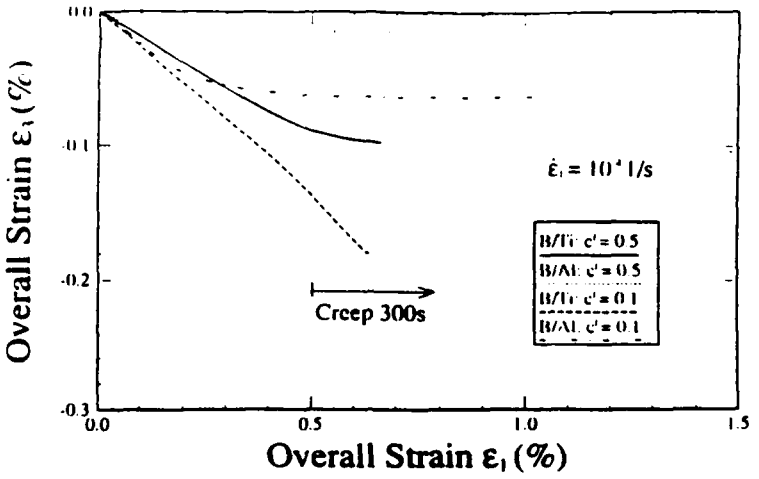

Figure 5. Strain in the fiber direction ϵ_3 vs. transverse strain ϵ_1 during some of the tests shown in Figure 4.

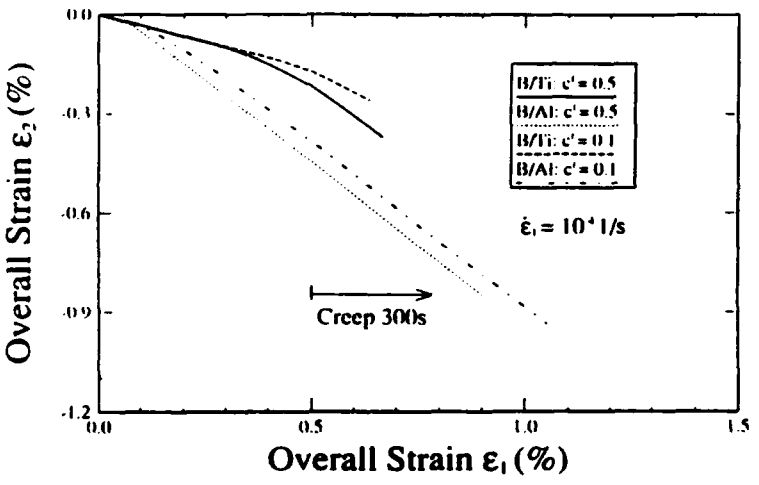

Figure 6. Transverse strain ϵ_2 vs. strain ϵ_1 during some of the tests shown in Figure 4.

both materials (see Figure 4). These are properties of the matrix constitutive equations and reflect observed experimental behavior.

The evolution of the axial strain ϵ_3 and of the transverse strain ϵ_2 is depicted in Figures 5 and 6, respectively. They show the influence of volume fraction on the induced strains. At the same strain in the 1-direction B/Ti exhibits a larger absolute value of the strain in the 3-direction than B/Al. The opposite is true for the 2-direction. Also, the trend of the influence of the volume fraction is opposite in Figures 5 and 6. It is shown in Figure 6 that Poisson's ratio increases with an increase in volume fraction; it decreases in Figure 5. The model predicts a minor influence of strain rate on Poisson's ratio. The numerical tests whose results are depicted in Figures 5 and 6, were repeated at a strain rate of 10^{-6} s^{-1} and the respective curves were almost indistinguishable from those obtained at 10^{-4} s^{-1} and shown in Figures 5 and 6.

Cyclic Loading with Creep of B/Ti

The TVBO constitutive equations used herein represent cyclic neutral behavior and the hysteresis loop closes after one cycle for cycling under symmetric stress or strain limits. This property is passed on to the composite model as depicted in Figure 7 (fiber direction) and Figure 8 (transverse direction). Each figure represents the response to a stress rate 1 MPa/s at a stress amplitude of ± 800 MPa with creep periods introduced at a stress magnitude of 500 MPa. When the stress magnitude increases the creep period is 300 s but is set to 100 hrs when the stress magnitude decreases.

It is observed that the loops close after one cycle and that almost twice as much strain develops in the transverse than in the fiber direction. Despite the differences in creep time the creep strain accumulation is much larger upon loading than upon unloading. This is an experimentally observed fact in monolithic materials and the TVBO model predicts this for the composite. The repository for modeling this behavior is the difference in the evolution of the matrix overstress during loading and unloading. Figures 7 and 8 show that this difference is larger on loading than on unloading. It should also be noted that the matrix stress in the fiber direction is not constant during the creep periods (see Figures 3 and 7).

Thermal Cycling of B/Al

The thermal cycling behavior of metal-matrix composite is of special interest since the almost always existing mismatch between the coefficients of thermal expansion of fiber and matrix can lead to the development of internal stresses and to very unusual thermal expansion behavior of the composite. This is especially true for composites with graphite fibers which have one negative coefficient of thermal expansion (see Wu et al. [7], Krempl and Yeh [2]). Here we illustrate the free thermal expansion of B/Al. Starting from room temperature the temperature is changed uniformly between $\pm 120°C$ at a rate of 0.033°C/s for five reversals.

The overall strain-in-the-fiber-direction vs. temperature hysteresis loop of B/Al is depicted in Figure 9. The composite expands on segment 0-1 but then changes slope in segment 1-2. Upon decrease of temperature from 120°C, the composite

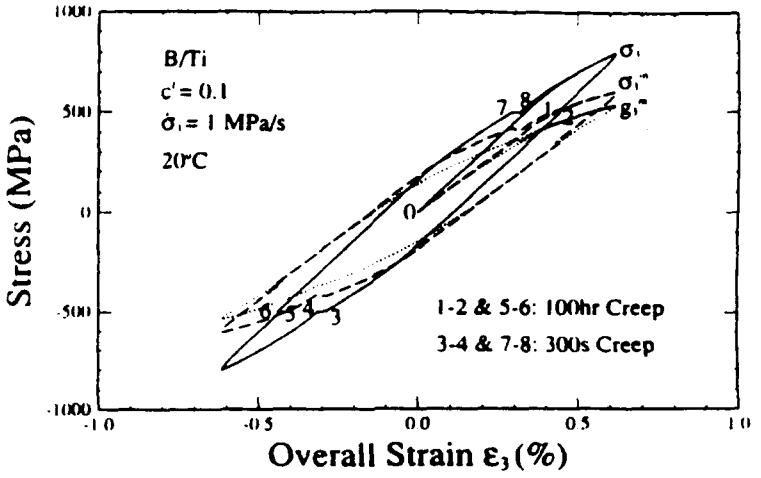

Figure 7. Uniaxial stress controlled, completely reversed cycling with unequal creep periods upon loading and unloading. Response in the fiber direction shows the overall stress σ_3, the matrix stress σ_3^m and the matrix equilibrium stress g_3^m vs. overall strain ε_3.

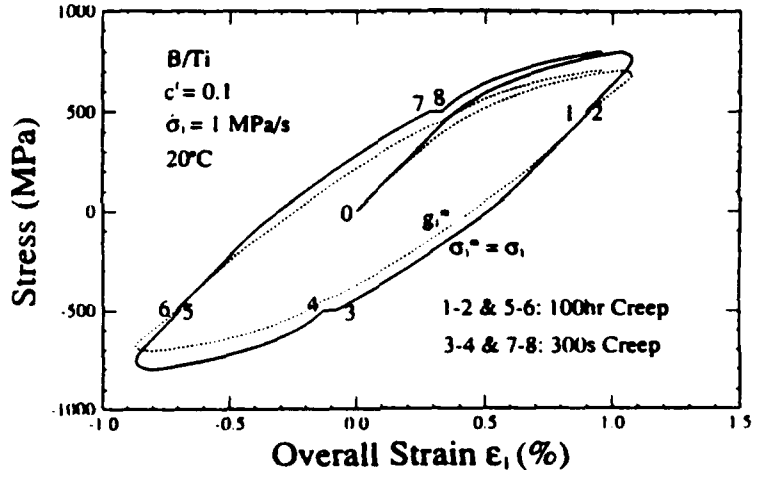

Figure 8. Same input as in Figure 7 but loading occurs in the transverse 1-direction. The response in the 1-direction is plotted.

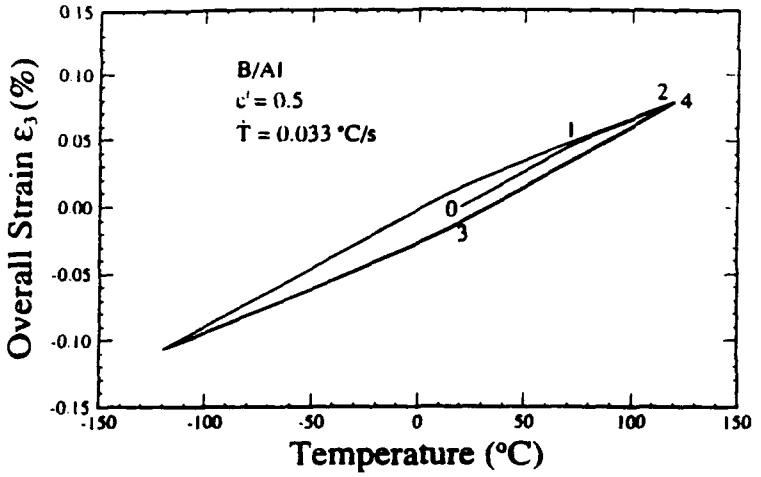

Figure 9. Temperature–fiber strain hysteresis loop thermal cycling of B/Al composite.

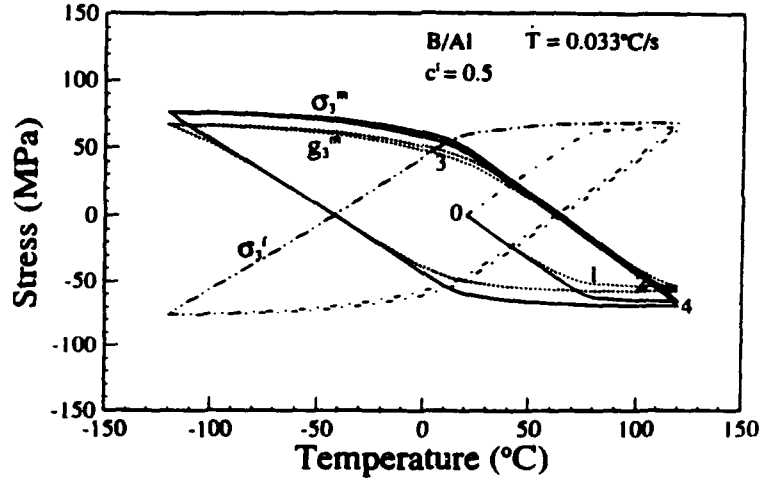

Figure 10. Fiber, matrix and matrix equilibrium stresses during temperature cycling shown in Figure 9.

shrinks in segment 2-3 but the rate of shrinking is reduced after point 3. A similar pattern evolves during the temperature increase from $-120°C$. The loop closes after one cycle.

The explanation of observed changes in slope can be found in the development of the fiber and matrix stresses during cycling as shown in Figure 10. At points 1 and 3 where the slope changes in Figure 9 the matrix starts to yield with a corresponding change in stiffness. After these points the fibers with their low coefficients of thermal expansion have a stronger influence than before these points.

DISCUSSION

Influence of Volume Fraction and of Loading Rate

An increase in fiber volume fraction increases the stress level in the fiber direction (see Figure 1) and decreases Poisson's ratio (see Figure 2). These results are to be expected. Also the accumulated creep strain in 300 s increases with decreasing volume fraction for both composites when straining occurs in the fiber direction (Figure 1). For transverse straining (see Figure 4), this is true for B/Al only. B/Ti, on the contrary, exhibits more creep strain accumulation for $c^f = 0.5$ than for $c^f = 0.1$. B/Ti with $c^f = 0.5$ yields earlier and thus has a larger prior overstress which drives the creep strain rate.

In Figure 1 the B/Ti composite develops more creep strain in 300 s than B/Al, but the opposite is true in Figure 4. This result is surprising at first since the model assumes that the Ti matrix is more rate sensitive than the Al matrix (the spacing between stress-strain curves at two different rates is larger for the Ti than for the Al matrix). However, at 0.5 percent strain inelastic flow is fully developed for the B/Al whereas B/Ti is in the transition from linear to nonlinear inelastic behavior. The creep stress levels are therefore not at an equivalent level and creep behavior can be different (the creep strain rate is a highly nonlinear function of stress level). For the loading in the direction of the fiber both composites exhibit almost linear behavior up to 0.5 percent strain (see Figure 1) and the creep stress levels can be considered equivalent.

For the TVBO model the observations can be explained in terms of the evolution of the matrix overstress. At 0.5 percent transverse strain the largest overstress, the asymptotic overstress characteristic of the strain rate has been reached for B/Al. In the knee of the transverse stress-strain curve the overstress increases and has not reached its asymptotic value for B/Ti. Further the tangent modulus at strains beyond 0.5 percent is small and nearly constant for B/Al but large and slowly decreasing for B/Ti. Creep rates increase with an increase of overstress and a decrease in tangent modulus.

These examples demonstrate that the evolution of creep strains is governed by a complex interaction between creep stress level and the material properties of the matrix. Aside from these considerations Equations (11) and (A15) in Reference [1] show that the inelastic strain rate which is caused by the viscosity of the matrix is also influenced by the elastic properties of the fiber.

At the same fiber volume fraction the accumulated creep strain in 300 s increases with an increase of the prior strain rate in the transverse direction (Figure 4). This is an experimentally observed behavior in monolithic materials and this behavior carries over to composite behavior.

The room temperature creep in the transverse direction predicted by the present model was observed by Min and Crossman [8] in Gr/Al composites.

The curves for B/Al in Figure 5 show almost no growth in induced axial strain beyond 0.4 percent strain. This implies that the plastic Poisson's ratio η_{13} is nearly zero. Evaluation of Equation (20) in Reference [1] using the pertinent values of the matrix overstress yields $\eta_{13} \approx 0$. Figure 6 of Sun and Chen [9] reports a plastic Poisson's ratio close to zero for transverse tensile tests of unidirectional B/Al. The inelastic Poisson's ratio $\eta_{31} = \eta_{32} = 0.83$ and obtained from Equation (18) in Reference [1] for $c^f = 0.475$ for B/Al compares favorably with the experimentally determined value for straining in the 3-direction as reported by Sun and Chen [9] in their Figure 6.

The theory permits the calculation of the variation of the total overall Poisson's ratio $\gamma_{ij} = -\dot{\epsilon}_j/\dot{\epsilon}$, for straining in the i-direction, $i,j = 1, 2, 3, i \neq j$. Figure 11 shows the variation of this quantity as well as the inelastic Poisson's ratio defined by Equation (17) in Reference [1] for the transverse tensile test on B/Al with $c^f = 0.5$ (see Figures 5 and 6). It is seen that both the inelastic and the total Poisson's ratio reach their limiting value before 0.5% strain. This behavior is due to the stress-strain behavior of B/Al as depicted in Figure 4. For the B/Ti composite which does not reach fully developed inelastic flow (see Figure 4), the variation of Poisson's ratios is quite different as shown in Figure 12 for $c^f = 0.5$. Immediately after the start of the creep test the inelastic and the total Poisson's ratios become equal as it should be since the elastic strain rates are zero in a creep test.

Cyclic Loading

In the presently used version of TVBO cyclic neutral behavior is modeled and the hysteresis loops close after one cycle (see Figures 7–10). The TVBO theory has been modified to account for cyclic hardening (see References [10] and [11]) and this feature can be implemented for composite analysis.

Figures 7 and 8 demonstrate that creep rate at the same stress level is much higher on loading than on unloading. Again this is a feature which is observed in monolithic materials and carries over to composites. This property is affected by the overstress dependence of the inelastic strain rate. It should be noted that the matrix stress is not constant during a creep test in the fiber direction. During creep with a positive stress, strain is increasing, the stress in the elastic fiber increases and to preserve equilibrium the matrix stress must decrease. This fact is demonstrated in Figures 3 and 7. When a creep test in the transverse direction is simulated, the matrix stress equals the overall stress and is therefore constant (see Figure 8). Comparison of the widths of the hysteresis loops at zero stress in Figures 7 and 8 shows the effect of fiber reinforcement. At the same stress amplitude much less strain develops in the fiber direction than in the transverse direction.

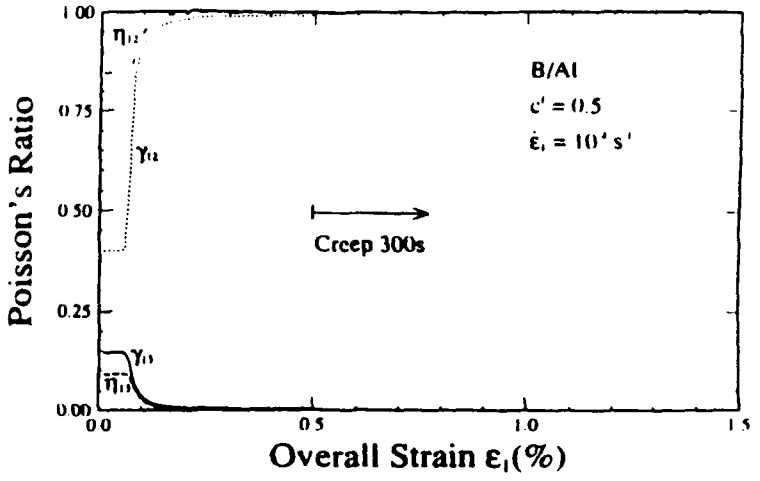

Figure 11. Inelastic (η_{ij}) and total ($\sim_{ij}$) Poisson's ratios vs. strain in the 1-direction for the B/Al test with c' = 0.5 depicted in Figures 4–6.

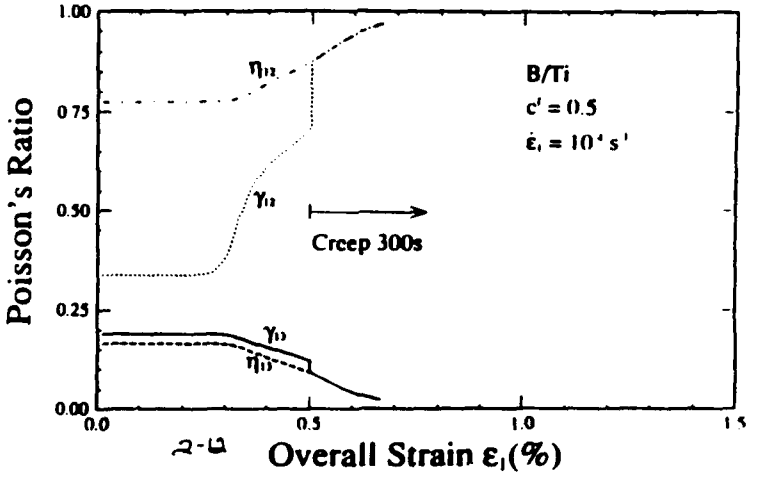

Figure 12. Same as Figure 11 except that the behavior of B/Ti is shown.

The unequal creep behavior upon loading and unloading is also evident from Figure 8.

During thermal cycling between $\pm 120°C$ of the freely expanding composite, the present theory predicts the axial strain–temperature hysteresis loop for B/Al as shown in Figure 9. There are changes in slope as indicated by the numerals 1 and 3 in Figure 9. Figure 10, which shows the matrix and fiber stress–temperature hysteresis loops, reveals that the change in slope in Figure 9 at points 1 and 3 coincides with the elastic-inelastic transition of the matrix. There is a coupling between the thermal expansion behavior and the stresses in the fiber and in the matrix which is caused by the mismatch of the coefficients of thermal expansion. The coupling is very pronounced in Gr/Al where a large difference between the coefficients of thermal expansion exists (see Krempl and Yeh [2]). It should be noted that the stress-strain behavior of the fiber is linear elastic, the fiber stress–temperature hysteresis loop notwithstanding.

At the same temperature range B/Ti only exhibits elastic thermal expansion. The yield stress of the Ti is much higher than the matrix stress resulting from the thermal strain mismatch of fiber and matrix.

ACKNOWLEDGEMENT

This research was supported by DARPA/ONR Contract N00014-86-k0770 with Rensselaer Polytechnic Institute.

REFERENCES

1. Yeh, N. M. and E. Krempl. In press. "Thermoviscoplasticity Based on Overstress Applied to the Analysis of Fibrous Metal-Matrix Composites," *Journal of Composite Materials*, 26(7).
2. Krempl, E. and N. M. Yeh. 1990. "Residual Stresses in Fibrous Metal-Matrix Composites. A Thermoviscoplastic Analysis," in *Proceedings IUTAM Symposium on Inelastic Deformation of Composite Materials*, G. J. Dvorak, ed., Springer-Verlag, pp. 411–443.
3. Lee, K. D. and E. Krempl. 1991. "An Orthotropic Theory of Viscoplasticity Based on Overstress for Thermomechanical Deformations," *International Journal of Solids and Structures*, 27:1445–1459.
4. Dvorak, G. J. and Y. A. Bahei-El-Din. 1982. "Plasticity Analysis of Fibrous Composites," *Journal of Applied Mechanics*, 49:327–335.
5. Yao, D. and E. Krempl. 1985. "Viscoplasticity Theory Based on Overstress. The Prediction of Monotonic and Cyclic Proportional and Non-Proportional Loading Paths of an Aluminum Alloy," *International Journal of Plasticity*, 1:259–274.
6. Krempl, E., M. Ruggles and D. Yao. 1987. "Viscoplasticity Theory Based on Overstress Applied to Ratchetting," *Symposium on Advances in Inelastic Analysis, ASME Winter Annual Meeting, Dec., 1987*, S. Nakasawa, K. Willam and N. Rebelo, eds., AMD–Vol. 88/PED–Vol. 28.
7. Wu, J. F., M. S. Shepherd, G. J. Dvorak and Y. A. Bahei-El-Din. 1989. "A Material Model for the Finite Element Analysis of Metal Matrix Composites," *Composites Science and Technology*, 35:347–366.
8. Min, B. K. and F. W. Crossman. 1982. "Analysis of Creep for Metal Matrix Composites," *Journal of Composite Materials*, 16:188–203.
9. Sun, C. T. and J. L. Chen. 1989. "A Simple Flow Rule for Characterizing Nonlinear Behavior of Fiber Composites," *Journal of Composite Materials*, 23:1009–1020.
10. Krempl, E. and D. Yao. 1987. "The Viscoplasticity Theory Based on Overstress Applied to

Ratchetting and Cyclic Hardening," in *Low Cycle Fatigue and Elasto-Plastic Behavior of Materials*, K.-T. Rie, ed., pp. 137-148.

11. Krempl, E. and S. H. Choi. In press. "Viscoplasticity Theory Based on Overstress: The Modeling of Ratchetting and Cyclic Hardening of AISI Type 304 Stainless Steel," *Nuclear Eng. and Design*.
12. Kreider, K. G. and K. M. Prewo. 1974. "Boron-Reinforced Aluminum," in *Composite Materials, Vol. 4, Metallic Matrix Composites*, K. G. Kreider, ed., Academic Press.
13. Tsirlin, A. M. 1985. "Boron Filaments," in *Handbook of Composites, Vol. 1, "Strong Fibers,"* W. Watt and B. V. Perov, eds., North-Holland.
14. Hillig, W. B. 1985. "Prospects for Ultra-High Temperature Ceramic Composites," Report No. 85CRD152, General Electric Research and Development Center.

Thermoviscoplasticity Based on Overstress Applied to the Analysis of Fibrous Metal-Matrix Composites

NAN-MING YEH AND ERHARD KREMPL
Mechanics of Materials Laboratory
Rensselaer Polytechnic Institute
Troy, NY 12180-3590

(Received September 10, 1990)
(Revised May 14, 1991)

ABSTRACT: The vanishing fiber diameter (VFD) model together with the thermoviscoplasticity theory based on overstress (TVBO) are used to analyse the thermomechanical behavior of unidirectional fibrous metal-matrix composites. Fiber and matrix can both be transversely-isotropic, thermoelastic-viscoplastic. All material constants can depend on current temperature. Yield surfaces and loading/unloading conditions are not used in the theory in which the inelastic strain rate is solely a function of the overstress, the difference between stress and the equilibrium stress, a state variable of the theory. The three-dimensional equations are derived and specialized for various simple loading cases such as isothermal uniaxial and biaxial proportional and nonproportional loadings. The predictions of this viscoplasticity theory during loading compare favorably with results from the rate-independent plasticity theory. In addition it is capable of predicting creep, relaxation and rate sensitivity.

INTRODUCTION

METAL-MATRIX COMPOSITES are being considered for room temperature and elevated temperature service and inelastic analyses are required to ascertain their behavior under load and variable temperature. The inelastic behavior is generally idealized as rate-independent elastic-plastic or by a creep model such as power law creep. The former is considered to be appropriate for low homologous temperature whereas the creep laws are used for high homologous temperature applications. In these approaches the transition from one representation to the other provides difficulties since creep laws are not mathematical limits of rate-independent plasticity and vice versa.

Unified material models do not separately postulate constitutive laws for creep and plasticity but consider all inelastic deformation rate dependent. Experiments with modern servocontrolled testing machines have shown rate dependence even at room temperature for engineering alloys, e.g., stainless steels, Krempl [1], 6061-T6 Al alloy, Krempl and Lu [2], and titanium alloys, Kujawski and Krempl

Reprinted from *Journal of* COMPOSITE MATERIALS, *Vol. 26, No. 7/1992*

[3]. The transition from low to high homologous temperature behavior is usually characterized by a decrease in strength and an increase in rate dependence. This behavior can be modeled easily by unified laws if certain material constants are made to depend on temperature. When material data are analyzed using separate laws for creep and rate-independent plasticity, identification problems arise since it is not always clear what portion of the inelastic deformation is to be attributed to creep or plasticity. This difficulty does not arise with unified constitutive laws. However, they are rather new and have not been used extensively.

The elastic-plastic isothermal behavior of fibrous metal-matrix composites has been analyzed by Min [4], Dvorak and Bahei-El-Din [5,6], Kenaga, Doyle and Sun [7], Teply and Dvorak [8], Dvorak, Bahei-El-Din, Macheret and Liu [9], and Sun and Chen [10].

Time (rate)-dependent isothermal analyses based on creep or creep/plasticity laws were performed by Min and Crossman [11], McLean [12,13], and Lilholt [14]. Min and Crossman [11] also showed that a Gr/Al exhibits primary creep at room temperature in the transverse direction.

Residual stresses between fiber and matrix can have a significant influence on the overall expansion and mechanical deformation behavior (see the experiments and analyses by Min and Crossman [15]). Dvorak [16] demonstrated that in the plastic range thermal and mechanical effects are coupled. Using the periodic hexagonal array model and the VFD model, the rate-independent thermomechanical behavior of composites was predicted by Wu et al. [17], and Bahei-El-Din [18], respectively. Longitudinal and transverse tensile tests on B/Al and B/epoxy plies reported by Meyn [19] showed some influence of strain rate on longitudinal strength. For the B/Al material the transverse tensile strength was strongly affected by rate of loading at room temperature. Surprisingly this dependence did not increase with increasing temperature.

A rate-dependent micromechanical analysis of metal matrix using the unified Bodner Model was performed by Aboudi [20]. In an extension of classical thermal laminate theory Krempl and Hong [21] used an orthotropic continuum viscoplasticity theory based on overstress to represent ply behavior. Subsequently Lee and Krempl [22] extended the treatment to the thermal, elastic-viscoplastic case. Application to the thermal cycling and thermomechanical loading followed [23,24]. The thermal viscoplastic behavior of a ply was idealized as an orthotropic continuum. With this theory the coupling between thermal and plastic material behavior could not be modeled.

The purpose of this paper is to apply the thermal orthotropic theory of viscoplasticity based on overstress (TVBO) which includes temperature-dependent material properties to a micromechanics analysis of fibrous metal matrix composites. The vanishing fiber diameter model (VFD) is employed which was proposed by Dvorak and Bahei-El-Din [5] in the context of a three-dimensional elastic-plastic analysis. The governing equations are derived and numerical experiments are performed under isothermal uniaxial and biaxial proportional loadings and compared with the predictions of the rate-independent plasticity theory of Reference [5]. The present approach can in addition model rate sensitivity, creep, relaxation and hysteresis and includes thermal-inelastic coupling.

MATERIAL AND COMPOSITE MODELS

Transversely-Isotropic, Thermoviscoplasticity Theory Based on Overstress (TVBO)

INTRODUCTION

The theory developed by Lee and Krempl [22] is for infinitesimal strain and orthotropy. It is of unified type and does not use a yield criterion and loading/unloading conditions. The elastic strain is formulated to be independent of thermomechanical path and the inelastic strain rate is a function of overstress, the difference between stress σ, and the equilibrium stress $\mathbf{g}$; it is a state variable of the theory.

The long term asymptotic values of stress, equilibrium stress, and kinematic stress rates, which can be obtained for a constant mechanical strain rate and ultimately constant temperature, are assumed to be independent of thermal history as are the ultimate levels of the rate-dependent overstress and of the rate-independent contribution to the stress (see Yao and Krempl [25]). Therefore the material functions and constants can in principle be obtained from isothermal tests within the temperature range of interest.

The model can predict not only the rate-dependent phenomena such as creep, relaxation, and rate sensitivity but includes inelastic incompressibility, tension/compression asymmetry, and invariance of the inelastic properties under superposed pressure as special cases [22].

Constant elastic and inelastic Poisson's ratios are defined for the uniaxial loading cases. The theory permits the computation of the actual Poisson's ratio which depends on the loading history [22].

All material constants can be functions of temperature. This dependence is not explicitly displayed. The temperature dependence can be the usual Arrhenius relation or can deviate from that model.

For the representation of the equations, vector notation is used where stress tensor components σ and the small strain tensor components ϵ are related to their vector components by

$$\sigma_1 = \sigma_{11} \quad \sigma_2 = \sigma_{22} \quad \sigma_3 = \sigma_{33} \quad \sigma_4 = \sigma_{23} \quad \sigma_5 = \sigma_{31} \quad \sigma_6 = \sigma_{12}$$

and

$$\epsilon_1 = \epsilon_{11} \quad \epsilon_2 = \epsilon_{22} \quad \epsilon_3 = \epsilon_{33} \quad \epsilon_4 = 2\epsilon_{23} \quad \epsilon_5 = 2\epsilon_{31} \quad \epsilon_6 = 2\epsilon_{12}$$

FLOW LAWS

In the context of an infinitesimal theory, the total strain rate, $d\epsilon/dt$, is considered to be the sum of elastic, $d\epsilon^{el}/dt$, inelastic, $d\epsilon^{in}/dt$, and thermal strain rates, $d\epsilon^{th}/dt$,

$$\dot{\epsilon} = \dot{\epsilon}^{el} + \dot{\epsilon}^{in} + \dot{\epsilon}^{th} \tag{1}$$

where the sum of the elastic and inelastic strain rate is called the mechanical strain rate,

$$\dot{\epsilon}^{me} = \dot{\epsilon}^{el} + \dot{\epsilon}^{in} \tag{2}$$

A superposed dot represents the total time derivative, d/dt.

For each strain rate, a constitutive equation is postulated. The elastic strain is assumed to be independent of thermal history, therefore,

$$\dot{\epsilon}^{el} = \frac{d}{dt}(\mathbf{C}^{-1}\sigma) \tag{3}$$

where $\mathbf{C}^{-1}$ is the temperature-dependent compliance matrix.

As in the case of isotropy, the inelastic strain rate is only a function of the overstress $\mathbf{X}$. It denotes the difference between the stress σ and the equilibrium stress $\mathbf{g}$, a vector state variable of the theory. Accordingly

$$\dot{\epsilon}^{in} = \mathbf{K}^{-1}\mathbf{X} \tag{4}$$

The viscosity matrix $\mathbf{K}^{-1}$ controls the rate dependence through the viscosity factors K_{ij} and the positive, decreasing viscosity function $k[\Gamma]$.

The thermal strain rate is given by

$$\dot{\epsilon}^{th} = \alpha\dot{T} \tag{5}$$

with α the coefficient of thermal expansion vector. T is the temperature difference from some datum temperature.

GROWTH LAWS FOR THE STATE VARIABLES

The growth law for g is the repository for modeling elastic regions and hysteresis. It is given by Reference [22]

$$\dot{\mathbf{g}} = q_1[\Gamma]\dot{\sigma} + \dot{T}\frac{\partial q_1[\Gamma]}{\partial T}\sigma + \{q_2[\Gamma] - \theta[q_2[\Gamma] - p(1 - q_1[\Gamma])]\}\frac{\mathbf{X}}{k[\Gamma]} \tag{6}$$

where the dimensionless modified shape functions q_1 and q_2 control the shape of stress-strain diagram. The dimensionless constant p represents the ratio of the tangent moduli at the maximum strain of interest to the corresponding viscosity

factors, $p \gtrless 0$. The invariant θ is related to the rate-independent contribution to the stress and is defined as

$$(\theta)^2 = \mathbf{Z}'\mathbf{P}\mathbf{Z} \tag{7}$$

where $\mathbf{P}$ is a matrix whose components have the dimension of reciprocal stress squared. The vector $\mathbf{Z}$ represents the difference between the equilibrium stress $\mathbf{g}$ and the kinematic stress $\mathbf{f}$

$$\mathbf{Z} = \mathbf{g} - \mathbf{f} \tag{8}$$

where $\mathbf{f}$ evolves according to

$$\dot{\mathbf{f}} = \frac{p}{k[\Gamma]}\mathbf{X} \tag{9}$$

Asymptotic analyses for the uniaxial isothermal case in References [25] and [26] show that $\dot{\mathbf{f}}$ determines $\dot{\sigma}$ ultimately. The purpose of Equation (9) is to set this slope which can be positive, zero or negative.

The representations of the material matrices for the transversely isotropic case and other explanations are given in Appendix 1; q_1, q_2 and p in Equation (6) are listed in Appendix 2. The above equations follow directly from Reference [22] by assuming tension/compression symmetry.

The theory given above represents cyclic neutral behavior. Rate sensitivity, relaxation and creep are represented. Since no recovery of state is modeled the creep behavior is controlled by the sign of p. If $p > 0$ the equations can only represent primary creep. Primary and secondary creep may be modeled for $p = 0$; primary, secondary and tertiary creep can be represented in principle if $p < 0$. Note also that p sets the slope of the stress-inelastic strain curve of the maximum inelastic strain of interest through Equation (9) (see the discussion of the properties of VBO in References [25]–[27]).

When recovery of state is included in the model [28] the creep behavior is no longer completely controlled by the sign of p and secondary creep can be reproduced at stress levels which are in the linear region of the stress-strain diagram. Also the isotropic formulation of VBO has been extended to cyclic hardening [29,30]. It is possible to include this property as well as recovery of state in the orthotropic theory. This will be done in a future paper.

Vanishing Fiber Diameter Model

For the representation of the fibrous composite the vanishing fiber diameter model (VFD) of Reference [5] is used. In this model uniform overall stresses and strains, perfect bonding between fiber and matrix, and vanishing fiber diameter are assumed even though fibers occupy a finite volume fraction of the composite [5]. This leads to a single constraint condition in the fiber direction which is assumed to be the 3-direction in this paper. In the transverse plane the fibers do

not interfere with the deformation of the matrix [5]. The following constraint equations hold

$$\begin{aligned} \dot{\sigma}_i &= \dot{\sigma}_i^f = \dot{\sigma}_i^m \qquad \text{for } i \neq 3 \\ \dot{\sigma}_3 &= c^f \dot{\sigma}_3^f + c^m \dot{\sigma}_3^m \\ \dot{\epsilon}_i &= c^f \dot{\epsilon}_i^f + c^m \dot{\epsilon}_i^m \qquad \text{for } i \neq 3 \\ \dot{\epsilon}_3 &= \dot{\epsilon}_3^f = \dot{\epsilon}_3^m \end{aligned} \tag{10}$$

In the above the superscripts f and m denote fiber and matrix, respectively. In the sequel the superscript r is used to denote either fiber or matrix. The volume fractions of fiber and matrix are c^f and c^m, respectively, with $c^f + c^m = 1$.

The Composite Model–Thermoviscoplasticity (TVBO) and Vanishing Fiber Diameter Model (VFD)

A unidirectional fibrous composite element is assumed where both the fiber and the matrix can be represented by the transversely isotropic, thermoviscoplasticity theory based on overstress (TVBO). On-axis representation and fiber orientation in the 3-direction are postulated. Thermoelastic fibers are a special case and the isotropic formulation of TVBO can be derived by making the substitutions given in Appendix 1.

The three-dimensional equations representing the composite which has transversely isotropic, thermoviscoplastic fiber and isotropic, thermoviscoplastic matrix result from using the constitutive Equations (1)–(9) and the VFD constraints [Equation (10)] together with the representations of the matrices given in Appendix 1. We then have

$$\dot{\epsilon} = \bar{\mathbf{C}}^{-1}\dot{\sigma} + (\mathbf{K}^f)^{-1}\mathbf{X}^f + (\mathbf{K}^m)^{-1}\mathbf{X}^m + (\dot{\mathbf{R}}^f)^{-1}\sigma^f + (\dot{\mathbf{R}}^m)^{-1}\sigma^m + \bar{\alpha}\dot{T} \tag{11}$$

together with a separate equation for the σ_3^m component of the matrix

$$\begin{aligned} \dot{\sigma}_3^m = {} & \frac{E^m}{E_{33}}\dot{\sigma}_3 - \frac{c^f}{E_{33}}L(\dot{\sigma}_1 + \dot{\sigma}_2) - \frac{c^f E_{33}^f E^m}{E_{33}} \\ & \times \left\{ \frac{1}{K^m k^m [\Gamma^m]}[X_3^m - 0.5(X_1^m + X_2^m)] + \frac{\eta_{31}^f}{K_{33}^f k^f [\Gamma^f]}(X_1^f + X_2^f) \right. \\ & \left. - \frac{X_3^f}{K_{33}^f k^f [\Gamma^f]} \right\} - \frac{c^f E_{33}^f E^m}{E_{33}} \left\{ \left[\frac{1}{(E_{33}^f)^2}(\dot{\nu}_{31}^f E_{33}^f - \nu_{31}^f \dot{E}_{33}^f \right. \right. \\ & \left. - \frac{1}{(E^m)^2}(\dot{\nu}^m E^m - \nu^m \dot{E}^m) \right](\sigma_1 + \sigma_2) + \frac{\dot{E}_{33}^f}{(E_{33}^f)^2}\sigma_3^f \\ & \left. - \frac{\dot{E}^m}{(E^m)^2}\sigma_3^m \right\} - \frac{c^f E_{33}^f E^m}{E_{33}}(\alpha^m - \alpha_3^f)\dot{T} \end{aligned} \tag{12}$$

In addition growth laws of equilibrium and kinematic stresses for fiber and matrix are needed which are obtained by rewriting Equations (6) and (9) in terms of matrix or fiber stresses,

$$\dot{\mathbf{g}}^r = q^r[\Gamma^r]\dot{\boldsymbol{\sigma}}^r + \dot{T}\frac{\partial q^r[\Gamma^r]}{\partial T}\boldsymbol{\sigma}^r + \{q^r[\Gamma^r] - \theta^r[q^r[\Gamma^r] - p^r(1 - q^r[\Gamma^r])]\}\frac{\mathbf{X}^r}{k^r[\Gamma^r]} \tag{13}$$

$$\dot{\mathbf{f}}^r = \frac{p^r}{k^r[\Gamma^r]}\mathbf{X}^r \tag{14}$$

where we have set $q_1 = q_2 = q$ for simplicity.

In the above $\bar{\mathbf{C}}^{-1}$ is the symmetric overall compliance matrix whose components are functions of the elastic properties of fiber and matrix. The viscosity matrices $(\mathbf{K}^f)^{-1}$, $(\mathbf{K}^m)^{-1}$ are not symmetric and their components together with those of $\bar{\mathbf{C}}^{-1}$ are listed in Appendix 3. In the representation of the matrix properties, isotropy and plastic incompressibility were assumed. The viscoplastic formulation and the rate-independent formulation [4,5] lead to a nonsymmetric matrix which relates the contributions of the matrix stresses to the overall inelastic strain rate. The matrices $(\dot{\mathbf{R}}^f)^{-1}$ and $(\dot{\mathbf{R}}^m)^{-1}$ contain time derivatives of the elastic constants of the fiber and the matrix, respectively. Both matrices are not symmetric (see Appendix 3). They are zero if the elastic constants are independent of temperature. These matrices are the "additional" terms which can play a significant role in modeling thermomechanical behavior (see Lee and Krempl [31]). Finally the coefficients $\bar{\alpha}$ are composed of the elastic constants and the coefficients of thermal expansion (see Appendix 3).

Equation (11) shows that the overall strain rate is the sum of the overall elastic strain rate, the overall inelastic strain rates contributed by the fiber and the matrix, and the overall thermal strain rate in the case of constant elastic properties. If temperature-dependent elastic properties are assumed then two additional terms contribute to the overall strain rate. They insure that the elastic behavior is path independent (see Lee and Krempl [22,31]). When the fibers deform only elastically their contribution to the inelastic strain rate vanishes.

Equation (12) is used to calculate the instantaneous axial matrix stress which cannot be obtained from the overall boundary conditions directly. $\dot{E}_{33}$ and L are defined in Appendix 3. σ_3^m is affected by mechanical and thermal loadings and their loading paths. For instance, for the isothermal case when $\dot{T} = 0$, matrix stresses in the fiber direction (σ_3^m, g_3^m, f_3^m) can evolve in unidirectional transverse loading, or may evolve in unidirectional shear loading provided the initial value of X_3^m is nonzero. For pure thermal loading (overall stresses are zero), σ_3^m together with g_3^m, f_3^m will develop due to the difference in the coefficients of thermal expansion of fiber and matrix; these matrix stresses in the fiber direction cause coupling between the mechanical and thermal loading in the inelastic range. If the fibers deform elastically and the elastic constants are independent of tempera-

ture, X_1', X_2', X_3', and the terms in the second brace vanish. For isothermal case, the temperature rate in the last term becomes zero.

From these general equations some properties of the model can be derived. We address inelastic dilatation and Poisson's ratio.

INELASTIC DILATATION AND INELASTIC POISSON'S RATIOS

Assuming constant temperature, the rate of inelastic dilatation of the composite $\dot{\epsilon}_{kk}^{in}$ can be computed from Equation (11). It consists of $(\dot{\epsilon}_{kk}^{in})^f$ and $(\dot{\epsilon}_{kk}^{in})^m$ with

$$(\dot{\epsilon}_{kk}^{in})^f = \frac{c^f}{E_{33}' K_{11}' k^f [\Gamma^f]} [(c^f - c^f \eta_{12}' - \eta_{13}' + 2c^m \nu^m \eta_{13}') E_{33}' + c^m (1 - \eta_{12}' - 2\nu_{31}' \eta_{13}') E^m](X_1' + X_2') + \frac{c^f}{E_{33}' K_{33}' k^f [\Gamma^f]} [(1 - 2c^f \eta_{31}' - 2c^m \nu^m) E_{33}' + 2c^m (\nu_{31}' - \eta_{31}') E^m] X_3' \tag{15}$$

$$(\dot{\epsilon}_{kk}^{in})^m = \frac{c^f c^m}{2E_{33}^m K^m k^m [\Gamma^m]} [(1 - 2\nu^m) E_{33}' - (1 - 2\nu_{31}') E^m](X_1^m + X_2^m - 2X_3^m) \tag{16}$$

where we have assumed isotropy and inelastic incompressibility for the matrix.

Even if the fibers deform only elastically, $(\dot{\epsilon}_{kk}^{in})^f = 0$, the overall inelastic dilatation still exists. Similar results were obtained for rate-independent plasticity (see References [4] and [32]).

For uniaxial loading in the i-direction the overall inelastic Poisson's ratio based on strain rates η_{ij} can be defined by

$$\eta_{ij} = -\frac{\dot{\epsilon}_j^{in}}{\dot{\epsilon}_i^{in}} \qquad (i,j = 1,2,3,\ i \neq j) \tag{17}$$

Elastic fibers and an isotropic matrix which exhibits inelastic incompressibility are assumed. The inelastic Poisson's ratios are

$$\eta_{31} = \frac{1}{2E^m}(E_{33}' + 2c^f L) = \eta_{32} \tag{18}$$

$$\eta_{12} = \frac{\left(0.5 - \frac{c^f L}{2E_{33}'}\right) X_1^m + \left(0.5 + \frac{c^f L}{E_{33}'}\right) X_3^m}{\left(1 + 0.5\frac{c^f L}{E_{33}'}\right) X_1^m - \left(0.5 + \frac{c^f L}{E_{33}'}\right) X_3^m} = \eta_{21} \tag{19}$$

$$\eta_{13} = \frac{E^m(X_1^m - 2X_3^m)}{2E_{33}' \left[\left(1 + 0.5\frac{c^f L}{E_{33}'}\right) X_1^m - \left(0.5 + \frac{c^f L}{E_{33}'}\right) X_3^m\right]} = \eta_{23} \tag{20}$$

It is seen that η_{31} and η_{32} are constant, i.e., for loading in the fiber direction the inelastic transverse strain rates are a fixed fraction of the inelastic strain rate in the loading direction. In all other cases the inelastic Poisson's ratio depends on deformation through the overstress components [see Equations (19) and (20)]. (It should be noted that the inelastic Poisson's ratio of the matrix is equal to 0.5.) When the overstress components are zero, indeterminate expressions result from Equations (19) and (20) which must be resolved.

The actual overall Poisson's ratios based on rates can be defined in analogy to Equation (17) (see Lee and Krempl [22]), and their values can be computed.

NUMERICAL EXPERIMENTS

Material Properties

To investigate the properties of the model the material constants appearing in Equations (11)–(14) must be identified and the appropriate boundary conditions have to be applied. A set of nonlinear coupled, first order differential equations must then be integrated under appropriate initial conditions. Closed form solutions are rare and numerical integration is the rule. In our case the IMSL routine DGEAR is used.

In this paper, isotropic, elastic fibers, and an isotropic, viscoplastic matrix are postulated. To affect a comparison with rate(time)-independent plasticity, hypothetical, but realistic material properties of fiber and matrix are assumed and are listed in Table 1. (For the fiber isotropic elastic properties close to boron are used, the isotropic matrix properties correspond closely to 6061 Al.) The elastic properties are in common for both models. The stress-plastic strain relation of the matrix for the rate-independent plasticity model is obtained from the viscoplastic model at a strain rate of $\dot{\epsilon} = 10^{-5}\ s^{-1}$.

Comparison of Plasticity (P) and Viscoplasticity (VBO) Composite Models

The two models are compared under uniaxial loading in the fiber direction (Figure 1), and under uniaxial as well as combined loadings in the transverse and shear directions in Figures 2 and 3, respectively. Close agreement between the two models is observed. For both theories, the stress-strain curves for biaxial loading are more compliant in the inelastic region than those for unidirectional loading. Also both theories predict almost linear behavior in the fiber direction as seen in Figure 1. Significant inelasticity is observed only in the transverse directions. For VBO a rate effect is evident and an adjustment of the rate within reasonable limits can improve the correspondence between the two theories.

Despite its different appearance and the absence of a yield surface and of loading and unloading conditions VBO can model typical plasticity effects. This is demonstrated for nonproportional loading paths in Figures 4 and 5. The strains at point 3 are highly dependent on the loading path. This can be easily seen when the relevant endpoints of Figures 2 through 5 are compared.

Table 1. Material properties for hypothetical MMC.

Properties	Fiber	Matrix
Volume Fraction	0.5	0.5
Elastic Properties		
E'_{33} (MPa)	4.0E + 5	7.0E + 4
ν'_{31}	0.21	0.33
G'_{44} (MPa)	1.65E + 5	2.63E + 4
E'_{11} (MPa)	4.0E + 5	7.0E + 4
G'_{66} (MPa)	1.65E + 5	2.63E + 4

Viscoplastic Properties

Viscosity Function:

$$k^m[\Gamma^m] = k_1[1 + (\Gamma^m/k_2)]^{-k_3}$$

k_1 = 314,200 (s) k_2 = 71.38 (MPa) k_3 = 52

Viscosity Factor:

$$K^m = E^m$$

Shape Function:

$$\Psi^m[\Gamma^m] = c_1 + (c_2 - c_1)\exp(-c_3\Gamma^m)$$

c_1 = 17,600 (MPa) c_2 = 69,300 (MPa) c_3 = 0.0868 (MPa^{-1})

E_i^m = 800 (MPa) A^m = 100 (MPa)

Inelastic Poisson's Ratio:

$$\eta^m = 0.5$$

Plastic Properties

Yield Stress:

$$\sigma_y^m = 77 \text{ MPa}$$

Isotropic elastic-plastic matrix with Prager-Ziegler kinematic hardening rule is assumed [5].

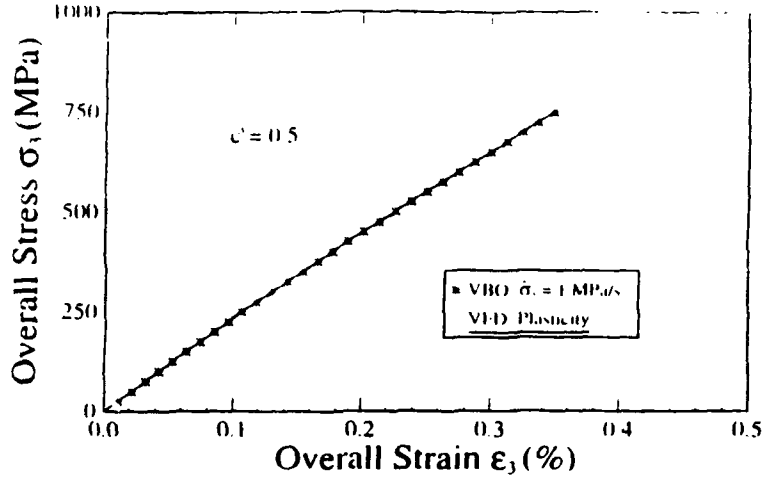

Figure 1. Stress-strain curves in the fiber direction of plasticity and viscoplasticity VFD models.

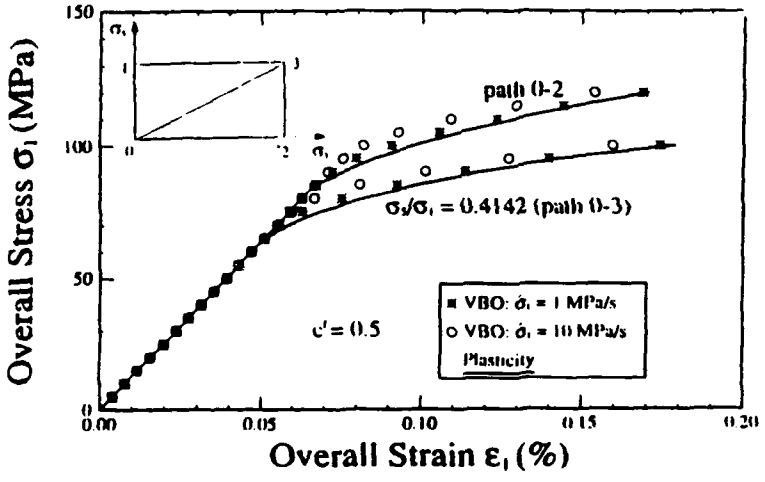

Figure 2. Uniaxial (path 0-2) and biaxial (path 0-3) transverse stress-strain curves of plasticity and viscoplasticity VFD models.

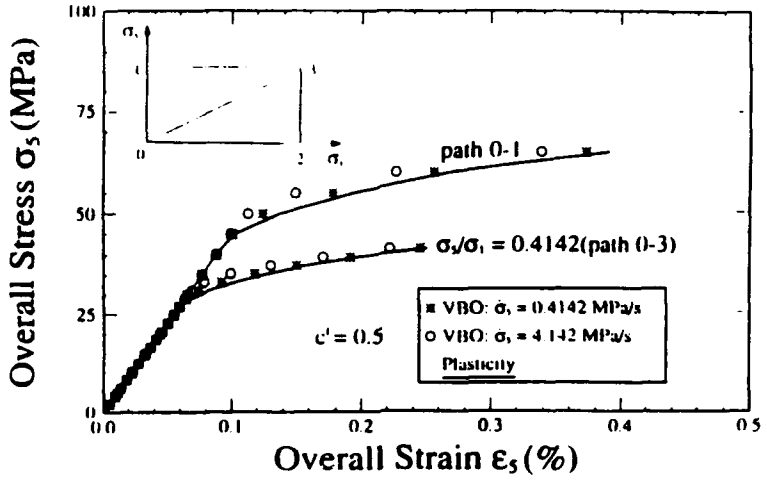

Figure 3. Uniaxial (path 0-1) and biaxial (path 0-3) shear stress-strain curves of plasticity and viscoplasticity VFD models.

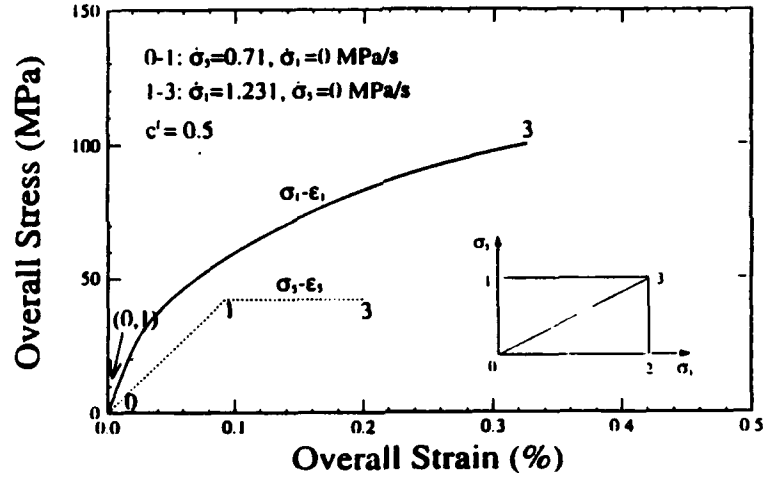

Figure 4. Transverse and shear stress-strain curves of viscoplasticity VFD model along the loading path 0-1-3.

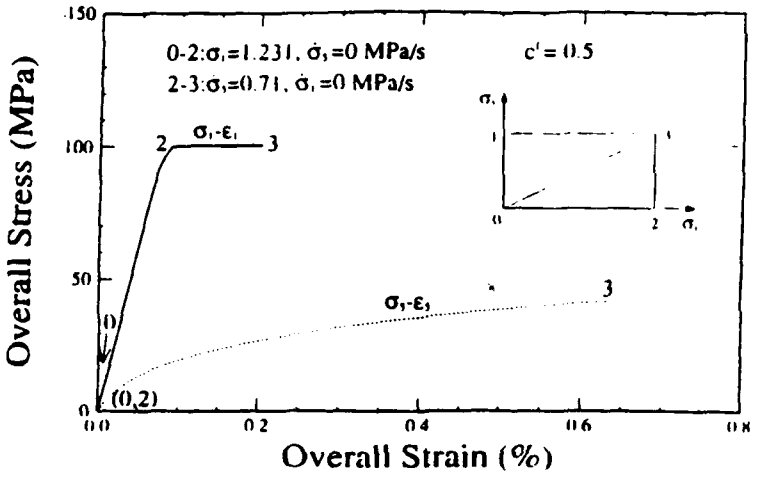

Figure 5. Transverse and shear stress-strain curves of viscoplasticity VFD model along the loading path 0-2-3.

DISCUSSION

Comparison with Rate-Independent Plasticity Theories

Figures 1-3 demonstrate that VBO can represent the same behavior as rate-independent plasticity theories which use yield surfaces. VBO can also model true plasticity phenomena, the path dependence of the response, as shown in Figures 4 and 5. This capability exists although the form of the flow law [Equation (4)] and the definition of the invariant Γ of Equation (A5) are quite different from the plasticity flow law. When, as it is usually done in rate-independent plasticity, the von Mises yield surface is used, the matrix which relates stress increments to plastic strain increments contains a term equivalent to $\mathbf{X}\mathbf{X}'$ which can become fully populated as the state of stress changes (see Equation (44) of Dvorak and Bahei-El-Din [5], where $\boldsymbol{\eta}$ is used instead of $\mathbf{X}$. Aside from the fact that the flow law is viscoplastic, Equation (4) contains the matrix $\mathbf{K}^{-1}$ whose coefficients do not change with the state of stress [see Equation (A2)]. Only the invariant Γ which appears as argument in the scalar viscosity function $k[\Gamma]$ varies with the state of stress. This apparent difference can be easily resolved by rewriting the flow law. After dividing and multiplying by Γ^2 Equation (4) can be rewritten as

$$\dot{\boldsymbol{\epsilon}}^{in} = 1/\Gamma^2(\mathbf{K}^{-1})(\mathbf{X}\mathbf{X}')(\mathbf{H}\mathbf{X}) \tag{21}$$

where we have used Equation (A5). It is seen that the term discussed previously

appears now in the flow law and the equivalence with regard to this aspect is demonstrated.

The capability of TVBO to model rate dependence, creep and relaxation is not emphasized in this paper. An indication of the influence of rate is given in Figure 2 where the stress-strain curves for two different stress rates are plotted. As expected the influence is small. A companion paper, Yeh and Krempl [35], considers the influence of creep periods during mechanical cycling and reports on numerical experiments under cyclic temperature changes for some metal matrix composites.

ACKNOWLEDGEMENT

This research was supported by DARPA/ONR Contract N00014-86-k0770 with Rensselaer Polytechnic Institute. Dr. Yehia A. Bahei-El-Din offered useful comments and provided the solutions of the P model.

APPENDIX 1

Matrices for Transverse Isotropy

It is assumed that the 3-direction is preferred. The symmetric elastic modulus matrix **C** and the symmetric viscosity matrix **K** are then represented by

$$\mathbf{C}^{-1} = \begin{bmatrix} \frac{1}{E_{11}} & \frac{-\nu_{12}}{E_{11}} & \frac{-\nu_{31}}{E_{33}} & 0 & 0 & 0 \\ \frac{-\nu_{12}}{E_{11}} & \frac{1}{E_{11}} & \frac{-\nu_{31}}{E_{33}} & 0 & 0 & 0 \\ \frac{-\nu_{13}}{E_{11}} & \frac{-\nu_{13}}{E_{11}} & \frac{1}{E_{33}} & 0 & 0 & 0 \\ 0 & 0 & 0 & \frac{1}{G_{44}} & 0 & 0 \\ 0 & 0 & 0 & 0 & \frac{1}{G_{44}} & 0 \\ 0 & 0 & 0 & 0 & 0 & \frac{1}{G_{66}} \end{bmatrix} \tag{A1}$$

where we have used the notation of Reference [5] and where $G_{66} = E_{11}/2(1 + \nu_{12})$, and

$$\mathbf{K}^{-1} = \frac{1}{k[\Gamma]} \begin{bmatrix} \frac{1}{K_{11}} & \frac{-\eta_{12}}{K_{11}} & \frac{-\eta_{31}}{K_{33}} & 0 & 0 & 0 \\ \frac{-\eta_{12}}{K_{11}} & \frac{1}{K_{11}} & \frac{-\eta_{31}}{K_{33}} & 0 & 0 & 0 \\ \frac{-\eta_{13}}{K_{11}} & \frac{-\eta_{13}}{K_{11}} & \frac{1}{K_{33}} & 0 & 0 & 0 \\ 0 & 0 & 0 & \frac{1}{K_{44}} & 0 & 0 \\ 0 & 0 & 0 & 0 & \frac{1}{K_{44}} & 0 \\ 0 & 0 & 0 & 0 & 0 & \frac{1}{K_{66}} \end{bmatrix} \tag{A2}$$

with $K_{66} = K_{11}/2(1 + \eta_{12})$. The positive decreasing viscosity function $k[\Gamma]$, dimension of time, controls the rate dependence together with the direction-dependent viscosity factors K_{ij}, dimension of stress.

The constant elastic Poisson's ratio based on rates for loading in the i-direction is

$$\nu_{ij} = -\frac{\dot{\epsilon}_j^{el}}{\dot{\epsilon}_i^{el}} \qquad (i,j = 1,2,3,\ i \neq j) \tag{A3}$$

similarly

$$\eta_{ij} = -\frac{\dot{\epsilon}_j^{in}}{\dot{\epsilon}_i^{in}} \qquad (i,j = 1,2,3,\ i \neq j) \tag{A4}$$

is the constant inelastic Poisson's ratio based on rates for loading in the i-direction. From these the actual Poisson's ratio can be calculated (see Reference [22]).

The overstress invariant Γ is

$$(\Gamma)^2 = \mathbf{X}' \mathbf{H} \mathbf{X} \tag{A5}$$

where $\mathbf{X} = \sigma - \mathbf{g}$ is the overstress. $\mathbf{H}$ is a dimensionless matrix, given by

$$\mathbf{H} = \begin{bmatrix} H_{11} & H_{12} & H_{13} & 0 & 0 & 0 \\ H_{12} & H_{11} & H_{13} & 0 & 0 & 0 \\ H_{13} & H_{13} & H_{33} & 0 & 0 & 0 \\ 0 & 0 & 0 & H_{44} & 0 & 0 \\ 0 & 0 & 0 & 0 & H_{44} & 0 \\ 0 & 0 & 0 & 0 & 0 & H_{66} \end{bmatrix} \tag{A6}$$

where $H_{12} = H_{11} - 0.5H_{66}$.

The rate-independent invariant is $(\theta)^2 = \mathbf{Z}' \mathbf{P} \mathbf{Z}$, where $\mathbf{P} = (\mathbf{A}^{-1})' \mathbf{P}_s \mathbf{A}^{-1}$. The representation of $\mathbf{P}_s$ is analogous to $\mathbf{H}$, and the diagonal matrix $\mathbf{A}$ is given by

$$\mathbf{A} = \begin{bmatrix} A_{11} & 0 & 0 & 0 & 0 & 0 \\ 0 & A_{11} & 0 & 0 & 0 & 0 \\ 0 & 0 & A_{33} & 0 & 0 & 0 \\ 0 & 0 & 0 & A_{44} & 0 & 0 \\ 0 & 0 & 0 & 0 & A_{44} & 0 \\ 0 & 0 & 0 & 0 & 0 & A_{66} \end{bmatrix} \tag{A7}$$

where A_{ii} (no sum on i, $i = 1,3,4,6$) is the difference between the equilibrium stress (g_{ii}) and the kinematic stress (f_{ii}) in the asymptotic state.

The coefficient of thermal expansion vector is $\boldsymbol{\alpha}$

$$\boldsymbol{\alpha}' = [\alpha_1 \quad \alpha_1 \quad \alpha_3 \quad 0 \quad 0 \quad 0] \tag{A8}$$

All components are material properties which must be identified for a given material.

Reduction to Isotropy

All directions in an isotropic body are equivalent. There are two independent elastic moduli, two independent inelastic moduli (for example, one viscosity factor and one inelastic Poisson's ratio), two shape functions, one tangent modulus, and two isotropic invariants. Thus, $E_{11} = E_{33} = E$, $G_{44} = G_{66} = G$, and $\nu_{12} = \nu_{13} = \nu_{31} = \nu$ are used in Equation (A1) together with $G = E/2(1 + \nu)$. Similarly in Equation (A2) $K_{11} = K_{33} = K$, $K_{44} = K_{66}$, and $\eta_{12} = \eta_{13} = \eta_{31} = \eta$ with $K_{66} = K_{33}/2(1 + \eta)$. In Equation (A6) the reductions $H_{11} = H_{33}$, $H_{44} = H_{66}$, and $H_{13} = H_{12}$ with $H_{12} = H_{33} - 0.5H_{66}$ hold, and $A_{11} = A_{33}$, $A_{44} = A_{66}$ in Equation (A7). If in addition Γ in Equation (A5) is to reflect invariance under superposed pressure then $3H_{11} = H_{66} = 3$. In this case the usual J_3 invariant results. Finally there is only one coefficient of thermal expansion in Equation (A8).

APPENDIX 2

Shape Functions q_1, q_2, and p

The modified shape functions q_1, q_2 and p are defined as

$$q_1 = \frac{\Psi_{11}[\Gamma]}{E_{11}} = \frac{\Psi_{33}[\Gamma]}{E_{33}} = \frac{\Psi_{44}[\Gamma]}{E_{44}} = \frac{\Psi_{66}[\Gamma]}{E_{66}} \tag{A9}$$

$$q_2 = \frac{\phi_{11}[\Gamma]}{K_{11}} = \frac{\phi_{33}[\Gamma]}{K_{33}} = \frac{\phi_{44}[\Gamma]}{K_{44}} = \frac{\phi_{66}[\Gamma]}{K_{66}} \tag{A10}$$

$$p = \frac{E_{r11}}{K_{11}} = \frac{E_{r33}}{K_{33}} = \frac{E_{r44}}{K_{44}} = \frac{E_{r66}}{K_{66}} \tag{A11}$$

The shape functions $\Psi_{ii}[\Gamma]$ and $\phi_{ii}[\Gamma]$ (no sum on i), have the dimensions of stress. It is possible to set $q_1 = q_2 = q$ which will be done in this paper. The quantity p represents the ratio of the tangent moduli at the maximum inelastic strain of interest E_{rii} to the viscosity factor K_{ii} (no sum on i), and sets the slope of the stress–inelastic strain diagram at the maximum strain of interest.

APPENDIX 3

Components of the Matrices in Equation (11)

For convenience the following quantities are defined

$$\begin{aligned} \bar{E}_{33} &= c^f E^f_{33} + c^m E^m \\ L &= \nu^f_{31} E^m - \nu^m E^f_{33} \\ \bar{\nu}_{31} &= c^f \nu^f_{31} + c^m \nu^m \end{aligned} \tag{A12}$$

The nonzero components of the overall elastic compliance matrix $\bar{\mathbf{C}}^{-1}$ are using a generally accepted notation

$$(\bar{\mathbf{C}}^{-1})_{11} = \frac{c^f}{E^f_{11}} + \frac{c^m}{E^m} - \frac{c^f c^m L^2}{E^f_{33} E^m \bar{E}_{33}} = (\bar{\mathbf{C}}^{-1})_{22}$$

$$(\bar{\mathbf{C}}^{-1})_{12} = -\left(c^f \frac{\nu^f_{12}}{E^f_{11}} + c^m \frac{\nu^m}{E^m} + \frac{c^f c^m L^2}{E^f_{33} E^m \bar{E}_{33}} \right) = (\bar{\mathbf{C}}^{-1})_{21}$$

$$(\bar{\mathbf{C}}^{-1})_{13} = \frac{-\bar{\nu}_{31}}{\bar{E}_{33}} = (\bar{\mathbf{C}}^{-1})_{23} = (\bar{\mathbf{C}}^{-1})_{31} = (\bar{\mathbf{C}}^{-1})_{32}$$

$$(\bar{\mathbf{C}}^{-1})_{33} = \frac{1}{\bar{E}_{33}}$$

$$(\bar{\mathbf{C}}^{-1})_{44} = \frac{c^f}{G^f_{44}} + \frac{c^m}{G^m} = (\bar{\mathbf{C}}^{-1})_{55}$$

$$(\bar{\mathbf{C}}^{-1})_{66} = \frac{c^f}{G^f_{66}} + \frac{c^m}{G^m} \tag{A13}$$

The nonzero components of the fiber viscosity matrix $(\mathbf{K}^f)^{-1}$ are (the argument of the viscosity function k^f is omitted)

$$(K^f)^{-1}_{11} = \frac{c^f}{K^f_{11}k^f} - \frac{c^f c^m L \eta^f_{31}}{K^f_{33}k^f \bar{E}_{33}} = (K^f)^{-1}_{22}$$

$$(K^f)^{-1}_{12} = -\frac{c^f}{k^f}\left(\frac{\eta^f_{12}}{K^f_{11}} + \frac{c^m L \eta^f_{31}}{K^f_{33}\bar{E}_{33}}\right) = (K^f)^{-1}_{21}$$

$$(K^f)^{-1}_{13} = \frac{c^f}{K^f_{33}k^f}\left(\frac{c^m L}{\bar{E}_{33}} - \eta^f_{31}\right) = (K^f)^{-1}_{23}$$

$$(K^f)^{-1}_{31} = -\frac{c^f \eta^f_{31} E^f_{33}}{\bar{E}_{33}K^f_{33}k^f} = (K^f)^{-1}_{32} \tag{A14}$$

$$(K^f)^{-1}_{33} = \frac{c^f E^f_{33}}{\bar{E}_{33}K^f_{33}k^f}$$

$$(K^f)^{-1}_{44} = \frac{c^f}{K^f_{44}k^f} = (K^f)^{-1}_{55}$$

$$(K^f)^{-1}_{66} = \frac{c^f}{K^f_{66}k^f}$$

Similarly for $(K^m)^{-1}$

$$(K^m)^{-1}_{11} = \frac{c^m}{K^m k^m}\left(1 + 0.5\,\frac{c^f L}{\bar{E}_{33}}\right) = (K^m)^{-1}_{22}$$

$$(K^m)^{-1}_{12} = \frac{-c^m}{2K^m k^m}\left(1 - \frac{c^f L}{\bar{E}_{33}}\right) = (K^m)^{-1}_{21}$$

$$(K^m)^{-1}_{13} = \frac{-c^m}{K^m k^m}\left(0.5 + \frac{c^f L}{\bar{E}_{33}}\right) = (K^m)^{-1}_{23}$$

$$(K^m)^{-1}_{31} = \frac{-c^m E^m}{2\bar{E}_{33} K^m k^m} = (K^m)^{-1}_{32} \tag{A15}$$

$$(K^m)^{-1}_{33} = \frac{c^m E^m}{\bar{E}_{33} K^m k^m}$$

$$(K^m)^{-1}_{66} = \frac{3c^m}{K^m k^m} = (K^m)^{-1}_{44} = (\mathbf{K}^m)^{-1}_{55}$$

The nonzero components of the "extra terms" $(\dot{\mathbf{R}}^f)^{-1}$ and $(\dot{\mathbf{R}}^m)^{-1}$ are

$$(\dot{R}^f)^{-1}_{11} = -c^f \frac{\dot{E}^f_{11}}{(E^f_{11})^2} - \frac{c^f c^m L}{(E^f_{33})^2 \bar{E}_{33}} (\dot{\nu}^f_{31} E^f_{33} - \nu^f_{31} \dot{E}^f_{33}) = (\dot{R}^f)^{-1}_{22}$$

$$(\dot{R}^f)^{-1}_{12} = -\left[\frac{c^f}{(E^f_{11})^2} (\dot{\nu}^f_{12} E^f_{11} - \nu^f_{12} \dot{E}^f_{11}) + \frac{c^f c^m L}{(E^f_{33})^2 \bar{E}_{33}} \times (\dot{\nu}^f_{31} E^f_{33} - \nu^f_{31} \dot{E}^f_{33})\right] = (\dot{R}^f)^{-1}_{21}$$

$$(\dot{R}^f)^{-1}_{13} = \frac{c^f}{E^f_{33} \bar{E}_{33}} (\bar{\nu}_{31} \dot{E}^f_{33} - \dot{\nu}^f_{31} \bar{E}_{33}) = (\dot{R}^f)^{-1}_{23} \tag{A16}$$

$$(\dot{R}^f)^{-1}_{31} = \frac{c^f}{E^f_{33} \bar{E}_{33}} (\nu^f_{31} \dot{E}^f_{33} - \dot{\nu}^f_{31} E^f_{33}) = (\dot{R}^f)^{-1}_{32}$$

$$(\dot{R}^f)^{-1}_{33} = -\frac{c^f \dot{E}^f_{33}}{E^f_{33} \bar{E}_{33}}$$

$$(\dot{R}^f)^{-1}_{44} = -c^f \frac{\dot{G}^f_{44}}{(G^f_{44})^2} = (\dot{R}^f)^{-1}_{55}$$

$$(\dot{R}^f)^{-1}_{66} = -c^f \frac{\dot{G}^f_{66}}{(G^f_{66})^2}$$

and

$$(\dot{R}^m)^{-1}_{11} = -c^m \frac{\dot{E}^m}{(E^m)^2} + \frac{c^f c^m L}{(E^m)^2 \bar{E}_{33}} (\dot{\nu}^m E^m - \nu^m \dot{E}^m) = (\dot{R}^m)^{-1}_{22}$$

$$(\dot{R}^m)^{-1}_{12} = \frac{c^m}{(E^m)^2} (\nu^m \dot{E}^m - \dot{\nu}^m E^m)\left(1 - \frac{c^f L}{\bar{E}_{33}}\right) = (\dot{R}^m)^{-1}_{21}$$

$$(\dot{R}^m)^{-1}_{13} = \frac{c^m}{E^m \bar{E}_{33}} (\bar{\nu}_{31} \dot{E}^m - \dot{\nu}^m \bar{E}_{33}) = (\dot{R}^m)^{-1}_{23}$$

$$(\dot{R}^m)^{-1}_{31} = \frac{c^m}{E^m \bar{E}_{33}} (\nu^m \dot{E}^m - \dot{\nu}^m E^m) = (\dot{R}^m)^{-1}_{32}$$

$$(\dot{R}^m)^{-1}_{33} = -\frac{c^m \dot{E}^m}{E^m \bar{E}_{33}}$$

$$(\dot{R}^m)^{-1}_{44} = -c^m \frac{\dot{G}^m}{(G^m)^2} = (\dot{R}^m)^{-1}_{44} = (\dot{R}^m)^{-1}_{55} \tag{A17}$$

Finally the overall coefficient of thermal expansion vector $\bar{\alpha}$ is represented by

$$(\bar{\alpha})_1 = c^f \alpha^f_1 + c^m \alpha^m - \frac{c^f c^m L}{\bar{E}_{33}} (\alpha^m - \alpha^f_3) = (\bar{\alpha})_2$$

$$(\bar{\alpha})_3 = (c^f \alpha^f_3 E^f_{33} + c^m \alpha^m E^m)/\bar{E}_{33} \tag{A18}$$

$$(\bar{\alpha})_4 = (\bar{\alpha})_5 = (\bar{\alpha})_6 = 0$$

REFERENCES

1. Krempl, E. 1979. "An Experimental Study of Room-Temperature Rate-Sensitivity, Creep and Relaxation of AISI Type 304 Stainless Steel," *Journal of the Mechanics and Physics of Solids*, 27:363–375.
2. Krempl, E. and H. Lu. 1983. "Comparison of the Stress Responses of an Aluminum Alloy Tube to Proportional and Alternate Axial and Shear Strain Paths at Room Temperature," *Mechanics of Materials*, 2:183–192.
3. Kujawski, D. and E. Krempl. 1981. "The Rate (Time)-Dependent Behavior of Ti-7Al-2Cb-1Ta Titanium Alloy at Room Temperature under Quasi-Static Monotonic and Cyclic Loading," *Journal of Applied Mechanics*, 48:55–63.
4. Min, B. K. 1981. "A Plane Stress Formulation for Elastic-Plastic Deformation of Unidirectional Composites," *Journal of the Mechanics and Physics of Solids*, 29:327–352.
5. Dvorak, G. J. and Y. A. Bahei-El-Din. 1982. "Plasticity Analysis of Fibrous Composites," *Journal of Applied Mechanics*, 49:327–335.
6. Dvorak, G. J. and Y. A. Bahei-El-Din. 1987. "A Bimodal Plasticity Theory of Fibrous Composite Materials," *Acta Mechanica*, 69:219–241.
7. Kenaga, D., J. F. Doyle and C. T. Sun. 1987. "The Characterization of Boron/Aluminum Composite in the Nonlinear Range as an Orthotropic Elastic-Plastic Material," *Journal of Composite Materials*, 21:516–531.
8. Teply, J. L. and G. J. Dvorak. 1988. "Bounds on Overall Instantaneous Properties of Elastic-Plastic Composites," *Journal of the Mechanics and Physics of Solids*, 36:29–58.
9. Dvorak, G. J., Y. A. Bahei-El-Din, Y. Macheret and C. H. Liu. 1988. "An Experimental Study of Elastic-Plastic Behavior of a Fibrous Boron-Aluminum Composite," *Journal of the Mechanics and Physics of Solids*, 6:655–687.
10. Sun, C. T. and J. L. Chen. 1989. "A Simple Flow Rule for Characterizing Nonlinear Behavior of Fiber Composites," *Journal of Composite Materials*, 23:1009–1020.

11. Min, B. K. and F. W. Crossman. 1982. "Analysis of Creep for Metal Matrix Composites," *Journal of Composite Materials*, 16:188–203.
12. McLean, M. 1982. "Creep Behavior of High Temperature Metal Matrix Composites," *Fatigue and Creep of Composites Materials; Proceedings of the Third Riso International Symposium on Metallurgy and Materials Science, Roskilde, Denmark*, Riso National Lab., pp. 77–88.
13. McLean, M. 1985. "Creep Deformation of Metal-Matrix Composites," *Composites Science and Technology*, 23:37–52.
14. Lilholt, H. 1985. "Creep of Fibrous Composite Materials," *Composites Science and Technology*, 22:277–294.
15. Min, B. K. and F. W. Crossman. 1982. "History-Dependent Thermomechanical Properties of Graphite/Aluminum Unidirectional Composites," in *Composite Materials: Testing and Design (Sixth Conference), ASTM STP 787*, I. M. Daniel, ed., American Society for Testing and Materials, pp. 371–392.
16. Dvorak, G. J. 1986. "Thermal Expansion of Elastic-Plastic Composite Materials," *Journal of Applied Mechanics*, 53:737–743.
17. Wu, J. F., M. S. Shepherd, G. J. Dvorak and Y. A. Bahei-El-Din. 1989. "A Material Model for the Finite Element Analysis of Metal Matrix Composites," *Composites Science and Technology*, 35:347–366.
18. Bahei-El-Din, Y. A. 1990. "Plasticity Analysis of Fibrous Composite Laminates under Thermomechanical Loads," *Thermal and Mechanical Behavior of Ceramic and Metal Matrix Composites, ASTM STP 1080*, J. M. Kennedy and W. S. Johnson, eds., American Society for Testing and Materials, pp. 20–39.
19. Meyn, D. A. 1974. "Effect of Temperature and Strain Rate on the Tensile Properties of Boron-Aluminum and Boron-Epoxy Composites," in *Composite Materials: Testing and Design (Third Conference), ASTM STP 546*, American Society for Testing and Materials, pp. 225–236.
20. Aboudi, J. 1982. "A Continuum Theory for Fiber-Reinforced Elastic-Viscoplastic Composites," *International Journal of Engineering Science*, 20:605–621.
21. Krempl, E. and B. Z. Hong. 1989. "A Simple Laminate Theory Using the Orthotropic Viscoplasticity Theory Based on Overstress. Part I: In Plane Stress-Strain Relations for Metal Matrix Composites," *Composites Science and Technology*, 35:53–74.
22. Lee, K. D. and E. Krempl. 1991. "An Orthotropic Theory of Viscoplasticity Based on Overstress for Thermomechanical Deformations," *International Journal of Solids and Structures*, 27:1445–1459.
23. Krempl, E. and K. D. Lee. 1988. "Thermal, Viscoplastic Analysis of Composite Laminates," *Materials Research Society, Symposium Proceedings*, 120:129–136.
24. Lee, K. D. and E. Krempl. 1990. "Thermomechanical, Time-Dependent Analysis of Layered Metal Matrix Composites," *Thermal and Mechanical Behavior of Ceramic and Metal Matrix Composites, ASTM STP 1080*, J. M. Kennedy and W. S. Johnson, eds., American Society for Testing and Materials, pp. 40–55.
25. Yao, D. and E. Krempl. 1985. "Viscoplasticity Theory Based on Overstress. The Prediction of Monotonic and Cyclic Proportional and Non-Proportional Loading Paths of an Aluminum Alloy," *International Journal of Plasticity*, 1:259–274.
26. Sutcu, M. and E. Krempl. 1990. "A Simplified Orthotropic Viscoplasticity Theory Based on Overstress," *International Journal of Plasticity*, 6:247–261.
27. Krempl, E., J. J. McMahon and D. Yao. 1986. "Viscoplasticity Based on Overstress with Differential Growth Law for the Equilibrium Stress," *Mechanics of Materials*, 5:35–48.
28. Choi, S. H. and E. Krempl. 1989. "The Orthotropic Viscoplasticity Theory Based on Overstress with Static Recovery Applied to the Modeling of Long Term High Temperature Creep Behavior of Cubic Single Crystals," Rensselaer Polytechnic Institute Report MML 89-3.
29. Krempl, E. and D. Yao. 1987. "The Viscoplasticity Theory Based on Overstress Applied to Ratchetting and Cyclic Hardening," in *Low Cycle Fatigue and Elasto-Plastic Behavior of Materials*, K.-T. Rie, ed., pp. 137–148.

30. Krempl, E. and S. H. Choi. In press. "Viscoplasticity Theory Based on Overstress: The Modeling of Ratchetting and Cyclic Hardening of AISI Type 304 Stainless Steel." *Nuclear Eng. and Design*.

31. Lee, K. D. and E. Krempl. 1991. "Uniaxial Thermomechanical Loading. Numerical Experiments Using the Thermal Viscoplasticity Theory Based on Overstress." *European Journal of Mechanics. A/Solids*, 10:175–194.

32. Dvorak, G. J. and M. S. M. Rao. 1976. "Axisymmetric Plasticity Theory of Fibrous Composites." *International Journal of Engineering Science*, 14:361–373.

33. Krempl, E., M. Ruggles and D. Yao. 1987. "Viscoplasticity Theory Based on Overstress Applied to Ratchetting," in *Symposium on Advances in Inelastic Analysis, ASME Winter Annual Meeting, Dec., 1987*, S. Nakasawa, K. Willam and N. Rebelo, eds., AMD–Vol. 88/PED–Vol. 28.

34. Krempl, E. and N. M. Yeh. 1990. "Residual Stresses in Fibrous Metal Matrix Composites. A Thermoviscoplastic Analysis," in *Proceedings IUTAM Symposium on Inelastic Deformation of Composite Materials*, G. J. Dvorak, ed., Springer-Verlag, pp. 411–443.

35. Yeh, N. M. and E. Krempl. 1992. "A Numerical Simulation of the Effects of Volume Fraction, Creep and Thermal Cycling on the Behavior of Fibrous Metal-Matrix Composites," *Journal of Composite Materials*, 26(6):899–914.

THE INFLUENCE OF COOL–DOWN TEMPERATURE HISTORIES ON THE RESIDUAL STRESSES IN FIBROUS METAL MATRIX COMPOSITES

Nan–Ming Yeh and Erhard Krempl

Mechanics of Materials Laboratory
Rensselaer Polytechnic Institute
Troy, NY 12180–3590

RPI Report MML 92–2

April 1992

submitted to J. Composite Mtls.

ABSTRACT

The vanishing fiber diameter model together with the thermoviscoplasticity theory based on overstress including a recovery of state formulation are introduced. They are employed to analyze the effects of temperature rate and of annealing at constant temperature on the residual stresses at room temperature when unidirectional fibrous metal–matrix composites are cooled down from 1000°C during the manufacturing process. For the present analysis the fibers are assumed to be transversely isotropic thermoelastic and the matrix constitutive equation is isotropic thermoviscoplastic including recovery of state. All material functions and constants can depend on current temperature. Yield surfaces and loading/unloading conditions are not used in the theory in which the inelastic strain rate is solely a function of the overstress, the difference between stress and the equilibrium stress, a state variable of the theory. Assumed but realistic material elastic and viscoplastic properties as a function of temperature which are close to W/9Cr–1Mo composite permit the computation of residual stresses. Due to the viscoplasticity of the matrix time–dependent effects such as creep and change of residual stresses with time are found. It is found that the residual stresses at room temperature change considerably with temperature history. The matrix residual stress, upon reaching room temperature, is highest for the fastest cooling rate, but after thirty days rest the influence of cooling rate is hardly noticeable since relaxation takes place. Annealing periods can reduce the residual stresses by more than 12% compared to continuous cooling.

INTRODUCTION

Metal matrix composites consist of a ductile, usually low strength matrix reinforced with elastic, brittle, and strong fibers. Ideally, the strength of the fiber and the ductility of the matrix combine to provide a new material with superior properties. Selecting the best combinations of fiber and matrix materials is a difficult task which involves conflicting demands and many compromises. To prevent self stresses from developing during cool down from the manufacturing temperature, it is desirable to have the same coefficient of thermal expansion for fiber and matrix. This ideal, however, is seldom achieved as other considerations have priority in selecting the constituent materials. Once different coefficients of thermal expansion are given, residual stresses are inevitable. The question arises whether process variables could be controlled so that residual stresses at room temperature could be minimized. One such variable is the temperature history in cooling down from manufacturing temperature. Intuitively, the rate of cooling and/or hold periods at constant temperature should have an influence on the residual stresses. When the temperature holds are introduced at high homologous temperature, high temperature creep could reduce the residual stresses. However, no quantitative information is available since experiments are costly and are not available for high temperature composites.

The residual stresses can, however, be obtained by analysis provided appropriate constitutive equations and a composite model are available. The material model must capture the time–dependent processes that take place at elevated temperature such as primary, secondary, possibly tertiary creep, relaxation, and loading rate dependence. In an early analysis, the complexity of the material model and the

available material data must be matched with the composite model; it is not advantageous to combine a very detailed composite model with a constitutive equation which does not capture the essence of real material behavior.

The viscoplasticity theory based on overstress with a static recovery of state (VBO) can reproduce primary, secondary, and tertiary creep at stress levels which are in the quasi–linear region of the stress–strain diagram; it also models loading rate sensitivity and relaxation. While these phenomena are built into the constitutive equation, specific materials are modeled by identifying the constants of the theory by appropriate tests reflecting the time(rate)–dependent behavior of the matrix (in general, the fiber is modeled as linear elastic but this is not a requirement of the theory).

In principle then, VBO cannot be applied since the time(rate)–dependent material properties of the matrix are not known. For high temperature composite matrices even stress–strain diagrams are not always available. Since VBO presents the above phenomena, the specific material properties are not important when general trends are being explored. To demonstrate the potential of the analysis, a hypothetical composite was created analytically. From a theoretical and experimental investigation at 538°C for a modified 9Cr–1Mo steel used in the power generation industry, the VBO model was available at that temperature. It was then natural to take advantage of this work and a W/Cr–Mo hypothetical composite was created analytically which is called MMC3. The temperature dependence of the mechanical properties of the matrix were established by reasonable guesses. The elastic properties of the W fiber were obtained from the literature [1]. This material model was then combined with the Vanishing Fiber Diameter Model (VFD) [2] in a thermoviscoplastic analysis. The theory is applicable for arbitrary thermomechanical loadings and is specialized here to the cool–down process in the absence of external loads. Although the results are strictly valid for MMC3 only, it is believed that the general trends are indicative of matrix materials whose strength decreases and whose time(rate)–dependent properties increase with an increase in temperature. (The trends may be different for some Nickel Aluminides which exhibit a strength increase with temperature before it decreases and whose time(rate)–dependent properties are largely unknown.)

In previous papers, analyses were performed using a version of VBO without the static recovery terms in the growth laws for the state variables. As a consequence, only "cold creep" was reproduced. It is shown that the residual stresses have an influence on the subsequent mechanical behavior as well as the thermal expansion behavior of metal matrix composites [3–5].

All the analyses reported in [3–5] were for VBO, which showed only primary creep for the matrix at stress levels corresponding to the quasi linear region of the matrix stress–strain diagram. It is known from the high temperature creep behavior of monolithic materials that, in these regions, secondary and tertiary creep can occur. To model such behavior, a static recovery of state term must be introduced in the growth law for the state variables following the Baily/Orowan concept of hardening/recovery competition in secondary creep. This has been done by Majors and Krempl [6] for modified 9Cr–1Mo steel. It is shown that secondary creep in the quasi elastic regions can be reproduced together with other phenomena found in the

experiments by Ruggles, Cheng, and Krempl [7]. These experiments include strain rate changes and repeated relaxation tests at 538°C.

The VBO model based on these experiments represents real high temperature behavior. It is the matrix constitutive equation in MMC3. The analysis shows the effects of temperature rate and of annealing at constant temperature during cool–down on the residual stresses at room temperature. The effect of recovery of modified 9Cr–1Mo steel during cool down is considered to be temperature–dependent and the transition from low to high homologous temperature behavior is characterized by a decrease in strength and a decrease in rate(time) dependence. No recovery of state takes place below 450°C.

First, the governing equations are stated. They are represented by a system of first order, nonlinear, coupled differential equations which must be solved for a given boundary condition and loading/temperature history. In this case, no mechanical loading with various cooling histories are simulated numerically. The model also includes cold–creep and changes of the residual stresses with time are observed at room temperature. It is assumed that perfect bonding starts at 1000°C and holds during the cool–down process.

THE COMPOSITE MODEL

Experimental Evidence of Deformation Behavior Influenced by Recovery of State

Evidence of recovery of state influencing the deformation behavior was presented by Ruggles, Cheng and Krempl [7] and discussed and modeled using VBO by Majors and Krempl [6]. Figure 1, taken from [7], shows the rate dependence of modified 9Cr–1Mo steel at 538°C. The stress level depends strongly on strain rate and the material exhibits strain softening. Of interest is the curve with the lowest strain rate which had relaxation periods introduced at points A, B and C. Due to the slow straining and the extended relaxation periods, the specimen was exposed to the elevated temperature environment for more than 140 hrs before straining resumed at C with a strain rate of 1.2E–5 1/s. The observed gap between this curve and the one for which the strain rate was 1.2E–5 1/s from the beginning (the total test duration for this test up to 4.8% strain was approximately 1.1 hrs) is attributed to the influence of static recovery as is the rate–dependent negative slope of the stress–strain curves in the inelastic region. Further evidence of the influence of static recovery is the cyclic softening of the initially annealed steel shown in Fig. 2. The hysteresis loops with relaxation drops at the first and at the 52nd cycle are shown in Fig. 2. These and other evidences of the influence of static recovery combined with the usual rate dependence, creep, and relaxation behavior are reported in [7] and modeled with VBO in [6].

A Thermal Version of the Viscoplasticity Theory Based on Overstress with Static Recovery of State.

The theory and the modeling given by Choi [8] and Majors and Krempl [6] is modified slightly to allow for the modeling of thermal behavior. This includes the addition of a temperature rate term and allowing the material constants to depend on temperature.

For the representation of the equations, the usual vector notation for the stress tensor components σ and the small strain tensor components ϵ are used. Boldface lower and upper case letters denote 6 × 1 and 6 × 6 matrices, respectively.

In the context of an infinitesimal theory, the total strain rate, $d\epsilon/dt$, is considered to be the sum of elastic, $d\epsilon^{el}/dt$, inelastic, $d\epsilon^{in}/dt$, and thermal strain rates, $d\epsilon^{th}/dt$,

$$\dot{\epsilon} = \dot{\epsilon}^{el} + \dot{\epsilon}^{in} + \dot{\epsilon}^{th} \tag{1}$$

For each strain rate, a constitutive equation is postulated. The elastic strain is assumed to be independent of thermal history, therefore,

$$\epsilon^{el} = \frac{d}{dt}(\mathbf{C}^{-1}\sigma) \tag{2}$$

where $\mathbf{C}^{-1}$ is the temperature dependent compliance matrix, and a superposed dot represents the total time derivative, d/dt.

The inelastic strain rate is only a function of the overstress $\mathbf{x}$. It denotes the difference between the stress σ and the equilibrium stress $\mathbf{g}$, a vector state variable of the theory. Accordingly

$$\dot{\epsilon}^{in} = \mathbf{K}^{-1}\mathbf{x} \tag{3}$$

The viscosity matrix $\mathbf{K}^{-1}$ controls the rate-dependence through the viscosity factors K_{ij} and the positive, decreasing viscosity function $k[\Gamma]$. The components of $\mathbf{K}^{-1}$ for isotropy and incompressibility are given in Appendix 1.

The thermal strain rate is given by

$$\dot{\epsilon}^{th} = \boldsymbol{\alpha}\dot{T} \tag{4}$$

with $\boldsymbol{\alpha}$ the coefficient of thermal expansion vector. T is the temperature difference from some datum temperature.

The growth law for the equilibrium stress with a temperature term and a term representing static recovery is

$$\dot{\mathbf{g}} = q[\Gamma,A](\dot{\sigma} + \frac{\mathbf{x}}{k[\Gamma]}) + \dot{T}\,\frac{\partial q[\Gamma,A]}{\partial T}\sigma - (\frac{q[\Gamma,A]E - E_t}{A})\mathbf{z}\dot{\phi} - R[\pi]\mathbf{g} \tag{5}$$

where

$$\Gamma^2 = \mathbf{x}^t\mathbf{H}\mathbf{x}, \quad \dot{\phi}^2 = (\dot{\epsilon}^{in})^t\mathbf{Q}\dot{\epsilon}^{in}, \quad \pi^2 = \mathbf{g}^t\mathbf{H}\mathbf{g}$$

and

$$\mathbf{x} = \sigma - \mathbf{g}\,, \quad \mathbf{z} = \mathbf{g} - \mathbf{f}$$

The viscosity function $k[\Gamma]$ and the dimensionless modified shape functions $q[\Gamma,A]$ are decreasing ($q[0,A] < 1$ is required) and control the rate dependence and the shape of stress–strain diagram, respectively. (Square brackets following a symbol denote "function of".) Γ is the overstress invariant and $\dot{\phi}$ is the rate of inelastic strain path length. E_t is the tangent modulus at the maximum strain of interest and can be positive, zero, or negative. The vector $\mathbf{s}$ represents the difference between the equilibrium stress $\mathbf{g}$ and the kinematic stress $\mathbf{f}$. $\mathbf{H}$ and $\mathbf{Q}$ are dimensionless matrices. For isotropy, their components are chosen to yield the von Mises effective stress and inelastic incompressibility, see Appendix 1. The recovery function R is positive and depends upon the current effective equilibrium stress π, see Cernocky and Krempl [17],

$$R[\pi] = \frac{RG_3}{2}[\tanh(UG) + \tanh(VG)] \tag{6}$$

where

$$UG = -3 + 6\left(\frac{\pi - RG_1}{RG_2 - RG_1}\right), \quad VG = 3 + 6\left(\frac{\pi + RG_1}{RG_2 - RG_1}\right).$$

RG_1, RG_2, and RG_3 are temperature–dependent material constants.

To model recovery induced softening, the recovery variable λ is taken to be

$$\lambda = hp - \eta \tag{7}$$

where

$$\dot{\eta} = h\dot{\phi} - R_1[\eta]\eta \ , \quad \text{and } p = \int_t \dot{\phi} d\tau.$$

In Eq. (7), p is the accumulated inelastic strain, and h is a dimensionless positive constant. The variable η grows proportionally to the effective inelastic strain rate, $\dot{\phi}$, but recovers by the function R_1. R_1 is same form as R with different constants called RA_1, RA_2, and RA_3. The isotropic variable A is influenced by λ

$$A = B + \frac{A_0 - B}{1 - G_1\lambda} \tag{8}$$

where B is the minimum value of A, A_0 is the initial value, and G_1 is a positive dimensionless material constant.

To improve modeling, the kinematic stresses and the shape function are modified and are made to depend on A

$$\mathbf{f} = \frac{E_t}{1 - \frac{E_t}{E}} \epsilon^{in} \left(\frac{A - B}{A_0 - B}\right). \tag{9}$$

The modified shape function $q[\Gamma,A] = \psi[\Gamma,A]/E$ with ψ, a positive decreasing function of Γ is

$$\psi[\Gamma,A] = c_1 + (c_2[A] - c_1)\exp(-c_3\Gamma) \tag{10}$$

where

$$c_2[A] = \frac{E}{\dfrac{A_0(E/c_{20} - 1)}{A\exp(c_4(A - A_0))} + 1}.$$

c_{20} is the initial value of c_2.

The capabilities of Eqs. (1–10) for modeling the material behavior include

- Stress level dependence on strain rate; recovery term decreases stress at slow rates.
- Primary, secondary and tertiary creep possible in quasi–elastic range.
- Qualitative modeling of relaxation drops and stress levels at the end of relaxation tests.
- Strain rate path dependence.
- Cyclic softening.
- Small permanent effect of rest time on subsequent stress–strain diagram.
- Tangent modulus in the inelastic range decreases with decreasing strain rate.

The details can be found in [6]. All constants can depend on temperature and this dependence is not explicitly displayed.

The Composite Model

For MMC3, it is assumed that the fiber of the unidirectional composite is transversely isotropic thermoelastic, the matrix is isotropic and thermoviscoplastic with recovery of state and represented by Eqs. (1–10). Fiber orientation in the 3–direction is postulated.

For the VFD model, Dvorak and Bahei–El–Din [2], the following constraint equations hold

$$\begin{aligned}
\dot\sigma_i &= \dot\sigma_i^f = \dot\sigma_i^m \quad \text{for } i \neq 3 \\
\dot\sigma_3 &= c^f\,\dot\sigma_3^f + c^m\,\dot\sigma_3^m \\
\dot\epsilon_i &= c^f\,\dot\epsilon_i^f + c^m\,\dot\epsilon_i^m \quad \text{for } i \neq 3 \\
\dot\epsilon_3 &= \dot\epsilon_3^f = \dot\epsilon_3^m.
\end{aligned} \tag{11}$$

In the above, stresses and strains without a superscript designate quantities imposed on the composite as a whole. Superscripts ^{f} and ^{m} denote fiber and matrix, respectively. The fiber volume fraction is c^f and c^m denotes the matrix volume fraction with $c^f + c^m = 1$. When the constraints [11] are combined with the VBO equations of Lee and Krempl [9], the composite response is given by (details can be found in Yeh and Krempl [10,13])

$$\dot\epsilon = \overline{C}^{-1}\dot\sigma + (K^m)^{-1}x^m + (\dot R^f)^{-1}\sigma^f + (\dot R^m)^{-1}\sigma^m + \overline{\alpha}\dot T \tag{12}$$

together with a separate equation for the σ_3^m component of the matrix

$$\dot{\sigma}_3^m = \frac{E^m}{E_{33}}\dot{\sigma}_3 - \frac{c^f}{E_{33}} L(\dot{\sigma}_1 + \dot{\sigma}_2) - \frac{c^f E_{33}^f E^m}{E_{33}}$$

$$\left\{\frac{1}{K^m k^m [\Gamma^m]} \left[x_3^m - 0.5(x_1^m + x_2^m)\right]\right\}$$

$$- \frac{c^f E_{33}^f E^m}{E_{33}} \left\{\left[\frac{1}{(E_{33}^f)^2}(\dot{\nu}_{31}^f E_{33}^f - \nu_{31}^f \dot{E}_{33}^f)\right.\right.$$

$$\left. - \frac{1}{(E^m)^2}(\dot{\nu}^m E^m - \nu^m \dot{E}^m)\right](\sigma_1 + \sigma_2) + \frac{\dot{E}_{33}^f}{(E_{33}^f)^2}\sigma_3^f - \left.\frac{\dot{E}^m}{(E^m)^2}\sigma_3^m\right\}$$

$$- \frac{c^f E_{33}^f E^m}{E_{33}}(\alpha^m - \alpha_3^f)\dot{T}. \qquad (13)$$

In addition, the growth laws for the state variables described previously are needed.

In the above, $\bar{C}^{-1}$ is the symmetric overall compliance matrix whose components are functions of the elastic properties of fiber and matrix. The viscosity matrix $(K^m)^{-1}$ is not symmetric and its components, together with those of $\bar{C}^{-1}$, are listed in Appendix 1. (Note, the matrix material is assumed to be isotropic and inelastically incompressible.) The matrices $(\dot{R}^f)^{-1}$ and $(\dot{R}^m)^{-1}$ contain time derivatives of the elastic constants of the fiber and the matrix, respectively. Both matrices are not symmetric, see Appendix 1. They are zero if the elastic constants are independent of temperature. These matrices represent the "additional" terms which can play a significant role in modeling thermomechanical behavior, see Lee and Krempl [11]. Finally, the components of $\bar{\alpha}$ are composed of the elastic constants and the coefficients of thermal expansion, see Appendix 1.

Equation (12) shows that the overall strain rate is the sum of the overall elastic strain rate, the overall inelastic strain rates contributed by the matrix, and the overall thermal strain rate in the case of constant elastic properties. If temperature dependent elastic properties are assumed, then two additional terms contribute to the overall strain rate. They insure that the elastic behavior is path independent, see Lee and Krempl [11].

Equation (13) is used to calculate the instantaneous axial matrix stress which cannot be directly obtained from the overall boundary conditions. E_{33} and L are defined in Appendix 1. σ_3^m is affected by mechanical and thermal loadings and their loading paths. For instance, for pure thermal loading (overall stresses are zero), σ_3^m

together with g_3^m, f_3^m will develop due to the difference in the coefficients of thermal expansion of fiber and matrix; these matrix stresses in the fiber direction cause coupling between the mechanical and thermal loading in the inelastic range.

NUMERICAL SIMULATION

Equations (1) through (13) constitute the model which must now be applied by specifying the boundary conditions and the uniform temperature history. In this paper we assume no overall stresses. Stresses arise when the temperature changes due to the different coefficients of thermal expansion for fiber and matrix. The properties of MMC3, a hypothetical unidirectional composite made of a modified 9Cr–1Mo steel matrix and W fibers are listed in Tables 1 and 2, respectively. The matrix properties give rise to the stress–strain diagrams shown in Fig. 3 at the indicated strain rate. A decrease in stress level with temperature is modeled. Long term creep curves at 538°C and 600°C at stress levels within the elastic range of the stress–strain curves in Fig. 3 are depicted in Fig. 4. It is seen that primary, secondary and tertiary creep are modeled. This capability is due to the recovery terms described previously. In the model it is assumed that static recovery is unimportant at temperatures below 450°C and only "cold" creep can be modeled below this temperature. Even at room temperature cold creep is found [12] which can give rise to residual stress changes while the composite is at rest at room temperature. Room temperature time–dependent behavior has been found in composites [15].

Residual Stresses upon Cool–Down from Manufacturing Temperature

The residual stresses at room temperature might be influenced by the cooling history. As a consequence, numerical experiments were performed involving the thermal histories listed in Table 3. They include continuous cooling at different temperature rates, Cases 1–3, change of temperature rates, Cases 4–6, and temperature holds at 600°C or at 800°C with rate changes, Cases 7–12. The results are graphed in Figs. 5–9.

The increase in the matrix stress in the fiber direction σ_3^m and of the equilibrium stress g_3^m in that direction with decreasing temperature is shown in Fig. 5. When the composite reaches room temperature at point b, relaxation sets in and the stress decreases while the equilibrium stress increases. As seen from the inset, the overstress, the difference of the stress and the equilibrium stress, decreases with time. After 30 days, the overstress is small and relaxation ceases for practical purposes. The residual stress which would be measured in a real composite would be close to that of point c since it takes some time before the composite can be tested. The stress redistribution at room temperature is caused by the presence of cold creep, i.e. the rate dependence of the matrix at room temperature found in alloys [12] and composites [15].

The influence of cooling rate is shown in Fig. 6 where only the matrix stress is plotted. Upon reaching room temperature, the stress is highest for the fastest cooling rate. It would appear then that a slow cooling rate would be beneficial. However,

the results in Table 4 show that the residual stresses after 30 days differs only by about 3 MPa. During the hold at room temperature, the relaxation is faster for the high than for the slow temperature rate so that the initial difference of 30 MPa between Cases 1 and 3 diminishes to 3 MPa. It is concluded that the final stress is nearly unaffected by the cooling rate.

The temperature rate changes do not appreciably alter the picture, see Fig. 7 and Table 4. It is, however, clearly noticeable that a slow cool in the high temperature region has a beneficial effect on the residual stresses, compare Cases 4 and 6 with Case 5.

It can be seen from Table 3 that the difference between Cases 7–9 and Cases 10–12 is the length of the temperature hold. The 30 day hold for Cases 7–9 produces up to 10% lower residual stresses than the one day hold, Cases 10–12, see Table 4. The lowest residual stress is found for Case 8 (Case 7 differs only by 1 MPa) with a hold at 600°C and fast cooling rates. When temperature holds are introduced at 800°C rather than at 600°C, the residual stresses are high, compare Cases 7 and 8 and Cases 11 and 12. The introduction of 30 day hold periods at 600°C is very effective and leads to the lowest residual stresses. It is also seen from Fig. 8 and Table 4 that using slow cooling to 600°C has no effect on the residual stresses. Figure 8 shows that the slow and the fast cooling rate curves relax to the same stress at the end of the 30 day hold at 600°C and that subsequent cooling starts from the same stress level. The situation is different for the one day hold of Fig. 9 for Cases 10 and 11. The fast cooling rate curve relaxes not quite as far as the slow one and the beneficial effect of slow cooling to 600°C is noticeable in the residual stress level, 204 vs 208 MPa. Comparing Cases 6 and 10 shows that the introduction of a one day hold has a very minor effect on the final residual stresses.

DISCUSSION

A composite model based on a "unified" viscoplasticity theory, the thermoviscoplasticity theory based on overstress (VBO), and the vanishing fiber diameter model (VFD) were used to analyse the effects of temperature rate and of annealing at constant temperature on the permanent residual stresses at room temperature. It was assumed that the unidirectional fibrous metal–matrix composite MMC3 was cooled down from 1000°C during the manufacturing process. Material properties based on a real alloy were used to create the hypothetical MMC3. Of special interest was the effect of recovery of state representing high temperature creep in the constitutive equation.

In a companion investigation, Yeh and Krempl [16], no recovery of state was included in the simulation of the behavior of Gr/Al. The same 12 Cases were computed and it was shown that the residual stresses at room temperature and long times differed by less than 3% for all 12 temperature histories. The present analysis, which includes high temperature creep, shows that there can be as much as 36 MPa difference in the final residual stress. As expected, the lowest residual stress is achieved with Case 8 which involves a 30 day hold at 600°C. It may be impractical to use such a history. Case 6, which involves slow cooling to 600°C followed by fast

cooling, is a cooling path which is practically feasible. It takes about 4.8 days as opposed to 30.3 days for Case 8. The results clearly show that an optimum path can be found and that high temperature creep has a beneficial effect on the final residual stress.

The residual stresses immediately after reaching room temperature range form 251 to 209 MPa, a 20% difference. These stresses relax with time spent at room temperature due to the presence of cold creep which has been observed in Al based metal matrix composites [15]. Since experiments have shown that cold creep is present with ferritic steels at room temperature [14], we have built it into the present model. Cold creep gives rise to the observed relaxation which is nearly over after 30 days. Cases 1–3 show that at the end the influence of rate is negligible since the final residual stresses are nearly identical. This observation corresponds to the results of a companion investigation without recovery of state [16] where temperature history effects are negligible after 30 days.

When extended periods of time are spent at temperatures where the influence of recovery of state is significant, its influence on the final residual stress is noticeable. However, the overall effect is not very large since the final stresses differ only by 18%.

Therefore, it appears therefore that variation of the thermal history does not have a very significant effect on the final residual stresses. However, it is clear that recovery of state or high temperature creep can be useful in reducing residual stresses. Holds in regions where recovery of state are significant are most beneficial. Since recovery of state is a long–term process, the beneficial effects can only be expected after long cooling times.

The present paper intends to show the capabilities of the proposed analysis in principle using a hypothetical composite MMC3. For the exact modeling of a metal matrix composite, various refinements are possible. Included are the determination of matrix and fiber properties as a function of temperature and the use of other micromechanical models. While the magnitude of the residual stresses are strongly dependent on the specific system, the general trends are expected to remain unaltered.

ACKNOWLEDGMENT

This research was supported by DARPA/ONR Contract N00014–86–k0770 with Rensselaer Polytechnic Institute. Some material properties of modified 9Cr–1Mo steel were provided by Dr. M. B. Ruggles.

REFERENCES

1 Wetherhold, R. C. and Westfall, L. J. "Thermal Cycling of Tungsten–fibre–reinforced Superalloy Composites," Journal of Material Science, 12:713–717 (1988).

2 Dvorak, G. J. and Bahei–El–Din, Y. A. "Plasticity Analysis of Fibrous Composites," ASME Journal of Applied Mechanics, 49:327–335 (1982).

3 Krempl, E. and Yeh, N. M. "Residual Stresses in Fibrous Metal Matrix Composites. A Thermoviscoplastic Analysis," Proceedings of IUTAM Symposium on Inelastic Deformation of Composite Materials, G. J. Dvorak, Ed., Spring–Verlag, 411–443 (1990).

4 Yeh, N. M. and Krempl, E. "A Thermoviscoplastic Analysis of Laminated Metal Matrix Composites using the Viscoplasticity Theory Based on Overstress," Proceedings of Symposium on the Mechanics of Composites at Elevated and Cryogenic Temperatures, ASME Applied Mechanics Division Meeting, W. F. Jones and S. Singhal, Eds., American Society of Mechanical Engineers, New York, NY, 9–22 (1991).

5 Krempl, E. and Yeh, N. M. "Residual Stresses Effect on Thermal Cycling Behavior of Laminated Metal Matrix Composites," to appear in Proceedings of 3rd International Conference on Residual Stresses, Tokushima, Japan, July 24–26 (1991).

6 Majors, P. S. and Krempl, E. "A Recovery of State Formulation for the Viscoplasticity Theory Based on Overstress," Proceedings of the Conference on High Temperature Constitutive Modeling: Theory and Application, A. D. Freed and K. P. Walker, Eds., American Society of Mechanical Engineers, New York, NY, 235–250 (1991).

7 Ruggles, M. B., Cheng, S., and Krempl, E. "The Rate (Time)–Dependent Mechanical Behavior of Modified 9Cr–1Mo Steel—I. Experiments at 538°C," Transactions of the 11th International Conference on Structural Mechanics in Reactor Technology, L06/2, Tokyo, Japan, 145–150 (1991).

8 Choi, S. H. and Krempl, E. "The Orthotropic Viscoplasticity Theory Based on Overstress with Static Recovery Applied to The Modeling of Long Term High Temperature Creep Behavior of Cubic Single Crystals," Rensselaer Polytechnic Institute Report MML 89–3 (1989).

9 Lee, K. D. and Krempl, E. "An Orthotropic Theory of Viscoplasticity Based on Overstress for Thermomechanical Deformations," International Journal of Solids and Structures, 27:1445–1459 (1991).

10 Yeh, N. M. and Krempl, E. "Thermoviscoplasticity Theory Based on Overstress Applied to the Analysis of Fibrous Metal–Matrix Composites," to appear in Journal of Composite Materials (1992).

11 Lee, K. D. and Krempl, E. "Uniaxial Thermomechanical Loading. Numerical Experiments Using the Thermal Viscoplasticity Theory Based on Overstress," European Journal of Mechanics A/Solids, 10:175–194 (1991).

12 Krempl, E. "An Experimental Study of Room–Temperature Rate Sensitivity, Creep and Relaxation of Type 304 Stainless Steel," Journal of the Mechanics and Physics of Solids, 27:363–375 (1979).

13 Yeh, N. M. and Krempl, E. "A Numerical Simulation of the effects of Volume Fraction, Creep and Thermal Cycling on the Behavior of Fibrous Metal Matrix Composites," to appear in Journal of Composite Materials (1992).

14 Krempl, E. and Lu, H. "The Rate(Time)–dependence of Ductile Fracture at Room Temperature," Engineering Fracture Mechanics, 20:629–632 (1984).

15 Min, B. K. and Crossman, F. W., "Analysis of Creep for Metal Matrix Composites," Journal of Composite Materials, 16:188–203 (1982).

16 Krempl, E. and Yeh, N.–M., "The Influence of Cooling Paths on the Residual Stress at Room Temperature of a Graphite/Aluminum Composite," Rensselaer Polytechnic Institute Report MML 92–2 (1992).

17 Cernocky, E. P. and Krempl, E., "Construction of Nonlinear Monotonic Functions with Selectable Intervals of Almost Constant or Linear Behavior," Journal of Applied Mechanics, 45:780–784 (1978).

APPENDIX 1

Matrices for Isotropy

The nonzero components of the symmetric elastic modulus matrix $\mathbf{C}^{-1}$ and the symmetric viscosity matrix $\mathbf{K}^{-1}$ are

$$\begin{aligned}(C^{-1})_{11} &= (C^{-1})_{22} = (C^{-1})_{33} = 1/E \\ (C^{-1})_{44} &= (C^{-1})_{55} = (C^{-1})_{66} = 1/G \\ (C^{-1})_{ij} &= -\nu/E,\ i,\ j = 1,\ 2,\ 3,\ \text{and}\ i \neq j \end{aligned} \tag{A1}$$

$$\begin{aligned}(K^{-1})_{11} &= (K^{-1})_{22} = (K^{-1})_{33} = 1/Ek[\Gamma] \\ (K^{-1})_{44} &= (K^{-1})_{55} = (K^{-1})_{66} = 3/Ek[\Gamma] \\ (K^{-1})_{ij} &= -1/2Ek[\Gamma],\ i,\ j = 1,\ 2,\ 3,\ \text{and}\ i \neq j \end{aligned} \tag{A2}$$

The coefficient of thermal expansion vector is

$$\alpha^t = [\alpha\ \alpha\ \alpha\ 0\ 0\ 0] \tag{A3}$$

H and **Q** are dimensionless matrices. For isotropy and independence of superposed hydrostatic terms the nonzero components are

$$\begin{aligned}H_{11} = H_{22} = H_{33}\ \ 1,\ H_{44} = H_{55} = H_{66} = 3 \\ H_{ij} = -0.5,\ i,\ j = 1,\ 2,\ 3,\ \text{and}\ i \neq j, \end{aligned} \tag{A4}$$

and

$$\begin{aligned}Q_{11} = Q_{22} = Q_{33} = 1,\ Q_{44} = Q_{55} = Q_{66} = 1/3 \\ Q_{ij} = -0.5,\ i,\ j = 1,\ 2,\ 3,\ \text{and}\ i \neq j, \end{aligned} \tag{A5}$$

respectively.

Components of the Matrices in Eq. (12)

For convenience the following quantities are defined

$$\begin{aligned}\bar{E}_{33} &= c^f E^f_{33} + c^m E^m \\ L &= \nu^f_{31} E^m - \nu^m E^f_{33} \\ \bar{\nu}_{31} &= c^f \nu^f_{31} + c^m \nu^m\ . \end{aligned} \tag{A6}$$

The nonzero components of the overall elastic compliance matrix $\bar{C}^{-1}$ are

$$
\begin{aligned}
(\bar{C}^{-1})_{11} &= \frac{c^f}{E^f_{11}} + \frac{c^m}{E^m} - \frac{c^f c^m L^2}{E^f_{33} E^m E_{33}} = (\bar{C}^{-1})_{22} \\
(\bar{C}^{-1})_{12} &= -\left(c^f \frac{\nu^f_{12}}{E^f_{11}} + c^m \frac{\nu^m}{E^m} + \frac{c^f c^m L^2}{E^f_{33} E^m E_{33}}\right) = (\bar{C}^{-1})_{21} \\
(\bar{C}^{-1})_{13} &= \frac{-\bar{\nu}_{31}}{E_{33}} = (\bar{C}^{-1})_{23} = (\bar{C}^{-1})_{31} = (\bar{C}^{-1})_{32} \\
(\bar{C}^{-1})_{33} &= \frac{1}{E_{33}} \\
(\bar{C}^{-1})_{44} &= \frac{c^f}{G^f_{44}} + \frac{c^m}{G^m} = (\bar{C}^{-1})_{55} \\
(\bar{C}^{-1})_{66} &= \frac{c^f}{G^f_{66}} + \frac{c^m}{G^m} .
\end{aligned}
\tag{A7}
$$

The nonzero components of the matrix $(K^m)^{-1}$ are (the argument of the viscosity function k^m is omitted)

$$
\begin{aligned}
(K^m)^{-1}_{11} &= \frac{c^m}{K^m k^m}\left(1 + 0.5\frac{c^f L}{E_{33}}\right) = (K^m)^{-1}_{22} \\
(K^m)^{-1}_{12} &= \frac{-c^m}{2K^m k^m}\left(1 - \frac{c^f L}{E_{33}}\right) = (K^m)^{-1}_{21} \\
(K^m)^{-1}_{13} &= \frac{-c^m}{K^m k^m}\left(0.5 + \frac{c^f L}{E_{33}}\right) = (K^m)^{-1}_{23} \\
(K^m)^{-1}_{31} &= \frac{-c^m E^m}{2E_{33} K^m k^m} = (K^m)^{-1}_{32} \\
(K^m)^{-1}_{33} &= \frac{c^m E^m}{E_{33} K^m k^m} \\
(K^m)^{-1}_{66} &= \frac{3c^m}{K^m k^m} = (K^m)^{-1}_{44} = (K^m)^{-1}_{55} .
\end{aligned}
\tag{A8}
$$

The nonzero components of the "extra terms" $(\dot{R}^f)^{-1}$ and $(\dot{R}^m)^{-1}$ are

$$(\dot{R}^f)_{\bar{1}\bar{1}} = -c^f\frac{\dot{E}^f_{11}}{(E^f_{11})^2} - \frac{c^f c^m L}{(E^f_{33})^2 E_{33}}(\dot{\nu}^f_{31}E^f_{33} - \nu^f_{31}\dot{E}^f_{33}) = (\dot{R}^f)_{\bar{2}\bar{2}}$$

$$(\dot{R}^f)_{\bar{1}\bar{2}} = -\left[\frac{c^f}{(E^f_{11})^2}(\dot{\nu}^f_{12}E^f_{11} - \nu^f_{12}\dot{E}^f_{11}) + \frac{c^f c^m L}{(E^f_{33})^2 E_{33}}(\dot{\nu}^f_{31}E^f_{33} - \nu^f_{31}\dot{E}^f_{33})\right] = (\dot{R}^f)_{\bar{2}\bar{1}}$$

$$(\dot{R}^f)_{\bar{1}\bar{3}} = \frac{c^f}{E^f_{33}E_{33}}(\bar{\nu}_{31}\dot{E}^f_{33} - \dot{\nu}^f_{31}E_{33}) = (\dot{R}^f)_{\bar{2}\bar{3}} \qquad \text{(A9)}$$

$$(\dot{R}^f)_{\bar{3}\bar{1}} = \frac{c^f}{E^f_{33}E_{33}}(\nu^f_{31}\dot{E}^f_{33} - \dot{\nu}^f_{31}E^f_{33}) = (\dot{R}^f)_{\bar{3}\bar{2}}$$

$$(\dot{R}^f)_{\bar{3}\bar{3}} = -\frac{c^f\dot{E}^f_{33}}{E^f_{33}E_{33}}$$

$$(\dot{R}^f)_{\bar{4}\bar{4}} = -c^f\frac{\dot{G}^f_{44}}{(G^f_{44})^2} = (\dot{R}^f)_{\bar{5}\bar{5}}$$

$$(\dot{R}^f)_{\bar{6}\bar{6}} = -c^f\frac{\dot{G}^f_{66}}{(G^f_{66})^2}$$

and

$$(\dot{R}^m)_{\bar{1}\bar{1}} = -c^m\frac{\dot{E}^m}{(E^m)^2} + \frac{c^f c^m L}{(E^m)^2 E_{33}}(\dot{\nu}^m E^m - \nu^m\dot{E}^m) = (\dot{R}^m)_{\bar{2}\bar{2}}$$

$$(\dot{R}^m)_{\bar{1}\bar{2}} = \frac{c^m}{(E^m)^2}(\dot{\nu}^m\dot{E}^m - \dot{\nu}^m E^m)(1 - \frac{c^f L}{E_{33}}) = (\dot{R}^m)_{\bar{2}\bar{1}}$$

$$(\dot{R}^m)_{\bar{1}\bar{3}} = \frac{c^m}{E^m E_{33}}(\bar{\nu}_{31}\dot{E}^m - \dot{\nu}^m E_{33}) = (\dot{R}^m)_{\bar{2}\bar{3}} \qquad \text{(A10)}$$

$$(\dot{R}^m)_{\bar{3}\bar{1}} = \frac{c^m}{E^m E_{33}}(\nu^m\dot{E}^m - \dot{\nu}^m E^m) = (\dot{R}^m)_{\bar{3}\bar{2}}$$

$$(\dot{R}^m)_{\bar{3}\bar{3}} = -\frac{c^m\dot{E}^m}{E^m E_{33}}$$

$$(\dot{R}^m)_{\bar{6}\bar{6}} = -c^m\frac{\dot{G}^m}{(G^m)^2} = (\dot{R}^m)_{\bar{4}\bar{4}} = (\dot{R}^m)_{\bar{5}\bar{5}}\ .$$

Finally the overall coefficient of thermal expansion vector $\overline{\alpha}$ is represented by

$$
\begin{aligned}
(\overline{\alpha})_1 &= c^f \alpha_1^f + c^m \alpha^m - \frac{c^f c^m L}{E_{33}}(\alpha^m - \alpha_3^f) = (\overline{\alpha})_2 \\
(\overline{\alpha})_3 &= (c^f \alpha_3^f E_{33}^f + c^m \alpha^m E^m)/E_{33} \\
(\overline{\alpha})_4 &= (\overline{\alpha})_5 = (\overline{\alpha})_6 = 0.
\end{aligned}
\tag{A11}
$$

Table 1. Thermoelastic and Thermoviscoplastic Properties of Modified 9Cr–1Mo Steel Matrix (MMC3) with Temperature–Dependent Recovery Function (*)

E	$= 237160 - 172.5T + 0.31T^2 - 3.43e{-}4T^3 + 1.1e{-}7T^4$ (MPa)	$298 \leq T \leq 1273°K$
G	$= 91572.1 - 68.924T + 0.1261T^2 - 1.386e{-}4T^3 + 4.421e{-}8T^4$ (MPa)	$298 \leq T \leq 1273°K$
α	$= 6.e{-}6 + 2.37e{-}8T - 3.78e{-}11T^2 + 3.2e{-}14T^3 - 9.2e{-}18T^4$ (m/m/°C)	$298 \leq T \leq 1273°K$
K^m	$= E$	
$k[\Gamma]$	$= k_1(1 + \frac{\Gamma}{k_2})^{-k_3(1 + \exp(k_5(\Gamma - k_4)))}$	
k_1	$= 2e{+}6$ (s), $k_2 = 250$ (MPa), $k_4 = 380$ (MPa), $k_5 = 0.01$ (1/MPa)	
k_3	$= 42.061 - 6.061e{-}2T$ (1/MPa)	$T \leq 364°K$
	$= 98.99 - 0.5775T + 1.525e{-}3T^2 - 1.723e{-}6T^3 + 6.968e{-}10T^4$	$364 \leq T \leq 873°K$
	$= -18.7271 + 0.0446625T - 6.25e{-}6T^2$	$T \geq 873°K$
E_t	$= -6214.62 + 126.257T - 0.2754T^2$ (MPa)	$T \leq 364°K$
	$= 11939.9 - 43.437T + 4.742e{-}2T^2 + 4.461e{-}5T^3 - 7.4763e{-}8T^4$	$364 \leq T \leq 811°K$
	$= 17624 - 33.236T - 6.185e{-}3T^2 + 3.76e{-}5T^3 - 1.689e{-}8T^4$	$T \geq 811°K$
A_0	$= 579.276 - 1.1393T + 9.886e{-}4T^2 + 2.111e{-}6T^3 - 2.833e{-}9T^4$	$T \leq 873°K$
	$= 304.391 - 0.34325T + 1.25e{-}4T^2$ (MPa)	$T \geq 873°K$
q	$= \psi/E$; see Eq. (10)	
c_1	$= 137212 - 212T$ (MPa)	$T \leq 364°K$
	$= 304327 - 1770.68T + 4.662T^2 - 5.283e{-}3T^3 + 2.123e{-}6T^4$	$364 \leq T \leq 873°K$
	$= 50231.8 - 1.35T - 0.025T^2$	$T \geq 873°K$
c_{20}	$= 228189 - 122.1T + 0.1728T^2 - 1.837e{-}4T^3 + 4.416e{-}8T^4$ (MPa)	$298 \leq T \leq 1273°K$
c_3	$= 2.424e{-}3 + 7.576e{-}5T$ (1/MPa)	$T \leq 364°K$
	$= 0.6561 - 4.978e{-}3T + 1.429e{-}5T^2 - 1.751e{-}8T^3 + 7.831e{-}12T^4$	$364 \leq T \leq 873°K$
	$= -0.3365 + 0.0005T$	$T \geq 873°K$
c_4	$= 0.5$ (1/MPa)	
h	$= 0$	$T \leq 723°K$
	$= 298.534 - 1.244T + 1.896e{-}3T^2 - 1.225e{-}6T^3 + 2.883e{-}10T^4$	$T \geq 723°K$
G_1	$= 0$	$T \leq 723°K$
	$= 298.534 - 1.244T + 1.896e{-}3T^2 - 1.225e{-}6T^3 + 2.883e{-}10T^4$	$T \geq 723°K$
B	$= 398.3 - 0.713T - 8.546e{-}4T^2 + 4.42e{-}6T^3 - 3.504e{-}9T^4$ (MPa)	$T \leq 873°K$
	$= 64.92 - 0.04T$	$T \geq 873°K$

Table 1. (continued)

$RG_1 = 0$ (MPa)	$298 \leq T \leq 1273°K$
$RG_2 = -589.57+12.04T-4.32e-2T^2+6.15e-5T^3-3.07e-8T^4$ (MPa)	$T \leq 873°K$
$= 209.125-0.125T$	$T \geq 873°K$
$RG_3 = 0$ (1/s)	$T \leq 723°K$
$= 4.1e-4-1.79e-6T+2.83e-9T^2-1.95e-12T^3+4.967e-16T^4$	$T \geq 723°K$
$RA_1 = 0$ (MPa)	$298 \leq T \leq 1273°K$
$RA_2 = 273.19-0.547T-4.8e-4T^2+2.55e-6T^3-1.906e-9T^4$ (MPa)	$T \leq 873°K$
$= 122.196-0.1716T+6.25e-5T^2$	$T \geq 873°K$
$RA_3 = 0$ (1/s)	$T \leq 723°K$
$= 4.1-1.785e-2T+2.829e-5T^2-1.95e-8T^3+4.967e-12T^4$	$T \geq 723°K$
$\nu = 0.3$, and inelastic Poisson's Ratio: 0.5	

* Estimated

Table 2. Thermoelastic Properties for W Fiber*

$E^f_{33} = E^f_{11}$ (MPa)	410920–40T	$298 \leq T \leq 1273^oK$
ν^f_{31}	0.29	$298 \leq T \leq 1273^oK$
$G^f_{44} = G^f_{66}$ (MPa)	159271–15.5T	$298 \leq T \leq 1273^oK$
$\alpha^f_3 = \alpha^f_1$ (m/m/°C)	4.198e–6+8.87e–10T	$298 \leq T \leq 1273^oK$

*From [1].

Table 3. Thermal Histories Used for MMC3

Case	Description	Cooling Rates °C/s	Hold Duration (Days)
1	Continuous	0.1	No
2	Continuous	0.033	No
3	Continuous	0.001	No
4	Rate Change (at 450 °C)	0.001/0.033	No
5	Rate Change (at 450 °C)	0.033/0.001	No
6	Rate Change (at 600 °C)	0.001/0.033	No
7	Temp. Hold (at 600 °C)	0.001/0.033	30
8	Temp. Hold (at 600 °C)	0.033/0.033	30
9	Temp. Hold (at 800 °C)	0.033/0.033	30
10	Temp. Hold (at 600 °C)	0.001/0.033	1
11	Temp. Hold (at 600 °C)	0.033/0.033	1
12	Temp. Hold (at 800 °C)	0.033/0.033	1

Table 4. Matrix Residual Stress for the Thermal Histories of Table 3

Case		1	2	3	4	5	6
σ_3^m (MPa)	(i)*	251	242	220	231	230	232
	(ii)*	217	216	214	207	224	206
Case		7	8	9	10	11	12
σ_3^m (MPa)	(i)*	210	209	225	229	234	239
	(ii)*	189	188	200	204	208	213

* Results in rows (i) and (ii) represent the residual stress immediately after reaching room temperature and after 30 days at room temperature, respectively.

FIGURE CAPTIONS:

Fig. 1. Rate and strain rate history dependence of modified 9Cr–1Mo steel at 538°C.

Fig. 2. Cyclic loading with repeated relaxation periods of modified 9Cr–1Mo steel at 538°C. Cyclic softening is indicative of recovery of state.

Fig. 3. Stress–strain diagrams of MMC3 matrix at various temperatures.

Fig. 4. Long term creep curves of MMC3 matrix at stress levels within the elastic range of the stress–strain curves in Fig. 3 at 538°C and 600°C.

Fig. 5. Development of matrix stress in fiber direction, and matrix equilibrium stress during cool–down from the assumed manufacturing temperature of 1000°C. The inset shows the decrease of the overstress during the room temperature hold b–c. MMC3

Fig. 6. Matrix residual stress developed during cool down of MMC3 from the assumed manufacturing temperature at 1000°C. The influence of cooling rate is apparent. After a hold of 30 days at room temperature the smallest residual stress of 214 MPa is obtained a cooling rate of 0.001°C/s. The model shows stress relaxation at room temperature.

Fig. 7. The effects of cooling rate change on the matrix residual stress at room temperature. The final residual stress for Case 4 is 207 MPa, compared to 224 MPa for Case 5.

Fig. 8. Influence of cooling rate and 30 days temperature holds at 600°C or at 800°C on the matrix residual stress at room temperature. In this case the lowest residual stress is 188 MPa for Case 8 about a 14% reduction compared to Fig. 6.

Fig. 9. Influence of cooling rate and 1 day temperature holds at 600°C or at 800°C on the matrix residual stress at room temperature. In this case the lowest residual stress is 204 MPa for Case 10.

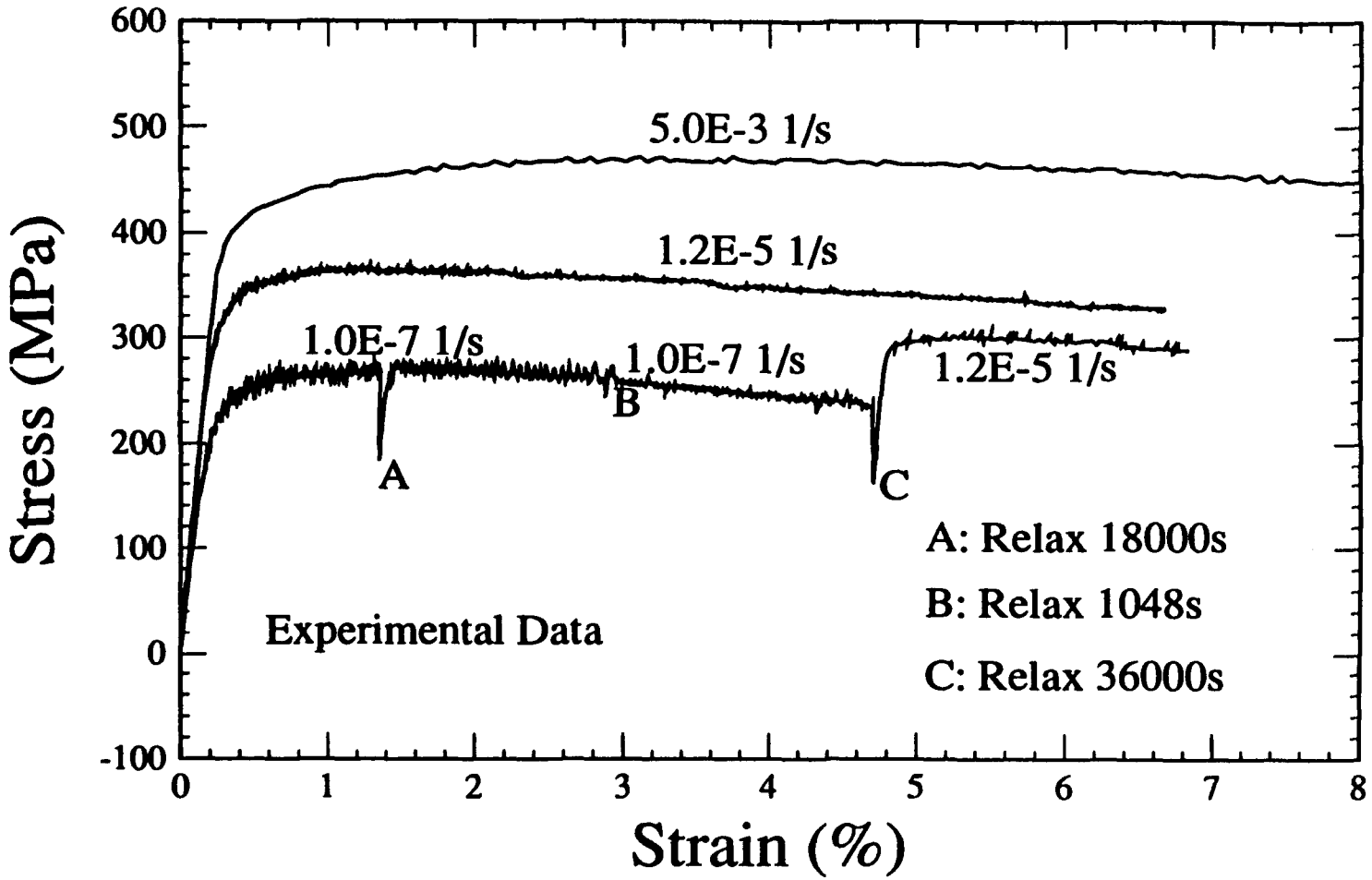
600
500
400
300
200
100
0
-100
0
1
2
3
4
5
6
7
8
Stress (MPa)
Strain (%)
5.0E-3 1/s
1.2E-5 1/s
1.0E-7 1/s
1.0E-7 1/s
1.2E-5 1/s
A
B
C
Experimental Data
A: Relax 18000s
B: Relax 1048s
C: Relax 36000s

Fig. 1

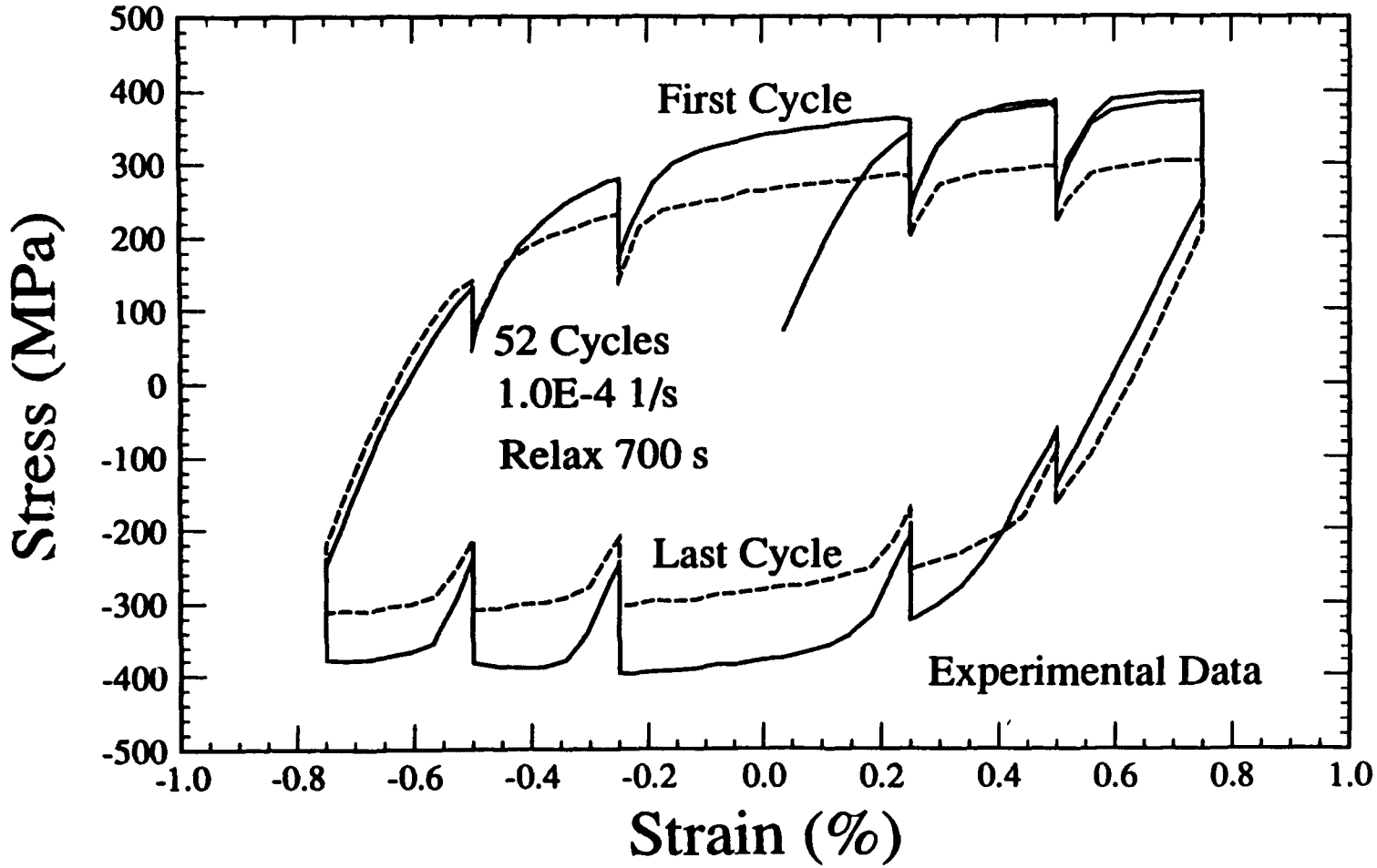
500
400
300
200
100
0
-100
-200
-300
-400
-500
-1.0
-0.8
-0.6
-0.4
-0.2
0.0
0.2
0.4
0.6
0.8
1.0
Stress (MPa)
Strain (%)
First Cycle
52 Cycles
1.0E-4 1/s
Relax 700 s
Last Cycle
Experimental Data

Fig. 2

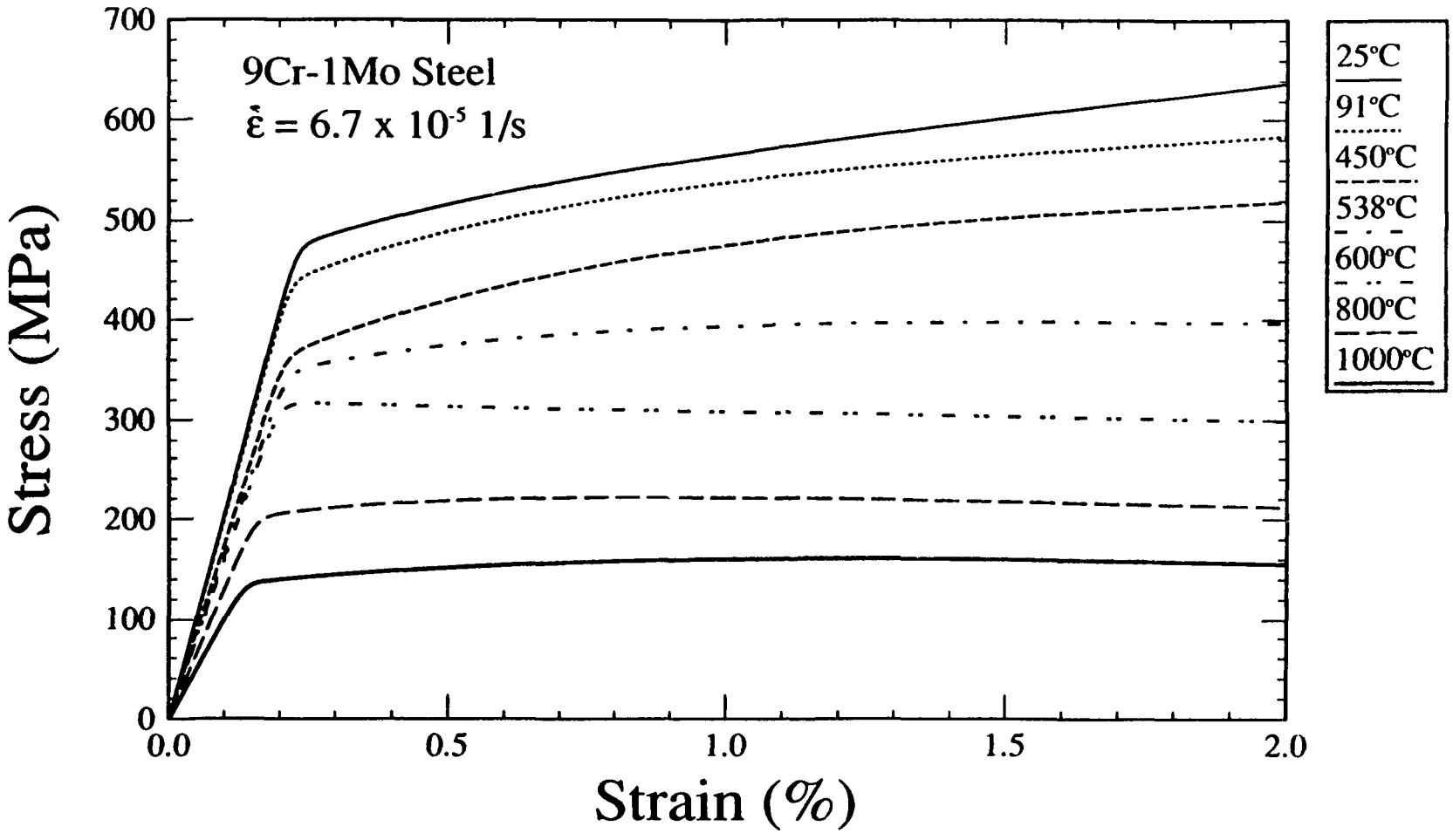
9Cr-1Mo Steel
$\dot{\varepsilon} = 6.7 \times 10^{-5}$ 1/s
Stress (MPa)
Strain (%)
0
100
200
300
400
500
600
700
0.0
0.5
1.0
1.5
2.0
25°C
91°C
450°C
538°C
600°C
800°C
1000°C

Fig. 3

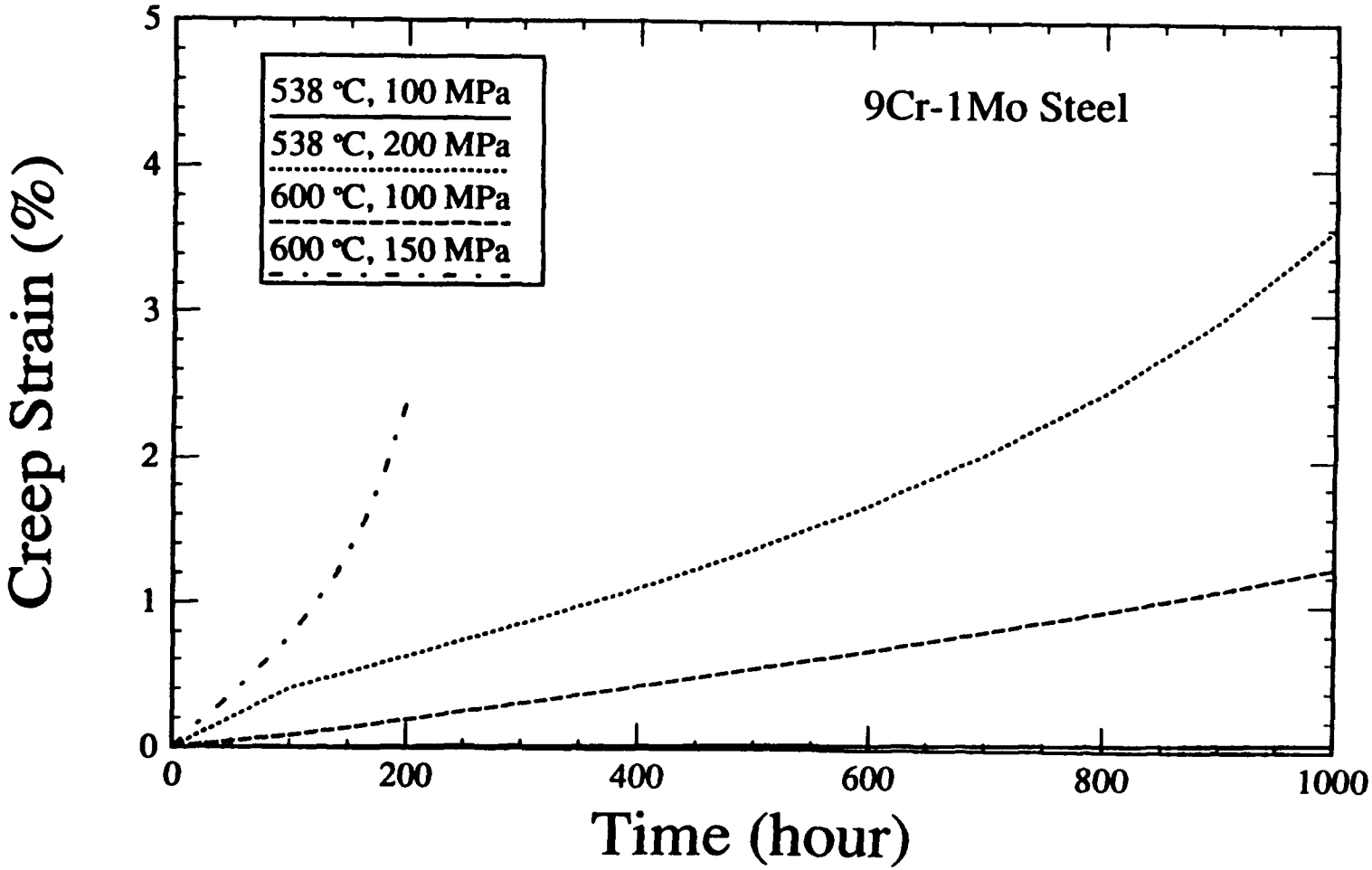
538 ℃, 100 MPa
538 ℃, 200 MPa
600 ℃, 100 MPa
600 ℃, 150 MPa
9Cr-1Mo Steel
Creep Strain (%)
Time (hour)
0
1
2
3
4
5
0
200
400
600
800
1000

Fig. 4

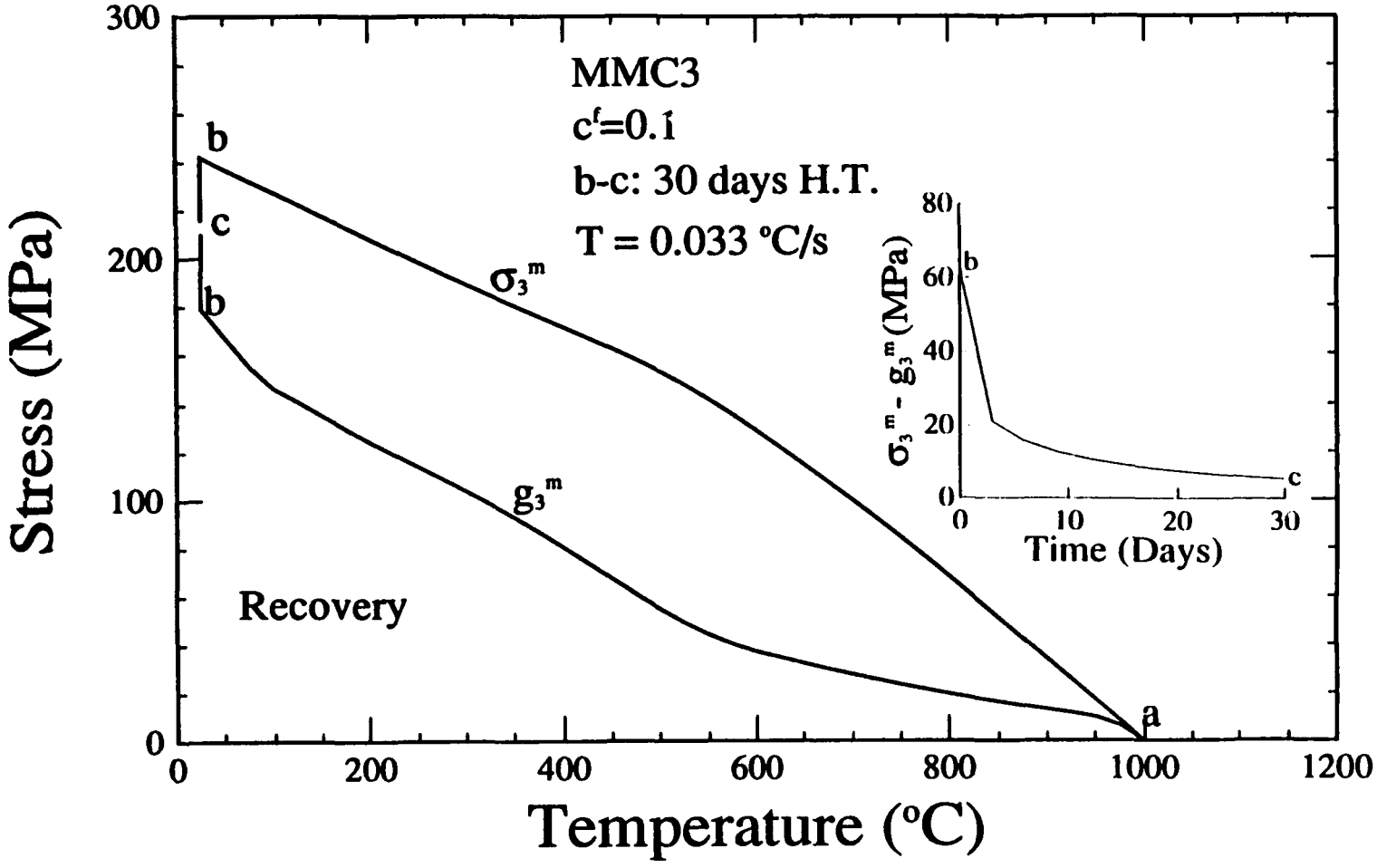
MMC3
c^f=0.1
b-c: 30 days H.T.
T = 0.033 °C/s
b
c
b
σ_3^m
g_3^m
Recovery
a
Stress (MPa)
Temperature (°C)
0
100
200
300
0
200
400
600
800
1000
1200
$\sigma_3^m - g_3^m$ (MPa)
Time (Days)
0
20
40
60
80
0
10
20
30
b
c

Fig. 5

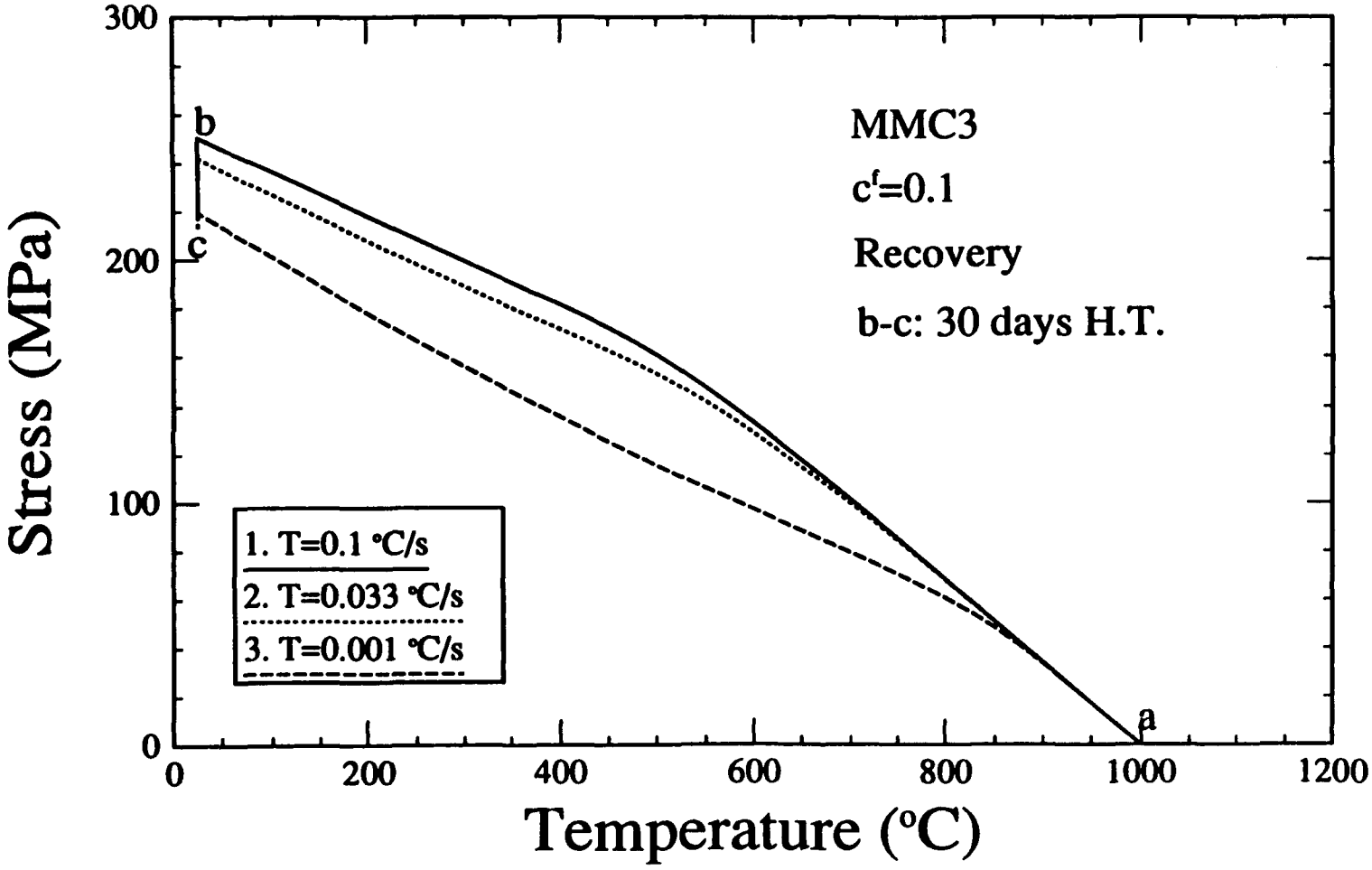
300
200
100
0
0
200
400
600
800
1000
1200
Stress (MPa)
Temperature (°C)
b
c
a
MMC3
c^f=0.1
Recovery
b-c: 30 days H.T.
1. T=0.1 °C/s
2. T=0.033 °C/s
3. T=0.001 °C/s

Fig. 6

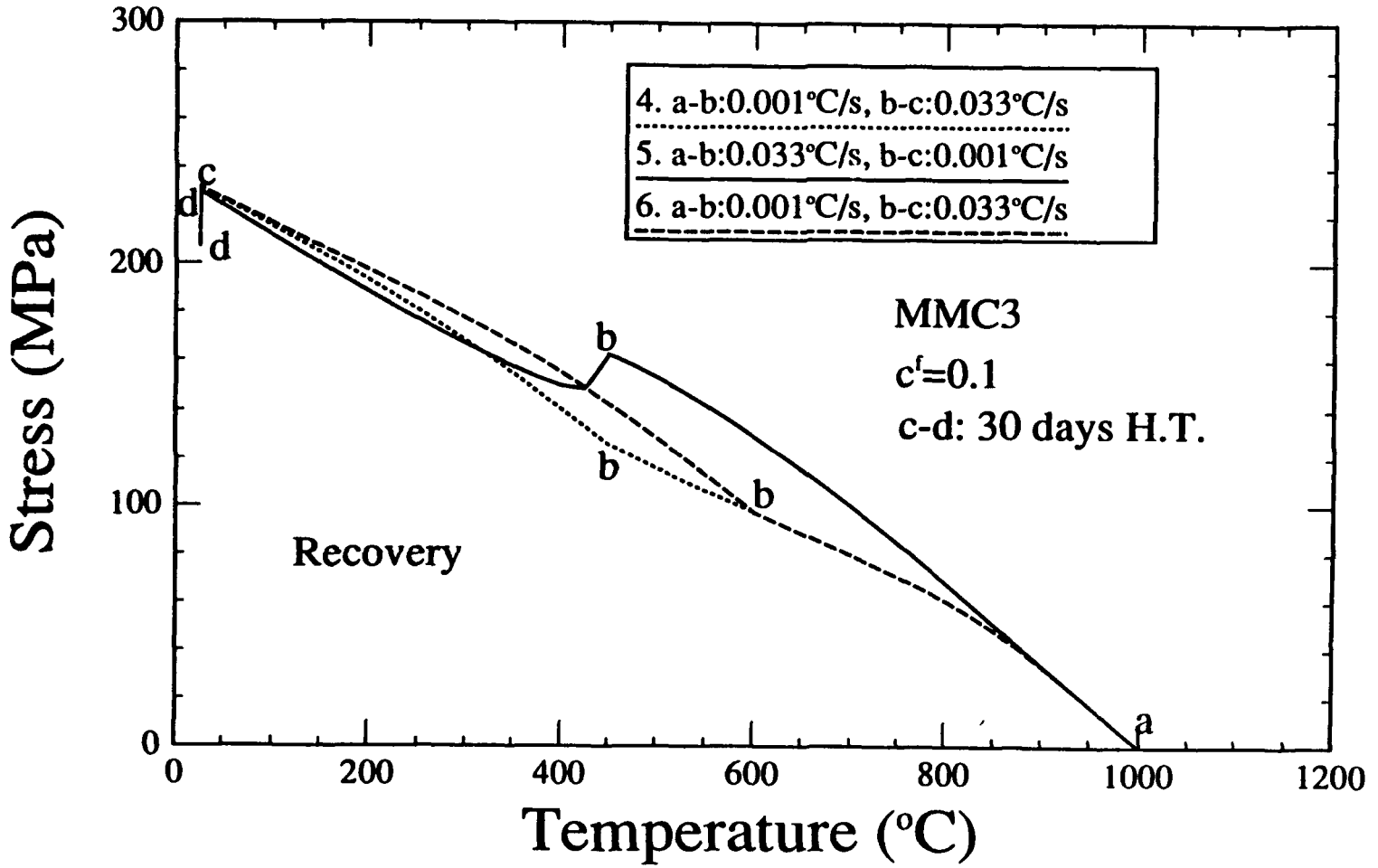
4. a-b:0.001°C/s, b-c:0.033°C/s
5. a-b:0.033°C/s, b-c:0.001°C/s
6. a-b:0.001°C/s, b-c:0.033°C/s
MMC3
c^f=0.1
c-d: 30 days H.T.
Recovery
Stress (MPa)
Temperature (°C)
300
200
100
0
0
200
400
600
800
1000
1200
a
b
b
b
c
d
d

Fig. 1

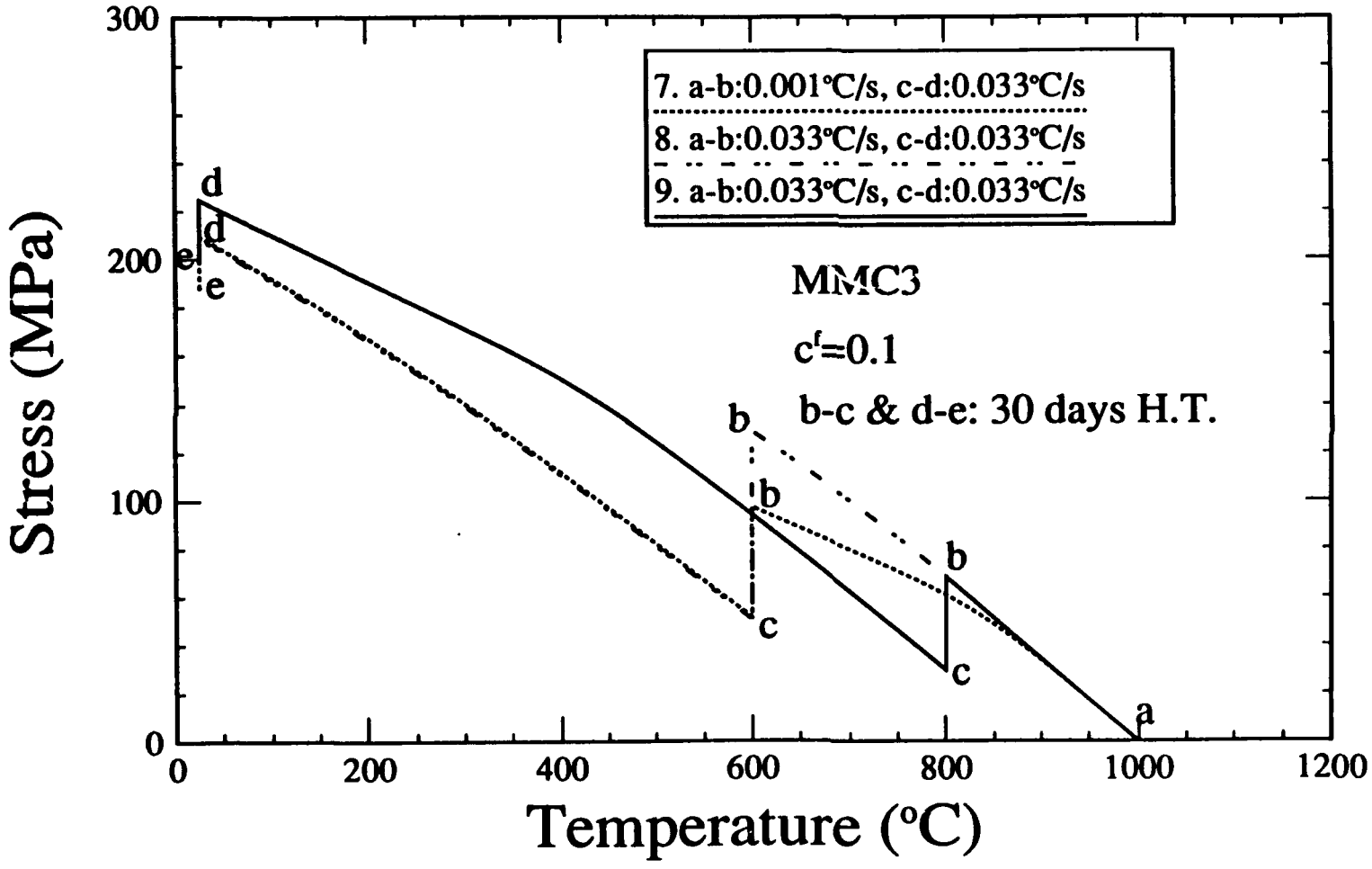
7. a-b:0.001°C/s, c-d:0.033°C/s
8. a-b:0.033°C/s, c-d:0.033°C/s
9. a-b:0.033°C/s, c-d:0.033°C/s
MMC3
c^f=0.1
b-c & d-e: 30 days H.T.
Stress (MPa)
Temperature (°C)
300
200
100
0
0
200
400
600
800
1000
1200
a
b
c
d
e

Fig. 8

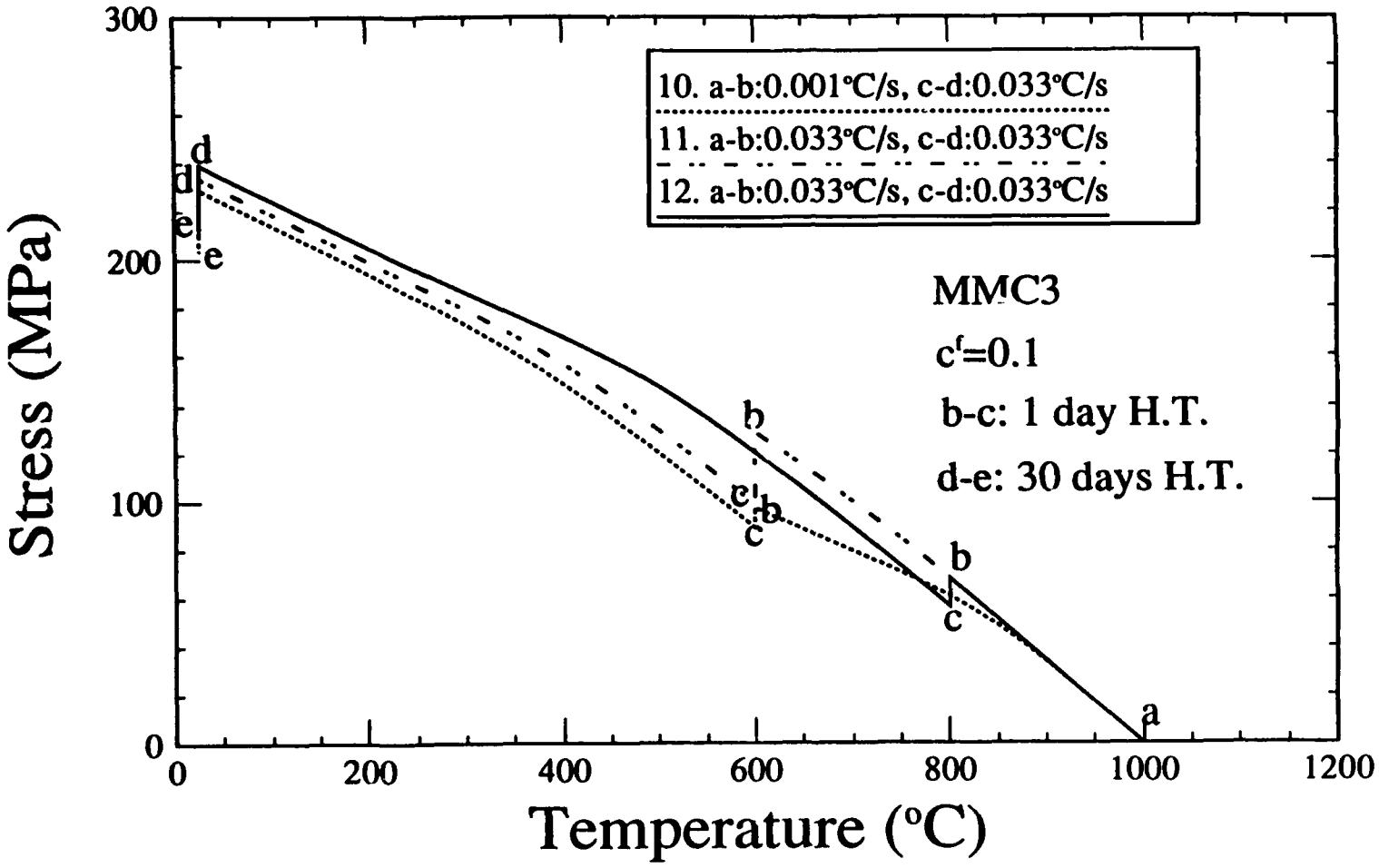
10. a-b:0.001°C/s, c-d:0.033°C/s
11. a-b:0.033°C/s, c-d:0.033°C/s
12. a-b:0.033°C/s, c-d:0.033°C/s
MMC3
c^f=0.1
b-c: 1 day H.T.
d-e: 30 days H.T.
Stress (MPa)
Temperature (°C)
300
200
100
0
0
200
400
600
800
1000
1200
a
b
c
d
e

Fig. 9

AN INCREMENTAL LIFE PREDICTION LAW FOR MULTIAXIAL CREEP–FATIGUE INTERACTION AND THERMOMECHANICAL LOADING

Nan–Ming Yeh and Erhard Krempl

Mechanics of Materials Laboratory

Rensselaer Polytechnic Institute

Troy, New York 12180–3590

RPI Report MML 91–8

October 1991

Presented at Symposium on Multiaxial Fatigue, ASTM, October 14–15, 1991, San Diego, CA.

to appear in the proceedings

TITLE OF SYMPOSIUM : Multiaxial Fatigue

AUTHORS' NAMES:

Nan-Ming Yeh[1] and Erhard Krempl[1]

TITLE OF PAPER:

An Incremental Life Prediction Law for Multiaxial
Creep-Fatigue Interaction and Thermomechanical Loading

AUTHORS' AFFILIATIONS:

Research Assistant and Professor of Mechanics, respectively, Mechanics of Materials Laboratory, Rensselaer Polytechnic Institute, Troy, N.Y. 12180-3590

ABSTRACT: An incremental multiaxial life prediction law (IMLP) is proposed which consists of the three-dimensional thermoviscoplasticity theory based on overstress (TVBO) combined with a multiaxial damage accumulation law (MDA) to compute the life-time or cycles-to-crack initiation. Crack growth is not considered in this paper but is needed to ascertain the useful life of a component. The method is intended for application to high temperature low-cycle fatigue with and without hold times and for triangular and trapezoidal waveforms when creep-fatigue interaction takes place.

The deformation behavior is determined by solving the coupled differential equations of TVBO for the strain variation of interest, i.e. continuous cycling, hold times or fast/slow or slow/fast loading. Only the cyclic neutral version of TVBO is used here although cyclic hardening and recovery of state formulations are available.

The incremental damage accumulation law consists of a fatigue and a creep damage rate equation. When the sum of creep and fatigue damage reaches one, crack initiation is said to occur. The damage accumulation equations assume that the combined actions of stress and inelastic strain rate contribute to damage and damage evolution does not influence the constitutive equation. Fatigue damage always accumulates but a negative creep damage rate is possible to allow for healing (creep damage is, however, always positive). In accordance with scarce experimental evidence, the maximum inelastic shear strain rate, a hydrostatic pressure modified effective stress as well as a parameter which depends on the multiaxiality of loading are used in each damage rate equation. The multiaxiality loading parameter depends on maximum inelastic shear strain rate for fatigue damage, while it is a function of maximum principal stress for creep damage.

All material constants for TVBO and MDA are determined from isothermal tests on Type 304 Stainless Steel (SS) at 538°C using data of Zamrik [1], Blass and Zamrik [2], and Blass [3]. The damage accumulation law correlates fatigue life under biaxial (tension-torsion) cycling with and without hold times. Only the results of one biaxial test series was available to compare the generally favorable predictions (correlations) with experiments.

KEY WORDS: thermoviscoplasticity, multiaxial creep-fatigue interaction, thermomechanical loading, 304 stainless steel, thermal fatigue

Introduction

The design of machines and devices for application in severe loading conditions such as variable temperature, multiaxial stress state, variable frequency, hold-times with creep and relaxation, is a problem of growing importance. The interrelationships between the thermal and the mechanical deformation, between creep and fatigue, and between the multiaxial stress state and the failure mode are very complicated and need to be modeled.

Creep-fatigue interaction is a problem occurring in high temperature nuclear vessels, jet engines, and steam and gas turbines due to temperature change such as startups and shutdowns and has been widely studied. In simulated service testings components are subjected to periodic sawtooth, trapezoidal, and other thermomechanical loadings, to study the time-dependent low-cycle fatigue damage development. Significant time(rate)-dependent effects are found. The analysis of the low-cycle fatigue life of these structural components must not only account for the time (rate) dependency but also for multiaxiality of the stress state.

Most of the creep-fatigue interaction problems were investigated at isothermal, uniaxial conditions. The approaches range from algebraic to incremental formulations. The former must assume a typical cycle whereas arbitrary loading histories can be considered using the incremental laws.

Coffin [4] introduced the frequency-modified Coffin-Manson equation with redefined frequency for hold-time fatigue tests to describe the low-cycle fatigue behavior under uniaxial trapezoidal waveform loadings. To account for slow-fast, fast-slow wave form effects Coffin [5] proposed the "frequency separating method", in which the tension-going frequency plays a major role in the fatigue life computation. Manson et al. [6] developed the "strain range partitioning" method to calculate the low-cycle fatigue life under uniaxial creep-fatigue interaction. This method is then extended to the analysis of multiaxial creep-fatigue interaction

conditions [1,7].

Majumdar and Maiya [8] introduced an incremental life prediction law for uniaxial creep-fatigue interaction. Later Majumdar extended it to a multiaxial version and correlated the biaxial time-dependent fatigue life of 304 SS at 1000°F [9]. Krempl et al. [10] modified Majumdar and Maiya's [8] law. Essentially, plastic strain was replaced by stress. This new law was combined with the viscoplasticity theory based on overstress (VBO) [11] to correlate and predict the low-cycle fatigue lives under uniaxial creep-fatigue interaction conditions.

Usually these approaches are isothermal and are applied to thermal fatigue by considering only the highest temperature (usually the worst). Unfortunately thermomechanical fatigue experiments [12] can exhibit a much lower fatigue life than those found at the highest temperature of the cycle under the same mechanical loading. Extension of life prediction to variable temperature conditions requires that material properties be introduced as a function of temperature and that the effects of thermal expansion be properly recognized. One such approach will be presented below.

Life prediction laws which lend themselves naturally to the evaluation of the life spent under variable loading are those formulated in incremental form [8,10,13]. By virtue of their incremental nature they can be integrated for any stress or strain path and give an indication of the life used up under such paths. In the case of periodic loading, only one cycle needs to be considered as in the case of algebraic laws.

Due to the path dependence of the inelastic deformation of metals, material models for the prediction of deformation must also be formulated in an incremental fashion. Such an incremental formulation couples naturally with an incremental life prediction law. However, it is also possible to integrate the constitutive equation for a certain typical cycle, to plot the results in terms of stress versus strain and to determine the quantities of interest for algebraic life prediction laws from the calculated hysteresis loops instead of from the experimental ones.

The purpose of this paper is to introduce an incremental multiaxial life prediction law (IMLP) for multiaxial creep-fatigue interaction under thermomechanical loading. IMLP consists

of the three-dimensional thermoviscoplasticity theory based on overstress (TVBO) [14] and a multiaxial damage accumulation law (MDA). Time-dependent thermomechanical behavior and temperature-dependent material properties are modeled by TVBO, and the multiaxial creep-fatigue damage is determined by integrating two temperature-dependent damage rate equations using the inelastic strain rates and stress computed from TVBO. The calculated cycles to failure are compared with the observed values and the results are discussed.

Theory

Thermoviscoplasticity Theory Based on Overstress (TVBO)

The theory developed by Lee and Krempl [14] is for infinitesimal strain and orthotropy. It is of unified type and does not use a yield criterion and loading/unloading conditions. The elastic strain is formulated to be independent of thermomechanical path and the inelastic strain rate is a function of overstress, the difference between stress $\hat{\sigma}$, and the equilibrium stress $\hat{g}$; it is a state variable of the theory.

The long term asymptotic values of stress, equilibrium stress, and kinematic stress rates, which can be obtained for a constant mechanical strain rate and ultimately constant temperature, are assumed to be independent of thermal history as are the ultimate levels of the rate-dependent overstress and of the rate-independent contribution to the stress, see Yao and Krempl [15]. Therefore the material functions and constants can in principle be obtained from isothermal tests within the temperature range of interest.

All material constants can be functions of temperature. This dependence is not explicitly displayed. The temperature dependence can be the usual Arrhenius relation or can deviate from that model.

For the representation of the equations, the usual vector notation for the stress tensor components $\hat{\sigma}$ and the small strain tensor components $\hat{\varepsilon}$ are used. Lower and upper case letters with a ^ denote 6 x 1 and 6 x 6 matrices, respectively.

Flow Laws -- In the context of an infinitesimal theory, the total strain rate, $d\hat{\varepsilon}/dt$, is considered to be the sum of elastic, $d\hat{\varepsilon}^{el}/dt$, inelastic, $d\hat{\varepsilon}^{in}/dt$, and thermal strain rates, $d\hat{\varepsilon}^{th}/dt$,

$$\dot{\hat{\varepsilon}} = \dot{\hat{\varepsilon}}^{el} + \dot{\hat{\varepsilon}}^{in} + \dot{\hat{\varepsilon}}^{th}. \tag{1}$$

A superposed dot represents the total time derivative, d/dt.

For each strain rate, a constitutive equation is postulated. The elastic strain is assumed to be independent of thermal history, therefore,

$$\dot{\hat{\varepsilon}}^{el} = \frac{d}{dt}(\hat{C}^{-1}\hat{\sigma}) = \hat{C}^{-1}\dot{\hat{\sigma}} + \dot{\hat{C}}^{-1}\hat{\sigma} \tag{2}$$

where $\hat{C}^{-1}$ is the compliance matrix. The additional term $\dot{\hat{C}}^{-1}\hat{\sigma}$ contributes to the total strain rate for temperature dependent elastic material properties. It insures that the elastic behavior is path-independent, see Lee and Krempl [16].

The inelastic strain rate is only a function of the overstress $\hat{x}$. It denotes the difference between the stress $\hat{\sigma}$ and the equilibrium stress $\hat{g}$, a vector state variable of the theory. Accordingly,

$$\dot{\hat{\varepsilon}}^{in} = \hat{K}^{-1}\hat{x}\,. \tag{3}$$

The viscosity matrix $\hat{K}^{-1}$ controls the rate dependence through the positive, decreasing viscosity function $k[\Gamma]$.

The thermal strain rate is given by

$$\dot{\hat{\varepsilon}}^{th} = \hat{\alpha}\dot{T} \tag{4}$$

with $\hat{\alpha}$ the coefficient of thermal expansion vector. T is the temperature difference from some datum temperature.

Growth Laws for the State Variables -- In addition growth laws for the two state variables of TVBO, the equilibrium stress $\hat{g}$ and the kinematic stress $\hat{f}$, are given as

$$\dot{\hat{g}} = q[\Gamma]\dot{\hat{\sigma}} + \dot{T}\frac{\partial q[\Gamma]}{\partial T}\hat{\sigma} + \{q[\Gamma] - \theta[q[\Gamma] - p(1 - q[\Gamma])]\}\frac{\hat{x}}{k[\Gamma]} \tag{5}$$

$$\dot{\hat{f}} = \frac{p}{k[\Gamma]}\dot{\hat{x}} \tag{6}$$

respectively, with

$$\Gamma^2 = \hat{x}^T\hat{H}\hat{x},\ \theta^2 = \frac{1}{A^2}\hat{z}^T\hat{H}\hat{z},\ \hat{x} = \hat{\sigma} - \hat{g},\ \text{and}\ \hat{z} = \hat{g} - \hat{f}\ . \tag{7}$$

In the above the dimensionless modified shape functions q controls the shape of stress-strain diagram. The dimensionless constant p represents the ratio of the tangent moduli at the maximum strain of interest to the corresponding viscosity factors, $p \geq 0$. The invariant θ is related to the rate independent contribution to the stress. The vector $\hat{z}$ represents the difference between the equilibrium stress $\hat{g}$ and the kinematic stress $\hat{f}$. Asymptotic analyses for the uniaxial isothermal case in [15,17] show that $\dot{\hat{f}}$ determines $\dot{\hat{\sigma}}$ ultimately. The purpose of (6) is to set this slope which can be positive, zero or negative. The representations of the material matrices for isotropy are given in Appendix I.

The theory given above represents cyclic neutral behavior. Rate sensitivity, relaxation and creep are modeled. Since no recovery of state is included the creep behavior is controlled by the sign of p. If $p > 0$ the equations can only represent primary creep. Primary and secondary creep may be modeled for $p = 0$; primary, secondary and tertiary creep can be represented in principle if $p < 0$. Note also that p sets the slope of the stress-inelastic strain curve of the maximum inelastic strain of interest through (6), see the discussion of VBO in [11,15,17].

When recovery of state is included in the model [18-20] the creep behavior is no longer completely controlled by the sign of p and secondary creep can be reproduced at stress levels which are in the linear region of the stress-strain diagram. Also the isothermal formulation of VBO has been extended to cyclic hardening [21-22]. It is possible to include this property as well as recovery of state in the TVBO theory. This will be done in a future paper.

The Incremental, Multiaxial Damage Accumulation Law

The multiaxial damage accumulation law (MDA) is proposed based on the modification of the incremental life prediction law for uniaxial creep-fatigue interaction [13]. The model

includes the effect of hydrostatic stress on creep and fatigue damage.

The importance of hydrostatic stress on the low-cycle fatigue life has been acknowledged [23-24]. The materials loose ductility and become brittle under hydrostatic tension while the brittle materials become more ductile under hydrostatic pressure. To model the hydrostatic effects the triaxiality factor TF ($= \sigma_{kk}/\sigma_{eff}$) is used in the model, where σ_{kk} is the first stress invariant and σ_{eff} is the von Mises effective stress. (Indicial tensor notation is used in this part.)

The present law is intended for the prediction of crack initiation, which is assumed to occur along the plane of maximum inelastic shear strain rate [25]. The creep damage is assumed to be cavity-type which initiates on grain boundaries normal to the maximum principal tensile stress direction [9,26]. The proposed incremental multiaxial damage accumulation law consists of a fatigue and a creep damage rate equation $\dot{D}_f$ and $\dot{D}_c$, respectively. Damage is only a counter and its evolution does not influence the constitutive equations. Fatigue and creep damage are set to be zero initially (for a virgin or fully annealed material), and crack initiation occurs if the sum of fatigue and creep damage reaches one. Following [13] the incremental law is given as

$$\dot{D}_f = \frac{L_f^{\pm}}{T_f}\left|\frac{\dot{\varepsilon}_{in}^{s}}{\dot{\varepsilon}_f}\right|^{n_f}\left|\frac{\sigma_{eff}^{*}}{\sigma_f}\right|^{m_f} \tag{8}$$

$$\dot{D}_c = \frac{L_c^{\pm}}{T_c}\left|\frac{\dot{\varepsilon}_{in}^{s}}{\dot{\varepsilon}_c}\right|^{n_c}\left|\frac{\sigma_{eff}^{**}}{\sigma_c}\right|^{m_c}. \tag{9}$$

Failure is said to occur when

$$D_f + D_c = 1. \tag{10}$$

$L_f^{\pm}$ is the fatigue loading function which models the effects of multiaxial loading and temperature T. It is assumed to be controlled by the ratio of $\dot{\varepsilon}_{in}^{n}$ and $\dot{\varepsilon}_{in}^{s}$, where $\dot{\varepsilon}_{in}^{s}$ is the normalized maximum inelastic shear strain rate, and where $\dot{\varepsilon}_{in}^{n}$ is the normalized inelastic strain rate perpendicular to $\dot{\varepsilon}_{in}^{s}$ [9,25]. The word "normalized" denotes that the multiaxial inelastic strain rates reduce to the uniaxial value for uniaxial loading. For the case considered here, (axial

and torsional loadings), $\dot{\varepsilon}^n_{in} = \dot{\varepsilon}_{in}$ and $\dot{\varepsilon}^s_{in} = [(\dot{\varepsilon}_{in})^2 + 4/9(\dot{\gamma}_{in})^2]^{.5}$, where $\dot{\varepsilon}_{in}$ and $\dot{\gamma}_{in}$ are the inelastic strain rates for axial and torsion, respectively. $L^{\pm}_c$ is the creep loading function which represents the effects of the multiaxial loading and temperature. $L^{\pm}_c$ is a function of the ratio of maximum principal stress σ_1 and the von Mises effective stress σ_{eff} [9]. We define

$$L^{\pm}_f \equiv L^{\pm}_f[\alpha, T] = \begin{cases} L^{+}_f[T], & \alpha \geq 0 \\ L^{-}_f[T], & \alpha < 0 \end{cases} \tag{11}$$

$$L^{\pm}_c \equiv L^{\pm}_c[\beta, T] = \begin{cases} L^{+}_c[T], & \beta \geq 0 \\ L^{-}_c[T], & \beta < 0 \end{cases} \tag{12}$$

where $$\alpha = \frac{\dot{\varepsilon}^n_{in}}{\dot{\varepsilon}^s_{in}}, \quad \beta = \frac{\sigma_1}{\sigma_{eff}}.$$

In addition two modified effective stresses σ^{*}_{eff} and σ^{**}_{eff} for fatigue and creep, respectively, and two multiaxiality factors MF_f and MF_c are defined as

$$\sigma^{*}_{eff} = \sigma_{eff}\{1 + a(1 - TF)\} \tag{13}$$

$$\sigma^{**}_{eff} = \sigma_{eff}\{1 + b(1 - TF)\} \tag{14}$$

$$MF_f = \{1 + a(1 - TF)\}^{m_f} \tag{15}$$

$$MF_c = \{1 + b(1 - TF)\}^{m_c}. \tag{16}$$

$L^{\pm}_f > 0$ is postulated and the fatigue damage always accumulates but a negative creep damage rate is allowed (creep damage is, however, always positive) through $L^{\pm}_c$. For instance, $L^{+}_c = 1$ and $L^{-}_c = -1$ are assumed for the uniaxial case in tension and compression, respectively [13]. Constants T_f, T_c, $\dot{\varepsilon}_f$, and $\dot{\varepsilon}_c$ in equations (9-16) are introduced for dimensional considerations. They are set equal to one in an appropriate units. The other constants n_f, m_f, σ_f, n_c, m_c, σ_c, a, and b must be determined from appropriate tests under multiaxial creep-fatigue interaction.

Numerical Experiments

Evaluation of constants

To model the multiaxial thermal time-dependent fatigue behavior the material properties of TVBO and MDA must be known as a function of temperature. For a complete determination of the viscoplastic properties strain rate change and relaxation tests are needed. Since such results are generally not available the present analysis uses whatever data are available augmented by "educated guesses" of the behavior to arrive at the material constants. The temperature-dependent material properties of TVBO and MDA are found from isothermal conditions and are interpolated for variable temperature. For instance a decrease in modulus, and flow stress with increasing temperature has been assumed in Fig. 1 for an Al alloy of Ref. [28].

TVBO together with equations (8-16) constitute the incremental multiaxial life prediction law and must now be applied. The boundary conditions and the material properties must be specified for calculation. For integration of the coupled set of differential equations the IMSL routine DGEAR is used on a SUN 3 work station.

The steady-state hysteresis loops under tension, torsion, and proportional biaxial loading with and without hold time for 304 SS at 538°C [1] are used to approximately determine the material constants of TVBO at 538°C. The constants are listed in Table 1.

Using TVBO and MDA life-time at 538°C can be calculated. Experimental failure points of uniaxial, torsional, and biaxial low-cycle fatigue tests with and without hold-time for 304 SS at 538°C [2,3] are used to identify the material constants of MDA. By virtue of the uniaxial low-cycle fatigue life at 538°C and the assumptions [13]

$$L_f^{\pm} = \begin{cases} L_f^{+} = 1, \ \dot{\varepsilon}_{in} \geq 0 \\ L_f^{-} = 0, \ \dot{\varepsilon}_{in} < 0, \end{cases} \qquad (17)$$

the material constants of fatigue damage n_f, σ_f, and m_f are obtained. The constant "a" in eq. (15) and fatigue loading function $L_f^{\pm}[\alpha,T]$ can be found using the data for torsional and proportional biaxial low-cycle fatigue tests at 538°C, respectively. Following the same procedures for the

determination of n_f, σ_f, and m_f and using the assumptions [13]

$$L_c^{\pm} = \begin{cases} L_c^{+} = 1, \ \sigma \geq 0 \\ L_c^{-} = -1, \ \sigma < 0 \end{cases} \tag{18}$$

for uniaxial case, the material constants n_c, σ_c, m_c, and b, and creep loading function $L_c^{\pm}[\beta, T]$ can be evaluated from uniaxial and biaxial hold-time low-cycle fatigue tests at 538°C.

For simplicity the multiaxiality factors MF_c and MF_f are assumed to be 0.5 for torsional fatigue tests with and without hold-time, respectively, to determine the constants a and b. The material properties for MDA are shown in Table 2.

The dependence of the fatigue loading function $L_f^{\pm}$ on $|\alpha|$ is shown in Fig. 1, where $|\alpha|$ is determined at the maximum strain of the cycle. In Fig. 1 L_f^{+} increases from 0.17 to 1 as $|\alpha|$ increases from 0 (pure torsion) to 1 (uniaxial), while the opposite is true for L_f^{-} which decreases from 0.17 to 0 whiled $|\alpha|$ increases from 0 to 1. For biaxial loading $0 \leq |\alpha| \leq 1$. $L_f^{+} = L_f^{-}$ for pure torsional loading, since the direction of shear should have no influence on crack initiation. The creep loading function L_c^{+} versus β is shown in Fig. 2. β is determined at the maximum strain of interest. L_c^{+} increases from 0.3 to 1 as β increases from 0.577 (pure torsion) to 1 (uniaxial). For biaxial cases β is between 0.577 and 1. L_c^{-} is assumed to be equal to -1 for the uniaxial compression to account for the healing effect observed in the experiments [12,26]. For torsional and biaxial cases $\beta \leq 0$ and L_c^{-} is postulated to be zero since no healing was reported in [9].

Deformation behavior

Deformation behavior computed using TVBO are shown in Figs. 3 and 4. In Fig. 3 two hysteresis loops for completely reversed strain-controlled loading at a strain amplitude of ±0.5% at steady state at 538°C are shown. Tensile and symmetric holds of 600s are introduced. The inelastic strain range of the symmetric hold test is slightly larger than that of tensile hold test. Steady-state hysteresis loops for slow-fast and fast-slow tests are shown in Fig. 4. The two loops are almost symmetric with respect to the origin. A near vertical drop is observed in the

transition of the changing from the fast strain rate 10^{-3} 1/s to the slow strain rate 10^{-6} 1/s.

Life prediction

The calculated and observed biaxial low-cycle fatigue lives together with two lines indicating a deviation of a factor of 2 in life are shown in Figs. 5 and 6 for the cases without and with hold-time, respectively. Because of the scarcity of the experimental data, only the data points for strain ratio R = 2 ($R = \Delta\gamma / \Delta\varepsilon$) are predictions in Fig. 5. The predicted lives in Fig. 5 are within the bounds and are acceptable. The results of the uniaxial, torsional, and biaxial hold-time tests are shown in Fig. 6. Although three points are outside of the bounds, the trend is correct and is thus acceptable.

6.2.3 Discussion

IMLP, which consists of the thermoviscoplasticity theory based on overstress (TVBO) and the multiaxial damage accumulation law (MDA), is applied to correlate and predict the low-cycle fatigue lives of 304 SS at 538°C under biaxial creep-fatigue interaction. The material constants of TVBO and MDA for 304 SS at 538°C are identified using the experimental data of [1] and [2-3], respectively. In TVBO theory used here, effects of recovery, aging, and cyclic hardening are neglected. There are some indications that recovery and aging are important at 538°C in 304 SS. A quantitative assessment of these effects, however, cannot be obtained from the available low-cycle fatigue data. They are consequently not modeled.

If IMLP is applied to thermal fatigue, both eqs. (1) and (5) have additional terms. These additional terms influence not only the elastic but also the inelastic behavior [16] and consequently affect the predicted low-cycle fatigue lives. The application of IMLP to predict the low-cycle fatigue life under thermal multiaxial creep-fatigue interaction will be presented in a future paper. The temperature-dependent material properties of TVBO and MDA can be determined from isothermal tests at different temperatures.

Although the calculated lives in Fig. 6 do show three points which are beyond the limits of a

factor of ±2 on life, the trends of the computed lives are in the proper direction. The three points are a uniaxial hold-time test, a biaxial R=1 hold-time test and a symmetric hold-time test in torsion. It can be seen from Table 2 in [9] that the fatigue life of the uniaxial test with 0.5% strain range and 60 minutes tensile hold-time (the first out-of-bound point) is unusually short. The biaxial test has the smallest effective strain range of all the tests and the deformation behavior shows very little inelasticity. In this region small deviations of the predicted stress-strain behavior from the real one can play an important role in the life calculation. It should be further considered that a complete data set was not available for determination of the constants. Some properties had to be assumed. Deviations have to be expected. The final unusual point is for torsional test with 0.55% effective strain range and 6 minutes symmetric hold time. The calculated value is much lower than the observed value. We have no explanation for this behavior.

The present paper intends to show the capabilities of modeling the time-dependent multiaxial thermal fatigue behavior using the thermoviscoplasticity theory based on overstress (TVBO) and multiaxial damage accumulation law (MDA). The trends are encouraging. For the complete evaluation of the predictive capability a consistent set of data is necessary. Some will be used to determine the needed material constants, others should be used to check on the predictive capability of the theory. Variable amplitude and thermal fatigue tests should be included in the latter set. Finally, MDA is not restricted to periodic loadings, it can in principle be applied to arbitrary deformation histories.

Acknowledgement

This research was supported by DARPA/ONR Contract N00014-86-k0770 with Rensselaer Polytechnic Institute.

References

[1] Zamrik, S. Y., "The Application of 'Strain range Partitioning Method' to Multiaxial Creep-Fatigue Interaction," AGARD Conference Proceedings No. 243, Apr., 1978, Paper No. 16.

[2] Blass, J. J. and Zamrik, S. Y., "Multiaxial Low-Cycle Fatigue of Type 304 Stainless Steel," Proceedings ASME-MPC Symposium on Creep-Fatigue Interaction, 1976, pp. 129-159.

[3] Blass, J. J., ORNL/TM-6438, 1979.

[4] Coffin, L. F., Jr., "The Concept of Frequency Separating in Life Prediction for Time-Dependent Fatigue," Proceedings ASME-MPC3 Symposium on Creep-Fatigue Interaction, R. M. Curran, Ed., American Society of Mechanical Engineers, New York, N.Y., 1976, pp. 349-363.

[5] Coffin, L. F., Jr., "Fatigue at High Temperature," Fatigue at Elevated Temperatures, ASTM STP 520, A. E. Carden, A. J. McEvily, and C. H. Wells, Eds., American Society for Testing and Materials, Philadelphia, 1972, pp. 5-34.

[6] Manson, S. S., Halford, G. R., and Hirschberg, M. H., "Creep-Fatigue Analysis by Strain-Range Partitioning," Proceedings of the First Symposium on Design for Elevated Temperature Environment, American Society of Mechanical Engineers, New York, N.Y., 1971, pp. 12-28.

[7] Manson, S. S. and Halford, G. R., "Multiaxial Creep-Fatigue Life Analysis using Strainrange Partitioning," Proceedings ASME-MPC3 Symposium on Creep-Fatigue Interaction, R. M. Curran, Ed., American Society of Mechanical Engineers, New York, N.Y., 1976, pp. 299-322.

[8] Majumdar, S. and Maiya, P. S., "A Damage Equation for Creep-Fatigue Interaction," Proceedings ASME-MPC3 Symposium on Creep-Fatigue Interaction, R. M. Curran, Ed., American Society of Mechanical Engineers, New York, N.Y., 1976, pp. 323-326.

[9] Majumdar, S., "Designing Against Low-Cycle Fatigue at elevated Temperature," Nuclear Engineering and Design, 63, 1981, pp. 121-135.

[10] Krempl, E., Lu, H., Satoh, and Yao, D., "Viscoplasticity Based on Overstress Applied to

Creep-Fatigue Interaction," Low Cycle Fatigue, ASTM STP 942, H. D. Solomon, G. R. Halford, L. R. Kaisand, and B. N. Leis, Eds., American Society for Testing and Materials, Philadelphia, 1987, pp. 123-139.

[11] Krempl, E. McMahon, J. J. and Yao, D., "Viscoplasticity Based on Overstress with Differential Growth Law for the Equilibrium Stress," Mechanics of Materials, 5, 1986, pp. 35-48.

[12] Bill, R. C., Verrilli, M. J., McGaw, M. A., and Halford, G. R., " A Preliminary Study of the Thermomechanical Fatigue of Polycrystalline Mar M-200," NASA TP-2280, AVSCOM TR 83-C-6, Feb. 1984.

[13] Satoh, M. and Krempl, E., "An Incremental Life Prediction Law for Creep-Fatigue Interaction," Material Behavior at Elevated Temperatures and Components Analysis, PVP-Vol. 60, Y. Yamada, R. L. Roche and F. L. Cho, Eds., 1982, pp. 71-79.

[14] Lee, K. D. and Krempl, E., "An Orthotropic Theory of Viscoplasticity Based on Overstress for Thermomechanical Deformations," International Journal of Solids and Structures, 27, 1991, 1445-1459.

[15] Yao, D. and Krempl, E., "Viscoplasticity Theory Based on Overstress. The Prediction of Monotonic and Cyclic Proportional and Nonproportional Loading Paths of an Aluminum Alloy," International Journal of Plasticity, 1, 1985, pp. 259-274.

[16] Lee, K. D. and Krempl, E., "Uniaxial Thermomechanical Loading. Numerical Experiments using the Thermal Viscoplasticity Theory based on Overstress," European Journal of Mechanics, A/Solids, 10, 1991, pp. 175-194.

[17] Sutcu, M. and Krempl, E., "A Simplified Orthotropic Viscoplasticity Theory Based on Overstress," International Journal of Plasticity, 6, 1990, pp. 247-261.

[18] Choi, S. H. and Krempl, E., "The Orthotropic Viscoplasticity Theory Based on Overstress with Static Recovery Applied to The Modeling of Long Term High Temperature Creep Behavior of Cubic Single Crystals," Rensselaer Polytechnic Institute Report MML 89-3 Dec. 1989.

[19] Majors, P. S. and Krempl, E., "A Recovery of State Formulation for the Viscoplasticity Theory Based on Overstress," to be presented at the Conference on High Temperature Constitutive Modeling: Theory and Application, A. D. Freed and K. P. Walker, Eds., American Society of Mechanical Engineers Winter Annual Meeting, Atlanta, GA.

[20] Yeh, N. M. and Krempl, E., "A Thermoviscoplastic Analysis of Uniaxial Ratchetting Behavior of SiC/Ti Fibrous Metal Matrix Composites," Proceedings of Sixth Technical Conference of American Society for Composites, pp. 329-337, 1991.

[21] Krempl, E. and Yao, D., "The Viscoplasticity Theory Based on Overstress Applied to Ratchetting and Cyclic Hardening," Low cycle Fatigue and Elasto-Plastic Behavior of Materials, K.-T. Rie, Ed., 1987, pp.137-148.

[22] Krempl, E. and Choi, S. H., "Viscoplasticity Theory Based on Overstress: The Modeling of Ratchetting and Cyclic Hardening of AISI Type 304 Stainless Steel," Rensselaer Polytechnic Institute Report MML 90-4 April 1990.

[23] Libertiny, G. Z., "Short-Life Fatigue under Combined Stresses," Journal of Strain Analysis, 2, 1967, pp. 91-97.

[24] Manson, S. S. and Halford, G. R., "Multiaxial Low-Cycle Fatigue of Type 304 Stainless Steel," Journal of Engineering Materials and Technology, 1977, pp. 283-285.

[25] Brown, M. W. and Miller, K. J., "A Theory for Fatigue Failure under Multiaxial Stress-Strain Conditions, Proc. Instn. mech. eng., 187, 1973, pp. 217-229.

[26] Hayhurst, D. R., "Creep Rupture under Multiaxial States of Stress," Journal of Mech. Phys. Solids, 20, 1972, pp. 381-390.

[27] Majumdar, S. and Maiya, P. S., "Waveshape Effects in Elevated Temperature Low-Cycle Fatigue of Type 304 Stainless Steel," Inelastic Behavior of Pressure Vessel and Piping Components, PVP-PB-028, American Society of Mechanical Engineers, New York, 1978, pp. 43-54.

[28] Krempl, E. and Yeh, N. M., "Residual Stresses in Fibrous Metal Matrix Composites. A Thermoviscoplastic Analysis," Proceedings IUTAM Symposium on Inelastic Deformation

of Composite Materials, 1990, pp. 411-443.

Appendix I

Matrices for Isotropy

The nonzero components of the symmetric elastic modulus matrix $\hat{C}^{-1}$ and the symmetric viscosity matrix $\hat{K}^{-1}$ are represented by

$$(C^{-1})_{11} = (C^{-1})_{22} = (C^{-1})_{33} = 1/E$$

$$(C^{-1})_{44} = (C^{-1})_{55} = (C^{-1})_{66} = 1/G$$

$$(C^{-1})_{ij} = -\nu/E,\ i, j = 1, 2, 3, \text{ and } i \neq j \qquad \text{(A-1)}$$

and

$$(K^{-1})_{11} = (K^{-1})_{22} = (K^{-1})_{33} = 1/Ek[\Gamma]$$

$$(K^{-1})_{44} = (K^{-1})_{55} = (K^{-1})_{66} = 3/Ek[\Gamma]$$

$$(K^{-1})_{ij} = -1/2Ek[\Gamma],\ i, j = 1, 2, 3, \text{ and } i \neq j \qquad \text{(A-2)}$$

where inelastic incompressibility is assumed and $G = \frac{E}{2(1+\nu)}$.

The positive decreasing viscosity function $k[\Gamma]$, dimension of time, controls the rate dependence. $\hat{H}$ is a dimensionless matrix, the nonzero components are given by

$$H_{11} = H_{22} = H_{33} = 1$$

$$H_{44} = H_{55} = H_{66} = 3$$

$$H_{ij} = -0.5,\ i, j = 1, 2, 3, \text{ and } i \neq j. \qquad \text{(A3)}$$

The coefficient of thermal expansion vector is $\hat{\alpha}$

$$\hat{\alpha}^t = [\alpha\ \alpha\ \alpha\ 0\ 0\ 0] \qquad \text{(A4)}$$

All components are material properties which must be identified for a given material.

Table 1--Material Properties of TVBO for AISI 304 SS

E (MPa) = 155000 $\quad \nu = 0.29$

$q[\Gamma] = \psi[\Gamma]/E \quad p = E_t/E$

Viscosity Function: $k[\Gamma] = k_1(1 + \frac{\Gamma}{k_2})^{-k_3}$

$k_1 = 314200$ (s), $k_2 = 60$ (MPa) $k_3 = 28$

Shape Function: $\psi[\Gamma] = c_1 + (c_2-c_1)\exp(-c_3\Gamma)$

$c_1 = 79500$ (MPa), $c_2 = 151900$ (MPa), $c_3 = 0.18$ (MPa^{-1})

$E_t = 2500$ (MPa), $A = 240$ (MPa), Inelastic Poisson's Ratio: $\eta = 0.5$

Table 2--Material Properties for Damage Accumulation Law

Fatigue Damage	Creep Damage
$T_f = 1$ (s)	$T_c = 1$ (s)
$\dot{\varepsilon}_f = 1$ (1/s)	$\dot{\varepsilon}_c = 1$ (1/s)
$n_f = 0.83$	$n_c = 0.274$
$\sigma_f = 1000$ (MPa)	$\sigma_c = 1021.6$ (MPa)
$m_f = 1.835$	$m_c = 5.667$
$a = -0.3146$	$b = -0.1184$

Figure Captions

Fig. 1 Fatigue loading functions vs. $|\alpha|$ for 304 SS at 538°C.

Fig. 2 Creep loading function vs. β for 304 SS at 538°C.

Fig. 3 Strain-control steady-state hysteresis loops of 304 SS at 538°C under tensile hold and symmetric hold loadings.

Fig. 4 Strain-control steady-state hysteresis loops of 304 SS at 538°C under slow/fast and fast/slow loadings. Near-vertical drops are at the transitions from fast to slow loadings.

Fig. 5 Observed fatigue lives versus calculated fatigue lives using the IMLP for different biaxial loadings. The data for R=2 are predictions.

Fig. 6 Observed fatigue lives versus calculated fatigue lives using the IMLP for different biaxial hold time loadings.

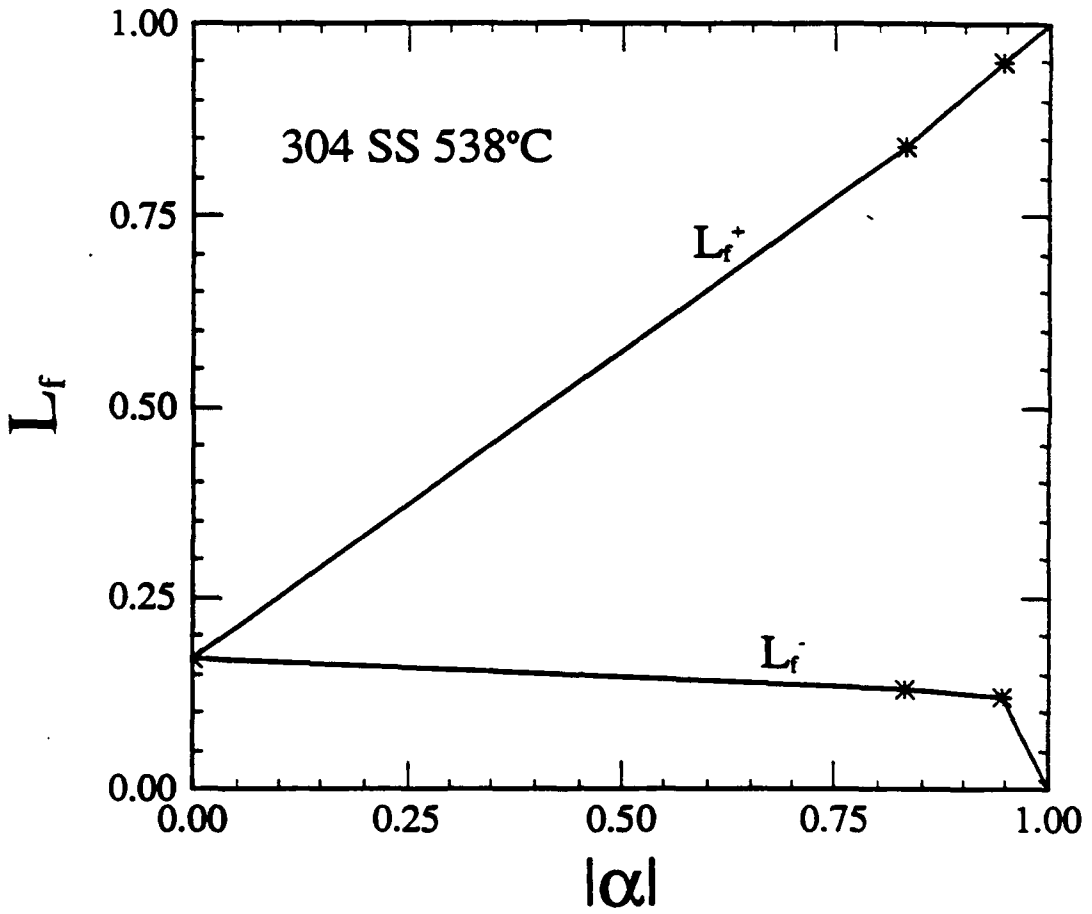

Fig. 1

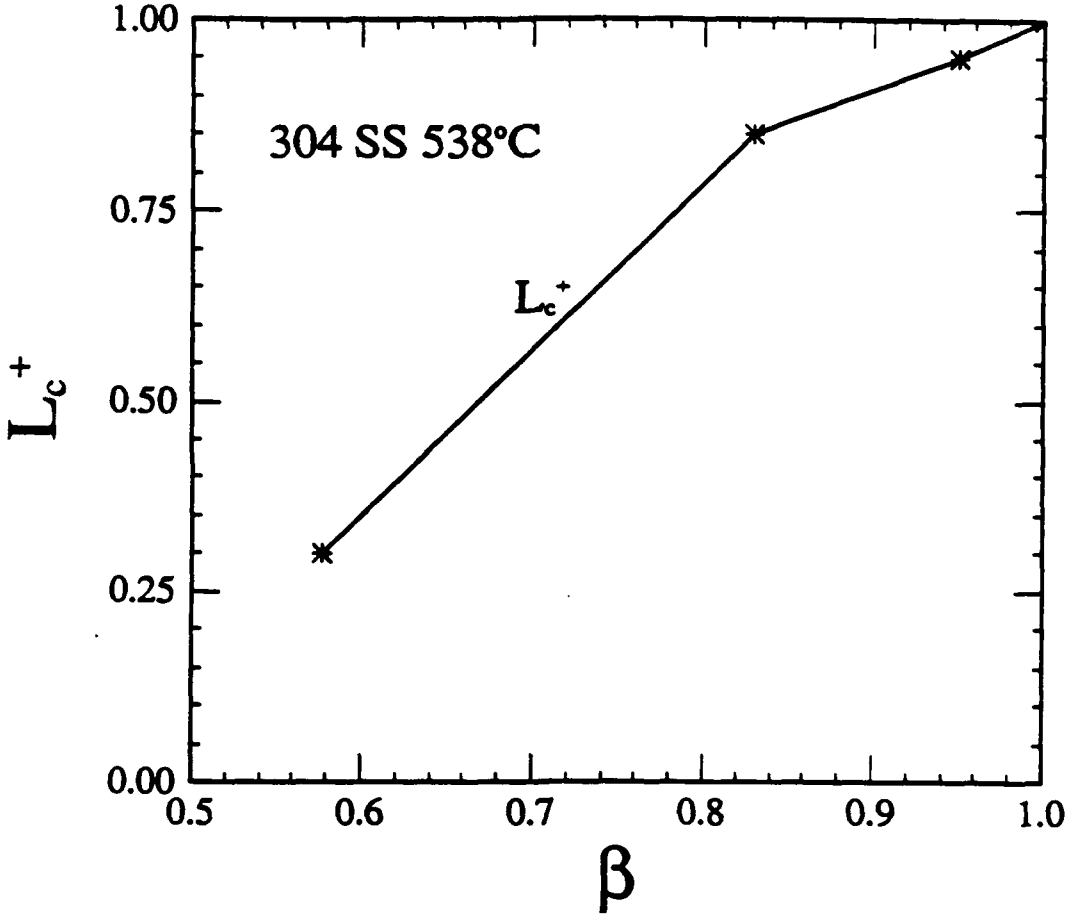
304 SS 538°C
L_c^+
L_c^+
β
1.00
0.75
0.50
0.25
0.00
0.5
0.6
0.7
0.8
0.9
1.0

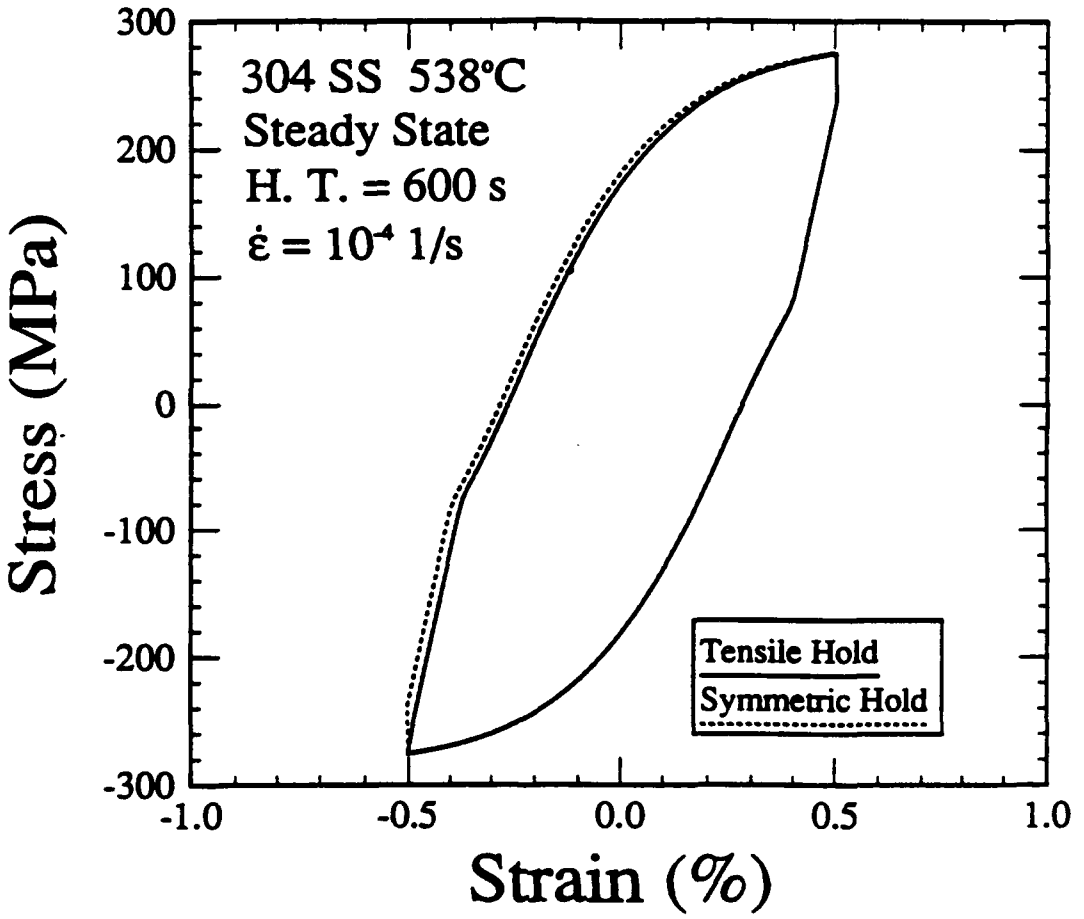
304 SS 538°C
Steady State
H. T. = 600 s
$\dot{\varepsilon} = 10^{-4}$ 1/s
Tensile Hold
Symmetric Hold
Stress (MPa)
Strain (%)
300
200
100
0
-100
-200
-300
-1.0
-0.5
0.0
0.5
1.0

Fig. 3

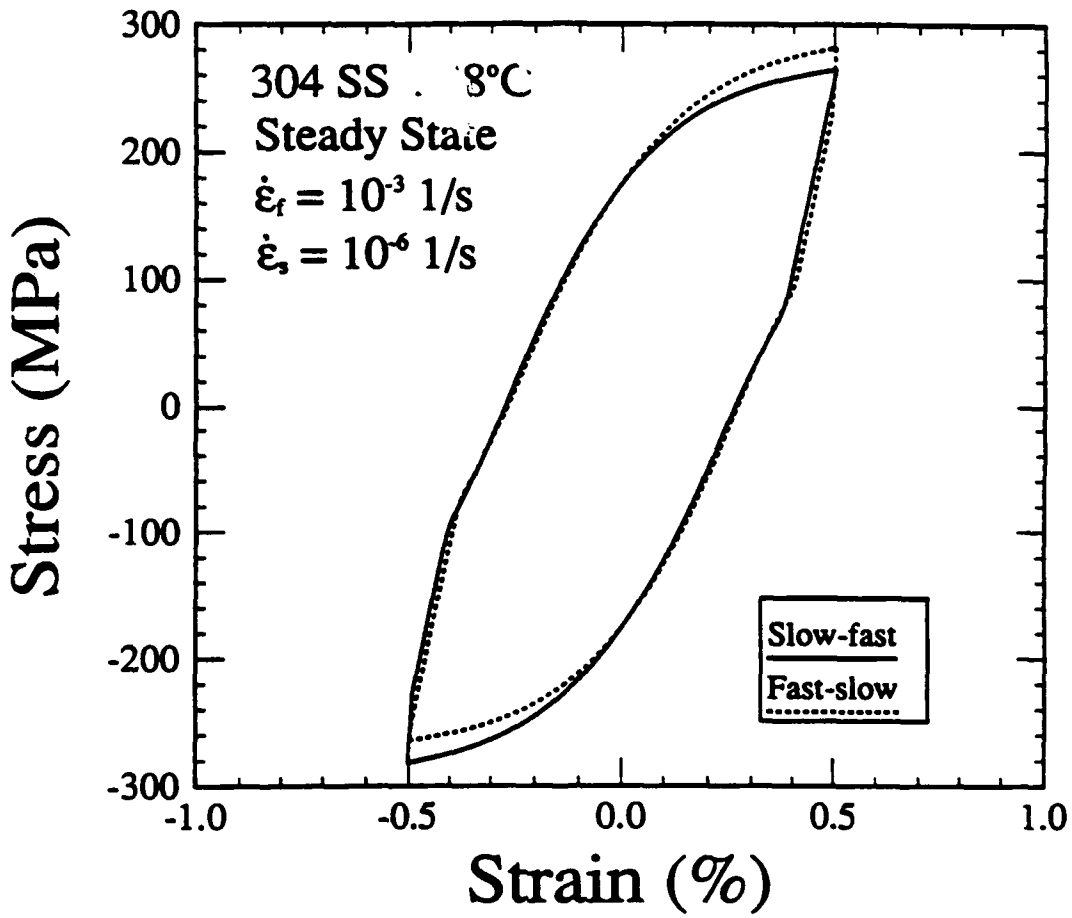
304 SS . 8°C
Steady State
$\dot{\varepsilon}_f = 10^{-3}$ 1/s
$\dot{\varepsilon}_s = 10^{-6}$ 1/s
Slow-fast
Fast-slow
Stress (MPa)
Strain (%)
300
200
100
0
-100
-200
-300
-1.0
-0.5
0.0
0.5
1.0

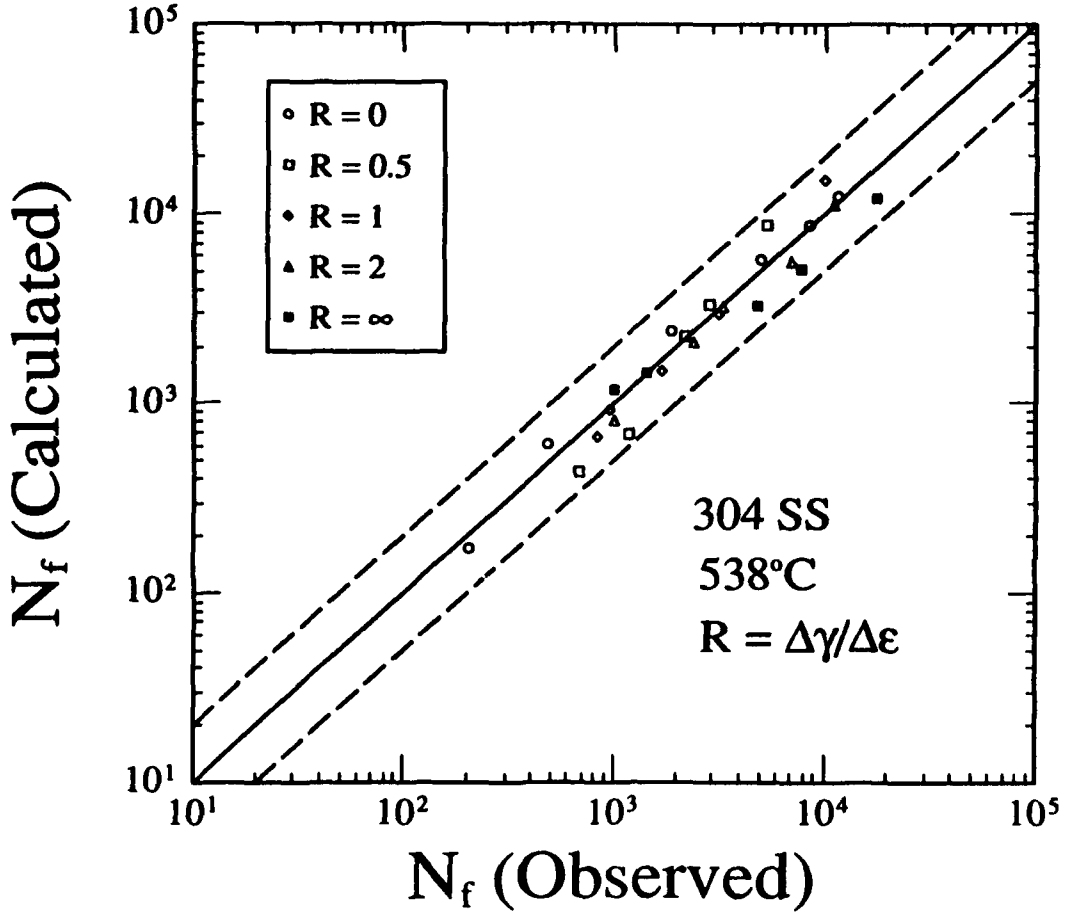
10^5
10^4
10^3
10^2
10^1
N_f (Calculated)
R = 0
R = 0.5
R = 1
R = 2
R = ∞
304 SS
538°C
R = Δγ/Δε
10^1
10^2
10^3
10^4
10^5
N_f (Observed)

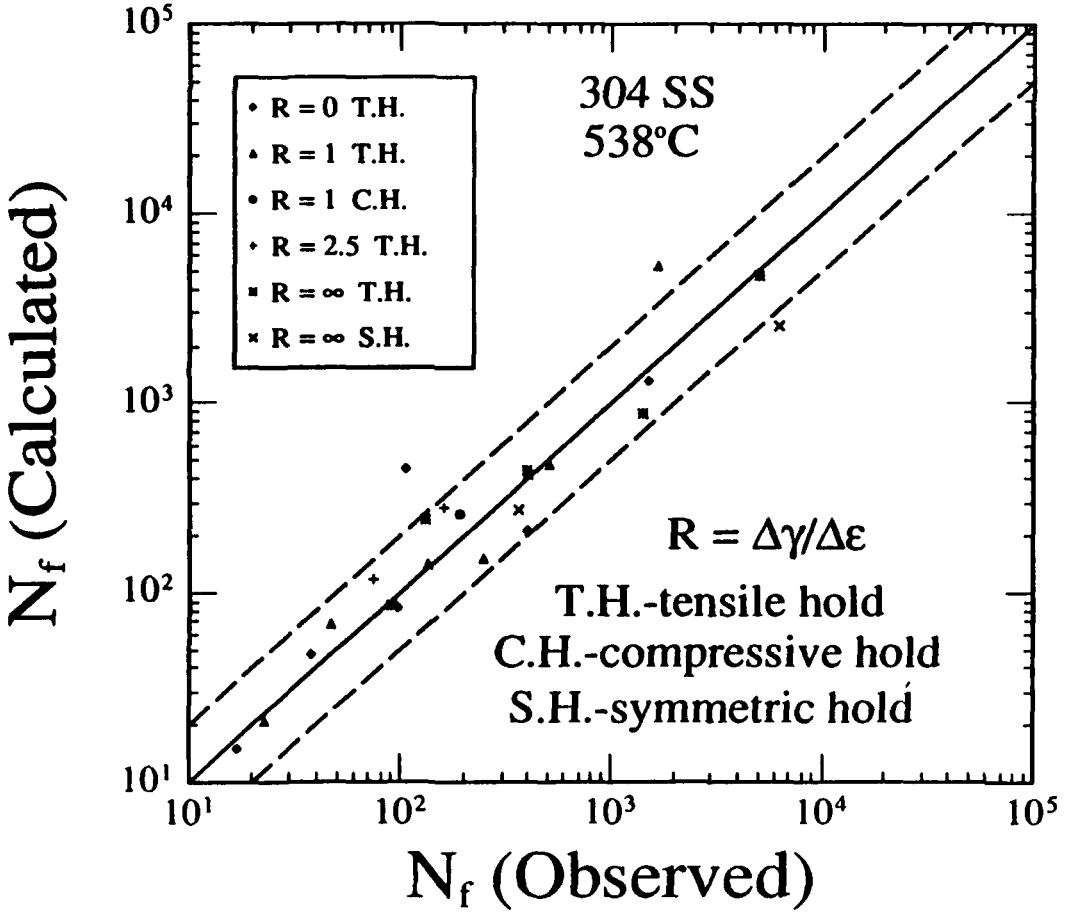
304 SS
538°C
R = 0 T.H.
R = 1 T.H.
R = 1 C.H.
R = 2.5 T.H.
R = ∞ T.H.
R = ∞ S.H.
R = Δγ/Δε
T.H.-tensile hold
C.H.-compressive hold
S.H.-symmetric hold
N_f (Calculated)
N_f (Observed)
10^1
10^2
10^3
10^4
10^5

Fig. 6

RESIDUAL STRESSES - III
Science and Technology

Volume 1

Edited by

H. FUJIWARA

Faculty of Engineering, Tokushima University, Japan

T. ABE

Department of Mechanical Engineering, Okayama University, Okayama, Japan

and

K. TANAKA

Department of Mechanical Engineering, Nagoya University, Japan

ELSEVIER APPLIED SCIENCE
LONDON and NEW YORK

RESIDUAL STRESSES EFFECTS ON THERMAL CYCLING BEHAVIOR OF LAMINATED METAL MATRIX COMPOSITES. A THERMOVISCOPLASTIC ANALYSIS.

Erhard KREMPL and Nan-Ming YEH

Mechanics of Materials Laboratory
Rensselaer Polytechnic Institute
Troy, NY 12180-3590 , USA

ABSTRACT

The vanishing fiber diameter model (VFD) and the thermoviscoplasticity theory based on overstress (TVBO) are combined to analyze the thermomechanical behavior of angle-ply laminates using classical laminate theory. TVBO is a "unified" theory which does not separately postulate constitutive equations for creep and rate independent plasticity. All inelastic deformation is considered rate-dependent and the concept of a yield surface is not used. Creep, relaxation, rate sensitivity and cyclic behavior are are included in this analysis tool where the composite is characterized by the fiber (matrix) volume fraction. As an example, numerical experiments illustrate the influence of residual stresses and ply angle on the free thermal expansion behavior of Gr/Al angle-ply laminates.

INTRODUCTION

Metal matrix composites are being considered for use over a wide range of temperature. This includes high temperature service where rate(time)-dependent effects such as creep, relaxation and rate sensitivity play an important role. These effects can also be found at low homologous temperature, but are not considered important. Elevated temperature service always implies variable temperature as the components have to be brought to the operating temperature at the start of the equipment and they will be cooling down when it ceases operation. Under variable temperature, the possible difference in the coefficients of thermal expansion (CTE) of the fiber and of the metal-matrix can cause internal stresses which affect the mechanical behavior and the lifetime of the metal matrix composites. Of specific interest here is the influence of residual stresses due to cool-down from manufacturing temperature on the subsequent thermal cycling behavior. Following previous developments for a single ply, see [1] and [2], we adopt the simple laminate model of [3] to formulate a theory of thermomechanical behavior of laminates. Each ply is characterized by the fiber volume fraction, the fiber and matrix mechanical properties. To compute the laminate behavior the lay-up must also be known. Here we restrict ourselves to the thermal cycling behavior of symmetric angle-ply composite laminates $(\pm\phi^\circ)_s$.

The matrix behavior is modeled by the thermoviscoplasticity theory based on overstress (TVBO) formulated for orthotropy in [4]. A simple composite model, the vanishing fiber diameter model (VFD) of [5] is combined with TVBO to obtain the three dimensional equations describing the thermomechanical behavior of the composite continuum represented by a ply with the fiber and matrix volume fractions

as parameters. This theory consists of 19 coupled, nonlinear differential equations which have to be solved under a given set of boundary conditions for the prescribed loading and temperature history. This theory is completely derived in [1] and applications are reported in [2]. The purpose of this paper is to investigate the effects of residual stresses and the ply angle (ϕ) on the thermal cycling behavior of angle-ply metal matrix laminates.

THE COMPOSITE MODEL AND NUMERICAL SIMULATION

Preliminaries

For the present investigation the fiber is assumed to be transversely isotropic, elastic with temperature-independent properties. The matrix is postulated to be isotropic and thermoviscoplastic and to be represented by TVBO [4]. When the VFD model [5] is combined with the TVBO the composite is characterized by a set of 19 coupled, first order, nonlinear differential equations which can be found in [1]. These equations are specialized for the case of plane stress to represent a lamina reducing the number of coupled nonlinear differential equations to 10. To obtain the laminate behavior, the usual coordinate transformation rules and the approximations known from simple laminate theory [3] are adopted. The overall stress rates are now obtained as a function of ply angle, ply thickness, laminate thickness and number of plies thus adding another set of three coupled, nonlinear differential equations. This theory enables the simulation of in-plane loading of composite angle-ply laminates under isothermal conditions or for uniformly changing temperature. For a continuum representation of the ply behavior, laminate theories have been published in [6,7]. Details of the present development can be found in [8].

For a single ply, the reference and material coordinate systems are denoted by 1, 2, 6 and x, y, s, respectively. Superscripts ^{f} and ^{m} denote fiber and matrix, respectively.

For numerical calculations material properties must be known as a function of temperature. Since all material constants of the theory can be functions of temperature a wide variety of thermomechanical behavior can be modeled. However, the fiber and matrix properties must be known from suitable experiments which must include the characterization of the rate(time)- dependent behavior. Such data is scarce, specifically for metal matrix composites intended for elevated temperature service. However, such data are being developed and the theory can be applied to these true high temperature systems in the future. For the purposes of this paper a Gr/Al metal matrix system is simulated, for which properties were found from test data and reasonable assumptions, see [2]. Since the Graphite fiber has a negative coefficient of thermal expansion interesting behaviors are found during experiments involving thermal cycling of a single ply, see [9].

In this paper only free thermal cycling is simulated, the ply or laminate is only subjected to a uniform temperature change which causes stresses to be developed between fiber and matrix and between the laminae. This interaction not only influences the mechanical behavior [2] but also affects the overall coefficient of thermal expansion which needs to be known. The set of governing differential equations is specialized for zero overall stresses. Since no closed form solution seems to be possible, the differential equations are integrated numerically, a numerical experiment is being performed. The numerical integration was done on a Sun 3/60 work station using the IMSL routine DGEAR. The output data file was then plotted using Templegraph. The plotted results can be compared with experimental results where available. To integrate the set of coupled differential equations for a laminate, about 30s running time on the Sun 3/60 is needed.

Residual Stresses upon Cool-Down from Manufacturing Temperature for a Gr/Al Laminate

Overall stresses are assumed to be zero and the temperature is decreased at a constant rate of 0.033 °C/s. It is assumed that the composite is stress free at 660 °C and that perfect bonding between fiber and matrix and between plies start at that temperature. Since the coefficient of thermal expansion is larger for the matrix than for the fibers, tensile matrix stresses and compressive fiber stresses in the 1-direction develop in a +12° ply as shown in Fig. 1 for Gr/Al with $c^f = 0.5$. At point 1 room temperature is reached. Due to the rate dependence of the matrix at room temperature, the stresses relax to point 2 with time. Fig. 1 also plots the evolution of the matrix equilibrium stress g_1^m, a state variable of TVBO (it is similar to the backstress of other theories). The difference $\sigma_1^m - g_1^m$ is the overstress of the matrix and it "drives" inelastic deformation. The inset shows the overstress $\sigma_1^m - g_1^m$, rapidly decreasing with time. After 30 days the overstress is nearly zero and the residual stress state is nearly constant at point 2. Small changes may still occur, but for practical purposes the residual stress state remains stationary from thereon.

All residual quantities, matrix stress and state variables enter as initial conditions for simulation of subsequent tests. They can affect the modeled behavior and therefore time appears to influence it until equilibrium is reached. Then the model predicts that the subsequent response is independent of the rest time at room temperature. In subsequent numerical experiments, the residual stress states at point 1 and at point 2 are designated as Case 1 and Case 2, respectively. The differences between the subsequent responses of Cases 1 and 2 represent the influence of the relaxation of the residual stresses.

The Influence of Residual Stresses on the Thermal Cycling Behavior of Gr/Al Composite.

The thermal cycling behavior of Gr/Al angle-ply laminates is of special interest due to the negative axial coefficient of thermal expansion (CTE) of Graphite. It gives rise

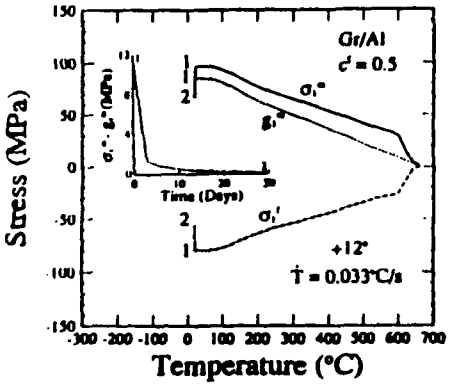

Fig. 1. Development of the constituent stresses σ_1^f, σ_1^m, and g_1^m in the + 12° Gr/Al ply during cool down from manufacturing temperature. The inset shows the decrease of the overstress during the room temperature hold.

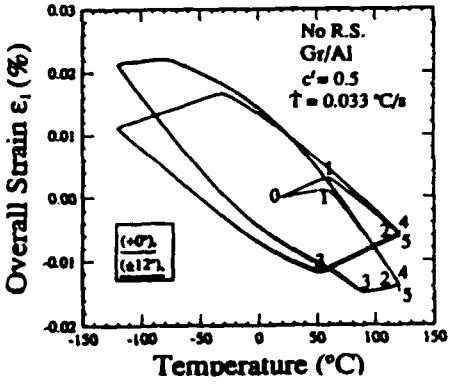

Fig. 2. Temperature-strain loops for (±0°), and (±12°), during temperature cycling of Gr/Al composites. No initial residual stresses

to some unusual expansion behavior, see [2,9]. The composite laminate is free to expand (overall stresses are zero) and is subjected to a temperature cycle starting from room temperature to ± 120 °C at a rate of 0.033 °C/s.

The resulting 1-direction strain-temperature hysteresis loops are depicted in Fig. 2 for a unidirectional and a $(\pm 12°)_s$ laminate. The hysteresis loops are similar, but the angle-ply laminate expands more than the unidirectional one. It is seen that both laminates expand on the segment 0-1 but then contract with increasing temperature, segment 1-2. Upon decrease of temperature from 120 °C the laminates shrink as expected but expand at point 3 although the temperature continues to decrease. This pattern continues in the subsequent reversals. At point 4 a 600 s temperature hold is introduced and the strain decreases by a small amount to point 5, the laminates "creep" under zero external load. For $(\pm 12°)_s$ laminate the strain increment is small in segment 0-1 but the strain decreases more in segment 1-2 than for the unidirectional laminate $(\pm 0°)_s$. During 600s temperature hold more creep strain accumulates for $(\pm 12°)_s$ than for $(\pm 0°)_s$. No residual stresses resulting from cool-down from manufacturing temperature are considered in Fig. 2.

To show the influence of residual stresses, Cases 1 and 2 are simulated in Figs. 3 and 4 for $(\pm 12°)_s$ laminates, respectively. Cooling down takes place on 0-1. While the composite rests free of overall stresses at room temperature, the overall strain increases on path 1-2, see Fig. 4 (this portion is absent in Fig. 3 which depicts Case 1). At 2 temperature cycling begins, the composite expands first, 2-3, but starts to shrink, 3-4 and then the pattern of Fig. 2 continues. However, this time the first part of the first cycle 2-5 is not inside the subsequent loop as it was the case for Fig. 2, see segment 0-3. Rather the first segment is shifted and the shift depends on the case considered. The residual stresses of the fiber, matrix, and plies alter the initial hysteresis loop.

This unusual behavior is due to the internal stresses between fiber and matrix. This is illustrated for Case 2 in Fig. 5 where the development the matrix and fiber stresses of a 12° ply during cycling (the cool-down portion 0-2 is omitted) is depicted. For identification the numbering scheme of Fig. 3 and in Fig. 4 is used. Cycling starts at point 2 with the residual stresses present from the previous history. As the temperature

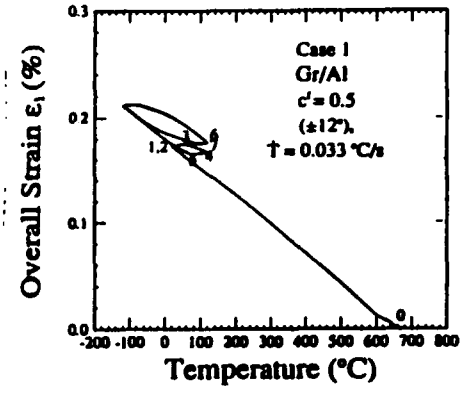

Fig. 3. Temperature-strain graph for $(\pm 12°)_s$ during cool down from 660° C and subsequent cycling as in Fig. 2. Case 1.

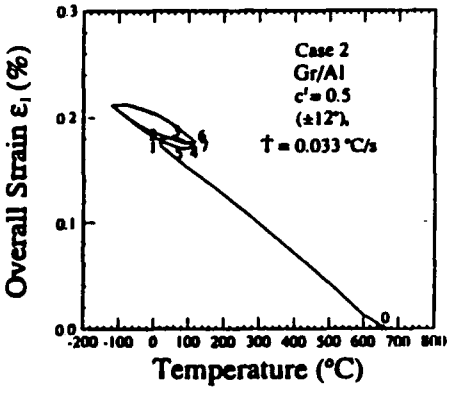

Fig. 4. Same as Fig. 3. for Case 2.

increases the magnitude of the matrix and the fiber stresses decrease almost linearly until yielding sets in at 3. It is also seen that the matrix overstress is nearly zero on the scale of the graph on path 2-3, indicative of the absence of time-dependent deformation in this region. The matrix starts yielding at points 3 and 5 where the breaks in Figs. 3 and 4 occur. During inelastic deformation the stiffness of the matrix is considerably reduced and its restraint on the graphite fibers which want to shrink with increasing temperature is reduced. The laminate shrinks on 3-4. Nearly elastic stiffness prevails on 4-5 until the matrix yields at point 5 where the temperature-overall strain loops show a distinctive break. It is clear that the unusual behavior is due to the matrix yielding and the negative axial CTE of Graphite.

The "micro creep strain" developed during a 600 s temperature hold at point 6 is not noticeable on Figs. 3 and 4 but the stress drop is observable in Fig. 5. For practical purposes the laminate behaves in a time-independent manner.

Due to the distinctive appearance of the overall strain-temperature hysteresis loops it is possible to define overall elastic and inelastic CTEs. For simplicity the elastic and inelastic CTEs are determined as tangents to the hysteresis loops during temperature increase in 20°-50°C and in the 100°-120°C ranges, respectively, at the first and the fifth reversals. The results are given in Fig. 6. While no residual stress effects are found in the elastic range, the inelastic CTEs in the first and fifth reversals are smaller than the CTEs without residual stresses. The inelastic CTEs are invariably negative and reach a maximum absolute value at $\phi = 30°$ for all cases.

DISCUSSION

The thermoviscoplasticity theory based on overstress is used in conjunction with the vanishing fiber diameter model in a simple analysis of the thermal cycling behavior of angle-ply composite laminates with and without residual stresses. Realistic but assumed material properties permit the execution of numerical experiments. The present theory exhibits rate-dependent behavior. The first example is the redistribution of the residual stresses while the composite element is sitting stress free at room temperature after cool-down from manufacturing temperature. The theory predicts that this redistribution will come to an end after some time which depends on material constants, especially the viscosity function used. In the present application the

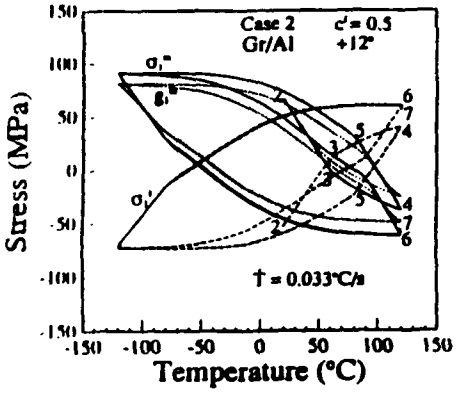

Fig. 5. The "internal stresses" developed during temperature cycling for Case 2. Curves start at room temperature, point 2 in Fig. 4.

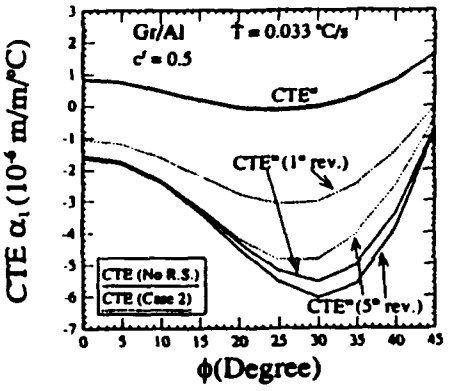

Fig. 6. Variation of axial CTE of angle-ply laminates (±φ°), as a function of laminate angle with and without residual stresses.

redistribution is almost finished after 30 days. While the stresses redistribute the time spent at room temperature appears to have an influence on the subsequent behavior. Another example is the creep strain accumulation during a 600s temperature hold in Fig.2. The creep strain, although small is larger for $(\pm 12°)_s$ than for $(\pm 0°)_s$. The matrix contribution to the deformation increases as the ply angle increases and as a consequence rate dependence is bound to increase with increasing ply angle.

The development of the internal stresses shown in Fig. 5 is the reason for the anomalous free thermal expansion of the Gr/Al composite laminates. The results of Figs. 3-5 suggest that residual stresses are responsible for the special shape of the hysteresis loop and the special form of the first cycle. The special form of the first cycle was found with experiments on a single ply in [9]. Our theory shows that this property carries over to angle-ply laminates.

Disregarding the first cycle, residual stresses are shown to have an effect on the overall inelastic CTE of a laminate, see Fig. 6. They decrease the absolute value of the inelastic CTEs. In this sense they are beneficial. A nonlinear relationship between CTE and ply angles exists in every case indicative of very complex interactions between CTEs of the constituents and the inelastic thermomechanical behavior of the matrix. For the case without residual stresses the CTEs vs. ϕ curves correspond to the trend of the results obtained with a time-independent plasticity, finite element model of the laminate [10].

The present analysis also permits to determine the fiber and matrix stresses in every ply and this information is useful for lifetime calculations which are not performed here but are considered elsewhere, see [8].

ACKNOWLEDGEMENT

This research was supported by DARPA/ONR Contract N00014-86-k0700 with Rensselaer Polytechnic Institute.

REFERENCES

1. Yeh, N. M. and Krempl, E., To appear in Journal of Composite Materials.
2. Krempl, E. and Yeh, N. M., Proceedings IUTAM Symposium on Inelastic Deformation of Composite Materials, G. J. Dvorak, Ed., Springer-Verlag, 1990, pp. 411-433.
3. Tsai, S. W. and Hahn, H. T., Introduction to Composite Materials, Technomic Publishing Company, Westport, Connecticut, 1980, pp. 116.
4. Lee, K. D. and Krempl, E., International Journal of Solids and Structures, 1991, 27, pp. 1445-1459.
5. Dvorak, G. J. and Bahei-El-Din, Y. A., Journal of Applied Mechanics, 1982, 49, pp. 327-335.
6. Lee, K. D. and Krempl, E., Thermal and Mechanical Behavior of Ceramic and Metal Matrix Composites, ASTM STP 1080, J. M., Kennedy and W. S. Johnson, Eds., American Society for Testing and Materials, 1990, pp. 40-55.
7. Krempl, E. and Hong, B. Z., Composites Science and Technology, 1989, 35, pp. 53-74.
8. Yeh, N. M., Ph.D. Thesis, Rensselaer Polytechnic Institute, Troy, New York, forthcoming.
9. Tompkins, S. S. and Dries, G. A., ASTM STP 964, P. R., DiGiovanni and N. R. Adsit, Eds., American Society and Testing Materials, 1988, pp. 248-258.
10. Wu, J. ., Shepherd, M. S., Dvorak, G. J., and Bahei-El-Din, Y. A., Composites Science and Technology, 1989, 35, pp. 347-366.

AMD-Vol. 118, Mechanics of Composites at
Elevated and Cryogenic Temperatures
ASME 1991

A THERMOMECHANICAL ANALYSIS OF LAMINATED METAL MATRIX COMPOSITES USING THE VISCOPLASTICITY THEORY BASED ON OVERSTRESS

Nan-Ming Yeh and Erhard Krempl
Mechanics of Materials Laboratory
Rensselaer Polytechnic Institute
Troy, New York

ABSTRACT

The vanishing fiber diameter model (VFD) and the thermoviscoplasticity theory based on overstress (TVBO) are used to analyse the thermo–mechanical behavior of angle–ply composite laminates using classical laminate theory. TVBO is a "unified" theory which does not separately postulate constitutive equations for creep and rate–independent plasticity. All inelastic deformation is considered rate–dependent and the concept of a yield surface is not used.

Assuming that fiber and matrix are stress free at the manufacturing temperature and remain perfectly bonded during cool down to room temperature the model permits the calculation of residual stresses between fiber and matrix which can influence the subsequent thermomechanical deformation behavior. A time–dependent, slowly diminishing redistribution of the residual stresses is predicted while the composite is sitting stress free at room temperature. As a consequence subsequent mechanical behavior depends on time spent at room temperature until the stress redistribution is complete which for the chosen material properties happens to occur after 30 days. Tension/compression asymmetry for a unidirectional and a $(\pm 12^{\circ})_s$ B/Al laminate are two examples for which detailed numerical analyses are performed. The results are encouraging and reflect the trends of the few available experimental results.

INTRODUCTION

Future airplanes and space structures need to be made of materials with high specific strength and stiffness as well as high fatigue and fracture resistance. Metal matrix composites are prime candidates for these applications. When thermal and mechanical cycling is involved as is frequently the case, stresses between fiber and matrix may develop when a mismatch of the coefficients of thermal expansion of matrix and fiber is present. These internal stresses may affect the mechanical behavior of the composite and may lead to premature failure. It is therefore necessary to develop analysis tools to predict and alleviate these internal stresses in the design stage. Since rate (time)–dependent effects are frequently present a thermoviscoplastic analysis is in order.

In an early experimental investigation Cheskis and Heckel [1970] used X–ray techniques to measure fiber and matrix stresses in a 2024 Al/W composite. They showed that the yield behavior of the composites is significantly influenced by manufacturing residual stresses.

Dvorak and Rao [1976] used a plasticity theory to compute the residual stresses in heat–treated metal matrix composites. They concluded that the residual stresses found

after heat–treatment are significant in magnitude and a high hydrostatic stress component in the matrix at the fiber–matrix interface may cause fracture or fatigue damage.

The purpose of this paper is to present a simple tool to analyze the thermomechanical behavior of metal matrix composite laminates for time dependent deformation including rate sensitivity, relaxation and creep. To this end the thermoviscoplasticity theory (TVBO) of Lee and Krempl [1991] is combined with the vanishing fiber diameter model (VFD) of Dvorak and Bahei–El–Din [1982] to determine the plane stress behavior of angle–ply laminates using standard classical laminate theory. Of special interest are the influences of fabrication residual stresses on the mechanical behavior. The residual stresses which develop during cool–down from manufacturing temperature and which can redistribute with time while the composite is stress free at room temperature are found to have a significant influence on the room temperature tension/compression behavior. The TVBO theory used here represents viscoplastic behavior which is sometimes called "cold creep", i.e. the creep behavior in metals seen at low homologous temperature. The growth laws for the state variables must be augmented by a suitable recovery of state term to represent secondary creep in the quasi elastic region of the stress–strain diagram. Such modifications are easily implemented but are not pursued here due to the lack of high temperature composite creep data.

THE COMPOSITE MODEL. THERMOVISCOPLASTICITY THEORY BASED ON OVERSTRESS (TVBO) AND THE VANISHING FIBER DIAMETER MODEL (VFD)

The Governing Equations

The three dimensional thermoviscoplasticity theory based on overstress has been developed by Lee and Krempl [1991]. In the present analysis a plane stress state in a fibrous ply is assumed. The usual vector notation for the stress tensor components σ and the small strain tensor components ϵ are used for the representation of the equations. Boldface capital letters denote 3x3 matrices.

Stresses and strains without a superscript designate quantities imposed on the composite as a whole. Superscripts ^{f} and ^{m} denote fiber and matrix, respectively. The fiber volume fraction is c^f and c^m denotes the matrix volume fraction with $c^f + c^m = 1$. The fiber is transversely isotropic thermoelastic, the matrix is isotropic, inelastically incompressible and thermoviscoplastic as represented by TVBO. Fiber orientation in the x–direction is postulated, see Fig. 1. The x y s is the preferred or on–axis coordinate system and 1 2 6 is the off–axis system. For convenience in writing we denote the vectors which are referred to be the off–axis system with a prime.

For the VFD model, Dvorak and Bahei–El–Din [1982], the following constraint equations hold

$$\begin{aligned} \dot{\sigma}_i &= \dot{\sigma}_i^f = \dot{\sigma}_i^m \quad \text{for } i = y, s \\ \dot{\sigma}_x &= c^f \dot{\sigma}_x^f + c^m \dot{\sigma}_x^m \\ \dot{\epsilon}_i &= c^f \dot{\epsilon}_i^f + c^m \dot{\epsilon}_i^m \text{ for } i = y, s \\ \dot{\epsilon}_x &= \dot{\epsilon}_x^f = \dot{\epsilon}_x^m. \end{aligned} \tag{1}$$

When they are combined with the TVBO equations by Lee and Krempl [1991] the composite is characterized by the following set of equations: (details can be found in Yeh and Krempl [1990])

$$\dot{\epsilon} = \overline{\mathbf{C}}^{-1}\dot{\sigma} + (\mathbf{K}^m)^{-1}\mathbf{X}^m + (\dot{\mathbf{R}}^f)^{-1}\sigma^f + (\dot{\mathbf{R}}^m)^{-1}\sigma^m + \overline{\alpha}\dot{T} \tag{2}$$

together with a separate growth law for the σ_x^m component of the matrix

$$\dot{\sigma}_x^m = \frac{E^m}{E_{xx}}\dot{\sigma}_x - \frac{c^f}{E_{xx}} L\dot{\sigma}_y - \frac{c^f E_{xx}^f E^m}{E_{xx}}\left[\frac{1}{K^m k^m[\Gamma^m]}(x_x^m - 0.5x_y^m)\right]$$
$$- \frac{c^f E_{xx}^f E^m}{E_{xx}}\left\{\left[\frac{1}{(E_{xx}^f)^2}(\dot{\nu}_{xy}^f E_{xx}^f - \nu_{xy}^f \dot{E}_{xx}^f) - \frac{1}{(E^m)^2}(\dot{\nu}^m E^m - \nu^m \dot{E}^m)\right]\sigma_y\right.$$
$$\left. + \frac{\dot{E}_{xx}^f}{(E_{xx}^f)^2}\sigma_x^f - \frac{\dot{E}^m}{(E^m)^2}\sigma_x^m\right\} - \frac{c^f E_{xx}^f E^m}{E_{xx}}(\alpha^m - \alpha_x^f)\dot{T}. \qquad (3)$$

In addition growth laws for the two state variables of TVBO, the matrix equilibrium stress g^m and the kinematic stress f^m, are given as

$$\dot{g}^m = q^m[\Gamma^m]\dot{\sigma}^m + \dot{T}\frac{\partial q^m[\Gamma^m]}{\partial T}\sigma^m + \left\{q^m[\Gamma^m] - \theta^m\left[q^m[\Gamma^m] - p^m(1-q^m[\Gamma^m])\right]\right\}\frac{x^m}{k^m[\Gamma^m]} \qquad (4)$$

and

$$\dot{f}^m = \frac{p^m}{k^m[\Gamma^m]}x^m, \qquad (5)$$

respectively, with

$$(\Gamma^m)^2 = (x^m)^t H (x^m)$$

$$(\theta^m)^2 = \frac{1}{(A^m)^2}(s^m)^t H (s^m)$$

$$x^m = \sigma^m - g^m$$

$$s^m = g^m - f^m$$

$$H = \begin{bmatrix} 1 & -0.5 & 0 \\ -0.5 & 1 & 0 \\ 0 & 0 & 3 \end{bmatrix} \qquad (6)$$

In the above inelastic incompressibility for the matrix is assumed. $\tilde{C}^{-1}$ is the overall compliance matrix and $(K^m)^{-1}$ is the viscosity matrix. The matrices $(\dot{R}^f)^{-1}$ and $(\dot{R}^m)^{-1}$ contain time derivatives of the elastic constants of the fiber and the matrix, respectively. All components of these four matrices are listed in Appendix I. The viscosity function $k^m[\Gamma^m]$ and the dimensionless shape function $q^m[\Gamma^m]$ are decreasing ($q^m[0] < 1$ is required, see Lee and Krempl [1991]) and control the rate dependence and the shape of the stress–strain diagram, respectively. (Square brackets following a symbol denote "function of".) The quantity p^m represents the ratio of the tangent modulus E_t^m at the maximum inelastic strain of interest to the viscosity factor K^m. It sets the slope of stress–inelastic strain diagram at the maximum strain of interest. E_{xx}, L, $\tilde{\alpha}$ are defined in Appendix I. An explanation of TVBO is given by Lee and Krempl [1991].

Eq. (3) is used to calculate the instantaneous axial matrix stress which can not be obtained from the overall boundary conditions directly. σ_x^m is affected by mechanical and thermal loadings and their loading paths. For instance for pure thermal loading (overall

stresses are zero), σ_x^m together with g_x^m, f_x^m will develop due to the difference in the coefficients of thermal expansion of fiber and matrix, see (3); these matrix stresses in the fiber direction cause coupling between the mechanical and thermal loading in the inelastic range. The details of derivation and explanation of equations (1–2) are given by Yeh and Krempl [1990].

In–Plane Deformation of a Single Ply

Transformation of strain, stress, and the state variable vector are defined by

$$\begin{aligned} \epsilon^r &= N\epsilon^{r'} \\ \sigma^r &= M\sigma^{r'} \\ g^m &= Mg^{m'}. \end{aligned} \tag{7}$$

The superscript r denotes fiber, matrix, or composite. The transformation matrices N and M are, see Tsai and Hahn [1980],

$$N = \begin{bmatrix} w^2 & n^2 & wn \\ n^2 & w^2 & -wn \\ -2wn & 2wn & w^2-n^2 \end{bmatrix} \tag{8}$$

$$M = \begin{bmatrix} w^2 & n^2 & 2wn \\ n^2 & w^2 & -2wn \\ -wn & wn & w^2-n^2 \end{bmatrix} \tag{9}$$

where $w = \cos\phi$ and $n = \sin\phi$, ϕ is defined in Figure 1. From equations (2) and (7) we then have, see Krempl and Lee [1988],

$$\begin{aligned} \dot{\epsilon}' = N^{-1}\bar{C}^{-1}M\,\dot{\sigma}' + N^{-1}(K^m)^{-1}Mx_m' + N^{-1}(\dot{R}^f)^{-1}M\sigma^{f'} \\ + N^{-1}(\dot{R}^m)^{-1}M\sigma^{m'} + N^{-1}\overline{\alpha}\dot{T} \end{aligned} \tag{10}$$

In–Plane Deformation of a Laminate

For description of laminates, the laminate code of Tsai and Hahn [1980] is adopted. The average stress of the laminate is defined as

$$\sigma_p = \frac{1}{h}\sum_{i=1}^{n}\sigma_i h_i \tag{11}$$

where h is the laminate thickness, h_i the ply thickness of the i–th ply, and p and n denote laminate and the number of plies, respectively. The strain is constant through the laminate thickness and is given by

$$\epsilon_i = \epsilon_p \;(\, i = 1, 2 \ldots\ldots, n\,) \tag{12}$$

The average stress rate $\dot{\sigma}_p'$ is obtained from (10) and (11)

$$\begin{aligned} \dot{\sigma}_p' = \sum_{i=1}^{n}[M^{-1}\bar{C}N]_i\frac{h_i}{h}\dot{\epsilon}' - \sum_{i=1}^{n}\Big[(M^{-1}\bar{C}(K^m)^{-1}Mx^{m'}) + (M^{-1}\bar{C}(\dot{R}^f)^{-1}M\sigma^{f'} \\ + M^{-1}\bar{C}(\dot{R}^m)^{-1}M\sigma^{m'}) + M^{-1}\bar{C}\overline{\alpha}\dot{T}\Big]_i\frac{h_i}{h}. \end{aligned} \tag{13}$$

Inspection reveals that the first term on the right hand side of (13) is the rate form of the elasticity equations found in Tsai and Hahn [1980] except that the elasticity matrix is replaced by the matrix obtained from the VFD model. This matrix has the same symmetries as the orthotropic matrix of elastic moduli. It is seen from the Appendix that the matrices $(K^a)^{-1}$, $(\dot{R}^f)^{-1}$ and $(\dot{R}^a)^{-1}$ are not symmetric. For specially stacked laminates, such as symmetric, antisymmetric, angle ply, the matrix products appearing in (13) have certain symmetries which for the first term are known from Tsai and Hahn [1980].

It is clear from (13) that the individual ply stresses cannot be prescribed, only the average stresses or the strains and the uniform temperature can be enforced. The following cases can be distinguished (the isothermal case is recovered when the temperature rate is zero).

Average Stress and Temperature Control. For average stress–temperature control, the average stress rates in all directions, the temperature rate, and the geometry of each layer must be specified. In addition, the initial overall stresses and strains and those of the fiber and the matrix and the initial temperature are needed. The ply or laminate strains as well as the ply stresses can then be obtained by integrating Eqs (2–13) simultaneously.

Strain and Temperature Control. For strain and temperature control the strain rates, the temperature rate, the geometry of each layer as well as appropriate initial conditions are needed. The average stress and the ply stresses are obtained simply by solving Eqs (2–13) simultaneously.

NUMERICAL SIMULATION

General Remarks

Eqs. (2–13) constitute the differential equations which describe the laminate behavior. Due to the nonlinearity a closed form integration is impossible for realistic material data. To show the capability of the theory numerical experiments must be performed using the same boundary and initial conditions as in real experiments. Once integrated all the variables appearing in the governing differential equations are known as a function of time. The variables of interest can be plotted and represent the response of the theory to the particular boundary conditions. For different boundary conditions a different response will be obtained since TVBO exhibits path dependence.

Also material properties must be known for the fiber and the matrix as a function of temperature. These material properties include the usual elastic properties and the coefficient of thermal expansion and the inelastic properties of the TVBO model. For the purposes of this paper a Boron/ Aluminum system is simulated. The matrix viscoplastic properties are known at room temperature from experiments reported by Yao and Krempl [1985] for a 6061–T6 Al alloy. An Al alloy of the same designation may have slightly different properties when used in a composite, but the general trend is reproduced. Since no experimental results were found at other temperatures a plausible temperature dependence was postulated. The elastic properties and the coefficient of thermal expansion for the B fiber are listed in Table 1. They are assumed to be independent of temperature for simplicity. The matrix properties which are close to 6061–T6 Al alloy are listed in Table 2. They yield the matrix stress–strain diagrams at a strain rate of 10^{-4} s^{-1} depicted in Fig. 2. A decrease in modulus, flow stress and the asymptotic tangent modulus with increasing temperature is modeled. The following numerical experiments represent tests with a material which has the stress–strain diagrams depicted in Fig. 2.

Two angle–ply laminates with plies of equal thickness, $(\pm 0^\circ)_s$ and $(\pm 12^\circ)_s$, are chosen for the numerical simulations.

The numerical integration was done on a Sun 3/60 work station using the IMSL routine DGEAR. The output data file was then plotted using Templegraph. To integrate the set of coupled differential equations for a laminate approximate 30s running time is needed.

Residual Stresses upon Cool–Down from Manufacturing Temperature

The composite cools down from the manufacturing temperature at a constant rate of 0.033 °C/s without the application of external forces. It is assumed that the composite is stress free at 660 °C and that perfect bonding between fiber and matrix and between plies start at that temperature. Fig. 3 shows the development of the matrix stresses in the 1–direction for +12° ply of a B/Al $(\pm 12°)_s$ laminate with $c^f = 0.1$. Since the coefficient of thermal expansion is larger for the matrix than for the fibers a tensile matrix stress is developed which increases with decreasing temperature. Also shown are the evolution of matrix equilibrium and matrix kinematic stress, the two state variables of the TVBO. At point 1 room temperature is reached. Due to the viscoplastic nature of the matrix the stresses relax to point 2 with time. The inset shows the overstress $\sigma - g$, which "drives" the inelastic deformation, rapidly decreasing with time at room temperature. After 30 days the residual stress state is nearly constant. The current value of the stress, equilibrium and kinematic stresses enter as initial conditions for simulation of subsequent tests. They can affect the modeled subsequent behavior and therefore time appears to influence it. During the first 30 days the model predicts that the subsequent response depends on time but becomes independent of the rest time thereafter. On the scale of this graph the kinematic variable f does not appear to change with time. However, the digital output confirms the slight increase predicted by Eq (5).

In the simulation of subsequent behavior the residual stresses at point 1 and at point 2 form the initial conditions for Case 1 and Case 2, respectively.

Influence of Residual Stresses on Room Temperature Mechanical Behavior

In this case $(\pm 0°)_s$ and $(\pm 12°)_s$ B/Al angle–ply composite laminates with $c^f = 0.1$ are considered and uniaxial numerical tensile and compressive tests in the 1–direction are performed at a strain rate of $10^{-4}\ s^{-1}$. When a strain magnitude of 0.5% is reached the overall stress is kept constant to allow creep deformation to evolve during a short period of 300s.

Fig. 4 shows tensile and compressive overall stress–strain behavior of tests of a $(\pm 0°)_s$ laminate in 1–direction (which is the fiber direction in this case) for no residual stresses and with residual stress states corresponding to Case 1 and Case 2.

A significant influence of residual stresses on the laminate stress–strain diagram is demonstrated. It can be seen that the stress–strain diagram with no residual stresses is point symmetric to the origin and that the residual stresses promote tension–compression asymmetry. Due to the high initial values of the matrix stresses for Case 1 more asymmetry is found for Case 1 than for Case 2. On the graph the initial slopes are equal but the transition to inelasticity and the initial inelastic slope are dependent on the residual stresses. The level of the tensile overall stress is considerably lower for Case 2 than for the case without residual stresses. However the opposite is true in the compressive direction. Since it is unlikely that a tensile test will be performed right after reaching room temperature and since the overstress decreases rapidly with time, see inset in Fig. 3, an experiment would likely yield the results of Case 2. During the 300s stress hold a small amount of creep strain develops which on the scale of the graph is equal in tension and compression and for all three cases. This creep strain is "cold creep" which is observed at room temperature, see Yao and Krempl [1985] and Ericksen [1973], and is modeled by TVBO.

The same tests are then performed on $(\pm 12°)_s$ laminates. The laminate stress, the matrix stress and matrix equilibrium stress of a ply are plotted vs. overall strain in the 1–direction in Figs. 5, 6, and 7. The laminate stress levels are somewhat lower than the corresponding tests for the $(\pm 0°)_s$. Again residual stresses promote tension/compression asymmetry. In Fig. 5 all stresses start from zero and initially the matrix overstress $\sigma_1^m - g_1^m$ is zero on the graph. Consequently the laminate stress–strain diagram is linear with the corresponding elastic slope. As overstress develops the stress–strain diagram bends

over and proceeds with a reduced slope. Simultaneously it is observed that the overstress is nearly constant. (A characteristic of TVBO is the attainment of an asymptotic solution for constant strain (stress) rate tests, see Yao and Krempl [1985] and papers cited therein.) When the stress is held constant creep develops and the overstress decreases. This indicates that creep is primary, i.e. the strain rate decreases. The creep strain of the three cases for $(\pm 0^\circ)_s$ is smaller than for $(\pm 12^\circ)_s$. For Cases 1 and 2 of both laminates more creep strain is accumulated in tension than in compression owing to a slightly larger tensile than compressive matrix overstress. The difference of creep strain accumulation between cases with and without residual stresses negligible on the scale of the graph. Also the final value of the overstress appears to be independent of the initial conditions. In Figs. 6 and 7 the initial values of the matrix stresses are clearly noticeable. Finally the characteristic overstress value is reached as straining continues.

DISCUSSION

The thermoviscoplasticity theory based on overstress was used in conjunction with the vanishing fiber diameter model in a simple analysis of the mechanical behavior of angle–ply composite laminates with and without residual stresses. Realistic but assumed material properties permitted the execution of numerical experiments. They show how the residual stresses develop during cool–down and subsequently influence the mechanical behavior. The validity of the analysis rests on the material properties used which were partially determined from experiments and partly established with plausible assumptions. While the magnitude of the stresses and strains may vary with material data the general trend of the results will not. When the stress level after cool down exceeds the elastic range TVBO will always predict a time–dependent redistribution of the residual stresses. The magnitude of the stress change will depend again on the material properties. The diminishing rate of redistribution which ultimately comes to rest is again a general property of TVBO. The same is true for the creep behavior, the present version of TVBO will always predict primary creep as long as the fiber is elastic and the constant $p^n > 0$. To represent high temperature creep where secondary creep can be observed at stress levels within the quasi linear region of the stress–strain diagram the growth laws for the state variables must be augmented by a static recovery term.

The tensile stress–strain diagrams reported in Fig. 4 correspond qualitatively with those reported by Cheskis and Heckel [1970]. In both cases a break in the slope of the overall stress–strain diagram is observed when the matrix starts to deform inelastically in an appreciable manner. The presence of residual stresses shift the location of this break point, see Fig. 4. Also residual stresses cause tension–compression asymmetry and larger tensile creep strain.

The initial residual matrix tensile stresses of a ply in 1–direction introduce the bias to model the tension/compression asymmetry. This can be seen in Figs. 5–7 for the laminates. The presence of tensile residual matrix stresses is responsible for the early yield in the tensile direction and the delay for the compression tests, see Figs. 6 and 7. In isothermal TVBO the growth laws for the stress and the equilibrium stress are formulated in such a way that the asymptotic equilibrium stress is independent of the initial conditions. This property seems to carry over to the present composite theory.

Another feature of the present theory is its ability to model rate dependence. The redistribution of the residual stresses while the composite element was sitting stress free at room temperature after cool–down from manufacturing temperature is caused by the rate–dependent constitutive equation. The theory predicts that this redistribution will nearly come to an end after some time which depends on material constants, especially the viscosity function used. In the present application the redistribution is almost finished after 30 days. While the stresses redistribute the time at room temperature appears to have an influence on the subsequent behavior. Experimental results confirming this behavior are not available. Since the changes in residual stresses are most rapid initially, see inset of Fig. 3, the changes are hard to detect experimentally. From a knowledge of the properties of TVBO it can be said that an increase in the cooling rate would increase the residual stresses at room temperature and their redistribution rate. However, the influence of rate is likely going to be small. Specifically, the stress cannot be lowered significantly by decreasing the cooling rate. The lowest stress that can be reached is the asymptotic

equilibrium stress. It is not known whether this corresponds to the equilibrium stress plotted in Fig. 3 exactly. But it would not be unreasonable to assume that it would be the stress reached in an infinitely slow cooling rate. It should also be noted that this is the limit in continuous cooling. The theory permits a stress drop below this limit when the temperature is held constant as can be seen in Fig. 3. The rate dependence will increase with an increase of the matrix mode of deformation. For the $(\pm 12^{\circ})_s$ laminates the creep strain in 300s is slightly higher than that for the corresponding tests in the fiber direction, compare Fig. 4 with Figs. 5 –7. An increase in the angle ϕ, would accentuate the creep behavior which will always be primary for the material properties postulated in Table 2.

The present paper intends to show the capabilities in principle. For the exact modeling of a metal matrix composite various refinements are possible. Included are the consideration of of modeling of cyclic hardening/softening of the matrix or the inclusion of "high temperature" creep by including a static recovery term in the growth law for the state variables, see Krempl and Majors [1990]. Also for a specific composite the determination of the matrix and fiber properties as a function of temperature is a formidable task. The simple VFD model could be replaced by an advanced one. However, the present simple approach has given some insight into the influence of residual stresses and of rate–dependence on the mechanical behavior of a metal matrix composite.

ACKNOWLEDGEMENT

This research was supported by DARPA/ONR Contract N00014–86–k0770 with Rensselaer Polytechnic Institute.

REFERENCES

Cheskis, H. P. and Heckel, R. W., 1970, "Deformation Behavior of Continuous–Fiber Metal–Matrix Composite Materials," Metallurgical Transactions, Vol 1, pp. 1931–1942.

Dvorak, G. J. and Rao, M. S. M., 1976, "Thermal Stresses in Heat–Treated Fibrous Composites," ASME Journal of Applied Mechanics, Vol. 43, pp. 619–624.

Dvorak, G. J. and Bahei–El–Din, Y. A., 1982, "Plasticity Analysis of Fibrous Composites," ASME Journal of Applied Mechanics, Vol. 49, pp. 327–335.

Ericksen, R. H., 1973, "Room Temperature Creep of Bosic–Aluminum Composites," Metallurgical Transactions, Vol. 4, pp. 1687–1693.

Hillig, W. B., 1985, "Prospects for Ultra–High–Temperature Ceramic Composites," Report No. 85CRD152, General Electric Research and Development Center.

Krempl, E. and Lee, K. D., 1988, "Thermal, Viscoplastic Analysis of Composite Laminates," Materials Research Society, Symposium Proceedings, 120:129–136.

Krempl, E. and Majors, P. S., 1990, "Modeling of Recovery of State Using the Viscoplasticity Theory Based on Overstress," Proceedings IUTAM Colloquium: Creep in Structures IV, Krakow, Poland, September.

Kreider, K. G. and Prewo, K. M., 1974, "Boron–Reinforced Aluminum," Composite Materials, Vol. 4, Metallic Matrix Composites, Edited by Kenneth G. Kreider, Academic Press.

Lee, K. D. and Krempl, E., 1990, "An Orthotropic Theory of Viscoplasticity Based on Overstress for Thermomechanical Deformations," to appear in International Journal of Solids and Structures.

Tsai, S. W. and Hahn, H. T., 1980, Introduction to Composite Materials, Technomic Publishing Company, Westport, Connecticut, pp. 116.

Tsirlin, A. M., 1985, "Boron Filaments," Handbook of Composites, Volume 1, "Strong Fibers," Editors: Watt, W. and Perov, B. V., North–Holland.

Yao, D. and Krempl, E., 1985, "Viscoplasticity Theory Based on Overstress. The Prediction of Monotonic and Cyclic Proportional and Nonproportional Loading Paths of an Aluminum Alloy," Int. Journal of Plasticity, Vol. 1, pp. 259–274.

Yeh, N. M. and Krempl, E., 1990, "Thermoviscoplastic Analysis of Fibrous Metal–Matrix Composites," MML Report 90–2, Rensselaer Polytechnic Institute, Troy, N.Y. 12180–3590, submitted for publication.

Table 1.

Elastic Properties for Boron Fiber

Properties	Boron	
E^f_3 (MPa)	413400	(*)
ν^f_{31}	0.21	(*)
G^f_{13} (MPa)	170830	(**)
α^f (m/m/°C)	6.3E-6	(***)
E^f_1 (MPa)	413400	(*)
G^f_{12} (MPa)	170830	(**)
α^f (m/m/°C)	6.3E-6	(***)

(*) Kreider and Prewo [1974]

(**) Estimate

(***) Tsirlin [1985]

Table 2.

Thermoelastic and Thermoviscoplastic Properties of the Matrix

$E^m = 74657[1 - (\frac{T}{933})^2]$ (MPa) (*), $\nu^m = 0.33$ (**)

$G^m = 28066[1 - (\frac{T}{933})^2]$ (MPa) (*)

$\alpha^m = 2.35E\text{-}5 + 2.476E\text{-}8(T - 273)$ (m/m/°C) (**)

$q^m[\Gamma^m] = \Phi^m[\Gamma^m]/E^m$, $p^m = E^T_1/K^m$

Viscosity function $k^m[\Gamma^m] = k_1(1+ \frac{\Gamma^m}{k_2})^{-k_3}$

$k_1 = 314200$ (s), $k_2 = 71.38$ (MPa) (***), $k_3 = 53 - 0.05(T-273)$ (**)(***)

Viscosity Factor $K^m = E^m$

$E^T_1 = 619[1 - (\frac{T}{933})^2]$ (MPa) (**), $A^m = 72.24[1 - (\frac{T}{933})^2]$ (MPa) (**)

Shape function $\Phi^m[\Gamma^m] = c_1 + (c_2-c_1)\exp(-c_3\Gamma^m)$

$c_1 = 16511[1 - (\frac{T}{933})^2]$ (MPa) (**), $c_2 = 73910[1 - (\frac{T}{933})^2]$ (MPa) (**)

$c_3 = 8.43E\text{-}2 + 1.06E\text{-}4(T-273) + 1.914E\text{-}6(T-273)^2 + 5.304E\text{-}9(T-273)^3$ (MPa^{-1}) (**)

Inelastic Poisson's Ratio: 0.5

T = °K, 153°K < T < 933°K

(*) Estimate. Temperature dependence due to Hillig [1985]

(**) Estimate

(***) Yao and Krempl [1985]

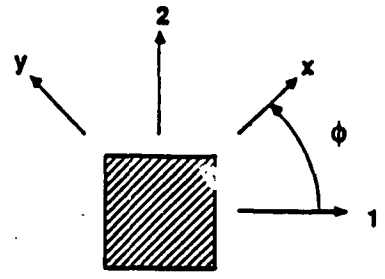

Fig. 1 Coordinate systems used in the analysis.

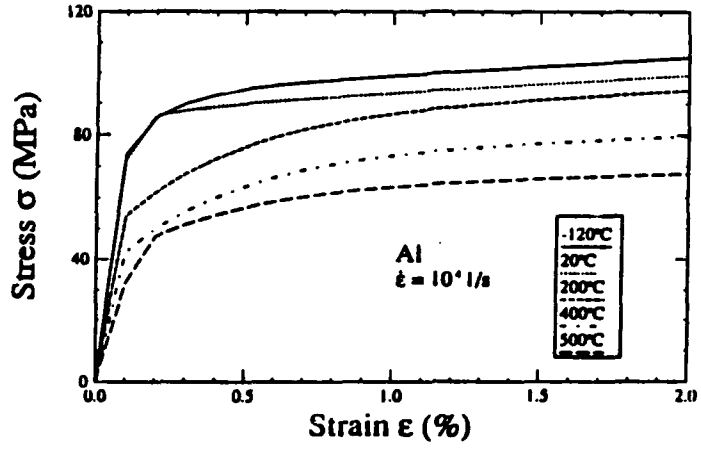

Fig. 2 Matrix stress–strain diagrams as a function of temperature. They are obtained by integrating the matrix constitutive equations for the strain rate of 10^{-4} 1/s.

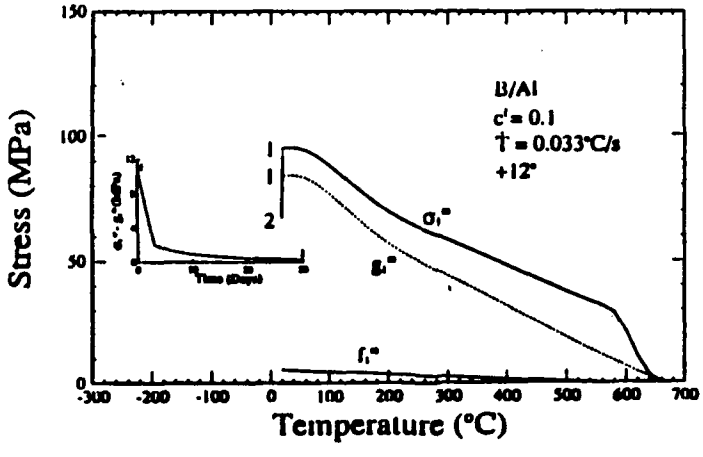

Fig. 3 Residual stresses in the 1-direction generated during the cool-down from manufacture to the +12° ply of a $(\pm 12°)_s$ laminate. The corresponding growth of the state variables of the matrix are also shown.

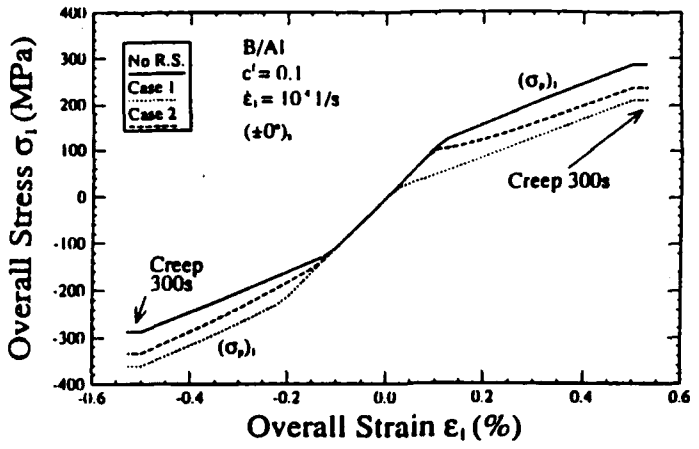

Fig 4 The influence of residual stresses on the subsequent behavior in tension/compression tests of a $(\pm 0^\circ)_s$ laminate. The strain accumulation during a 300s creep test shows the viscoplastic nature of the deformation.

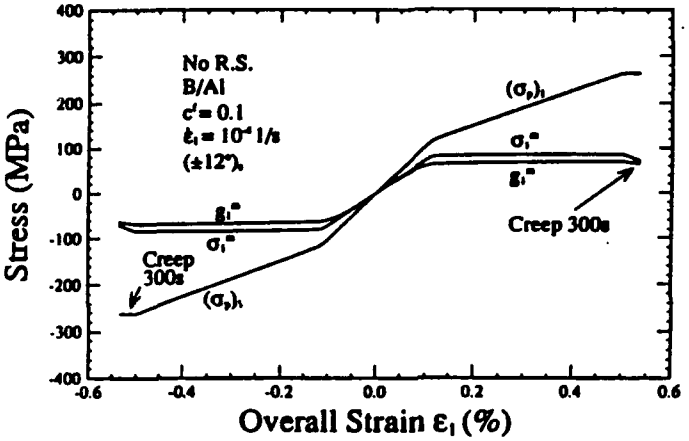

Fig 5 Tension/compression stress–strain diagrams for a $(\pm 12^\circ)_s$ laminate at a constant strain rate with a creep period of 300 s duration. In addition to the laminate stress $(\sigma_p)_1$ the corresponding matrix stress σ_1^m and matrix equilibrium stress g_1^m of a ply are also shown. No residual stresses from cool–down.

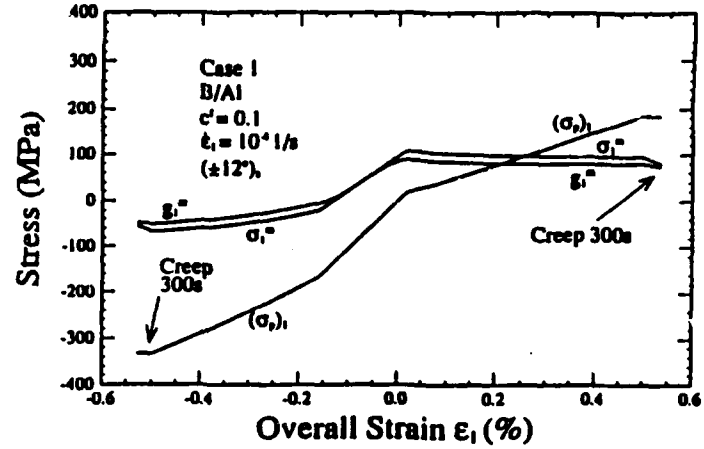

Fig. 6 Same as Fig. 5 except that residual stresses corresponding to Case 1 are used.

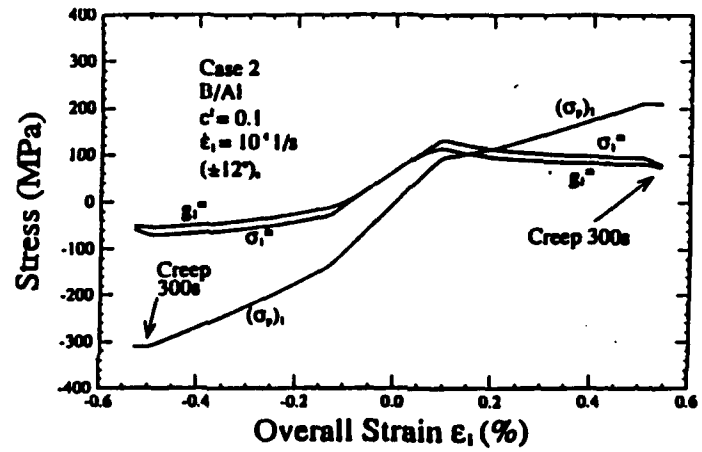

Fig. 7 Same as Fig. 5 except that residual stresses corresponding to Case 2 are used.

APPENDIX

For the transversely isotropic (fiber) and the isotropic (matrix) elastic properties the usual designations are employed. For convenience the following quantities are defined and used

$$E_{xx} = c^f E^f_{xx} + c^m E^m$$
$$L = \nu^f_{xy} E^m - \nu^m E^f_{xx}$$
$$\overline{\nu}_{xy} = c^f \nu^f_{xy} + c^m \nu^m .$$

The components of the overall elastic compliance matrix $\overline{C}^{-1}$ are

$$(\overline{C}^{-1})_{xx} = \frac{1}{E_{xx}}$$
$$(\overline{C}^{-1})_{yy} = \frac{c^f}{E^f_{yy}} + \frac{c^m}{E^m} - \frac{c^f c^m L^2}{E^f_{xx} E^m E_{xx}}$$
$$(\overline{C}^{-1})_{xy} = \frac{-\overline{\nu}_{xy}}{E_{xx}} = (\overline{C}^{-1})_{yx}$$
$$(\overline{C}^{-1})_{ss} = \frac{c^f}{G^f_{ss}} + \frac{c^m}{G^m}$$

with all other $(\overline{C}^{-1})_{ij} = 0$.

The viscosity matrix $(K^m)^{-1}$ is given by the components (the argument of the viscosity function k^m is omitted)

$$(K^m)^{-1}_{xx} = \frac{c^m E^m}{E_{xx} K^m k^m}$$
$$(K^m)^{-1}_{yy} = \frac{c^m}{K^m k^m}\left(1 + 0.5\frac{c^f L}{E_{xx}}\right)$$
$$(K^m)^{-1}_{yx} = \frac{-c^m}{K^m k^m}\left(0.5 + \frac{c^f L}{E_{xx}}\right)$$
$$(K^m)^{-1}_{xy} = \frac{-c^m E^m}{2 E_{xx} K^m k^m}$$
$$(K^m)^{-1}_{ss} = \frac{3 c^m}{K^m k^m} .$$

All other $(K^m)^{-1}_{ij} = 0$.

The components of the "extra terms" $(\dot{R}^f)^{-1}$ and $(\dot{R}^m)^{-1}$ are

$$(\dot{R}^f)^{-1}_{xx} = -\frac{c^f \dot{E}^f_{xx}}{E^f_{xx} E_{xx}}$$
$$(\dot{R}^f)^{-1}_{yy} = -c^f \frac{\dot{E}^f_{yy}}{(E^f_{yy})^2} - \frac{c^f c^m L}{(E^f_{xx})^2 E_{xx}}\left(\nu^f_{xy} \dot{E}^f_{xx} - \nu^f_{xy} \dot{E}^f_{xx}\right)$$
$$(\dot{R}^f)^{-1}_{yx} = \frac{c^f}{E^f_{xx} E_{xx}}\left(\overline{\nu}_{xy} \dot{E}^f_{xx} - \nu^f_{xy} E_{xx}\right)$$

$$(\dot{R}^f)_{xy}^{-1} = \frac{c^f}{E_{xx}^f E_{xx}}(\nu_{xy}^f \dot{E}_{xx}^f - \dot{\nu}_{xy}^f E_{xx}^f)$$

$$(\dot{R}^f)_{ss}^{-1} = -c^f \frac{\dot{G}_{ss}^f}{(G_{ss}^f)^2}$$

with all other $(\dot{R}^f)_{ij}^{-1} = 0$.

$$(\dot{R}^m)_{xx}^{-1} = -\frac{c^m \dot{E}^m}{E^m E_{xx}}$$

$$(\dot{R}^m)_{yy}^{-1} = -c^m \frac{\dot{E}^m}{(E^m)^2} + \frac{c^f c^m L}{(E^m)^2 E_{xx}}(\nu^m E^m - \nu^m \dot{E}^m)$$

$$(\dot{R}^m)_{yx}^{-1} = \frac{c^m}{E^m E_{xx}}(\bar{\nu}_{xy} \dot{E}^m - \nu^m E_{xx})$$

$$(\dot{R}^m)_{xy}^{-1} = \frac{c^m}{E^m E_{xx}}(\nu^m \dot{E}^m - \dot{\nu}^m E^m)$$

$$(\dot{R}^m)_{ss}^{-1} = -c^m \frac{\dot{G}^m}{(G^m)^2}$$

All other $(\dot{R}^m)_{ij}^{-1} = 0$.

The overall coefficient of thermal expansion vector $\bar{\alpha}$ is represented by

$$(\bar{\alpha})_x = (c^f \alpha_x^f E_{xx}^f + c^m \alpha^m E^m)/E_{xx}$$

$$(\bar{\alpha})_y = c^f \alpha_y^f + c^m \alpha^m - \frac{c^f c^m L}{E_{xx}}(\alpha^m - \alpha_x^f)$$

$$(\bar{\alpha})_s = 0$$

A THERMOVISCOPLASTIC ANALYSIS OF UNIAXIAL RATCHETTING BEHAVIOR OF SiC/Ti FIBROUS METAL MATRIX COMPOSITES

Nan–Ming Yeh and Erhard Krempl

Mechanics of Materials Laboratory

Rensselaer Polytechnic Institute

Troy, New York 12180–3590

RPI Report MML 91–5

June 1991

~~To appear in~~ Proceedings, American Society for Composites 6th Technical Conference on Composite Materials, Albany, New York, October 6–9, 1991, pp. 329–337

A THERMOVISCOPLASTIC ANALYSIS OF UNIAXIAL RATCHETTING BEHAVIOR OF SiC/Ti FIBROUS METAL MATRIX COMPOSITES

Nan–Ming Yeh and Erhard Krempl
Mechanics of Materials Laboratory
Rensselaer Polytechnic Institute
Troy, New York 12180–3590

ABSTRACT

The vanishing fiber diameter model together with the thermoviscoplasticity theory based on overstress are used to analyze the thermomechanical ratchetting behavior of a SiC/Ti unidirectional metal matrix composite. For the present analysis the fibers are assumed to be isotropic thermoelastic and the matrix constitutive equation is the isotropic thermoviscoplasticity theory based on overstress with temperature–dependent recovery of state. Yield surfaces and loading/unloading conditions are not used in the viscoplasticity theory for the matrix in which the inelastic strain rate is solely a function of the overstress, the difference between stress and equilibrium stress, a state variable of the theory. All material functions and constants can depend on current temperature. Assumed but realistic material elastic and viscoplastic properties as a function of temperature which are close to SiC and Ti, respectively, permit the computation of the stresses of the constituents and mechanical, thermal, creep, and ratchetting strains.

Numerical experiments of in–phase and out–of–phase thermomechanical loadings are performed in fiber and transverse directions. In the fiber direction very little difference is found in the ratchetting behavior for in–phase and out–of–phase loadings, while in the transverse direction in–phase loading accumulates more mechanical ratchetting strain than out–of–phase loading. In the fiber direction very little deviation from linear behavior and very small ratchetting strain are observed. Rate dependence of the matrix is the driving force of the significant transverse ratchetting strain.

INTRODUCTION

Inelastic strain accumulation under cyclic stress controlled loading (ratchetting behavior) is a special design concern. Chaboche [1] introduced cyclic time–independent plasticity theory to interpret the ratchetting behavior of 316 stainless steel. He concluded that an increase of stress range for a given mean stress will increase ratchetting strain. Ruggles and Krempl, [2,3] studied the zero–to–tension ratchetting behavior of 304 stainless steel and found that, in this case, rate dependence is the major driving force of the inelastic strain accumulation.

The purpose of this paper is to investigate the ratchetting behavior of SiC/Ti fibrous metal matrix composite in both fiber and transverse directions under thermomechanical loading by numerical experiments. The fiber is assumed to be thermoelastic and isotropic, and the matrix is assumed thermoviscoplastic and isotropic including static recovery of state. The vanishing fiber diameter model [4] is combined with the thermoviscoplasticity theory based on overstress (TVBO) [5] for a composite model.

Numerical experiments of uniaxial zero–to–tension mechanical loading (stress–control) with simultaneous temperature changes are performed. In this case the temperature and the load can be made to increase simultaneously (in–phase loading) or mechanical loading and temperature can move in different directions (out–of–phase

loading), see Fig. 1. Of specific interest is the difference in ratchetting behavior in in–phase and out–of–phase loadings. Both the fiber direction behavior and the transverse direction behavior for a SiC/Ti composite are investigated.

THE COMPOSITE MODEL

For the representation of the equations, the usual vector notation for the stress tensor components σ and the small strain tensor components ϵ are used. Boldface capital letters denote 6x6 matrices.

Stresses and strains without a superscript designate quantities imposed on the composite as a whole. *Superscripts* ^{f} and ^{m} *denote* fiber and matrix, respectively. The fiber volume fraction is c^f and c^m denotes the matrix volume fraction with $c^f + c^m = 1$.

A unidirectional fibrous composite element is assumed with fiber orientation in the 3–direction. When the VFD [4] model is combined with the TVBO model [5] the composite is characterized by the following set of equations: (details can be found in [6])

$$\dot{\epsilon} = \bar{\mathbf{C}}^{-1}\dot{\sigma} + (\mathbf{K}^m)^{-1}\mathbf{x}^m + (\dot{\mathbf{R}}^f)^{-1}\sigma^f + (\dot{\mathbf{R}}^m)^{-1}\sigma^m + \bar{\alpha}\dot{T} \tag{1}$$

together with a separate growth law for the σ_3^m component of the matrix

$$\begin{aligned}\dot{\sigma}_3^m = {} & \frac{E^m}{E_{33}}\dot{\sigma}_3 - \frac{c^f}{E_{33}}L(\dot{\sigma}_1 + \dot{\sigma}_2) - \frac{c^f E_{33}^f E^m}{E_{33}} \\ & \left\{\frac{1}{K^m k^m[\Gamma^m]}\left[x_3^m - 0.5(x_1^m + x_2^m)\right]\right\} \\ & - \frac{c^f E_{33}^f E^m}{E_{33}}\left\{\left[\frac{1}{(E_{33}^f)^2}(\nu_{31}^f E_{33}^f - \nu_{31}^f \dot{E}_{33}^f)\right.\right. \\ & \left.\left. - \frac{1}{(E^m)^2}(\nu^m E^m - \nu^m \dot{E}^m)\right](\sigma_1 + \sigma_2) + \frac{\dot{E}_{33}^f}{(E_{33}^f)^2}\sigma_3^f - \frac{\dot{E}^m}{(E^m)^2}\sigma_3^m\right\} \\ & - \frac{c^f E_{33}^f E^m}{E_{33}}(\alpha^m - \alpha_3^f)\dot{T}.\end{aligned} \tag{2}$$

In addition growth laws for the two state variables of TVBO, the matrix equilibrium stress g^m and the kinematic stress f^m, are given as

$$\begin{aligned}\dot{g}^m = {} & q^m[\Gamma^m]\dot{\sigma}^m + \dot{T}\frac{\partial q^m[\Gamma^m]}{\partial T}\sigma^m + \left\{q^m[\Gamma^m] - \theta^m\left[q^m[\Gamma^m] - \right.\right. \\ & \left.\left. p^m(1-q^m[\Gamma^m])\right]\right\}\frac{x^m}{k^m[\Gamma^m]} - \frac{g^m}{\Pi^m}R^m[\Pi^m]\end{aligned} \tag{3}$$

$$\dot{f}^m = \frac{p^m}{k^m[\Gamma^m]}x^m. \tag{4}$$

with

$$(\Gamma^m)^2 = (x^m)^t\, H\, (x^m)$$
$$(\theta^m)^2 = \frac{1}{(A^m)^2}(z^m)^t\, H\, (z^m)$$
$$(\Pi^m)^2 = (g^m)^t\, H\, (g^m)$$
$$x^m = \sigma^m - g^m$$
$$z^m = g^m - f^m \qquad (5)$$

The recovery function R^m for the matrix is postulated to be

$$R^m[\Pi^m] = \frac{R_3}{2}\left\{\text{sign}(U)\left[1-(1+|U|)^{1-\zeta}\right] + \text{sign}(V)\left[1-(1+|V|)^{1-\zeta}\right]\right\} \qquad (6)$$

where

$$U = -R4 + R5\left(\frac{\Pi^m - R_1}{R_2 - R_1}\right),$$
$$V = R4 + R5\left(\frac{\Pi^m + R_1}{R_2 - R_1}\right),$$

and R_1, R_2, R_3 are functions of temperature. The recovery function depends on temperature and equilibrium stress, and is assumed to activate at 400° C when equilibrium stress reaches 300 MPa (threshold), and to become saturated if equilibrium stress is larger than 360 MPa. The threshold value decreases and the saturated value increases as the increase of the temperature. Recovery is negligible when the current temperature is lower than 400° C. A discussion of the recovery of state formulation within TVBO is given in [7].

In the above $\bar{C}^{-1}$ is the overall compliance matrix and $(K^m)^{-1}$ denotes the viscosity matrix. The matrices $(\dot{R}^f)^{-1}$ and $(\dot{R}^m)^{-1}$ contain time derivatives of the elastic constants of the fiber and the matrix, respectively. All components of the matrices $\bar{C}^{-1}$, $(K^m)^{-1}$, $(\dot{R}^f)^{-1}$, $(\dot{R}^m)^{-1}$, and H, and the definition of the quantities $\bar{E}_{33}$, L, $\bar{\alpha}$ are given in [6]. The viscosity function $k^m[\Gamma^m]$ and the dimensionless shape function $q^m[\Gamma^m]$ are decreasing ($q^m[0] < 1$ is required) and control the rate dependence and the shape of the stress–strain diagram, respectively. (Square brackets following a symbol denote "function of".) The quantity p^m represents the ratio of the tangent modulus E_t^m at the maximum inelastic strain of interest to the viscosity factor K^m. It sets the slope of stress–inelastic strain diagram at the maximum strain of interest. A detailed explanation of the TVBO and the composite model are given in [5] and [6], respectively.

NUMERICAL SIMULATION

Eqs. (1) – (5) constitute the three dimensional model which must be reduced to the one dimensional case. The boundary conditions must be specified in addition to the uniform temperature history. Also the material properties of the composite constituents must be known as a function of temperature. Only the elastic properties of the SiC fibers

are known reasonably well, see Table 1. The thermoviscoplastic properties of the Ti–matrix were assumed by using data from Krempl et al. [8] of Ti–alloy at room temperature and by postulating that the stress level at a given strain and strain rate decreases with increasing temperature. The temperature dependence of the constants is given in Table 2. When TVBO is integrated for the tensile test with a constant strain rate of 10^{-4} s^{-1} the isothermal stress–strain diagrams depicted in Fig. 2 result. They represent the postulated matrix properties.

For the integration of the coupled set of differential equations the IMSL routine DGEAR is used.

Numerical experiments of uniaxial zero–to–tension mechanical loading (stress–control) with simultaneous temperature changes are performed in both fiber and transverse directions. In Fig. 3 in–phase stress and temperature controlled thermomechanical loading is applied in fiber direction to reach 450 MPa and 320° C using the indicated rates. The rates are then changed to impose five cycles of in–phase loading in the fiber direction. In Fig. 3 both the total and the mechanical strain are used to plot the stress–strain diagrams. Only little ratchetting strain is accumulated, and some matrix stress relaxation is observed. Matrix stress range and matrix mean stress of the first cycle are 378 MPa and 84 MPa, respectively. In Fig. 4 the same initial loading is performed followed by five cycles out–of–phase loading. The matrix stress range (504 MPa) and the matrix mean stress (100 MPa) is increased compared to Fig. 3. Although the ratchetting strain is higher than in Fig. 3 it is still small and does not appear to be progressive. The same numerical processes are now applied in transverse direction and the results are shown in Fig. 5, 6 for in–phase and out–of–phase cases, respectively. The matrix stress ranges and the matrix mean stresses are the same for both cases. Significant ratchetting strain is accumulated during the five cycles of in–phase loading in Fig. 5, while only little ratchetting strain for the out–of–phase case is shown in Fig. 6.

DISCUSSION

Ratchetting, the accumulation of strain under cyclic loading involving stress boundary conditions, is driven by inelasticity, it is not a phenomenon of linear elasticity. Isothermal, time(rate)–independent analyses, see Chaboche [1], and rate dependent, viscoplastic analyses, see Krempl and Ruggles [3], have been performed. Depending on loading conditions plasticity or viscoplasticity effects may dominate.

In the present case variable temperature and composites are considered. For in–phase and out–of–phase loading in the fiber direction, the cyclic stress range used is such that very little inelasticity develops. This is mostly due to the stiffening effects of the fibers. As a consequence insignificant ratchetting strain is seen to develop in Figs. 3 and 4. Although one would expect more ratchet strain accumulation for the in–phase case than for the out–of–phase case on account of the simultaneous increase of stress and temperature and a simultaneous decrease in strength, this expectation is not borne out by the calculations.

However, the results for the transverse direction confirm this expectation, see Figs. 5 and 6, where in–phase loading shows considerably larger ratchetting strains than the out–of–phase case. In the absence of any reinforcement effects of the fibers, the behavior is completely determined by the matrix properties and ratchetting turns out to be significant in Fig.5. The decrease in temperature while the stress increases results in a considerable reduction of the ratchet strain in Fig. 6. From this analysis it appears that the transverse direction is more susceptible to ratchetting than the fiber direction. At the same time it

has to be realized that the VFD model provides no restraint in the transverse direction so that the computations give certainly a worst case scenario.

In Figs. 3 through 6 we have plotted both the total and the mechanical strain for illustrative purposes. Due to the stress–controlled loading the thermal strain simply adds to the mechanical strain. As a consequence the stress–strain diagrams using the total and the mechanical strain are very similar. The situation would be different in strain controlled loading which could be simulated as well.

It has to be realized that the simulation has been performed with assumed material properties, this is especially so for the inelastic properties of the matrix material. The predictions, which appear to be reasonable, are, of course, only as good as these assumptions. For an application the fiber and matrix properties should be determined by suitable mechanical tests at various temperatures (isothermal tests suffice for TVBO) before the model is used to numerically predict the behavior of the composite. These predictions should then be compared with actual tests performed under the same boundary conditions as the numerical experiments. If both results agree reasonably the theory is validated for design use. Unfortunately no such experiments appear to be available.

Although recovery of state was included in the formulation, the numerical experiments involve only short times in which recovery of state does not significantly contribute to the deformation behavior. A discussion of recovery of state formulations and their effects on model predictions can be found in Majors and Krempl [7]. The present formulation includes the recovery term only in the growth law for the matrix equilibrium stress, see Eq. (3). It enables the modeling of secondary creep in the quasi–linear region of the temperature above the thresholds given after Eq. (6).

ACKNOWLEDGEMENT

This research was supported by DARPA/ONR Contract N00014–86–k0770 with Rensselaer Polytechnic Institute

REFERENCES

1 Chaboche, J. L., 1987, "Cyclic Plasticity Modeling and Ratchetting Effects," Proceedings of the Second International Conference on Constitutive Laws for Engineering Materials: Theory and Applications, Vol. 1, Desai, C. S., Krempl E., Kiousis, P. D., and Kundu, T., Eds., Elsevier Publishers, pp. 47–58.

2 Ruggles, M. B. and Krempl, E., 1990, "The Interaction of Cyclic Hardening and Ratchetting for Aisi Type–304 Stainless Steel at Room Temperature. I. Experiments," Journal of the Mechanics and Physics of Solids, Vol. 38, pp. 575–585.

3 Krempl, E. and Ruggles, M. B., 1990, "The Interaction of Cyclic Hardening and Ratchetting for Aisi Type–304 Stainless Steel at Room Temperature. II. Modeling with the Viscoplasticity Theory Based on Overstress," Journal of the Mechanics and Physics of Solids, Vol. 38, pp. 587–597.

4 Dvorak, G. J. and Bahei–El–Din, Y. A., 1982, "Plasticity Analysis of Fibrous Composites," Journal of Applied Mechanics, Vol. 49, pp. 327–335.

5 Lee, K. D. and Krempl, E., 1990, "An Orthotropic Theory of Viscoplasticity Based on Overstress for Thermomechanical Deformations," International Journal of Solids and Structures, Vol. 27, pp. 1445–1459.

6 Yeh, N. M. and Krempl, E., 1990, " Thermoviscoplastic Analysis of Fibrous Metal–Matrix Composites," to appear, Journal of Composite Materials.

7 Majors, P. S. and Krempl, E., 1991, "A Recovery of State Formulation for the Viscoplasticity Theory Based on Overstress," to appear in Proceedings of the Conference on High Temperature Constitutive Modeling: Theory and Application, A. D. Freed and K. P. Walker, Eds., American Society of Mechanical Engineers Winter Annual Meeting, Atlanta, GA.

8 Krempl, E., Ruggles, M. B., and Yao, D., 1987, "Viscoplasticity Theory Based on Overstress Applied to Ratchetting," Symposium on Advances in Inelastic Analysis, AMD–Vol. 88/PED–Vol. 28, S. Nakasawa, K. Willam, and N. Rebelo, Eds. American Society for Mechanical Engineers, New York, N.Y., pp. 1–11.

9 Hillig, W. B., 1985, "Prospects for Ultra–High–Temperature Ceramic Composites," Report No. 85CRD152, General Electric Research and Development Center.

10 Lara–Curzio, E. and Sternstein, S. S., 1991, "On the Anomalous Thermal Expansion Behavior of CVD SiC Fibers," to appear, J. Am. Ceram. Soc.

Table 1 Thermoelastic Properties for SiC Fiber

$E^f_{33} = E^f_{11}$ (MPa)	$374000[1 - (\frac{T}{933})^3]$ (*)	
ν^f_{31}	0.2 (**)	
$G^f_{44} = G^f_{66}$ (MPa)	$155833[1 - (\frac{T}{933})^3]$ (*)	
$\alpha^f_3 = \alpha^f_1$ (m/m/°C)	4.3E–6	R.T. → 1000°C
(***)	5.6E–6	1000°C → 1350°C
	–4.9E–6	1350°C → 1410°C
	5.6E–6	> 1410°

(*): Estimated, temperature dependence due to Hillig [9]
(**): Estimate
(***): Lara–Curzio and Sternstein [10]

Table 2 Thermoelastic and Thermoviscoplastic Properties of the Ti Matrix with Temperature–Dependent Recovery Function (*)

$E^m = 51149 + 696.7T - 2.205T^2 + 0.0025T^3 - 1.017T^4$ (MPa), $T \leq 773°K$
$= 297251 - 668.7T + 0.693T^2 - 3.41E{-}4T^3 + 6.26E{-}8T^4$, $T \geq 773°K$

$G^m = 19523 + 266T - 0.842T^2 + 9.52E{-}4T^3 - 3.88E{-}7T^4$ (MPa), $T \leq 773°K$
$= 113455 - 255T + 0.265T^2 - 1.3E{-}4T^3 + 2.39E{-}8T^4$, $T \geq 773°K$

$\nu^m = 0.31$, $\alpha^m = 9.0E{-}6$ (m/m/°C)

$k_1 = 314200$ (s), $k_2 = 117$ (MPa)
$k_3 = 20.64 - 7.3E{-}3T$ (MPa), $T \leq 773°K$
$= 16.52 - 0.013T + 3.53E{-}5T^2 - 3.64E{-}8T^3 + 1.25E{-}11T^4$, $T \geq 773°K$

$E_t^m = 1333.3 - 0.6937T$ (MPa)

$A^m = -44 + 8.82T - 0.034T^2 + 4.86E{-}5T^3 - 2.45E{-}8T^4$ (MPa), $T \leq 773°K$
$= 2712 - 6.3T + 0.0057T^2 - 2.31E{-}6T^3 + 3.53E{-}10T^4$, $T \geq 773°K$

$c_1 = 152941 - 954T + 4.56T^2 - 9.37E{-}3T^3 + 6.57E{-}6T^4$ (MPa), $T \leq 573°K$
$= -846653 + 4706T - 8.87T^2 + 7.11E{-}3T^3 - 2.08E{-}6T^4$, $573 \leq T \leq 1073°K$
$= 157042 - 263T + 0.146T^2 - 2.58E{-}5T^3 - 5.22E{-}10T^4$, $T \geq 1073°K$
$c_2 = 166382 - 612T + 3.2T^2 - 7.12E{-}3T^3 + 5.19E{-}6T^4$ (MPa), $T \leq 573°K$
$= 160341 - 99.6T - 0.104T^2 - 6.8E{-}5T^3 + 1.57E{-}8T^4$, $573 \leq T \leq 1073°K$
$= 71000 + 6.11T - 0.0455T^2 + 7.91E{-}6T^3 + 2.35E{-}9T^4$, $T \geq 1073°K$
$c_3 = -0.124 + 9.8D{-}4T - 2D{-}6T^2 + 1.57E{-}9T^3$ (MPa^{-1}), $T \leq 573°K$
$= -1.634 + 8.98E{-}3T - 1.6E{-}5T^2 + 9.67E{-}9T^3$, $573 \leq T \leq 1073°K$
$= -14.44 + 0.017T - 1.41E{-}6T^2 - 7.42E{-}10T^3$, $T \geq 1073°K$

$R1 = 2773 - 15.6T + 0.044T^2 - 5.47E{-}5T^3 + 2.39E{-}8T^4$ (MPa), $T \leq 773°K$
$= 906 - 1.82T + 1.22E{-}3T^2 - 2.69E{-}7T^3$, $T \geq 773°K$
$R2 = 5355 - 38.7T + 0.116T^2 - 1.55E{-}4T^3 + 7.42E{-}8T^4$ (MPa), $T \leq 773°K$
$= 929 - 0.55T - 1.21E{-}3T^2 + 1.26E{-}6T^3 - 3.2E{-}10$, $T \geq 773°K$
$R3 = 9.4E{-}4 + 5.9E{-}6T$

Inelastic Poisson's Ratio: 0.5

(*) Estimated and Krempl et al., [8]

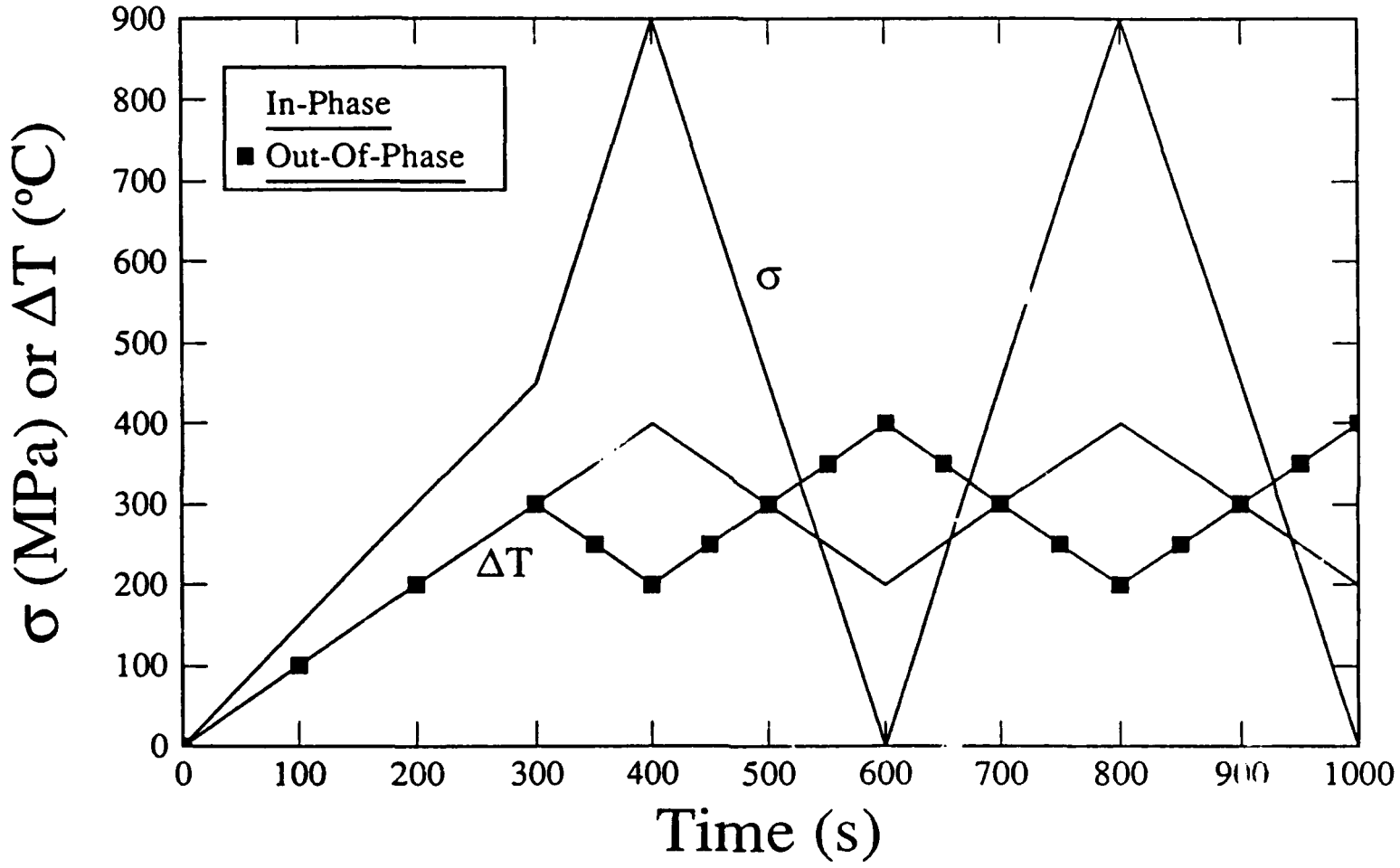

Fig. 1 Stress and temperature difference vs. time for in-phase and out-of-phase loading.

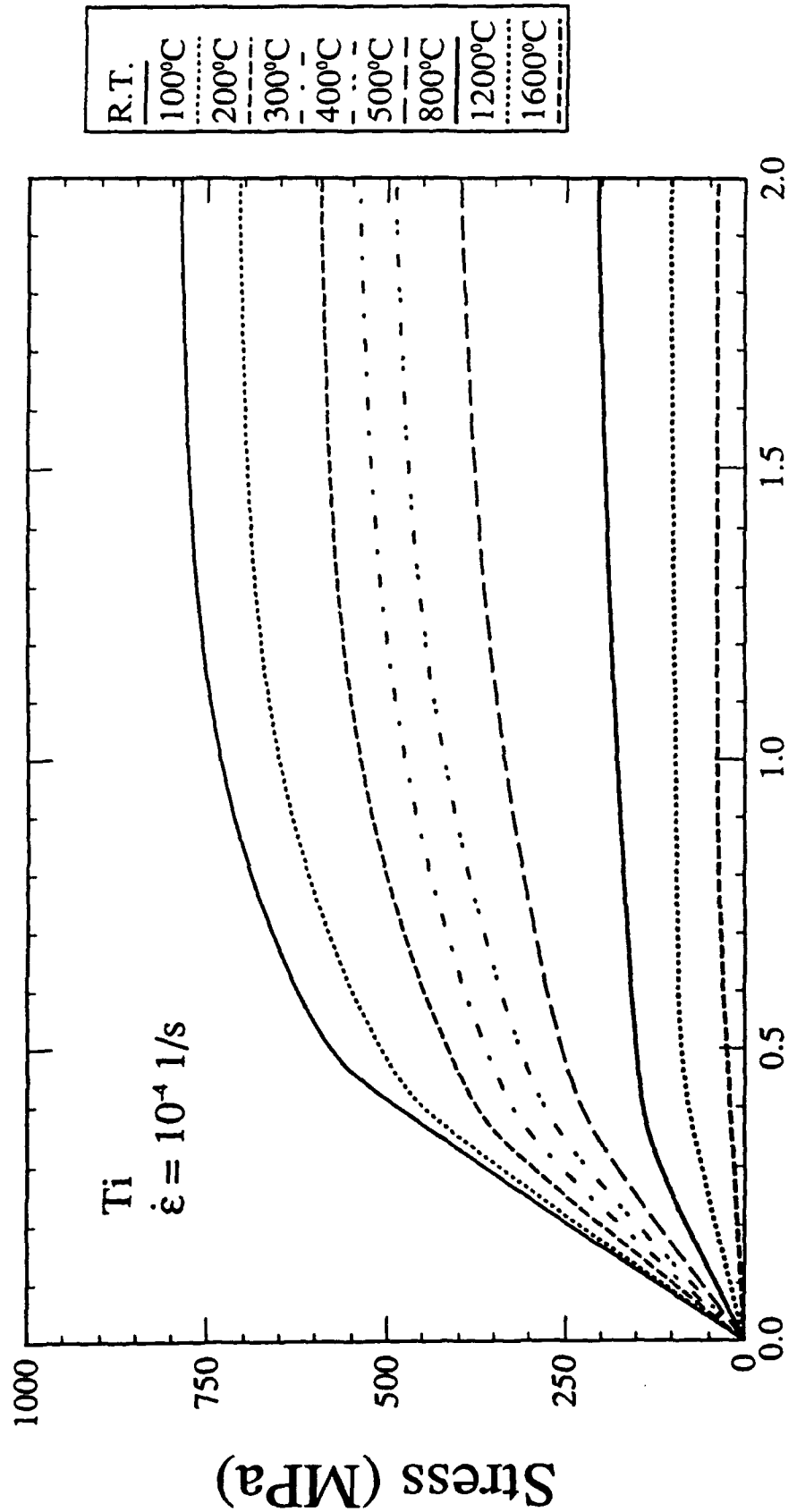

Fig. 2 Stress-strain diagrams of matrix at various temperatures.

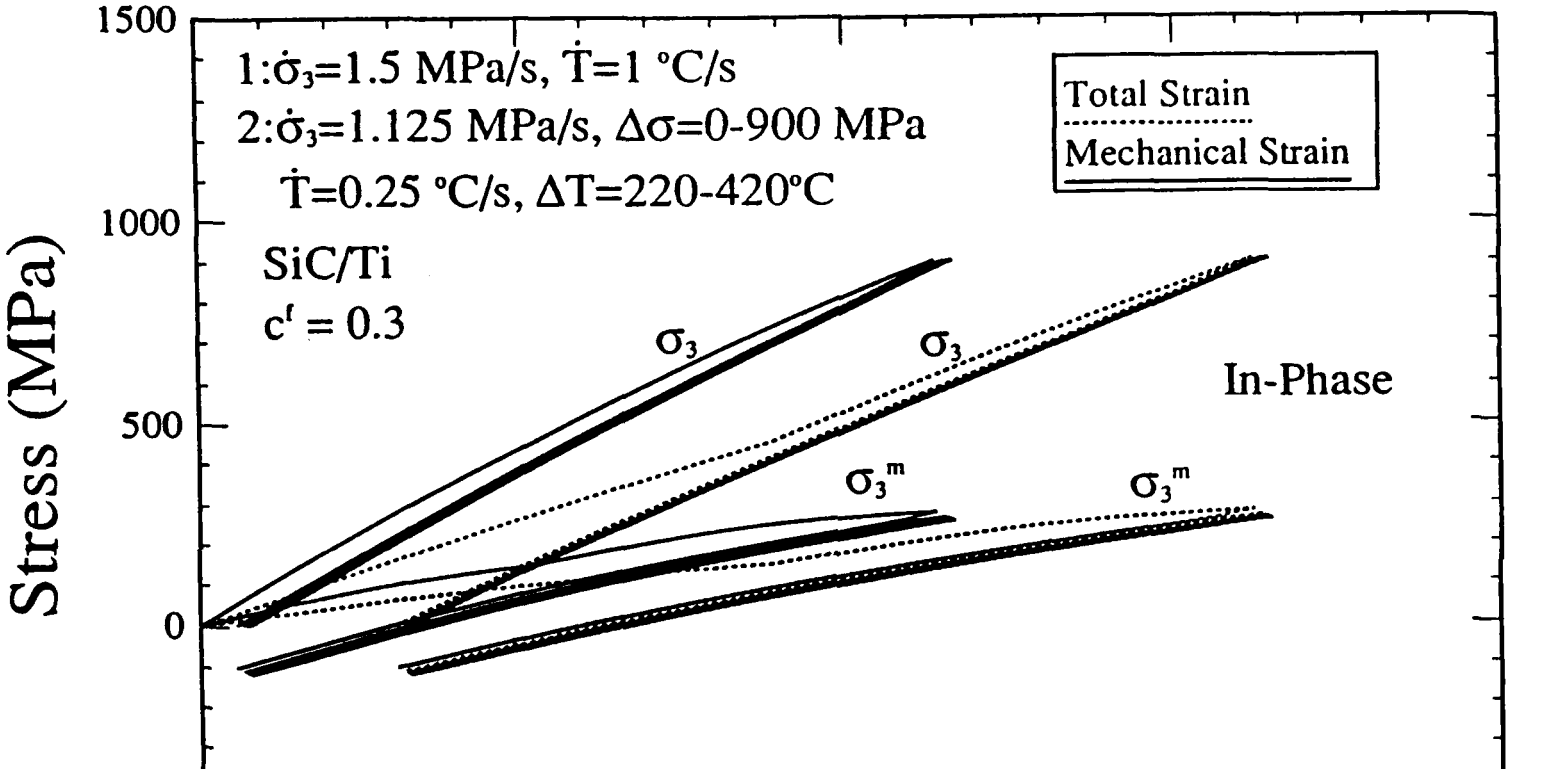

Fig. 3 Axial stress-total strain and axial stress-mechanical strain curves for SiC/Ti under stress and temperature controlled cyclic in-phase thermomechanical loading; see Fig. 1 for a definition of the loading history.

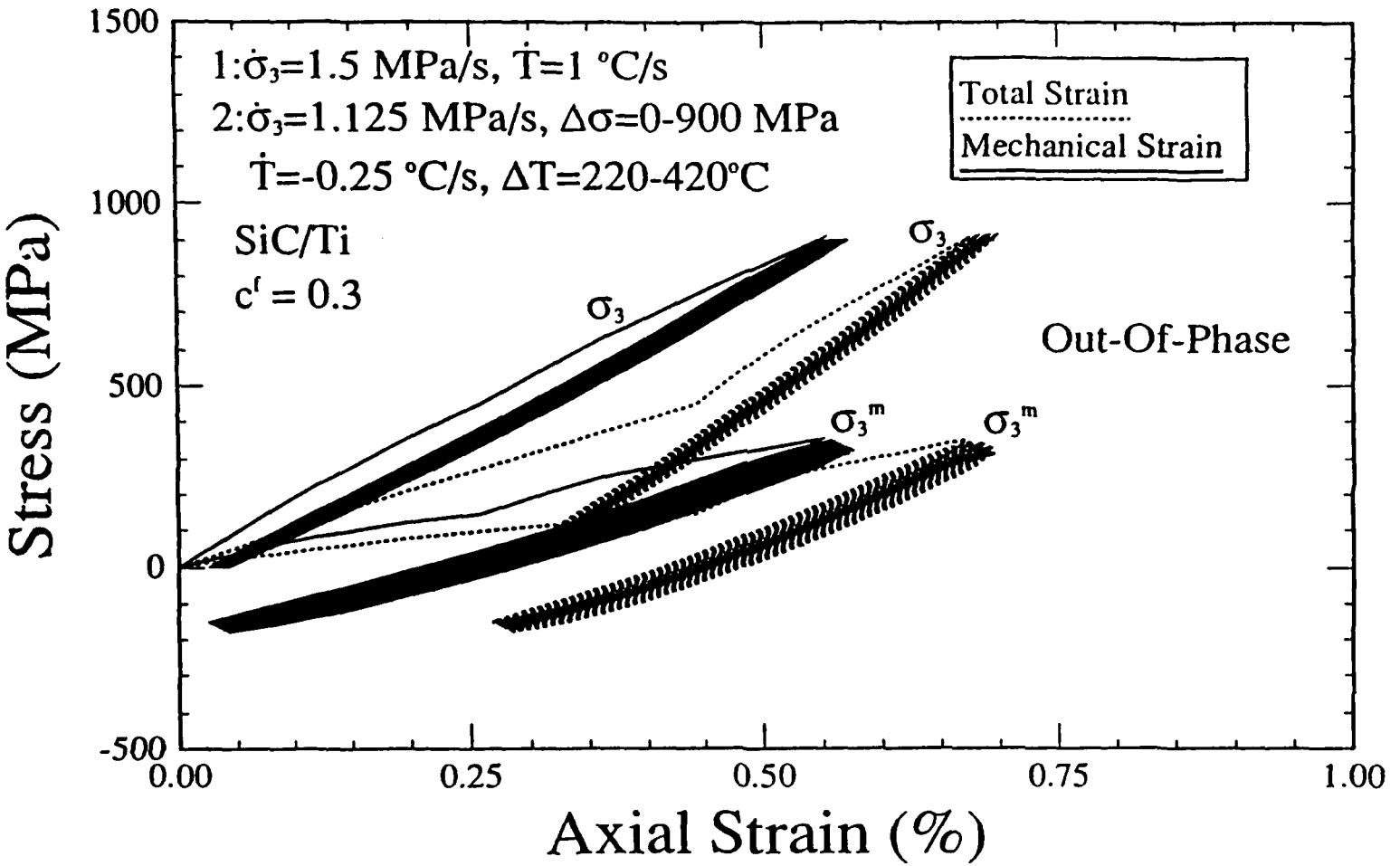

Fig. 4 Same as Fig. 3 except for out-of-phase loading.

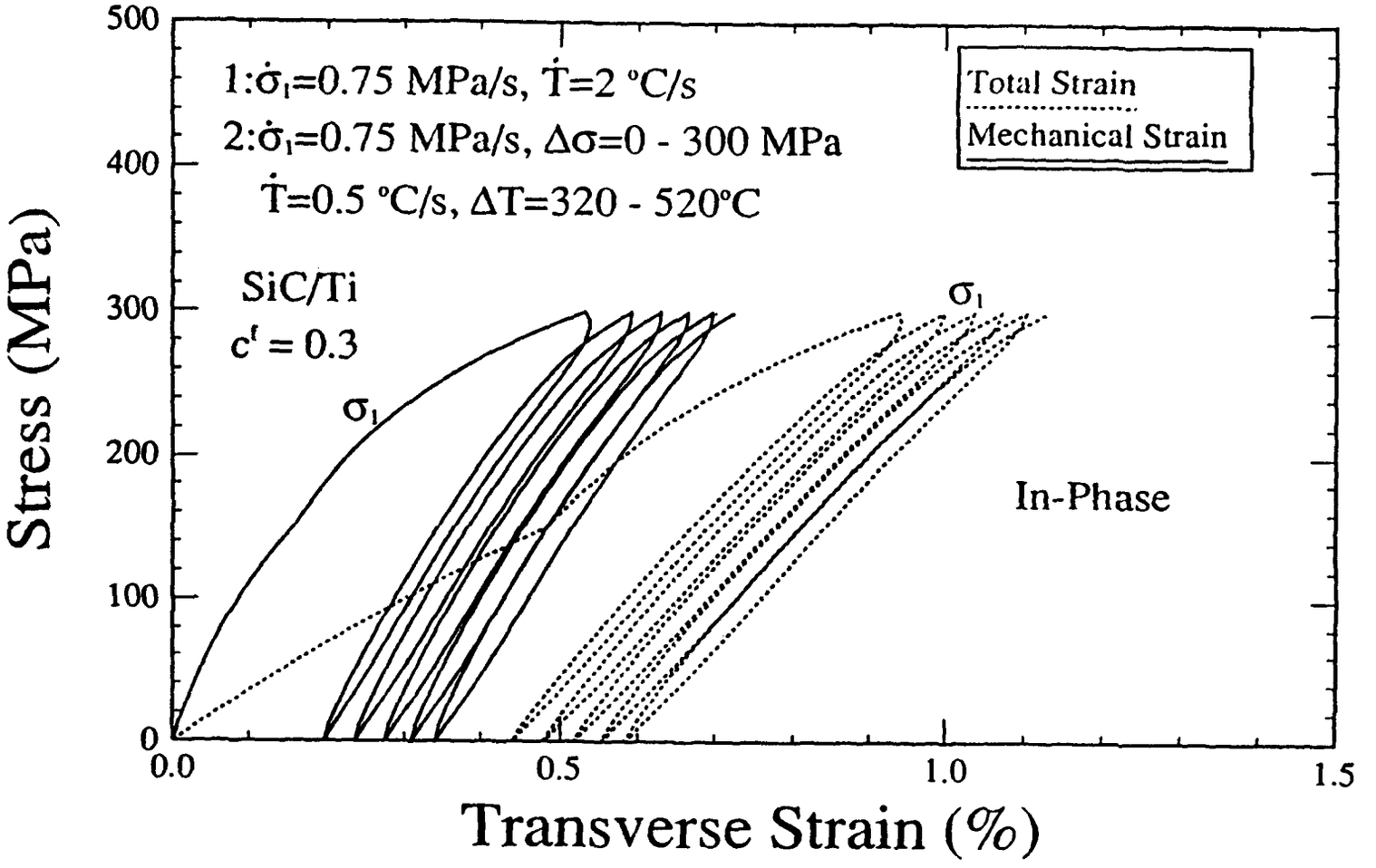

Fig. 5 Transverse stress-total strain and transverse stress-mechanical strain curves for SiC/Ti under stress and temperature controlled ..ic in-phase thermomechanical loadin.. see Fig. 1 for a definition of the loading history.

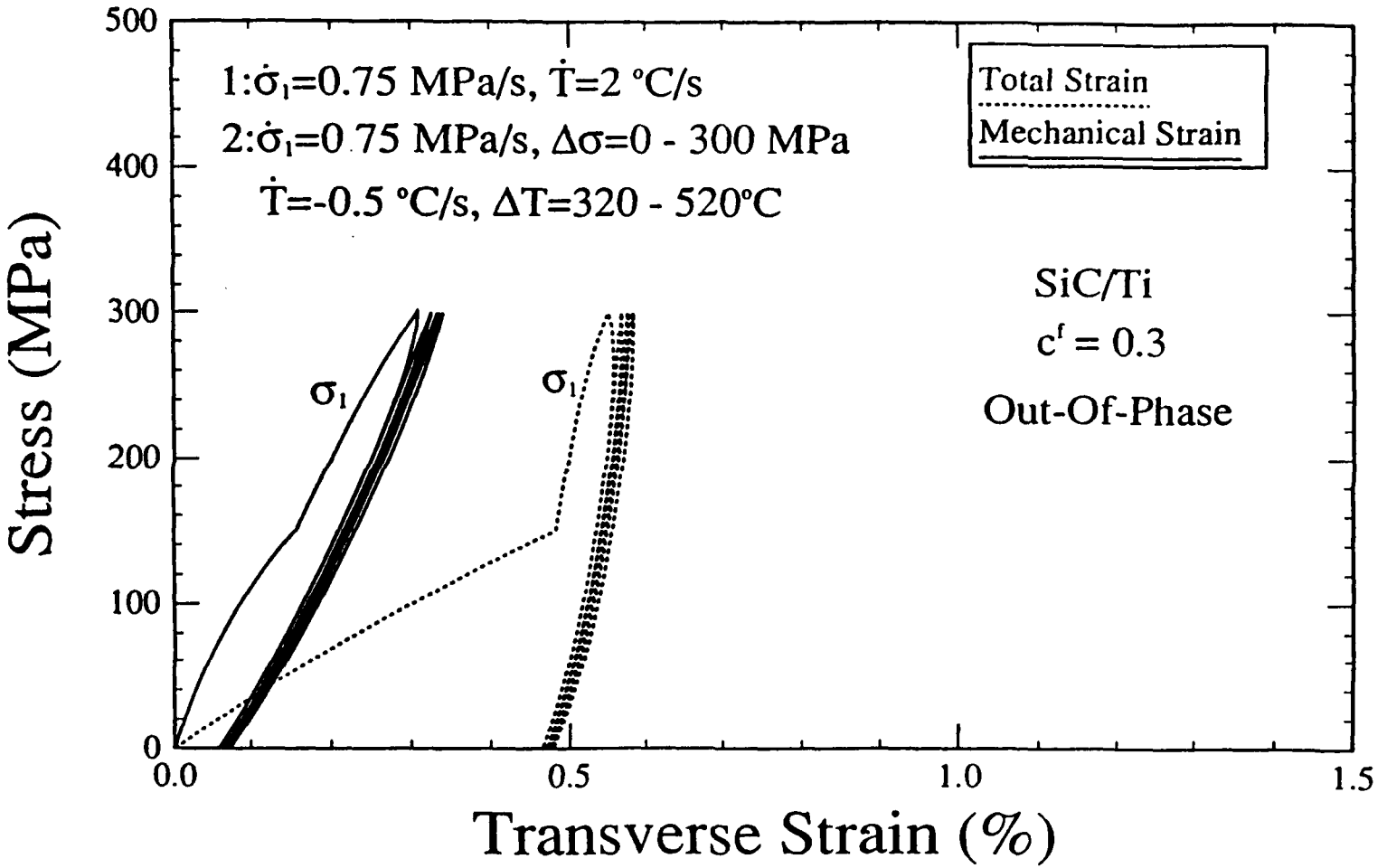

Fig. 6 Same as Fig. 5 except for out-of-phase loading.